

Stereocontrolled approaches to  $\beta$ -fluoroamines and  
a formal synthesis of the anti-HIV and antibacterial peptide (-)-feglymycin

By

Jade A. Bing

Dissertation

Submitted to the Faculty of the  
Graduate School of Vanderbilt University  
in partial fulfillment of the requirements

for the degree of

DOCTOR OF PHILOSOPHY

in

CHEMISTRY

June 30, 2020

Nashville, Tennessee

Approved:

Jeffrey N. Johnston, Ph.D.

Gary A. Sulikowski, Ph.D.

Steven D. Townsend, Ph.D.

Shaun R. Stauffer, Ph.D.

*In loving memory of Milton Bing Jr. (1957-2014)*

## ACKNOWLEDGMENTS

*“It takes a village to raise a child.”*

African proverb

My time in graduate school has not been just an academic journey, but one of mind, body and spirit. The challenges I've faced both in and out of graduate school would certainly have overcome me if I did not have my support system. There have been a lot of people along the way that have gone above and beyond to help me get to this point, and I am forever grateful for your support.

First, I must acknowledge my advisor and mentor, Dr. Jeffrey Johnston. Since the beginning Jeff has always been willing to go out of his way to help both inside and outside of lab. He has gone to extreme ends to ensure that obstacles encountered outside of the lab would never affect my success as a scientist. Thank you for leading by example and for your unending work ethic. Jeff is a teacher to his core and will do *whatever it takes* to make sure his students have a solid foundation and comprehensive understanding of chemistry. He is also empathetic and a problem-solver, and I have been blessed to have him in my corner.

Thank you to my committee, Dr. Gary Sulikowski, Dr. Steven Townsend, and Dr. Shaun Stauffer for your guidance, suggestions and open doors throughout my time at Vanderbilt. We have had quite the unusual circumstances over the last few months of my PhD while the world is in lockdown put in place by the COVID-19 pandemic. I appreciate your flexibility and patience as I conducted my Independent Research Proposal and dissertation during this time.

It unlikely that I would have pursued organic chemistry if it wasn't for Dr. Danielle Jacobs-Duda. My first year and a half in college at Rider University I was an undecided major. It wasn't until I took Dr. Jacobs' class that I found a home in chemistry. She gave me the opportunity to work in her lab for more than two years, including for some time after graduation while I figured things out before coming to graduate school. At a PUI there are no graduate students, and as such Dr. Jacobs was essential not only as a professor, but as a mentor in and out of the laboratory. Thank you, Dr. J, for teaching me how to push arrows, collect fractions and take a TLC. Thank you for your consistently high expectations of both me and of yourself, for your keen attention to detail, all of the red ink early on and for never giving up on me.

I had the pleasure of working with Dr. Robert Knowles at Princeton, who went out of his way to make sure I succeeded. I learned a lot working in his lab and sitting in on some lectures. He was really important for making sure I started on a level playing field when I came to graduate school.

I must say thank you to Angelica Benitez & the Ronald E. McNair Post-Baccalaureate Achievement Program, without whom I wouldn't even know what graduate school was, let alone how to prepare for and get into a PhD program. They exposed me to the world of academia and showed me that someone who checks all the boxes (low-income, first-generation, minority, woman in STEM), has every right to exist and succeed in that world. The program gave me the support needed (both financially and otherwise) to go to several conferences and supplied me with everything from business attire and a suitcase to a well-prepared presentation.

Thank you also to Dean Don Brunson for recruiting me and keeping his promise to do whatever is within his power to make sure I see this degree through to the end. Thank you to all of my friends in the Organization of Black Graduate and Professional Students (OBGAPS) for providing a sense of home and community throughout my time at Vanderbilt.

Thank you to Markus Voehler and Don Stec for maintaining the NMR facilities and for going out of their way to help me with extensive characterization. Thanks to Don STec also for always coming in as a relief pitcher

in IM softball. Thank you to Dr. Nathan Schley for his time and efforts with running and solving X-ray structures.

I want to acknowledge all of the past Johnston lab members, for their feedback, guidance, and a lot of great soccer games. Ken Schwieter showed me the ropes in the beginning, and was always there to answer questions, proofread, and brainstorm. I learned a lot from Sergey Tsukanov, Roosbeh Yusefi, Yasunori Toda, and Mahesh Vishe who were exemplary post-docs, with model work ethic and the patience to teach younger students. Brandon, thank you for being a great first bench mate! Thank you to Matt Knowe, who is one the kindest people I have ever met and will go out of his way to help anyone. Thank you to Thomas Struble, who has always been a humble genius, for his guidance in chemistry, for maintaining all of the lab instruments, and for being a great friend. Thank you to Dan Sprague for the chemistry discussions and for passing on the legacy of the intramural softball team to me. Karan Goyal, thank you for always bringing positive energy to the table, I look forward to seeing you succeed in graduate school.

I must give a special thanks to Dr. Kazuyuki Tokumaru, a visiting scientist, with whom I worked closely during my first two years. He was fundamental in my development as a scientist, a patient teacher, a fantastic leader, and a great guy to grab a beer with.

Suzanne Batiste, thank you for always being willing to talk science, for being a great friend, confidant and roommate. I have always admired your excitement for chemistry and unwavering curiosity and determination to figure things out. And of course, a special shout out to Mr. Mo the NMR cat, who had a strong paw in solving complicated multiplets and always being a great couch and tv buddy.

To the current Johnston lab members, Dr. Rashanique Quarels, Michael Crocker, Jenna Payne, Abigail Smith, Jade Izaguirre, Jade Williams, Paige Thorpe, David Almond and Zihang Deng, it has been a pleasure working and learning with you. Rashanique, thank you for your commitment to feglymycin, and for always offering to lend an ear and support in difficult times. Michael Crocker is one of the most patient and kind people I have ever worked with. Thank you for your discussions about chemistry and for hosting some great events outside of lab, and for being a great friend. Jenna Payne is an extremely hardworker, and I appreciate your dedication to your labmates and to science. I never thought I would have the pleasure of working alongside not one, but two other Jades. Jade Izaguirre, it's been wonderful having you as a bench mate. Jade Williams, thank you for your friendship, support and for editing my documents. I know I can always count on Abigail Smith to get things done. I have watched her grow into a confident, brilliant scientist with a keen attention to detail and excellent leadership skills. A special thanks to Abby and Jenna for leading the force to get our laboratory organized in a way I would never imagine possible. Y'all really wore that label maker out! To the new students, Paige, David and Zihang, I'm excited to see all that you will accomplish in the future!

Outside of the Johnston laboratory, Katie Chong was a great friend and role model. Katie is an absolutely brilliant scientist, empathetic and fun to be around, and made sure I felt included during my time at Vanderbilt. Thank you to Louie Thal and his pups Mo and Olive for being awesome roommates. I will always cherish the times we shared at Snyder Ave.

Graduate school would have been a much more difficult time if I hadn't begun the journey with Audrey Yñiguez-Gutierrez and Kelly Craft by my side. I can always go to them with the science questions that I'd be embarrassed to ask anyone else. But even more than that, Audrey and Kelly have been great friends, always willing to listen and commiserate. They have been there for every celebration, and for every low throughout graduate school, and helped me keep my sanity throughout this process. I am so happy to have made life-long friends like them.

Thank you to Kate Moore and my family at GetFit615 and Shakti Power Yoga for being my 'third place'. They have helped me redefine my understanding of fitness, given me a place to vent my frustrations, and provided me with the nourishing and committed community I didn't realize I needed.

Thank you to my friends back home - Jamie Spampinato, Lanie Alden, Rachel Schwartz and Sam Masters. Your unconditional love, support and encouragement has been essential to my success here in Nashville. To the honorary Bings – Larry Alexander and Kevin Wiley - thank you for being there not just for me, but for our whole family. It has been a great challenge to be away from home when things are not at their best, but knowing that I have people there to help and watch over things while I'm away makes it the slightest bit easier to focus on something like a PhD.

Ron Benning – you have been my anchor and my rock since our undergraduate days at Rider University. Thank you for your patience, selflessness, and for always being Mr. Fix-it. Thank you for working so hard for us and always giving your all despite the obstacles life has thrown your way. I am grateful that you have taught me so much, about chemistry and about life. I appreciate your encouragement and willingness to listen. I am inspired by your constant desire to learn and gain a true understanding of things both in and outside of the laboratory. I would not have made it through this if it weren't for your love and support and I look forward to all the future has to bring us. Thank you also to the Benning family – Mama Yolanda, Pops and Chaz – for welcoming me into your family and for sharing your home, love, and support.

Finally, I must acknowledge my immediate family. Along with the good times, together we have endured a lot of loss and misfortunes, and together we moved forward. Thank you to my siblings. To my big brother Lenny, for always taking the road less travelled with me and being a great cheerleader and role model. To my big sister Tara, for always lending an understanding ear - we will always be connected with that MMC. I will always have your backs. We've been climbing this mountain for our whole lives, and I'm blessed to have siblings like you to take the journey with me.

I have been blessed to have loving and supporting parents. To my buddy, my role model, my hard-working, humble, always down for a good time, Dad; and to the beautiful, compassionate and resilient woman that is my mother – Thank you. To my family, we have been through plenty of tragedy, and finally we see some triumph. Dear family, we have endured and along the way you have taught me so much. Together we instill values in one another and I am blessed to have you all on my side. Thank you for teaching me the value of the little things, and for helping me understand that you don't always get what you want, things aren't always easy don't always work out as planned, and sometimes you just have to suck it up, deal with it, move forward and believe. Thank you for teaching me to be respectful, and teaching me not to just do things, but to do them right. Thank you for instilling within me a hard work ethic, and for working yourself to the bone; for showing me the true value of skinned knees and calloused hands, and that hard work, diligence, and attention to detail pays off. Thank you for teaching me to be humble, to work with what you've got, to see the good in what you have, to find a light in all things and people. This dissertation would never have come to fruition without these lessons, your love and support.

And a big thanks to you, dear reader, for taking the time to peruse this document.

## TABLE OF CONTENTS

	Page
ACKNOWLEDGMENTS .....	iii
LIST OF FIGURES .....	viii
LIST OF SCHEMES .....	x
LIST OF TABLES.....	xiv
I. STEREOSELECTIVE SYNTHESIS OF B-FLUOROAMINES .....	15
Chapter	
1.1 INTRODUCTION .....	15
1.1.1 PROPERTIES AND PRESENCE OF FLUORINE.....	15
1.1.2 CHANGES IN PHYSIOCHEMICAL PROPERTIES MEDIATED BY B-FLUORINATION OF AN AMINE.....	19
1.1.3 FLUORINATED CARBOCYCLES .....	23
1.1.4 EXISTING METHODS TO FOR ENANTIOSELECTIVE SYNTHESIS OF B-FLUOROAMINES.....	23
1.2 DISCOVERY OF FLUORINE-INDUCED DIASTEREODIVERGENCE IN A RARE <i>SYN</i> -SELECTIVE AZA-HENRY REACTION .....	29
1.2.1 INTRODUCTION TO THE AZA-HENRY REACTION .....	29
1.2.2 THE ANTI PARADIGM IN AZA-HENRY REACTIONS.....	33
1.2.3 PROJECT OVERVIEW .....	36
1.2.4 CATALYZED AZA-HENRY REACTIONS: TYPE I (AR/AR).....	38
1.2.5 CATALYZED AZA-HENRY REACTIONS: TYPE II (ALKYL/AR).....	40
1.2.6 CATALYZED AZA-HENRY REACTIONS: TYPE III (AR/ALKYL) .....	43
1.2.7 CATALYZED AZA-HENRY REACTIONS: TYPE IV (ALKYL/ALKYL).....	44
1.2.8 CATALYST SELECTION .....	46
1.2.9 DISCUSSION .....	47
1.2.9 CONCLUSION .....	51
1.3 PHASE TRANSFER CATALYZED AZA-HENRY REACTIONS FOR ALKYL B-FLUOROAMINES.....	52
1.3.1 INTRODUCTION & OBJECTIVES.....	52
1.3.2 ENANTIOSELECTIVE SYNTHESIS OF ALIPHATIC B-FLUORO-B-NITRO AMINES. ....	56
1.4 SYNTHESIS OF STEREODEFINED CARBOCYCLIC B-FLUOROAMINES .....	62
1.4.1 INTRODUCTION & OBJECTIVES.....	62
1.4.2 TOWARD 8-MEMBERED CARBOCYCLIC B-FLUOROAMINES: INITIAL ATTEMPTS AND OBSERVATIONS .....	64
1.4.3 TOWARD 7-MEMBERED CARBOCYCLIC B-FLUOROAMINES: PREVENTING ISOMERIZATION .....	67
<i>Endgame strategy for cycloheptyl <math>\beta</math>-fluoroamines</i> .....	73
1.4.4 TOWARD 6-MEMBERED CARBOCYCLIC B-FLUOROAMINES .....	74
<i>Initial attempt: Intramolecular aza-Henry</i> .....	74
<i>Revised strategy: ring closing metathesis</i> .....	76
<i>Reductive denitration of the 6-membered ring</i> .....	79
1.4.5 TOWARD BENZANNULATED RING SYSTEMS: ACCESS TO LARGER RING SIZES.....	81
II. EPIMERIZATION-FREE SYNTHESIS OF ELECTRON-RICH ARYL GLYCINAMIDES.....	84
2.1 INTRODUCTION & BACKGROUND .....	84
2.1.1 AMIDE BOND FORMATION .....	84

2.1.2 INTRODUCTION TO UMPOLUNG AMIDE SYNTHESIS .....	88
2.1.3 PROPERTIES OF ARYL GLYCINAMIDES .....	91
2.1.4 EXISTING METHODS FOR THE ASYMMETRIC SYNTHESIS OF ARYL GLYCINES .....	97
<i>Methods developed for <math>\alpha</math>-aryl glycinamide synthesis during the pursuit of vancomycin and related therapeutic peptides</i> .....	98
2.2 UMPOLUNG AMIDE SYNTHESIS WITH ELECTRON-RICH $\alpha$ -BROMO NITROALKANES .....	115
2.2.1 PROJECT OVERVIEW .....	115
2.2.2 SYNTHESIS OF $\beta$ -AMIDO $\alpha$ -BROMONITROALKANES .....	119
2.2.2 DEGRADATION PROFILES OF $\beta$ -AMIDO $\alpha$ -BROMONITROALKANES .....	129
2.2.3 ATTEMPTS TO CHANGE ELECTRONICS OF THE $\alpha$ -BROMONITROALKANES .....	134
2.2.4 ADDRESSING THE TER MEER REACTION – EXAMINATION OF $\alpha$ -FLUORONITROALKANES .....	140
2.2.5 ADDRESSING UNDESIRED OXIDATION OF GLYCINAMIDE PRODUCTS .....	143
2.2.6 GAME-CHANGING TACTICS IN UMAS TOWARD ELECTRON-RICH ARYL GLYCINAMIDES .....	146
III. THE FORMAL SYNTHESIS OF (-)-FEGLYMYCIN .....	158
3.1 INTRODUCTION TO FEGLYMYCIN .....	158
3.1.1 ISOLATION AND STRUCTURE .....	158
3.1.2 BIOLOGICAL ACTIVITY .....	160
<i>Anti-HIV activity</i> .....	160
<i>Antibacterial activity</i> .....	165
3.1.3 BIOSYNTHESIS OF FEGLYMYCIN .....	170
3.1.4 PREVIOUS SYNTHESIS OF (-)-FEGLYMYCIN .....	174
<i>Süssmuth's synthesis of feglymycin</i> .....	174
<i>Fuse's synthesis of feglymycin</i> .....	184
3.2 FORMAL SYNTHESIS OF (-)-FEGLYMYCIN .....	190
3.2.1 PREVIOUS WORK IN THE JOHNSTON GROUP .....	190
3.2.2 RETROSYNTHETIC PROPOSAL AND BUILDING BLOCK SYNTHESIS .....	198
3.2.3 SYNTHESIS OF FRAGMENT B .....	201
<i>DMF as a solvent in UmAS</i> .....	204
<i>TIPS protected phenols change solubility of Fragment B</i> .....	205
<i>DEPBT couplings to homologate the tetra- and pentapeptides</i> .....	207
<i>N<math>\rightarrow</math>C Convergent 4+2 approach to hexapeptide 349 via UmAS</i> .....	215
<i>Convergent 4+2 approach to hexapeptide 349 via DEPBT coupling</i> .....	217
<i>Completion and purification of the hexapeptide central fragment of (-)-feglymycin</i> .....	219
3.2.4 SYNTHESIS OF FRAGMENT A .....	222
3.2.5 SYNTHESIS OF FRAGMENT C & ENDGAME STRATEGIES .....	224
<i>Synthesis of Fragment C with C-terminal TSE protecting groups</i> .....	224
<i>Endgame attempts using C-terminal TSE protecting groups</i> .....	227
<i>Synthesis of Fragment C with C-terminal benzyl protecting groups</i> .....	230
<i>Endgame attempt using C-terminal benzyl protecting groups</i> .....	233
<i>Second generation synthesis of Fragment C with C-terminal benzyl protecting groups</i> .....	234
<i>Second generation endgame attempts using C-terminal benzyl protecting groups</i> .....	235
3.2.6 COMPLETION OF THE FORMAL SYNTHESIS OF (-)-FEGLYMYCIN .....	236
3.2.7 FEGLYMYCIN FORMAL SYNTHESIS: SUMMARY & COMPARISON OF FINAL ROUTES .....	238
IV. EXPERIMENTAL SECTION .....	245
4.1 CHARACTERIZATION OF ORGANIC MOLECULES .....	245
4.2 X-RAY CRYSTALLOGRAPHIC DATA .....	322

## LIST OF FIGURES

Figure	Page
1. FLUORINATED NATURAL PRODUCTS.	15
2. FLUORINE CONTAINING PHARMACEUTICALS.	17
3. THE FLUORINE <i>GAUCHE</i> EFFECT.	18
4. STRUCTURE OF FENTANYL & NFEPP.	20
5. FLUORINATION CHANGES $PK_A$ AND SAFETY PROFILE OF AN ASTRAZENECA NBTI ANTIBACTERIAL AGENT.	22
6. REAGENTS FOR DEOXYFLUORINATION.	23
7. EXAMPLES OF STRUCTURAL DIVERSIFICATION IN BAM CATALYST SYSTEMS.	31
8. STRUCTURES OF CATALYSTS USED FOR EACH ‘TYPE’ OF AZA-HENRY ADDITION.	37
9. CATEGORIZATION OF AZA-HENRY REACTIONS BY THE TYPE (ARYL VS. ALKYL) OF THE AZOMETHINE ELECTROPHILE SUBSTITUENT, AND THE NITROMETHANE SUBSTITUENT(S). X-RAY ANALYSIS FOR MAJOR (RELATIVE AND ABSOLUTE) STEREOISOMER FORMED IN EXPERIMENTS DETAILED BY TABLE 2.	43
10. CATALYST SELECTION CHART FOR TYPE I-IV AZA-HENRY REACTIONS.	46
11. WORKING MODELS TO IDENTIFY DOMINANT EFFECTS PRESENT DURING C-C BOND FORMATION AS A FUNCTION OF NITRONATE SUBSTITUENT COMBINATION (ARYL/ALKYL, H/F).	49
12. STEREOCHEMICAL ASSIGNMENT OF MAJOR AND MINOR DIASTEREOMERS OF AZA-HENRY ADDUCT 66. <sup>A</sup>	61
13. OCCURRENCE OF DIFFERENT TYPES OF REACTIONS FROM 1984 COMPARED TO 2014. <sup>115</sup>	84
14. OCCURRENCE OF DIFFERENT TYPES OF REACTIONS USED IN NATURAL PRODUCT SYNTHESIS COMPARED TO MEDICINAL CHEMISTRY IN 2014. <sup>115</sup>	85
15. STRUCTURES OF COMMON PHENYL GLYCINAMIDE MOTIFS.	91
16. EXAMPLES OF NATURAL PRODUCTS AND THERAPEUTICS CONTAINING ELECTRON-RICH ARYL-GLYCINE RESIDUES.	92
17. STRUCTURES OF VANCOMYCIN AND RELATED GLYCOPEPTIDE ANTIBIOTICS.	99
18. TIMELINE OF METHODS USED FOR THE SYNTHESIS OF (GLYCO)PEPTIDE ANTIBIOTICS.	100
19. SUMMARY OF CLASSICAL METHODS USED TO SYNTHESIZE ARYL GLYCINE RESIDUES IN GLYCOPEPTIDE ANTIBIOTICS. <sup>A</sup>	109
20. STRUCTURES OF TARGETED PHENYL GLYCINAMIDE DERIVATIVES.	115
21. STRUCTURES OF ( <i>R,R</i> )- AND ( <i>S,S</i> )-PBAM.	116
22. FACTORS EXAMINED TO OPTIMIZE UMAS WITH ELECTRON-RICH ARYL GLYCINAMIDE PRECURSORS.	150
23. COMPARISON OF CRUDE <sup>1</sup> H-NMRS FROM UMAS WITH KI/UHP AND NIS.	156
24. STRUCTURE OF (-)-FEGLYMYCIN (153).	158
25. CRYSTAL STRUCTURE OF FEGLYMYCIN.	159
26. CLASSES OF FDA-APPROVED ANTI-HIV DRUGS. <sup>A</sup>	161
27. HIV INFECTION AND REPLICATION.	162
28. REPRESENTATION OF VIRAL SYNCYTIA FORMATION.	164
29. DIAGRAM OF PEPTIDOGLYCAN BIOSYNTHESIS.	167
30. RESIDUES THAT IMPACT FEGLYMYCIN’S ANTIMICROBIAL ACTIVITY.	169
31. BIOSYNTHESIS OF FEGLYMYCIN BY NRPS.	174
32. SÜSSMUTH’S CONVERGENT RETROSYNTHETIC ANALYSIS OF FEGLYMYCIN.	175
33. SÜSSMUTH’S ITERATIVE RETROSYNTHESIS OF FEGLYMYCIN.	179
34. COMPARISON OF FUSE’S LINEAR APPROACH AND SÜSSMUTH’S CONVERGENT APPROACH TO FEGLYMYCIN.	185
35. REPRESENTATIVE SCHEMATIC FOR MICRO-FLOW AMIDATION.	186
36. CHALLENGES IN FRAGMENT PREPARATION DETERMINED BY PRIOR WORK.	190
37. RETROSYNTHESIS OF THE PARTIALLY TIPS-PROTECTED CENTRAL FRAGMENT OF (-)-FEGLYMYCIN.	205



38. DEPROTECTION AND PROTODESILYLATION OF TSE PROTECTING GROUP.	230
39. REVISED RETROSYNTHESIS FOR C-TERMINAL BENZYL PROTECTED FRAGMENT C.	234
40. KEY NMR CORRELATIONS FOR THE STEREOCHEMICAL ASSIGNMENT OF 67A.	261
41. KEY NMR CORRELATIONS FOR THE STEREOCHEMICAL ASSIGNMENT OF THE MAJOR AND MINOR DIASTEREOMERS FROM REDUCTIVE DENITRATION OF 67.	266
42. LOWEST ENERGY CONFORMATIONS OF CIS AND TRANS CYCLOHEPTENYL B-FLUOROAMINES 89 AND 90.	267
43. KEY <sup>19</sup> F- <sup>1</sup> H HOESY INTERACTION FOR THE BENZANNULATED CYCLOHEPTENE 127	271
44. KEY <sup>1</sup> H- <sup>13</sup> C HSQC CROSSPEAKS FOR THE STRUCTURAL ASSIGNMENT OF HEXAPEPTIDE 349.	310
45. KEY <sup>1</sup> H- <sup>1</sup> H COSY CROSSPEAKS FOR THE STRUCTURAL ASSIGNMENT OF HEXAPEPTIDE 349.	310
46. KEY <sup>1</sup> H- <sup>13</sup> C HMBC CROSSPEAKS FOR THE STRUCTURAL ASSIGNMENT OF DECAPEPTIDE 348.	319

## LIST OF SCHEMES

Scheme	Page
1. EXISTING METHODS FOR SYNTHESIZING B-FLUOROAMINES. ....	24
2. MERCK'S SYNTHESIS OF B-FLUOROCYCLOHEXYL AMINE DEMONSTRATES THE NEED FOR IMPROVED ENANTIOSELECTIVE METHODOLOGY. ....	25
3. DOYLE'S SYNTHESIS OF <i>TRANS</i> B-FLUOROAMINES. ....	26
4. LINDSLEY'S STEREOSELECTIVE A-FLUORINATION OF ALDEHYDES AND ALDIMINES USING MACMILLAN'S IMIDAZOLIDINONE. ....	27
5. ENANTIOSELECTIVE AMINOFLUORINATION CASCADE BY BRENNER-MOYER. ....	28
6. PHASE-TRANSFER CATALYZED ENANTIOSELECTIVE FLUORINATION OF BENZOYL ENAMINES. ....	29
7. THE AZA-HENRY (NITRO-MANNICH) REACTION. ....	30
8. SEMINAL BAM CATALYZED AZA-HENRY REACTION. ....	30
9. SELECTED EXAMPLES OF PUBLISHED AZA-HENRY ADDUCTS FROM THE JOHNSTON LABORATORY. ....	33
10. SHIBASAKI'S <i>SYN</i> SELECTIVE AZA-HENRY REACTION. ....	34
11. PROPOSED CATALYTIC CYCLE AND STEREOCHEMICAL MODEL FOR SHIBASAKI'S <i>SYN</i> -SELECTIVE AZA-HENRY REACTION. ....	34
12. MODELS FOR STEREOSELECTIVITY IN THE BAM CATALYZED AZA-HENRY REACTION. ....	35
13. DESCRIPTION OF CATEGORIES FOR TYPE I-TYPE IV AZA-HENRY REACTIONS. ....	36
14. REPRESENTATIVE EXAMPLES OF SELECTIVITY IN TYPE I AZA-HENRY REACTIONS. ....	39
15. STEREOCHEMICAL ASSIGNMENT MAPS FOR TYPE IV AZA-HENRY REACTIONS. ....	44
16. RELATIVE REACTIVITY OF A-FLUORONITROALKANES IN AZA-HENRY REACTIONS. ....	55
17. GENERAL SYNTHETIC SCHEME FOR THE SYNTHESIS OF A-FLUORONITROALKANE AND A-AMIDO SULFONE AZA-HENRY PARTNERS. ....	56
18. CONDITIONS SURVEYED FOR THE BAM CATALYZED AZA-HENRY REACTION WITH ALKYL A-FLUORONITROALKANE 61. ....	57
19. PHASE-TRANSFER CATALYZED AZA-HENRY REACTION OF ALKYL A-FLUORONITROALKANES AND ALKYL <i>N</i> -BOC A-AMIDO SULFONES. ....	60
20. RCM APPROACH TO CARBOCYCLIC B-FLUOROAMINES. ....	62
21. OBSERVED ISOMERIZATION PRIOR TO RING CLOSING METATHESIS. ....	64
22. ETHEREAL SOLVENT PROMOTES ISOMERIZATION PRIOR TO METATHESIS TO AFFORD CYCLOHEPTYL B-FLUOROAMINES. ....	65
23. LACK OF SUBSTRATE CONTROL FOR ISOMERIZATION. ....	66
24. STUDY OF ISOMERIZATION USING RU(H) ....	66
25. PROPOSED MECHANISMS OF ALKENE ISOMERIZATION DURING RU-CATALYZED METATHESIS. ....	67
26. STRUCTURES OF RUTHENIUM HYDRIDE FORMED FROM THE GRUBBS II CATALYST. ....	68
27. ISOMERIZATION PREVENTION DURING THE SYNTHESIS OF 7-MEMBERED CARBOCYCLIC B-FLUOROAMINES. ....	72
28. REDUCTIVE DENITRATION AND HYDROGENATION TO AFFORD <i>CIS</i> - AND <i>TRANS</i> CYCLOHEPTYL B-FLUOROAMINES. ....	73
29. REDUCTIVE DENITRATION OF CYCLOHEPTYL ALKENE REGIOISOMER 68. ....	73
30. PREPARATION OF AZA-HENRY PRECURSOR 97. ....	74
31. ATTEMPTED INTRAMOLECULAR AZA-HENRY REACTION USING HOMOGENEOUS CATALYSIS. ....	75
32. RETROSYNTHETIC STRATEGIES TO FORM 6-MEMBERED B-FLUORO-B-NITRO CYCLOHEXYLAMINE. ....	76
33. ATTEMPTED '5+3' SYNTHESIS OF THE RCM PRECURSOR FOR THE 6-MEMBERED RING. ....	77
34. ATTEMPTED ALLYLIC SULFONE FORMATION FOR '3+5' APPROACH TO 6-MEMBERED RING PRECURSOR. ....	78
35. ATTEMPTED SULFONE FORMATION FOR '4+4' APPROACH TO 6-MEMBERED RING PRECURSOR. ....	78

36. ONE-POT TANDEM ISOMERIZATION/RCM STRATEGY FOR CYCLOHEXENYL B-FLUORO-B-NITROAMINES. ....	79
37. DENITRATION OF 6-MEMBERED CARBOCYCLIC B-FLUOROAMINE. ....	80
38. ALKENE REDUCTION PRIOR TO DENITRATION OF 6-MEMBERED RING. ....	80
40. POTENTIAL STRUCTURES OF MAJOR PRODUCTS FROM DENITRATION OF 6-MEMBERED RING. ....	81
39. SYNTHESIS OF BENZANNULATED CYCLOHEPTENYL B-FLUORO-B-NITROAMINE 127. ....	81
41. AZA-HENRY REACTION TOWARD BENZANNULATED CYCLOOCTENE PRECURSOR 129. ....	82
42. GRUBBS RCM PROVIDES BENZANNULATED CYCLOOCTENE 130. ....	82
43. REDUCTION OF NITRO AND ALKENE MOTIFS TO FURNISH <i>CIS</i> AND <i>TRANS</i> CYCLOOCTYL B-FLUOROAMINES. ....	83
44. A-AMINO ACID EPIMERIZATION PATHWAYS DURING CONDENSATIVE AMIDE FORMATION. ....	87
45. COMPARISON OF UMPOLUNG AMIDE SYNTHESIS (UMAS) AND CONDENSATIVE AMIDE SYNTHESIS. ....	88
46. PROPOSED UMAS MECHANISM. ....	89
47. ANAEROBIC & AEROBIC PATHWAYS OF UMAS. ....	90
48. OUTLINE OF THE RACEMIZATION OF ARYL GLYCINES AND TYPICAL SUBSTITUENT EFFECTS. <sup>142</sup> .....	94
49. SHARPLESS' OPENING OF CHIRAL EPOXIDES BY AZIDE. ....	97
50. CONVERSION OF 3-AZIDO 1,2-DIOLS INTO A-ARYL GLYCINES. ....	98
51. GENERAL STRECKER AMINO ACID SYNTHESIS. ....	101
52. CHAKRABORTY'S KINETIC ASYMMETRIC STRECKER REACTION USING A-PHENYL GLYCINOL AS A CHIRAL AUXILIARY. ....	102
53. OGURA'S THERMODYNAMIC ASYMMETRIC STRECKER REACTION USING A-PHENYL GLYCINOL AS A CHIRAL AUXILIARY. ....	103
54. ZHU'S APPLICATION OF THE ASYMMETRIC STRECKER REACTION TO THE SYNTHESIS OF VANCOMYCIN. ....	104
55. SHARPLESS ASYMMETRIC DIHYDROXYLATION. ....	105
56. SHARPLESS ASYMMETRIC AMINOHYDROXYLATION. ....	106
57. NICOLOAU'S SYNTHESIS OF AA-4 OF VANCOMYCIN AGLYCON. ....	106
58. EVANS' CHIRAL-AUXILIARY BASED ENOLATE AZIDATION. ....	107
59. HOVEYDA'S APPLICATION OF AN ENANTIOSELECTIVE TI-CATALYZED STRECKER REACTION TO CHLOROPEPTIN I. ....	111
60. ENANTIOSELECTIVE PHASE-TRANSFER CATALYZED STRECKER REACTION. ....	112
61. CATALYTIC ASYMMETRIC HYDROGENATION OF A-IMINO ESTERS. ....	113
62. FU'S ASYMMETRIC N-H INSERTION. ....	113
63. AZA-HENRY REACTION FOLLOWED BY A NEF REACTION PROVIDES A-ARYL AMINO ACIDS. ....	114
64. RAWALS' USE OF "MASKED ACYL CYANIDES" TO SYNTHESIZE ARYL GLYCINAMIDES. ....	115
65. UMAS BASED APPROACH TO ACCESS A-ARYL GLYCINE DERIVATIVES. ....	116
66. UMAS COUPLINGS WITH THE CANONICAL AMINO ACIDS. ....	117
67. STRUCTURES OF FEGLYMYCIN AND FFEGLYMYCIN. ....	118
68. TARGETED A-AMIDO BROMONITROALKANES. ....	119
69. PREPARATION OF <i>A</i> -AMIDO SULFONES. ....	120
70. BAM CATALYZED ENANTIOSELECTIVE AZA-HENRY. ....	121
71. UMAS REACTION WITH BROMONITROALKANE XX AND ( <i>S</i> )-A-METHYL BENZYLAMINE. ....	122
72. UMAS REACTION OF BROMONITROALKANE 220 AND VALINE BENZYL ESTER. ....	126
73. REACTIVITY OF BROMONITROALKANE 218 UNDER CONDITIONS OPTIMIZED FOR 220. ....	128
74. COMPETITION EXPERIMENT OF UMAS BETWEEN BROMONITROALKANES 220 AND 218. ....	129
75. DEGRADATION OF BROMONITROALKANES UNDER BASIC, AEROBIC CONDITIONS. ....	129
76. RETRO AZA-HENRY REACTION. ....	130
77. PROPOSED PATHWAYS FOR SIDE REACTIONS OF BROMONITROALKANES 56. ....	131
78. MECHANISM OF THE TER MEER REACTION. ....	132
79. OXIDATION OF NITROALKANES. ....	133
80. ALTERNATE PROTECTING GROUPS TO CHANGE ELECTRON DENSITY OF AROMATIC RING. ....	134
SCHEME 81. SYNTHESIS OF BROMONITROALKANE 239. ....	135

82. COMPETITION EXPERIMENT BETWEEN BROMONITROALKANES 218 AND 239 IN UMAS.....	137
83. APPLICATION OF ONE-POT $\alpha$ -AMIDATION REACTION TO NITROALKANE 61C.....	138
84. ATTEMPT TO SYNTHESIZE TRIFLATE PROTECTED BROMONITROALKANE 240.....	138
85. SYNTHESIS OF PERFLUOROTOLYL-PROTECTED BROMONITROALKANE 243.....	139
86. TARGETED $\alpha$ -FLUORONITROALKANES.....	140
87. DISSOCIATION INVOLVED IN THE TER MEER REACTION.....	140
88. FLUORINATION OF NITROALKANES.....	141
89. FLURONITROALKANES AS ACYL DONORS IN UMAS.....	142
90. ATTEMPTED IODINATION OF GLYCINAMIDE 227 AND BROMONITROALKANE PRECURSOR 220.....	143
91. BROMINATION OF GLYCINAMIDE 221 AND BROMONITROALKANE PRECURSOR 220.....	144
92. EXCLUSION OF $K_2CO_3$ AND WATER IN THE UMAS REACTION WITH $\alpha$ -BROMO NITROALKANE 220.....	148
93. BIOSYNTHESIS OF HPG AND DPG. <sup>A</sup> .....	172
94. MECHANISM OF DEPBT-MEDIATED AMIDE COUPLING.....	176
95. SÜSSMUTH'S SYNTHESIS OF 3,5-DIHYDROXYPHENYLGLYCINE.....	176
96. SÜSSMUTH'S SYNTHESIS OF DIPEPTIDES 277 AND 279.....	177
97. SÜSSMUTH'S SYNTHESIS OF C-TERMINAL HEXAPEPTIDE 275.....	177
98. SÜSSMUTH'S SYNTHESIS OF TETRAPEPTIDE AND TRIPEPTIDE PRECURSORS TO <i>N</i> -TERMINAL HEPTAPEPTIDE 274.....	181
99. SÜSSMUTH'S SYNTHESIS OF <i>N</i> -TERMINAL HEPTAPEPTIDE 274.....	182
100. NICOLAOU'S COMPARISON OF CONDITIONS FOR METHYL ESTER HYDROLYSIS.....	183
101. SÜSSMUTH'S COMPLETION OF (-)-FEGLYMYCIN.....	184
102. FUSE'S SYNTHESIS OF C-TERMINAL HEXAPEPTIDE 305.....	187
103. FUSE'S SYNTHESIS OF <i>N</i> -TERMINAL HEPTAPEPTIDE 299.....	188
104. FUSE'S COMPLETION OF (-)-FEGLYMYCIN.....	189
105. GENERAL RETROSYNTHETIC ANALYSIS OF FEGLYMYCIN.....	191
106. <i>N</i> -TMS ALDIMINE APPROACH TO DPG $\alpha$ -BROMONITROALKANE DONORS. <sup>229</sup> .....	192
107. PREVIOUS IMPROVEMENTS TOWARD THE C-TERMINAL TETRAPEPTIDE.....	193
108. PREVIOUS SYNTHESIS OF TRIPEPTIDE 328.....	193
109. KEY OBSERVATION TOWARD THE SYNTHESIS OF TETRAPEPTIDE 329.....	194
110. EFFORTS TOWARD C-TERMINAL TETRAPEPTIDE.....	195
111. STRUCTURE OF MODEL PEPTIDE FFEGLYMYCIN (210).....	196
112. RETROSYNTHETIC ANALYSIS AND SUMMARY OF FRAGMENT PREPARATION FOR FFEGLYMYCIN.....	197
113. COMPLETION OF FFEGLYMYCIN (210).....	198
114. THIS WORK: RETROSYNTHESIS OF (-)-FEGLYMYCIN.....	199
115. SYNTHESIS OF $\alpha$ -BROMO NITROALKANE BUILDING BLOCKS FOR FEGLYMYCIN.....	201
116. SYNTHESIS OF CENTRAL FRAGMENT B VIA UMAS.....	203
117. DMF AS A SOLVENT IN UMAS.....	204
118. PROTECTING GROUP SWAP TOWARD THE PARTIALLY TIPS-PROTECTED CENTRAL FRAGMENT OF (-)-FEGLYMYCIN.....	207
119. RETROSYNTHESIS OF $\alpha$ -ARYL AMINO ACIDS.....	208
120. DEBROMINATION OF $\alpha$ -BROMO NITROALKANES.....	209
121. UNSUCCESSFUL NEF ATTEMPTS.....	212
122. PROPOSED MECHANISM OF THE MIOSKOWSKI-NEF REACTION.....	213
123. SYNTHESIS OF ARYL GLYCINE AMINO ACIDS VIA THE MIOSKOWSKI-NEF REACTION.....	214
124. DEPBT COUPLINGS TO MAKE PENTA- AND HEXAPEPTIDE B.....	214
125. ALTERNATE RETROSYNTHESIS OF HEXAPEPTIDE B: UMAS 4+2 APPROACH.....	215
126. SYNTHESIS OF TERMINAL AMIDE 374.....	216
127. REVISED 4+2 APPROACH TO FRAGMENT B.....	217
128. EVANS' USE OF AN <i>N</i> -METHYL AMIDE AS A MASKED CARBOXYLIC ACID IN THE SYNTHESIS OF VANCOMYCIN.....	218
129. MASKED CARBOXYLIC ACID APPROACH.....	218

130. CONVERGENT 4+2 APPROACH TO HEXAPEPTIDE 349.....	219
131. HYDROGENOLYSIS OF HEXAPEPTIDE 349 AFFORDS FRAGMENT B.....	221
132. RESIDUAL NH <sub>4</sub> OAC CAUSES <i>N</i> -TERMINAL CAPPING IN AMIDE COUPLING. ....	222
133. SYNTHESIS OF FRAGMENT A.....	223
134. SYNTHESIS OF <i>C</i> -TERMINAL TSE PROTECTED TRIPEPTIDE C. ....	224
135. COMPARISON OF UMAS AND DEPBT COUPLINGS TO COMPLETE FRAGMENT C. ....	226
136. <i>N</i> -TERMINAL DEPROTECTION OF TSE-PROTECTED TETRAPEPTIDE 332.....	227
137. SYNTHESIS OF <i>C</i> -TERMINAL TSE PROTECTED DECAPEPTIDE 382.....	227
138. ENDGAME STRATEGY WITH <i>C</i> -TERMINAL TSE PROTECTING GROUPS. ....	229
139. TOWARD THE SYNTHESIS OF <i>C</i> -TERMINAL BENZYL PROTECTED FRAGMENT C. ....	231
140. SOLUBILITY ISSUES IN SYNTHESIS OF FULLY BENZYL PROTECTED FRAGMENT C. ....	232
141. ATTEMPT TO SYNTHESIZE DECAPEPTIDE 386.....	233
142. 2+2 AMIDE COUPLING TO SYNTHESIZE <i>C</i> -TERMINAL TETRAPEPTIDE 290. ....	235
143. SYNTHESIS OF <i>C</i> -TERMINAL BENZYL PROTECTED DECAPEPTIDE 387.....	235
144. PROTECTING GROUP SWAP ON FRAGMENT A. ....	236
145. COMPLETION OF THE FORMAL SYNTHESIS OF (-)-FEGLYMYCIN. ....	237
146. SÜSSMUTH'S TOTAL SYNTHESIS DIAGRAM.....	238
147. FUSE'S TOTAL SYNTHESIS DIAGRAM. <sup>A</sup> .....	239
148. JOHNSTON LABORATORY FORMAL SYNTHESIS: FIRST-GENERATION SYNTHESIS DIAGRAM.....	241
149. JOHNSTON LABORATORY FORMAL SYNTHESIS: SECOND-GENERATION SYNTHESIS DIAGRAM. <sup>A</sup> .....	242
150. JOHNSTON LABORATORY FORMAL SYNTHESIS: THIRD-GENERATION SYNTHESIS DIAGRAM. .....	244

## LIST OF TABLES

Table	Page
1. EFFECT OF FLUORINATION ON ACTIVITY OF T-TYPE CA <sup>2+</sup> CHANNEL INHIBITION & OFF-TARGET EFFECTS. <sup>21</sup> .....	21
2. CATALYZED AZA-HENRY REACTIONS VARYING AROMATIC/ALIPHATIC SUBSTITUENTS OF AZOMETHINE AND NITRONATE/FLUORONITRONATE (TYPES I-IV). <sup>A</sup> .....	42
3. PREVIOUS STUDIES IN THE JOHNSTON LABORATORY ON THE BAM-CATALYZED AZA-HENRY WITH A-FLUORONITROALKANES. <sup>A,B</sup> .....	54
4. OPTIMIZATION OF PHASE-TRANSFER CATALYZED AZA-HENRY REACTION WITH ALKYL A-FLUORONITROALKANE (61) <sup>A</sup> .....	58
5. BOURGEOIS' PRODUCT DISTRIBUTION FOR COMPETING RCM & ISOMERIZATION REACTIONS IN PURSUIT OF TAXOL (74).....	65
6. DE BO'S PRODUCT DISTRIBUTION FOR COMPETING RCM & ISOMERIZATION REACTIONS IN PURSUIT OF PENTALENENE.....	70
7. PRODUCT DISTRIBUTION DURING RCM OF A 10-CARBON PRECURSOR.....	71
8. PHASE TRANSFER CATALYZED INTRAMOLECULAR AZA-HENRY REACTION. ....	75
9. ALANINE SCAN OF RAMOPLANIN AGLYCON AGAINST <i>S. AUREUS</i> ATCC 25923. <sup>144</sup> .....	96
10. PREVIOUS STUDIES ON THE SCOPE OF ARYL BROMONITROALKANES IN UMAS. ....	117
11. EFFECT OF SOLVENT AND TEMPERATURE ON UMAS. ....	123
12. EFFECT OF CATALYTIC NIS, TEMPERATURE, AND SOLVENT ON PRODUCT YIELD. ....	124
13. EFFECT OF NIS EQUIVALENTS.....	125
14. COMPETITION REACTION BETWEEN (S)-A-METHYL BENZYLAMINE AND VALINE BENZYL ESTER. ....	127
15. UMAS REACTIONS WITH BROMONITROALKANE 239 AND (S)-A-METHYLBENZYLAMINE. ....	135
16. GLYCINAMIDE FORMATION USING PERFLUOROTOLYL-PROTECTED BROMONITROALKANE XX. ....	139
17. ELECTRON AFFINITIES OF HALOGENS AND C-X BOND DISSOCIATION ENERGIES. ....	141
18. SYNTHESIS OF BROMINATED GLYCINAMIDE 260. ....	145
19. PREVIOUSLY REPORTED EFFECTS OF WATER AND BASE ON THE YIELD OF UMAS.....	147
20. SYNTHESIS OF GLYCINAMIDES VIA THE <i>IN SITU</i> GENERATION OF A-HALO NITROALKANES. <sup>A</sup> .....	149
21. SELECTED EXAMPLES OF OXIDANTS EXAMINED IN UMAS WITH 3,5-(OBN) <sub>2</sub> -DPG (218) AND AMBA.....	151
22. SELECTED EXAMPLES FROM THE EXAMINATION OF PEROXIDES FOR THE COUPLING OF 3,5-(OBN) <sub>2</sub> -BROMONITROALKANE 218 TO VALINE BENZYL ESTER. ....	152
23. FURTHER OPTIMIZATION OF KI/UHP PROTOCOL. <sup>A</sup> .....	154
24. EXAMINATION OF VARIOUS AMINES USING THE KI/UHP PROTOCOL FOR UMAS. <sup>A</sup> .....	155
25. GENES OF THE FEGLYMYCIN BIOSYNTHESIS GENE CLUSTER AND THEIR PREDICTED FUNCTIONS. <sup>A</sup> .....	171
26. FEEDING STUDIES WITH FEGLYMYCIN MUTANT AND ROLE OF THE <i>FEGC</i> GENE. ....	173
27. CATALYST SCREEN AND PRODUCT DISTRIBUTION IN BAM CATALYZED AZA-HENRY REACTIONS. ....	210
28. OPTIMIZATION OF BAM-CATALYZED AZA-HENRY REACTION FOR AMINO ACID PRECURSORS. ....	211
29. ATTEMPTS TO SYNTHESIZE SULFONES FOR 4+2 UMAS .....	216
30. EPIMERIZATION STUDIES FOR DIPEPTIDE 325. ....	225

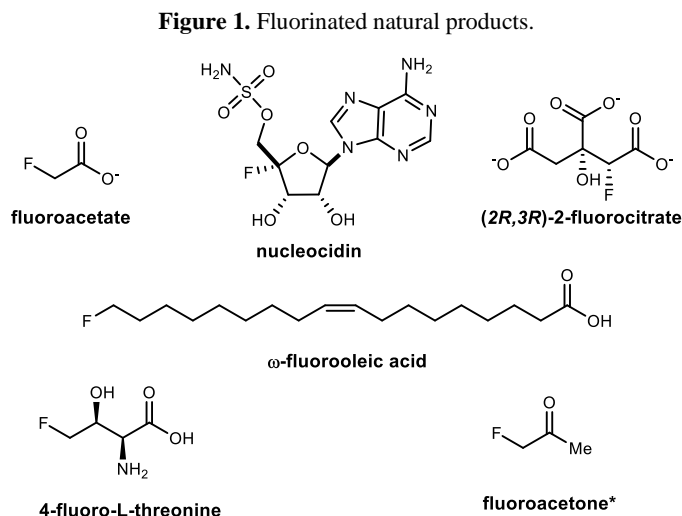
# I. Stereoselective synthesis of $\beta$ -fluoroamines

## 1.1 Introduction

### 1.1.1 Properties and presence of fluorine

The fluorine atom possesses many unique traits, such as being the most electronegative of all the atoms, and its incorporation into an organic molecule can have a significant stereoelectronic influence. The carbon-fluorine bond is the strongest of the covalent bonds to carbon, weighing in with a bond dissociation energy of  $\sim 115$  kcal/mol (*c.f.* BDE of  $\text{H}_3\text{C-H}$  is 105 kcal/mol). The distinct nature of the fluorine atom and resultant C-F bond has allowed for its implementation in drug design, agrochemistry, organocatalysis, and material science as a tool for controlling a compound's molecular conformation,  $\text{p}K_a$ , pharmacokinetic, and biological properties.

Fluorine exists as the 13<sup>th</sup> most abundant element in the Earth's crust and the most abundant halogen on earth, and yet fluorinated natural products are scarce.<sup>1,2,3</sup> In fact, to date, there have only been 13 natural products identified that contain a carbon-fluorine bond. Eight of these are



<sup>1</sup>Chan, K. K. J.; O'Hagan, D. In *Methods Enzymol.*; Hopwood, D. A., Ed.; Academic Press: 2012; Vol. 516, p 219.

<sup>2</sup>O'Hagan, D.; Harper, D. B. *J. Fluorine Chem.* **1999**, *100*, 127.

<sup>3</sup>Emsley, J. *Nature's building blocks : an A-Z guide to the elements*; New ed.; Oxford University Press: Oxford ; New York, 2011.

homologues of the same fatty acid from the same plant source, which decreases the count to a formal 6 compounds.<sup>1</sup> Moreover, as of 2009 there were only 5 of these products whose structures are considered defined, with the most recent discovery being more than 30 years ago (4-fluoro-L-threonine, **Figure 1**). Their structures are shown in **Figure 1**. Fluoroacetate is the most abundant and has been found in both plants and bacteria.<sup>1,4</sup> This compound's toxicity is attributed to its ability to be converted into fluorocitrate, which interestingly is only produced enzymatically as the (2*R*,3*R*) diastereomer, which is the only toxic one of the 4 possible isomers.<sup>1,5</sup> Nucleocidin<sup>6</sup> presents one of the more structurally interesting natural organofluorine compounds, and has antibiotic activity.  $\omega$ -Fluorooleic acid was isolated from the seeds of a West African shrub, *Dichapetalum toxicarium*,<sup>7</sup> and is toxic upon ingestion, a property once exploited by witchdoctors to conduct trial by ordeal.<sup>2</sup> Isomers and metabolites of this fatty acid were also identified by GC/MS and <sup>1</sup>H-NMR.<sup>8</sup> 4-Fluorothreonine was isolated from *S. cattleya* and has been shown by total synthesis to have the same (2*S*,3*S*) configuration as the natural L-threonine.<sup>9</sup> The final compound fluoroactone, was originally proposed by Peters and Shorthouse,<sup>10</sup> but there has been some speculation as to whether the compound is actually a natural product since it was not directly observed.<sup>1,2</sup>

These few examples notwithstanding, the occurrence of fluorinated natural products is few and far between. Even so, this has not stopped scientists from developing, nor the general population from reaping the benefits of, fluorinated compounds.

---

<sup>4</sup> First identification: Marais, J. S. C. D. T., P.J. *Onderstepoort Journal of Veterinary Science and Animal Industry* **1943**, *18*, 203.; Marais, J. S. C. D. T., P.J. *Onderstepoort Journal of Veterinary Science and Animal Industry* **1944**, *20*, 67. For reviews see refs 1 and 2

<sup>5</sup> Keck, R.; Haas, H.; János, R. *FEBS Lett.* **1980**, *114*, 287.

<sup>6</sup> Isolation: Thomas, S. O. S., V.L.; Lowery, J.A.; Sharpe, R.W.; Preuss, L.M.; Porter, J.N.; Mowat, J.H.; Bohonos, N. *Antibiotics Ann.* **1956**, *1956-1957*, 716.; Structure elucidation: Morton, G. O.; Lancaster, J. E.; Van Lear, G. E.; Fulmor, W.; Meyer, W. E. *J. Am. Chem. Soc.* **1969**, *91*, 1535.

<sup>7</sup> Peters, R. A.; Hall, R. J.; Ward, P. F. V.; Sheppard, N. *Biochem. J.* **1960**, *77*, 17.; Ward, P. F. V.; Hall, R. J.; Peters, R. A. *Nature* **1964**, *201*, 611.

<sup>8</sup> Hamilton, J. T. G.; Harper, D. B. *Phytochemistry* **1997**, *44*, 1129.; Christie, W. W.; Hamilton, J. T. G.; Harper, D. B. *Chem. Phys. Lipids* **1998**, *97*, 41.; Harper, D.; T.G. Hamilton, J.; O' Hagan, D. *Tetrahedron Lett.* **1990**, *31*, 7661.

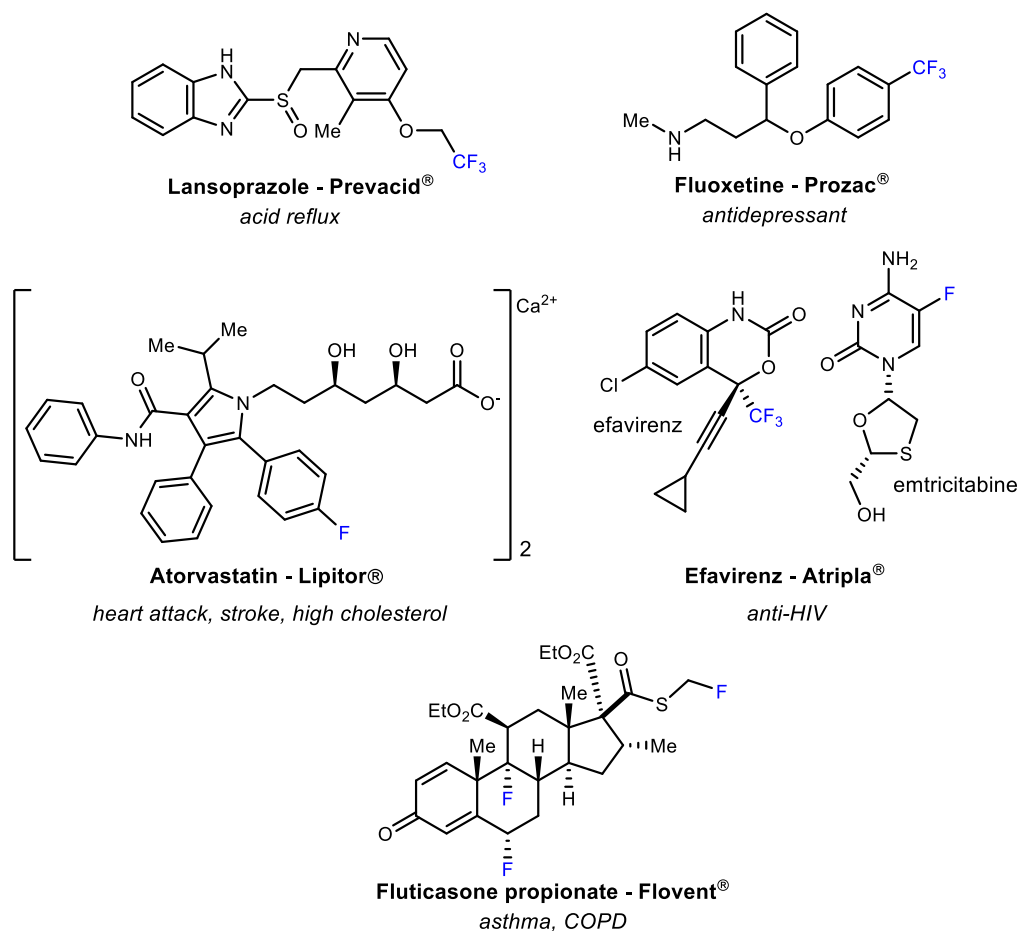
<sup>9</sup> Isolation: Sanada, M.; Miyano, T.; Iwaware, S.; Williamson, J. M.; Arison, B. H.; Smith, J. L.; Douglas, A. W.; Liesch, J. M.; Inamine, E. *J. Antibiot.* **1986**, *39*, 259.; Total synthesis: R. Amin, M.; B. Harper, D.; M. Moloney, J.; D. Murphy, C.; A. K. Howard, J.; O'Hagan, D. *Chem. Commun.* **1997**, 1471.; refer to reference 2 for a review of 4-fluorothreonine's biosynthesis and activity

<sup>10</sup> Peters, R. A.; Shorthouse, M. *Nature* **1967**, *216*, 80.; Peters, R. A.; Shorthouse, M. *Nature* **1971**, *231*, 123.



During lead optimization, fluorination may beneficially impact metabolic stability, off-target effects, penetration of the blood-brain barrier, potency, and bioavailability. As such, an increasing number of fluorinated compounds are making their way into clinical trials and beyond. It is

**Figure 2.** Fluorine containing pharmaceuticals.

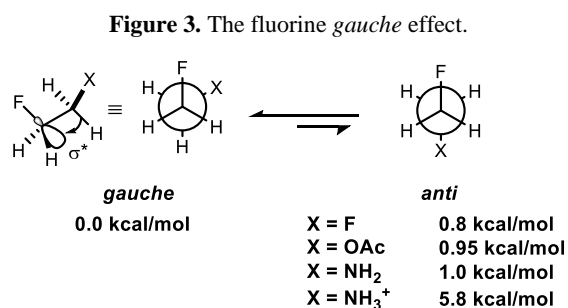


estimated that in 2014 approximately 25% of the drugs on the market contained fluorine, including three out of the five top selling pharmaceuticals (Lipitor®, Flovent®, and Prevacid®) (**Figure**

2).<sup>11</sup> **Figure 2** shows just some of these medicinally relevant compounds and demonstrates the structural diversity and myriad applications of fluorine containing pharmaceuticals.

The small covalent C-F radius in conjunction with fluorine's small atomic radius makes it a suitable isostere for hydrogen. Accordingly, substitution of a C-H bond for a strong C-F bond is a tactic commonly used in drug design to increase metabolic stability by blocking sites prone to oxidation.<sup>12</sup>

The carbon-fluorine bond is highly polarized which bears consequences for both the compound at hand as well as its environment. The large dipole can cause both intra- and intermolecular dipole-dipole and charge-dipole interactions, leading to a greater energy difference between conformers



and relative interactions. A key phenomenon associated with fluorine's ability to drive conformational steering results from its preference for a *gauche* relationship with a vicinal electron-withdrawing or electropositive functionality. The so-called *gauche* effect is dependent upon the stabilization of the low lying  $\sigma^*$  orbital of the C-F bond through hyperconjugation with adjacent  $\sigma$ -bonds, as observed in the  $\sigma_{C-H} \rightarrow \sigma^*_{C-F}$  donation from electron-rich C-H bonds (Figure 3). This can be further reinforced when the vicinal group is positively charged through charge-dipole/electrostatic interactions with the polarized  $C^{\delta+}-F^{\delta-}$  bond. The effect is significant – the *gauche* conformation is favored by 0.8 kcal/mol for a vicinal electron-withdrawing group as in

<sup>11</sup>Wang, J.; Sánchez-Roselló, M.; Aceña, J. L.; del Pozo, C.; Sorochinsky, A. E.; Fustero, S.; Soloshonok, V. A.; Liu, H. *Chem. Rev.* **2014**, *114*, 2432.

<sup>12</sup>Böhm, H.-J.; Banner, D.; Bendels, S.; Kansy, M.; Kuhn, B.; Müller, K.; Obst-Sander, U.; Stahl, M. *ChemBioChem* **2004**, *5*, 637.

1,2-difluoroethane (Figure 3, X=F). In addition to the hyperconjugative effects, an electrostatic enhancement is evoked by an adjacent positively charged motif as evidenced by the large 5.8 kcal/mol *gauche* preference for 2-fluoroethylammonium.<sup>13</sup>

### ***1.1.2 Changes in physicochemical properties mediated by $\beta$ -fluorination of an amine***

In biological systems fluorine-induced conformational bias may alter a compound's potency, binding, and off-target effects. In fact, this has been used to identify and study the biologically active conformations of the neurotransmitter GABA<sup>14</sup> as well as NMDA.<sup>15</sup> This has also been exploited in the field of organocatalysis. For example, fluorinated proline catalysts have been shown to be more rigid than non-fluorinated derivatives, and the structural preorganization can result in increased selectivity.<sup>16</sup>

Another important consequence of fluorination is the ability to alter a compound's  $pK_a$  in a generally predictable manner. Changes in acidity are significant in lead optimization as they can alter physicochemical properties such as solubility and permeability, as well as binding affinity and potency. Of crucial significance to a compound's viability as a drug candidate are its absorption, distribution, metabolism, excretion, and toxicity (ADMET) properties, which can also be modulated by changes in acidity.<sup>17</sup> Specifically, fluorine installation adjacent to a heteroatom, such as the amine functionality that is frequently encountered in pharmaceuticals, renders the amine less basic. In open-chain systems,  $\beta$ -fluorination results in a  $pK_a$  decrease of about 1.7 units for each fluorine installed.<sup>17</sup> **In cyclic amines, the change differs based upon conformation**, with an equatorial fluorine providing a greater decrease in  $pK_a$  than its axial congener.<sup>17</sup>

---

<sup>13</sup> Briggs, C. R. S.; Allen, M. J.; O'Hagan, D.; Tozer, D. J.; Slawin, A. M. Z.; Goeta, A. E.; Howard, J. A. K. *Org. Biomol. Chem.* **2004**, *2*, 732.

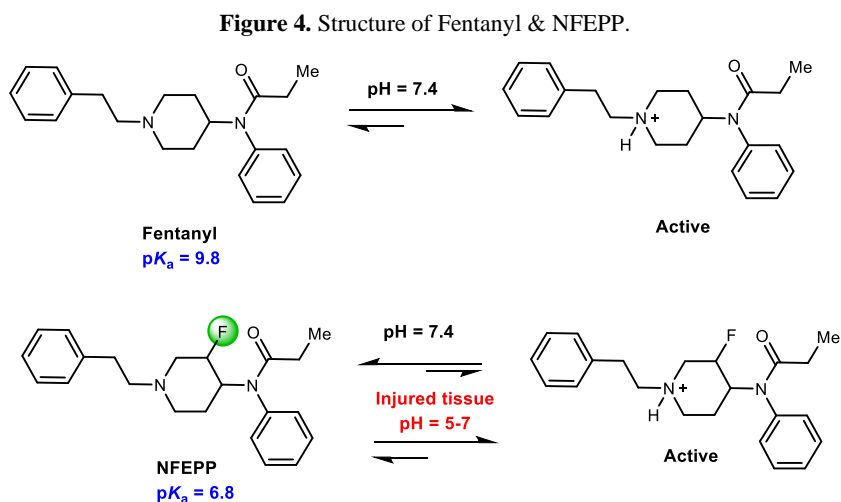
<sup>14</sup> Deniau, G.; Slawin, A. M. Z.; Lebl, T.; Chorki, F.; Issberner, J. P.; van Mourik, T.; Heygate, J. M.; Lambert, J. J.; Etherington, L.-A.; Sillar, K. T.; O'Hagan, D. *ChemBioChem* **2007**, *8*, 2265.; Clift, M. D.; Ji, H.; Deniau, G. P.; O'Hagan, D.; Silverman, R. B. *Biochemistry* **2007**, *46*, 13819.

<sup>15</sup> Chia, P. W.; Livesey, M. R.; Slawin, A. M. Z.; van Mourik, T.; Wyllie, D. J. A.; O'Hagan, D. *Chem. Eur. J.* **2012**, *18*, 8813.

<sup>16</sup> Tanzer, E.-M.; Zimmer, L. E.; Schweizer, W. B.; Gilmour, R. *Chem. Eur. J.* **2012**, *18*, 11334.; For a review see Zimmer, L. E.; Sparr, C.; Gilmour, R. *Angew. Chem. Int. Ed.* **2011**, *50*, 11860.

<sup>17</sup> For a review see: Morgenthaler, M.; Schweizer, E.; Hoffmann-Roder, A.; Benini, F.; Martin, R. E.; Jaeschke, G.; Wagner, B.; Fischer, H.; Bendels, S.; Zimmerli, D.; Schneider, J.; Diederich, F.; Kansy, M.; Muller, K. *ChemMedChem* **2007**, *2*, 1100.

The use of fluorination as a tool for modulating  $pK_a$  has powerful implications as illustrated by Stein's work with the opioid analgesic Fentanyl and its fluorinated analog NFEPP (Figure 4).<sup>18</sup> In America, the number of opioid related deaths continues to rise so much so that it has been deemed an epidemic. From 2016 to 2017 synthetic opioid-involved overdose death rates increased by 45%.<sup>19</sup> Fentanyl in particular has been a leading contributor, and in 2017 the CDC reports more than 28,000 deaths involving synthetic opioids other than methadone, which accounts for more deaths than any other type of opioid.<sup>20</sup> Fentanyl is known to have a host of side-effects, which the team sought to mitigate. They aimed to develop a compound that only acts in damaged and inflamed tissues, and not in normal environments. For Fentanyl to be active, it must be protonated, and with a  $pK_a$  of 9.8, it will always be protonated at physiological pH, leading to its excellent potency, but also to its side effects. Stein hypothesized that improved selectivity might result from an adjustment of Fentanyl's basicity. To accomplish this,  $\beta$ -Fluorination of the core piperidine ring (NFEPP, Figure 4) lowered the  $pK_a$  by  $\sim 3$  units. Within injured tissue, the pH is lower, and thus



NFEPP is only protonated and active at the more acidic sights of injury. The authors found that

<sup>18</sup> Spahn, V.; Del Vecchio, G.; Labuz, D.; Rodriguez-Gaztelumendi, A.; Massaly, N.; Temp, J.; Durmaz, V.; Sabri, P.; Reidelbach, M.; Machelska, H.; Weber, M.; Stein, C. *Science* **2017**, 355, 966.

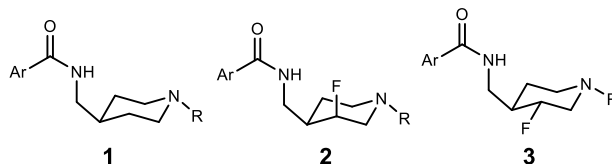
<sup>19</sup> Scholl L, S. P., Kariisa M, Wilson N, Baldwin G.; Services, U. S. D. o. H. a. H., Ed.; MMWR Morb Mortal Wkly Rep: 2019; Vol. 67, p 1419.

<sup>20</sup> Centers for Disease Control and Prevention, National Center for Injury Prevention and Control. Synthetic Opioid Overdose Data, 2019. <https://www.cdc.gov/drugoverdose/data/fentanyl.html#overdose-deaths-synthetic> (accessed Feb 21, 2020)

this provided a pain killer that produces injury-restricted analgesia without causing respiratory depression, sedation, constipation, or addiction in rat models.

The benefits of informed structural modification are further evinced by  $\beta$ -fluorination of a piperidine motif in a T-type calcium channel inhibitor (Table 1, Compound **1**), which increased its likelihood to serve as a potential treatment for CNS disorders such as epilepsy.<sup>21</sup> This discrete change decreased the compound's  $pK_a$  by approximately 1 unit, which resulted in both a two-fold decrease in negative off-target hERG channel activity and a two fold increase in potency (Table 1, FLIPR IP). *This work also highlights the influence of chirality of the fluorine-bearing carbon.* The *trans* isomer **3**, featuring an equatorial fluorine, lowered the  $pK_a$  an additional unit and was

**Table 1.** Effect of fluorination on activity of T-type  $Ca^{2+}$  channel inhibition & off-target effects.<sup>21</sup>



compound	pKa	T-Type, FLIPR IP (nM)	hERG IP (nM)	L-type binding IC50 (nM)
1	8.7	61	1934	1191
2	7.9	32	4114	2134
3	6.7	411	3034	1049

significantly less potent and less selective than its C-3 epimer **2**.

AstraZeneca has worked to develop novel (non-fluoroquinoline) bacterial type II topoisomerase inhibitors (NBTIs) for use as antibacterial agents that would be viable against fluoroquinolone resistant bacteria.<sup>22</sup> Lead optimization resulted in *N*-linked aminopiperidines such as compound **4** (Figure 5) as promising targets. However, while these compounds were active, they had poor

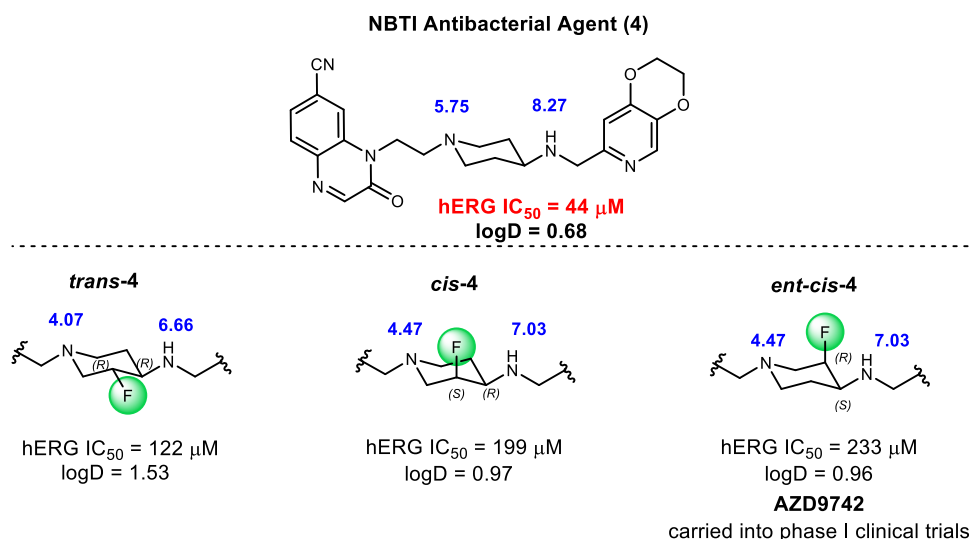
<sup>21</sup>Yang, Z.-Q.; Barrow, J. C.; Shipe, W. D.; Schlegel, K.-A. S.; Shu, Y.; Yang, F. V.; Lindsley, C. W.; Rittle, K. E.; Bock, M. G.; Hartman, G. D.; Uebele, V. N.; Nuss, C. E.; Fox, S. V.; Kraus, R. L.; Doran, S. M.; Connolly, T. M.; Tang, C.; Ballard, J. E.; Kuo, Y.; Adarayan, E. D.; Prueksaritanont, T.; Zrada, M. M.; Marino, M. J.; Graufelds, V. K.; DiLella, A. G.; Reynolds, I. J.; Vargas, H. M.; Bunting, P. B.; Woltmann, R. F.; Magee, M. M.; Koblan, K. S.; Renger, J. J. *J. Med. Chem.* 2008, 51, 6471.

<sup>22</sup>Reck, F.; Alm, R. A.; Brassil, P.; Newman, J. V.; Ciaccio, P.; McNulty, J.; Barthow, H.; Goteti, K.; Breen, J.; Comita-Prevoir, J. L.; Cronin, M.; Ehmann, D. E.; Geng, B.; Godfrey, A. A.; Fisher, S. L. *J. Med. Chem.* 2012, 55, 6916.

safety profiles as demonstrated by potent human *Ether-a-go-go* (hERG) inhibition, which can lead to cardiac issues and predispose individuals to sudden cardiac death.<sup>23</sup> In this study, the researchers expected that fluorination would reduce the  $pK_a$  of the amines, thereby reducing hERG binding affinity.

As shown in **Figure 5**, both of the *cis* diastereomers of **4** decreased the  $pK_a$  of the secondary amine as well as the tertiary piperidine nitrogen. Importantly, these compounds also demonstrate approximately 5-fold improvement with respect to hERG  $IC_{50}$  (233 and 199  $\mu M$ ) over the original compound **4** (44  $\mu M$ ). Interestingly, the *trans*-**4** isomer decreased the  $pK_a$  even more than the *cis* isomer, but it was a stronger hERG inhibitor (hERG  $IC_{50}$  = 122  $\mu M$ ). The researchers ultimately attributed this to a substantial increase in logD. While both *cis* isomers increased logD from 0.68 to 0.96-0.97, the *trans* isomer more than doubled it to 1.53, and it is known that higher logD is

**Figure 5.** Fluorination changes  $pK_a$  and safety profile of an AstraZeneca NBTI antibacterial agent.



Numbers in blue indicate the  $pK_a$  determined by pH metric titration as detailed in reference 22.

correlated to increased hERG activity.<sup>23</sup> The *ent-cis*-**4** diastereomer was ultimately carried into Phase I clinical trials, and clearly demonstrated the importance of being able to synthesize all stereoisomers of  $\beta$ -fluoroamines.

<sup>23</sup>Yu, H.-b.; Zou, B.-y.; Wang, X.-l.; Li, M. *Acta Pharmacol. Sin.* **2016**, *37*, 111.

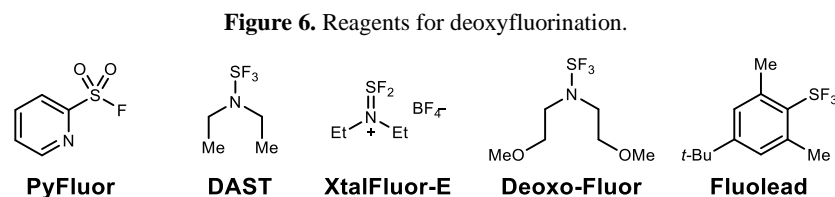
### 1.1.3 Fluorinated carbocycles

Fluorination of aromatic rings, linear aliphatic compounds, and *N*-heterocycles, can often have beneficial effects. It is less common to see fluorinated cycloalkyl amines, perhaps due to the lack of methods to access these motifs. Such structures could find utility in organocatalysis or serve as important biological probes by providing an additional element of conformational control. The crucial effects demonstrated by preorganization to the *gauche* conformer in acyclic systems could be further emphasized if the motif existed in a cyclic scaffold.

In this work, we proposed the synthesis of  $\beta$ -fluoroamines that are constrained to a carbocyclic backbone. To provide access to a variety of ring sizes and all stereoisomers, we have developed a synthetic approach that enables the fine-tuning of amine basicity & conformation. In comparison to  $\beta$ -fluorinated *N*-heterocycles,  $\beta$ -fluoroamines with a carbocyclic backbone are more difficult to prepare. These motifs would however provide a way to utilize conformationally restricted  $\beta$ -fluoroamines without the introduction of an additional basic nitrogen. These also grant a means by which the nitrogen in a fluorinated *N*-heterocycle can be compared directly to its carbocyclic analog for probing biological activity and mechanism of action. Our proposed methods will grant access to these structures with points of divergence throughout the synthesis, allowing for discrete manipulations for intentional evaluations.

### 1.1.4 Existing methods to for enantioselective synthesis of $\beta$ -fluoroamines

Methods to synthesize fluorinated aryl motifs are rather well precedented and applied on commercial scale. Additionally, many of these subunits are commercially available. However, mono-fluorinated aliphatic compounds are fewer in number, with those containing fluorine at a

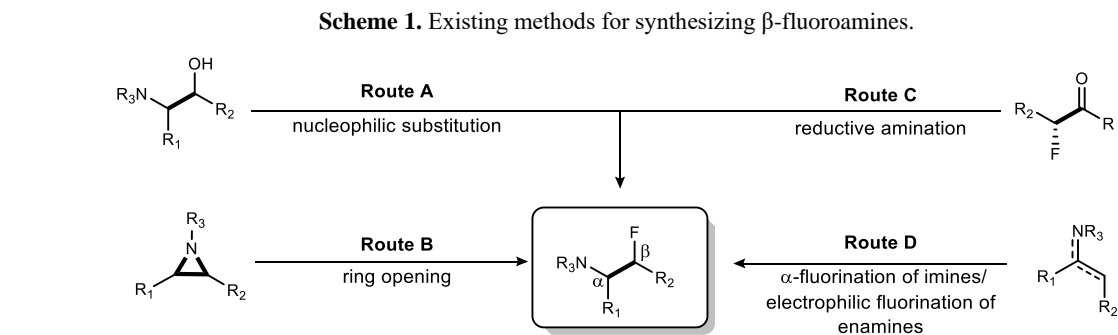


chiral center being among the most elusive. Currently, industry is still mainly reliant on deoxyfluorination of chiral alcohols to access these motifs. Diethylaminosulfur trifluoride (DAST,

**Figure 6**) is one of the most commonly-used reagents for this transformation. However, DAST presents several hazards in that it reacts very violently with water, can be explosive, and its decomposition products can be highly reactive.<sup>24</sup> Moreover, it has limited functional group tolerance and often results in elimination-related side products. Other reagents such as Deoxo-Fluor, XtalFluor and Fluolead (**Figure 6**) are more thermally stable, but do not provide great improvement in chemoselectivity. In 2015, PyFluor (**Figure 6**) was introduced by Doyle and coworkers as a superior reagent in terms of both selectivity and safety.<sup>25</sup> It suffers less from undesired elimination than its competitors and is claimed to be more amenable to larger scale productions.

Despite the associated hazards and selectivity issues, deoxyfluorination is still the most common method to access aliphatic fluorides. Some examples of substitution methods specific to  $\beta$ -fluoroamines include nucleophilic fluoride displacement of  $\beta$ -amino alcohols and nucleophilic azide displacement of activated fluorohydrins followed by Staundinger reduction.<sup>26</sup> The most commonly employed **methods for stereodefined cyclic  $\beta$ -fluoroamines rely on racemic methods followed by chiral separation of stereoisomers.**<sup>27</sup>

Nucleophilic ring opening of aziridines is often used to generate racemic *trans*-products (**Scheme 1**, Route B). The racemic *cis*-products are obtained via fluorination of an enolate equivalent followed by reductive amination (**Scheme 1**, Route C). One example from Merck demonstrates



<sup>24</sup> Baumann, M.; Baxendale, I. R.; Ley, S. V. *Synlett* **2008**, 2008, 2111.

<sup>25</sup> Nielsen, M. K.; Ugaz, C. R.; Li, W.; Doyle, A. G. *J. Am. Chem. Soc.* **2015**, 137, 9571.

<sup>26</sup> Cresswell, A. J.; Davies, S. G.; Lee, J. A.; Roberts, P. M.; Russell, A. J.; Thomson, J. E.; Tyte, M. J. *Org. Lett.* **2010**, 12, 2936.

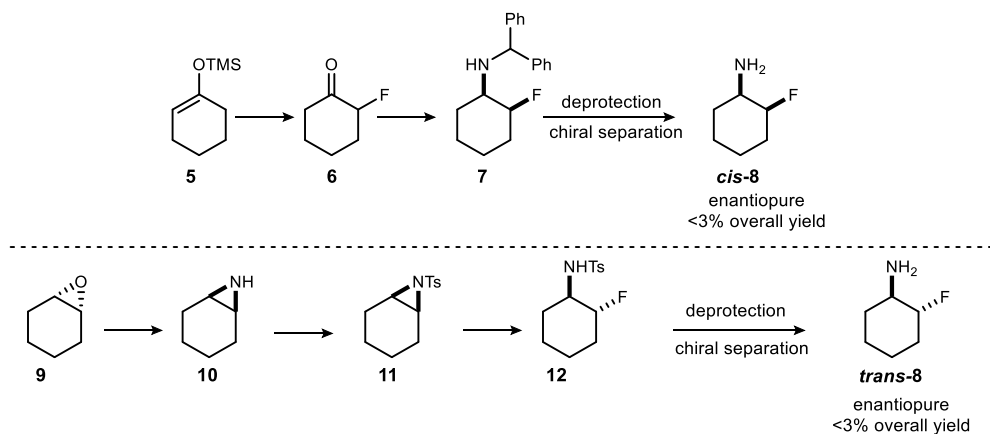
<sup>27</sup> Coburn, C. A.; Egbertson, M. S.; Graham, S. L.; Mcgaughey, G. B.; Stauffer, S. R.; Yang, W.; Lu, W.; Fahr, B.; Patent WO/2007/011810: 2007. Coburn, C. A.; Egbertson, M. S.; Graham, S. L.; Mcgaughey, G. B.; Stauffer, S. R.; Rajapakse, H. A.; Nantermet, P. G.; Stachel, S. R.; Yang, W.; Lu, W.; Patent WO/2007/011833 A2: 2007.



the need for improved stereoselective methods as chiral separation techniques provide diastereo- and enantiopure compounds in <3% overall yield *en route* to synthesizing potential  $\beta$ -secretase inhibitors as therapeutics for Alzheimer's disease (**Scheme 2**).<sup>27</sup>

Several groups have strived to achieve the goal of stereoselective synthesis of  $\beta$ -fluoroamines. For example, catalytic hydrofluorination of aziridines was accomplished by Doyle and coworkers using Lewis base catalysis to generate an amine-HF source *in situ* from benzoyl fluoride (**13**) and

**Scheme 2.** Merck's synthesis of  $\beta$ -fluorocyclohexyl amine demonstrates the need for improved enantioselective methodology.

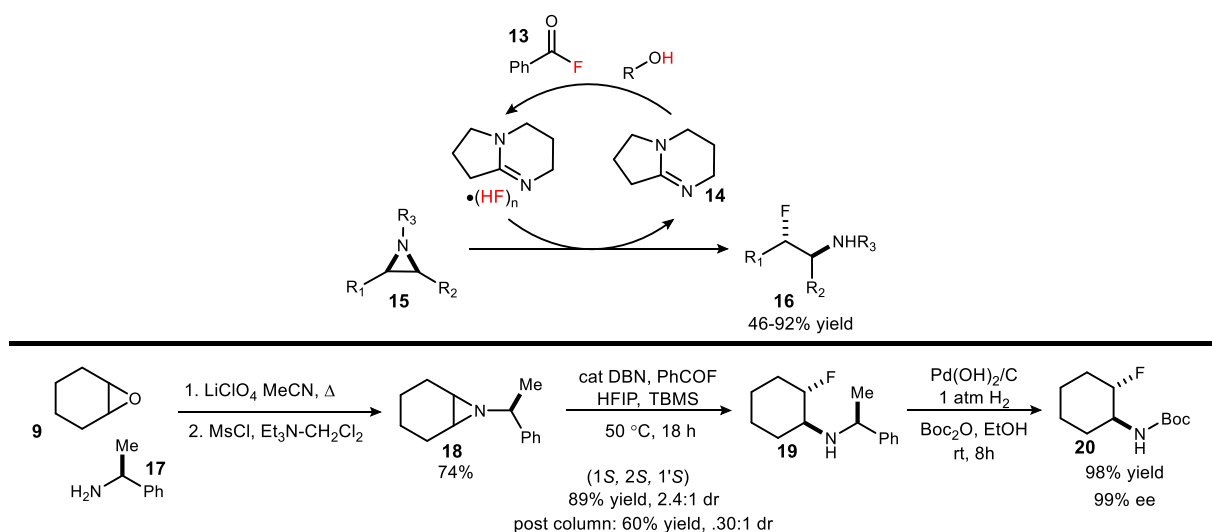


1,1,1,3,3,3,-hexafluoroisopropanol (HFIP) (**Scheme 3**).<sup>28</sup> This method provided various cyclic *trans*- $\beta$ -fluoroamines, and the enantioenriched  $\beta$ -fluorocyclohexyl amine could be obtained by means of employing  $\alpha$ -methyl benzylamine (**17**) as a chiral auxiliary (**Scheme 3**).

The same group later found that using a chelating aziridine protecting group in conjunction with the same PhCOF/HFIP HF source, and a combination of the chiral (salen)Co and Ti(IV) Lewis acid catalysts, could achieve the enantioselective ring opening in up to 84% ee. However, with both the Lewis base and cooperative Lewis acid catalyst systems, issues of regioselectivity arise in the case of unsymmetrical aziridines. It is expected that “fluorination occurs at the carbon that best stabilizes a positive charge”,<sup>28</sup> but when a significant difference is not present between sites

<sup>28</sup> Kalow, J. A.; Schmitt, D. E.; Doyle, A. G. *J. Org. Chem.* **2012**, *77*, 4177.

**Scheme 3.** Doyle's synthesis of *trans*  $\beta$ -fluoroamines.



of ring opening, regioselectivity presents an ongoing challenge. Additionally, this method only provides access to the *trans* diastereomer.

In other respects, several methods rely on the enantioselective synthesis of  $\alpha$ -fluoro carbonyl compounds, which are subsequently transformed into the desired  $\beta$ -fluoroamine. Lindsley and coworkers utilized Macmillan's imidazolidinone (**22**)<sup>29</sup> to catalyze the enantioselective fluorination of aldehydes. Extension of this methodology provided access to chiral  $\beta$ -fluoro amines by reductive amination (**Scheme 4, A**).<sup>30</sup> Diastereoselectivity was achieved using the Ellman *N*-sulfinyl amine chiral auxiliary to provide the aldimine in >20:1 dr, which was converted to either the *cis* or *trans*- $\beta$ -fluoroamine **26** or **27** (**Scheme 4, B**).<sup>31</sup> Furthermore, this was applied to provide  $\beta$ -fluoro-cyclohexyl amine (**8**) in 48% yield over 5 steps from the aldehyde (70% in 4 steps from  $\beta$ -fluoro-*N*-sulfinyl aldimine) (**Scheme 4, C**).

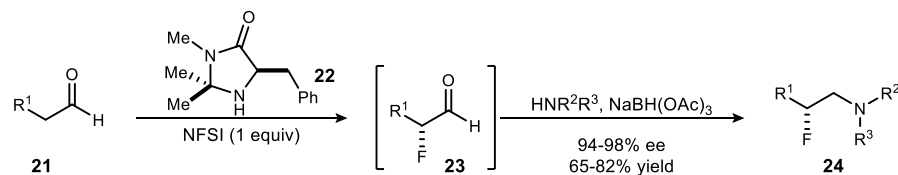
<sup>29</sup> Beeson, T. D.; MacMillan, D. W. C. *J. Am. Chem. Soc.* **2005**, *127*, 8826.

<sup>30</sup> Fadeyi, O. O.; Lindsley, C. W. *Org. Lett.* **2009**, *11*, 943.

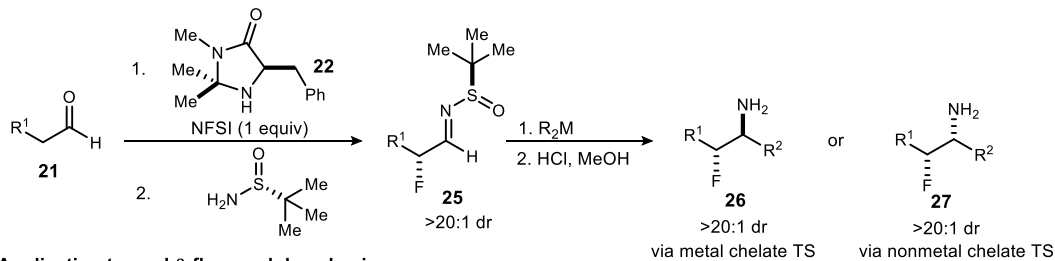
<sup>31</sup> Schulte, M. L.; Lindsley, C. W. *Org. Lett.* **2011**, *13*, 5684.

**Scheme 4.** Lindsley's stereoselective  $\alpha$ -fluorination of aldehydes and aldimines using Macmillan's imidazolidinone.

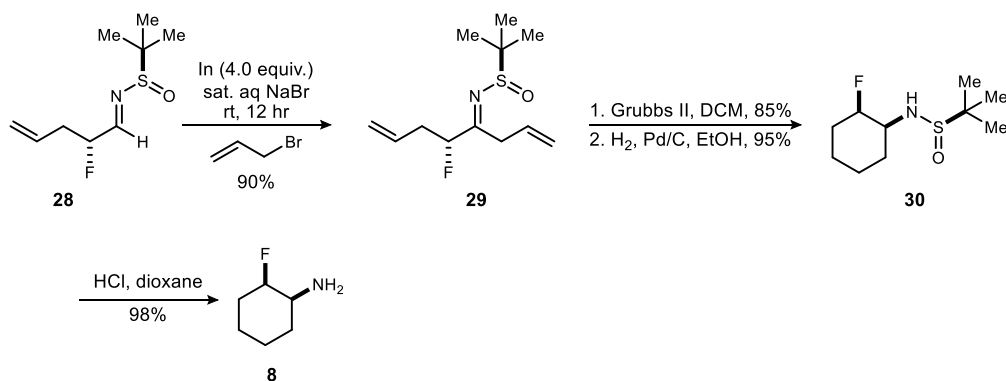
**A) Enantioselective  $\alpha$ -fluorination of aldehydes**



**B) Diastereoselective variant using Ellman *N*-sulfinyl aldimines**



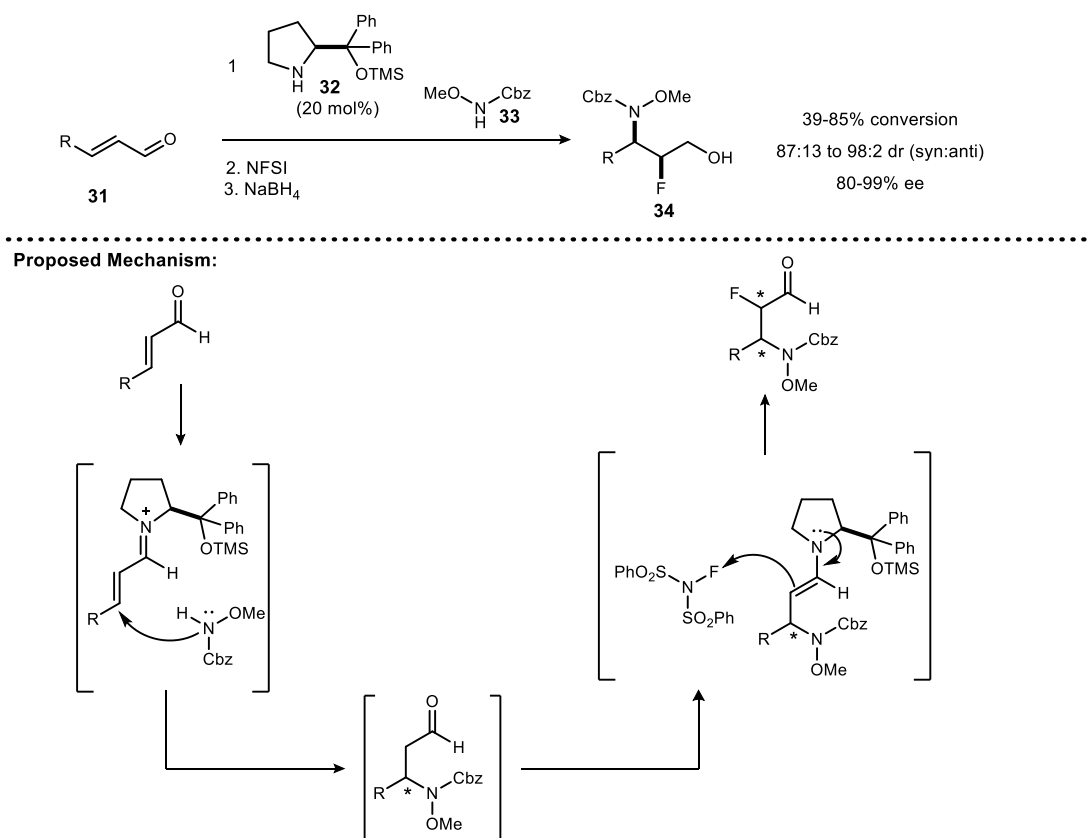
**C) Application toward  $\beta$ -fluorocyclohexylamine**



As an alternate approach, Brenner-Moyer and coworkers developed an elegant one-pot organocascade reaction of  $\alpha,\beta$ -unsaturated aldehydes to effect the enantioselective aminofluorination of olefins (**Scheme 5**).<sup>32</sup> This approach takes advantage of both iminium and enamine catalysis in a single pot as shown in the mechanism in **Scheme 5**. In this work, a single organocatalyst promotes the selective conjugate addition of the amine nucleophile, as well as the selective electrophilic fluorination of the enamine. While the group did explore the use of various Macmillan imidazolidinone catalysts, they ultimately found success with the chiral diarylprolinol

<sup>32</sup> Appayee, C.; Brenner-Moyer, S. E. *Org. Lett.* **2010**, *12*, 3356.

**Scheme 5.** Enantioselective aminofluorination cascade by Brenner-Moyer.



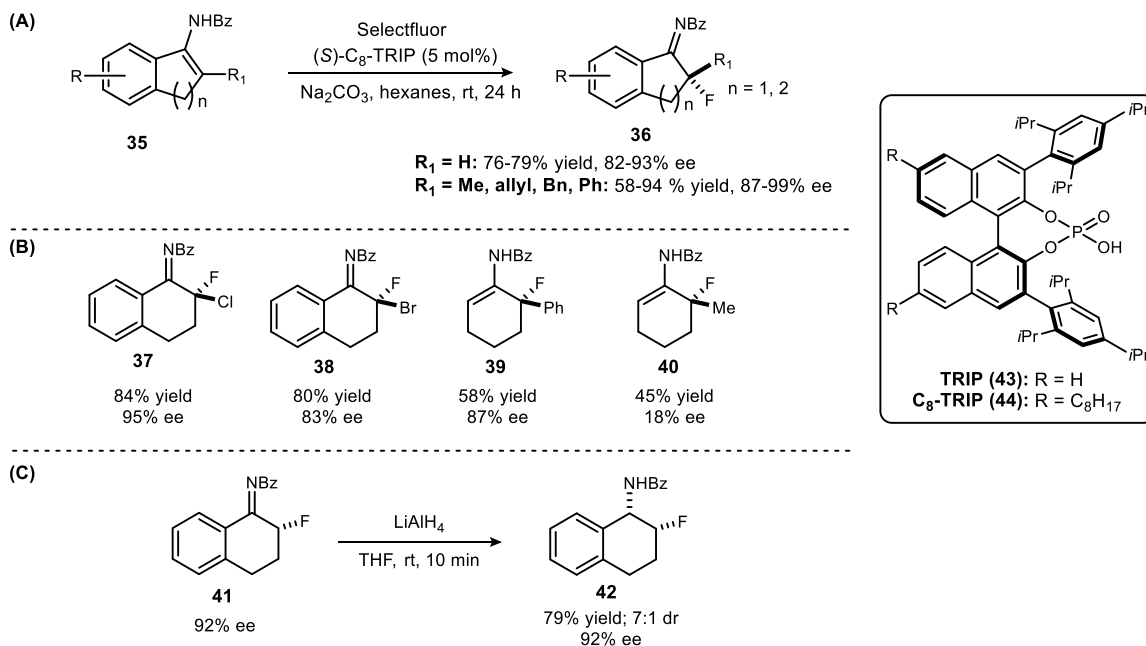
catalyst **32**.<sup>33</sup> However, the scope of this reaction has not yet been expanded to include cyclic structures.

Another avenue toward cyclic  $\beta$ -fluoroamines involves chiral phase-transfer catalysis for the enantioselective fluorination of cyclic benzoyl enamines (**Scheme 6**).<sup>34</sup> The use of phosphoric acid-based catalysts **43** and **44** provided a broad range of cyclic  $\alpha$ -(fluoro)benzoylimines with high enantioselection. This method works well for carbocycles with a tethered aromatic ring (e.g. **37**, **38**), however cyclohexanone-derived enamines, while accessible, suffered from a significant decrease in yield and enantioselection (**39-40**, **Scheme 6**). Importantly, hydride reduction of the resultant imine could afford the *cis*  $\beta$ -fluoroamines without erosion of ee (**Scheme 6, C**).

<sup>33</sup> Vesely, J.; Ibrahim, I.; Rios, R.; Zhao, G.-L.; Xu, Y.; Córdova, A. *Tetrahedron Lett.* **2007**, *48*, 2193.

<sup>34</sup> Phipps, R. J.; Hiramatsu, K.; Toste, F. D. *J. Am. Chem. Soc.* **2012**, *134*, 8376.

**Scheme 6.** Phase-transfer catalyzed enantioselective fluorination of benzoyl enamines.



## 1.2 Discovery of fluorine-induced diastereodivergence in a rare *syn*-selective aza-Henry reaction

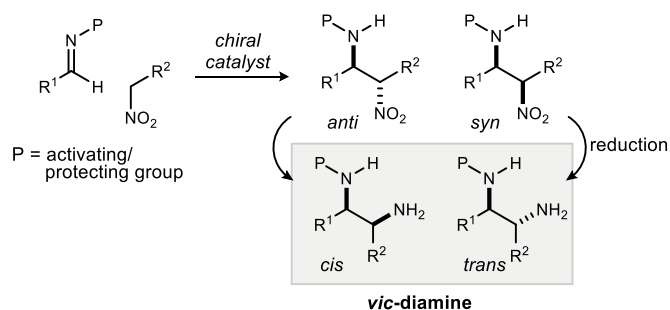
### 1.2.1 Introduction to the aza-Henry reaction

The addition of nitroalkanes to azomethines is often referred to as the aza-Henry or nitro-Mannich reaction. It has been successfully developed into a leading method for the stereocontrolled synthesis of *vic*-diamines<sup>35</sup> owing to the ease of subsequent nitro reduction (**Scheme 8**).<sup>36</sup>

<sup>35</sup> Lucet, D.; Le Gall, T.; Mioskowski, C. *Angew. Chem., Int. Ed.* **1998**, *37*, 2580.

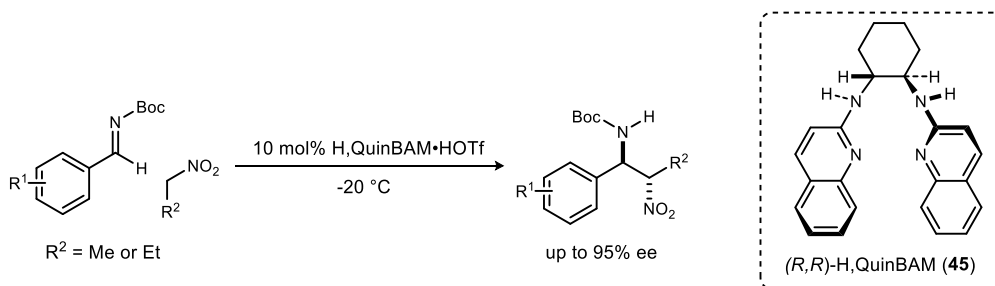
<sup>36</sup> For reviews see: a) Ana, M. F. P. *Current Organocatalysis* **2016**, *3*, 222.; b) Marqués-López, E.; Merino, P.; Tejero, T.; Herrera, R. P. *Eur. J. Org. Chem.* **2009**, *2009*, 2401.; c) Westermann, B. *Angew. Chem. Int. Ed.* **2003**, *42*, 151.

**Scheme 8.** The aza-Henry (nitro-mannich) reaction.



The discovery of a wide array of Lewis acid and metal-free chiral catalysts that accelerate the aza-Henry reaction has greatly expanded the amine products readily accessed, in particular diamine and secondary amine precursors to small molecules with relevance to therapeutic development.<sup>37,38</sup> One of the many ways that the Johnston group has contributed to this field is through the advent of ‘chiral proton catalysis.’<sup>39</sup> The seminal work published in 2004 highlighted the use of a chiral organocatalyst to effect the enantioselective addition of nitromethane or nitroethane into electron-deficient *N*-Boc aldimines (**Scheme 7**).

**Scheme 7.** Seminal BAM catalyzed aza-Henry reaction.



<sup>37</sup> Sukhorukov, A. Y.; Sukhanova, A. A.; Zlotin, S. G. *Tetrahedron* **2016**, 72, 6191.

<sup>38</sup> Noble, A.; Anderson, J. C. *Chem. Rev.* **2013**, 113, 2887.

<sup>39</sup> Nugent, B. M.; Yoder, R. A.; Johnston, J. N. *J. Am. Chem. Soc.* **2004**, 126, 3418.



aza-Henry<sup>39,40,41,42,43,44</sup> and halocyclization<sup>45</sup> reactions. The ligand structure features three primary sites for diversification (**Figure 7, A-C**). What is shown as the chiral *trans*-1,2-cyclohexanediamine backbone (**Figure 7, C**), can be exchanged, typically for a *trans*-stillbenediamine or anthracenyldiamine backbone, to change the size of the chiral pocket. Substitution at the 4-position of the quinoline ring alters reactivity and selectivity (**Figure 7, A**). It was found that placing pyrrolidine at the 4-position increased Brønsted basicity and reactivity.<sup>41</sup> This pyrrolidine *bis*(amidine) catalyst (PBAM, **46**) has been effective for a number of transformations, and was even made commercially available.<sup>46</sup> Substituents can be added to the 6- and 7-positions (and sometimes 8) on the quinoline ring to impart steric and/or electronic changes on the catalyst (**Figure 7, B**). For example, <sup>6,7</sup>(MeO)<sub>2</sub>PBAM (**47**) was found to be more Brønsted basic than the unsubstituted congener PBAM (**46**), and has thus seen applications for the activation of less reactive substrates. In the context of the aza-Henry reaction, the Johnston laboratory has demonstrated the utility of these ligands for the activation of a number of pro-nucleophiles (**Scheme 9**). This scope has been shown to include nitroalkanes,<sup>40d,e</sup>  $\alpha$ -halonitroalkanes,<sup>42,44, 47</sup>  $\alpha$ -nitroesters,<sup>40a,b,g</sup> and  $\alpha$ -nitrophosphonates<sup>40c</sup> (**Scheme 9**).

---

<sup>40</sup> a) Singh, A.; Yoder, R. A.; Shen, B.; Johnston, J. N. *J. Am. Chem. Soc.* **2007**, *129*, 3466.; b) Singh, A.; Johnston, J. N. *J. Am. Chem. Soc.* **2008**, *130*, 5866.; c) Wilt, J. C.; Pink, M.; Johnston, J. N. *Chem. Commun.* **2008**, 4177.; d) Davis, T. A.; Johnston, J. N. *Chem. Sci.* **2011**, *2*, 1076.; e) Davis, T. A.; Vilgelm, A. E.; Richmond, A.; Johnston, J. N. *J. Org. Chem.* **2013**, *78*, 10605.; f) Vara, B. A.; Mayasundari, A.; Tellis, J. C.; Danneman, M. W.; Arredondo, V.; Davis, T. A.; Min, J.; Finch, K.; Guy, R. K.; Johnston, J. N. *J. Org. Chem.* **2014**, *79*, 6913.; g) Sprague, D. J.; Singh, A.; Johnston, J. N. *Chem. Sci.* **2018**, *9*, 2336.

<sup>41</sup> Davis, T. A.; Wilt, J. C.; Johnston, J. N. *J. Am. Chem. Soc.* **2010**, *132*, 2880.

<sup>42</sup> Shen, B.; Makley, D. M.; Johnston, J. N. *Nature* **2010**, *465*, 1027.

<sup>43</sup> Makley, D. M.; Johnston, J. N. *Org. Lett.* **2014**, *16*, 3146.

<sup>44</sup> Schwieter, K. E.; Johnston, J. N. *ACS Catal.* **2015**, *5*, 6559.

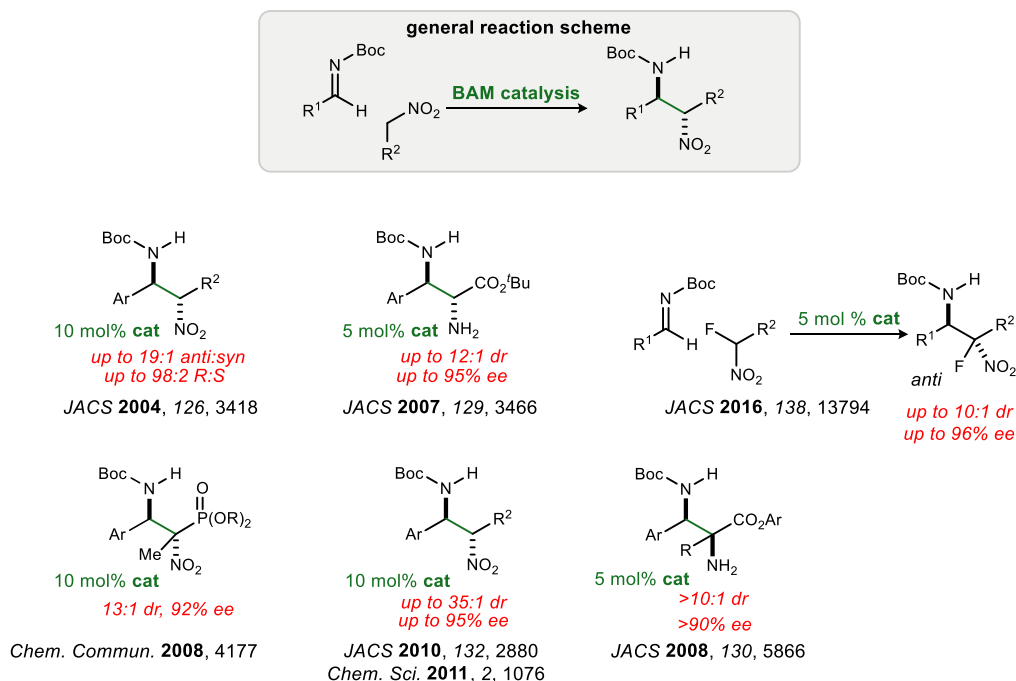
<sup>45</sup> a) Yousefi, R.; Struble, T. J.; Payne, J. L.; Vishe, M.; Schley, N. D.; Johnston, J. N. *J. Am. Chem. Soc.* **2019**, *141*, 618.; b) Struble, T. J.; Lankswert, H. M.; Pink, M.; Johnston, J. N. *ACS Catal.* **2018**, *8*, 11926.; c) Knowe, M. T.; Danneman, M. W.; Sun, S.; Pink, M.; Johnston, J. N. *J. Am. Chem. Soc.* **2018**, *140*, 1998.; d) Toda, Y.; Pink, M.; Johnston, J. N. *J. Am. Chem. Soc.* **2014**, *136*, 14734.; e) Dobish, M. C.; Johnston, J. N. *J. Am. Chem. Soc.* **2012**, *134*, 6068.

<sup>46</sup> Aldrich catalog number 799599

<sup>47</sup> Vara, B. A.; Johnston, J. N. *J. Am. Chem. Soc.* **2016**, *138*, 13794.



**Scheme 9.** Selected examples of published aza-Henry adducts from the Johnston Laboratory.



### 1.2.2 The *anti* paradigm in aza-Henry reactions

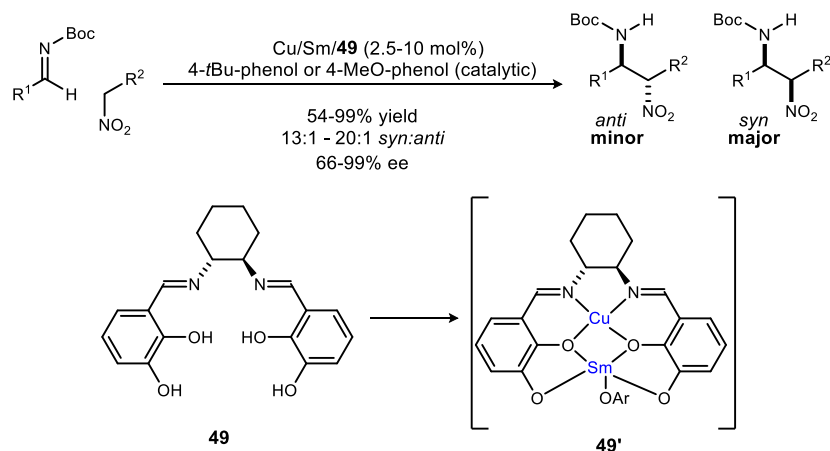
Nearly all aza-Henry reactions promoted by chiral catalysts favor the *anti* diastereomer.<sup>48,49</sup> The absence of general *syn*-selective aza-Henry reactions diminishes the otherwise broad utility of *trans-vic*-diamines in therapeutic development and asymmetric synthesis.<sup>35</sup> Simultaneous observation of high *syn*-diastereoselection and high enantioselection has been achieved only once by the Shibasaki group (**Scheme 10**).<sup>50</sup> Their work uses a bimetallic system with a chiral Schiff base ligand to catalyze the aza-Henry reaction. The Schiff base ligand accommodates both a transition metal and a rare-earth metal in the fashion described by structure **49'** (**Scheme 10**), and the observation of nonlinear effects suggest that the active catalyst species is not a monomer.

<sup>48</sup> The use of relative stereochemical terms (*anti*, *syn*) here conforms to the most common convention: the aza-Henry product is drawn in zigzag form using the carbon backbone, and *anti* characterizes this drawing when the nitrogens of amine and nitro reside on opposite sides.

<sup>49</sup> Ketimine electrophiles in enantioselective aza-Henry reactions are far less common, but *syn*-selective variants are known: Hong, G.; Mao, D.; Zhu, X.; Wu, S.; Wang, L. *Org. Chem. Front.* **2015**, 2, 985.

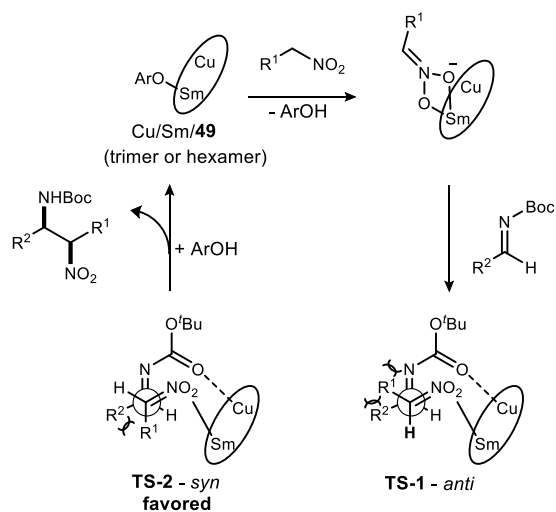
<sup>50</sup> a) Handa, S.; Gnanadesikan, V.; Matsunaga, S.; Shibasaki, M. *J. Am. Chem. Soc.* **2007**, 129, 4900.; b) Handa, S.; Gnanadesikan, V.; Matsunaga, S.; Shibasaki, M. *J. Am. Chem. Soc.* **2010**, 132, 4925.

**Scheme 10.** Shibasaki's *syn* selective aza-Henry reaction.



The mechanism and model for stereoselection is shown in **Scheme 11**. Shibasaki proposes that the Sm-aryl oxide moiety in the catalyst (either the exogenous phenoxide or one from the Schiff base) would serve as a Brønsted base to form the nitronate species. The Cu(II) behaves as a Lewis acid to coordinate the imine in the chiral pocket. It is suspected that due to steric interaction, the less-hindered transition state-2 is favored, resulting in the *syn* diastereomer and catalyst regeneration upon protonation.

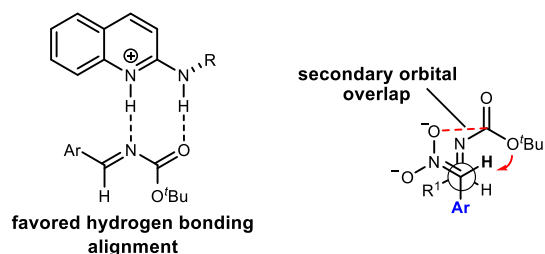
**Scheme 11.** Proposed catalytic cycle and stereochemical model for Shibasaki's *syn*-selective aza-Henry reaction.



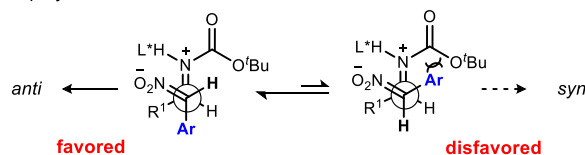
With the BAM catalyst systems, it is hypothesized that the observed *anti*-selectivity arises from a transition state such as that depicted in **Scheme 12**. One of the key differences between Shibasaki's bimetallic catalyst activation and BAM catalysis is that in BAM catalysis, stereoselectivity is controlled primarily through hydrogen-bonding interactions in the chiral pocket. Thus, in these Newman projections, both the nitro group and iminium N-H are positioned on the same side to account for the dual activation by the catalyst. Calculations performed by the Dudding group also suggest the alignment of the Boc group shown in **Scheme 12**.<sup>51,52</sup> From there, it is hypothesized that the transition state leading to the *anti*-diastereomer would be favored because of steric interactions between the nitroalkane substituent (Ar) and the Boc group. The Boc group is oriented as shown, allowing for 2-point binding by the carbamate N/O atoms. Calculations performed by the Dudding group also indicate that the sterics in the *syn* transition state force the imine to be less planar, which is disfavorable because it disrupts the conjugation. Additionally, they found that the *anti* transition state is stabilized by interactions between the Boc alkoxy oxygen lone pair and the allylic nitronate C-H antibonding  $\sigma^*$  orbital. Our findings described below also suggest favorable orbital interactions between the aryl substituent and the iminium  $\pi^*$  in the *anti* transition state.

**Scheme 12.** Models for stereoselectivity in the BAM catalyzed aza-Henry reaction.

A) favored alignments



B) Newman projections



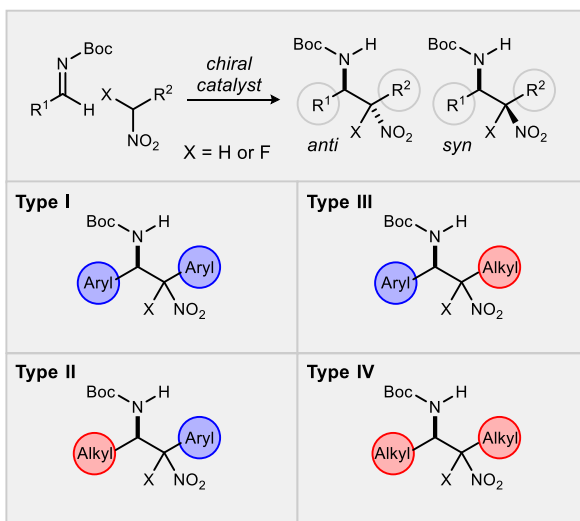
<sup>51</sup> Belding, L.; Taimoory, S. M.; Dudding, T. *ACS Catal.* **2015**, *5*, 343.

<sup>52</sup> Taimoory, S. M.; Dudding, T. *J. Org. Chem.* **2016**, *81*, 3286.

### 1.2.3 Project overview

In this work we discovered an unusual reversal of diastereoselectivity, favoring the *syn*-aza-Henry product, that arises within a subset of  $\alpha$ -fluoro nitroalkane pronucleophiles. An additional unusual feature is that the reversal is mediated, but not determined by the catalyst, leading to the discovery of an example of fluorine-based diastereodivergence.<sup>53</sup> This behavior is outlined by a methodical investigation of this substrate control using aryl and aliphatic aldimines, combined with aryl and

**Scheme 13.** Description of categories for Type I-Type IV aza-Henry reactions.

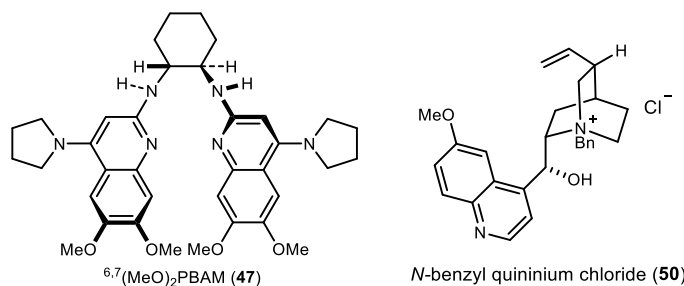


aliphatic  $\alpha$ -fluoro nitromethane derivatives. To this end, we divided these combinations into four different ‘types’: Type I, consisting of an aryl electrophile and aryl nucleophile; Type II, consisting of an alkyl electrophile and an aryl nucleophile; Type III, consisting of an aryl electrophile and an alkyl nucleophile, and finally, Type IV consisting of an alkyl nucleophile and electrophile (**Scheme 13**).

<sup>53</sup> Adolph, H. G.; Kamlet, M. J. *J. Am. Chem. Soc.* **1966**, 88, 4761.

Each type was evaluated for both fluoronitroalkanes and unsubstituted nitroalkanes. Moreover, to determine the role that the catalyst may play, each Type and substitution pattern was evaluated using both the homogeneous catalyst **47** and the phase transfer catalyst **50** (Figure 8). An underlying hierarchy has been uncovered in these additions whereby fluorine reverses the inherent *anti*-selectivity of nitroalkane additions except when using aryl nitromethanes. The nitronates bearing geminal aryl and fluorine remain unaffected when changing from hydrogen to fluorine at the nitronate carbon, suggesting a dominant directing effect provided by the aromatic ring.

**Figure 8.** Structures of catalysts used for each ‘type’ of aza-Henry addition.



As previously discussed, our laboratory has reported the catalyzed addition of  $\alpha$ -fluoro nitroalkanes to *N*-Boc aldimines using chiral bis(amidine) [BAM] catalyst **47**.<sup>47</sup> The inclusion of fluorine in the nitroalkane pronucleophile provided for the synthesis of  $\beta$ -fluoro-stilbene amines,<sup>54</sup> albeit with an attenuated overall rate relative to non-fluorinated aryl nitromethanes.<sup>40d-f,55</sup> The relative configuration of the  $\beta$ -amino nitroalkanes<sup>56</sup> was assigned by X-ray diffractometry, establishing that the fluorine’s effect on rate did not affect *anti*-selectivity in this case. Other cases exhibited similarly high selectivity (Types II-IV), encouraging a tentative assignment of configuration for many cases by analogy.

<sup>54</sup> Some stilbene  $\beta$ -fluoroamines can be prepared by enantioselective phase transfer catalysis of aziridine ring-opening. Leading reference: Pupo, G.; Vicini, A. C.; Ascough, D. M. H.; Iba, F.; Christensen, K. E.; Thompson, A. L.; Brown, J. M.; Paton, R. S.; Gouverneur, V. *J. Am. Chem. Soc.* **2019**, *141*, 2878.

<sup>55</sup> For a general review of fluorine effects on fluoroalkylation reactions, see: Ni, C.; Hu, J. *Chem. Soc. Rev.* **2016**, *45*, 5441.

<sup>56</sup> The Type framework is based on the hypothesis that the relative stereoselectivity may be influenced by the nature of the reactive functionality’s substituents, organized into four categories, Types I-IV, determined by the *N*-Boc aldimine and nitroalkane substituents (aryl vs. alkyl). For example, a Type I aza-Henry involves an aryl nitromethane addition to aryl aldimine, while a Type III addition involves a nitroalkane addition to an aryl aldimine.

During our pursuit of applications requiring Type IV additions (*vide infra*), we continued to observe high diastereo- and enantioselectivity. These studies provided an additional opportunity to rigorously determine absolute and relative stereochemistry by X-ray diffraction. In doing so, we made the surprising discovery that selectivity favored the *syn*- $\beta$ -amino- $\alpha$ -fluoro nitroalkane. This led us to launch a thorough study of each aza-Henry addition Type with the objective to identify the control element(s) leading to *syn*-selectivity, and ultimately an understanding of this phenomenon of diastereodivergence. In some cases, determination of the absolute and relative configuration of the minor stereoisomer was possible, for which remarkably little is known from the extensive studies to-date reported in the literature. The sum of these results indicates that *syn*-selectivity for these aza-Henry reactions derives from a hierarchy of interactions, favoring a *syn*-transition state model wherein the fluorine and aryl (when present) compete for control.<sup>57</sup>

#### 1.2.4 Catalyzed aza-Henry reactions: Type I (Ar/Ar)

Aryl nitromethanes undergo diastereo- and enantioselective addition to *N*-Boc benzaldimines using bis(amidine) [BAM] catalysis, providing *anti*-addition products with high yield and selectivity (**Scheme 14**). In addition to assignment of the favored stereoisomer by X-ray diffraction ( $R_1=3\text{-Br-4-MeOC}_6\text{H}_3$ ,  $R_2=\text{C}_6\text{H}_5$ ), a key analogue ( $R_1=R_2=4\text{-ClC}_6\text{H}_4$ ) was converted to the p53/MDM2 inhibitor Nutlin-3a,<sup>40e</sup> and its potency recapitulated *in vitro*.<sup>58</sup> Additionally, Ooi developed the chiral ammonium betaine **51** that further improves the selectivity of this addition, providing the Type I product (Ph/Ph) in 98% ee (**Scheme 14**).<sup>71</sup> Ooi's investigation of aryl nitromethane, and  $\alpha$ -vinyl- $\alpha$ -aryl-nitromethane addition to imines exhibited highly conserved *anti*-selectivity (**Scheme 14**).<sup>59</sup> Kozłowski identified cinchonidinium acetate as an effective homogeneous catalyst for Type I products (**Scheme 14**). Finally, Duan used a urea/tetralkyl

---

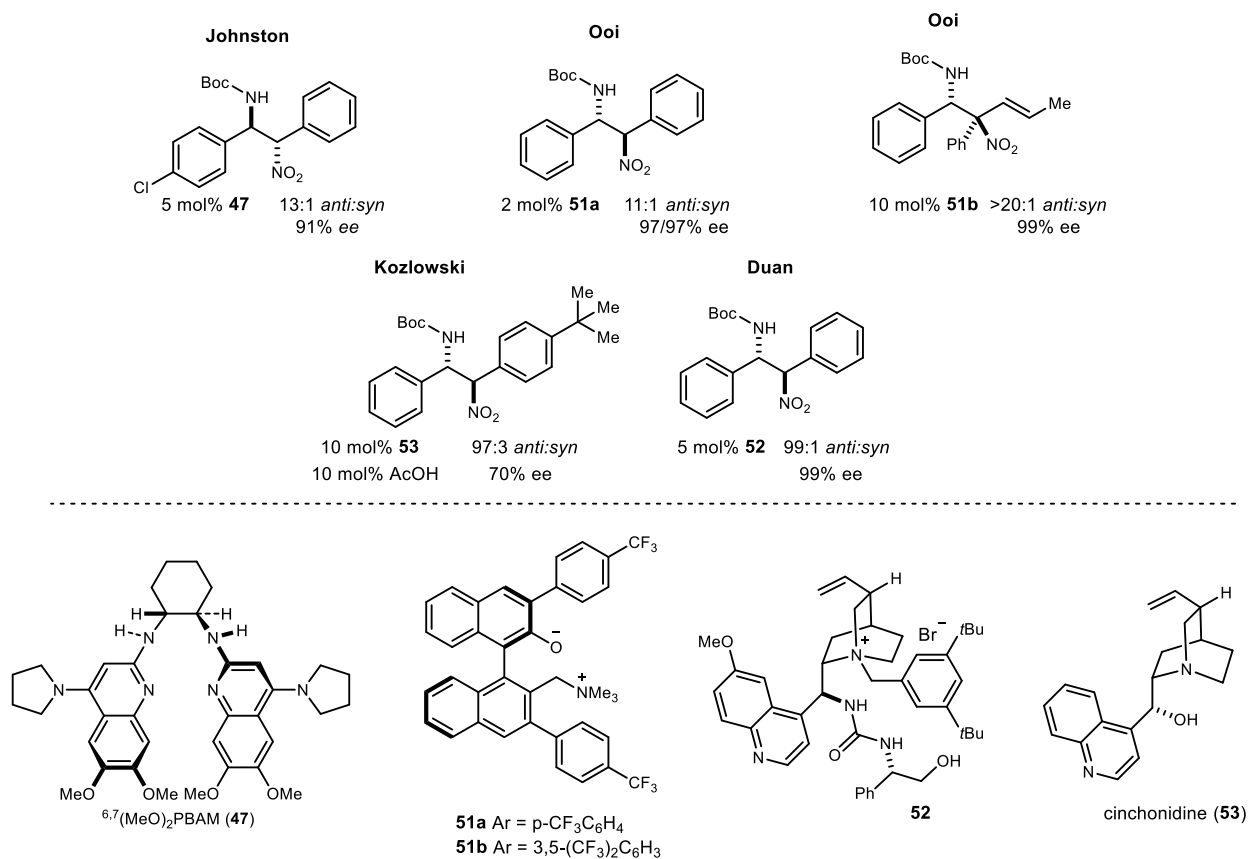
<sup>57</sup> In total, three cases (**56h-j**) in ref. 47 must be reassigned as *syn*-diastereomers. See Supporting Information for complete experimental data.

<sup>58</sup> For use of this material *in vivo*, see: a) Vilgelm, A. E.; Pawlikowski, J. S.; Liu, Y.; Hawkins, O. E.; Davis, T. A.; Smith, J.; Weller, K. P.; Horton, L. W.; McClain, C. M.; Ayers, G. D.; Turner, D. C.; Essaka, D. C.; Stewart, C. F.; Sosman, J. A.; Kelley, M. C.; Ecsedy, J. A.; Johnston, J. N.; Richmond, A. *Cancer Res.* **2015**, *75*, 181. b) Vilgelm, A. E.; Saleh, N.; Shattuck-Brandt, R.; Riemenschneider, K.; Slesur, L.; Chen, S.-C.; Johnson, C. A.; Yang, J.; Blevins, A.; Yan, C.; Johnson, D. B.; Al-Rohil, R. N.; Halilovic, E.; Kauffmann, R. M.; Kelley, M.; Ayers, G. D.; Richmond, A. *Science Translational Medicine* **2019**, *11*, eaav7171.

<sup>59</sup> Oyaizu, K.; Uraguchi, D.; Ooi, T. *Chem. Commun.* **2015**, *51*, 4437.

ammonium bifunctional catalyst **62** to provide the Type I adduct in 99:1 *anti:syn* and 99% ee (**Scheme 14**).

**Scheme 14.** Representative examples of selectivity in Type I aza-Henry reactions.



We examined the selectivity for Type I systems using both phase-transfer catalysis and homogeneous catalysis. In our hands, *N*-benzyl quininium chloride (**50**, 12 mol %) and cesium hydroxide applied to the  $\alpha$ -amido sulfone precursor to *N*-Boc imine provided the addition product with similarly high diastereoselectivity, but low enantioselection for the major (*anti*) diastereomer (**Table 2**, entry 2: **56a**, 15:1 dr, 39% ee). Catalysts **1** (homogeneous) and **50** (heterogeneous) not only exhibited similar behavior with phenyl nitromethane, but also  $\alpha$ -fluoro phenyl nitromethane (**Table 2**, entries 3-4). This suggested a robust correlation between nitronate-azomethine orientation during catalyst activation, and relative insensitivity of this stereochemistry-determining arrangement to the presence of fluorine at a reacting carbon. It should be noted, however, that fluorine notably slowed the aza-Henry additions relative to those of non-fluorinated aryl

nitromethanes. This is a phenomenon already noted for BAM catalyst **1** (including the effects of ligand protonation), consistent with a combination of rate-limiting nitroalkane deprotonation, and the higher effective  $pK_a$  exhibited by  $\alpha$ -fluoronitroalkanes.<sup>60</sup> In summary, homogeneous catalyst **47** is superior to heterogeneous catalyst **50** in Type I additions, but both favor the same relative configuration, as well as absolute configuration for the major and minor diastereomers.

### 1.2.5 Catalyzed aza-Henry reactions: Type II (Alkyl/Ar)

Additions of aryl nitronates to alkyl aldimines have also been established as *anti*-selective. Aliphatic *N*-Boc aldimines are best addressed by phase transfer-catalysis since the formation of *N*-Boc enamide by tautomerization is minimized.<sup>66,61</sup> Duan extended the catalyst effective for Type I additions to a single example involving an aliphatic aldimine, which provided the product in 91% yield (PhCH<sub>2</sub>CH<sub>2</sub>/Ph: 94:6 dr, 97% ee). The stereochemical assignment of this example was made by analogy to the associated Type I cases, specifically **56a**.

We investigated the Type II addition shown in **Table 2**, observing high levels of selectivity. Our results using catalysts **1** and **2** favored the same relative and absolute configurations. The level of diastereoselection during formation of **6c** was highest using BAM catalysis (**Table 2**, entry 5 vs. entry 6), but enantioselection was higher using PTC (89% ee vs. 60% ee). Extending this examination to  $\alpha$ -fluoronitroalkane **54b**, both catalysts **47** and **50** featured *anti*-selective additions for  $\alpha$ -fluoro aryl nitromethane additions to aliphatic aldimines (Type II). For example,  $\alpha$ -fluoro phenyl nitromethane provided the  $\beta$ -amino- $\alpha$ -fluoro-nitroalkane in 5.2:1 *anti:syn*, 83% ee (**Table 2**, entry 7).

Our need for rigorous assignment of the major stereoisomer for the non-fluorinated adduct was attempted, but crystalline *anti*-**6c** formed only thin, feathery needles. In the absence of this, Duan's assignment of a Type II example by analogy to a Type I case remains.<sup>62</sup> Absolute and relative stereochemistry for the *major* isomer of the fluorinated substrate was assigned by X-ray diffraction

---

<sup>60</sup> a) Bordwell, F. G.; Bartmess, J. E. *J. Org. Chem.* **1978**, *43*, 3101. b) Adolph, H. G.; Kamlet, M. J. *J. Am. Chem. Soc.* **1966**, *88*, 4761. c) Slovetskii, V. I.; Okhlobystina, L. V.; Fainzil'berg, A. A.; Ivanov, A. I.; Biryukova, L. I.; Novikov, S. S. *Bulletin of the Academy of Sciences of the USSR, Division of chemical science* **1965**, *14*, 2032.

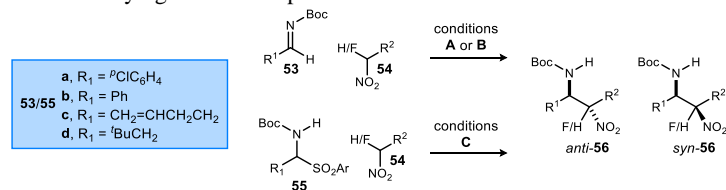
<sup>61</sup> Fini, F.; Sgarzani, V.; Pettersen, D.; Herrera, R. P.; Bernardi, L.; Ricci, A. *Angew. Chem., Int. Ed.* **2005**, *44*, 7975.

<sup>62</sup> Lu, N.; Li, R.; Wei, Z.; Cao, J.; Liang, D.; Lin, Y.; Duan, H. *J. Org. Chem.* **2017**, *82*, 4668.



(*anti*-**56d**, **Figure 9**). This confirmed that Type II additions exhibit robust *anti*-selectivity regardless of fluorine substitution of the intermediate aryl nitronate. Importantly, these results also establish that this behavior is independent of catalyst type (homo- vs. heterogeneous), although under these standard conditions, PTC catalyst **50** provides **56d** with slightly higher enantioselection (91% vs. 83% ee) at the expense of slightly lower diastereoselection (2.7:1 vs. 5.2:1 *anti-syn*).

**Table 2.** Catalyzed aza-Henry reactions varying aromatic/aliphatic substituents of azomethine and nitronate/fluoronitronate (Types I-IV).<sup>a</sup>



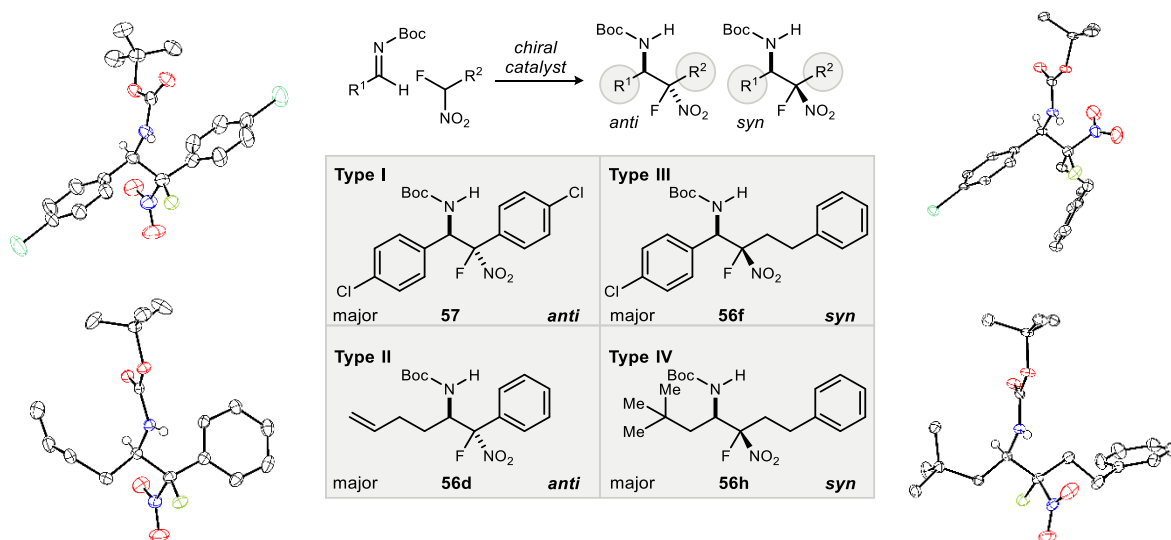
entry	type	R <sup>1</sup>	conditions	R <sup>2</sup>	H/F	54→56	temp (°C)	catalyst	anti:syn <sup>b</sup>	ee (%) <sup>b</sup>		yield (%) <sup>c</sup>	
										anti	syn	NMR	isol
1	I	Ph	<b>B</b>	Ph	H	<b>54a/56a</b>	-55	<b>47</b>	>20:1	78	99	79	
2	I	Ph	<b>C</b>	Ph	H	<b>54a/56a</b>	-50	<b>50</b>	15:1	39	99	30	
3 <sup>d</sup>	I	Ph	<b>B</b>	Ph	F	<b>54b/56b</b>	0	<b>47·HNTf<sub>2</sub></b>	3.5:1	94	84		88
4	I	Ph	<b>C</b>	Ph	F	<b>54b/56b</b>	-55	<b>50</b>	4.2:1	52	31	60	
5	II	CH <sub>2</sub> =CHCH <sub>2</sub> CH <sub>2</sub>	<b>A</b>	Ph	H	<b>54a/56c</b>	-55	<b>47</b>	>20:1	60	99	35	35
6	II	CH <sub>2</sub> =CHCH <sub>2</sub> CH <sub>2</sub>	<b>C</b>	Ph	H	<b>54a/56c</b>	-35	<b>50</b>	11:1	89	99	33	31
7 <sup>e</sup>	II	CH <sub>2</sub> =CHCH <sub>2</sub> CH <sub>2</sub>	<b>A</b>	Ph	F	<b>54b/56d</b>	-20	<b>47·HNTf<sub>2</sub></b>	5.2:1	83	99		53
8	II	CH <sub>2</sub> =CHCH <sub>2</sub> CH <sub>2</sub>	<b>C</b>	Ph	F	<b>54b/56d</b>	-35	<b>50</b>	2.7:1	91	93		43
9	III	<sup>p</sup> ClC <sub>6</sub> H <sub>4</sub>	<b>B</b>	PhCH <sub>2</sub> CH <sub>2</sub>	H	<b>54c/56e</b>	-20	<b>47·HNTf<sub>2</sub></b>	20:1	87	51		49
10	III	<sup>p</sup> ClC <sub>6</sub> H <sub>4</sub>	<b>C</b>	PhCH <sub>2</sub> CH <sub>2</sub>	H	<b>54c/56e</b>	-55	<b>50</b>	3:1	33	7	86	
11 <sup>d</sup>	III	<sup>p</sup> ClC <sub>6</sub> H <sub>4</sub>	<b>B</b>	PhCH <sub>2</sub> CH <sub>2</sub>	F	<b>54d/56f</b>	25	<b>47·HNTf<sub>2</sub></b>	1:5.0	99	93		85
12	III	<sup>p</sup> ClC <sub>6</sub> H <sub>4</sub>	<b>C</b>	PhCH <sub>2</sub> CH <sub>2</sub>	F	<b>54d/56f</b>	-35	<b>50</b>	1:2.5	24	60	89	79
13	IV	<sup>t</sup> BuCH <sub>2</sub>	<b>A</b>	PhCH <sub>2</sub> CH <sub>2</sub>	H	<b>54c/56g</b>	-55	<b>47</b>	1:1	20	11		21
14	IV	<sup>t</sup> BuCH <sub>2</sub>	<b>C</b>	PhCH <sub>2</sub> CH <sub>2</sub>	H	<b>54c/56g</b>	-55	<b>50</b>	>20:1	99	-	94	90
15	IV	<sup>t</sup> BuCH <sub>2</sub>	<b>A</b>	PhCH <sub>2</sub> CH <sub>2</sub>	F	<b>54d/56h</b>	0	<b>47·HNTf<sub>2</sub></b>	1:2.4	81	80	47	
16	IV	<sup>t</sup> BuCH <sub>2</sub>	<b>C</b>	PhCH <sub>2</sub> CH <sub>2</sub>	F	<b>54d/56h</b>	-35	<b>50</b>	1:7.2	76	91		84

<sup>a</sup>Conditions: **A**: The  $\alpha$ -amido sulfone **55** is treated with Cs<sub>2</sub>CO<sub>3</sub> in toluene to form imine **53**. After filtration, this solution is used directly in the aza-Henry reaction which is carried out in toluene (0.1 M) using the nitro- or fluoronitroalkane (1.2 equiv) and <sup>6,7</sup>(MeO)<sub>2</sub>PBAM (**47**) or <sup>6,7</sup>(MeO)<sub>2</sub>PBAM·HNTf<sub>2</sub> (**47·HNTf<sub>2</sub>**, 10 mol%) for 24 hours. **B**: Using **53** (neat, preformed from **55**), the aza-Henry reaction is run in dry toluene (0.1 M) under argon using the nitro- or fluoronitroalkane (1.2 equiv) with **47** or **47·HNTf<sub>2</sub>**. **C**: Reaction run in dry toluene (0.1 M) under argon using the nitro- or fluoronitroalkane (4.5 equiv), *N*-benzylquininium chloride (**50**, 12 mol%), and CsOH·H<sub>2</sub>O (1.3 equiv) for 48-72 hours. See Supporting Information for complete details. <sup>b</sup>Diastereomeric ratios measured by <sup>1</sup>H NMR analysis of the crude reaction mixture. Enantiomeric excess determined by HPLC using a chiral stationary phase. In cases where diastereoselection is high, the ee determined for the minor diastereomer is often based on two very small peaks. Therefore, values of 99% ee may contain more error since they are based on the observance of only one small peak. However, the observed (major) peak is consistent between the two catalysts. <sup>c</sup>Yields for conditions are calculated over 2 steps (from  $\alpha$ -amido sulfone). NMR: Yield measured using internal standard. Isol: Isolated yield. <sup>d</sup>Data from ref 47. <sup>e</sup>20 mol% catalyst. Using 10 mol% catalyst provides **56d** with 5.8:1 dr, 87/>99% ee, and 43% yield.

### 1.2.6 Catalyzed aza-Henry reactions: Type III (Ar/Alkyl)

Type III additions are undoubtedly the most studied cases, thereby providing a greater pool of catalysts for comparison. Among these, the catalysts **47**·HNTf<sub>2</sub> and **50** have been shown to be highly effective. However, the high degree of consistency exhibited by Type I-II additions using non-fluorinated and fluorinated nitroalkanes **54** did not accurately forecast the behaviors to be uncovered by Type III additions. Non-fluorinated, alkyl-substituted nitronates provided addition products with aryl aldimines with good selectivity (20:1 dr, 87% ee) when using **47**·HNTf<sub>2</sub> (**Table 2**, entry 9). Dixon<sup>63</sup> and Palomo<sup>66</sup> have independently assigned *anti*-selectivity to this type of addition. In the case of **56e**, catalyst **50** was not competitive, providing low diastereoselection (3:1) and enantioselection (33% ee, **Table 2**, entry 10) relative to BAM catalysis. Despite the low selectivity, both catalysts favor the same stereoisomer. Our interest in  $\alpha$ -fluoro nitroalkane additions led us to examine aromatic aldimine electrophiles, and these proceeded with good diastereo- and enantioselectivity (5.0:1 dr, 99% ee: **Table 2**, entry 11). This behavior followed the trends outlined for all of the additions described to this point. Fortunately, we did not rely on analogy for stereochemical assignment since it would have predicted conservation of *anti*-

**Figure 9.** Categorization of aza-Henry reactions by the type (aryl vs. alkyl) of the azomethine electrophile substituent, and the nitromethane substituent(s). X-Ray analysis for major (relative and absolute) stereoisomer formed in experiments detailed by **Table 2**.

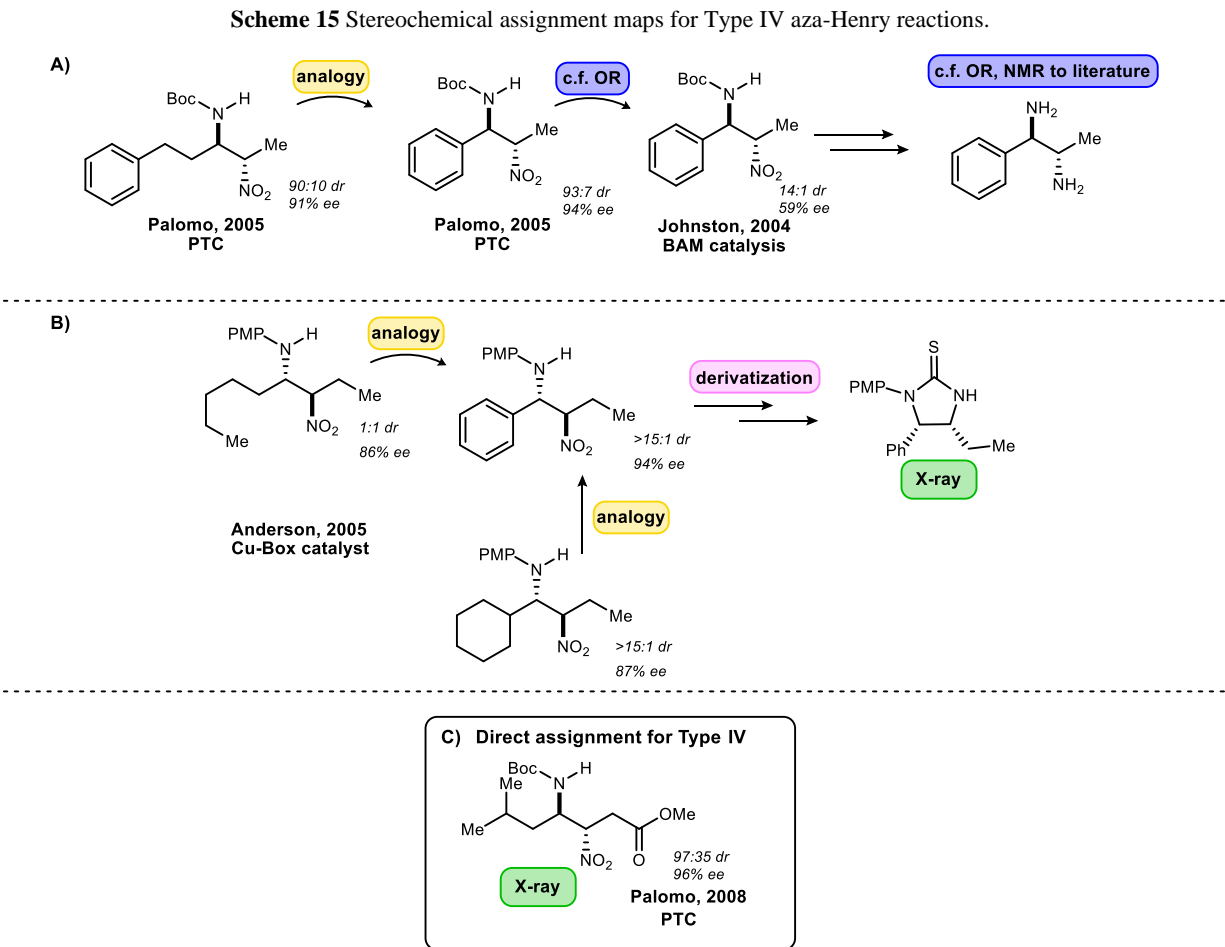


<sup>63</sup> A Type III addition product was assigned by analogy to a Type IV product: Johnson, K. M.; Rattley, M. S.; Sladojevich, F.; Barber, D. M.; Nunez, M. G.; Goldys, A. M.; Dixon, D. J. *Org. Lett.* **2012**, *14*, 2492.

selectivity based on all Type I/II additions, and non-fluorinated Type III additions. We instead sought rigorous stereochemical assignment by X-ray diffraction. Single crystals of the *major* diastereomer for **56f** revealed its *syn*-relationship (**Figure 9**). Comparison of homo- and heterogeneous catalysis confirmed again that both methods favored the same relative and absolute stereochemistry in the product, albeit with low dr and ee for **50** (**Table 2**, entry 12).

### 1.2.7 Catalyzed aza-Henry reactions: Type IV (Alkyl/Alkyl)

Limited literature precedent exists for the favored stereoisomer in additions of alkyl-substituted nitronates to aliphatic aldimines. This includes the early examples (2005) by Palomo citing *anti*-selectivity when drawing analogy to Type III additions (**Scheme 15**). This Type IV selectivity was more rigorously established in 2008 using X-ray diffraction (**Scheme 15**, C).<sup>66b</sup> Shibasaki's *syn*-selective Type IV additions featured a Cu(II)/Sm(III) protocol for nitroethane addition to an



aliphatic aldimine (65% yield, 20:1 dr, 80% ee), and this product was converted to nemonapride, an antipsychotic agent.<sup>50</sup> In other cases, Shibasaki's bimetallic catalyst provided the typical *anti*-selectivity with good enantioselection.<sup>64</sup> Anderson rigorously assigned silyl nitronate addition products within the Type III class for which a copper(II)-bis(oxazoline) system provided high dr/ee. These were assigned by derivatization to crystalline thiourea and subsequent X-ray analysis (**Scheme 15, B**). Analogy was then used to assign those belonging to the Type IV class, which included two cases: the product from cyclohexanal *N*-PMP imine, and hexanal imine.<sup>65</sup> Finally, Duan used a phase transfer catalyst equipped with hydrogen bonding ability to report a single example: the addition of nitroethane to the cyclohexaldehyde imine, with up to 99:1 dr, 97% ee.

We selected 3-phenyl-1-nitropropane to evaluate in both hetero- and homogeneous catalyst protocols, delivering the product of addition to **53d** with high selectivity only when using **50** (**Table 2**, entries 13-14). A strength of phase transfer catalysis is the pairing of rates for imine formation and consumption, a feature that is particularly impactful when the imine can tautomerize to the *N*-acyl enamide. In this comparison, catalyst **47** provided **56g** in low yield and with minimal stereoselection. However, PTC **50** delivered **56g** with exceptional selectivity (>20:1 dr, 99% ee) and yield (**Table 2**, entry 14). Rigorous assignment of *anti*-selectivity for this reaction was made by X-ray diffraction analysis of the major product, *anti*-**56g**.

Our examination of the corresponding  $\alpha$ -fluoronitroalkane addition using either homogeneous BAM catalysis (**47**·HNTf<sub>2</sub>) and heterogeneous catalysis (**50**) revealed similar selectivity trends again, with the former providing product with low diastereoselection (2.4:1) and moderate enantioselection (81% ee) at 0 °C. Catalyst **50** led to the same major diastereomer with high selectivity (7.2:1), and moderate enantioselection (76% ee) at -35 °C (**Table 2**, entry 16). In this case, both the major and minor diastereomers of **56h** formed quality single crystals that allowed the major to be assigned as *syn*-**56h** and the minor to be assigned as *anti*-**56h**. This also allowed us to further confirm that the stereochemistry at the azomethine carbon is conserved. Once again, the addition of alkyl-substituted  $\alpha$ -fluoro nitronates displayed a reversal of diastereoselection,

---

<sup>64</sup> Nitabaru, T.; Kumagai, N.; Shibasaki, M. *Molecules* **2010**, *15*, 1280.

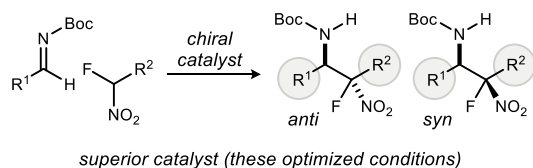
<sup>65</sup> Anderson, J. C.; Howell, G. P.; Lawrence, R. M.; Wilson, C. S. *J. Org. Chem.* **2005**, *70*, 5665.

favoring *syn*-selectivity. And again, this behavior stands in contrast to the *anti*-selectivity observed with non-fluorinated alkyl-substituted nitronates **54c**.

### 1.2.8 Catalyst selection

A goal of this study was to identify, if not understand the factors that determined diastereoselection using standard protocols that required little deviation to quantify selectivity (dr, ee). These standard protocols may not be optimal for individual cases, and further optimization could lead to higher yield and selectivity. These caveats notwithstanding, **Figure 10** is a selection table based on the catalysts used in this study. Importantly, the crystallinity that is typical of the products not only allowed the use of X-ray diffractometry to directly assign configuration for the adducts, but it also provided a means to enrich products further. For example, adduct **56e** could be recrystallized (ethyl acetate/hexanes) from 15:1 dr, 87/51% ee to >20:1 dr, 96% ee material.

**Figure 10.** Catalyst selection chart for Type I-IV aza-Henry reactions.



Type I - H	<b>47</b>	Type III - H	<b>47</b> ·HNTf <sub>2</sub>
Type I - F	<b>47</b> ·HNTf <sub>2</sub>	Type III - F	<b>47</b> ·HNTf <sub>2</sub>
Type II - H	<b>50</b>	Type IV - H	<b>50</b>
Type II - F	<b>47</b> ·HNTf <sub>2</sub>	Type IV - F	<b>50</b>

Superior Protocol	Type I		Type II		Type III		Type IV	
	H	F	H	F	H	F	H	F
catalyst	<b>47</b>	<b>47</b> ·HNTf <sub>2</sub>	<b>50</b>	<b>47</b> ·HNTf <sub>2</sub>	<b>47</b> ·HNTf <sub>2</sub>	<b>47</b> ·HNTf <sub>2</sub>	<b>50</b>	<b>50</b>
selectivity	<i>anti</i>	<i>anti</i>	<i>anti</i>	<i>anti</i>	<i>anti</i>	<b><i>syn</i></b>	<i>anti</i>	<b><i>syn</i></b>
entry (Table 2)	1	3	6	7	9	11	14	16

### 1.2.9 Discussion

The results outlined in **Table 2** illustrate clear trends that align with existing reports of *anti*-selective aza-Henry reactions when using either a hetero- or homogeneous catalyst, regardless of the nature of the azomethine and nitronate substituents. In order to highlight the trends, variants are organized here into four types based on aromatic and (primary) alkyl variants that are most common. Across Types I-IV, *anti*-diastereoselection is observed when using non-fluorinated nitroalkanes. This is observed regardless of catalyst (**1** or **2**), reaffirming reports with PTC,<sup>66</sup> BAM,<sup>39,40a,b</sup> and a wide range of other catalysts<sup>67,68,69,70</sup> with alkyl-substituted nitronates, and PTC<sup>62,71,72</sup> or BAM<sup>40d-f</sup> catalysts applied to aryl-substituted nitronates.

Departing from this behavior for enantioselective aza-Henry reactions, Shibasaki's report is a standout, and to-date is the most successful *syn*-diastereo- and enantioselective reaction. Using a mixed Cu(II)/Sm(III) complex, excellent *syn*-diastereoselection was achieved, with high enantioselection (43-83% ee). Aliphatic aldimines were less successful, reaching as high as 81% ee, and the scope was also limited to three linear aldimines.<sup>50</sup> The *syn*-selectivity in this work is attributed to reagent control by formation of a samarium(III) nitronate and copper(II)-activated Boc-imine supported simultaneously by the same chiral ligand (see **Scheme 11**).

The majority of new catalytic, enantioselective aza-Henry additions that feature new chiral catalysts have focused rather narrowly on a subset of substrates, often using the aryl aldimine-nitroethane combination to probe diastereoselection. Extrapolation of these assignments to other variations by analogy, a broadly accepted and generally reliable practice, has served as a substitute for rigor that might otherwise benefit the field. A departure from this practice was key to the discovery that  $\alpha$ -fluoronitroalkanes can favor either *anti*- or *syn*-aza-Henry products under catalyst

---

<sup>66</sup> a) A Type III product assigned by optical rotation: Palomo, C.; Oiarbide, M.; Laso, A.; Lopez, R. *J. Am. Chem. Soc.* **2005**, *127*, 17622. b) Gomez-Bengoa, E.; Linden, A.; Lopez, R.; Mugica-Mendiola, I.; Oiarbide, M.; Palomo, C. *J. Am. Chem. Soc.* **2008**, *130*, 7955.

<sup>67</sup> Friestad, G. K.; Mathies, A. K. *Tetrahedron* **2007**, *63*, 2541.

<sup>68</sup> Noble, A.; Anderson, J. C. *Chem. Rev.* **2013**, *113*, 2887.

<sup>69</sup> Akiyama, T.; Itoh, J.; Fuchibe, K. *Adv. Synth. Catal.* **2006**, *348*, 999.

<sup>70</sup> Vilaivan, T.; Bhanthumnavin, W.; Sritana-Anant, Y. *Curr. Org. Chem.* **2005**, *9*, 1315.

<sup>71</sup> Uraguchi, D.; Oyaizu, K.; Noguchi, H.; Ooi, T. *Chem. - Asian J.* **2015**, *10*, 334.

<sup>72</sup> Walvoord, R. R.; Kozlowski, M. C. *Tetrahedron Lett.* **2015**, *56*, 3070.

control using the most successful and broadly applied homogeneous (**47**, **47**·HNTf<sub>2</sub>) and heterogeneous (**50**) catalyst classes reported to-date.

The observation of *syn*-selective aza-Henry additions includes cases where an achiral catalyst and/or racemic product is formed.<sup>73</sup> Additionally, Anderson found that solvent can effect a change in diastereoselection, rationalized by an open transition state. This work attributed selectivity to the use of ether solvent in which the Lewis acid was minimally soluble.<sup>74</sup> *syn*-Selective aza-Henry reactions beyond those cited already are of uncertain relevance due to the substrate differences. For example, Xu used a thiourea catalyst derived from cyclohexane diamine to achieve high *syn*-selectivity in a deconjugative aza-Henry reaction of nitroalkenes with tosyl imines.<sup>75</sup> The Xu protocol delivered up to 97:3 *syn:anti*, 91% ee, for aromatic aldimines, and 81:19 *syn:anti*, 84% ee, for a single aliphatic aldimine. Boc-aldimines retained good *syn:anti* selectivity, but at the expense of lower enantioselection.

The fluorine-substituted nitronate diastereodivergent behavior observed here is both surprising and sharply defined. In cases where the nitroalkane is *aryl*-substituted (Types I-II), *anti*-selectivity prevails for both non-fluorinated and  $\alpha$ -fluorinated nitroalkanes (**Table 2**, entries 3-4 & 7-8). In contrast, *alkyl*-substituted nitronates of *fluoronitroalkanes* are *syn*-selective, regardless of the nature of the azomethine substituent (**Table 2**, entries 11-12 & 15-16). There is minimal literature related to the effect of fluorine on the diastereo- and enantioselective addition of nitroalkanes bearing alternative activating groups, including Tan's use of  $\alpha$ -fluoro- $\alpha$ -sulfonyl nitromethane leading to *anti*-adducts.<sup>76</sup> Those studies have not uncovered unusual stereochemical features of the reaction.<sup>77, 78</sup> Still other activated nitroalkane additions ( $\alpha$ -nitrophosphonates) have been attempted, but are not sufficiently selective to identify a paradigm in diastereoselection.<sup>79</sup>

---

<sup>73</sup> Kundu, D.; Debnath, R. K.; Majee, A.; Hajra, A. *Tetrahedron Lett.* **2009**, *50*, 6998.

<sup>74</sup> Anderson, J. C.; Stepney, G. J.; Mills, M. R.; Horsfall, L. R.; Blake, A. J.; Lewis, W. J. *Org. Chem.* **2011**, *76*, 1961.

<sup>75</sup> Wang, X.; Chen, Y.-F.; Niu, L.-F.; Xu, P.-F. *Org. Lett.* **2009**, *11*, 3310.

<sup>76</sup> Pan, Y.; Zhao, Y.; Ma, T.; Yang, Y.; Liu, H.; Jiang, Z.; Tan, C.-H. *Chem. Eur. J.* **2010**, *16*, 779.

<sup>77</sup> Enantioselective  $\alpha$ -fluoro- $\alpha$ -sulfonyl nitroalkanes additions to isatin-derived ketimines catalyzed by cinchonine are also known: Urban, M.; Franc, M.; Hofmanová, M.; Čísařová, I.; Veselý, J. *Org. Biomol. Chem.* **2017**, *15*, 9071.

<sup>78</sup> For enantioselective Michael additions of  $\alpha$ -fluoro nitroester to enones, see: Cui, H.-F.; Li, P.; Wang, X.-W.; Chai, Z.; Yang, Y.-Q.; Cai, Y.-P.; Zhu, S.-Z.; Zhao, G. *Tetrahedron* **2011**, *67*, 312.

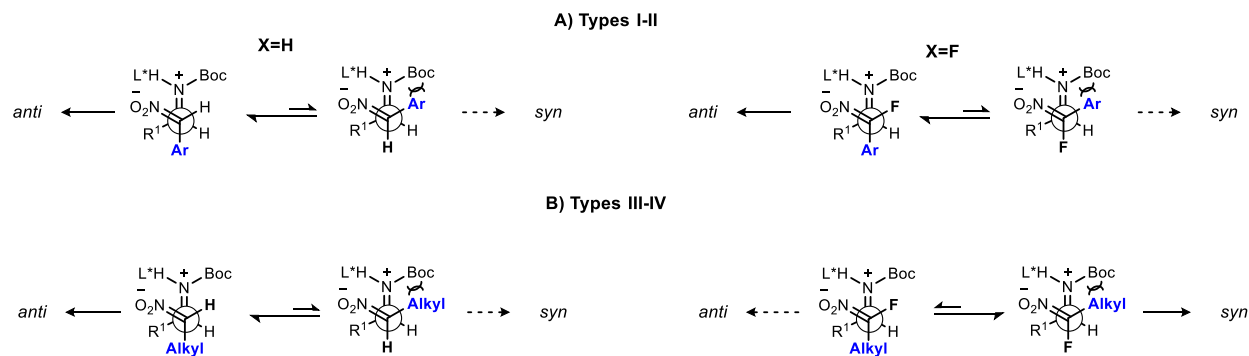
<sup>79</sup> Blaszczyk, R.; Gajda, A.; Zawadzki, S.; Czubačka, E.; Gajda, T. *Tetrahedron* **2010**, *66*, 9840.



Two basic stereochemistry-determining arrangements of azomethine and nitronate are summarized in **Figure 11**: pre-*anti* and pre-*syn*. Regardless of catalyst deployed in experiments here, the azomethine *Si* face is favored. A notable feature of aza-Henry reactions using BAM or PTC catalysis is that the major and minor diastereomer are homochiral at the amine carbon, indicating that the azomethine-catalyst binding is relatively conserved (this was further confirmed in this work by X-ray analysis, see SI for details). Therefore, each Newman projection in **Figure 11** illustrates nitronate approach to the azomethine *Si* face. A second guiding principle is the bifunctional activation of azomethine and nitronate which favors a synclinal arrangement of azomethine nitrogen and nitronate-NO<sub>2</sub> units. This feature has been supported by Dudding's analysis,<sup>51,52</sup> it is consistent with the bifunctional character of BAM catalysis, and it is also invoked elsewhere.<sup>50,66b</sup> Type I-II aza-Henry reactions are *anti*-selective and insensitive to the presence of fluorine (H vs. F). The arrangement in **Figure 11A** provides for the first two factors, and placement of the aromatic ring of the nitronate between the smaller aldimine-hydrogen and Ar/Alkyl substituents of the azomethine predicts *anti*-selectivity on purely steric grounds. The case of alkyl-substituted nitronates are more nuanced (**Figure 11B**), with the non-fluorinated nitronate favoring *anti*-selectivity for the same reasons as listed above.

Fluorine-substituted nitronates favor *syn*-selectivity (**Figure 11B**) when geminally-substituted with an alkyl substituent, but not aryl. Contemporary models advancing the gauche effect for

**Figure 11.** Working models to identify dominant effects present during C-C bond formation as a function of nitronate substituent combination (aryl/alkyl, H/F).



fluorine<sup>80</sup> align with *anti*-selectivity, wherein iminium and fluorine are gauche (**Figure 11**) to allow  $\sigma_{CC} \rightarrow \sigma^*_{CF}$  overlap involving the aldimine R<sub>2</sub>-carbon bond. While this reasoning is consistent with Type I-II (R<sub>1</sub>=F) additions, it should also apply to Type III-IV additions (R<sub>1</sub>=F), but these lead to *syn*-selectivity instead.

The origin of diastereodivergence may emanate from a secondary interaction between the iminium and the nitronate substituent in an *anti*-relationship in the transition state, favoring Ar>F>alkyl. We speculated that the extensive literature describing the Diels-Alder reaction might harbor fluorine-based diastereodivergence, particularly in cases where directing groups compete in a thermal reaction. Indeed, the competition between phenyl and fluorine for *endo*-positioning in Diels-Alder reactions favors slightly (2-3:1) *endo*-fluorine with an electron-rich benzoisofuran and  $\alpha$ -fluoro styrene.<sup>81</sup> Moreover, (*E*)- $\beta$ -fluoro styrene is also slightly *endo*-fluorine selective, while (*Z*)- $\beta$ -fluoro styrene produces only *endo*-product (both Ph and F are positioned *endo*).<sup>82</sup> The substituent effect of fluorine (vs. hydrogen) is perhaps most pronounced in enantioselective catalysis with  $\alpha$ -fluoro enones and esters. In these cases, fluorine overrides ketone and ester carbonyl for *endo*-positioning by 3:1.<sup>83</sup> Computational methods have been applied to thermal and Lewis acid-promoted Diels-Alder cycloadditions of cyclopentadiene with enones, leading to the conclusion that destabilization of the *endo*-pathway for 3-fluorobutenone is primarily responsible for its *endo*-fluorine (*exo*-C=O) selectivity.<sup>84</sup> Overall, these substituent effects follow a hierarchy F>Ph/carbonyl>H consistent across cyclopentadiene and diphenyl isobenzofuran.

Unlike the thermal Diels-Alder reactions where fluorine effected diastereodivergence when competitive with both phenyl (aryl) and carbonyl geminal substituents, the hierarchy here is Ar>F>alkyl. Of course, the transition states for nitronate additions to imines with catalysis are quite different, and the role of fluorine in the transition state would be expected to be more pronounced than an alkyl group. The unusual behavior lies in the contrasting effects when phenyl

---

<sup>80</sup> Briggs, C. R. S.; Allen, M. J.; O'Hagan, D.; Tozer, D. J.; Slawin, A. M. Z.; Goeta, A. E.; Howard, J. A. K. *Org. Biomol. Chem.* **2004**, *2*, 732. Tanzer, E.-M.; Zimmer, L. E.; Schweizer, W. B.; Gilmour, R. *Chem. Eur. J.* **2012**, *18*, 11334. For reviews see: O'Hagan, D. *Chem. Soc. Rev.* **2008**, *37*, 308.; Hunter, L. *Beilstein J. Org. Chem.* **2010**, *6*, 38.

<sup>81</sup> Ernet, T.; Haufe, G. *Tetrahedron Lett.* **1996**, *37*, 7251.

<sup>82</sup> Landelle, G.; Turcotte-Savard, M.-O.; Angers, L.; Paquin, J.-F. *Org. Lett.* **2011**, *13*, 1568.

<sup>83</sup> Shibatomi, K.; Futatsugi, K.; Kobayashi, F.; Iwasa, S.; Yamamoto, H. *J. Am. Chem. Soc.* **2010**, *132*, 5625.

<sup>84</sup> Merzoud, L.; Saal, A.; Moussaoui, R.; Ouamerali, O.; Morell, C.; Chermette, H. *Phys. Chem. Chem. Phys.* **2018**, *20*, 16102.

nitromethane derivatives are involved. We speculate that in these cases the electronic nature of an aryl ring prevails, perhaps through a secondary interaction between *anti*-aryl or *anti*-F and imine  $\pi^*$  orbitals:  $\pi_{\text{Ar}} \rightarrow \pi^* \text{-imine} > n_{\text{F}} \rightarrow \pi^* \text{-imine} > \sigma_{\text{C-alkyl}} \rightarrow \pi^* \text{-imine}$ .

### 1.2.9 Conclusion

Despite extensive investigation of the aza-Henry reaction using a broad range of chiral catalysts, highly enantio- and *syn*-selective variations are rare.<sup>37</sup> Moreover, with one exception, the only known examples require an  $\alpha$ -nitro ester [Shibasaki, Johnston] or  $\alpha$ -nitro phosphonate.<sup>79</sup> Only one *syn*-selective aza-Henry of a nitroalkane without an additional activating group has been reported, with enantioselection as high as 98%.<sup>50</sup> Based on a thorough study of catalyzed nitronate additions to *N*-Boc imines derived from aliphatic and aromatic aldehydes, exceptions have been uncovered to the otherwise common finding of *anti*-selectivity that is broadly observed in enantioselective, catalyzed aza-Henry reactions. This selectivity is particularly characteristic of terminal nitroalkanes lacking activating groups, and we replicated and extended this trend, using X-ray diffraction to rigorously assign product stereochemistry when needed. The exceptions were found among fluorine-substituted nitronates, but only those with an aliphatic substituent. In cases where an aromatic ring substituent was geminal to the C-F bond, *anti*-selectivity prevailed. The fluorine effect, and its compartmentalization into a subset of nitronates is unprecedented. We speculate that a hierarchy of directing effects is responsible for the selectivity, with the nitro group's position conserved among Type I-IV, but a phenyl ring overriding the fluorine's additional effect in Type I-II additions. Remarkable aspects of this discovery include the turnover in diastereoselection to *syn*-selectivity simultaneous with high enantioselection, in some cases setting it apart from prior highs established by others.<sup>50</sup> That these trends are relatively independent of catalysis method (hetero- vs. homogeneous) when using  $\alpha$ -fluoronitroalkane pronucleophiles suggests that the behavior may be more generally observed. Examples of diastereodivergence associated with substrate control, using a single catalyst, are increasing.<sup>85,86</sup> As solutions the stereocontrolled aza-

---

<sup>85</sup> Hernández-Toribio, J.; Gómez Arrayás, R.; Carretero, J. C. *Chem. Eur. J.* **2010**, *16*, 1153.

<sup>86</sup> Ding, R.; De los Santos, Z. A.; Wolf, C. *ACS Catal.* **2019**, *9*, 2169.

Henry reaction increase, so will their impact on concise preparations of small molecules in drug development, and innovative entry to peptides based solely on catalytic, enantioselective methods.

### **1.3 Phase transfer catalyzed aza-Henry reactions for alkyl $\beta$ -fluoroamines**

#### ***1.3.1 Introduction & objectives***

Generally, two distinct approaches to mono-fluorinated compounds are utilized; late stage fluorination and early-stage fluorination (building block approach). Late stage fluorination involves construction of the majority of compound's scaffold followed by electro- or nucleophilic fluorination. This approach is beneficial for applications such as PET imaging, which utilizes  $^{18}\text{F}$  radioisotope tracers for imaging. Given the short half-life of  $^{18}\text{F}$ , it must be installed as close to administration of the compound as possible. However, the late-stage approach does, in general, possess liability in terms of selectivity issues and functional group tolerance which pose a special risk when working with precious frontline material. Conversely, a more convergent approach incorporates the fluorinated fragment of the target compound as a building block. A greater number of structural modifications can be made without impacting other portions of the compound. Similarly, changes in distant parts of the molecule can be made without the danger of affecting the carefully constructed fluorine-containing motif.

We devised a strategy for the catalytic, enantioselective synthesis of cyclic building blocks bearing  $\beta$ -fluoroamines. This strategy allows for variety in ring size and functional groups present in the backbone. Many of the approaches toward stereodefined cyclic  $\beta$ -fluoroamines depend on the use of a chiral auxiliary, pre-installed stereocenters, substrate control/directing groups or only provide either the *cis* or the *trans* isomers (see Section 1.1.4, page 23). What is lacking is an approach to all stereoisomers in pure form from a common starting material, which can be manipulated as desired for backbone modifications. Enantioselective methods exist for  $\beta$ -fluorination of an amine,  $\beta$ -amination of a fluoromethine, and aminofluorination of an olefin. Notwithstanding, construction of the carbon-carbon bond joining the aminomethyl and fluoromethyl motifs in a stereoselective manner is underdeveloped.

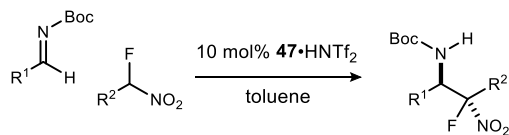
In 2016 our group addressed this gap via the aza-Henry reaction.<sup>47</sup> This involves the addition of a nitroalkane into an imine, providing an efficient means of constructing carbon-carbon bonds in an

enantioselective fashion. It was shown that chiral proton catalysis<sup>39,41,51,52</sup> promotes the enantioselective aza-Henry reaction between aryl  $\alpha$ -fluoro nitroalkanes and *N*-Boc aldimines. As such, the aforementioned C-C bond is formed, and the nitro group serves as a functional handle for derivatization.

It was found that while aryl  $\alpha$ -fluoro nitroalkanes and aryl *N*-Boc imines react to provide the products in good yields, diastereo- and enantioselection, their aliphatic counterparts are not as well behaved. For example, the aryl aldimine reacted with the  $\alpha$ -aryl- $\alpha$ -fluoronitroalkane in a promising fashion (**Table 3**, entry 1). However, its reaction with an alkyl fluoronitroalkane had to be run at room temperature due the decreased reactivity of the alkyl pronucleophile (**Table 3**, entry 2). On the other hand, while phenyl fluoronitromethane is known to be a viable and reactive nucleophile, the alkyl imine is not long-lived due to competitive tautomerization to the enamine. This resulted in a lower yield, although d.r. and ee were maintained (**Table 3**, entries 3-4). Finally, reaction of an alkyl imine with an alkyl fluoronitroalkane could be achieved with high d.r. and good enantioselection, but only in 21% yield (**Table 3**, entry 5). With the alkyl imines, a two-step, one-pot procedure was used to avoid its isolation and depress tautomerization to the enamine.

**Table 3.** Previous studies in the Johnston laboratory on the BAM-catalyzed aza-Henry with  $\alpha$ -fluoronitroalkanes.<sup>a,b</sup>

(as reported in reference 47)



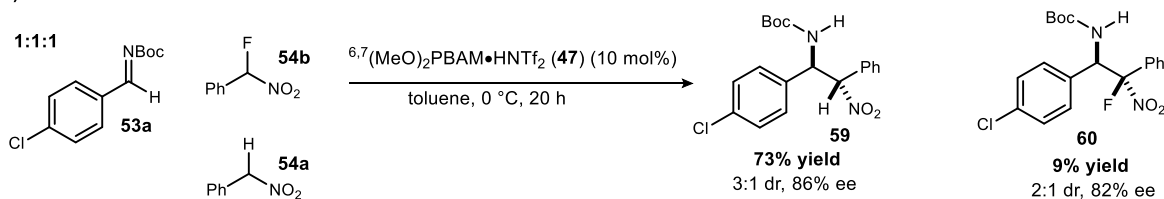
entry	product	product	temp	yield <sup>c</sup>	dr <sup>d</sup>	ee(%) <sup>d</sup>
1		<b>57</b>	0 °C	97	4.8:1	91
2		<b>56f</b>	24 °C	85	5.0:1	93
3		<b>58</b>	0 °C	21 <sup>e</sup>	6.1:1	84
4		<b>58</b>	-20 °C	70 <sup>e,f</sup>	9.0:1	93
5		<b>56h</b>	24 °C	21 <sup>f</sup>	>10:1	84

<sup>a</sup> This table is reproduced using the data reported in reference 47. Later studies (reported here) have revised the assignment of the relative stereochemistry, and thus the associated yield, dr and ee for entries 2 and 5. (see **Table 4**) <sup>b</sup> Catalyst prepared as the 1:1 acid salt. Reactions were 0.1 M in dry toluene for 18 h, unless otherwise noted. Relative and absolute configuration assigned by analogy to **57** (X-ray). <sup>c</sup> Isolated yield. <sup>d</sup> Diastereomeric ratios determined by <sup>1</sup>H NMR, and enantiomeric excess (ee, major enantiomer shown) determined by HPLC using a chiral stationary phase. <sup>e</sup> 48 h Reaction time. <sup>f</sup> Yield over 2-steps from  $\alpha$ -amido sulfone.

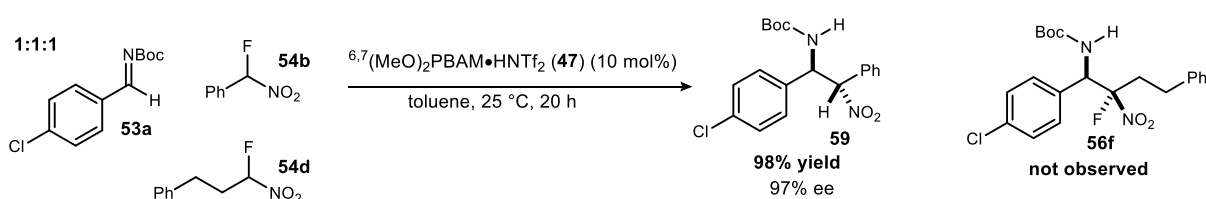
These observations were consistent with competition experiments that were conducted with the objective of determining the relative reactivity of  $\alpha$ -fluoronitroalkanes in the aza-Henry reaction (**Scheme 16**). When phenylnitromethane (**54a**) and  $\alpha$ -fluoro phenylnitromethane (**54b**) were used in a 1:1:1 ratio with *para*-chloro imine **53a**, it was clear that the nonfluorinated nitroalkane was significantly more reactive. The adduct **59** resulting from the addition of phenylnitromethane (**54a**) was formed in 73% yield, while the adduct **60** resulting from  $\alpha$ -fluoro phenylnitromethane (**54b**) was only formed in 9% yield (**Scheme 16**). A similar reaction was conducted to observe the relative reactivity of alkyl fluoronitroalkanes and aryl fluoronitroalkanes. It was found that the only product observed in the competition experiment was the aryl fluoronitroalkane adduct **59**

**Scheme 16.** Relative reactivity of  $\alpha$ -fluoronitroalkanes in aza-Henry reactions.

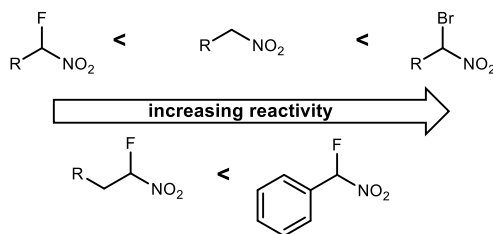
**A) nitroalkane vs. fluoronitroalkane**



**B) aryl vs. alkyl fluoronitroalkane**



**C) relative reactivity of fluoronitroalkanes**



(Scheme 16). The relative reactivity is depicted in **Scheme 16**: the fluoronitroalkanes are less reactive than nitroalkanes, and  $\alpha$ -bromonitroalkanes. Additionally, aryl  $\alpha$ -fluoronitroalkane pronucleophiles are much more reactive than alkyl  $\alpha$ -fluoronitroalkanes.

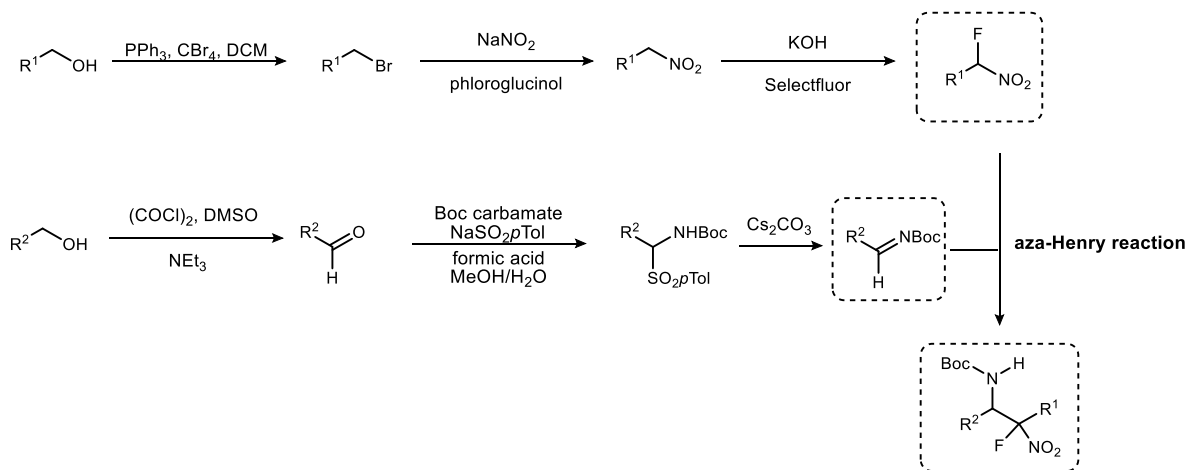
Thus, this work addressed the challenges associated with the aza-Henry reaction of alkyl  $\alpha$ -fluoro nitroalkanes and alkyl *N*-Boc aldimines, such as (a) the lower reactivity of alkyl fluoronitroalkanes as compared to their aryl counterparts and corresponding nitroalkanes, and (b) the propensity of the alkyl aldimine to tautomerize to the unreactive enamide. To this end, a general catalytic and stereoselective route to access alkyl  $\beta$ -fluoro- $\beta$ -nitro amines using chiral phase-transfer catalysis was developed. Of particular interest were the analogs containing two terminal dienes, which might be used as precursors for ring closing metathesis in a strategy to prepare cyclic  $\beta$ -fluoro- $\beta$ -nitro amines. The nitro group can serve as a functional handle for further manipulation, and the alkene can either be functionalized, reduced, or left unchanged. These methods provide a

convergent pathway to collections of stereoisomerically-pure carbocyclic  $\beta$ -fluoroamines for use as scaffolds in drug development and material science.

### 1.3.2 Enantioselective synthesis of aliphatic $\beta$ -fluoro- $\beta$ -nitro amines.

We proposed a route toward stereodefined  $\beta$ -fluoro- $\beta$ -nitro amines from readily available starting materials via the catalytic, enantioselective aza-Henry reaction. The fluoronitroalkane pronucleophiles were synthesized in high yield and in multigram quantities by electrophilic fluorination of their nitroalkane precursors, which were acquired by nitrite substitution of readily available bromides (**Scheme 17**).<sup>87</sup> The  $\alpha$ -amido sulfones were synthesized in one step from commercially available aldehydes and served as bench-stable precursors to the *N*-Boc aldimines (**Scheme 17**).

**Scheme 17.** General synthetic scheme for the synthesis of  $\alpha$ -fluoronitroalkane and  $\alpha$ -amido sulfone aza-Henry partners.

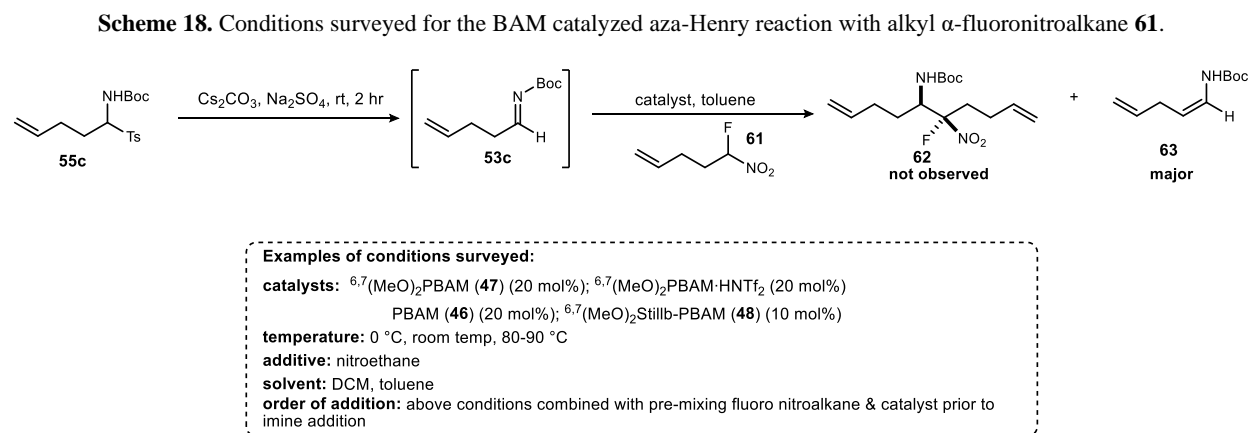


In the case of aryl pro-electrophiles, discrete formation and isolation of the aryl imines generally proceeds uneventfully, allowing the imine to be stored for future use or carried forward into the aza-Henry reaction. **However, with alkyl imines possessing an enolizable carbon, we observed tautomerization to the more stable enamide during isolation attempts.** It was expected that tautomerization could be limited using a two-step one-pot approach that proved successful for the

<sup>87</sup> Kornblum, N.; Larson, H. O.; Blackwood, R. K.; Mooberry, D. D.; Oliveto, E. P.; Graham, G. E. *J. Am. Chem. Soc.* **1956**, *78*, 1497.



addition of bromonitromethane into aliphatic imines (**Scheme 18**).<sup>44</sup> This circumvents imine isolation by passing the elimination reaction mixture through Celite to remove the inorganic base, and into a reaction flask containing catalyst and pronucleophile. In this work, as expected, treatment of the  $\alpha$ -amido sulfone **55c** with base provides the *N*-Boc aldimine **53c** as determined by <sup>1</sup>H-NMR (**Scheme 18**).



However, the aliphatic imine was short-lived. This approach as well as other variants of the two-step procedure proved ineffective, providing in all cases the enamide **63** as the major product with little to no aza-Henry adduct (**Scheme 18**). Many conditions were screened, including the catalyst, the temperature, the use of additives (e.g. nitroethane), and the solvent, however none proved fruitful. Efforts to achieve reactivity through the enamide were also unsuccessful. It became evident that while the aldimine can be pre-formed, the rate of tautomerization is faster than the rate of addition of the alkyl  $\alpha$ -fluoronitroalkane.

Consequently, routes were pursued with the intention of mitigating the observed disparity in rates between addition of the fluoronitroalkane and tautomerization to the enamide. Phase-transfer catalysis is an attractive alternative to the two-step approach and has been shown to facilitate aza-Henry reactions between aliphatic aldimines and nitroalkanes as well as bromonitromethane.<sup>88, 89</sup> This variant utilizes an insoluble inorganic base with a cinchona alkaloid-derived catalyst and

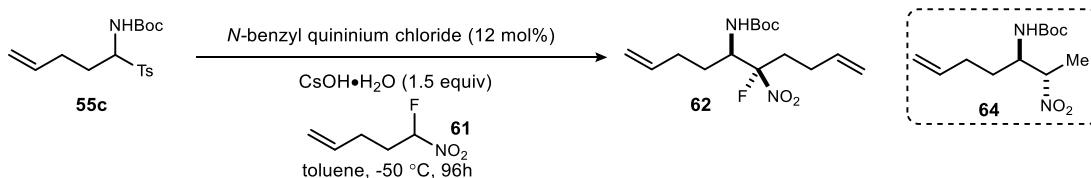
<sup>88</sup> Gomez-Bengoa, E.; Linden, A.; López, R.; Múgica-Mendiola, I.; Oiarbide, M.; Palomo, C. *J. Am. Chem. Soc.* **2008**, *130*, 7955.; Palomo, C.; Oiarbide, M.; Laso, A.; López, R. *J. Am. Chem. Soc.* **2005**, *127*, 17622.

<sup>89</sup> Schwieter, K. E.; Johnston, J. N. *Chem Sci* **2015**, *6*, 2590.

limits the amount of imine present at any one time via slow *in situ* sulfonate elimination. The (bromo)nitroalkane quickly traps the resultant imine to form the aza-Henry adduct. The chiral ion pair between the nitronate and the catalyst controls stereoselectivity. This had never been extended to the less reactive fluoronitroalkanes, and it remained to be seen if nitronate formation and subsequent imine sequestration would occur at a rate that exceeds tautomerization.

Initial attempts modeled conditions previously used in the Johnston laboratory for the phase-transfer catalyzed addition of bromonitromethane into aliphatic aldimines.<sup>89</sup> To this end, the aza-Henry reaction was carried out using 1.5 equivalents of  $\alpha$ -fluoronitroalkane in toluene (0.3 M) (Table 4, entry 1), but no conversion of the starting  $\alpha$ -amido sulfone was observed. It was hypothesized that the addition of an exogenous nitroalkane may serve to increase the rate of elimination to the imine and also help with solubility. Upon addition of nitroethane, conversion was observed, but only to the nitroethane adduct **64** (Table 4, entry 2). Studies by the Palomo group on the phase transfer catalyzed aza-Henry reaction with nitroethane or nitromethane typically used a larger excess of the nitroalkane (at least 5.0 equiv) in the reactions.<sup>88</sup> Gratifyingly, application of the molar ratio used by the Palomo group resulted in full conversion of the  $\alpha$ -amido sulfone. The desired aza-Henry adduct **62** was obtained with good yield (87%), good dr (6.8:1), and high ee (>99/>99%) (Table 4, entry 3). For gram-scale reactions it was found that 4.0

**Table 4.** Optimization of phase-transfer catalyzed aza-Henry reaction with alkyl  $\alpha$ -fluoronitroalkane (**61**)<sup>a</sup>



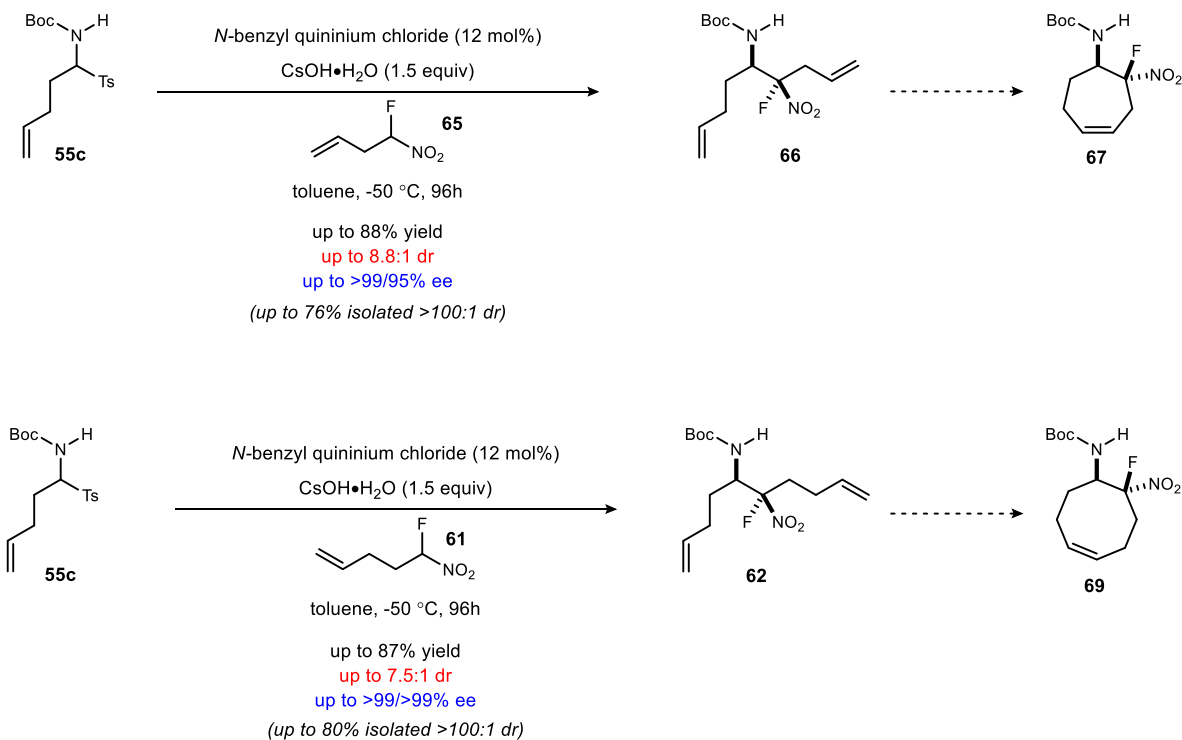
entry	<b>61</b> (equiv)	toluene [M]	dr <sup>b</sup>	ee <sup>c</sup>	yield <sup>d</sup>
1	1.5	0.3	--	--	no conversion
2	1.5 + nitroethane (10 equiv)	0.3	--	--	<b>55c</b> , <b>61</b> and <b>64</b> observed <sup>e</sup>
3	5.0	0.3	6.8:1	99/99	87% (70% <i>syn</i> , 17% <i>anti</i> )
4	5.0	0.15	4.7:1	99/99	96% (81% <i>syn</i> , 15% <i>anti</i> )

<sup>a</sup>Reactions were in dry toluene under argon for 96 h, unless otherwise noted. Relative and absolute configuration assigned by analogy to **66** (X-ray). <sup>b</sup>Diastereomeric ratios determined by <sup>19</sup>F NMR. <sup>c</sup>Enantiomeric excess (ee) determined by HPLC using a chiral stationary phase. <sup>d</sup>Isolated yield. Diastereomers separated by flash column chromatography (SiO<sub>2</sub>) <sup>e</sup>**64** is observed by <sup>1</sup>H NMR

equivalents of the fluoronitroalkane was sufficient to achieve similar yields. Decreasing the concentration improved solubility and resulted in higher yield of the aza-Henry adduct (96%, **Table 4**, entry 3). Throughout the optimization studies (including experiments not shown in **Table 4**) it was evident that this heterogeneous reaction was very sensitive to physical conditions such as stirring and heat transfer. For example, on a small-scale reaction that was conducted in a vial, the conversion and stereoselection was higher for reactions run in the reaction freezer as compared to those run in the Cryocool. In the reaction freezer, the vial is in direct contact with the stir-plate (efficient stirring), whereas in the Cryocool the vial is suspended about an inch above the stir-plate (poor stirring). On the other hand, when conducting large-scale reactions in a round-bottom flask, selectivity and yield were consistently higher for reactions run in the Cryocool. With the larger flask, stirring is not an issue in the Cryocool, and more efficient heat transfer is achieved because the flask is submerged in a cold bath, instead of cold air as it would be in the reaction freezer.

In this work, we aimed to specifically utilize this reaction to conjoin an imine and fluoronitroalkane that both possess a terminal diene. This was done for the purpose of employing the resultant unsaturated  $\beta$ -fluoro- $\beta$ -nitro amines in ring closing metathesis for the synthesis of 6, 7, and 8-membered carbocyclic  $\beta$ -fluoroamines. To this end, the syntheses of some of the RCM precursors are described in **Scheme 19**. The addition of 4-fluoro-4-nitrobut-1-ene (**65**) and 5-fluoro-5-nitropent-1-ene (**61**) into the pentenyl imine (**53c**, generated *in situ* from **55c**) was performed on multigram scale to access to their respective aza-Henry adducts with good d.r., high yield, and excellent enantioselection. These adducts serve as precursors of the 7- and 8-membered ring systems.

**Scheme 19.** Phase-transfer catalyzed aza-Henry reaction of alkyl  $\alpha$ -fluoronitroalkanes and alkyl *N*-Boc  $\alpha$ -amido sulfones.

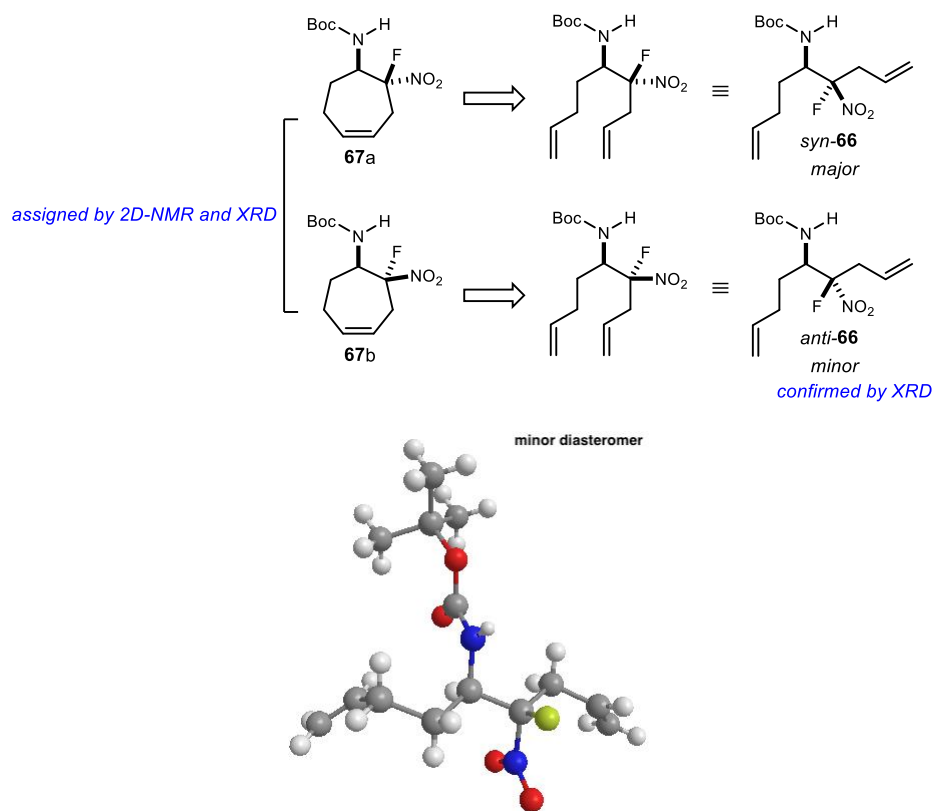


Importantly, the diastereomers formed in this reaction were separable by flash column chromatography. Theoretically, both diastereomers could be carried through the proposed sequence together as they would converge at the denitration step, where radical reductive denitration would not retain stereointegrity at the  $\beta$ -fluoro- $\beta$ -nitro carbon. However, I wanted to first carry each diastereomer through the sequence separately to ensure proper stereochemical assignments and to observe whether the diastereomers behaved different in the RCM or denitration reactions. What began as a small nuanced curiosity would ultimately open the door to the significant discovery that the major diastereomer formed in this reaction has *syn* relative stereochemistry between the amine and nitro functional groups. This would become one of three known *syn* selective aza-Henry reactions that also provides the adducts with high enantioselectivity (see section 1.2, page 29).

As will be described below, each diastereomer was carried through the RCM and the relative stereochemistry of the carbocyclic products was assigned by 1D and 2D NMR studies. It was observed that the carbocycle resulting from the major diastereomer has the amine and nitro groups

*anti* to one-another while the carbocycle resulting from the minor diastereomer was *syn*. This would imply that the major diastereomer from the aza-Henry reaction was *syn* as illustrated in **Figure 12**. An in-depth analysis of the relative stereochemistry for the aza-Henry reaction with  $\alpha$ -fluoronitroalkanes and the factors by which it is influenced was conducted and required more evidence via X-ray analysis (see section 1.2, page 29).<sup>90</sup> As such, we were able to confirm the absolute and relative stereochemistry of the minor diastereomer through X-ray analysis, which was indeed found to be *anti*.

**Figure 12.** Stereochemical assignment of major and minor diastereomers of aza-Henry adduct **66**.<sup>a</sup>



<sup>a</sup>X-ray crystallography performed by Dr. Nathan Schley, Vanderbilt University.

<sup>90</sup> XRD performed and analyzed by Dr. Nathan Schley.

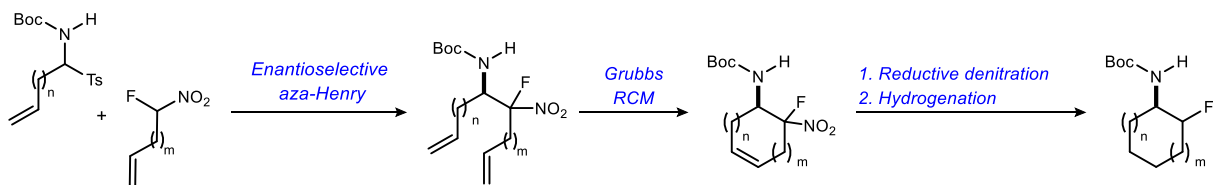
## 1.4 Synthesis of stereodefined carbocyclic $\beta$ -fluoroamines

### 1.4.1 Introduction & objectives

This work pursued the synthesis of carbocyclic  $\beta$ -fluoroamines for their use as building blocks in medicinal chemistry and asymmetric catalysis. Our approach is outlined in **Scheme 20**, and utilized ring-closing metathesis (RCM)<sup>91</sup> of the linear diene precursor produced by an asymmetric aza-Henry reaction, to confine the  $\beta$ -fluoro amine to a carbocyclic backbone. This approach provided access to small- and medium-sized rings, and addresses the reactivity issues shown to plague the synthesis of medium-sized rings from unconstrained linear precursors.

It is well-known that the RCM rates for macrocycles and medium sized rings are slower than for 5 or 6-membered rings.<sup>92</sup> RCM reactions toward medium sized rings are typically conducted

**Scheme 20.** RCM Approach to carbocyclic  $\beta$ -fluoroamines.



under dilute conditions to bias the catalyst toward intra- vs. intermolecular reactions. However, this dilution slows the overall reaction rate and provides additional time for catalyst decomposition. This can lead to lower yields and side reactions. Dimers and oligomers are often observed as byproducts in RCM reactions with medium-sized rings. Their formation however, is not a dead end to the reaction, since the process can be reversible. If the catalyst supports back-binding and survives long enough to reach equilibrium, the oligomers can be recycled and ultimately form the RCM product. However, this requires a catalyst with significant longevity under the reaction conditions, and premature catalyst deactivation often outcompetes oligomer recycling.

<sup>91</sup> For a review see: Vougioukalakis, G. C.; Grubbs, R. H. *Chem. Rev.* **2010**, *110*, 1746.

<sup>92</sup> Van Lierop, B. J., Lummiss, Justin A. M., Fogg, Deryn E. In *Olefin Metathesis* 2014, p 85.

Catalyst decomposition can also result in the formation of species capable of catalyzing alkene isomerization. While this phenomenon is not fully understood, a significant amount of work has been put forth to illuminate the structure of these species and the mechanisms associated with their formation,<sup>93,94,95,96</sup> the mechanisms by which they catalyze isomerization,<sup>97,98</sup> and their potential synthetic utility.<sup>99,100</sup>

Fogg divides these isomerizations into three classes:<sup>92</sup>

- (i) **Class A:** RCM is faster than isomerization so the desired ring size is obtained, but isomerization of the double bond results in various alkene regioisomers
- (ii) **Class B:** isomerization is faster than metathesis and RCM of the isomerized internal olefin leads to ring-contracted products
- (iii) **Class C:** isomerization occurs without metathesis, which is typically the result of the catalyst being unable to accommodate the increased steric bulk of the internal (isomerized) olefin.

In these studies toward the synthesis of carbocyclic  $\beta$ -fluoroamines, isomerizations belonging to **Class B** were the primary type observed, and our attempts to both suppress and promote these isomerizations are discussed below.

---

<sup>93</sup> Higman, C. S.; Plais, L.; Fogg, D. E. *ChemCatChem* **2013**, *5*, 3548.

<sup>94</sup> Yue, C. J.; Liu, Y.; He, R. *J. Mol. Catal. A: Chem.* **2006**, *259*, 17.

<sup>95</sup> Trnka, T. M.; Morgan, J. P.; Sanford, M. S.; Wilhelm, T. E.; Scholl, M.; Choi, T.-L.; Ding, S.; Day, M. W.; Grubbs, R. H. *J. Am. Chem. Soc.* **2003**, *125*, 2546.

<sup>96</sup> Hong, S. H.; Day, M. W.; Grubbs, R. H. *J. Am. Chem. Soc.* **2004**, *126*, 7414.

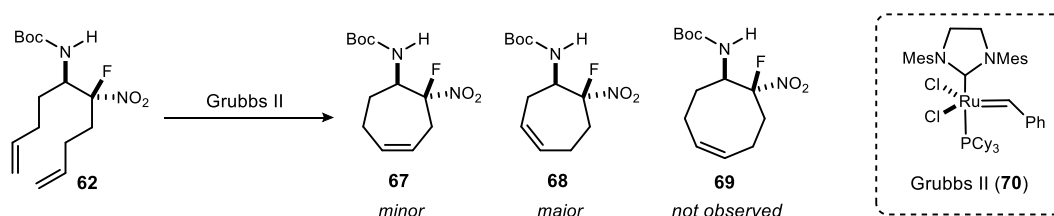
<sup>97</sup> Courchay, F. C.; Sworen, J. C.; Ghiviriga, I.; Abboud, K. A.; Wagener, K. B. *Organometallics* **2006**, *25*, 6074.; Ashworth, I. W.; Hillier, I. H.; Nelson, D. J.; Percy, J. M.; Vincent, M. A. *Eur. J. Org. Chem.* **2012**, *2012*, 5673.; Nelson, D. J.; Percy, J. M. *Dalton Trans.* **2014**, *43*, 4674.

<sup>98</sup> Biswas, S. *Comments Inorg. Chem.* **2015**, *35*, 300.

<sup>99</sup> For reviews see: a) Schmidt, B. *Eur. J. Org. Chem.* **2004**, *2004*, 1865.; b) Donohoe, T. J.; O'Riordan, T. J. C.; Rosa, C. P. *Angew. Chem. Int. Ed.* **2009**, *48*, 1014.

<sup>100</sup> Prunet, J. *Synthesis of heterocycles by metathesis reactions*; Springer Berlin Heidelberg: New York, NY, 2016.;

**Scheme 21.** Observed isomerization prior to ring closing metathesis.



#### 1.4.2 Toward 8-membered carbocyclic $\beta$ -fluoroamines: initial attempts and observations

The medium-sized 8-membered ring was pursued first, which was expected to be a significant challenge based on literature precedence.<sup>101,102</sup> To this end, it was not particularly surprising when the ring closing metathesis reaction using the 10-carbon precursor did not proceed as expected. This reaction did not yield the desired 8-membered ring, but instead isomerization of the terminal alkene prior to RCM occurred to afford a mixture of cycloheptenes **67** and **68** in a 1:2.8 ratio in favor of the homoallylic amine (**Scheme 21**). Using benzene as the solvent instead of DCM, rigorously degassing the solution, and varying the concentration gave slightly cleaner reactions with yields of the cycloheptenes ranging from 5-20%. Despite many optimization attempts, the eight-membered ring was never observed.

In 2000, Bourgeois *et al* also encountered isomerization when attempting to use RCM to access the eight-membered ring in the Taxol BC ring systems (**Table 5**).<sup>103</sup> A notable solvent effect has been observed in cases where RCM was slow and isomerization was observed. The findings of Bourgeois and coworkers paralleled those from early studies by the Fürstner group<sup>104</sup> and showed that isomerization was less aggressive in chlorinated solvents (e.g. dichloroethane (DCE), **Table 5**, entry 3) than in benzene or toluene ((**Table 5**, entries 1-2). Interestingly, they discovered that isomerization was even more likely to occur when a coordinating solvent such as 1,2-dimethoxy ethane (DME) was used (**Table 5**, entry 5) as compared to non-coordinating solvents such as benzene or dichloroethane (**Table 5**, entries 1&3). The authors proposed that the solvent

<sup>101</sup> a) Michalak, K.; Michalak, M.; Wicha, J. *Tetrahedron Lett.* **2005**, *46*, 1149.; b) Michalak, M.; Wicha, J. *Synlett* **2005**, *2005*, 2277.; c) Mizutani, R.; Miki, T.; Nakashima, K.; Sono, M.; Tori, M. *Heterocycles* **2009**, *78*, 2295.

<sup>102</sup> For reviews see: a) Michaut, A.; Rodriguez, J. *Angew. Chem. Int. Ed.* **2006**, *45*, 5740.; b) Tori, M.; Mizutani, R. *Molecules* **2010**, *15*, 4242.

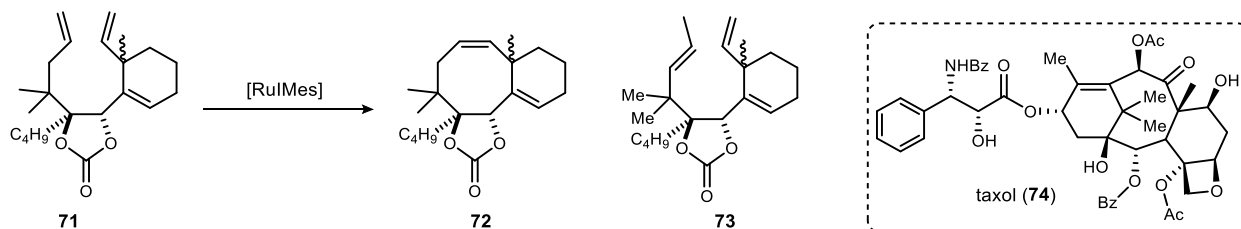
<sup>103</sup> Bourgeois, D.; Pancrazi, A.; Nolan, S. P.; Prunet, J. *J. Organomet. Chem.* **2002**, *643-644*, 247.

<sup>104</sup> Fürstner, A.; Thiel, O. R.; Kindler, N.; Bartkowska, B. *J. Org. Chem.* **2000**, *65*, 7990.



coordinates to the metal center, slowing the coordination of the second double bond, thereby preventing RCM and promoting isomerization. Future studies would suggest that the ethereal solvent increases the rate of decomposition to the Ru-H, which would increase isomerization (*vide infra*).

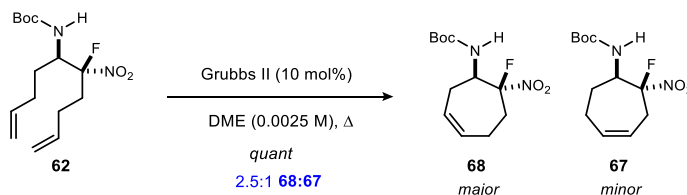
**Table 5.** Bourgeois' product distribution for competing RCM & isomerization reactions in pursuit of Taxol (**74**)



entry	solvent	yield <b>72</b> (%)	yield <b>73</b> (%)
1	Benzene	50-70	30-50
2	toluene	20	80
3	DCE	90	10
4	DCE + POCy <sub>3</sub> (5 or 0.5%)	100	0
5	DME	0	100

In our studies, given that the cycloheptene was the major product, we sought to exploit the observed isomerization and optimize the reaction to provide **68** in synthetically useful quantities. The aforementioned findings using DME translated well to the reaction at hand, and complete conversion of the 10-carbon RCM precursor **62** to a mixture of cycloheptenes was observed with little to no detectable oligomerization (**Scheme 22**). Rigorous degassing was found to be necessary

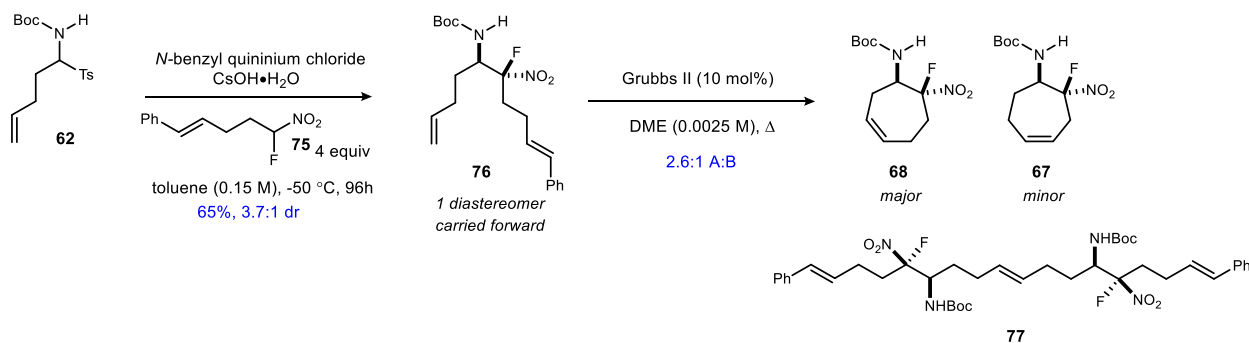
**Scheme 22.** Ethereal solvent promotes isomerization prior to metathesis to afford cycloheptyl  $\beta$ -fluoroamines.



to prevent the formation of oligomers. While the pair of regioisomers was formed in quantitative yield on small scale (25 mg), their separation proved challenging. At best, chromatography could afford a 16:1 mixture of **68**:**67**. On a slightly larger scale (150 mg), the pair was isolated in 75% yield after column chromatography.

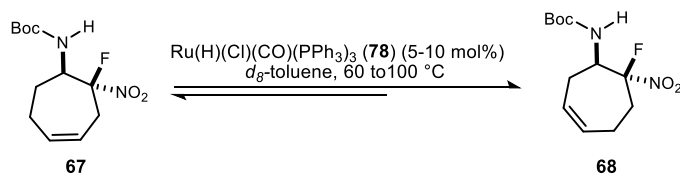
As isomerization to the homoallylic amine proved to be the favored process, we sought to push this isomerization by adding steric bulk to the right-hand portion of the molecule to provide a single regioisomer in RCM. It was hypothesized that the driving force for isomerization was the

**Scheme 23.** Lack of substrate control for isomerization.



formation of a disubstituted alkene, and perhaps it could be attenuated by incorporation of a terminal styrene. The styrene motif, a Type I ligand, would still be reactive in the RCM reaction, but may be more stable towards isomerization. To this end, styrenyl fluoronitroalkane **75** was prepared and used in the phase transfer catalyzed aza-Henry reaction. This provided the RCM precursor **76** in 65% yield and 3.7:1 dr (**Scheme 23**). The major diastereomer was subjected to the RCM reaction, and proved to be a less than stellar substrate. Isomerization was not inhibited. In fact, when compared to the reaction with **61**, an identical ratio of regioisomers was obtained.

**Scheme 24.** Study of isomerization using Ru(H)



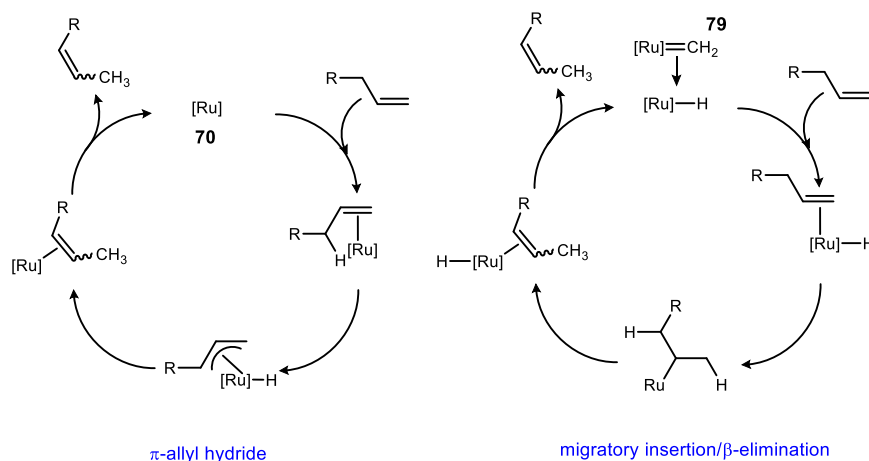
Moreover, the more reactive monosubstituted alkene underwent cross metathesis to form the dimer **77**.

The possibility of converging the isomeric mixture to a single isomer by addition of an exogenous ruthenium hydride was explored. To probe this possibility the minor regioisomer **67** was subjected to isomerization by Ru(H)(Cl)(PPh<sub>3</sub>)<sub>3</sub> (**78**) and monitored by <sup>19</sup>F and <sup>1</sup>H-NMR (**Scheme 24**).<sup>105</sup> After 6.5 hours the isomerization plateaued, despite heating to a higher temperature, adding additional catalyst, or starting with 20 mol% catalyst instead of 5 mol%. Ultimately it was determined that there was a thermodynamic mixture of approximately 1:3 **67:68**.

#### 1.4.3 Toward 7-membered carbocyclic $\beta$ -fluoroamines: preventing isomerization

It was evident that attempting to achieve substrate-controlled optimization was unprofitable for this system. At this point our attention turned towards preventing isomerization instead of promoting it. The two most widely accepted proposals for the mechanism of isomerization are the  $\pi$ -allyl hydride mechanism (**Scheme 25**, left) and the migratory insertion/ $\beta$ -hydride elimination pathway (**Scheme 25**, middle).<sup>98</sup> While both mechanisms proceed through a Ru-H intermediate, the latter mechanism involves a discrete, exogenous Ru-H source.

**Scheme 25.** Proposed mechanisms of alkene isomerization during Ru-catalyzed metathesis.

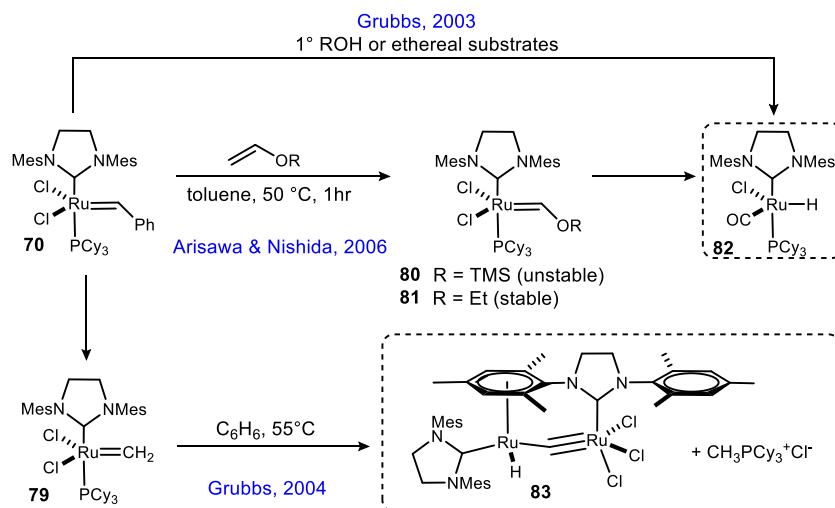


<sup>105</sup> Dieltiens, N.; Stevens, C. V.; Masschelein, K.; Hennebel, G.; Van der Jeught, S. *Tetrahedron*. **2008**, *64*, 4295.; Wakamatsu, H.; Nishida, M.; Adachi, N.; Mori, M. *J. Org. Chem.* **2000**, *65*, 3966.

On a quest to provide the community with a means to prevent unwanted isomerization during olefin metathesis, Grubbs and coworkers found  $\text{Cy}_3\text{PO}$  to be an ineffective additive. They did however, determine that weak acids such as acetic acid as well as quinone compounds were useful additives for isomerization arrest.<sup>106</sup> Ultimately, 1,4-benzoquinones and their more electron deficient variants (e.g. tetrafluoro-1,4-benzoquinone) championed acetic acid as more powerful and encompassing inhibitors of isomerization during ring closing-, self- and cross-metathesis of several susceptible substrates. It is postulated that 1,4-benzoquinones are able to preclude unwanted isomerization by intercepting the suspected culprits, ruthenium hydrides.

Several putative structures of such hydrides have been proposed. Significant evidence has been provided for the formation and activity of species **82** and **83** (Scheme 26).<sup>107</sup> When investigating

**Scheme 26.** Structures of ruthenium hydride formed from the Grubbs II catalyst.



the synthesis of **70**, Grubbs and coworkers identified the hydrido-carbonyl derivative **82** (Scheme 26) from the reaction of methanol with the ruthenium alkylidene complex, and also upon its prolonged exposure to oxygen-containing substrates.<sup>95</sup> Arikawa and Nishida synthesized the same ruthenium hydride **82** for the purpose of catalytic olefin isomerization (Scheme 26).<sup>108</sup> This was

<sup>106</sup> Hong, S. H.; Sanders, D. P.; Lee, C. W.; Grubbs, R. H. *J. Am. Chem. Soc.* **2005**, *127*, 17160.

<sup>107</sup> Higman, C. S.; Plais, L.; Fogg, D. E. *ChemCatChem* **2013**, *5*, 3548.

<sup>108</sup> Arisawa, M.; Terada, Y.; Takahashi, K.; Nakagawa, M.; Nishida, A. *J. Org. Chem.* **2006**, *71*, 4255.

achieved by reacting the Grubbs II catalyst with vinyloxytrimethylsilane to first form intermediate **80**, which collapses to the desired ruthenium hydride. Given the instability of **80**, vinyloxyethane was used to make a more stable version of the intermediate (**81**) for characterization. These observations notwithstanding, under typical metathesis conditions that use aprotic solvents under an inert atmosphere, the species **82** is unlikely to form. Grubbs and coworkers therefore set out to unveil the decomposition product responsible for isomerization during RCM. The dinuclear ruthenium hydride complex **83** (**Scheme 26**) was isolated and characterized as a decomposition product of methyldiene complex **79**.<sup>96</sup> This complex was shown to catalyze isomerization – specifically that of allyl benzene to  $\beta$ -methyl styrene. While these hydride species are a nuisance in RCM reactions where isomerization is undesirable, they can be quite useful in synthesis for performing mild, selective, and catalytic olefin isomerizations that bear no risk of hydrogenation.<sup>109</sup>

When pursuing the synthesis of pentalenene, De Bo and Marko encountered a phenomenon similar to the one at hand, where a 7-membered ring was observed during the RCM targeting an 8-membered ring.<sup>110</sup> They conducted an investigation into the mechanism of the isomerization reaction that utilized some of the aforementioned additives. As shown in **Table 6**, initial attempts to use Grubbs II in benzene resulted in almost equal amounts of the 8- and 7-membered rings. Reducing the catalyst loading slightly increased the yield, but the product distribution was unchanged (**Table 6**, entry 2). Changing to a chlorinated solvent did not significantly improve the product ratio and resulted in a lower yield (**Table 6**, entry 3). Addition of Cy<sub>3</sub>PO also did not change the distribution and lowered the yield (**Table 6**, entry 4). Finally, using 1,4-benzoquinone as an additive drastically improved the product distribution, affording the desired 8-membered ring as the major product (>20:1 **85:86**) in 57% yield (**Table 6**, entry 5).

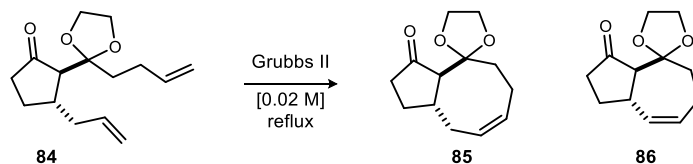
---

<sup>109</sup> Donohoe, T. J.; O'Riordan, T. J. C.; Rosa, C. P. *Angew. Chem. Int. Ed.* **2009**, *48*, 1014.

<sup>110</sup> De Bo, G.; Markó, I. E. *Eur. J. Org. Chem.* **2011**, *2011*, 1859.

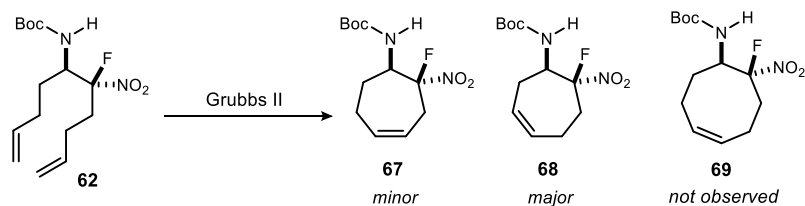
With these studies in mind, we examined the effect of additives on the reaction. Similar to the results seen by the Grubbs group and De Bo, in our hands, Cy<sub>3</sub>PO proved to be ineffective at

**Table 6.** De Bo's product distribution for competing RCM & isomerization reactions in pursuit of pentalenene.



entry	Grubbs II (mol%)	additive	solvent	time (hr)	yield (%)	85:86
1	10 mol%	-	benzene	20	53	1.1:1
2	3 mol%	-	benzene	4	62	1:1
3	3 mol%	-	DCE	24	49	1.4:1
4	3 mol%	Cy <sub>3</sub> PO (5 mol%)	DCE	24	30	1.4:1
5	3 mol%	1,4-benzoquinone (5 mol%)	DCE	24	57	>20:1

inhibiting isomerization. Instead, a mixture of starting material, isomerized cycloheptenes and adducts of poly/oligomerization were observed (**Table 7**, entry 3). However, an important result was observed upon the addition of 1,4-benzoquinone (**Table 7**, entry 4). While the reaction incorporating this additive did not yield any of the desired 8- membered ring, isomerization was greatly inhibited and the majority of starting material remained intact. This was exciting as it provided evidence that the additive suppresses the competing reaction pathways (cross metathesis and isomerization).

**Table 7.** Product distribution during RCM of a 10-carbon precursor.

entry	solvent	relative ratios <sup>a</sup>			yield XX <sup>b</sup>
		<b>62</b>	<b>67</b>	<b>68</b>	
1	DCM	0	1.0	2.8	20%
2	DME	0	1.0	2.5	quant
3 <sup>c</sup>	DCE + Cy <sub>3</sub> PO	1.0	1.0	1.3	<i>nd</i>
4 <sup>d</sup>	DCE + 1,4-benzoquinone	94	1.6	1.0	<i>nd</i>

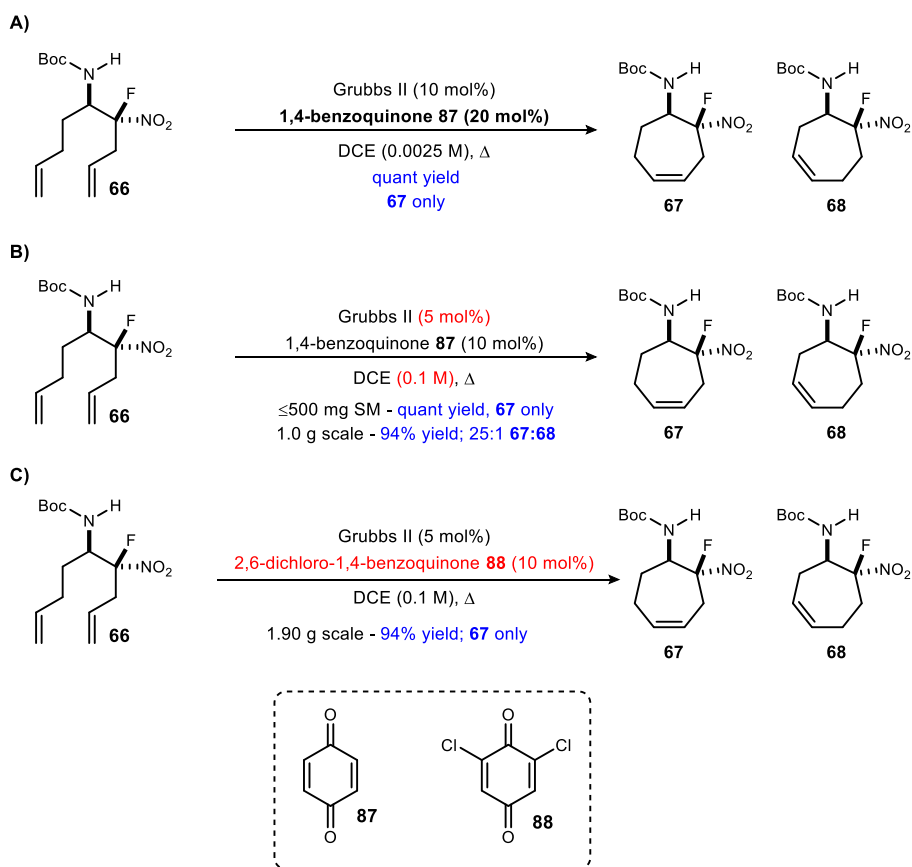
<sup>a</sup> Relative product ratio determined by <sup>19</sup>F-NMR integration. <sup>b</sup> Isolated yields. <sup>c</sup> 10 mol% Cy<sub>3</sub>PO added. <sup>d</sup> 20 mol% 1,4-benzoquinone added.

Our attention was redirected to the cycloheptene **67**, which we now hypothesized could be obtained from RCM of the 9-carbon linear precursor with the use of the benzoquinone additive. Fluoronitrobutene was prepared and employed in the phase transfer catalyzed aza-Henry reaction to afford the desired adduct in good yield, dr and high enantiomeric excess. The addition of 1,4-benzoquinone (**87**) (10 mol%) attenuated isomerization on scales up to 500 mg, resulting in quantitative yield of a single regioisomer (**Scheme 27**). Optimization studies were performed, making the procedure more amenable to larger scale. Increasing the concentration four-fold from 0.025M to 0.1M had no effect on yield or reaction outcome. This was quite gratifying as it is four times more concentrated than the recommended concentration for the formation of 7-membered rings, which is very desirable from both a green-chemistry and bench-chemist's perspectives.<sup>92</sup> Importantly, catalyst loading was decreased from 10 to 5 mol% with no negative impact.<sup>111</sup> Extension of optimized conditions to a 1 gram-scale resulted in 91% yield, but mild alkene

<sup>111</sup> Decreasing the catalyst loading even further, to 2 mol%, provided 94% conversion to a single isomer on a 25 mg scale.

isomerization to the homoallylic amine is observed (Scheme 27, B). This was eluded by adding the more electron rich 2,6-dichloro-1,4-benzoquinone (88), which provided the desired cycloheptene in 94% yield on multigram scale, a vast improvement over current methods (Scheme 27, C). For example, Fustero and coworkers applied RCM towards cycloheptyl  $\gamma,\gamma$ -difluoro  $\beta$ -amino acids.<sup>112</sup> Despite having the *gem*-difluoro motif to leverage a Thorpe-Ingold-like effect, they obtained at best 27% yield of the racemic *cis* or *trans* cycloheptenes using a very high catalyst loading (15 mol%) and dilute conditions.

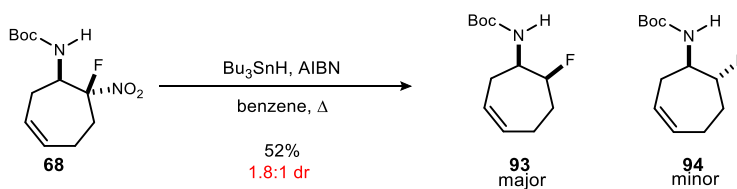
**Scheme 27.** Isomerization prevention during the synthesis of 7-membered carbocyclic  $\beta$ -fluoroamines.



<sup>112</sup> Fustero, S.; Bartolomé, A.; Sanz-Cervera, J. F.; Sánchez-Roselló, M.; Soler, J. G.; Ramírez de Arellano, C.; Fuentes, A. S. *Org. Lett.* **2003**, *5*, 2523.



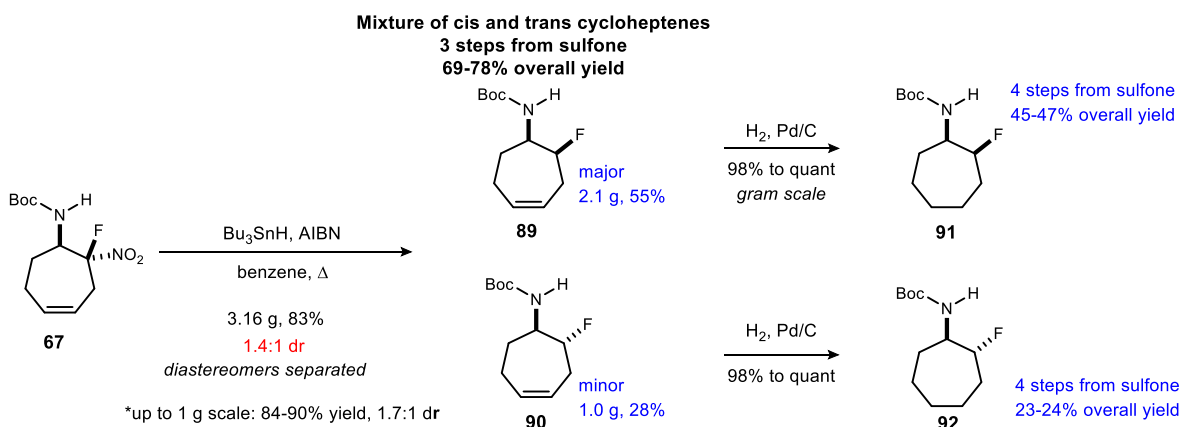
**Scheme 29.** Reductive denitration of cycloheptyl alkene regioisomer **68**.



## Endgame strategy for cycloheptyl $\beta$ -fluoroamines

With the cycloheptene in hand, the nitro group was removed via reductive radical denitration. On scales up to one gram, this reaction provided a 1.7:1 mixture of diastereomers in 84-90% yield

**Scheme 28.** Reductive denitration and hydrogenation to afford *cis*- and *trans* cycloheptyl  $\beta$ -fluoroamines.



(**Scheme 28**). Using  $\text{Bu}_3\text{SnH}$  and AIBN, the reduced substrates **89** and **90** were afforded in 84-90% yield with 1.7:1 dr in favor of the *cis*  $\beta$ -fluoroamine on scales up to one gram.<sup>113</sup> On multigram scale, a 1.4:1 mixture of diastereomers was provided in 83% yield. Reductive denitration of the major alkene isomer from RCM in DME **68** was carried out with similar diastereoselection (1.8:1 dr), in favor of the *cis* diastereomer, but with lower yield (52%, **Scheme 29**).<sup>113</sup>

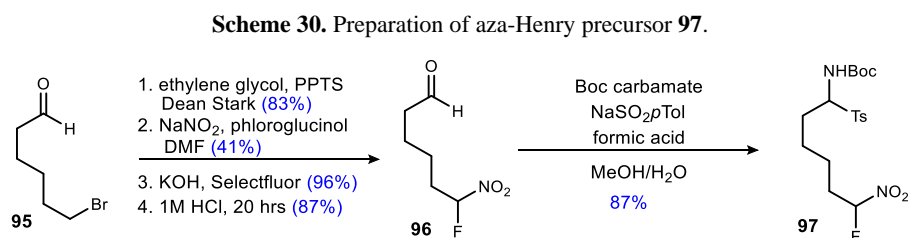
<sup>113</sup> Relative and absolute stereochemistry assigned by 2D NMR and X-ray crystallography. See Supporting Information for details.

The diastereomers were separated for each regioisomer. In the gram-scale synthesis shown in **Scheme 29**, the diastereomers were independently subjected to alkene hydrogenation using Pd/C. Ultimately, the *cis*- and *trans*-cycloheptyl  $\beta$ -fluoramines were obtained in four steps from the  $\alpha$ -amido sulfone in 45-47% and 23-24%, respectively (**Scheme 28**).

#### 1.4.4 Toward 6-membered carbocyclic $\beta$ -fluoroamines

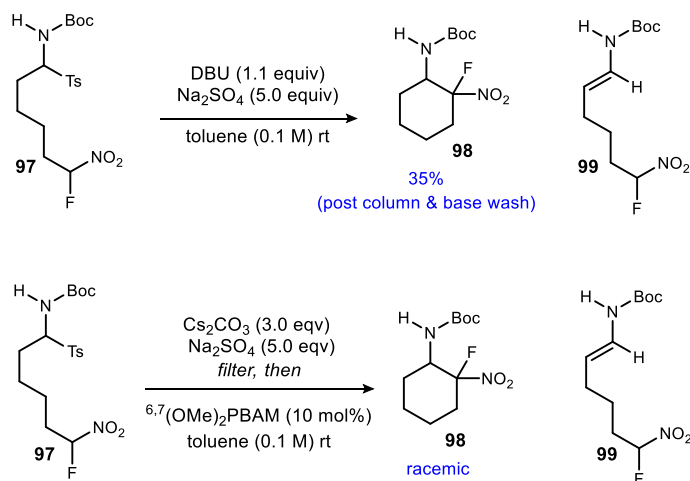
##### Initial attempt: Intramolecular aza-Henry

The first attempts to synthesize  $\beta$ -fluoroamine carbocycles did not feature ring closing metathesis, but instead focused an intramolecular aza-Henry reaction to close the ring. The  $\alpha$ -amido sulfone aza-Henry precursor **97** was prepared in 5 steps from commercially available aldehyde **95** (**Scheme 30**). The aldehyde was protected as the acetal, then nitrite substitution of the bromide provided the nitroalkane. This was subjected to electrophilic fluorination followed by acetal deprotection and sulfone formation (**Scheme 30**). Acetal protection was necessary to avoid decomposition during the fluorination step.



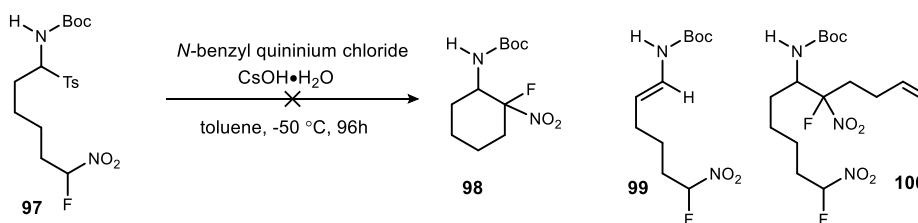
Attempts to employ this substrate in the intramolecular aza-Henry reaction commenced with DBU as the base, which provided a mixture of cyclization product **98** and enamide **99** (**Scheme 31**). The two are very difficult to separate by chromatography due to similar retention factors, but flash column chromatography followed by a base wash worked to remove the enamide. Subjecting the imine to the BAM catalyzed aza-Henry reaction also provided a mixture of **98** and **99**. However, in this case, washing with base could not completely remove the enamide, even after three attempts. Chiral HPLC analysis of the mixture showed that the product was racemic so attention was turned to other methods.

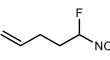
**Scheme 31.** Attempted intramolecular aza-Henry reaction using homogeneous catalysis.



Phase transfer catalysis (PTC) is a particularly attractive way to perform the aza-Henry with alkyl electrophiles as the imine is generated *in situ* from the  $\alpha$ -amido sulfone and then quickly trapped by the nucleophile. In this case, when **62** was subjected to PTC conditions, no enamide was observed. However, no product was observed either. Additives were tried that had been useful in our previous examinations of PTC conditions,<sup>89</sup> however none of these proved beneficial (**Table**

**Table 8.** Phase transfer catalyzed intramolecular aza-Henry reaction.



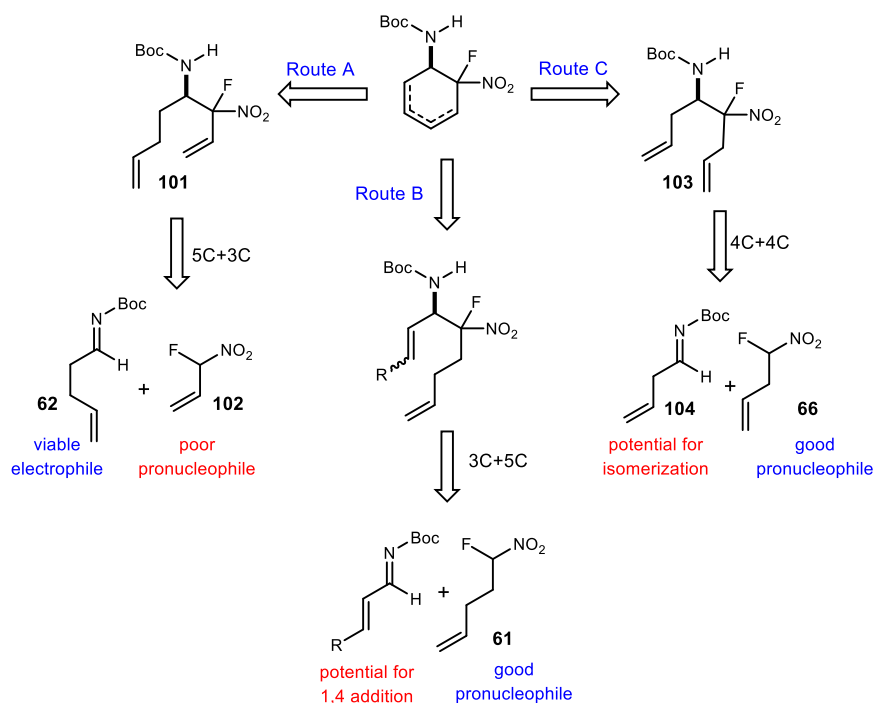
entry	additive	result
1	none	little conversion
2	EtNO <sub>2</sub> (5.0 equiv)	no conversion
3	nitrobenzene (10.0 equiv)	no conversion
4	 (3.0 equiv)	<b>97</b> and <b>100</b> (34%)

**8**, entries 2-3). It was interesting that while the addition of nitroethane nor nitrobenzene helped with conversion, using an exogenous fluoronitroalkane did convert of the sulfone, but resulted only in the intermolecular addition product **100** in 34% yield (**Table 8**, entry 4).

### Revised strategy: ring closing metathesis

We next attempted to apply the ring closing metathesis methodology used to make the seven-membered ring to the six-membered homolog. However, issues in reactivity at the aza-Henry stage were encountered. To access the 8-carbon linear precursor to the cyclohexene, one could envision the aza-Henry reaction between two 4-carbon units (**Scheme 32**, Route C), between a 5-carbon electrophile and 3 carbon nucleophile (**Scheme 32**, Route A), or vice versa (**Scheme 32**, Route B).

**Scheme 32.** Retrosynthetic strategies to form 6-membered  $\beta$ -fluoro- $\beta$ -nitro cyclohexenylamine.



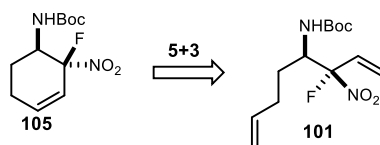
Ultimately it was found that none of these approaches were suitable to make the desired ring.

The attempts to utilize Route A are summarized in **Scheme 33**. While the pentenyl imine **62** was a viable electrophile in other reactions, 1-fluoro-1-nitroprop-3-ene (**102**) proved to be a sluggish pro-nucleophile. Attempts to use the homogenous BAM catalyzed aza-Henry reaction provided

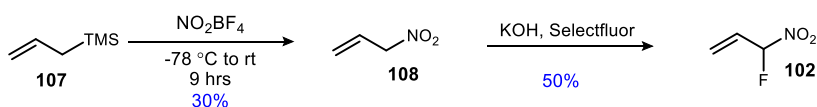
the enamide **63** as the major product, with only trace amounts of the aza-Henry adduct (**Scheme 33, B**). Product was not formed under phase-transfer catalyzed aza-Henry conditions (**Scheme 33, C**). In fact, no conversion was observed. The sulfone remained and the fluoronitroalkene decomposed. The fluoronitroalkene **102** was inherently unstable. It was prone to decomposition and isomerization, and also was difficult to synthesize without isomerization or polymerization. The sulfone **62** works in other reactions, but has little conversion here. This could be due to the low reactivity of the allyl nitronate, which is stabilized by conjugation. The nitronate has been postulated to behave as the base for sulfinate elimination, and thus if it is not reactive, elimination

**Scheme 33.** Attempted '5+3' synthesis of the RCM precursor for the 6-membered ring.

**A) retrosynthesis**



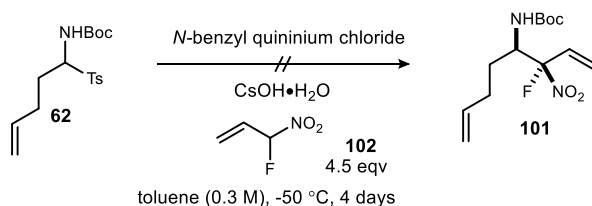
**B) synthesis of  $\alpha$ -fluoronitropropene**



**C) homogeneous aza-Henry attempt**



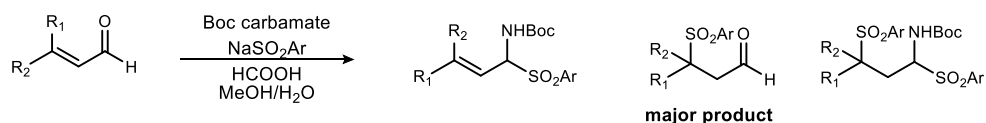
**D) phase-transfer catalyzed aza-Henry attempt**



will not occur, allowing for competing decomposition and side reactions to take place.

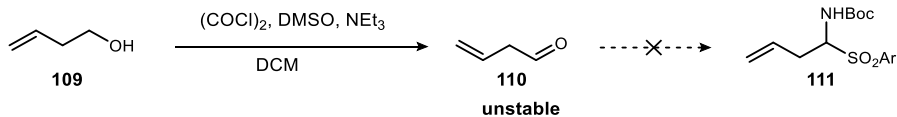
In contrast, in the ‘3+5’ approach, fluoro-nitrobutene is a reactive nucleophile and was shown to behave as a viable reactant in aza-Henry reactions. However, in the ‘Route B’ approach, the electrophilic partner bears the potential for 1,4-addition. It was postulated that the rate of 1,2-addition would be faster than 1,4-addition, but unfortunately, we were unable to get to the point of testing the aza-Henry reaction due to issues with the sulfone formation (**Scheme 34**). Conjugate addition was observed in all attempts to make the sulfone, resulting in a complex mixture of products (**Scheme 34**).

**Scheme 34.** Attempted allylic sulfone formation for ‘3+5’ approach to 6-membered ring precursor.



Lastly, in the case of joining two 4-carbon units, the butenyl imine **104**, bears a strong potential for isomerization of the terminal alkene, and also for tautomerization to the enamide due to the resultant conjugation. Ultimately, as shown in **Scheme 35**, the sulfone was not accessible due to

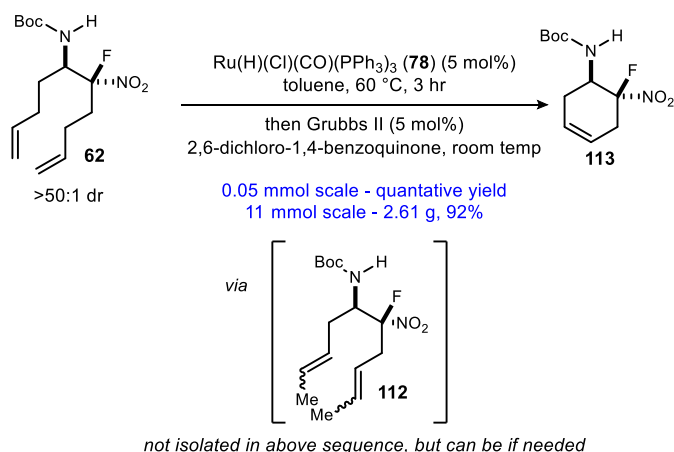
**Scheme 35.** Attempted sulfone formation for ‘4+4’ approach to 6-membered ring precursor.



the quick isomerization and decomposition of the aldehyde **110**.

These results prompted an inquiry into other avenues through which a viable and stable aza-henry adduct for RCM could be accessed. Inspiration was drawn from the isomerization reactions observed en route to the seven-membered ring. To this end, a one-pot tandem isomerization/ring closing metathesis approach to synthesize the 6-membered ring was developed (**Scheme 36**). By addition of an exogenous Ru-H source, both terminal double bonds were isomerized to the adjacent carbons. This provided the in situ formation of a butenyl or allyl group from stable and accessible precursors. Thus, the  $\beta$ -fluoro- $\beta$ -nitro cyclohexenyl amide was synthesized as a single enantiomer with >50:1 dr in quantitative yield on small scale, and 92% yield on multi-gram scale (**Scheme 36**)!

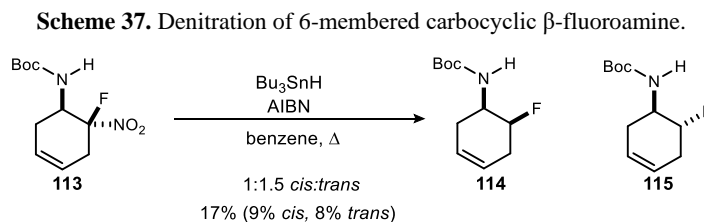
**Scheme 36.** One-pot tandem isomerization/RCM strategy for cyclohexenyl  $\beta$ -fluoro- $\beta$ -nitroamines.



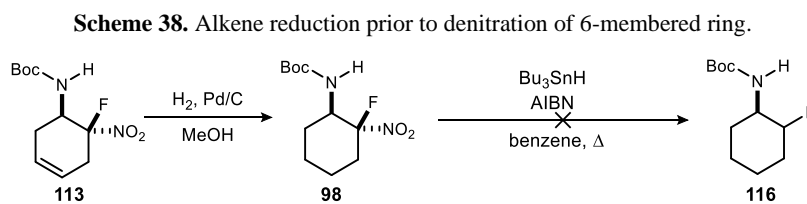
### Reductive denitration of the 6-membered ring

Attempts to denitrate the six-membered ring were not as straightforward as those to denitrate the 7-membered rings. As shown in **Scheme 37**, reductive denitration using tributyl tin hydride and AIBN provided the targets **114** and **115** in only 17% yield. Extensive efforts were made to improve the yield based on procedural adjustments. The equivalents of  $\text{Bu}_3\text{SnH}$  and AIBN were varied, as well as the order and rate of addition. The reagents were added independently, as the same or separate solutions, and with or without degassing, however no improvements were observed. We also examined the use of toluene instead of benzene, the use of ABCN instead of AIBN as the

initiator as well as different temperatures and reaction times. Notwithstanding, the yield and reaction profile did not improve. The substrate also did not react with allylSnBu<sub>3</sub> and AIBN.



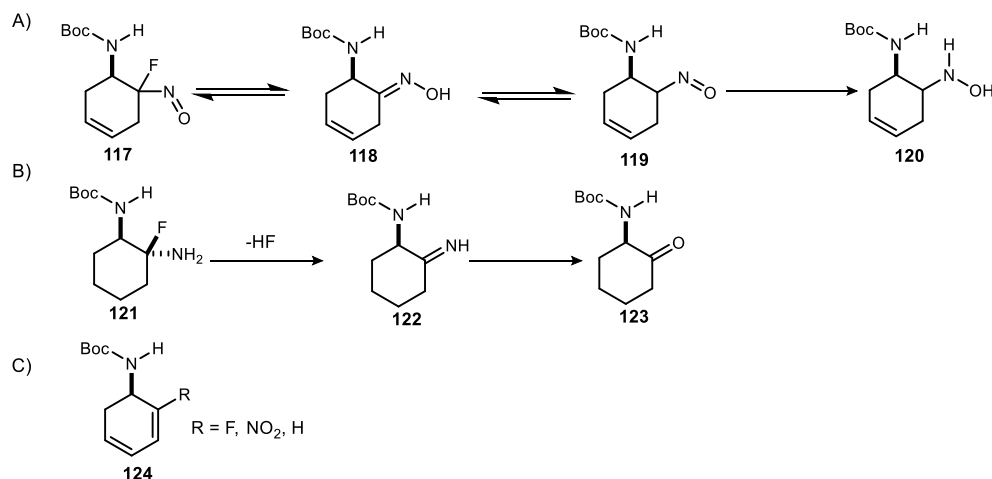
It was hypothesized that conformational restriction may be contributing to the low yields, so the alkene was reduced prior to denitration (**Scheme 38**). This however, did not provide any improvements.



There were other major products formed in the reductive denitration reactions, but efforts to isolate and characterize them were not fruitful. It appeared that whatever species were formed would interconvert between isomers or decompose upon attempted purification. Some of the potential products that could form result from incomplete reduction of the nitro group. For example, partial reduction to the nitroso species **117** could occur, and fluoride elimination could form the oxime **118** (**Scheme 39, A**). The oxime could convert to the nitroso species **119**, which could be reduced to the N-oxide **120**. Alternatively, if partial reduction to the amine occurred, the species would likely be short-lived as elimination of HF to form **122** would likely be fast (**Scheme 39, B**). The imine formed has the potential to undergo hydrolysis to the ketone **123** (**Scheme 39, B**). Finally, elimination could also occur to generate the diene **124** (**Scheme 39, C**). Further studies are needed to isolate and identify the major byproducts from the denitration reaction so that their mechanism of formation can be understood and ultimately shut down.



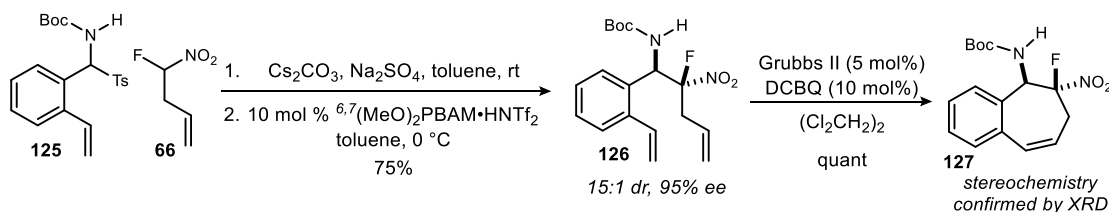
**Scheme 39.** Potential structures of major products from denitration of 6-membered ring.



#### 1.4.5 Toward benzannulated ring systems: access to larger ring sizes

To further expand the scope of these reactions, aryl derivatives of the cyclic  $\beta$ -fluoroamines were synthesized. The conformational constraint provided by the pendant aryl ring allowed for facile ring closing metathesis of precursors to medium sized rings. For example, the cyclooctene derivative could now be formed by RCM in high yield! Moreover, the absence of an adjacent enolizable carbon precludes the issue of tautomerization, and yields a more stable imine intermediate. For this series of benzyl aldimines, chiral homogeneous organocatalysis proved to be superior to phase-transfer catalysis in terms of reactivity, reaction time and diastereoselectivity. To this end, the aza-Henry worked well to provide the RCM precursor for the 7-membered benzannulated ring in high dr and with excellent enantioselection (**Scheme 40**). Ring closing

**Scheme 40.** Synthesis of benzannulated cycloheptenyl  $\beta$ -fluoro- $\beta$ -nitroamine **127**.

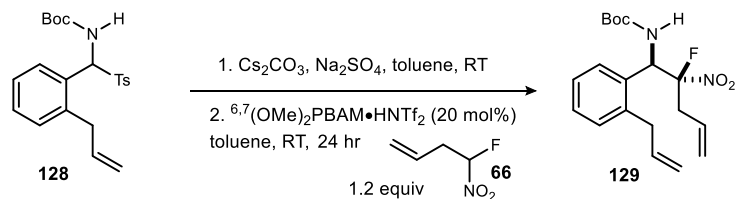


metathesis proceeded in quantitative yield (**Scheme 40**). The stereochemistry of the cycloheptene

was assigned by 2D-NMR and confirmed by X-ray crystallography. The observed stereochemistry was consistent with our previous findings for Type III aza-Henry reactions.

In a similar fashion, the aza-Henry reaction provided benzannulated cyclooctene precursor **129** in high dr with good enantioselection and yield (**Scheme 41**). Gratifyingly, subjecting the aza-Henry

**Scheme 41.** Aza-Henry reaction toward benzannulated cyclooctene precursor **129**.

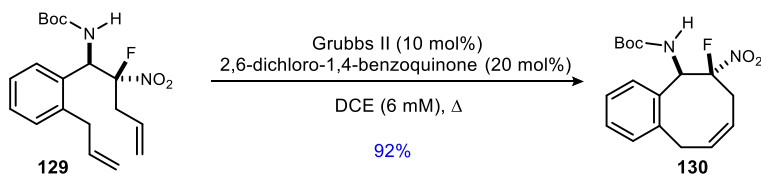


20 mol% catalyst - 76% yield, 15.9:1 dr, 96/88% ee  
10 mol% catalyst - 59% yield, 16.4:1 dr, 95/62% ee

adduct **129** to Grubbs RCM with 2,6-dichloro-1,4-benzoquinone as an additive provided the benzannulated cyclooctene **130** in high yield (**Scheme 42**). Importantly, no isomerization was observed! There was no evidence for the formation of ring-contracted products nor of alkene isomers of the cyclooctene.

If no benzoquinone was used, the reaction yield was not significantly affected, further supporting the benefit of conformational restraint for RCM of medium-sized rings. A test reaction run in

**Scheme 42.** Grubbs RCM provides benzannulated cyclooctene **130**.

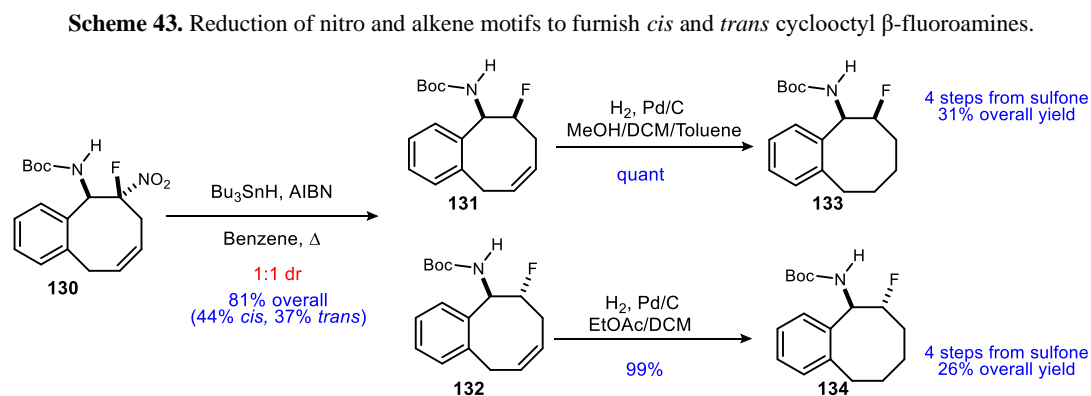


\*5 mol% Grubbs, no benzoquinone, toluene- $d_8$  gives 89%

toluene- $d_8$  showed the product was formed in 89% yield without benzoquinone. It should be noted however that this reaction was monitored by  $^{19}\text{F}$ -NMR and the yield was calculated as soon as the starting material was consumed. Without benzoquinone present, it is possible that catalyst decomposition to a Ru-H species could occur if exposed to the reaction conditions for too long,

which risks alkene isomerization of the product. Further studies would need to be done to test the limits of this reaction in terms of isomerization.

Notwithstanding, the benzannulated cyclooctene **130** was carried forward through denitration to provide the *cis* and *trans*  $\beta$ -fluoroamines **131** and **132** in good yield (81%, **Scheme 43**). The diastereomers were separated and hydrogenation provided their respective diastereomers in 99-quantitative yield (**Scheme 43**). Overall, this approach provided *cis* and *trans* cyclooctanes with high ee in 57% total yield over 4 steps from the  $\alpha$ -amido sulfone.



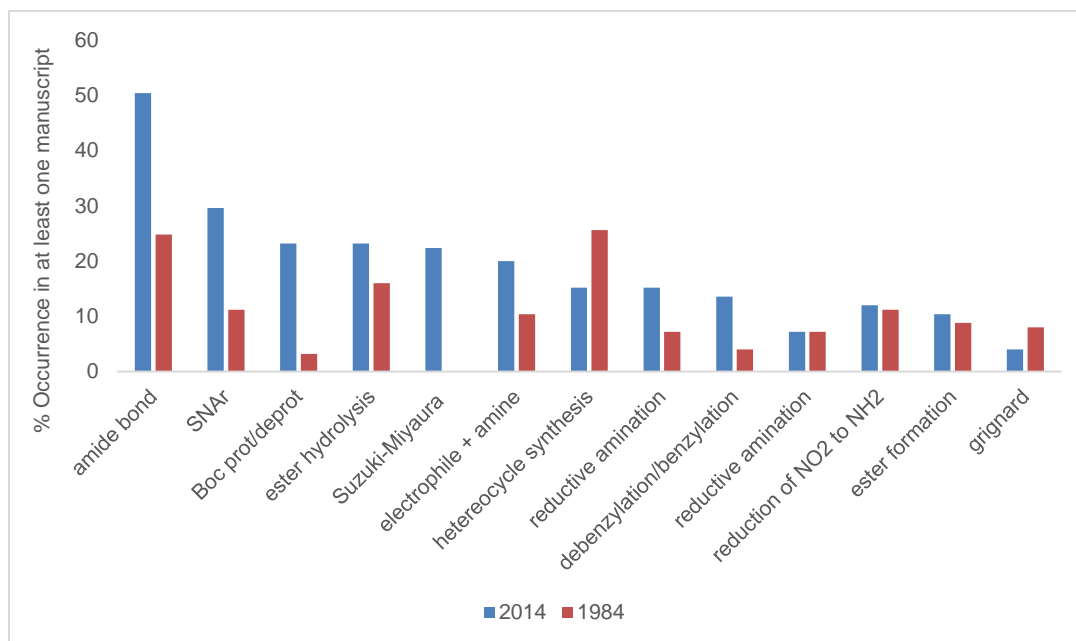
## II. Epimerization-free synthesis of electron-rich aryl glycinamides.

### 2.1 Introduction & background

#### 2.1.1 Amide bond formation

Amide bonds comprise the backbone of proteins and peptides, and are commonly found in medically relevant natural products and therapeutics. As of 2018, over 60 peptide drugs had been approved in the United States, Europe, and Japan; more than 500 are in preclinical trials; more than 150 are in current clinical trials, and an additional 260 have been tested in human clinical trials.<sup>114</sup> Not surprisingly, amide bond formation is a popular reaction in the field of medicinal chemistry. A study was published in 2016 that analyzed the frequency with which particular reactions were used in publications from the *Journal of Medicinal Chemistry* (**Figure 13**).<sup>115</sup>

**Figure 13.** Occurrence of different types of reactions from 1984 compared to 2014.<sup>115</sup>



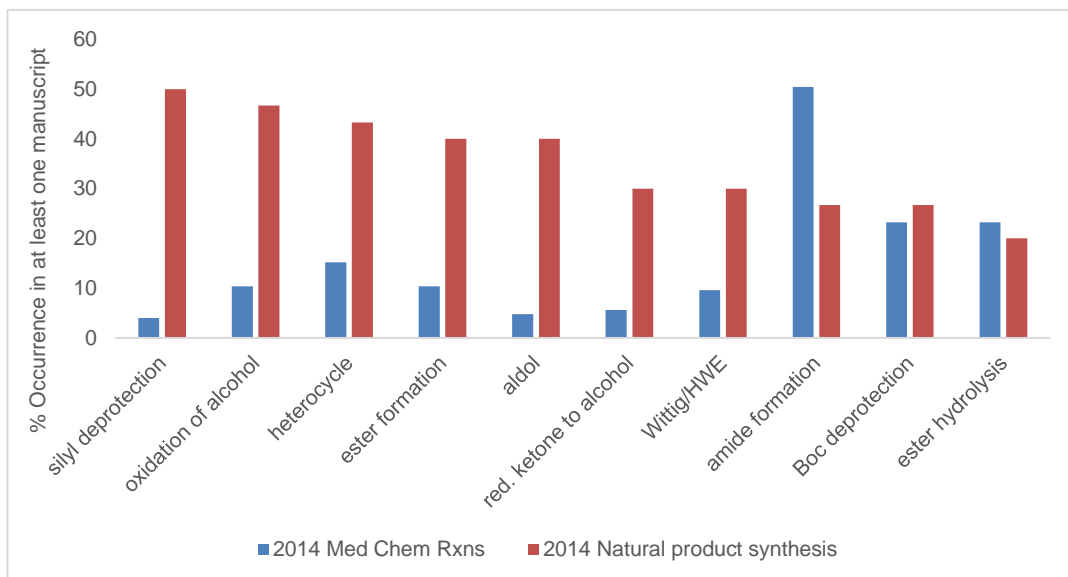
<sup>114</sup> For reviews on peptide therapeutics see: a) Lau, J. L.; Dunn, M. K. *Bioorg. Med. Chem.* **2018**, *26*, 2700.; b) Fosgerau, K.; Hoffmann, T. *Drug Discovery Today* **2015**, *20*, 122.; c) Kaspar, A. A.; Reichert, J. M. *Drug Discovery Today* **2013**, *18*, 807.

<sup>115</sup> Brown, D. G.; Boström, J. *J. Med. Chem.* **2016**, *59*, 4443.

This paper also conducted this analysis for 1984. Among the top reactions used were  $S_NAr$  reactions, protecting group manipulations, Suzuki-Miyaura couplings, and amide bond formation. In 1984 amide bond formation was tied with heterocycle synthesis for the most commonly used reaction type. Thirty years later, amide bond formation is still the most frequently used reaction type, having been used in more than 50% of publications in 2014. Importantly, the relative occurrence has almost doubled in that time. It should be noted that the 50% occurrence does not include cases where solid-phase or automated methods were used (7%). Thus, if both categories were combined, amide bond formation would have been seen in at least once in ~60% of the manuscripts published in *J. Med. Chem.* in 2014. This study also showed that amide bond formation appeared as the final synthetic step in more than 30% of the manuscripts analyzed, making it the most common “production” step in 2014.

Oftentimes the goals and strategies for in medicinal chemistry differ significantly from those used in (chemical) natural product synthesis. Brown and coworkers conducted an analysis similar to the one previously described, using instead natural product publications from the *J. Am. Chem. Soc.* and *Angew. Chem., Int. Ed.* That comparison is shown in **Figure 14**. As shown, there are

**Figure 14.** Occurrence of different types of reactions used in natural product synthesis compared to medicinal chemistry in 2014.<sup>115</sup>



significant differences in the types and frequency of reactions used, but amide bond formation still occurs at least once in more than 20% of the natural product papers analyzed.

To this extent, there has been a long and sustained interest in the preparation of natural product derivatives, or analogs for medicinal chemistry ‘hits’ that may serve as probes for understanding biological mechanisms, or as therapeutics with enhanced activity.<sup>116</sup> The targets that contain amide bonds often source  $\alpha$ -amino acids for their size, structural and functional diversity, and their defined stereochemistry. Reliance on the chiral pool alone, however, imposes a severe constraint on access to chemical space. Specifically, the incorporation of noncanonical amino acids into peptides is in high demand as we learn more about biological systems and interactions, and understand the benefits of peptidomimetics. Perturbations and manipulations to such systems can lead to new discoveries; however, the synthesis of substrates containing unnatural amino acids in a manner that is both efficient (fast) and highly selective (yield and stereochemical purity) has remained a challenge for scientists. The ease of a synthesis, and the reliability of its execution, are directly proportional to its widespread adoption.

Traditionally, peptides have been synthesized through the condensation of an amine and a carboxylic acid to generate amide bonds. The most common approach is to use a coupling reagent to generate an activated ester from the carboxylic acid. Inherent to this approach is the generation of an intermediate with a more acidic  $\alpha$ -proton. This intermediate opens a pathway to  $\alpha$ -epimerization through azlactone or ketene formation (**Scheme 44**).<sup>117</sup> Chemists have long recognized this liability, resulting in the development of a wide variety of reagent combinations and protocols whose aim is to accelerate the amide formation relative to the rate of epimerization.<sup>118</sup> Typically, with the use of modern coupling reagents and additives such as HOBT or HATU, epimerization can be minimized.<sup>119</sup>

---

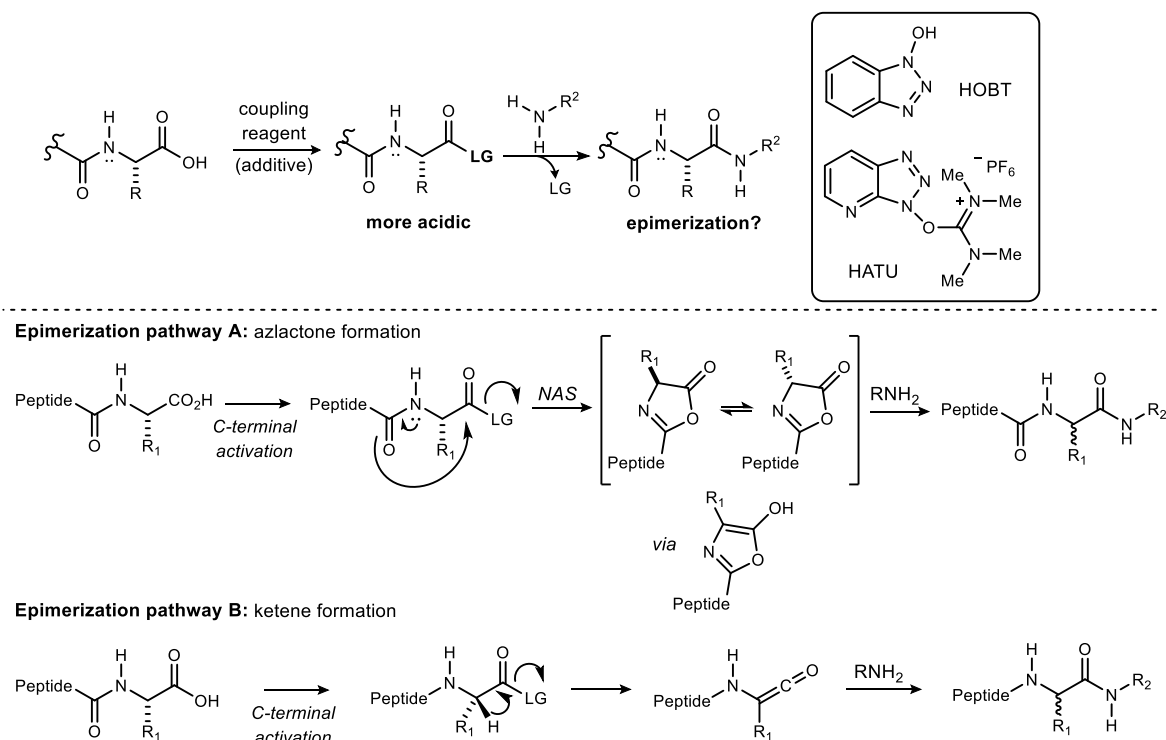
<sup>116</sup> Noisier, A. F. M.; Brimble, M. A. *Chem. Rev.* **2014**, *114*, 8775.

<sup>117</sup> Pattabiraman, V. R.; Bode, J. W. *Nature* **2011**, *480*, 471.

<sup>118</sup> Valeur, E.; Bradley, M. *Chem. Soc. Rev.* **2009**, *38*, 606.

<sup>119</sup> For reviews see: El-Faham, A.; Albericio, F. *Chem. Rev.* **2011**, *111*, 6557.; Al-Warhi, T. I.; Al-Hazimi, H. M. A.; El-Faham, A. *Journal of Saudi Chemical Society* **2012**, *16*, 97.

**Scheme 44.**  $\alpha$ -Amino acid epimerization pathways during condensative amide formation.



Over a half-century of research, advances have been made to address the issues often encountered in condensative peptide synthesis, which may include limited functional group tolerance, low stereoselectivity, and harsh or wasteful reaction conditions. Progress in solid phase peptide synthesis<sup>120</sup> as well as the development of native chemical ligation<sup>121</sup> and the Staudinger ligation<sup>122</sup> has improved our ability to synthetically access useful peptides. However, each of these approaches comes with unique limitations. Staudinger ligation can suffer epimerization, and solid phase peptide synthesis requires excess reagents to drive reactions to completion, which leads to the generation of waste. Traditionally, native chemical ligation was limited to peptides that include a cysteine residue, however significant advances in post-ligation desulfurization strategies<sup>123,124</sup> have since made this approach amenable for use at non-cysteine residues. In these studies, the thiol

<sup>120</sup> Palomo, J. M. *RSC Adv.* **2014**, *4*, 32658.

<sup>121</sup> Dawson, P.; Muir, T.; Clark-Lewis, I.; Kent, S. *Science* **1994**, *266*, 776.

<sup>122</sup> Saxon, E.; Armstrong, J. I.; Bertozzi, C. R. *Org. Lett.* **2000**, *2*, 2141.

<sup>123</sup> Wan, Q.; Danishefsky, S. J. *Angew. Chem. Int. Ed.* **2007**, *46*, 9248.

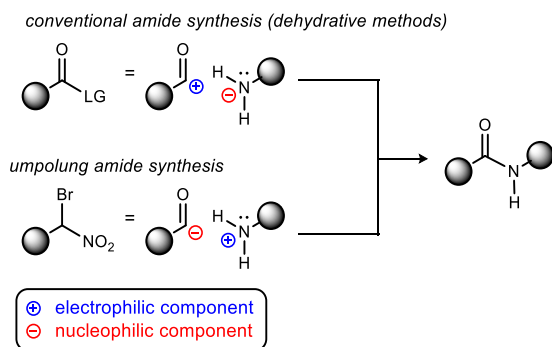
<sup>124</sup> Yan, L. Z.; Dawson, P. E. *J. Am. Chem. Soc.* **2001**, *123*, 526.

(or selenide) is incorporated at the amino acid of choice (e.g. Ala,<sup>124</sup> Phe,<sup>125</sup> Pro<sup>126</sup>), ligation is carried out, and then the side-chain sulfur or seleno-functionality is removed.

### 2.1.2 Introduction to Umpolung Amide Synthesis

In 2010, advances were made to address the inherent demand for methods that are accessible, catalytic, stereoselective and tolerant to sterically demanding and functionally diverse substrates. This was achieved through the discovery of a novel amide bond forming reaction between a bromonitroalkane and an amine (**Scheme 45**).<sup>42</sup> This reaction was coined Umpolung Amide Synthesis as it was understood to reverse the electronic roles (German, *umpolung*) of the conventional coupling partners in amide synthesis. The traditionally electron-rich amine was hypothesized to be activated by conversion to an electron deficient *N*-haloamine (or equivalent). Under the mildly basic reaction conditions, an electron-rich, nucleophilic  $\alpha$ -bromonitronate was formed, ultimately serving as an acyl donor equivalent.

**Scheme 45.** Comparison of Umpolung Amide Synthesis (UmAS) and condensative amide synthesis.



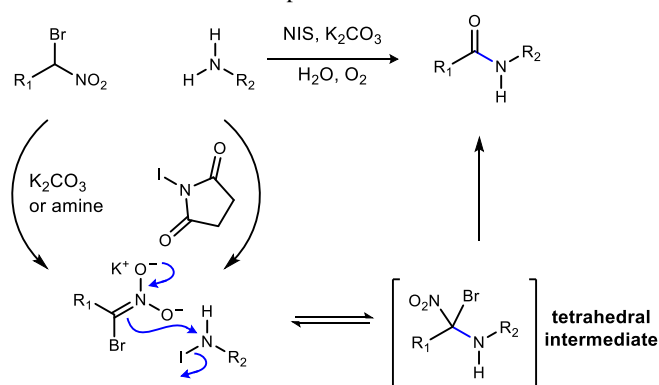
Importantly, this reaction mechanistically *avoids* an active ester intermediate and the associated pathways to epimerization. Moreover, the mild conditions utilize a weak base, which is important for retaining the stereochemical integrity of acidic amino acid residues during coupling. Overall, the reaction is proposed to proceed through nucleophilic nitronate attack on the electrophilic amine intermediate, the latter formed from reaction of the amine with a halonium source such as NIS

<sup>125</sup> Crich, D.; Banerjee, A. *J. Am. Chem. Soc.* **2007**, *129*, 10064.

<sup>126</sup> Townsend, S. D.; Tan, Z.; Dong, S.; Shang, S.; Brailsford, J. A.; Danishefsky, S. J. *J. Am. Chem. Soc.* **2012**, *134*, 3912.



**Scheme 46.** Proposed UmAS mechanism.



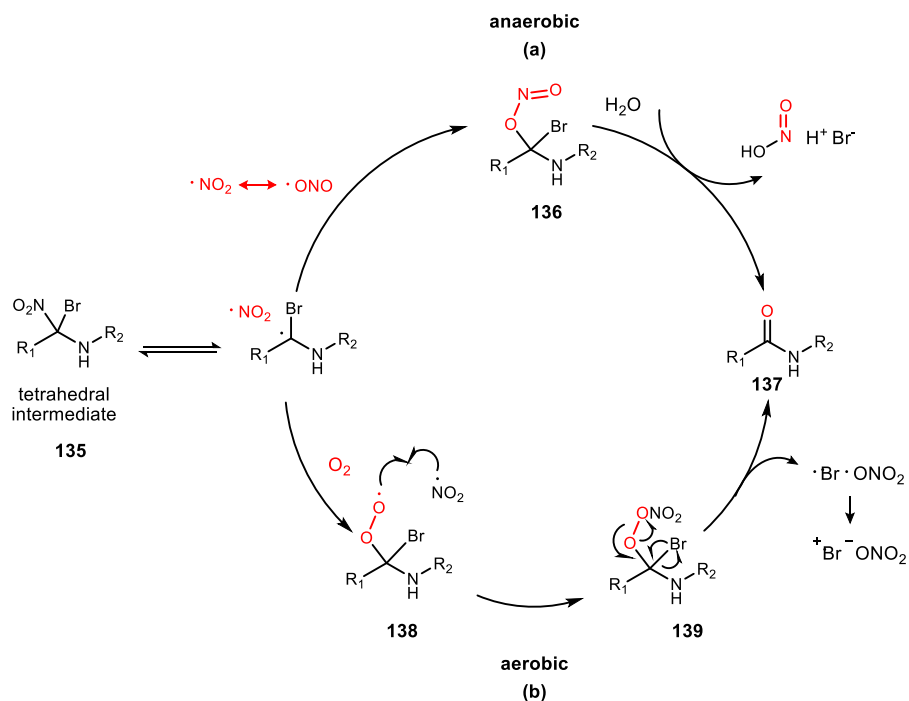
(Scheme 46). The amide is generated upon collapse of the resultant tetrahedral intermediate.<sup>42,,127,128</sup>

Elucidation of the mechanism behind the collapse of the tetrahedral intermediate was obtained through <sup>18</sup>O-labeling studies.<sup>127</sup> It was observed that two potential pathways – one anaerobic, and one aerobic – to amide formation exist, which diverge after the formation of the tetrahedral intermediate (**135**) (**Scheme 47**). Both pathways begin with C-O bond formation, however the oxygen source and subsequent reaction pathway differs. In the absence of dioxygen (O<sub>2</sub>), the nitro group functions as the oxygen source for the amide carbonyl (**Scheme 47**, pathway a). The nitrogen dioxide/amino methyl radical pair can recombine with C-O bond formation (via overall nitro-nitrite isomerization) to form nitrite **136**, which upon hydrolysis liberates nitrite, bromide, and the amide (**137**). Under aerobic conditions (**Scheme 47**, pathway b) the amino methyl radical combines with triplet oxygen to form the tetrahedral peroxide radical intermediate (**138**). Reaction with the nitrogen dioxide radical to form **139** followed by homolytic cleavage of the carbon-bromine and oxygen-oxygen bonds results in amide formation and release of the elements of bromonium nitrate.

<sup>127</sup> Shackleford, J. P.; Shen, B.; Johnston, J. N. *Proc. Natl. Acad. Sci. U. S. A.* **2012**, *109*, 44.

<sup>128</sup> Crocker, M. S.; Foy, H.; Tokumaru, K.; Dudding, T.; Pink, M.; Johnston, J. N. *Chem* **2019**, *5*, 1248.

**Scheme 47.** Anaerobic & aerobic pathways of UmAS.



A key demonstration in the original report of UmAS was the enantioselective synthesis of  $\alpha$ -bromo nitroalkane donors that convert to  $\alpha$ -amino amide products with high enantiomeric excess (ee). This finding relied on the use of bis(amidine) catalysis (BAM) to affect the enantioselective addition of commercial bromonitromethane to *N*-Boc aldimines. The success of this approach requires an effective and robust method for producing  $\alpha$ -bromo nitroalkane donors with diverse side chains. These nitroalkane donors also exhibit reactivity that provides a diverse array of amide products. To this point, investigations have demonstrated the efficacy of UmAS chemistry in the stereoselective catalytic formation of derivatives of  $\alpha$ -aryl  $\alpha$ -aminoamides (aryl glycinamides),  $\alpha$ -oxy amides, and  $\alpha$ -alkyl  $\alpha$ -aminoamides.<sup>43,89, 129</sup> It has been applied to the synthesis of LY411575,<sup>129</sup> a drug used for the treatment of Alzheimer's disease, and to the synthesis of the cyclodepsipeptide insecticides *nat*-verticilide<sup>130</sup> and bassianolide.<sup>131</sup>

<sup>129</sup> Leighty, M. W.; Shen, B.; Johnston, J. N. *J. Am. Chem. Soc.* **2012**, *134*, 15233.

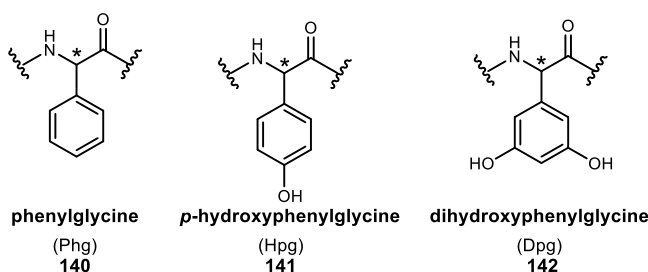
<sup>130</sup> Batiste, S. M.; Blackwell, D. J.; Kim, K.; Kryshal, D. O.; Gomez-Hurtado, N.; Rebbeck, R. T.; Cornea, R. L.; Johnston, J. N.; Knollmann, B. C. *Proc. Natl. Acad. Sci. U. S. A.* **2019**, *116*, 4810.

<sup>131</sup> Batiste, S. M.; Johnston, J. N. *Unpublished Results* **2016**.

### 2.1.3 Properties of aryl glycinamides

The aza-Henry/Umpolung amide synthesis approach is ideal for the preparation of  $\alpha$ -aryl glycinamides without risk of epimerization, an observation consistent with the unique *umpolung* mechanism. Of particular interest is the ability to incorporate the non-proteinogenic amino amide residues such as phenylglycine (Phg, **140**), hydroxyphenyl glycine (Hpg, **141**), and dihydroxyphenylglycine (Dpg, **142**), due to their unique reactivity as well as structural and biological properties (**Figure 15**).

**Figure 15.** Structures of common phenyl glycinamide motifs.



These residues represent a family of noncanonical amino acids common to many peptide therapeutics and natural products such as the  $\beta$ -lactam antibiotics norcardicin A-G,<sup>132</sup> chlorocardicin,<sup>133</sup> penicillin,<sup>134</sup> amoxicillins,<sup>135</sup> MDL 19592,<sup>136</sup> and cefadroxil,<sup>137</sup> as well as the glycopeptide class of antibiotics<sup>138</sup> (**Figure 16**). Highlighted in **Figure 16** are some of the compounds that contain contain electron-rich aryl glycine residues as these will be the primary focus of this work (*vide infra*).

<sup>132</sup> Aoki, H.; Sakai, H.; Kohsaka, M.; Konomi, T.; Hosoda, J.; Kubochi, Y.; Iguchi, E.; Imanaka, H. *J. Antibiot.* **1976**, *29*, 492.; Hashimoto, M.; Komori, T.; Kamiya, T. *J. Antibiot.* **1976**, *29*, 890.

<sup>133</sup> Chan, J. A.; Shultis, E. A.; Dingerdissen, J. J.; Debrosse, C. W.; Roberts, G. D.; Snader, K. M. *J. Antibiot.* **1985**, *38*, 139.

<sup>134</sup> Baldwin, J. E.; Schofield, C. J.; Smith, B. D. *Tetrahedron* **1990**, *46*, 3019.

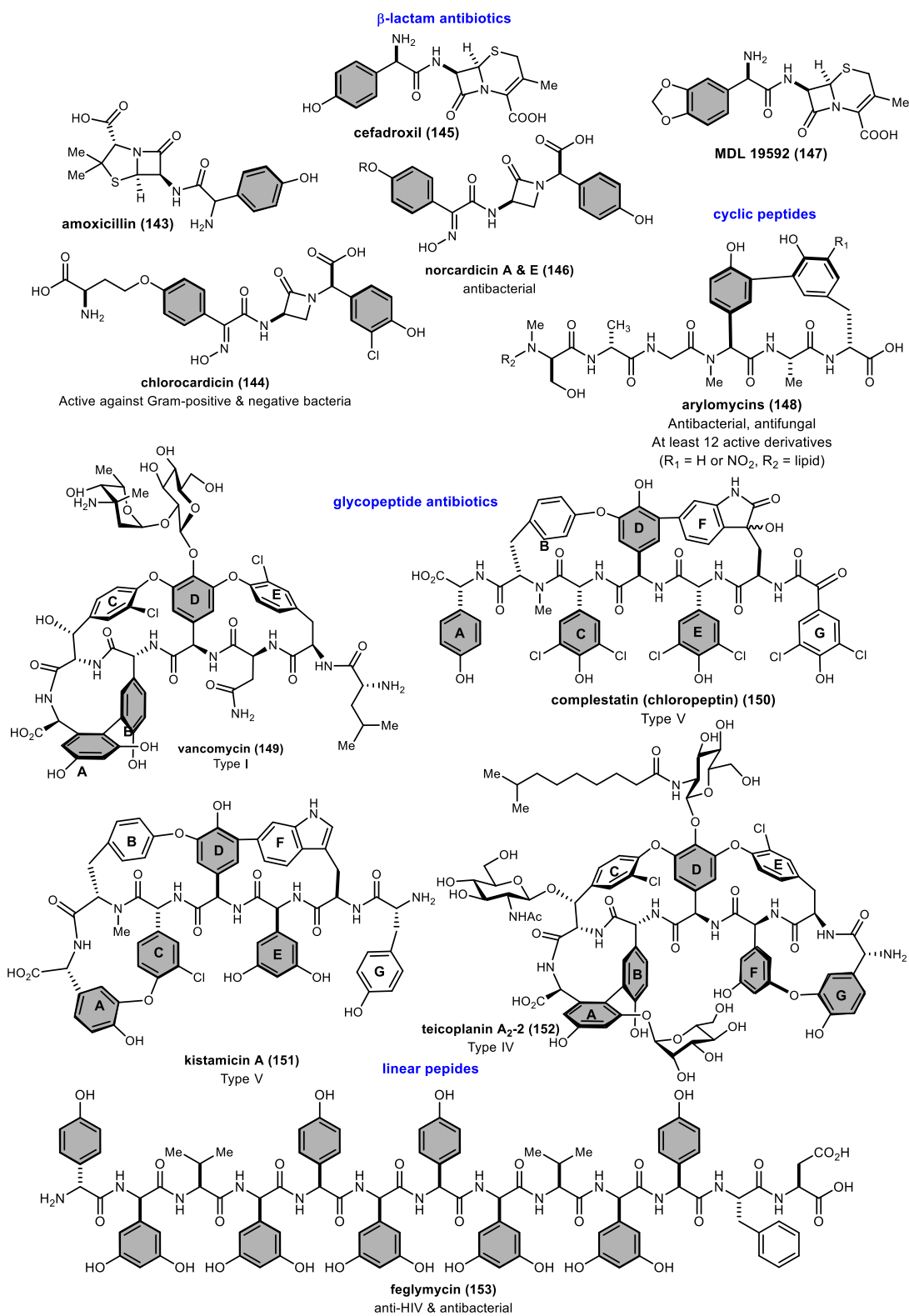
<sup>135</sup> Ball, P. *Int. J. Antimicrob. Agents* **2007**, *30*, 113.

<sup>136</sup> a) Erickson, R. C.; Baumann, R. J.; Gibson, C. B.; Hoffman, P. F. *J. Antibiot (Tokyo)* **1983**, *36*, 1345. b) Jones, R. N.; Barry, A. L. *Diagnostic Microbiology and Infectious Disease* **1988**, *11*, 159.

<sup>137</sup> Campagna, J. D.; Bond, M. C.; Schabelman, E.; Hayes, B. D. *The Journal of Emergency Medicine* **2012**, *42*, 612.

<sup>138</sup> For review see a) Williams, R. M.; Hendrix, J. A. *Chem. Rev.* **1992**, *92*, 889. b) Nicolaou, K. C.; Boddy, C. N. C.; Bräse, S.; Winssinger, N. *Angew. Chem. Int. Ed.* **1999**, *38*, 2096.

**Figure 16.** Examples of natural products and therapeutics containing electron-rich aryl-glycine residues.



The aryl glycine motif typically contributes to a peptide's conformation and thus to its biological properties. Without the presence of a  $\beta$ -carbon spacer (such as Tyr or Phe), they impart unique restrictions on peptide conformation, thereby limiting the amount of inactive conformations in which the peptide may exist. Moreover, aryl moieties in peptides provide a functional handle for cyclization. The Hpg, Dpg and related residues are distinct in that they may be amenable to  $\pi$ -stacking while serving as hydrogen bond donors. Biosynthetically, electron-rich aryl glycinamides offer the possibility of ether bridges and aryl-aryl C-C bonds, such as those found in the glycopeptide antibiotics. These are formed through oxidative coupling steps performed by members of the cytochrome P450 family.<sup>139</sup> Synthetically, the construction of these bonds has prompted the development of novel chemistry such as aryl-aryl couplings, macrocyclizations, and etherifications.<sup>140</sup> The increased opportunity for cyclization when oxygenated aryl glycine units are present is an important feature when considering the adaptation of natural products to therapeutic development. It is well known that cyclic peptides can have improved properties for drug development in comparison to their linear relatives as they are less susceptible to proteolytic degradation,<sup>141</sup> their rigid structure can provide better binding affinity due to minimal entropy loss upon binding, and they can have increased membrane permeability. The lack of a C or N terminus renders cyclic peptides more stable to exopeptidases, and their enhanced rigidity makes them less recognizable to endopeptidases.

---

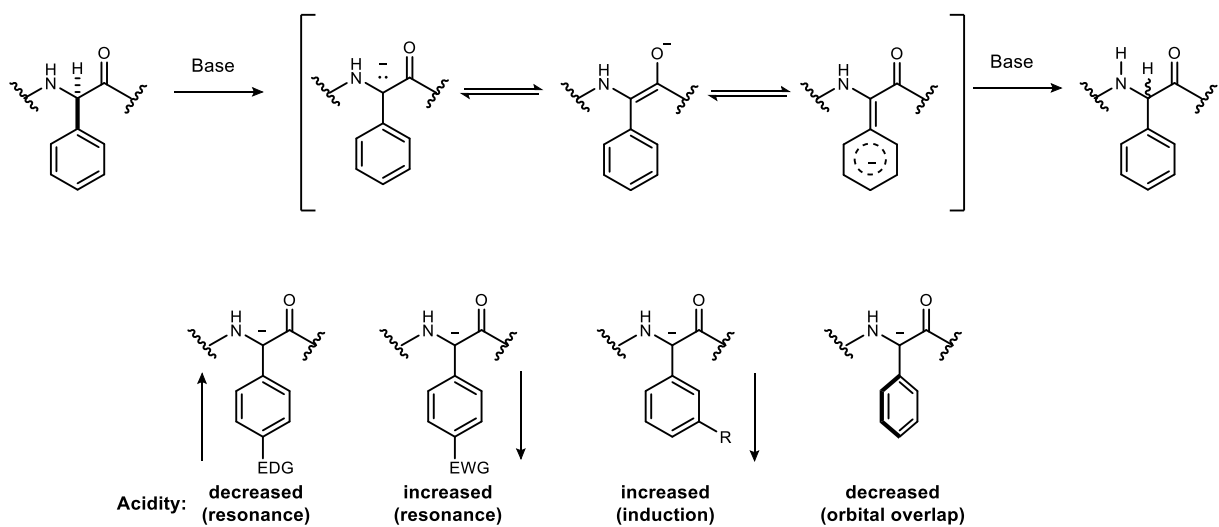
<sup>139</sup> Cryle, M. J.; Brieke, C.; Haslinger, K. In *Amino Acids, Peptides and Proteins: Volume 38*; The Royal Society of Chemistry: 2014; Vol. 38, p 1.

<sup>140</sup> For a review of macrocyclizations see: Gulder, T.; Baran, P. S. *Nat. Prod. Rep.* **2012**, *29*, 899. For a review on biaryl and biaryl ether linkages in peptides see: Feliu, L.; Planas, M. *Int. J. Pept. Res. Ther.*, *11*, 53.

<sup>141</sup> For review see Andrew, T. B.; Cayla, M. M.; Lokey, R. S. *Curr. Top. Med. Chem.* **2013**, *13*, 821. Joo, S.-H. *Biomolecules and Therapeutics* **2012**, *20*, 19.

A notable trait of the aryl glycines that makes their synthesis and incorporation into peptides difficult, is their increased propensity for epimerization of the  $\alpha$ -carbon over the canonical amino acids. For example, it has been shown that Hpg undergoes racemization at a rate 9-fold faster than alanine.<sup>142</sup> This is attributed to the increased acidity of the  $\alpha$ -proton, as the charge in the conjugate base is delocalized over the  $\pi$ -system of the aromatic ring. Substitution on the aryl moiety can affect the rate of epimerization through resonance and induction. The congestion around the aryl-carbon bond also introduces steric congestion ( $A^{1,3}$ -strain) that affects the propensity for epimerization by destabilization of the ground state (**Scheme 48**).<sup>142</sup> With these factors in mind, it can be understood why the relative rates of racemization for the phenylglycine residues is in the

**Scheme 48.** Outline of the racemization of aryl glycines and typical substituent effects.<sup>142</sup>



order of Hpg<Phg<Dpg, with Dpg being the most prone to racemization.

Questioning the necessity of complexity in a natural product is an important step toward its use in therapeutic development. Structural simplification, however, is typically a labor- and time-intensive process that requires careful hypothesis-driven structure-activity relationship studies. These studies can be more straightforward in peptides since each residue is well-defined, and syntheses are more clearly envisioned as a connection of ‘building blocks’. For example, the

<sup>142</sup> Al Toma, R. S.; Brieke, C.; Cryle, M. J.; Sussmuth, R. D. *Nat. Prod. Rep.* **2015**, *32*, 1207.

dependence of biological activity on aryl glycine residues in natural products has been documented in several instances, including feglymycin. An alanine scan is often used to determine the contribution of specific residues to the structure or function of a peptide or protein. This process generates a library of derivatives, where each residue is exchanged for an alanine. Alanine is typically selected because it will retain some conformational rigidity associated with a substituted  $\alpha$ -amino amide (vs. glycine), and because its side chain is chemically inert. To this end, iterative substitutions are performed, until an X-mer peptide has had each position replaced by an alanine, producing X unique peptides for comparison in an assay. This procedure was performed with feglymycin (**153**, **Figure 16**), and documented a >32 fold increase in MIC upon replacement of a single Hpg residue. The authors proposed that a disruption of  $\pi$ - $\pi$  interactions in the 13-mer caused a significant change in secondary structure, leading to the diminution of activity.<sup>143</sup>

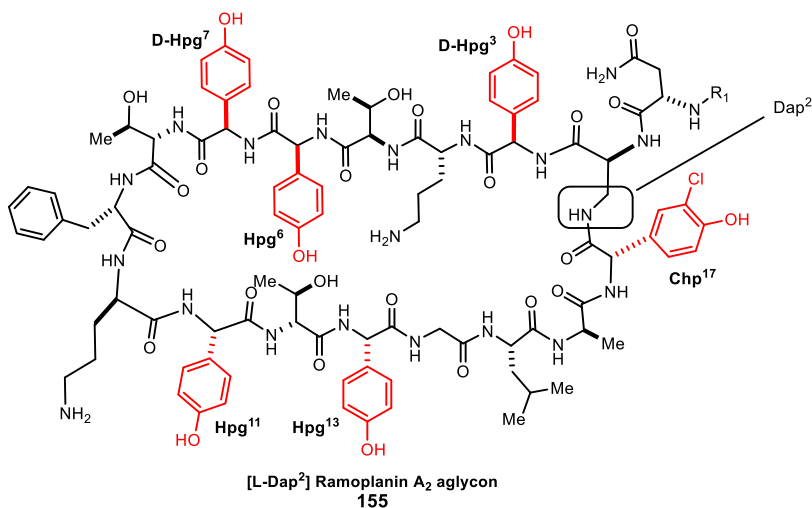
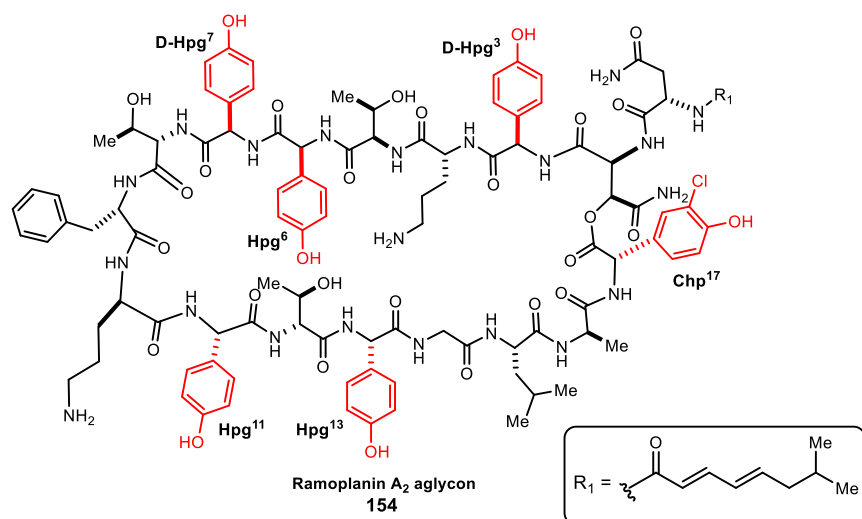
The alanine scan may also be restricted to specific residues of interest. The structures of both ramoplanin A2 aglycon (**154**) and the derivative [Dap<sup>2</sup>]-ramoplanin A2 aglycon (**155**) are shown above **Table 9**. The [Dap<sup>2</sup>] analogue replaces the labile ester linkage between HAsn<sup>2</sup> and Chp<sup>17</sup> with a more stable amide bond and also replaces HAsn<sup>2</sup> with L-2,3-diamino propionic acid (Dap). This change results in a more stable and more synthetically accessible version of ramoplanin with little change in biological activity or tertiary structure. An alanine scan was conducted on [Dap<sup>2</sup>]-ramoplanin A2 aglycon and showed that replacing selected Hpg and Dpg residues exhibited a 13-74 fold increase in MIC (**Table 9**).<sup>144</sup> In solution, ramoplanin A2 is a dimer consisting of two antiparallel  $\beta$ -strands that are stabilized by H-bonds and aromatic side chains. This causes ramoplanin A2 to exist in a U-shape topology. It was proposed that replacement of the aromatic residues disrupts the formation of the dimer and also may disrupt the formation of a hydrophobic membrane binding domain, resulting in decreased activity.

---

<sup>143</sup> Hanchen, A.; Rausch, S.; Landmann, B.; Toti, L.; Nusser, A.; Sussmuth, R. D. *ChemBioChem* **2013**, *14*, 625.

<sup>144</sup> Nam, J.; Shin, D.; Rew, Y.; Boger, D. L. *J. Am. Chem. Soc.* **2007**, *129*, 8747.

**Table 9.** Alanine scan of ramoplanin aglycon against *S. aureus* ATCC 25923.<sup>144</sup>



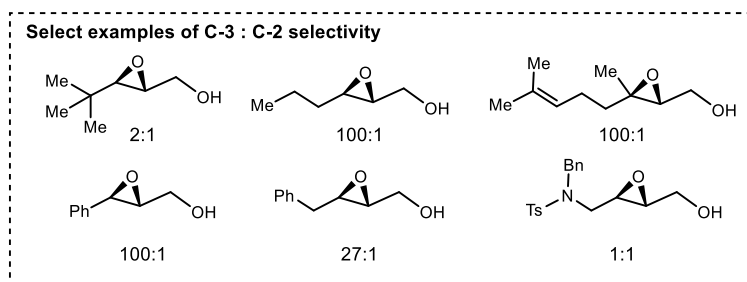
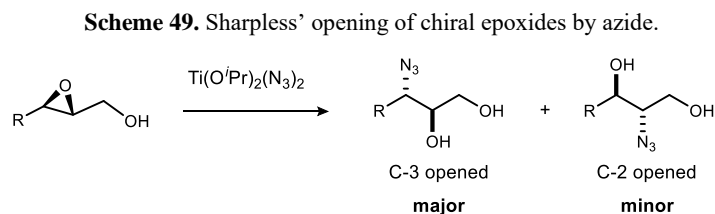
entry	compound	authentic residue	MIC (μg/mL)	fold difference
1	Ramoplanin A2 aglycon	--	0.11	1.6
2	[Dap <sup>2</sup> ]ramoplanin A2 aglycon	--	0.07	1
2	[Dap <sup>2</sup> , D-Ala <sup>3</sup> ]ramoplanin A2 aglycon	D-Hpg <sup>3</sup>	5.2	74
3	[Dap <sup>2</sup> , D-Ala <sup>6</sup> ]ramoplanin A2 aglycon	Hpg <sup>6</sup>	0.9	13
4	[Dap <sup>2</sup> , D-Ala <sup>7</sup> ]ramoplanin A2 aglycon	D-Hpg <sup>7</sup>	3.7	53
5	[Dap <sup>2</sup> , D-Ala <sup>11</sup> ]ramoplanin A2 aglycon	Hpg <sup>11</sup>	2.5	36
6	[Dap <sup>2</sup> , D-Ala <sup>13</sup> ]ramoplanin A2 aglycon	Hpg <sup>13</sup>	1.4	20



### 2.1.4 Existing methods for the asymmetric synthesis of aryl glycines

The synthesis of aryl glycine derivatives has been studied rather extensively due to their presence in many natural products and therapeutics. However, the ability to (i) synthesize these amino acids enantioselectively and (ii) use them in peptide coupling without epimerization, presents a significant challenge (*vide supra*). Since the synthesis of an aryl glycinamide normally converges at the  $\alpha$ -amino acid precursor, this discussion will focus on the synthesis of aryl glycine  $\alpha$ -amino acids or their precursor. Note that comparisons made later during discussions of UmAS must account for the fundamental difference that UmAS does not use a carboxylic acid or activated derivative at any point in its mechanism.<sup>145</sup>

An early and straightforward method for the asymmetric synthesis of non-canonical amino acids involves the nucleophilic ring-opening of enantioenriched epoxy alcohols, themselves prepared by Sharpless epoxidation by treatment with  $[\text{Ti}(\text{O}-i\text{-Pr})_2(\text{N}_3)_2]$ .<sup>146</sup> The ring opening of *trans*-epoxy



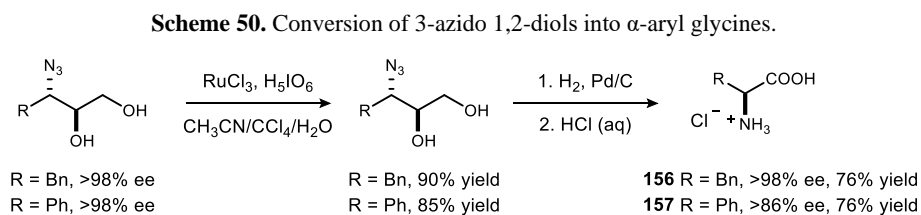
alcohols was found to proceed with preference for C-3 attack, with varying degrees of C-3:C-2

<sup>145</sup> In one exception, however, BAM catalysis and the Mioskowski-Nef reaction will be used to prepare *N*-Boc aryl glycines, and then use these for traditional amide synthesis.

<sup>146</sup>Caron, M.; Carlier, P. R.; Sharpless, K. B. *J. Org. Chem.* **1988**, 53, 5185.

regioselectivity that ranged from 1:1 to 100:1 (**Scheme 49**). High selectivity for benzylic azide formation (100:1) makes this method particularly suitable for aryl glycine synthesis.

The resultant 3-azido-1,2-diols can be transformed into the corresponding amino acids by ruthenium tetroxide oxidation and catalytic hydrogenation (**Scheme 50**). Stereochemistry was maintained throughout this transformation to obtain L-phenylalanine (**156**) with >98% ee. However, while the precursor to L-phenylglycine (**157**), 3-azido 3-phenyl 1,2-diol, was formed with 100:1 C-3:C-2 selectivity and 100% yield, the stereochemistry was compromised during its conversion to the amino acid, specifically at the oxidation stage. It is not a rare occurrence for methods that are fruitful when applied to the synthesis and coupling of amino acids to have a less than stellar application for, or to simply be inapplicable to, the synthesis of  $\alpha$ -aryl glycines and their derivatives.



## Methods developed for $\alpha$ -aryl glycinamide synthesis during the pursuit of vancomycin and related therapeutic peptides

A significant portion of the contributions made to stereoselective aryl glycine synthesis came during the ‘vancomycin era’ of the 1990’s to early 2000s.<sup>147</sup> Vancomycin (**149**) is a potent antibiotic that is used as the last line of defense against methicillin-resistant staphylococcus aureus (MRSA). It is also used to treat infections in patients with allergies to other antibiotics. Vancomycin belongs to the class of glycopeptide antibiotics, which contains a number of related compounds such as those shown in **Figure 17**. Vancomycin became a well sought-after synthetic target for both its medicinal relevance and striking structural features. With several aryl glycine residues, bi-aryl and bi-aryl ether linkages, as well as several atropisomeric sites, it is no wonder

<sup>147</sup> For a recent review on synthetic strategies toward vancomycin see: Okano, A.; Isley, N. A.; Boger, D. L. *Chem. Rev.* **2017**, *117*, 11952.

there was such a heavy push by synthetic organic chemists to improve and invent state-of-the-art techniques to achieve its total synthesis. As highlighted in **Figure 17**, each of these antibiotics contain multiple aryl glycine residues, and therefore new methodology had to be developed to make the required amino acid derivatives.

**Figure 17.** Structures of vancomycin and related glycopeptide antibiotics.

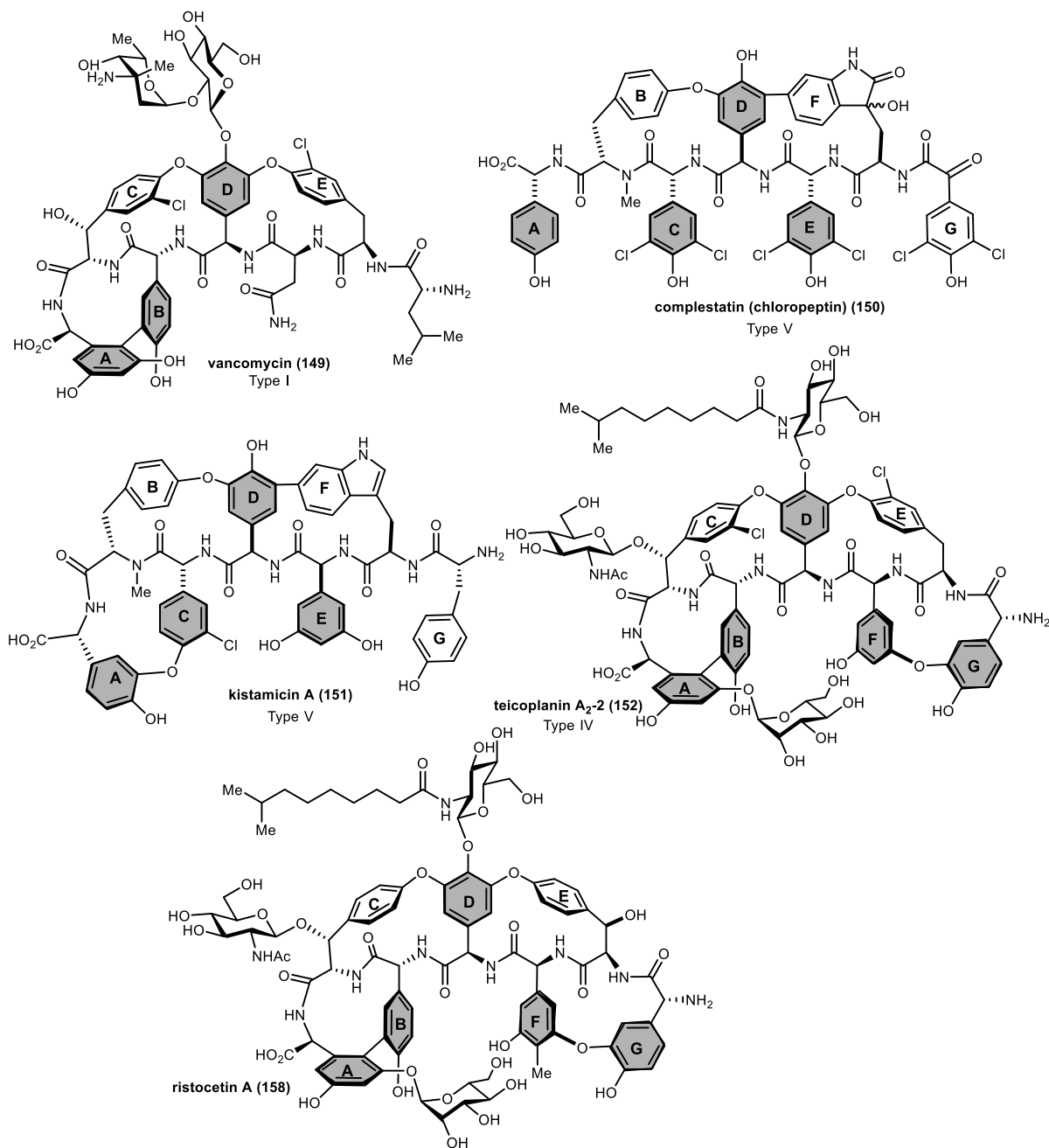
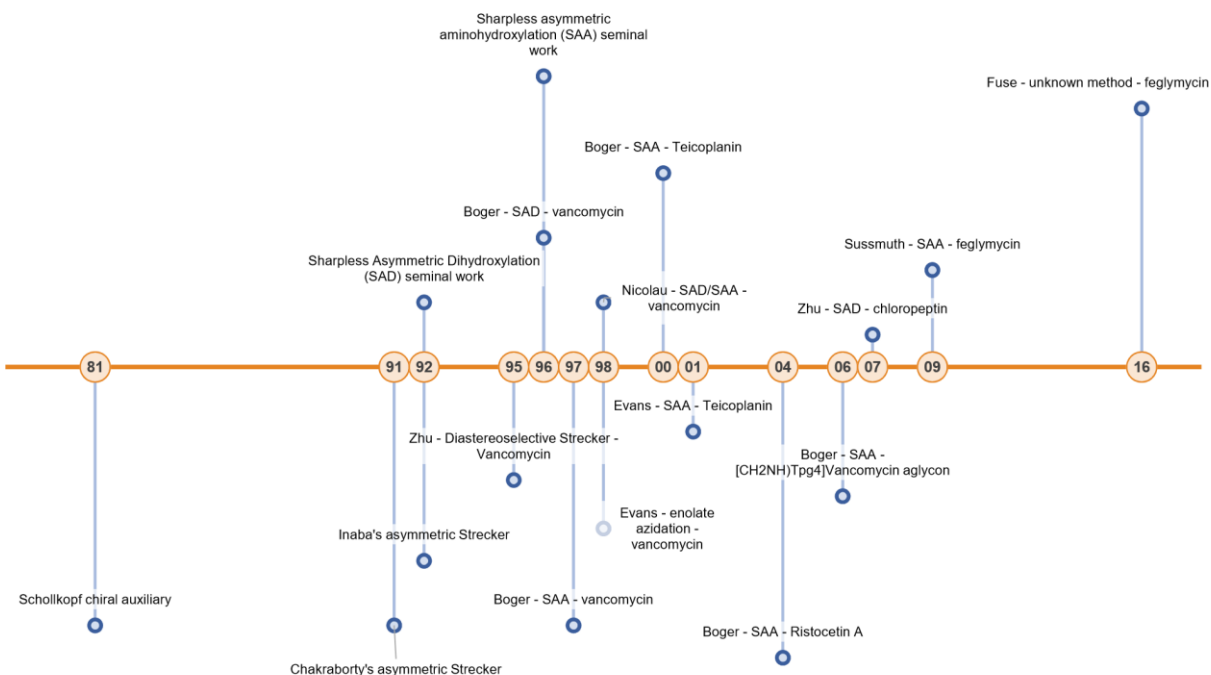


**Figure 18** shows some of the main contributions to aryl glycine synthesis as well as the completion of the syntheses of the glycopeptide targets. As shown, early work primarily utilized the Strecker reaction, while later work took advantage of developments made by the Sharpless group in the area of asymmetric alkene functionalization. Each of these approaches, as well as other significant

**Figure 18.** Timeline of methods used for the synthesis of (glyco)peptide antibiotics.

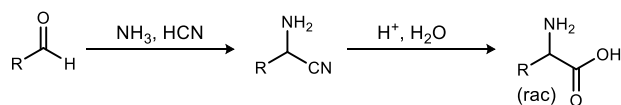


contributions will be discussed in this section.

Many of the first discoveries in the field of asymmetric aryl glycine synthesis relied on substrate or auxiliary induced diastereoselectivity. Chiral auxiliary-based approaches to access optically active  $\alpha$ -aryl glycines have been broadly explored as seen by the use of the auxiliary-based Strecker synthesis, oxazolidinone based enolate azidations, the addition of arene-metal complexes to the

Schöllkopf auxiliary,<sup>148</sup> and addition to electrophilic chiral glycine equivalents,<sup>149</sup> among others.<sup>138</sup> Chiral auxiliaries have also been used in diastereoselective Strecker reactions. The

**Scheme 51.** General Strecker amino acid synthesis.



Strecker synthesis was first developed in 1850 and has been proposed to be the method by which amino acids were made in primordial Earth.<sup>150, 151</sup> This two-step reaction sequence has been a reliable method for the synthesis of amino acids, and proceeds via imine formation by condensation with an aldehyde, followed by the addition of cyanide. The resulting nitrile is then hydrolyzed to provide the amino acid (**Scheme 51**).<sup>152</sup>

Diastereoselective variants that employed  $\alpha$ -methyl benzylamine as a chiral auxiliary proved to be advantageous for the synthesis of many amino acids.<sup>152</sup> Unfortunately, this auxiliary is unsuitable for the synthesis of aryl glycines, sulfur, or alkene containing amino acids, or any non-canonical amino acids containing side chain groups that are sensitive to the hydrogenation conditions needed to remove the  $\alpha$ -methyl benzyl amine.

However, while pursuing the synthesis of vancomycin, Chakraborty identified  $\alpha$ -phenylglycinol (**14**) as an effective chiral auxiliary for the diastereoselective Strecker synthesis of amino acids, specifically the  $\alpha$ -aryl glycine residues present in vancomycin, as it can be oxidatively cleaved with lead tetraacetate.<sup>153</sup> Both enantiomers of  $\alpha$ -phenyl glycinol are readily available, allowing

<sup>148</sup> a) Schöllkopf, U.; Groth, U.; Deng, C. *Angew. Chem. Int. Ed. Engl.* **1981**, *20*, 798. b) Pearson, A. J.; Lee, S.-H.; Gouzoules, F. *J. Chem. Soc., Perkin Trans. 1* **1990**, 2251. c) Pearson, A. J.; Bruhn, P. R.; Gouzoules, F.; Lee, S.-H. *J. Chem. Soc., Chem. Commun.* **1989**, 659.

<sup>149</sup> a) Ermert, P.; Meyer, J.; Stucki, C.; Schneebeli, J.; Obrecht, J.-P. *Tetrahedron Lett.* **1988**, *29*, 1265. b) Sinclair, P. J.; Zhai, D.; Reibenspies, J.; Williams, R. M. *J. Am. Chem. Soc.* **1986**, *108*, 1103. c) Williams, R. M.; Hendrix, J. A. *J. Org. Chem.* **1990**, *55*, 3723.

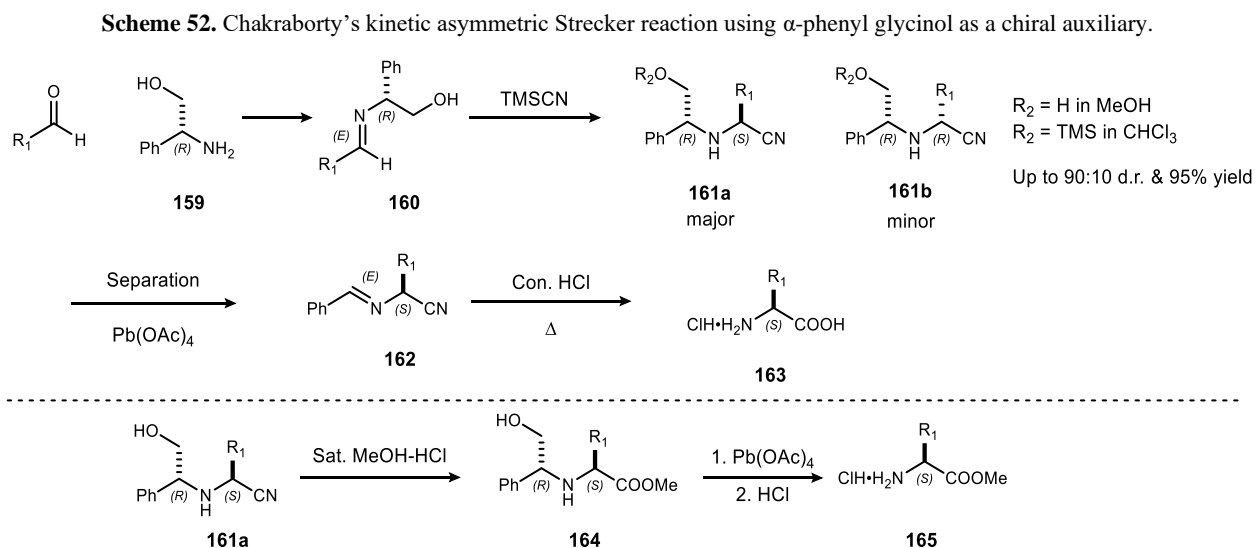
<sup>150</sup> Strecker, A. *Ann.* **1850**, *75*, 27.

<sup>151</sup> Miller, S. L. *Science* **1953**, *117*, 528.; Parker, E. T.; Zhou, M.; Burton, A. S.; Glavin, D. P.; Dworkin, J. P.; Krishnamurthy, R.; Fernández, F. M.; Bada, J. L. *Angew. Chem. Int. Ed.* **2014**, *53*, 8132.

<sup>152</sup> Harada, K. *Nature* **1963**, *200*, 1201.

<sup>153</sup> Chakraborty, T. K.; Reddy, G. V.; Azhar Hussain, K. *Tetrahedron Lett.* **1991**, *32*, 7597.

access to both L- and D-amino acids. The amino acids were synthesized through the condensation between (*R*)-2-phenylglycinol (**14**) and an aldehyde (**13**) to generate the imine (**15**). Addition of trimethylsilyl cyanide generated the  $\alpha$ -amino carbonitrile (**16**) with up to 90:10 dr in favor of the



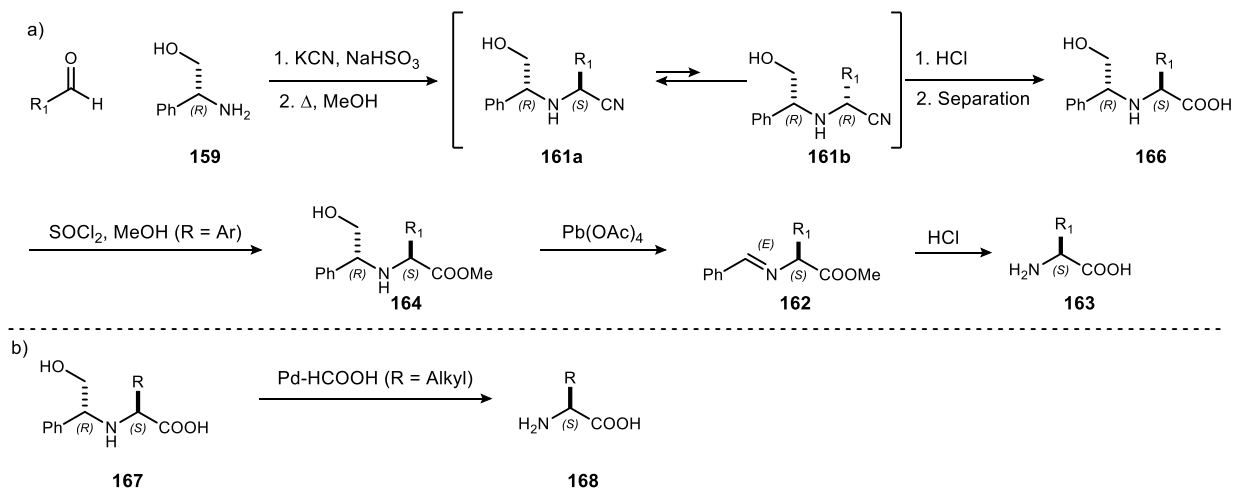
(*R,S*) diastereomer and up to 95% yield for the combination of both diastereomers (**Scheme 52**).

The preference for the transition state leading to the (*R,S*) diastereomer by *Re*-face attack on the imine, over that which leads to the (*S,S*) diastereomer, is presumably dictated not only by sterics, but also by stabilization provided by an intramolecular 5-membered cyclic hydrogen-bond interaction between the alcohol and imine. As such, employment of  $\alpha$ -phenylglycinol provided better diastereoselectivity in comparison to  $\alpha$ -methyl benzyl amine. Separation of diastereomers by column chromatography, oxidative cleavage with lead tetraacetate yields the imine (**162**), and subsequent hydrolysis of cyano and imine groups provided the  $\alpha$ -amino acids (**163**). Alternatively, nitrile hydrolysis with methanolic-HCl followed by removal of the chiral auxiliary afforded the enantiopure  $\alpha$ -amino acid methyl esters (**165**) in 5 steps overall from the aldehyde.

Ogura and coworkers simultaneously reported the use of  $\alpha$ -phenylglycinol as a chiral auxiliary in the asymmetric Strecker reaction.<sup>154</sup> The diastereoselectivity using their conditions is controlled

<sup>154</sup> Inaba, T.; Kozono, I.; Fujita, M.; Ogura, K. *Bull. Chem. Soc. Jpn.* **1992**, *65*, 2359.

**Scheme 53.** Ogura's thermodynamic asymmetric Strecker reaction using  $\alpha$ -phenyl glycinol as a chiral auxiliary.

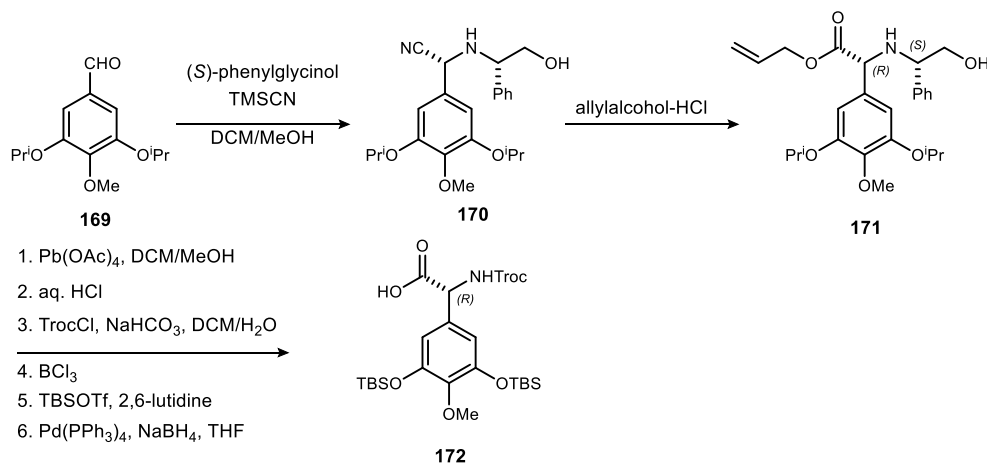


thermodynamically as opposed to the kinetically controlled selectivity described above. Ogura prepared the  $\alpha$ -amino carbonitrile as a mixture of diastereomers from an aldehyde,  $\alpha$ -phenylglycinol **159**, potassium cyanide and sodium bisulfite (**Scheme 53**). Heating the mixture in methanol produced an equilibrium mixture with a diastereomeric ratio of up to 84:16 in favor of the (*R,S*) diastereomer **161a**, which was hydrolyzed to carboxylic acid **166** and separated by column chromatography.  $\alpha$ -Aryl amino acids **163** were obtained in three steps from the protected  $\alpha$ -amino acid by conversion to the methyl ester **164**, oxidation to the imine (**162**), and hydrolysis. Ogura also found that  $\alpha$ -alkyl amino acids **168** could be obtained in one step from the protected  $\alpha$ -amino acid (**167**) by a palladium catalyzed hydrogenolysis in the presence of formic acid.

This methodology later proved to be practical and effective as demonstrated by Jieping Zhu and coworkers in their synthesis of the C-D-E ring of vancomycin.<sup>155</sup> Treatment of 4-methoxy-3,5-diisopropoxy benzaldehyde **169** (prepared in 6 steps from methyl gallate) with (*S*)-phenylglycinol followed by addition of TMSCN provided the  $\alpha$ -amino carbonitrile **170** as a mixture of diastereomers, which were separated by chromatography to afford the (*R,S*) diastereomer in 86% yield (**Scheme 54**). However, acidic hydrolysis of the cyano group to the amino acid in this case proved not to be as straightforward and facile as described by Chakraborty

<sup>155</sup> Zhu, J.; Bouillon, J.-P.; Singh, G. P.; Chastanet, J.; Bengelmans, R. *Tetrahedron Lett.* **1995**, *36*, 7081.

**Scheme 54.** Zhu's application of the asymmetric Strecker reaction to the synthesis of vancomycin.



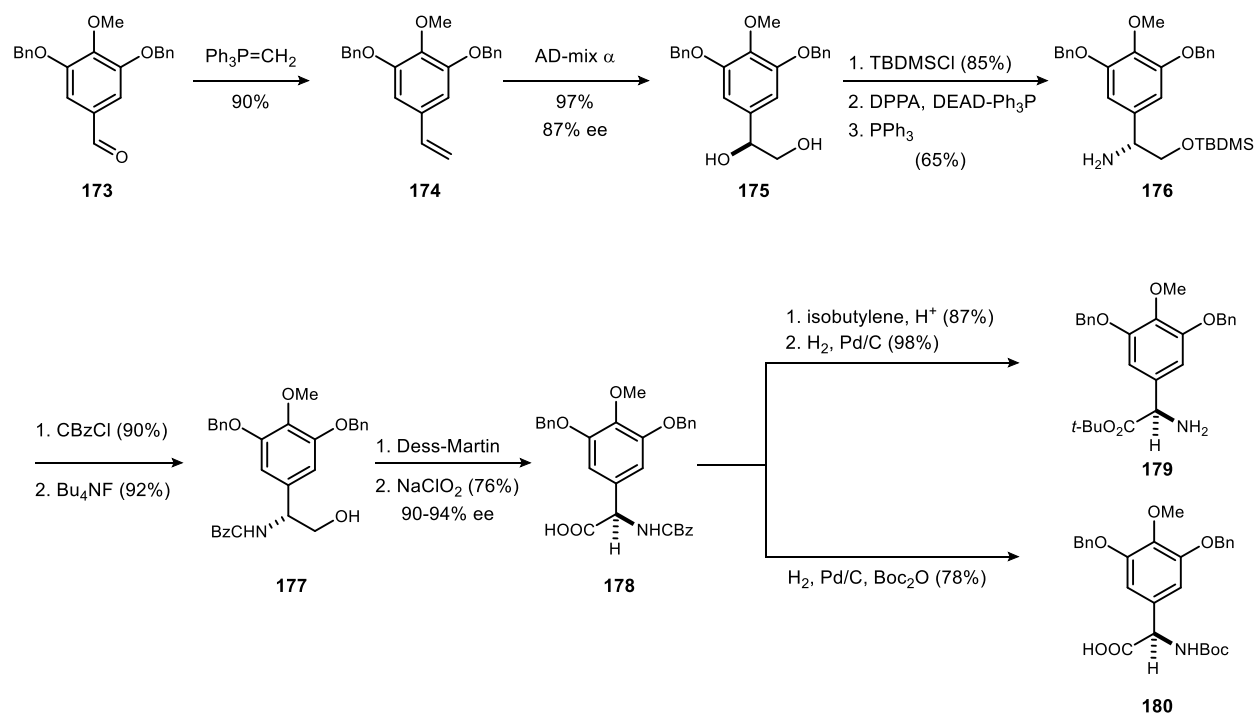
or Ogura. Instead, the cyano group was transformed into the  $\alpha$ -amino allyl ester **171** using gaseous HCl-saturated allyl alcohol. Ultimately, a subsequent series of protections and deprotections afforded the *N*-Troc amino acid (**172**) in 6 steps from the aldehyde with 80% ee as determined by a 9:1 dr when reacted with optically pure  $\alpha$ -methyl benzylamine.

Shortly after Zhu demonstrated the efficacy of the asymmetric Strecker reaction for the synthesis of the core aryl glycine motif of vancomycin, Boger and coworkers, also in pursuit of the highly sought-after glycopeptide, implemented the Sharpless asymmetric dihydroxylation to access the aforementioned amino acid.<sup>156</sup> Wittig olefination of aldehyde **173** provides styrene **174**, which was treated with AD-mix- $\alpha$  to give diol **175** with excellent yield and good enantioselectivity (**Scheme 55**). The primary alcohol was protected as the TBDMS ether, and the secondary alcohol was activated under Mitsunobu conditions, which allowed for inversion of the stereocenter by azide displacement. Staudinger reduction of the azide followed by protection of the amine (**176**) and deprotection of the alcohol afforded the Cbz-amino alcohol **177** with stereochemical integrity maintained at 85-87% ee. Recrystallization provided enantioenriched **33** (>94% ee), and the alcohol was oxidized to the acid (**178**). Further protecting group manipulations provided either the *t*-butyl amino ester (**179**) or the *N*-Boc amino acid (**180**) in 10 and 9 steps, respectively, from the aldehyde.

<sup>156</sup> Boger, D. L.; Borzilleri, R. M.; Nukui, S. *J. Org. Chem.* **1996**, *61*, 3561.



**Scheme 55.** Sharpless asymmetric dihydroxylation.



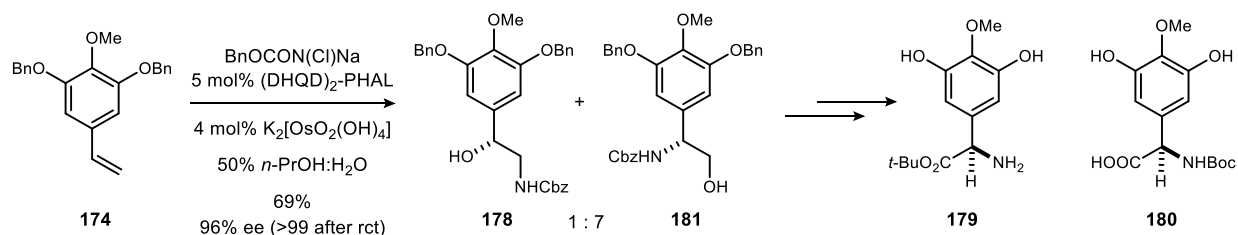
One year later, Boger reported the synthesis of the vancomycin CD and DE ring systems.<sup>157</sup> Therein, the syntheses of amino acid derivatives **179** and **180** were shortened by four steps and the ee was improved from 87% ee (AD) to 96% after the development and application of the Sharpless asymmetric aminohydroxylation (AA) (Scheme 56). The Sharpless Asymmetric Aminohydroxylation<sup>158</sup> has seen extensive application in synthesis over the years,<sup>159</sup> and in this case the reaction improved enantioselectivity. However, methods have not perfected regioselectivity, always leading to some of the undesired regioisomer **181**.

<sup>157</sup> Boger, D. L.; Borzilleri, R. M.; Nukui, S.; Beresis, R. T. *J. Org. Chem.* **1997**, *62*, 4721.

<sup>158</sup> (a) Li, G.; Chang, H.-T.; Sharpless, K. B. *Angew. Chem. Int. Ed. Engl.* **1996**, *35*, 451. (b) Li, G.; Angert, H. H.; Sharpless, K. B. *Angew. Chem. Int. Ed. Engl.* **1996**, *35*, 2813.

<sup>159</sup> For reviews on synthetic applications see: Heravi, Majid M.; Lashaki, T. B.; Fattahi, B.; Zadsirjan, V. *RSC Adv.* **2018**, *8*, 6634.; Bodkin, J. A.; McLeod, M. D. *J. Chem. Soc., Perkin Trans. 1* **2002**, 2733. O'Brien, P. *Angew. Chem. Int. Ed.* **1999**, *38*, 326.

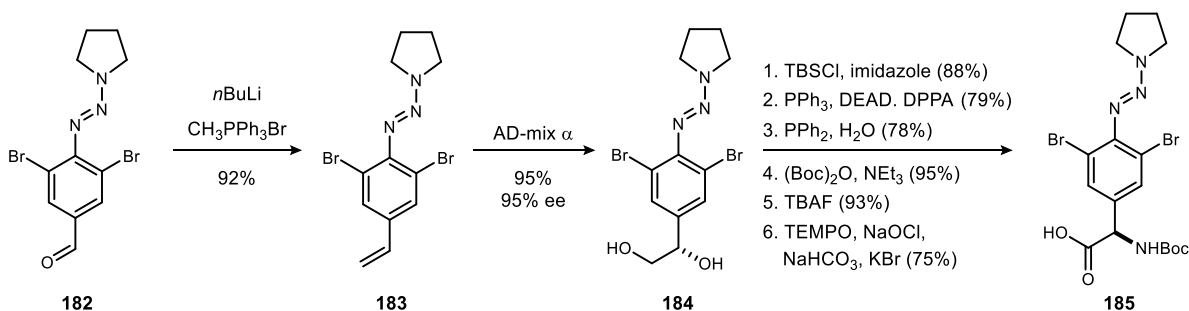
**Scheme 56.** Sharpless asymmetric aminohydroxylation.



In 1998, concomitant, independent reports on the total synthesis of vancomycin aglycon were published as consecutive articles in *Angewandte Chemie* by both Evans and Nicolaou.<sup>160,161</sup> Nicolaou utilized both the Sharpless asymmetric aminohydroxylation as well as the Sharpless dihydroxylation in this synthesis. In the case of the core  $\alpha$ -aryl glycine derivative (AA-4), derivatization of *para*-amino benzoic acid afforded aldehyde **182** (Scheme 57). Wittig olefination to styrene **183** followed by asymmetric dihydroxylation gave diol **184**. Mitsunobu activation, azide displacement, and subsequent protection/deprotection and oxidation sequences ultimately afforded amino acid **185** in 8 steps from the aldehyde with 95% ee.

Evans applied oxazolidinone-based methodology towards the asymmetric synthesis of residues contained within the vancomycin aglycon as well as eremomycin aglycon.<sup>161</sup> The chiral-auxiliary

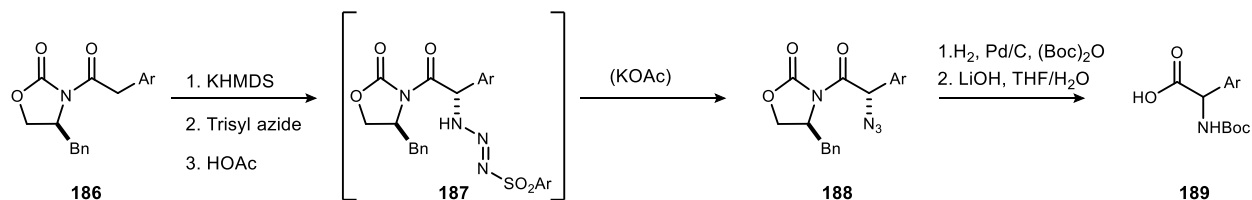
**Scheme 57.** Nicolaou's synthesis of AA-4 of vancomycin aglycon.



<sup>160</sup> a) Nicolaou, K. C.; Natarajan, S.; Li, H.; Jain, N. F.; Hughes, R.; Solomon, M. E.; Ramanjulu, J. M.; Boddy, C. N. C.; Takayanagi, M. *Angew. Chem. Int. Ed.* **1998**, *37*, 2708.; b) Nicolaou, K. C.; Jain, N. F.; Natarajan, S.; Hughes, R.; Solomon, M. E.; Li, H.; Ramanjulu, J. M.; Takayanagi, M.; Koumbis, A. E.; Bando, T. *Angew. Chem. Int. Ed.* **1998**, *37*, 2714.; c) Nicolaou, K. C.; Takayanagi, M.; Jain, N. F.; Natarajan, S.; Koumbis, A. E.; Bando, T.; Ramanjulu, J. M. *Angew. Chem. Int. Ed.* **1998**, *37*, 2717.

<sup>161</sup> !!! INVALID CITATION !!! Evans, D. A.; Wood, M. R.; Trotter, B. W.; Richardson, T. I.; Barrow, J. C.; Katz, J. L. *Angew. Chem. Int. Ed.* **1998**, *37*, 2700. Evans, D. A.; Wood, M. R.; Trotter, B. W.; Richardson, T. I.; Barrow, J. C.; Katz, J. L. *Angew. Chem. Int. Ed.* **1998**, *37*, 2700.

**Scheme 58.** Evans' chiral-auxiliary based enolate azidation.



based electrophilic enolate azidation effected the synthesis of Dpg residues as well as the previously reported synthesis of echinocandin.<sup>162</sup> This process generates the carboximide enolate of **186**, which will add to the “(+)-N<sub>3</sub> synthon”, trisyl azide, to generate the triazene intermediate (**187**) (Scheme 58).

Diastereoselectivity is dictated by the benzyl moiety of the chiral auxiliary, which promotes attack on the azide from the least hindered side of the enolate plane.<sup>163</sup> Potassium acetate, produced during the reaction quench, will promote triazene decomposition to afford the azide (**188**). Reduction of the azide by hydrogenolysis, *in situ* amine protection, and cleavage of the chiral auxiliary ultimately affords the protected *N*-Boc amino acid (**189**). Furthermore, this endgame sequence can be adjusted to cater to functional groups sensitive to hydrogenolysis, such as the benzyl ethers commonly used for protecting DPG residues. This is achieved in three steps by reducing the azide with SnCl<sub>2</sub> in dioxane/H<sub>2</sub>O, followed by Boc protection and chiral auxiliary removal. This chiral-pool based approach holds the advantage of readily accessible starting materials, and access to many functionalized derivatives of aryl glycines from the corresponding carboxylic acid.

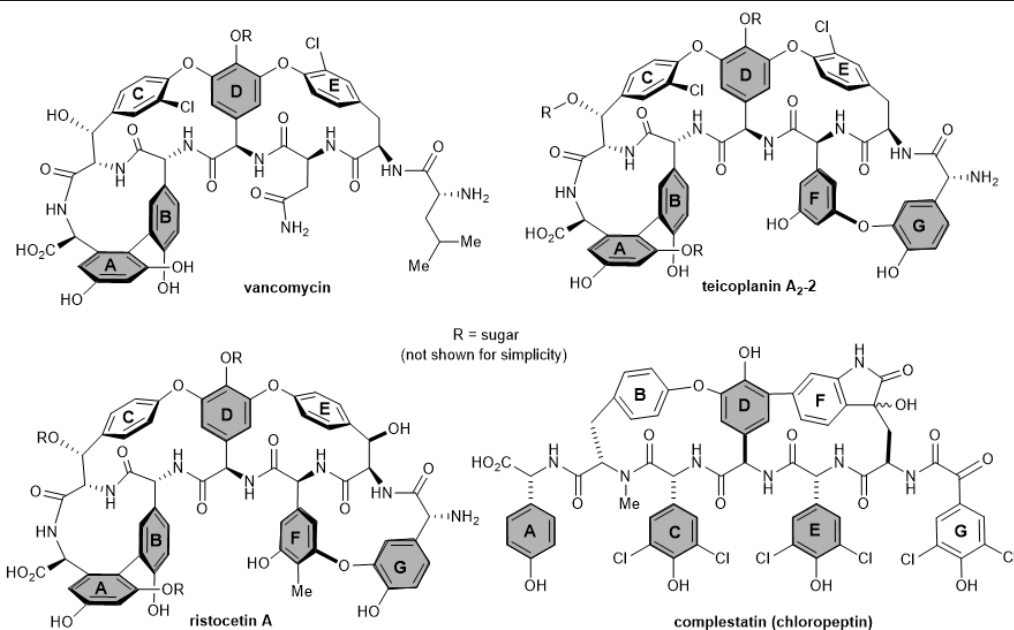
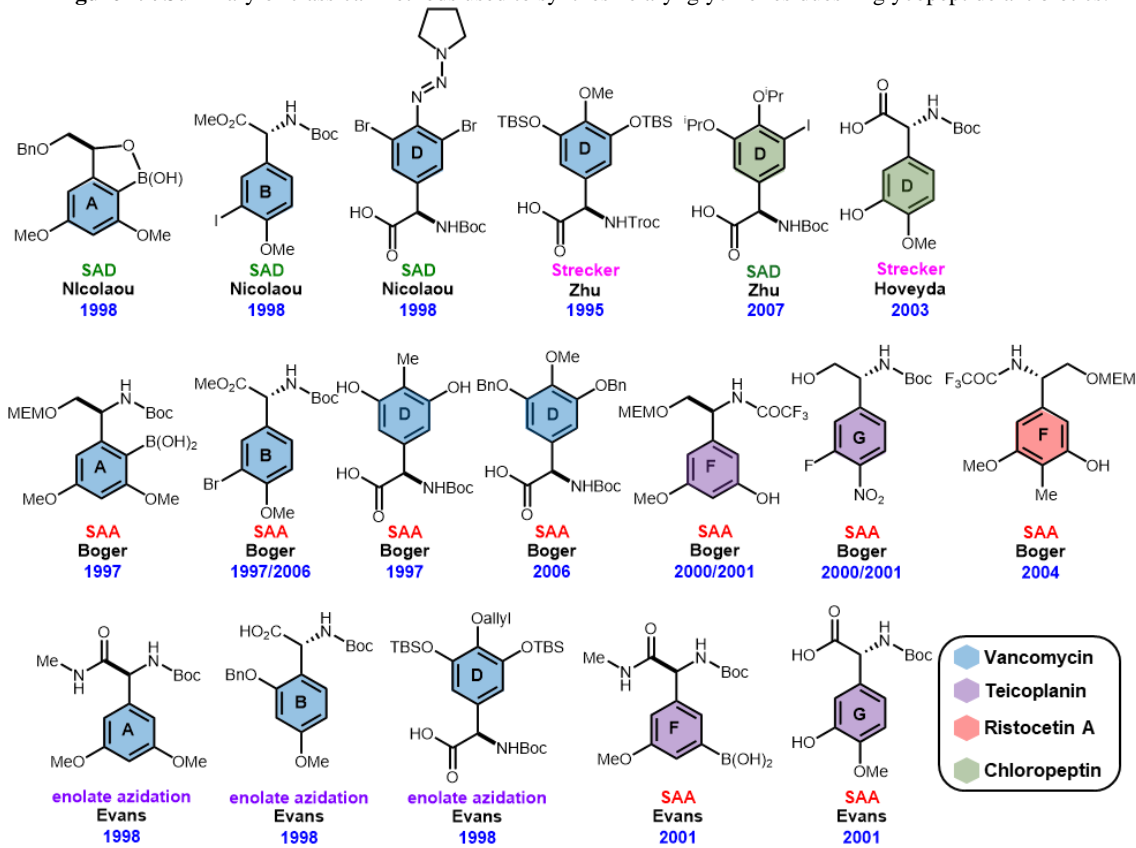
Ultimately, a limited number of reactions have been used toward the requisite  $\alpha$ -aryl amino acids for the synthesis of glycopeptide antibiotics (Figure 19). A summary of methods used is presented in Figure 19, which shows that over the course of a decade (1997-2007), only four reactions had been employed to make the amino acids. Even more so, the majority of methods that have been

<sup>162</sup> Evans, D. A.; Weber, A. E. *J. Am. Chem. Soc.* **1987**, *109*, 7151.

<sup>163</sup> a) Evans, D. A.; Britton, T. C.; Ellman, J. A.; Dorow, R. L. *J. Am. Chem. Soc.* **1990**, *112*, 4011.; b) Evans, D. A.; Evrard, D. A.; Rychnovsky, S. D.; Fruh, T.; Whittingham, W. G.; Devries, K. M. *Tetrahedron Lett.* **1992**, *33*, 1189.

developed in the past twenty years to make  $\alpha$ -aryl glycine residues (post 2000) have not been applied in total synthesis.

**Figure 19.** Summary of classical methods used to synthesize aryl glycine residues in glycopeptide antibiotics.<sup>a</sup>



<sup>a</sup>The represented glycopeptides all share common core structures & amino acids, thus if methodology was applied by the same research group to make the same amino acid but for a different target, it is not included here. SAD = Sharpless asymmetric dihydroxylation; SAA = Sharpless asymmetric aminohydroxylation.

For example, the diastereoselective Strecker reaction has seen extensive application in total synthesis<sup>164</sup> and has even been used to generate radio-labeled amino acids through the use of  $K^{14}CN$ .<sup>165</sup> However, while enantioselective variants of the Strecker reaction have also been developed, most methods have not yet seen application in total synthesis.<sup>166</sup> An exception has been the development and application of a Ti-catalyzed Strecker reaction<sup>167</sup> toward the synthesis of chloropeptin I<sup>168</sup> by the Hoveyda group. This reaction employs a chiral Schiff base as a ligand and was shown to provide the aryl glycine to be used as the D ring in chloropeptin (**Scheme 59**). The cyanide addition provided **191** with 93% ee, which was further converted to arrive at amino acid **192** (98% ee, 50% over 4 steps). Chai and coworkers were also successful in using titanium to catalyze an asymmetric Strecker reaction using an amino alcohol ligand.<sup>169</sup>

---

<sup>164</sup> For select examples of the diastereoselective Strecker applied in total synthesis see: a) chloropeptin: Roussi, G.; Zamora, E. G.; Carbonnelle, A.-C.; Beugelmans, R. *Tetrahedron Lett.* **1997**, *38*, 4401.; Roussi, G.; Zamora, E. G.; Carbonnelle, A. C.; Beugelmans, R. *Heterocycles* **1999**, *51*, 2041.; b) (-)-hemiasterlin: Vedejs, E.; Kongkittingam, C. *J. Org. Chem.* **2001**, *66*, 7355.; c) 7-methoxybenzolactam-V8: Sakamuri, S.; Kozikowski, A. P. *Chem. Commun.* **2001**, 475.

<sup>165</sup> Song, F.; Salter, R.; Weaner, L. E. *Journal of Labelled Compounds and Radiopharmaceuticals* **2015**, *58*, 173.

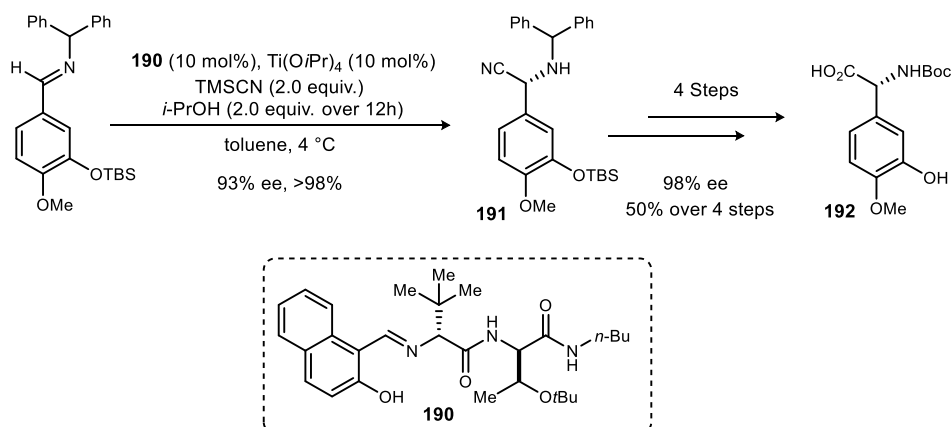
<sup>166</sup> For reviews see: a) Nájera, C.; Sansano, J. M. *Chem. Rev.* **2007**, *107*, 4584.; b) Wang, J.; Liu, X.; Feng, X. *Chem. Rev.* **2011**, *111*, 6947.; c) Cai, X.-H., Bing, Xie *Arkivoc* **2014**, 205.

<sup>167</sup> Krueger, C. A.; Kuntz, K. W.; Dzierba, C. D.; Wirschun, W. G.; Gleason, J. D.; Snapper, M. L.; Hoveyda, A. H. *J. Am. Chem. Soc.* **1999**, *121*, 4284.; Josephsohn, N. S.; Kuntz, K. W.; Snapper, M. L.; Hoveyda, A. H. *J. Am. Chem. Soc.* **2001**, *123*, 11594.

<sup>168</sup> Deng, H.; Jung, J.-K.; Liu, T.; Kuntz, K. W.; Snapper, M. L.; Hoveyda, A. H. *J. Am. Chem. Soc.* **2003**, *125*, 9032.

<sup>169</sup> Ramalingam, B.; Seayad, A. M.; Chuanzhao, L.; Garland, M.; Yoshinaga, K.; Wadamoto, M.; Nagata, T.; Chai, C. L. *Adv. Synth. Catal.* **2010**, *352*, 2153.

**Scheme 59.** Hoveyda's application of an enantioselective Ti-catalyzed Strecker reaction to chloropeptin I.

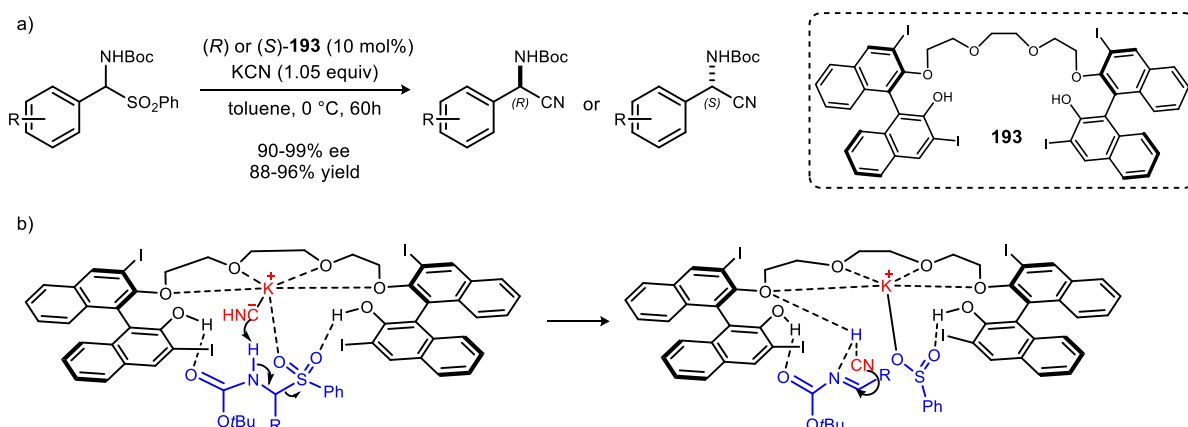


Many other metal-catalyzed Strecker reactions have been successful and have been summarized in several reviews.<sup>170</sup> In those reviews one can also find reports on organocatalyzed enantioselective Strecker reactions. One example of methodology that could see significant application on an industrial scale was developed by Yan et al. They discovered a unique phase-transfer catalyzed enantioselective Strecker reaction wherein the chiral bis-hydroxy polyether **193** is used as a chiral anion generator (**Scheme 60**).<sup>171</sup> Control experiments showed that the using the  $\alpha$ -amido sulfone (vs. preformed aldimine) was important for both enantioselection and reactivity. It was also demonstrated that excess potassium cyanide decreased ee. Yan postulated that cyanide anion plays the role of both the base and nucleophile and that the sulfinate anion is essential to making the necessary chiral cage for enantioselection as shown in **Scheme 60**. This reaction proceeded with high ee over a range of substrates and the catalyst can be recycled and easily separated, making it amenable to application on large scale. Moreover, the catalyst is easily prepared and both enantiomers are readily available making this reaction a particularly attractive option for the synthesis of  $\alpha$ -aryl amino acids.

<sup>170</sup> Cai, X.-H., Bing, Xie *Arkivoc* **2014**, 205.; Wang, J.; Liu, X.; Feng, X. *Chem. Rev.* **2011**, *111*, 6947.; Groger, H. *Chem. Rev.* **2003**, *103*, 2795.

<sup>171</sup> Yan, H.; Suk Oh, J.; Lee, J.-W.; Eui Song, C. *Nat. Commun.* **2012**, *3*, 1212.

**Scheme 60.** Enantioselective phase-transfer catalyzed Strecker reaction.



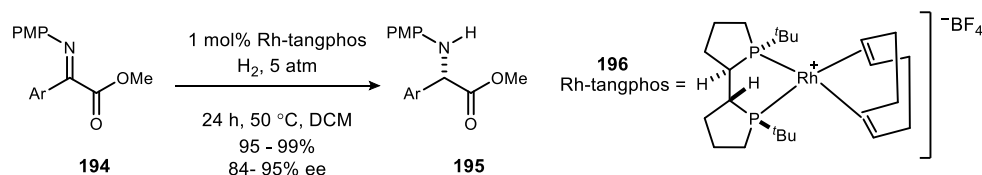
In addition to the methods described *vide supra*, a number of unique approaches to aryl glycine synthesis have presented themselves. Asymmetric hydrogenation of  $\alpha$ -dehydroamino acids has proven an effective method for the stereoselective synthesis of  $\alpha$ -alkyl amino acids, generally providing good yields and excellent enantioselectivity. Given the absence of a  $\beta$ -hydrogen, and therefore the inability to access  $\alpha$ -dehydroamino acids of  $\alpha$ -aryl glycines, this method is not applicable for their synthesis.<sup>172,173</sup> However, asymmetric hydrogenation to provide  $\alpha$ -aryl glycines may be performed by instead reducing the C=N bond of  $\alpha$ -imino acids or esters.<sup>173</sup> Zhang achieved this transformation on PMP-protected  $\alpha$ -aryl imino esters **194** using a Rh-tangphos catalyst (**196**) to afford aryl glycine derivatives **195** with 95-99% conversion and 84-95% ee (**Scheme 61**). While catalyst loadings and difficult imine preparation may limit the application of this work, the one step transformation is applicable to a range of aryl groups. Notably, electronic factors respective to the aryl moiety did not impact yield or selectivity, and the PMP group can be removed by CAN with no effect on the ee. Additionally, use of the (*R,R,S,S*) catalyst in lieu of (*S,S,R,R*) (shown) allows for access to both enantiomers.

<sup>172</sup> Tang, W.; Zhang, X. *Chem. Rev.* **2003**, *103*, 3029.

<sup>173</sup> Shang, G.; Yang, Q.; Zhang, X. *Angew. Chem. Int. Ed.* **2006**, *45*, 6360.

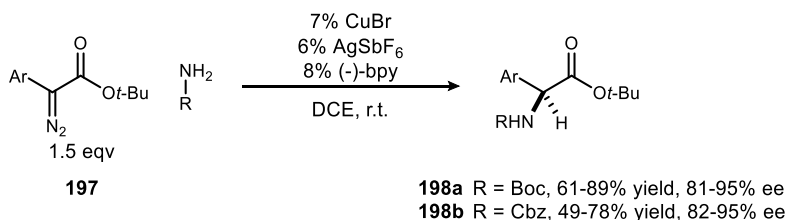


**Scheme 61.** Catalytic asymmetric hydrogenation of  $\alpha$ -imino esters.



Stereocontrol in aryl glycine synthesis has also been achieved by Fu and Lee.<sup>174</sup> With the use of a chiral copper/bipyridine catalyst, they effected the asymmetric N-H insertion of carbamates into  $\alpha$ -aryl- $\alpha$ -diazo esters (**197**) as a means to access *N*-Boc aryl glycine derivatives **198a**. This transformation provides the aryl glycines in one step with 61-89% yield and good to excellent ee (**Scheme 62**). This procedure is also applicable to the synthesis of *N*-Cbz-protected aryl glycines **198b**, albeit with lower yields (49-78%).

**Scheme 62.** Fu's asymmetric N-H insertion.

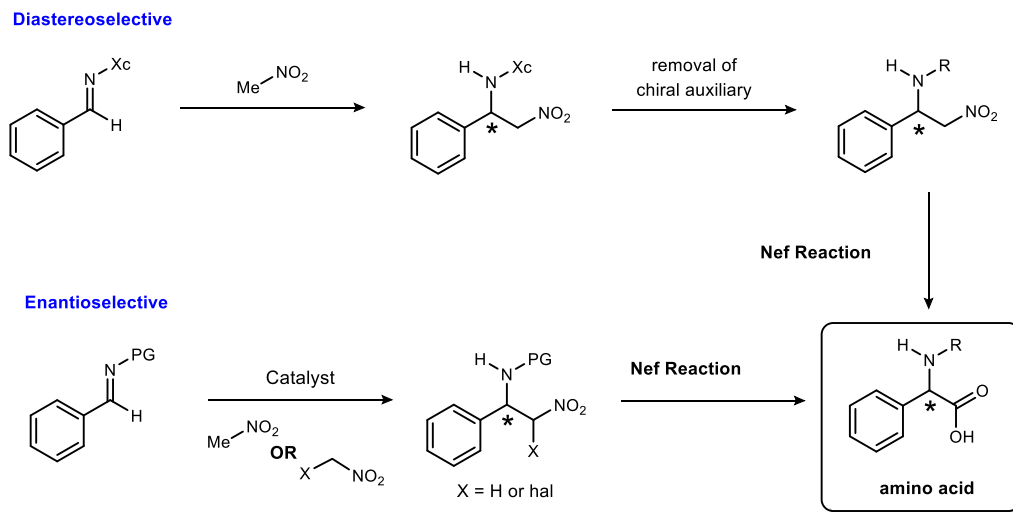


Another useful procedure to make  $\alpha$ -aryl amino acids is through the stereoselective aza-Henry reaction, followed by a nitro to carbonyl (Nef) reaction. The general reaction scheme shown in **Scheme 63**. The aza-Henry reaction can be carried out in a diastereo- or enantioselective fashion

<sup>174</sup> Lee, E. C.; Fu, G. C. *J. Am. Chem. Soc.* **2007**, *129*, 12066.

using a variety of catalysts and conditions.<sup>175</sup> Similarly, many conditions and variations of the Nef reaction exist.<sup>176,177</sup> A more in-depth discussion of this approach can be found in Chapter 3.

**Scheme 63.** Aza-Henry reaction followed by a Nef reaction provides  $\alpha$ -aryl amino acids.



An interesting two-step approach to aryl glycinamides was developed by Rawal and coworkers.<sup>178</sup> This strategy used a cinchona alkaloid-based catalyst (**199**) to catalyze the addition of ‘masked acyl cyanides’ into *N*-Boc aldimines in high yield and with good enantioselection. The “unmasking” event takes place upon treatment with TASF to generate the acyl cyanide. This is performed in the presence of an amine, which reacts with the active ester to form the amide (**Scheme 64**). This reaction has a wide functional group tolerance for both the aldimine and amine used. However, one of the drawbacks to this approach is the choice of catalyst. It is a well-known phenomenon that psuedoenantiomers of cinchona-alkaloid based catalysts don’t always perform

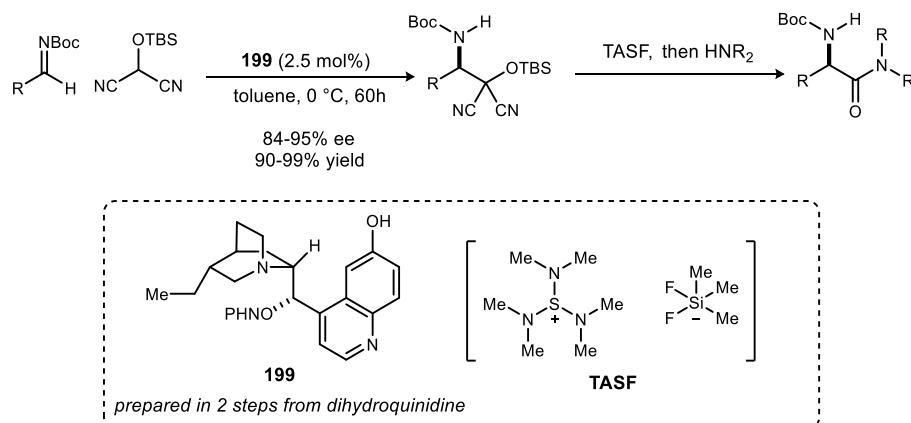
<sup>175</sup> For reviews see a) Ana, M. F. P. *Current Organocatalysis* **2016**, 3, 222.; b) Marqués-López, E.; Merino, P.; Tejero, T.; Herrera, R. P. *Eur. J. Org. Chem.* **2009**, 2009, 2401.; c) Westermann, B. *Angew. Chem. Int. Ed.* **2003**, 42, 151.

<sup>176</sup> Discovery & pioneering studies: a) Konovalov, M. *J. Russ. Phys. Chem. Soc.* **1893**, 25, 509.; b) Meyer, V.; Wurster, C. *Berichte der deutschen chemischen Gesellschaft* **1873**, 6, 1168.; c) Nef, J. U. *Ann.* **1894**, 280, 263.; d) Konowalow, M. *Berichte der deutschen chemischen Gesellschaft* **1896**, 29, 2193.; e) Bamberger, E.; Rüst, E. *Berichte der deutschen chemischen Gesellschaft* **1902**, 35, 45.; f) Lippincott, S. B.; Hass, H. B. *Industrial & Engineering Chemistry* **1939**, 31, 118.; g) Kamlet, M. J.; Kaplan, L. A.; Dacons, J. C. *J. Org. Chem.* **1961**, 26, 4371.; h) Kornblum, N.; Brown, R. A. *J. Am. Chem. Soc.* **1965**, 87, 1742.

<sup>177</sup> For reviews on the Nef reaction see: Noland, W. E. *Chem. Rev.* **1955**, 55, 137.; Ballini, R.; Petrini, M. *Tetrahedron* **2004**, 60, 1017.; Ballini, R.; Petrini, M. *Adv. Synth. Catal.* **2015**, 357, 2371.

<sup>178</sup> Yang, K. S.; Rawal, V. H. *J. Am. Chem. Soc.* **2014**, 136, 16148.

**Scheme 64.** Rawals' use of "masked acyl cyanides" to synthesize aryl glycinamides.



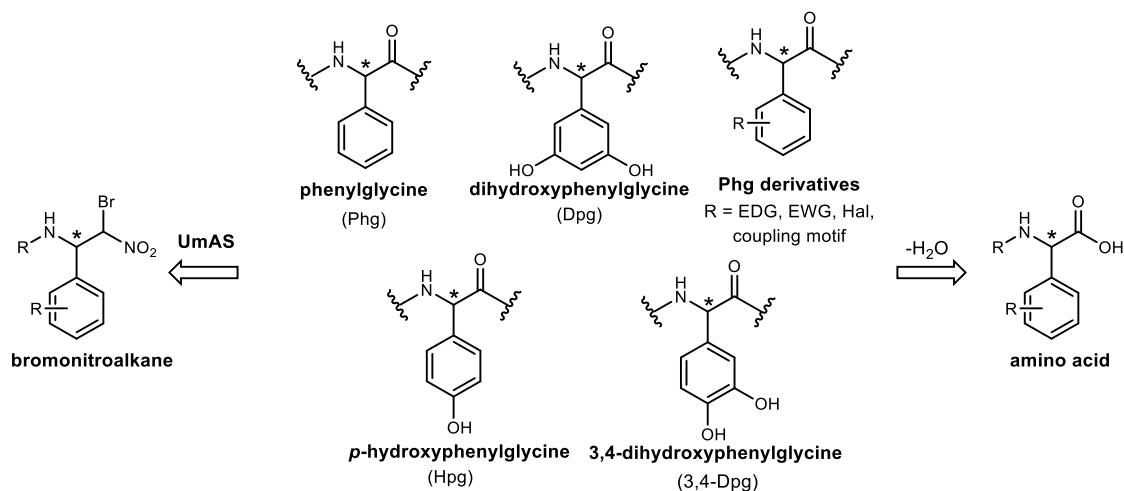
with the same selectivity or turnover. This typically results in one enantiomer of the product being much more readily available than the other. In this work, however, the pseudoenantiomer only slightly lowered the ee & reactivity.

## 2.2 Umpolung Amide Synthesis with electron-rich $\alpha$ -bromo nitroalkanes

### 2.2.1 Project overview

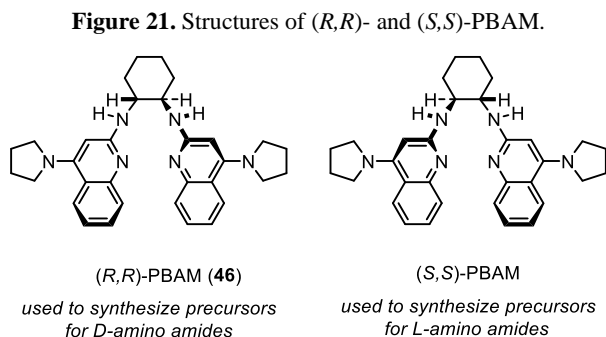
Umpolung Amide Synthesis is a uniquely attractive method for the synthesis of aryl glycine containing peptides, due to the mild reaction conditions and mechanistic avoidance of an activated ester. We have examined the generalization of peptide homologation with aryl glycinamides, with

**Figure 20.** Structures of targeted phenyl glycinamide derivatives.



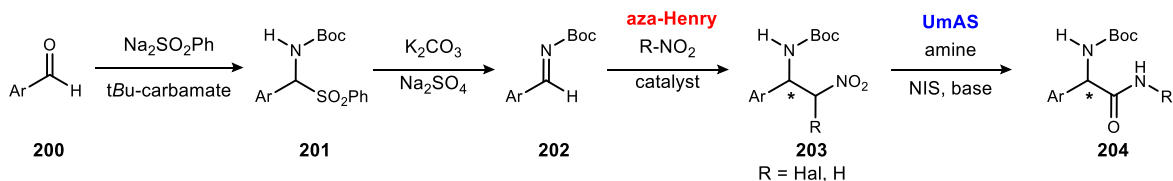
the aims of (i) streamlining the process to abbreviate the sequence length, (ii) utilizing readily available and inexpensive starting materials (aldehydes), and (iii) perfecting the stereochemical aspects of the process overall. Specifically, we sought to develop a short synthesis of  $\alpha$ -bromonitroalkane donors for the on-demand synthesis of peptides that contain non-natural Phg, Dpg, and 3,4-Dpg derivatives (**Figure 20**).

The development of the enantioselective addition of nitroalkanes<sup>39,40,41</sup> and bromonitromethane<sup>42,43, 44,89,127</sup> into imines via the chiral bis-amidine (BAM) catalyzed aza-Henry reaction has provided precedent for the synthesis of the acyl donors in high yield and high ee. Moreover, the availability of (*R,R*) and (*S,S*) catalysts (e.g. PBAM, **Figure 21**) allows for access to both enantiomers of the product.



The UmAS approach allows for the catalytic and stereoselective access to amides containing aryl glycine residues in four steps from an aldehyde. As described in **Scheme 65**, the aldehyde (**200**) is converted to the  $\alpha$ -amido sulfone (**201**), which serves as a bench-stable intermediate for the synthesis of imines **202**. Chiral proton catalysis using the BAM-catalyzed aza-Henry reaction provides optically active  $\beta$ -amino  $\alpha$ -halo nitroalkanes **203**. These will serve as acyl anion

**Scheme 65.** UmAS based approach to access  $\alpha$ -aryl glycine derivatives.

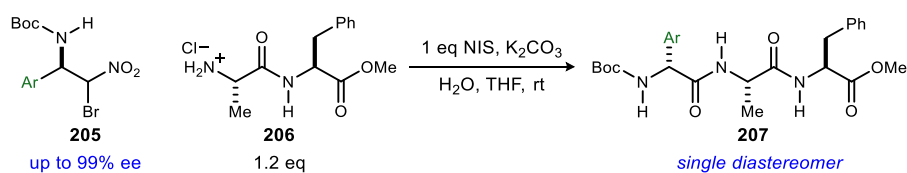


equivalents in the subsequent Umpolung Amide Synthesis reaction to provide the desired glycinamides (**204**).

Previous studies in our laboratory conducted by Dawn Makley showed that UmAS worked well for coupling various substituted aryl bromonitroalkanes as shown in **Table 10**.<sup>179</sup> The seminal paper on UmAS also showed that the *para*-chloro substituted aryl bromonitroalkane **208** was successfully coupled to all 20 canonical amino acids, with the exception of cysteine(**Scheme 66**).<sup>42</sup>

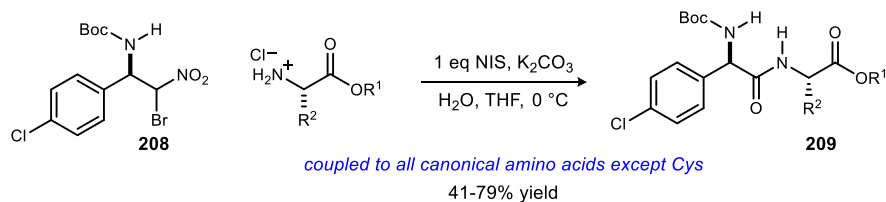
*However, the synthesis of peptides containing electron-rich aryl glycine residues such as hydroxyphenylglycine (Hpg) and dihydroxyphenylglycine (Dpg) using UmAS has presented a*

**Table 10.** Previous studies on the scope of aryl bromonitroalkanes in UmAS.



entry	Ar	yield (%)
1	<i>p</i> -Cl-(C <sub>6</sub> H <sub>5</sub> )	72
2	<i>p</i> -Br-(C <sub>6</sub> H <sub>5</sub> )	87
3	<i>p</i> -I-(C <sub>6</sub> H <sub>5</sub> )	58
4	<i>p</i> -NO <sub>2</sub> -(C <sub>6</sub> H <sub>5</sub> )	47
5	<i>p</i> -CF <sub>3</sub> -(C <sub>6</sub> H <sub>5</sub> )	60
6	<i>p</i> -MeO-(C <sub>6</sub> H <sub>5</sub> )	72
7	<i>p</i> -AcO-(C <sub>6</sub> H <sub>5</sub> )	49
8	naphthyl	50

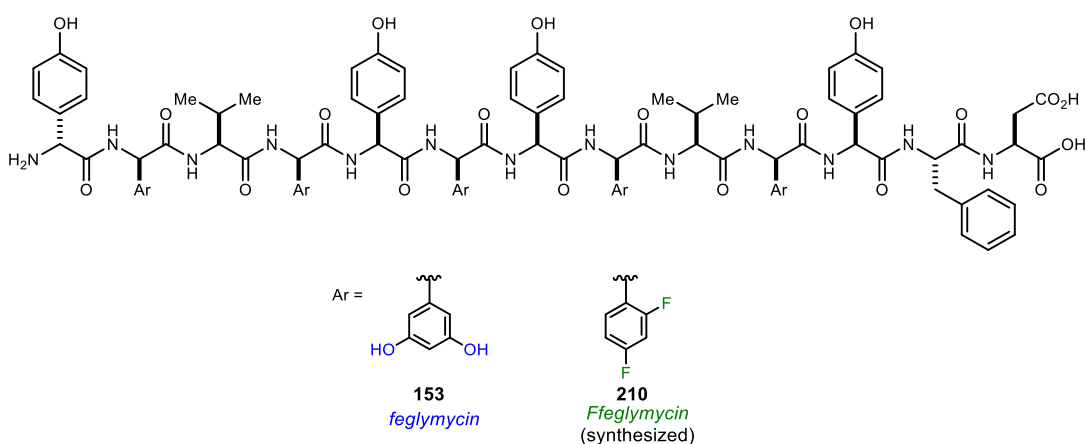
**Scheme 66.** UmAS couplings with the canonical amino acids.



<sup>179</sup> Makley, D. M., Vanderbilt University, 2012.

*unique and continuing challenge.* For example, extensive efforts in our laboratory have been directed toward the synthesis of the antibacterial and anti-HIV linear peptide feglymycin (**Scheme 67**).<sup>180</sup> The synthesis of the target has been pursued using iterative UmAS coupling for the sensitive aryl-glycine residues, in conjunction with traditional peptide couplings at natural  $\alpha$ -amino amide residues to achieve strategy-level convergence. Despite extensive hypothesis-driven investigations to solve problems as they arose, the synthesis of feglymycin could not previously be realized due to several aspects that affected overall reactivity, including poor product solubility. The solubility characteristics further complicated purifications, seemingly specific to the incorporation of benzyl-protected electron-rich Dpg residues. It became apparent however, that the difficulty in making this compound did not lie in the applicability of UmAS coupling to large peptide fragments, as the synthesis of the fluorinated derivative Ffeglymycin (**210**, **Scheme 67**)

**Scheme 67.** Structures of feglymycin and Ffeglymycin.



was achieved.

Synthesis of natural feglymycin remained the ultimate goal, owing to its documented biological activity and an opportunity for us to compare an UmAS-based approach to two syntheses dependent on standard techniques and reagents (see Chapter 3).<sup>181,182</sup> A successful synthesis would

<sup>180</sup> Doody, A. B.; Tsukanov, S. V.; Schwieter, K. E.; Makley, D. M.; Shen, B.; Johnston, J. N. *Unpublished Results*.

<sup>181</sup> Dettner, F.; Hänchen, A.; Schols, D.; Toti, L.; Nußer, A.; Süßmuth, R. D. *Angew. Chem. Int. Ed.* **2009**, *48*, 1856.

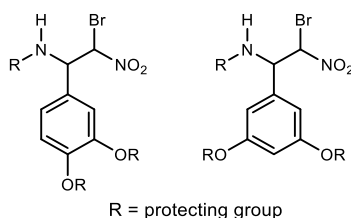
<sup>182</sup> Fuse, S.; Mifune, Y.; Nakamura, H.; Tanaka, H. *Nature Communications* **2016**, *7*, 13491.

also codify the applicability of UmAS for the synthesis of peptides containing aryl glycinamides such as the previously described glycopeptide antibiotics.

### 2.2.2 Synthesis of $\beta$ -amido $\alpha$ -bromonitroalkanes

As stated earlier, we have examined the optimization of the UmAS reaction using  $\alpha$ -bromo nitroalkanes that contain an electron-rich aryl moiety, specifically those bearing oxygen atoms at either the 3 and 5 or 3 and 4 positions (**Scheme 68**).

**Scheme 68.** Targeted  $\alpha$ -amido bromonitroalkanes.

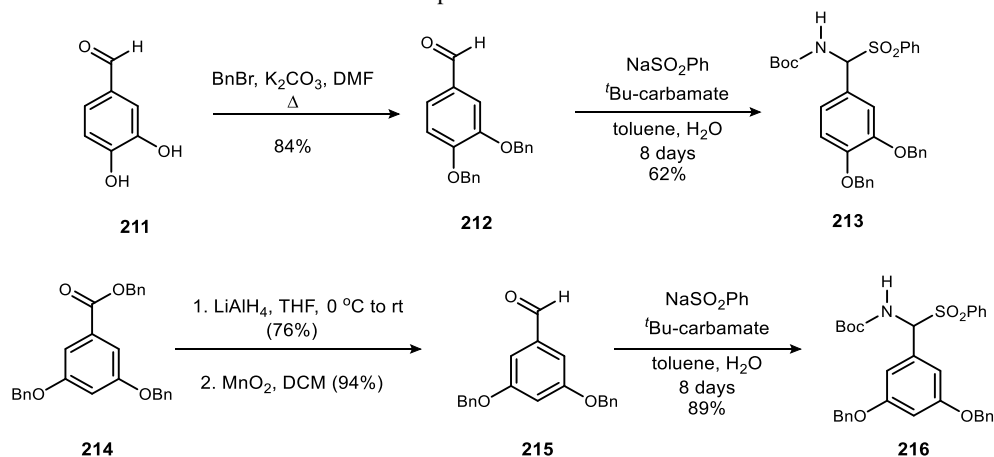


Previous efforts in our lab have explored the use of Fmoc, Cbz and Alloc nitrogen protecting groups for aryl glycinamide precursors.<sup>43,179, 183,184</sup> Based on those previous findings, we opted to Boc protect the nitrogen and protect the oxygens as benzyl ethers. The *N*-Boc and *O*-benzyl groups can be removed under epimerization-free conditions by HCl in dioxane and hydrogenolysis, respectively. To this end, the requisite aldehydes were prepared as described in **Scheme 69**. The (3,4)-bis(benzyloxy)benzaldehyde (**212**) was synthesized in good yield on multigram scale by alkylation of the commercially available (3,4)-dihydroxy benzaldehyde (**211**). Reduction of (3,5)-bis(benzyloxy)phenyl-benzyl ester **214** by LAH and subsequent oxidation of the alcohol using MnO<sub>2</sub> afforded the desired (3,5)-bis(benzyloxy)benzaldehyde **215**, also in good yield on multigram scale. With the protected aldehydes in hand, reaction with Boc-carbamate and the arylsulfinate salt provided the  $\alpha$ -amido sulfones (**213**, **216**).

<sup>183</sup> Doody, A. B., Vanderbilt University, 2014.

<sup>184</sup> Schwieter, K. E., Vanderbilt University, 2016.

**Scheme 69.** Preparation of  $\alpha$ -amido sulfones.

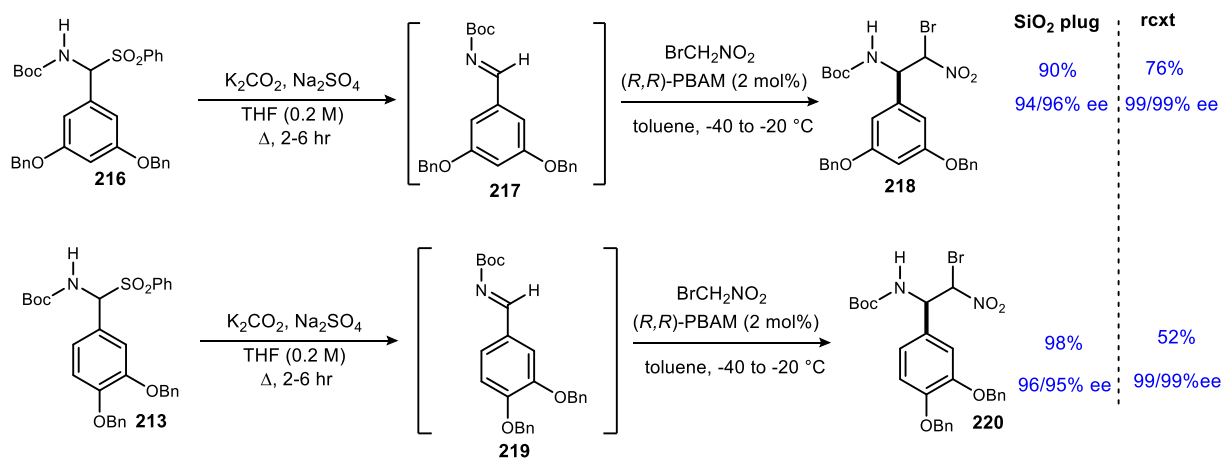


Elimination of sulfinate under basic conditions afforded the *N*-Boc aldimines (**217**, **219**) (**Scheme 70**). These imines are susceptible to hydrolysis, and were thus carried through immediately to the aza-Henry reaction following filtration and concentration (**Scheme 70**). The PBAM free base was selected to provide a baseline for enantioselection for the addition of bromonitromethane into the *N*-Boc imines. Gratifyingly, we did not need to look much further as PBAM provided the desired aza-Henry adducts in good yield, and with good enantioselection (**Scheme 70**). The 3,4-bis(benzyloxy) bromonitroalkane **220** was obtained in 96/95% ee and the 3,5-bis(benzyloxy) bromonitroalkane **218** was obtained in 94/96% ee.<sup>185</sup> Recrystallization of both bromonitroalkanes provided enantioenriched material with >99/>99% ee. Overall, this provided us with the optically active carboxylic acid surrogate in 3 steps, with high enantiomeric excess, from the corresponding aldehyde.

<sup>185</sup> Racemic *N*-Boc bromonitroalkane donors were synthesized for the development of chiral HPLC assays by activation of the imine with DMAP followed by addition of bromonitromethane ((*rac*)-**220**, 48%; (*rac*)-**218** 25% yield)



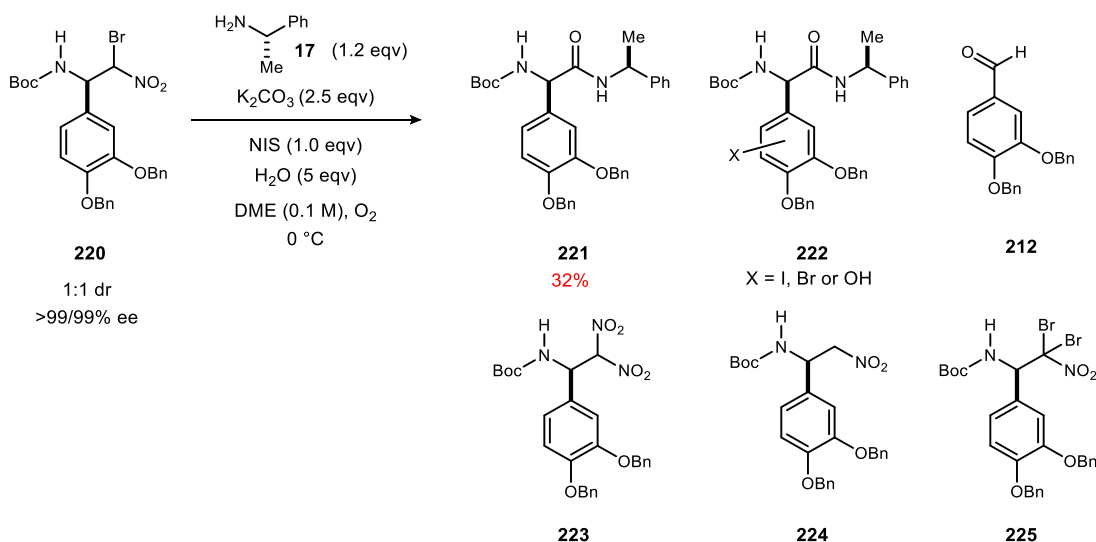
**Scheme 70.** BAM catalyzed enantioselective aza-Henry.



After the syntheses of the  $\alpha$ -bromonitroalkanes, attention was turned to the Umpolung Amide Synthesis reaction. To determine how to best improve the yield and purification process, extensive efforts were directed towards complete mass recovery from the reaction and towards the isolation and characterization of the byproducts formed. If the byproducts and route to their formation could be identified, we may find a way to circumvent or limit these reaction pathways to increase product yield. I worked toward this goal with visiting scientist Dr. Kazuyuki Tokumaru. Initially, his primary focus was on the 3,5-disubstituted aryl glycinamide precursors while I worked mainly with the 3,4-disubstituted regioisomer. Using this parallel approach, we were able to directly compare conditions, byproducts, and conclusions between two aromatic systems that have similar yet distinct electronic and steric properties. For example, the 3,5-aryl substitution pattern adds more steric bulk relative to the amide backbone, while the 3,4-aryl substitution adds more electron density to the  $\alpha$ -amido carbon. Later in the project we both transitioned to focusing on the 3,5-aryl substitution pattern for the purpose of optimizing conditions with the total synthesis of feglymycin in mind.

Toward understanding the 3,4-disubstituted system, bromonitroalkane **220** was reacted with (*S*)- $\alpha$ -methylbenzylamine (**17**) – a monosubstituted secondary amine often used in our studies as a benchmarking amine – under standard UmAS conditions,<sup>42</sup> and the byproducts were carefully examined (**Scheme 71**).

**Scheme 71.** UmAS reaction with bromonitroalkane XX and (*S*)- $\alpha$ -methyl benzylamine.



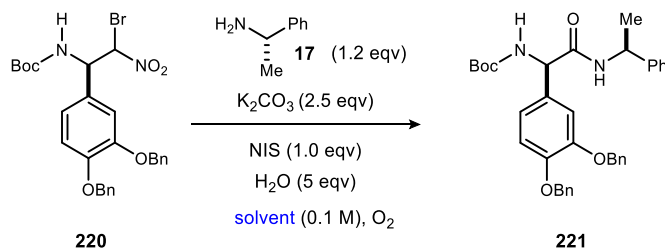
The desired amide **221** formed, but only in 32% yield. After 48 hours some starting material was recovered, indicating incomplete conversion. Moreover, evidence for derivatization of the electron-rich aryl ring was collected in the form of amide derivatives **222**.<sup>186</sup> The aldehyde (**212**), dinitroalkane (**223**), nitroalkane (**224**), and dibromonitroalkane (**225**) were also identified. These are additional fates for the bromonitroalkane starting material under basic aerobic conditions (see section 2.2.2 Degradation profiles of  $\beta$ -amido  $\alpha$ -bromonitroalkanes). As some starting material was recovered, the temperature of the reaction was increased to speed the rate of amide formation. This could increase selectivity for amide formation if the lifetime of reagents necessary for UmAS is short, but decomposition pathways endured over longer reaction times. Moreover, 2-methyl-THF was examined as a different polar, aprotic solvent as it is less prone to oxidation by NIS at warmer temperatures and the longer reaction times examined throughout these studies.

Increasing the temperature from 0 °C to room temperature gave a higher yield of desired amide for reactions run in either DME or in 2-Me-THF (**Table 11**). It was also observed that the yields were overall lower for reactions in 2-Me-THF in comparison to DME. In the 3,5-disubstituted

<sup>186</sup> Changes in the aromatic region corresponding to a loss of a proton from the central aromatic ring, accompanied by a distinct change in chemical shift, were observed by <sup>1</sup>H-NMR. The structures of the iodinated and brominated amides are supported by <sup>1</sup>H-NMR and LCMS analysis and the structure of the oxygenated amide is supported by <sup>1</sup>H-NMR and HRMS (ESI) analysis. The brominated amide was later confirmed by direct synthesis.

system, temperature did not significantly affect the yield, and DME was also found to be superior to 2-Me-THF.

**Table 11.** Effect of solvent and temperature on UmAS.



entry	solvent	temp	yield <sup>a</sup>
1	DME	0 °C	32
2	DME	24 °C	39
3	2-Me-THF	0 °C	23
4	2-Me-THF	24 °C	28

<sup>a</sup> Isolated yield.

Next, given the potential for the central electron-rich ring to undergo electrophilic aromatic substitution with NIS, we sought to limit the amount of electrophilic iodine available to the substrate. It has previously been demonstrated in our laboratory that UmAS can proceed with a catalytic amount (as little as 1 mol %) of NIS.<sup>187</sup> Under catalytic, aerobic conditions, an equivalent of bromonium (in the form of bromonium nitrate) is released during amide formation. This can serve as the halonium source for the amine, or as an

oxidant to iodine to generate iodonium, thereby providing reaction turnover.

Reactions were run in either DME or 2-Me-THF at 0 °C or room temperature, with either 10 mol% or 100 mol% NIS (**Table 12**). Consistent with the aforementioned results, 2-Me-THF provided lower yields in every case when compared to otherwise identical reactions run in DME. Perhaps this is because 2-Me-THF is not miscible with water. This may cause a slower reaction rate by reducing the amount of base capable of interacting with the starting material or by limiting the solubility of intermediate ions necessary for the putative reaction pathway.

Furthermore, all reactions conducted at room temperature, regardless of the amount of NIS or the solvent used, provided higher yields than those conducted at 0 °C (**Table 12**, Entries 2,4,6,8).<sup>188</sup> The yield was lower for reactions run with 10 mol% NIS at 0 °C compared to those run under identical conditions with 100 mol% NIS. Using substoichiometric NIS at low temperatures

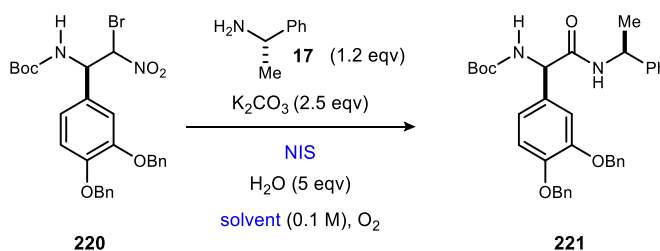
<sup>187</sup> Schwieter, K. E.; Shen, B.; Shackelford, J. P.; Leighty, M. W.; Johnston, J. N. *Org. Lett.* **2014**, *16*, 4714.

<sup>188</sup> Entries 1,3,5,7 (**Table 12**) did not have complete conversion as evidenced by recovered starting material.

decreased the reaction rate, as evidenced by the recovery of starting material in each of these reactions.<sup>189</sup> However, for reactions at room temperature, yields of the desired product increased with the use of substoichiometric NIS (34% vs. 28%, 2-Me-THF and 42% vs. 39%, DME). Overall, these results indicate the following:

1. DME is a preferable solvent to 2-Me-THF.
2. Reactions proceed faster and with better yields at room temperature (compared to 0 °C).
3. The use of substoichiometric NIS seems to improve yield and decrease presence of side products.

**Table 12.** Effect of catalytic NIS, temperature, and solvent on product yield.



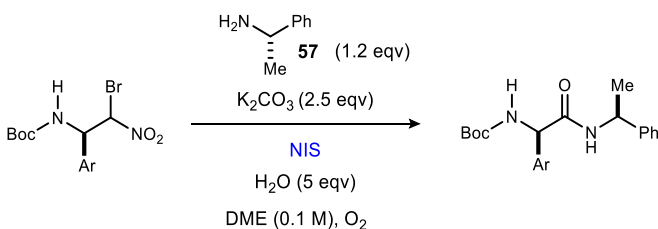
entry	solvent	NIS (mol %)	temp. (°C)	yield (%)	entry	solvent	NIS (mol %)	temp. (°C)	yield (%)
1	DME	100	0	32	5	2-Me-THF	100	0	25
2	DME	100	25	39	6	2-Me-THF	100	25	28
3	DME	10	0	25	7	2-Me-THF	10	0	11
4	DME	10	25	42	8	2-Me-THF	10	25	34

At this point, the highest yield (42%, **Table 12**, entry 4) of desired amide was obtained using 10 mol % NIS, 1.2 equiv. of amine and 2.5 equiv. of base under aerobic conditions at room

<sup>189</sup> With a reaction time >72 h, full conversion was not achieved for entries 3,4,7 & 8 (**Table 12**).

temperature. Given these results, the amount of NIS was varied between 10 and 100 mol % to try to increase the rate of amide production while keeping substrate iodination and byproduct formation at bay. The results are summarized in **Table 13**, showing a rather quadratic relationship between the yield and the amount of NIS used. Given these results, it seems that using more than 10 mol% of NIS is beneficial for increasing the rate and amount of desired amide that is formed, and also potentially for decreasing the amount of desbromo nitroalkane **224**. However, if more than 0.5 equivalents are used, the yield decreases, which may be attributed to competition for NIS between the amine and the electron-rich ring, leading to debromination of the starting material to provide the nitroalkane. As the rate of re-bromination of the nitroalkane (**224**) is very slow relative to UmAS, it is unlikely for it to contribute to product formation.<sup>187</sup> This trend did not however hold true for the 3,5-substituted analog as evidenced by entries 6-8 (Table 13).

**Table 13.** Effect of NIS equivalents.



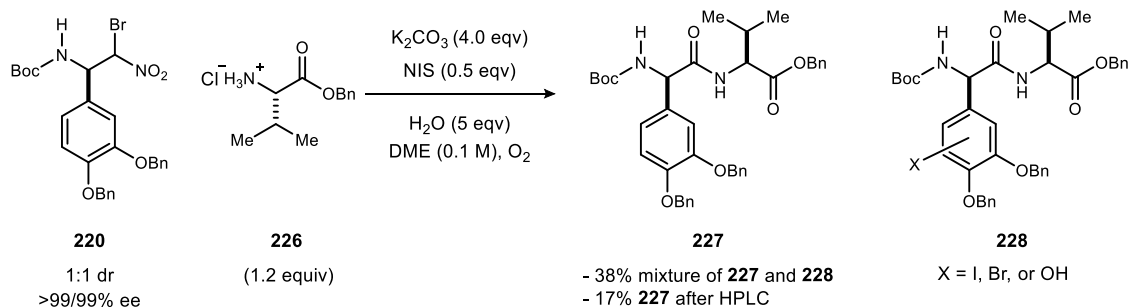
entry	Ar	NIS (mol%)	yield <sup>a</sup>
1	3,4-(OBn) <sub>2</sub> C <sub>6</sub> H <sub>4</sub>	10	42
2	3,4-(OBn) <sub>2</sub> C <sub>6</sub> H <sub>4</sub>	25	48
3	3,4-(OBn) <sub>2</sub> C <sub>6</sub> H <sub>4</sub>	50	49
4	3,4-(OBn) <sub>2</sub> C <sub>6</sub> H <sub>4</sub>	75	41
5	3,4-(OBn) <sub>2</sub> C <sub>6</sub> H <sub>4</sub>	100	39 <sup>b</sup>
6	3,5-(OBn) <sub>2</sub> C <sub>6</sub> H <sub>4</sub>	10	24 <sup>b</sup>
7	3,5-(OBn) <sub>2</sub> C <sub>6</sub> H <sub>4</sub>	100	35 <sup>b</sup>
8	3,5-(OBn) <sub>2</sub> C <sub>6</sub> H <sub>4</sub>	240	25

<sup>a</sup>Isolated yield. <sup>b</sup>Isolated product contains some oxidized glycnamide

With the yield of the 3,4-disubstituted system now increased to 49%, the work-up conditions of the reaction were examined. Standard workup procedure involved diluting the reaction mixture with ethyl acetate, and quenching with 1 N HCl followed by extraction and washing with aqueous sodium thiosulfate and brine. The use of sodium thiosulfate was necessary to remove excess iodine and prevent degradation of the crude reaction mixture. After examination of several work-up procedures, it was found that using acetic acid to bring the pH to neutral instead of acidic (as with HCl), resulted in an increase of yield to a workable 59%.

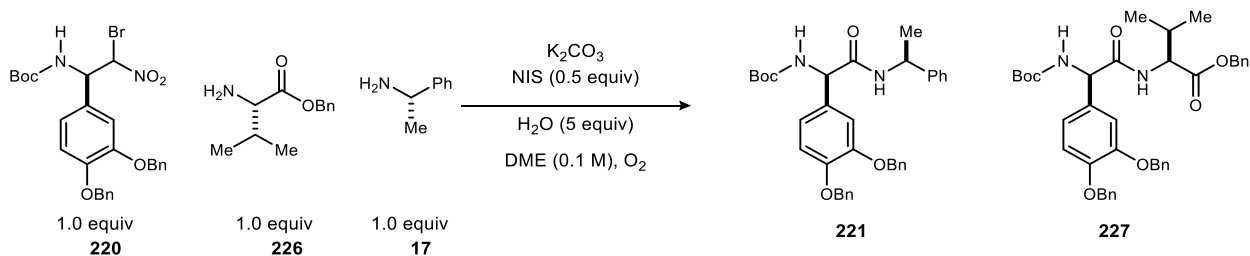
With a useful yield of desired amide in hand, attention was turned towards coupling the bromonitroalkane with a more demanding amine. The HCl salt of L-valine benzyl ester (**226**) was reacted with bromonitroalkane **220** using the optimized conditions (**Scheme 72**). The amount of base added was increased to 4.0 equivalents to account for the generation of the free base of the amine. The reaction profile was similar to the reaction with  $\alpha$ -methyl benzylamine, providing the desired amide, but also giving much higher yields of amide derivatives **228**, which proved to be difficult to separate during column chromatography. Flash column chromatography resulted in a 38% yield of desired amide **227** with some of the oxidized derivatives. Reversed-phase HPLC purification ultimately provided the desired amide in 17% yield. The steric bulk of the valine benzyl ester may lead to a slower formation of halo-amine in comparison to  $\alpha$ -methyl benzylamine, and overall decrease the rate of amide formation. The steric bulk may also decrease its accessibility during nitronate attack, and slow amide formation. The yield of the observed amide derivatives may have increased as a result of the rate of amide formation being slower than or comparable to the rate of electrophilic aromatic substitution of either the starting bromonitroalkane, or of the desired amide. Generating the free base of the amine prior to the reaction did not improve the yield.

**Scheme 72.** UmAS reaction of bromonitroalkane **220** and valine benzyl ester.



To determine how much of an impact the amine had on the reaction, a competition experiment between (*S*)- $\alpha$ -methyl benzylamine **17** and valine benzyl ester **226** was conducted. This revealed nearly equal reactivity of the amines as shown by approximately equal formation of both **221** and **227** after 24 hours, as indicated by  $^1H$ -NMR (**Table 14**, entry 1). However, when the HCl salt of the valine benzyl ester was used,  $^1H$ -NMR showed a 1.4:1 ratio of **221**:**227** after 24 hours, suggesting that the rate of nitronate formation is competitive with generation of the free base.

**Table 14.** Competition reaction between (*S*)- $\alpha$ -methyl benzylamine and valine benzyl ester.



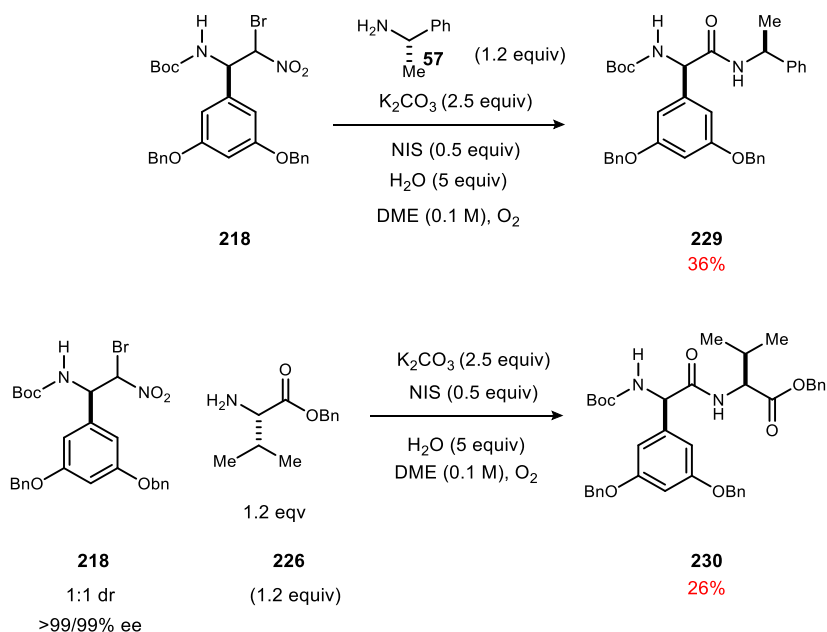
entry	$K_2CO_3$ (equiv)	product ratio ( <b>58:64</b> ) <sup>a</sup>
1	2.5	1:1
2 <sup>b</sup>	3.5	1.4:1

<sup>a</sup>Ratio determined by  $^1H$  NMR integration prior to purification. <sup>b</sup>Reaction used the HCl salt of valine benzyl ester.

Ultimately, this demonstrated that optimization efforts should continue to be directed towards increasing the reactivity of the bromonitroalkane or limiting byproduct formation, instead of being directed towards the amine.

The optimized conditions were also applied to the 3,5-bis(benzyloxy) bromonitroalkane substrate **218**. Yields were comparable to previous reactions (on average ~35% yield of amide and halogenated derivatives) but gave lower yields than bromonitroalkane **220** upon reaction with both (*S*)- $\alpha$ -methyl benzylamine and valine benzyl ester (**Scheme 73**).

**Scheme 73.** Reactivity of bromonitroalkane **218** under conditions optimized for **220**.

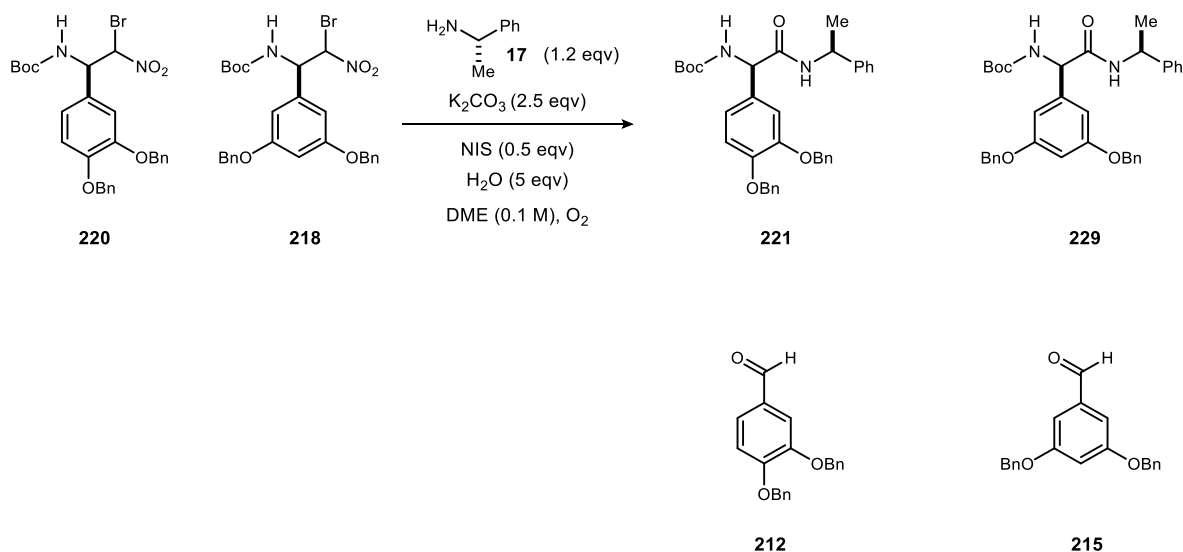


To examine the relative reactivity of the bromonitroalkane donors **218** and **220**, a competition experiment was run (**Scheme 74**). This reaction led to the production of glycinamides **221** and **229**, aldehydes **212** and **215**, recovered starting material, and other byproducts that were unable to be quantified. It was found that more of the 3,5-dibenzyloxy derived glycinamide **229** was formed (1.4:1 **229:221**).<sup>190</sup> We also observed that the 3,4-dibenzyloxy bromonitroalkane (**220**) is more susceptible to retro-aza-Henry than the 3,5-dibenzyloxy bromonitroalkane (**218**) as evidenced by a 2:1 ratio of aldehyde **212** to aldehyde **215** in the crude reaction mixture. This could be attributed to the presence of the *para*-benzyloxy substituent. As this possesses the ability to donate electron density via resonance, it may increase the propensity for bromonitromethane to leave during retro-aza-Henry (see Scheme 76). **Overall, while these optimization studies manipulating the standard reaction conditions led to an incremental increase in yield, it was clear that more prominent changes to the system or to the substrates needed to be made to make this widely applicable.**

<sup>190</sup> Ratio determined by <sup>1</sup>H NMR integration of material post-column.



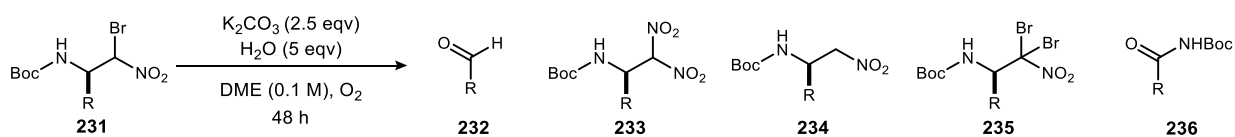
**Scheme 74.** Competition experiment of UmAS between bromonitroalkanes **220** and **218**.



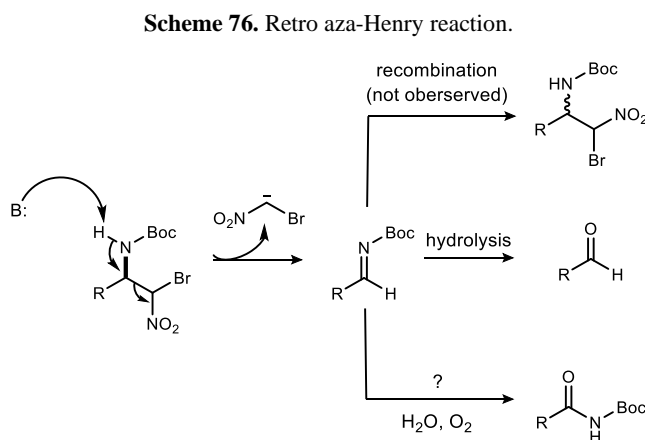
### 2.2.2 Degradation profiles of $\beta$ -amido $\alpha$ -bromonitroalkanes

It was evident that the competing side reactions leading to decomposition of the bromonitroalkane should be investigated. To this end, the amine and NIS were removed from the reaction conditions, and the degradation profile (rate and array of products) of  $\alpha$ -bromo nitroalkanes under basic, aerobic conditions was examined. After 48 hours the bromonitroalkane (**231**) reacted with potassium carbonate and oxygen to form a range of degradation products. The most significant of these were the aldehyde (**232**), the  $\beta$ -amido  $\alpha,\alpha$ -dinitroalkane (**233**),  $\beta$ -amido nitroalkane (**234**), the  $\beta$ -amido  $\alpha,\alpha$ -dibromonitroalkane (**235**), and the imide (**236**) (**Scheme 75**). In the case of the bromonitroalkane **220**, no starting material was recovered, and the reaction profile was the same at room temperature and 0 °C. With bromonitroalkane **218**, less than 28% of the starting material remained after 48 hours at 0 °C.

**Scheme 75.** Degradation of bromonitroalkanes under basic, aerobic conditions.



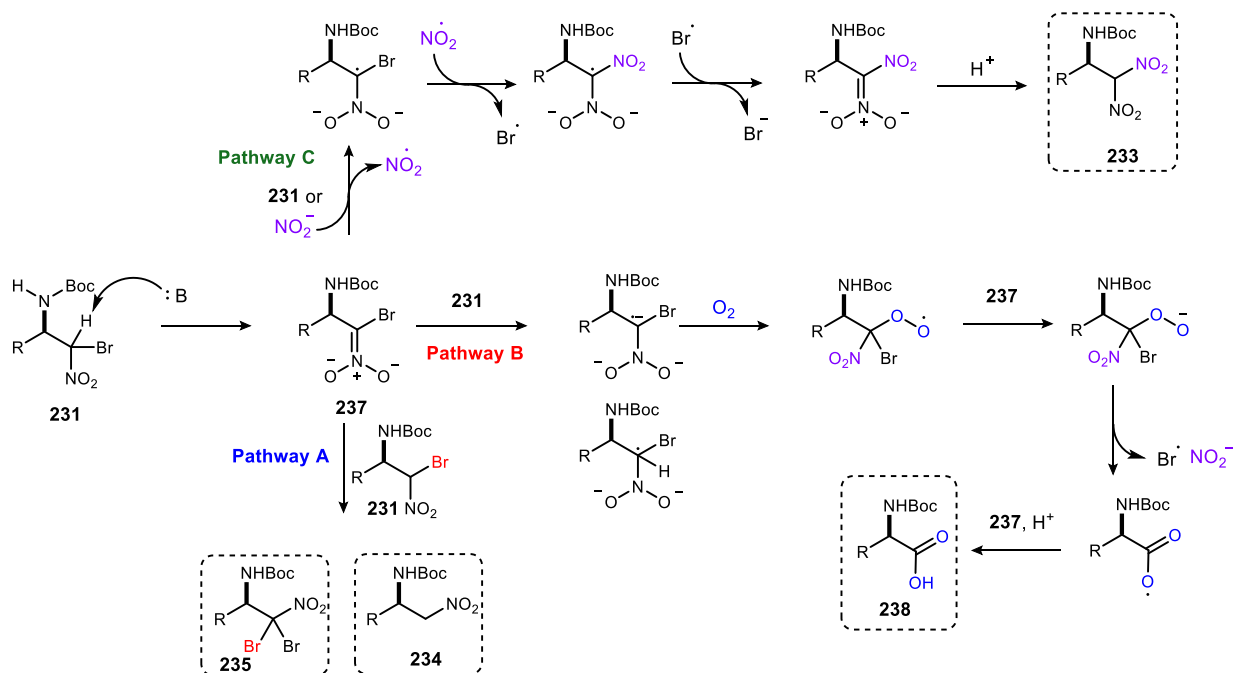
The aldehyde (**232**) is the most commonly observed and the most abundant byproduct formed whenever  $\alpha$ -bromo nitroalkanes **220** and **218** are subjected to basic conditions. It is suspected that the aldehyde is formed by the retro aza-Henry reaction where deprotonation of the amide nitrogen and elimination of bromonitromethane leads to the formation of the imine (**Scheme 76**). The imine can then undergo hydrolysis to form the aldehyde. Alternatively, recombination of bromonitromethane can lead to the racemic bromonitroalkane. While the aldehyde was often isolated, whenever starting material was recovered the enantioenrichment was maintained, suggesting that recombination does not occur.



While recombination was not observed, the hypothesized retro aza-Henry reaction can be further supported by observation of imide **236**. The most probable pathway to its formation would require imine **55** to be produced (presumably by retro aza-Henry), followed by the addition of oxygen to form a peroxide adduct and further oxidation to the amide. Alternatively, water could add to the imine to form the hemiaminal, which could be oxidized to the amide. This compound was also observed when the imine (**217**) was stored at room temperature while exposed to moisture and atmosphere, which supports the presence of imine **217** as an intermediate to byproduct formation.

The formation of nitroalkane **234** and dibromonitroalkane **235** can be formally envisioned as a result of nitronate attack on bromonitroalkane (**Scheme 77**, pathway A).  $\alpha,\alpha$ -Dibromo nitroalkane could also be formed by attack of the nitronate on the  $\alpha,\alpha$ -dibromo nitroalkane **235**, or several other brominated intermediates.

**Scheme 77.** Proposed pathways for side reactions of bromonitroalkanes 56.



Presumably, the dinitro compound **233** forms as a result of the ter Meer reaction between nitrite and the starting bromonitroalkane. The ter Meer reaction is generally used to synthesize 1,1-dinitroalkanes from 1-halo-1-nitroalkanes and a nitrite source. Under the current conditions, where no amine or NIS is present, nitrite can be formed, as proposed by Shugalei, through pathway B (**Scheme 77**).<sup>191</sup> A redox reaction between the nitronate and another equivalent of starting halonitroalkane generates the alkyl nitro radical and the radical anion. The latter can be captured by triplet oxygen to form the tetrahedral peroxide radical intermediate. The nitronate can reduce the peroxide radical to the peroxide anion, which can collapse to release nitrite, bromine radical, and the carboxylate radical, which is reduced again by nitronate to the carboxylate and protonated

<sup>191</sup> Shugalei, I. V.; Tselinskii, I. V.; Bazanov, A. G. *Zh. Org. Khim.* **1986**, 22, 2496.



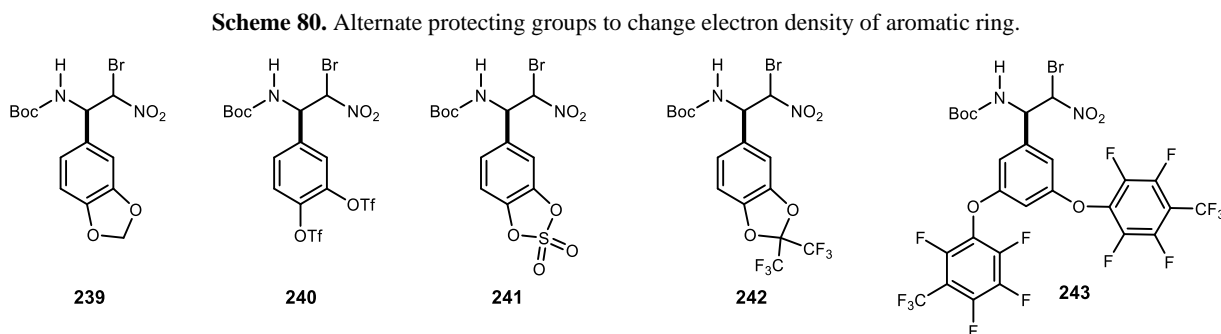


for each equivalent of dinitroalkane **233** formed, two equivalents of the starting bromonitroalkane **231** are consumed, which contributes to the moderate to low yields of the desired amide in UmAS. Our next steps were planned based on the hypothesis that the moderate to low yields obtained from UmAS reactions with bromonitroalkanes **220** and **218** could be attributed to the following:

1. low reactivity of the donors along the UmAS pathway
2. competing decomposition pathways of the starting material
3. oxidation of glycinamide products

### 2.2.3 Attempts to change electronics of the $\alpha$ -bromonitroalkanes

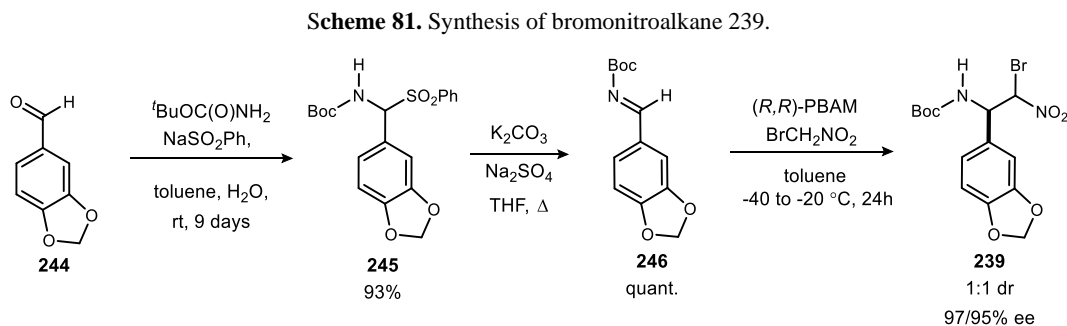
The UmAS reactions using electron rich aryl glycine donors are uniquely slow, with optimized yields ranging from 30% to 58%. We hypothesized that these reactions could be improved if we could change the reactivity of the nitronate in the UmAS pathway by altering the electronic nature of the aryl group. Thus, efforts were directed towards synthesizing bromonitroalkane donors with different protecting groups to alter and/or attenuate the electron rich nature of the aryl ring. We identified the potential donors in **Scheme 80** to test this hypothesis.



To this end, triflate, sulfate, methylene, and trifluoromethylene protecting groups were pursued for the 3,4-dihydroxy substrate. The perfluorinated tolyl protected derivative **243** was also explored for the 3,5-dihydroxy substrate.<sup>196</sup>

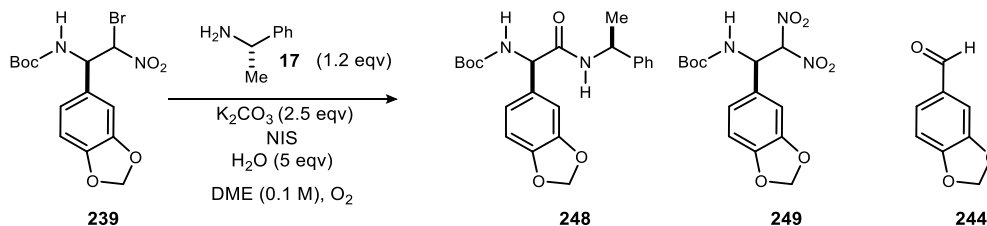
<sup>196</sup> Designed and synthesized by Dr. Kazuyuki Tokumaru.

To our delight, synthesis of the bromonitroalkane donor **239** proved uneventful and provided the desired product from commercially available piperonal (**244**) with 1:1 dr and excellent ee (up to 97/95%) (**Scheme 81**). As with the other donors, this substrate could be recrystallized to provide the product as a 1:1 mixture of diastereomers with >99/99% ee.



This substrate was next employed in UmAS under standard conditions (**Table 15**, entries 1 & 2) as well as the conditions optimized for bromonitroalkane **220** (**Table 15**, entry 3). All reactions showed a similar profile, and were overall less complex than the reactions conducted using bromonitroalkanes **220** or **218**. The aldehyde **244** was produced in about a 1:3 ratio relative to the

**Table 15.** UmAS reactions with bromonitroalkane **239** and (*S*)- $\alpha$ -methylbenzylamine.



entry	NIS (mol %)	temp (°C)	yeld of <b>248</b> (%)
1 <sup>a,b</sup>	100	0	28
2 <sup>b,c</sup>	100	25	24
3 <sup>c,d</sup>	50	25	24

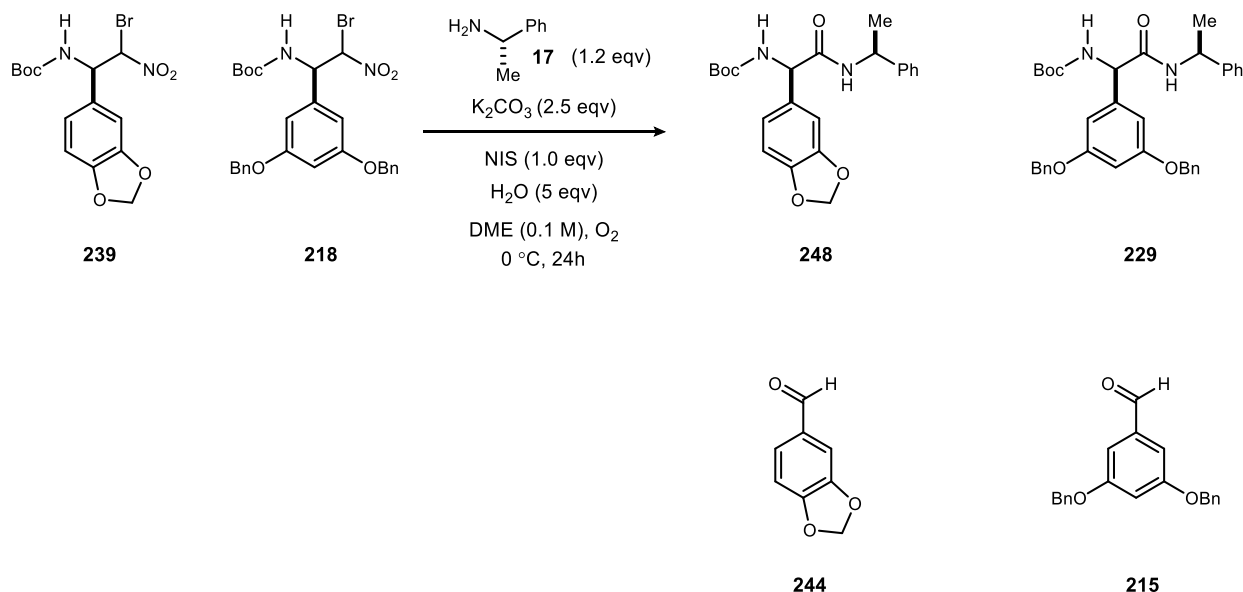
<sup>a</sup>Reaction run for 48 h. <sup>b</sup>Work up conditions used 1 N HCl and Na<sub>2</sub>S<sub>2</sub>O<sub>3</sub>. <sup>c</sup>Reaction run for 28 h. <sup>d</sup>Work up conditions used AcOH and Na<sub>2</sub>S<sub>2</sub>O<sub>3</sub>.

desired glycinamide **248** as determined by the crude  $^1\text{H-NMR}$ . Among the byproducts formed, the dinitroalkane **249** was the most abundant, and formed in approximately 20% yield in all reactions. These reactions provided a much lower yield of desired amide than those run with the 3,4- and 3,5-dibenzyloxy substrates **220** and **218**, but the reaction was overall cleaner. There is a possibility that the substrate **239** is light sensitive as the white solid becomes discolored if left exposed to light. To determine the stability of this substrate, its degradation profile was examined by subjecting the material to basic, aerobic conditions in the absence of NIS and amine. After 48 hours at 0 °C, the substrate showed complete decomposition into the same products (*vide supra*) for the benzyl protected bromonitroalkanes (**Scheme 75**).

To determine the relative reactivity of this substrate in UmAS as compared to bromonitroalkanes **220** and **218**, competition experiments were leveraged again. When bromonitroalkane **218** was pit against bromonitroalkane **239**, approximately equal amounts of amides **229** and **248** formed (**Scheme 82**). Starting material was recovered for both of the substrates, but more than twice as much of bromonitroalkane **218** was recovered. Moreover, as per the crude  $^1\text{H-NMR}$ , bromonitroalkane **239** was slightly more prone to the retro aza-Henry/hydrolysis sequence as shown by a 1:1.3 ratio of 3,5-dibenzyloxy-benzaldehyde (**215**) to piperonal (**244**). The same competition was conducted between bromonitroalkanes **220** and **239** but the reaction proved to be extremely messy. Little information could be gathered from this experiment, with the exception that the bromonitroalkane **220** is much more susceptible to the retro aza-Henry/hydrolysis sequence than the piperonal derived bromonitroalkane **239** as evidenced by the presence of 3,4-dibenzyloxy-benzaldehyde (**212**) and absence of piperonal (**244**) in the crude reaction mixture.



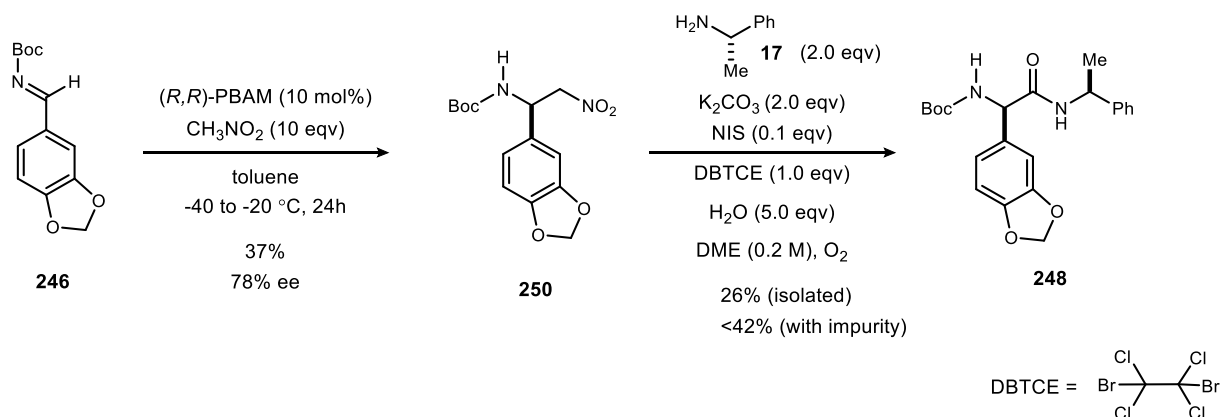
**Scheme 82.** Competition experiment between bromonitroalkanes 218 and 239 in UmAS.



Given that the piperonal derived substrate provided a cleaner reaction profile, with larger amounts of identifiable byproducts (namely the dinitroalkane), it was pursued further. As the dinitroalkane was the major byproduct, it was postulated that if we generated the bromonitroalkane *in situ* from the nitroalkane it would be less prone to ter Meer reaction. This would be expected since the nitrite necessary for the ter Meer reaction would not yet be formed (as it is only formed from the bromonitroalkane). To this end, nitroalkane **61c** was prepared in 37% yield and 78% ee by aza-Henry with nitromethane (Scheme 83). The one-pot amidation of nitroalkanes using DBTCE to brominate the substrate *in situ* recently reported in our laboratory,<sup>197</sup> was applied to this substrate. The crude reaction mixture was essentially unchanged as compared to that conducted under standard UmAS conditions (Table 15), and the yield was comparable. **Overall, while this substrate did seem to give a cleaner reaction profile than its benzyl-protected cousins, it did not help reach the overarching goal of generating an improved yield of desired amide.**

<sup>197</sup> Schwieter, K. E.; Johnston, J. N. *Chem. Commun.* **2016**, 52, 152.

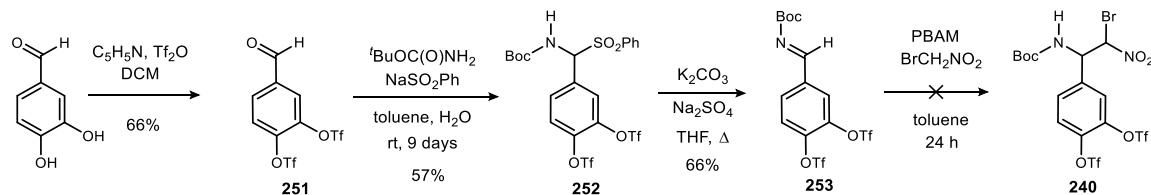
**Scheme 83.** Application of one-pot  $\alpha$ -amidation reaction to nitroalkane 61c.



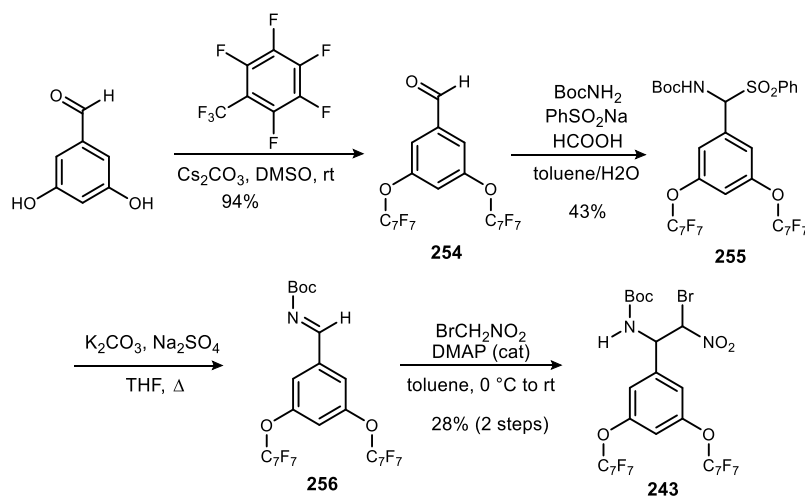
To this end, the triflate-protected substrate **240** was pursued. 3,4-Dihydroxybenzaldehyde was treated with pyridine and triflic anhydride to afford the triflate-protected aldehyde (**251**), which was used to form the sulfone (**252**) (**Scheme 84**). However, there was some impurity present that resisted removal by trituration, which is one of the few workable methods for sulfone purification. Ultimately, elimination was affected, but the impurities from the sulfone were still present. When the crude material was subjected to the aza-Henry reaction, a very complicated reaction mixture resulted, from which no product could be isolated. Efforts were also directed towards the synthesis of sulfate **241** (**Scheme 80**), but difficulty in synthesizing the protected aldehyde precursor precluded access to the bromonitroalkane.

The perfluorotolyl-protected bromonitroalkane **243** was synthesized in a straightforward fashion from the aldehyde (**Scheme 85**).

**Scheme 84.** Attempt to synthesize triflate protected bromonitroalkane 240.

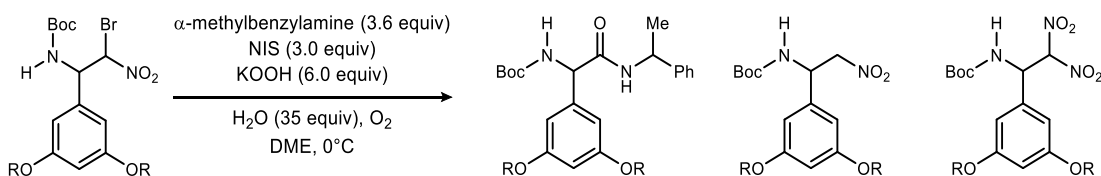


**Scheme 85.** Synthesis of perfluorotolyl-protected bromonitroalkane **243**.



Its activity in the UmAS reaction was compared to the benzyl-protected substrate using the conditions shown in **Table 16**. The pathway and rationale that led to the development of these particular reaction conditions will be discussed in the next section. However, in this context, we are examining the effect of protecting group changes. LCMS showed no signs of halogenation on the aryl ring of the *p*-CF<sub>3</sub>(C<sub>6</sub>F<sub>5</sub>)-glycinamide under the conditions shown in **Table 16**, nor under conditions using K<sub>2</sub>CO<sub>3</sub> (not shown). TLC implied the formation of the dinitro derivative but it was not isolated. Overall, this substrate worked just as well as the benzyl ether-protected bromonitroalkane. It would be suitable to apply if it served a purpose for a particular protecting

**Table 16.** Glycinamide formation using perfluorotolyl-protected bromonitroalkane **243**.



entry	R	time (hr)	bromonitroalkane (%)	amide (%)	nitroalkane (%)	dinitroalkane (%)
1	Bn	40	21	53	21	trace
2	4-CF <sub>3</sub> (C <sub>6</sub> F <sub>5</sub> )-	2	-- <sup>a</sup>	54	16	trace

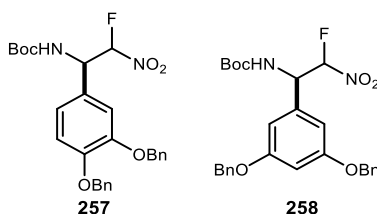
<sup>a</sup> Full conversion observed.

group scheme, but for our objectives it did not significantly improve the yield of the desired amide and thus was not pursued further.

#### 2.2.4 Addressing the *ter Meer* reaction – examination of $\alpha$ -fluoronitroalkanes

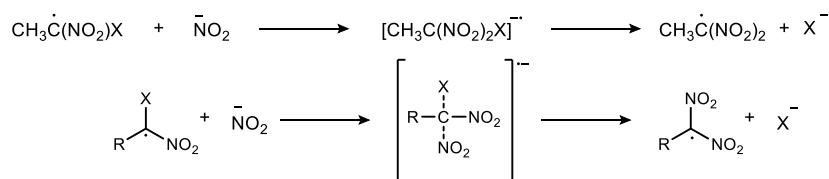
To further address the byproducts formed through the *ter Meer* reaction and related pathways, the reactivity of fluoronitroalkanes **73** and **74** (**Scheme 86**) in UmAS was examined.

**Scheme 86.** Targeted  $\alpha$ -fluoronitroalkanes.



It is known that fluoronitroalkanes do not undergo the *ter Meer* reaction due to the stability of the C-F bond in the radical anion of *geminal* halonitroalkanes.<sup>194d</sup> Generally, in the case of the chloro-, bromo-, and iodo-nitroalkanes, the radical anion species is quite unstable and will readily decompose to form the dinitro radical and the halide (**Scheme 87**)

**Scheme 87.** Dissociation involved in the *ter Meer* reaction.



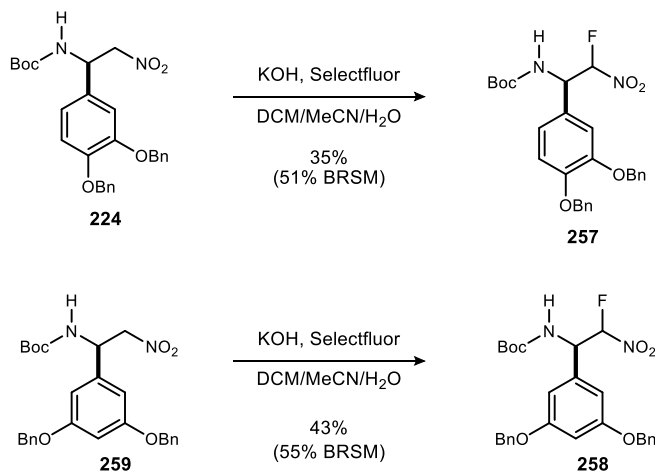
The rate of this propagation step varies depending on the halogen leaving group, its electron affinity, and the C-X bond dissociation energy. As expected, the rate increases in the order of  $\text{Cl} \ll \text{Br} < \text{I}$ , as the difference between the two factors increases (**Table 17**). While fluorine does have high electron affinity, it is not enough to override the strength of the C-F bond, resulting in a difference of -25 kcal/mol. As such, a fluoronitroalkane will not undergo the *ter Meer* reaction. If it is proven that the starting bromonitroalkane is the source for bromination of the glycinamide, the fluoronitroalkane may be beneficial as electrophilic aromatic fluorination is highly unlikely

**Table 17.** Electron affinities of halogens and C-X Bond dissociation energies.

entry	halogen	electron affinity	BDE	$\Delta(\text{EA} - \text{BDE})$ (kcal)
1	Cl	85	80	5
2	Br	79	68	11
3	I	72	53	19
4	F	81	106	-25

under the reaction conditions. To this extent, the observed dehalogenation of the starting material to form the nitroalkane should not occur with the fluoronitroalkane, thereby increasing the lifetime of the acyl donor equivalent and its likelihood to participate in amide bond formation.

Therefore, the fluoronitroalkanes (**257** and **258**) were prepared by electrophilic fluorination of the corresponding nitroalkane (**Scheme 88**).<sup>198</sup> This afforded the fluoronitroalkane (**257**) in 35% yield (51% brsm),<sup>199</sup> with the only major byproduct being the aldehyde (**Scheme 88**). The fluoronitroalkane **258** was produced in 43% yield (55% brsm) (**Scheme 88**).

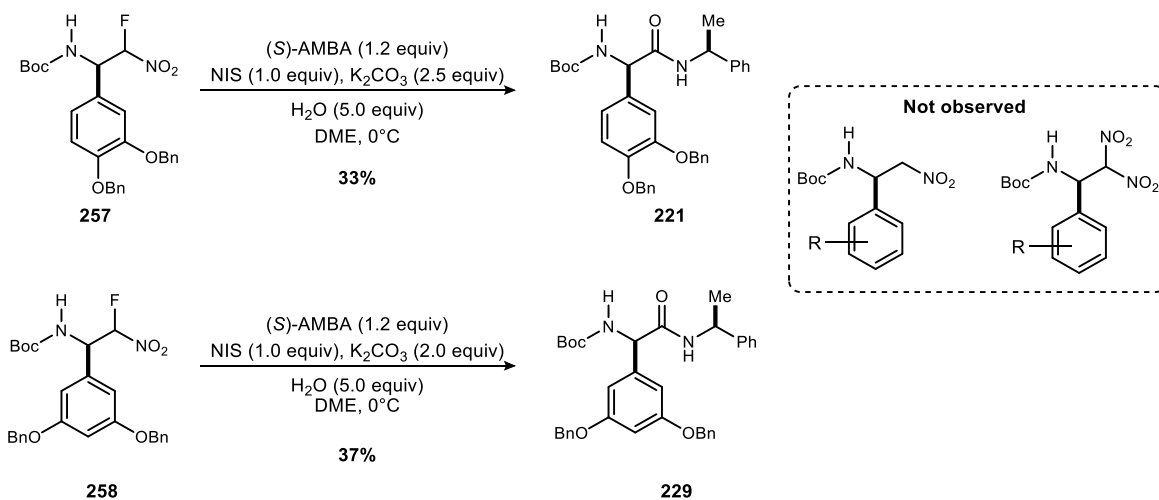
**Scheme 88.** Fluorination of nitroalkanes.

<sup>198</sup> Hu, H.; Huang, Y.; Guo, Y. *J. Fluorine Chem.* **2012**, *133*, 108.

<sup>199</sup> Recovered 49% of the starting nitroalkane **61a**

The efficacy of these  $\alpha$ -fluoro nitroalkanes as an acyl donor in UmAS was evaluated (**Scheme 89**). In stark contrast to the reactions using the  $\alpha$ -bromo nitroalkanes, neither the nitroalkane nor the dinitroalkane were observed. This supported our hypotheses regarding the decreased likelihood of the  $\alpha$ -fluoro nitroalkane to undergo dehalogenation and the ter Meer reaction. These intriguing results notwithstanding, the  $\alpha$ -fluoro nitroalkane was slow to react and the yield of the amide was not improved. This slow reactivity may be a result of the lower effective  $pK_a$  of  $\alpha$ -fluoronitroalkanes relative to  $\alpha$ -bromonitroalkanes as observed in previous studies in our laboratory, which would slow nitronate formation.<sup>47</sup> It may also be that the  $\alpha$ -fluoro substituent deactivates the nitronate once it is formed, leading to a slower attack in the UmAS step.

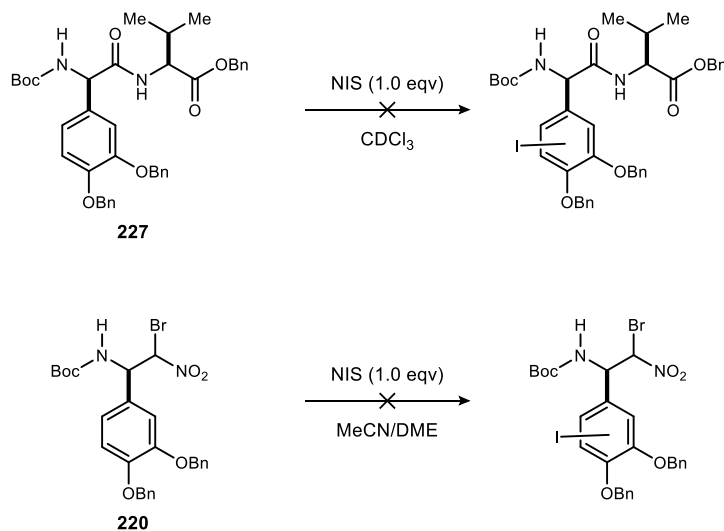
**Scheme 89.** Fluoronitroalkanes as acyl donors in UmAS.



### 2.2.5 Addressing undesired oxidation of glycinamide products

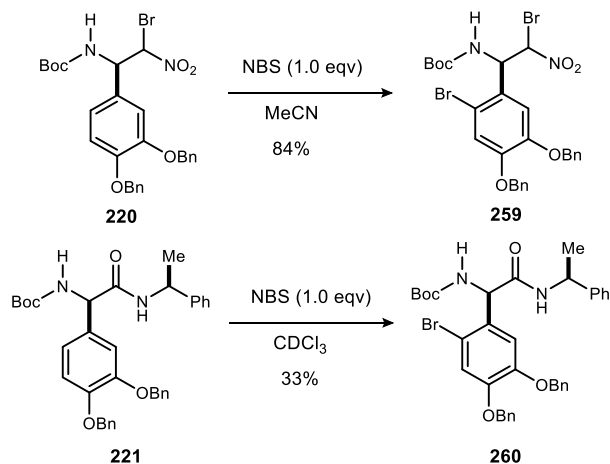
The instability of the UmAS product to the reaction conditions was considered as a contributor to the low yields. To determine the structure of the putative amide derivatives that might result, we conducted an NMR experiment in which the amide **227** was mixed with NIS in  $\text{CDCl}_3$  (**Scheme 90**). No iodination was observed after 12 hours of mixing at room temperature, and heating at  $60^\circ\text{C}$  overnight only led to decomposition of NIS. Similarly, no reaction was observed when bromonitroalkane **220** was stirred with NIS at room temperature in MeCN/DME, even after 48 hours.

**Scheme 90.** Attempted iodination of glycinamide **227** and bromonitroalkane precursor **220**.



An identical reaction of the bromonitroalkane **220** was run using NBS instead of NIS, and the starting material was fully consumed (**Scheme 91**). Given this observation, glycinamide **221** was stirred with NBS in  $\text{CDCl}_3$ , and after 18 hours full consumption of NBS and approximately 50% conversion of the glycinamide to the brominated glycinamide **260** was observed.

**Scheme 91.** Bromination of glycinamide 221 and bromonitroalkane precursor 220.



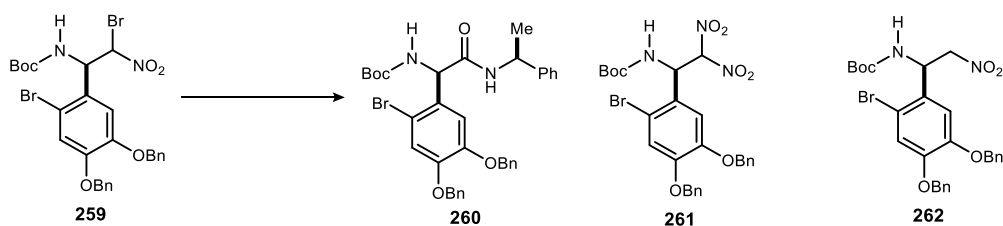
While these experiments suggest that direct iodination of the glycinamide products by NIS may be unlikely, the iodination of the amide cannot be ruled out as there are many factors attributed to UmAS reaction conditions not present in the NMR experiment. Similarly, while bromination was observed using reactive NBS, the precise source for bromination of glycinamides in UmAS is yet to be determined. The bromonitroalkane is one potential bromine source for the electron-rich ring. Other sources may include the *N*-bromo amine generated from the amine coupling partner as well as the bromonium nitrate produced during collapse of the tetrahedral intermediate in UmAS (see section 2.1.2 *Introduction to Umpolung Amide Synthesis*). Additional control experiments would be needed to determine the true factors contributing to the formation of **260** in UmAS.

It was also of interest to carry the 2-bromo-3,4-dibenzyloxy bromonitroalkane forward into the UmAS reaction. In addition to fulfilling the need for isolation and characterization of brominated glycinamides, use of this substrate may reduce the observed byproducts. If the starting bromonitroalkane acts as the halogen transfer agent, then consumption of the starting material by bromination of the glycinamide (or starting bromonitroalkane) would be circumvented. This could limit the amount of the debrominated nitroalkane (**234**) formed in the reaction, which, as described above, is unlikely to re-enter the pathway to amide formation. Moreover, if this substrate proved to improve the reaction profile and yield, it could be used in place of bromonitroalkanes **220** and **239**, as the bromine can be removed during the hydrogenolysis used for benzyl deprotection of the phenol moieties. As shown in **Table 18**, the standard UmAS conditions gave a low yield of the



amide product (**Table 18**, entry 1). Excluding  $K_2CO_3$  and using an excess of amine to act as both the base and coupling partner gave a significant increase in yield. However, the dinitro and desbromo adducts were still observed. Piperidine was added to act as a potential nitroso scavenger, and this increased the yield of the amide (**Table 18**, entry 3). No additional amide derivatives were observed in any of these reactions. From these experiments we learned that the *ortho*-bromo substituent did serve to block a site prone to oxidation, which improved our ability to cleanly isolate the amide product. We were also able to confirm the presence of this brominated amide species in previous reactions. However, mechanistically this change did not seem to decrease the formation of off-target derivatives of the starting bromonitroalkane and thus was not pursued further.

**Table 18.** Synthesis of brominated glycinamide 260.



entry	conditions <sup>a</sup>	yield 260 (%) <sup>b</sup>	yield 261 (%) <sup>b</sup>	yield 262 (%) <sup>b</sup>
1	(S)-AMBA (1.2 equiv) NIS (1.0 equiv) $K_2CO_3$ (2.5 equiv) $H_2O$ (5.0 equiv) DME (0.2 M)	27	12	Not isolated
2	(S)-AMBA (4.0 equiv) NIS (1.0 equiv) DME (0.2 M)	50	13	12
3 <sup>c</sup>	(S)-AMBA (4.0 equiv) NIS (1.0 equiv) Piperidine (1.0 equiv) DME (0.2 M)	56	15	13

<sup>a</sup>All reactions run at 0 °C for 24 h. <sup>b</sup>Isolated yields. <sup>c</sup>The nitroalkane was also isolated from this reaction (13%).

### *2.2.6 Game-changing tactics in UmAS toward electron-rich aryl glycinamides*

As previously described, many manipulations to the existing reaction parameters to make aryl glycinamides were made by myself as well as several coworkers.<sup>200</sup> With all of our results in hand, along with the identification of the primary byproducts of this reaction, we made a few more hypothesis-driven optimization attempts.

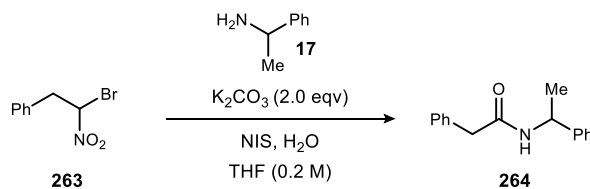
For example, a slight excess of amine (1.2 equiv.) was originally used. It was hypothesized that since the bromonitroalkane degrades without amine present, the use of excess amine may be beneficial. Furthermore, the dibromonitroalkane (**235**) was observed, which has been shown to be a viable reactant in UmAS, albeit at slower rates than the bromonitroalkane. To this extent, we thought that the presence of excess amine may drive the consumption of dibromonitroalkane and lead to improved conversion. Moreover, we hypothesized that decreasing the amount of water could help prevent hydrolysis of the starting materials. However, this would have likely limited the reactivity due to the low solubility of potassium carbonate in organic solvents. Alternatively, the amount of water may be decreased and an alternative base, such as cesium carbonate, which has an increased solubility in organic solvents, could be used. Cesium carbonate had previously been effective in our laboratory's synthesis of a fluorinated derivative of feglymycin, Ffeglymycin, but has little effect on the current reaction at hand.<sup>184</sup>

---

<sup>200</sup> Dawn Makley, Amanda Doody, Ken Schwieter, Sergey Tsukanov, Kazuyuki Tokumaru, Jade Bing

The effect that the amount of water and the use of an exogenous base ( $K_2CO_3$ ) had on the yield in UmAS was also previously examined (**Table 19**).<sup>42</sup> It has been shown that UmAS will proceed in the absence of an added base if an excess of amine is used (**Table 19**, entry 1). While dry conditions (**Table 19**, entry 4), led to a decrease in yield, the exclusion of water was only examined when

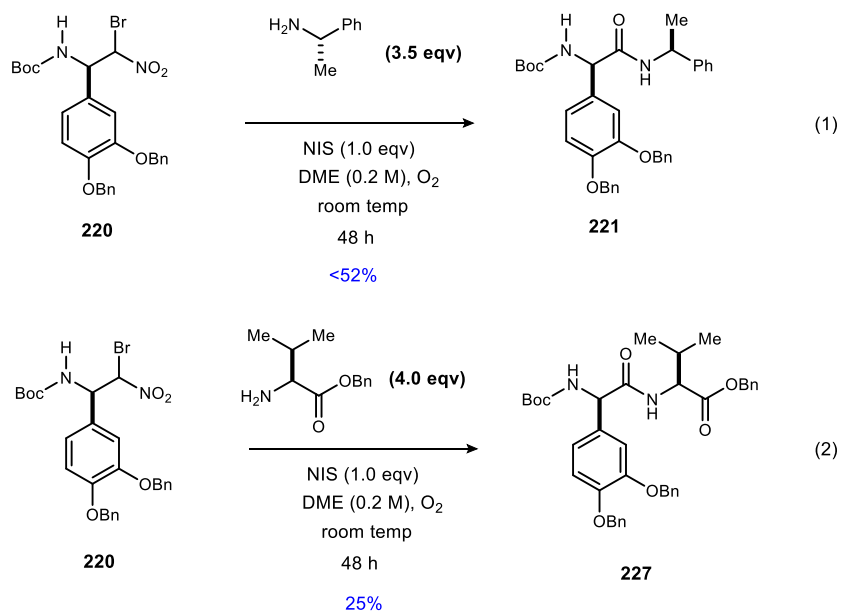
**Table 19.** Previously reported effects of water and base on the yield of UmAS.



entry	amine (equiv.)	NIS (equiv.)	$H_2O$ (equiv.)	$K_2CO_3$ (equiv.)	yield (%)
1	2.0	1.2	93	0	61
2	1.2	1.0	93	2	58
3	1.2	1.0	5	2	70
4	1.2	1.0	0	2	55

$K_2CO_3$  was used as an added base. Thus, in the current investigation we examined the reactivity when water is excluded and 2.0 equiv. or more of amine are used instead of additional base. We hypothesized that decreasing the equivalents of water used may serve an additional purpose in that it could decrease the solubility of nitrite ion, the main proponent of the ter Meer reaction. Indeed, **Scheme 92** shows that using an excess of amine and excluding water and  $K_2CO_3$  significantly improved the yield when coupling the  $\alpha$ -bromo nitroalkane and AMBA. Unfortunately, this effect did not hold when coupling to valine benzyl ester, nor when using the 3,5-aryl substituted  $\alpha$ -bromo nitroalkane. Additionally, if an inorganic base is used, the exclusion of water typically decreased the yield of the desired amide. The effect of water on the reaction would become more prevalent later in our optimization studies toward the synthesis of (-)-feglymycin (see Chapter 3).

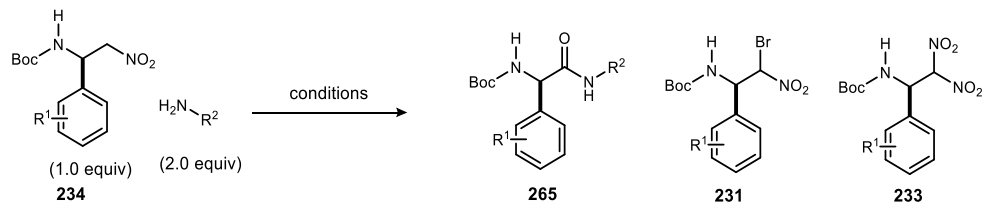
**Scheme 92.** Exclusion of  $K_2CO_3$  and water in the UmAS reaction with  $\alpha$ -bromo nitroalkane **220**.



Next, we examined methods that use the nitroalkane as the starting material and generate the  $\alpha$ -halo nitroalkane *in situ*. Efforts from both our laboratory<sup>201</sup> and the Hayashi laboratory<sup>202</sup> identified two sets of conditions suitable for this transformation. **Table 20** shows our results when employing both of these conditions. We found that under the one-pot amidation protocol developed in our lab, no amide product was observed when using the 3,4-aryl substituted  $\alpha$ -bromo nitroalkane (**Table 20**, entry 1). The primary product was the bromonitroalkane (68%), even when excess amine was added and the reaction time was 72 hours. We also tried the 3,5-disubstituted  $\alpha$ -bromo nitroalkane and observed some amide formation (34%), but incomplete conversion (**Table 20**, entry 2). These reactions were rather messy and although we observed some of the bromonitroalkane and dinitroalkane, the yields could not be quantified by crude <sup>1</sup>H-NMR. Full conversion of the nitroalkane was also not observed using Hayashi's conditions (**Table 20**, entry 3). The desired amide was observed in 36% yield, but the dinitroalkane was also formed in significant amounts (~27%).

<sup>201</sup> Schwieter, K. E.; Johnston, J. N. *Chem. Commun.* **2016**, 52, 152.

<sup>202</sup> Li, J.; Lear, M. J.; Kawamoto, Y.; Umemiya, S.; Wong, A. R.; Kwon, E.; Sato, I.; Hayashi, Y. *Angew. Chem. Int. Ed.* **2015**, 54, 12986.

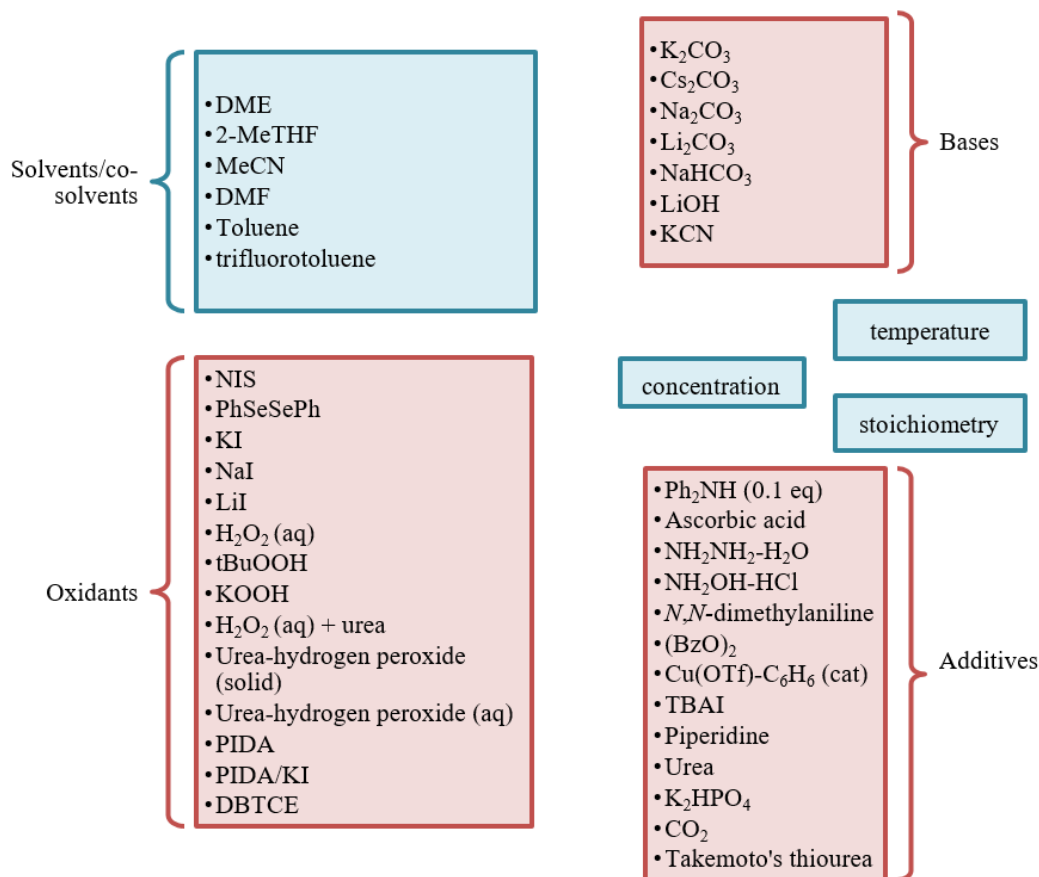
**Table 20.** Synthesis of glycinamides via the *in situ* generation of  $\alpha$ -halo nitroalkanes.<sup>a</sup>

entry	R <sup>1</sup>	amine (equiv)	conditions	temp, time	234 (%)	265 (%)	231 (%)	233 (%)
1	3,4-(OBn) <sub>2</sub>	 H <sub>2</sub> N-CH(Me)-Ph (2.0)	K <sub>2</sub> CO <sub>3</sub> (1.0 equiv) DBTCE (1.0 equiv) NIS (0.1 equiv) H <sub>2</sub> O (5.0 equiv) DME (0.2 M)	rt, 72 hr	nd	-- <sup>b</sup>	68	-- <sup>c</sup>
2	3,5-(OBn) <sub>2</sub>	 H <sub>2</sub> N-CH(Me)-CH <sub>2</sub> -C(=O)OBn (2.0)	K <sub>2</sub> CO <sub>3</sub> (1.0 equiv) DBTCE (1.0 equiv) NIS (0.1 equiv) H <sub>2</sub> O (5.0 equiv) DME (0.2 M)	rt, 24 hr	29	34	-- <sup>d</sup>	-- <sup>d</sup>
3	3,5-(OBn) <sub>2</sub>	 H <sub>2</sub> N-CH(Me)-CH <sub>2</sub> -C(=O)OBn (1.0)	K <sub>2</sub> CO <sub>3</sub> (2.0 equiv) NIS (1.0 equiv) MeCN (0.1 M)	0 °C, 24 hr	31	36	na	~27

<sup>a</sup>All yields determined by <sup>1</sup>H NMR using an internal standard. <sup>b</sup>Not observed. <sup>c</sup>Yield not determined. <sup>d</sup>Observed but NMR too messy to quantify.

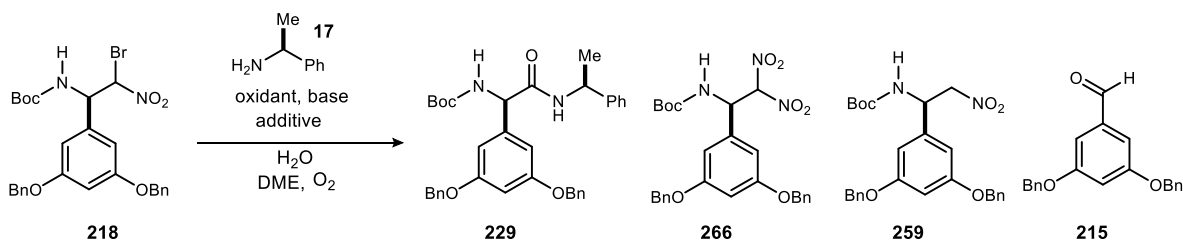
At this stage in the project, we shifted our efforts to focus solely on the 3,5-disubstituted aryl donor, due its presence in (-)-feglymycin. To this extent, we examined the use of new oxidants, additives and bases, as well as their combined effects with changes in temperature, stoichiometry, and concentration. Dr. Kazuyuki Tokumaru contributed a Herculean effort toward the execution of this exhaustive number of permutations. **Figure 22** presents a partial summary of the factors examined. Of the possible combinations, the most effective was the use of a nitroso scavenger such as *N,N*-dimethylaniline or piperidine. Additionally, the use of peroxide oxidant systems was essential to the study. The nitroso scavengers resulted in an increase in yield – a possible result of aiding in the collapse of the alkyl nitrite isomer of the tetrahedral intermediate, or for preventing the degradation of the  $\alpha$ -bromo nitroalkane starting material. They did not, however, significantly improve the overall reaction profile and purification was still immensely difficult.

**Figure 22.** Factors examined to optimize UmAS with electron-rich aryl glycinamide precursors.



The presence of peroxide however, caused a momentous shift in the reaction profile. The reactions were tremendously cleaner. Thus, we focused on improving the yield of this variety of reactions. Table 21 shows some selected examples that led to the initial observation of cleaner reactions and an increase in yield. Using KOOH as a base and co-oxidant significantly decreased the amount of decomposition observed. While the yield of desired amide was relatively low using two equivalents of KOOH (23%), only trace amounts of oxidized amide product were observed, and importantly, 30% of the starting  $\alpha$ -bromo nitroalkane was recovered (Table 21, entry 3). An increase in the amount of KOOH caused a large jump in yield to 53% (Table 21, entry 4). However, the amount of dinitroalkane was unchanged and less of the  $\alpha$ -bromo nitroalkane was recovered.

**Table 21.** Selected examples of oxidants examined in UmAS with 3,5-(OBn)<sub>2</sub>-DPG (**218**) and AMBA.



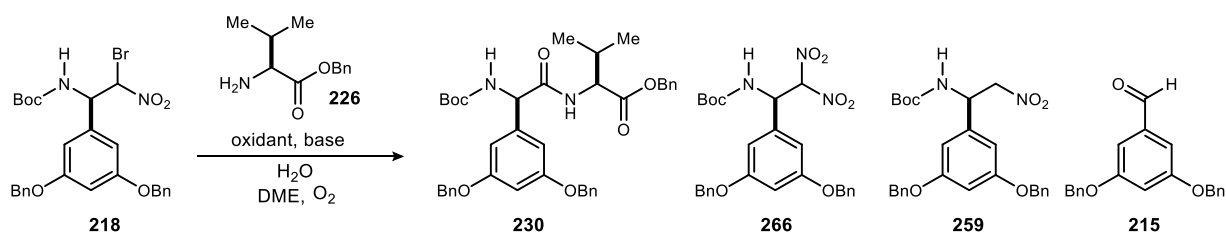
entry	218 (equiv)	17 (equiv)	base (equiv)	oxidant (equiv)	H <sub>2</sub> O (equiv)	218 (recovered)	229 (yield)	266 (yield)	259 (yield)	215 (yield)	notes
1 <sup>a</sup>	1.0	1.2	K <sub>2</sub> CO <sub>3</sub> (2.0)	Ph(OAc) <sub>2</sub> (2) + KI (1.2)	5	6	35	7	12	6	0 °C, 36 hr
2	1.0	1.2	K <sub>2</sub> CO <sub>3</sub> (2.0)	PhSeSePh (0.2)	5	nd	<10%	nd	19	nd	0 °C 24 hr then rt 48 hr
3	1.0	1.2	KOOH (2)	NIS (1)	35	30	23	13	12	--	0 °C 24 hr then rt 72 hr
4	1.0	1.2	KOOH (6)	NIS (3)	35	7	53	13	10	2	0 °C, 48 hr
5	1.0	3.6	KOOH (6)	NIS (3)	35	21	53	Trace	21	nd	0 °C, 48 hr
6	1.0	1.2	KOOH (6)	NIS (3)	35	10	40	7	30	3	Using MeCN 0 °C, 48 hr
7	1.0	1.2	K <sub>2</sub> CO <sub>3</sub> (2)	NIS (1), UHP (2)	0	17	44	15	12	1	0 °C, 48 hr
8	1.0	1.2	K <sub>2</sub> CO <sub>3</sub> (2)	NIS (1), UHP (2)	0	5	48	17	3	21	Using MeCN 0 °C, 48 hr
9	1.0	1.2	K <sub>2</sub> CO <sub>3</sub> (2)	NIS (1), tBuOOH (2)	5	-- (full conversion)	<51	37	--	--	0 °C, 24 hr
10	1.0	1.2	K <sub>2</sub> CO <sub>3</sub> (2)	NIS (1), UHP (2)	5	<9	47	23	--	9	0 °C, 72 hr
11	1.0	3.6	K <sub>2</sub> CO <sub>3</sub> (6)	NIS (3) 30% aq H <sub>2</sub> O <sub>2</sub> (6)	With oxidant	11	55	--	14	--	rt, 2 hr
12	1.0	3.6	K <sub>2</sub> CO <sub>3</sub> (6)	NIS (3) 30% aq H <sub>2</sub> O <sub>2</sub> (6) Urea (6)	With oxidant	Full conversion	62	15	0	nd	rt, 2 hr

<sup>a</sup>Also isolated from this reaction: dibromonitroalkane (17%).

Gratifyingly, drawing inspiration from previous studies and using a larger excess of amine provided the same 53% yield, but only trace dinitroalkane was observed and more starting material could be recovered (**Table 21**, entry 5). Removing water from the system, returning to the carbonate base, and using solid urea-hydrogen peroxide gave similar results to the reactions using

KOOH (**Table 21**, entries 7-8, 10). Ultimately, a return to a semi-aqueous system, combined with the presence of peroxide and urea as a stabilizing agent led to the best yield observed at the time, with complete conversion of the starting  $\alpha$ -bromo nitroalkane and a rather clean reaction profile (62% yield of amide, **Table 21**, entry 12). This reaction was also complete in two hours at room temperature. We postulate that the urea contributes to the increased yield by stabilizing the peroxide, and also may help with solubility and aggregation through interactions with the substrates or with the solvent.

**Table 22.** Selected examples from the examination of peroxides for the coupling of 3,5-(OBn)<sub>2</sub>-bromonitroalkane **218** to valine benzyl ester.



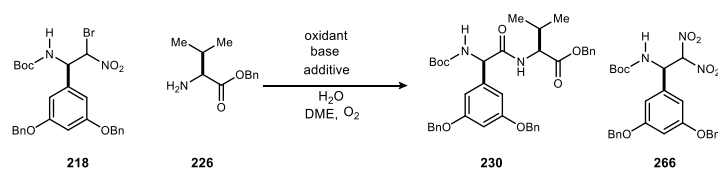
entry	218 (equiv)	226 (equiv)	base (equiv)	oxidant (equiv)	230 (yield)	266 (yield)	temp, time
1 <sup>a</sup>	1.0	3.6	K <sub>2</sub> CO <sub>3</sub> (6)	NIS (3) 30% aq H <sub>2</sub> O <sub>2</sub> (6)	49 <sup>b</sup>	29 <sup>b</sup>	rt, 2 hr
2	1.0	3.6	K <sub>2</sub> CO <sub>3</sub> (6)	NIS (3) 30% aq H <sub>2</sub> O <sub>2</sub> (6) Fe(BF <sub>4</sub> ) <sub>2</sub>	229	23 <sup>b</sup>	rt, 2hr
3	1.0	3.6	K <sub>2</sub> CO <sub>3</sub> (6)	NIS (3) 30% aq H <sub>2</sub> O <sub>2</sub> (3)	51 <sup>b</sup>	nd	rt, 2 hr
4	1.0	3.6	K <sub>2</sub> CO <sub>3</sub> (6)	NIS (3) 30% aq H <sub>2</sub> O <sub>2</sub> (12)	57 <sup>b</sup>	nd	rt, 2 hr
5	1.0	1.2	K <sub>2</sub> CO <sub>3</sub> (6)	KI (2) 30% aq H <sub>2</sub> O <sub>2</sub> (3)	51 <sup>b</sup>	nd	0 °C, 22 hr
6	1.5	1.0	K <sub>2</sub> CO <sub>3</sub> (3)	NIS (1) 30% aq H <sub>2</sub> O <sub>2</sub> (1)	18 <sup>b</sup>	nd	rt, 2 hr
7	1.0	1.2	K <sub>2</sub> CO <sub>3</sub> (6)	KI (2) 3M aq UHP (3) <sup>c</sup>	57 <sup>b</sup>	8 <sup>b</sup>	0 °C, 24 hr
8	1.0	1.2	Cs <sub>2</sub> CO <sub>3</sub> (6)	KI (2) 3M aq UHP (3) <sup>c</sup>	43 <sup>b</sup>	nd	0 °C, 24 hr
9	1.0	1.2	Na <sub>2</sub> CO <sub>3</sub> (6)	KI (2) 3M aq UHP (3) <sup>c</sup>	47 <sup>b</sup>	nd	0 °C, 48 hr
10	1.0	1.2	Li <sub>2</sub> CO <sub>3</sub> (6)	LiI (2) 3M aq UHP (3) <sup>c</sup>	17 <sup>b</sup>	nd	0 °C, 24 hr
11	1.05	1.0	K <sub>2</sub> CO <sub>3</sub> (6)	KI (2) 3M aq UHP (3) <sup>c</sup>	58 <sup>d</sup>	<13 <sup>d</sup>	0 °C, 24 hr
12	1.05	1.0	K <sub>2</sub> CO <sub>3</sub> (6)	KI (2) 3M H <sub>2</sub> O <sub>2</sub> (3) <sup>c</sup>	61 <sup>d</sup>	<11 <sup>d</sup>	0 °C, 24 hr
13	1.2	1.0	K <sub>2</sub> CO <sub>3</sub> (6)	KI (2) 3M H <sub>2</sub> O <sub>2</sub> (3) <sup>c</sup>	72 <sup>d</sup>	not isolated	0 °C, 24 hr

<sup>a</sup>Also isolated from this reaction were **218** (16%) and **259** (17%). <sup>b</sup>Yield determined by <sup>1</sup>H-NMR. <sup>c</sup>Added as a 3 M aqueous solution over 2 hours. <sup>d</sup>Isolated yield.



This incited a closer look at the effect of peroxides in this reaction (**Table 22**). We observed that using more than 3 equivalents of peroxide did not significantly increase the yield. Interestingly, making a change from NIS to KI allowed for the reduction of the amount of amine used back to 1.2 equivalents with little effect on the yield (**Table 22**, entries 5&7). This implies that the peroxide is oxidizing the iodide to iodonium *in situ*. Moreover, a solution of urea-hydrogen peroxide was a suitable substitute for aqueous H<sub>2</sub>O<sub>2</sub> (**Table 22**, entry 7). Alternative carbonate bases were examined and K<sub>2</sub>CO<sub>3</sub> performed the best (**Table 22**, entries 7-10). It was found that dropwise addition of the peroxide solution was beneficial. Lastly, and perhaps most importantly, when using the amine as the limiting reagent we saw, for the first time, a very 'clean' reaction with a 72% isolated yield (**Table 22**, entry 13).

With these results in hand the reaction could be fine-tuned to fit some procedural preferences. A solution of urea-hydrogen peroxide is preferable to aqueous H<sub>2</sub>O<sub>2</sub> on larger scale as it is more stable and can be freshly prepared. It also gives us the freedom to change the amount of water if necessary. As shown in **Table 23**, the relative stoichiometry of all the reagents, the rate of addition of the peroxide solution, as well as time, temperature, and atmosphere were examined. It was found that the reaction was often complete after approximately 3 hours if excess  $\alpha$ -bromonitroalkane was used (**Table 23**, entries 5-7). Ultimately, a 72% yield was obtained using the conditions described in entry 8 (**Table 23**). Typically, these reactions are run using an atmosphere of oxygen, but we found that running the reaction open to air was not detrimental (**Table 23**, entry 9). Perhaps one of the biggest benefits of this protocol is that solubility is much improved as compared to the standard NIS/K<sub>2</sub>CO<sub>3</sub> conditions. This was crucial to improve the ease of set up for large-scale reactions. Previously an overhead stirrer was necessary to get good mixing, but in this case we are able to run reactions using a simple stir bar with only a minor decrease in yield (**Table 23**, entry 10). The efficiency of this reaction on multi-gram scale will be described in our formal synthesis of (-)-feglymycin (Chapter 3).

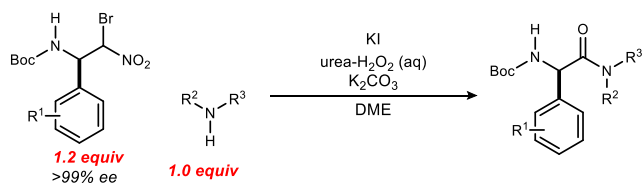
**Table 23.** Further optimization of KI/UHP protocol.<sup>a</sup>

entry	218 (equiv)	226 (equiv)	base (equiv)	oxidant (equiv)	oxidant addition	230 (yield)	266 (yield)	temp, time	atmosphere
1	1.0	1.2	K <sub>2</sub> CO <sub>3</sub> (6)	KI (2) 3M aq UHP (3)	dropwise	61	nd	0 °C, 22 hr	O <sub>2</sub>
2	1.0	1.2	K <sub>2</sub> CO <sub>3</sub> (3)	KI (2) 3M aq UHP (1.5)	dropwise	48	nd	0 °C, 22 hr	O <sub>2</sub>
3	1.0	1.2	K <sub>2</sub> CO <sub>3</sub> (6)	KI (2) 3M aq UHP (3)	dropwise	57	nd	0 °C, 22 hr	air
4	1.0	1.05	K <sub>2</sub> CO <sub>3</sub> (6)	KI (2) 3M aq UHP (3)	dropwise	58	nd	0 °C, 22 hr	air
5	1.2	1.0	K <sub>2</sub> CO <sub>3</sub> (6)	KI (2) 3M aq UHP (3)	dropwise	57	20	0 °C, 2 hr UHP addition, then 1 hr	O <sub>2</sub>
6	1.2	1.0	K <sub>2</sub> CO <sub>3</sub> (6)	KI (2) 3M aq UHP (3)	one portion	64	10-20% (not isolated)	0 °C, 2 hr	O <sub>2</sub>
7	1.2	1.0	K <sub>2</sub> CO <sub>3</sub> (3)	KI (2) 3M aq UHP (1.5)	dropwise	57	10-20% (not isolated)	0 °C, 2 hr UHP addition, then 1 hr	O <sub>2</sub>
8	1.2	1.0	K <sub>2</sub> CO <sub>3</sub> (6)	KI (2) 3M aq UHP (3)	dropwise	72	nd	0 °C, 22 hr	O <sub>2</sub>
9	1.2	1.0	K <sub>2</sub> CO <sub>3</sub> (6)	KI (2) 3M aq UHP (3)	dropwise	72	nd	0 °C, 22 hr	air
10 <sup>b</sup>	1.2	1.0	K <sub>2</sub> CO <sub>3</sub> (6)	KI (2) 3M H <sub>2</sub> O <sub>2</sub> (3)	dropwise	66	not isolated	0 °C to rt 24 hr	O <sub>2</sub>

<sup>a</sup>All reactions run on 0.1 mmol scale unless otherwise noted. <sup>b</sup>0.5 mmol scale

We were very pleased to see that these results were not specific to this particular combination of  $\alpha$ -bromo nitroalkane and amine. Using the 3,4-aryl substituted substrate gave results identical to the 3,5-aryl substituted system (entry 3, **Table 24**). Several amines were also examined and we observed that these conditions tolerated the free primary alcohol in ethanolamine (**Table 24**, entry 4) and the electron-poor nature of aminoacetonitrile (**Table 24**, entry 5). Disubstituted and secondary amines also worked well (**Table 24**, entries 6-8). Even the sterically encumbered adamantamine was incorporated, albeit in lower yield (**Table 24**, entry 8). Finally, we demonstrated that coupling to simple primary amines is quite facile as exhibited by the coupling to allylamine in quantitative yield (**Table 24**, entry 9).

**Table 24.** Examination of various amines using the KI/UHP protocol for UmAS.<sup>a</sup>

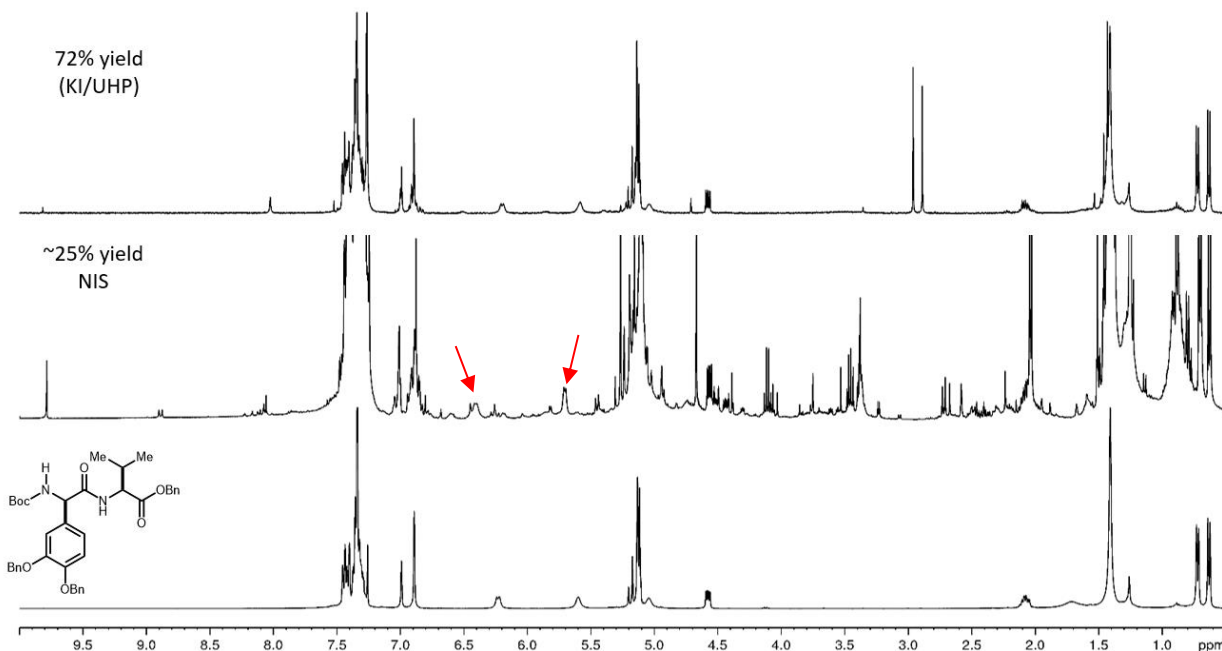


entry	amine	product	product	temp	yield <sup>b</sup>
1			<b>230</b>	0 °C	72 <sup>c</sup>
2	HCl • H <sub>2</sub> N-CH(Me)-CH2-C(=O)OBn		<b>227</b>	0 °C	65 <sup>c,d</sup>
3	HCl • H <sub>2</sub> N-CH(Me)-CH2-C(=O)OBn		<b>267</b>	0 °C	72
4	H <sub>2</sub> N-CH2-CH2-OH		<b>268</b>	24 °C	97
5 <sup>e</sup>	H <sub>2</sub> SO <sub>4</sub> • H <sub>2</sub> N-CH2-CN		<b>269</b>	24 °C	55
6	HNEt <sub>2</sub>		<b>270</b>	24 °C	67
7	HCl • HN(CH <sub>2</sub> ) <sub>2</sub> CO <sub>2</sub> Me		<b>271</b>	24 °C	77
8	HCl • HN(CH <sub>2</sub> ) <sub>2</sub> CO <sub>2</sub> Me		<b>272</b>	24 °C	76
9	H <sub>2</sub> N-Cyclohexane		<b>273</b>	24 °C	37
9	H <sub>2</sub> N-Bicyclo[2.2.1]heptane		<b>273</b>	0 °C	quant
9	H <sub>2</sub> N-CH2-CH=CH <sub>2</sub>		<b>273</b>	0 °C	quant

<sup>a</sup> Unless otherwise noted, reactions were on 0.1 mmol scale for 18 hours using the amine (1.0 equiv),  $\alpha$ -bromonitroalkane (1.2 equiv), KI (2.0 equiv.) and K<sub>2</sub>CO<sub>3</sub> (6.0 equiv) in DME (0.1 M). A freshly prepared 3 M aqueous solution of urea-hydrogen peroxide (3.0 equiv) was added over 2 hours by syringe pump. <sup>b</sup> Yield determined by <sup>1</sup>H-NMR using an internal standard. <sup>c</sup> Isolated yield. <sup>d</sup> Reaction run on 12 mmol scale. <sup>e</sup> Using 8.0 equiv. K<sub>2</sub>CO<sub>3</sub>. Refer to the Chapter 4 for more details.

The improvements in the reaction profile and ease of purification can be deduced from a comparison of the crude  $^1\text{H}$ -NMRs of the reactions using KI/UHP and those using NIS (**Figure 23**). As shown, the desired glycinamide is the main product in the KI/UHP reaction, and the relative amounts of byproducts are drastically decreased.

**Figure 23.** Comparison of crude  $^1\text{H}$ -NMRs from UmAS with KI/UHP and NIS.



All spectra obtained on a 400 MHz NMR in  $\text{CDCl}_3$ . Arrows indicate the NH and  $\alpha$ -CH protons of the glycinamide product, which shift in the crude NMR from the reaction run using NIS.

Ultimately, the discovery of the KI/urea-hydrogen peroxide system holds many benefits, some of which are listed below.

1. Reaction is typically complete in 3-24 hours.
2. The aqueous solution of UHP improves solubility
3. Mechanical stirring is not necessary on mutigram scale (up to 12 mmol of amine tested).
4. The amine is the limiting reagent.
5. Cleaner reaction profile is observed.

With this we now have a reliable, epimerization-free means to access aryl glycinamides. We have demonstrated the relevance and robustness of this transformation in our formal synthesis of (-)-feglymycin (see Chapter 3).

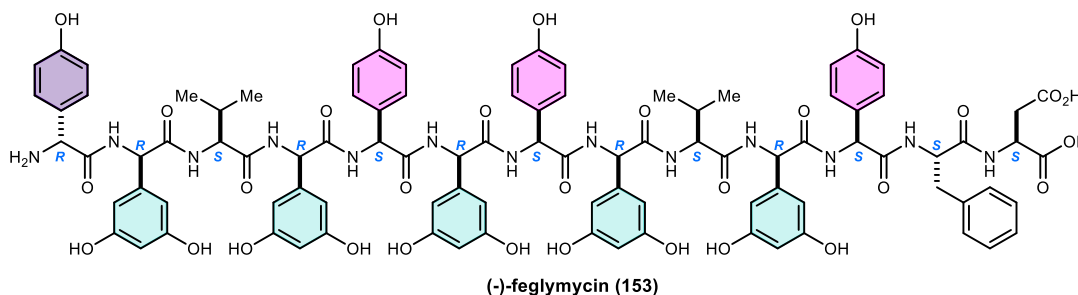
### III. The formal synthesis of (-)-feglymycin.

#### 3.1 Introduction to feglymycin

##### 3.1.1 Isolation and structure

Feglymycin (**153**, **Figure 24**) is a stereochemically unusual, aryl glycine-rich, helical tridecapeptide natural product with antiviral and antibacterial properties. It was first isolated in 1998 by Vertésy and coworkers from cultures of *Streptomyces* sp. DSM 11171 by solid phase extraction, size exclusion chromatography and reversed-phase chromatography.<sup>203</sup> It was found to have a  $[M+H]^+$   $m/z$  at 1900.6 and an  $[M+2H]^{2+}$   $m/z$  at 950.9, and its molecular formula was determined to be  $C_{95}H_{97}N_{13}O_{30}$ . The structure was elucidated by 1D and 2D NMR spectroscopy, which showed the 13  $\alpha$ -amino amides displayed in **Figure 24**. The amino acid sequence was further confirmed by its fragmentation pattern in mass spectroscopy, and it was determined that feglymycin contains the rare noncanonical amino acid residues 4-hydroxyphenylglycine (Hpg) and 3,5-dihydroxyphenylglycine (Dpg).

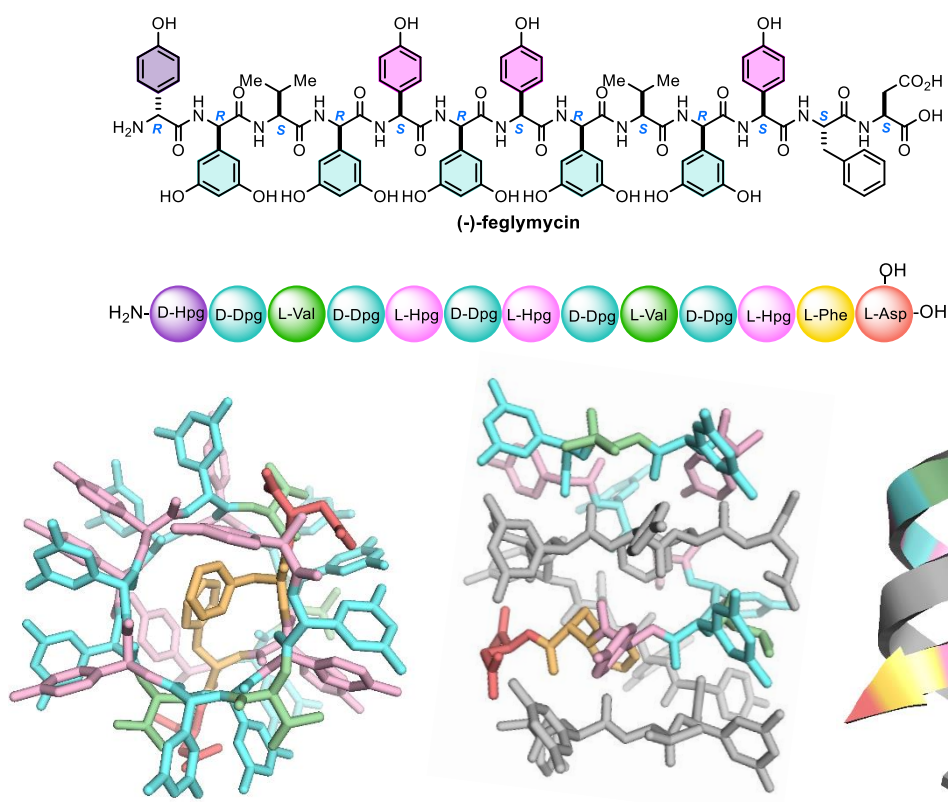
**Figure 24.** Structure of (-)-feglymycin (**153**).



<sup>203</sup> Vertesy, L.; Aretz, W.; Knauf, M.; Markus, A.; Vogel, M.; Wink, J. *J. Antibiot.* **1999**, 52, 374.

Six years after the report of its isolation, the crystal structure was solved, which provided stereochemical assignments of the amino acids.<sup>204</sup> Impressively, at the time of publication this crystal structure was the largest equal-atom structure solved by direct methods. In fact, with 1033 unique non-hydrogen atoms, it was 50% larger than the biggest solved structure at the time. The solved structure showed that with the exception of the termini, all of the residues alternate stereochemistry. Feglymycin, like gramicidin, which also has alternating D/L configurations, exists as a wide, antiparallel, double-stranded  $\beta$ -

**Figure 25.** Crystal structure of feglymycin.



helical dimer (**Figure 25**).<sup>204,205</sup>

<sup>204</sup> Bunkóczi, G.; Vértesy, L.; Sheldrick, G. M. *Angew. Chem. Int. Ed.* **2005**, *44*, 1340.

<sup>205</sup> Langs, D. A. *Science* **1988**, *241*, 188.; Di Blasio, B.; Benedetti, E.; Pavone, V.; Pedone, C.; Gerber, C.; Lorenzi, G. P. *Biopolymers* **1989**, *28*, 203.; Di Blasio, B.; Benedetti, E.; Pavone, V.; Pedone, C.; Spiniello, O.; Lorenzi, G. P. *Biopolymers* **1989**, *28*, 193.

The dimers align to form infinite right-handed helical chains. The channel formed by feglymycin is shorter and wider than that of the transmembrane spanning pentadecapeptide gramicidin. Bunkóczi and coworkers speculated that it is improbable that feglymycin would behave as a membrane channel since it is likely too short to span a biological membrane, and the phenylalanine side chains may prevent transportation. However, the authors do suggest that it could certainly act as an ion carrier, which may contribute to its biological activity. Its structure certainly informs its biological properties, to which significant efforts have been dedicated to understanding.

### **3.1.2 Biological activity**

Upon its isolation, feglymycin was identified as having anti-HIV and antibacterial activity.<sup>203</sup> This was confirmed by the Süßmuth group following their seminal total synthesis of feglymycin.<sup>206</sup> As of 2020, unique mechanisms of action have been attributed to feglymycin for both its antibacterial and anti-HIV activity. This is important as bacterial and viral mutations continue to diminish the effectiveness of current treatments. Currently, there is a critical need for new antibiotics to target resistant microbes such as methicillin resistant *Staphylococcus aureus* (MRSA) and vancomycin resistant enterococci (VRE). In a similar vein, HIV drug resistance can develop within a patient and make treatment ineffective. Moreover, this can lead to the transmission of drug-resistant HIV. As viral and bacterial mutations occur in response to current therapies, other drugs with similar mechanisms of action become compromised as well due to cross-resistance. One way to combat this is through the discovery and development of drugs with novel mechanisms of action.

#### **Anti-HIV activity**

Feglymycin was found to have an uncommon mechanism of action with regard to its anti-HIV properties. It was found to target the entry process, specifically the binding, of HIV to host cells. The vast majority of HIV treatments target post-entry processes (**Figure 26**). In fact, as of January 2020 only 3 FDA-approved drugs are in use that target the entry process: T20 (enfuvirtide, Fuzeon®, fusion inhibitor), maraviroc (Selzentry®, CCR5 antagonist) and ibalizumab-uiyk (Trogarzo®, post-attachment inhibitor).<sup>207</sup> **Feglymycin was shown to not only engage this**

---

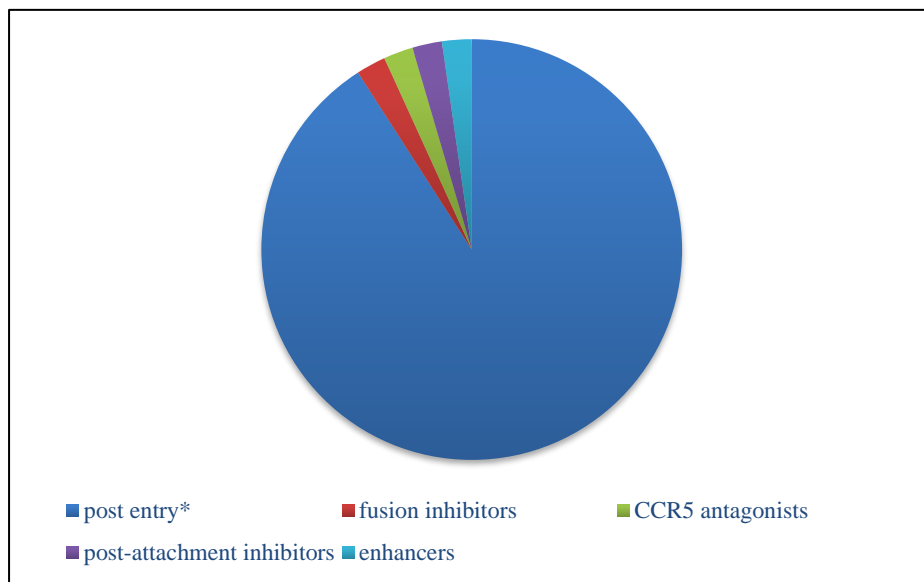
<sup>206</sup> Dettner, F.; Hänchen, A.; Schols, D.; Toti, L.; Nußer, A.; Süßmuth, R. D. *Angew. Chem. Int. Ed.* **2009**, *48*, 1856.

<sup>207</sup> Services, U. S. D. O. H. A. H.; National Institutes of Health: 2020; Vol. 2020.



under-developed target, but it does so in a manner distinct from current viral entry therapies.

Figure 26. Classes of FDA-approved anti-HIV drugs.<sup>a</sup>



<sup>a</sup>Graph is current as of January 2020 and represents only FDA-approved drugs currently in use  
\*post-entry drugs include NNRTIs, NRTIs, PIs, integrase inhibitors and combination drugs

As previously stated, feglymycin displayed anti-HIV activity upon its isolation.<sup>203</sup> Süßmuth and coworkers determined that both feglymycin and its enantiomer had  $\mu\text{M}$  anti-HIV activity and no cytotoxicity at 100  $\mu\text{M}$  in the human MT-4 cell line.<sup>206</sup> In 2012, Férir and coworkers expanded our understanding with an in-depth look at feglymycin's antiviral activity.<sup>208</sup> Overall, the researchers found that feglymycin has broad activity against many strains of HIV and a unique mechanism of action.

The life cycle of HIV is depicted in **Figure 27**. Cluster of differentiation 4 (CD4) is a glycoprotein found on the surface of cells involved in the immune response. In general, HIV will attack and destroy CD4<sup>+</sup> cells. The virus will hijack the machinery within the CD4<sup>+</sup> cell to replicate and

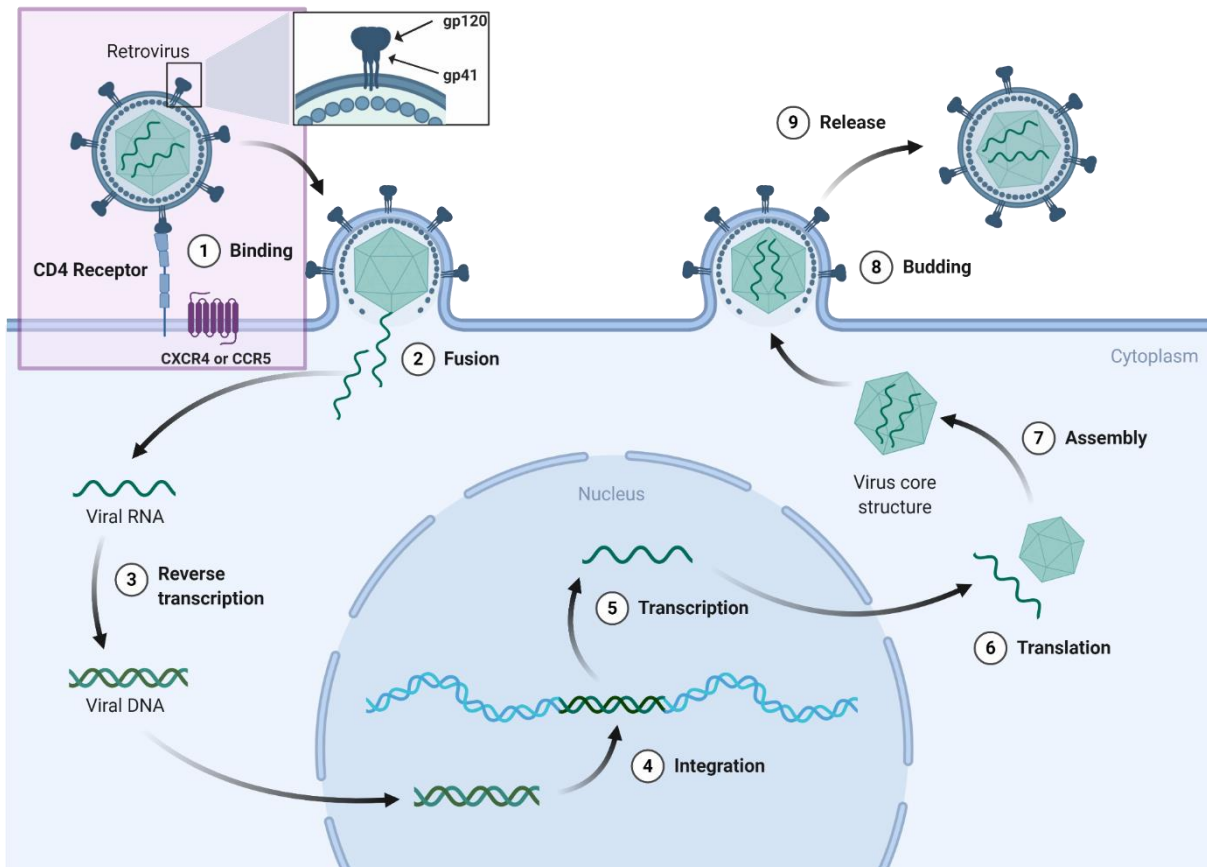
---

<sup>208</sup> Férir, G.; Hänchen, A.; François, K. O.; Hoorelbeke, B.; Huskens, D.; Dettner, F.; Süßmuth, R. D.; Schols, D. *Virology* **2012**, 433, 308.

spread throughout the body. There are nine steps shown in **Figure 27**, but the first step, binding, is of most importance to this discussion as that is the process associated with feglymycin's activity.

The HIV virus has an envelope that is derived from host cell membranes, and incorporated into that envelope are two glycoproteins: gp41 and gp120 (**Figure 27**). The virus uses gp120 to bind to the CD4 receptor. This causes a conformational change in gp120, allowing it to adsorb to a chemokine coreceptor (C-X-C motif chemokine receptor 4; CXCR4 or C-C chemokine receptor type 5; CCR5). This adsorption elicits an additional conformational change that exposes the fusion protein, gp41. This action allows the viral envelope to fuse with the host cell membrane (2, **Figure 27**). After fusion, the single stranded viral RNA is released from the capsid into the cytoplasm of

**Figure 27.** HIV infection and replication.<sup>209</sup>



<sup>209</sup> Figure created using BioRender.

the host cell. A process called reversed transcription converts RNA into single-stranded DNA and then double-stranded DNA. The viral DNA is brought into the nucleus and incorporated into the host's chromosomes. At this stage the provirus can lie latent or can be active. If it is active, the processes of transcription and translation will occur, the virus core structure is assembled, and the immature virus pushes itself out of the host cell (budding, **Figure 27**). After release, maturation occurs and the virus is free to infect more cells.

In order to determine feglymycin's role in intervening in this complex life cycle, Férir and coworkers began by evaluating its activity against a diverse set of HIV strains. This included cell-line adapted, mutant, and clinically isolated HIV-1 and HIV-2 strains. The researchers also examined cell lines with distinct coreceptors that work with the CD4 receptor and gp120 to bring HIV into the cell, namely CXCR4 and CCR5.

Drugs that target the entry process of HIV typically involve inhibition of gp120, gp41, or the co-receptor (CXCR4 or CCR5). Thus, feglymycin was tested against strains that are resistant to each of these mechanisms. If feglymycin is active, that would imply that it acts by a different mechanism than the one to which the mutant is resistant. As such, feglymycin was active ( $EC_{50}=0.9-2.4 \mu\text{M}$ ) against three mutant HIV-1 strains: (i) gp41 fusion inhibitor T20, (ii) carbohydrate binding anti-gp120 monoclonal antibody (mAb) 2G12, and (iii) CXCR4 antagonist AMD3100. This demonstrates that feglymycin has a unique mechanism of action as compared to other viral-entry inhibiting drugs. Importantly, feglymycin also showed broad spectrum anti-HIV activity against clinical strains that represent members of different viral clads regardless of their coreceptor tropism (CXCR4 or CCR5). In another experiment, feglymycin maintained consistent activity with increasing viral titer (measured as  $TCID_{50}$ ). This was significant as the gp41 fusion inhibitor T20 and the anti-gp120 mAb 2G12 completely lost antiviral activity under the same conditions.

In an effort to understand the SAR of feglymycin, the group conducted an alanine scan and found that only [D-Ala13]-feglymycin had a significant change (6.5-fold decrease). Interestingly, this is also the only derivative that contributed to feglymycin's inhibition of the cytoplasmic ligase enzymes MurA and MurC (*vide infra*).<sup>210</sup>

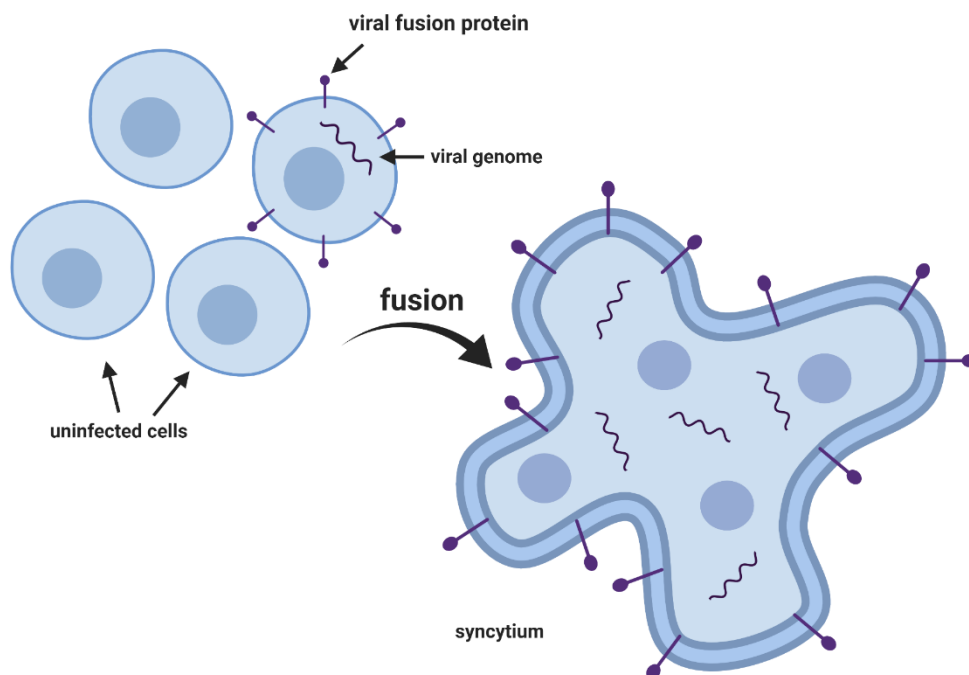
---

<sup>210</sup> Hänchen, A.; Rausch, S.; Landmann, B.; Toti, L.; Nusser, A.; Süßmuth, R. D. *ChemBioChem* **2013**, *14*, 625.

A *time of drug addition* experiment helped to narrow down feglymycin's mechanism of action. In this experiment a compound is added at specific time points after infection – if the compound targets the binding process it would have no effect, whereas if the compound targets reverse transcription or is a protease inhibitor, then it would retain activity. To this extent, when added one hour after infection, feglymycin's activity diminished, suggesting that it acts as an early viral binding/adsorption inhibitor.

It is known that CD4<sup>+</sup> T-cells can be infected by free virions and also by cell-to-cell contact. This results in the formation of syncytia or “giant cells” as shown in **Figure 28**. Vértesy and coworkers originally found that feglymycin inhibited the formation of HIV syncytia *in vitro*.<sup>203</sup> An IC<sub>50</sub> of ~5

**Figure 28.** Representation of viral syncytia formation.<sup>211</sup>



μM was identified by microscope, which was further tuned to 3.6 μM by p24 antigen test. Férir and coworkers found that feglymycin prevented the appearance of syncytia in a dose-dependent

<sup>211</sup> Figure created with BioRender.

manner. Similar to its consistency in activity with increased viral titer, feglymycin's activity against cell to cell transmission was also comparable to its activity against general HIV infection, with an EC<sub>50</sub> of 5.4 μM. Conversely, the AMD3100 and T20 reference compounds lost at least 1000-fold of their inhibitory activity in these experiments. It should be noted however, that these compounds are changing from nM to μM EC<sub>50</sub> values.

Another series of experiments used ELISA to show that feglymycin inhibited the act of binding of HIV-1 to the CD4<sup>+</sup> T-cell surface. Moreover, surface plasmon resonance was used to measure the affinity constant (K<sub>D</sub>) for the interaction between feglymycin and gp120 with both the CXCR4 and CCR5 coreceptors. Feglymycin has a K<sub>D</sub> of 6.1 nM and 2.2 nM for gp120-CXCR4 and gp120-CCR5 respectively. The group also measured the K<sub>D</sub> for [D-Ala13]-feglymycin and found it has 8-fold less affinity for gp120 than feglymycin. This is in accordance with the previously observed loss of activity for [D-Ala13]-feglymycin.

To further confirm the hypothesis that feglymycin works by inhibiting the binding of HIV to CD4<sup>+</sup> cells, Férir and coworkers sought to identify a feglymycin-resistant strain of HIV. After 44 passages they were successful in this feat. Intriguingly, only two mutations existed in the gp120 of the resistant strain; I153L and K457I – both of which are located near the CD4 binding domain. There were no changes in gp41. This further supports the aforementioned hypothesis.

Overall, these experiments indicate that feglymycin has a rare mechanism of action that targets HIV entry. Given the propensity for viral mutation, the development of drugs with unique mechanisms of action is a crucial process for the treatment of HIV, which makes feglymycin an appealing anti-HIV prototype that should be further explored.

### **Antibacterial activity**

Many antibiotics, including the β-lactam and glycopeptide antibiotics, target peptidoglycan (PG) biosynthesis, a key step of bacterial cell-wall construction that is essential for microbial survival.<sup>212,213</sup> The arylglycine-containing antibiotics vancomycin<sup>147</sup> and ramoplanin<sup>144</sup> are known

---

<sup>212</sup> For a review on peptidoglycan biosynthesis as a target for drug development see: Gautam, A.; Vyas, R.; Tewari, R. *Critical Reviews in Biotechnology* **2011**, *31*, 295.

<sup>213</sup> For reviews on the cytoplasmic steps of peptidoglycan biosynthesis and their roles as drug targets see: a) Kouidmi, I.; Levesque, R. C.; Paradis-Bleau, C. *Mol. Microbiol.* **2014**, *94*, 242. b) El Zoeiby, A.; Sanschagrín, F.; Levesque, R.

to inhibit the later stages of peptidoglycan biosynthesis.<sup>214</sup> Given its structural similarity to these glycopeptide antibiotics as well as its large size, it was originally postulated that feglymycin may have a similar mechanism of action. However, Süßmuth ultimately found that feglymycin did not affect the later stages of peptidoglycan biosynthesis and instead actually possesses a unique mechanism of action.<sup>215</sup>

**Figure 29** shows a general overview of the complex peptidoglycan biosynthesis pathway.<sup>212,213</sup> The PG layer is essential for bacterial survival as it provides structural strength and combats the high internal osmotic pressure in the cytoplasm. The core pieces of the peptidoglycan layer are made up of long polysaccharide chains with alternating *N*-acetylglucosamine (GlcNAc) and *N*-acetylmuramic acid (MurNAc) motifs that are cross-linked by peptides. The overall process of PG synthesis can be split into three main stages. Stage I occurs in the cytoplasm and involves the synthesis of UDP-MurNAc-l-Ala- $\gamma$ -d-Glu-m-Dap-d-Ala-d-Ala, or the so-called Park's nucleotide<sup>216</sup> (highlighted in the pink box, **Figure 29**). Stage II occurs in the inner membrane and consists of the synthesis of undecaprenyl-pyrophosphoryl-MurNAc-(pentapeptide)-GlcNAc, aka lipid II (**Figure 29**). In the final stage, lipid II is transported across the membrane, glycosyltransferase catalyzes its polymerization (GT, **Figure 29**), and transpeptidase carries out the crosslinking between the peptide chains (TP, **Figure 29**).

---

C. *Mol. Microbiol.* **2003**, *47*, 1. c) Barreteau, H.; Kovač, A.; Boniface, A.; Sova, M.; Gobec, S.; Blanot, D. *FEMS Microbiol. Rev.* **2008**, *32*, 168.

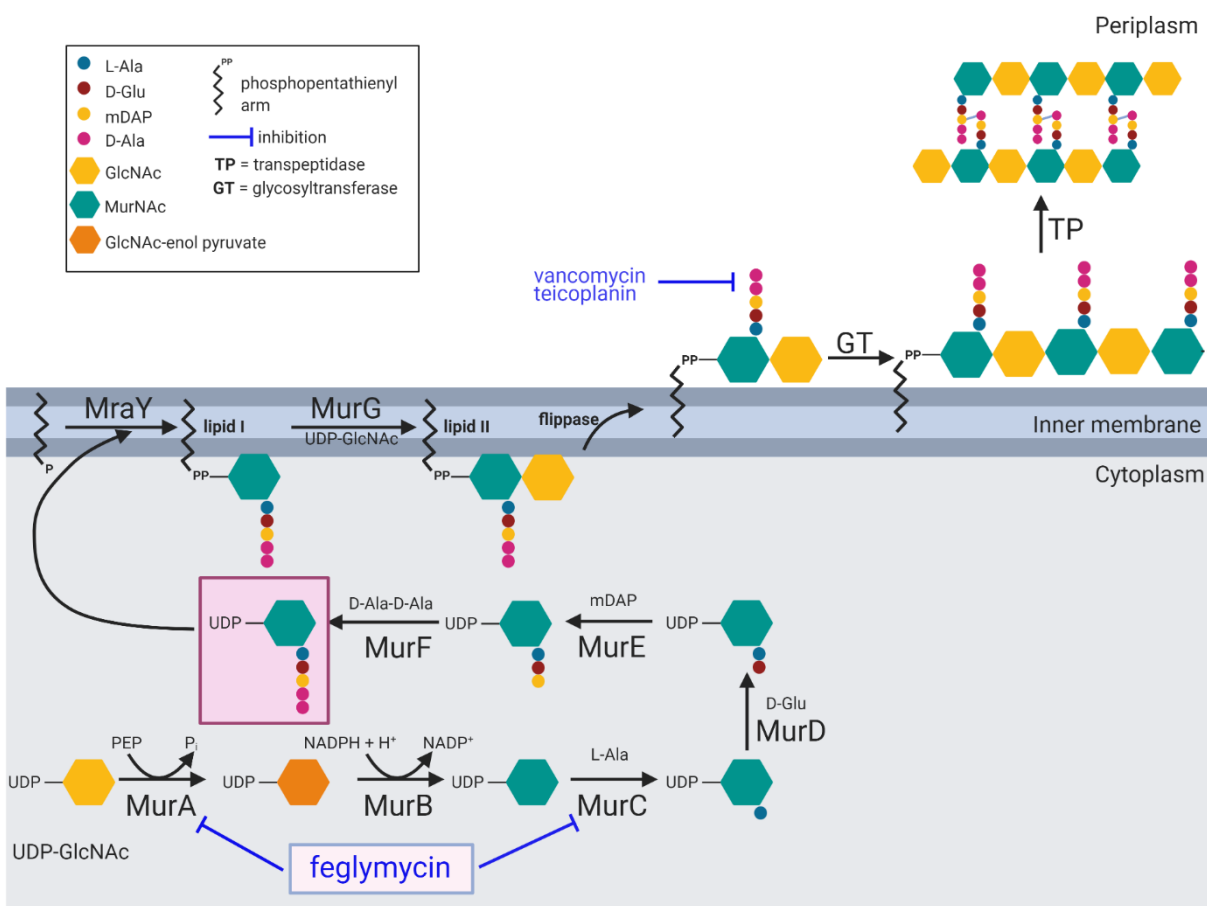
<sup>214</sup> Reynolds, P. E. *European Journal of Clinical Microbiology and Infectious Diseases* **1989**, *8*, 943.

<sup>215</sup> Rausch, S.; Hänchen, A.; Denisiuk, A.; Löhken, M.; Schneider, T.; Süßmuth, R. D. *ChemBioChem* **2011**, *12*, 1171.

<sup>216</sup> Identification and isolation: Park, J. T. *J. Biol. Chem.* **1952**, *194*, 885. Total synthesis: Hitchcock, S. A.; Eid, C. N.; Aikins, J. A.; Zia-Ebrahimi, M.; Blaszcak, L. C. *J. Am. Chem. Soc.* **1998**, *120*, 1916.

The cytoplasmic ligases MurC, MurD, MurE, and MurF catalyze the formation of the pentapeptide chain that will become the base for crosslinking in the peptidoglycan layer. MurA and MurB synthesize the UDP-*N*-acetylmuramic acid (UDP-MurNAc) precursor.<sup>218</sup> More specifically, MurA couples UDP-GlcNAc with PEP (phosphoenolpyruvate) to provide GlcNAc-enol pyruvate (**Figure 27**). MurB then uses NADPH to reduce the enol to provide UDP-MurNAc. MurC catalyzes the addition of L-Ala in an ATP dependent fashion. MurD, MurE, and MurF then extend

**Figure 29.** Diagram of peptidoglycan biosynthesis.<sup>217</sup>



<sup>217</sup> Figure created using BioRender.

<sup>218</sup> Reddy, S. G.; Waddell, S. T.; Kuo, D. W.; Wong, K. K.; Pompliano, D. L. *J. Am. Chem. Soc.* **1999**, *121*, 1175.

the peptide chain using ATP to ultimately provide Park's nucleotide. As previously mentioned, Park's nucleotide goes on to Stages II and III to make the peptidoglycan layer.

Upon its isolation, Vértessy originally found feglymycin to have weak antibacterial activity against Gram-positive bacteria (MIC ~32-64 for different strains of *S. aureus*).<sup>203</sup> However, studies years later by Süßmuth showed that feglymycin actually has potent antibacterial activity (MIC = 1-4  $\mu$ M against *S. aureus*).<sup>206</sup> Importantly, it is quite active against strains that are resistant to current therapies, such as MRSA (IC<sub>80</sub> = ~2  $\mu$ M).

As previously stated, feglymycin's antibacterial properties may stem from interactions with cytoplasmic enzymes involved in cell wall biosynthesis. *In vitro* inhibition experiments were conducted to probe feglymycin's impact on the MurA-F pathway.<sup>215</sup> This study used enzymes from both Gram-positive and Gram-negative bacteria. Interestingly, feglymycin selectively inhibited only MurA and MurC and did not have an effect on the other cytoplasmic enzymes. Feglymycin operated with non-competitive inhibition and has IC<sub>50</sub> values in the low  $\mu$ M (MurA) to upper nM (MurC) range. Using enzymes from both *E. coli* and *S. aureus* demonstrates that the enzymes in both Gram-positive and Gram-negative bacteria are inhibited by feglymycin. However, *in vivo* experiments show that feglymycin has no effect on Gram-negative bacteria such as *E. coli*. **It was thus proposed that feglymycin cannot cross the outer membrane in Gram-negative bacteria, but may cross the inner cell membrane either nonspecifically or by a transport/uptake system present in *S. aureus*.** Later studies will show that additional experiments are certainly needed to confirm or deny this hypothesis.<sup>210</sup>

Overall, within the cytoplasmic processes of peptidoglycan biosynthesis, feglymycin specifically targets MurA and MurC and displays no effect on the other Mur enzymes.<sup>215</sup> MurC is about 10 times more sensitive to feglymycin than MurA and thus it was proposed to be its main target. **This makes feglymycin the first known natural inhibitor of MurC.** While the exact mechanism of feglymycin's inhibition is still unknown, we do know that its inhibition is non-competitive and it does not bear structural similarity to the enzymes' natural substrates. Interestingly, MurA and MurC have similar three-dimensional features, especially when compared to the other Mur enzymes.<sup>213</sup> MurB and MurD-F all have a three-domain structure where as MurC forms dimers and MurA has two similar domains connected by a linker.

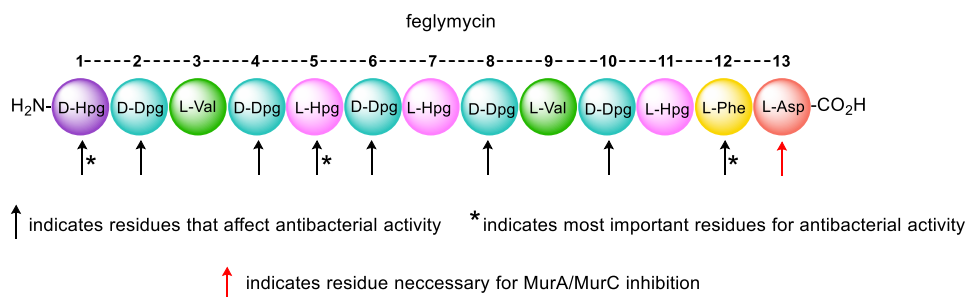


To gain further understanding of feglymycin's MOA, the Süssmuth group took on the challenge of conducting a synthetic alanine scan of feglymycin. They synthesized 13 derivatives, exchanging each amino acid for alanine, and explored the biological activity of each one.<sup>210</sup> The experiments were designed to retain the wild-type D-L configuration to control for effects on the secondary structure of the peptide. To this extent, CD spectra were recorded for each derivative and with the exception of [L-Ala13]-feglymycin, all compounds gave similar spectra to that of natural feglymycin, suggesting that the antiparallel  $\beta$ -helical dimer<sup>204</sup> was not disrupted.

**Figure 30** highlights the residues that contribute to the antibacterial properties of feglymycin as determined by the alanine scan. The study revealed that substitution of any Dpg residue resulted in 4- to 16-fold decreased activity. The most pronounced effects were observed for [D-Ala<sup>1</sup>]-feglymycin (MIC = 8  $\mu$ M), [L-Ala<sup>5</sup>]-feglymycin (MIC > 32  $\mu$ M), and [L-Ala<sup>12</sup>]-feglymycin (MIC > 32  $\mu$ M).

Perhaps the most unanticipated find from this study is that there is a difference in the results from in vitro antibacterial assays and in vitro assays for MurA and MurC inhibition. While three residues (D-Hpg1, L-Hpg5, L-Phe12) were vital for antibacterial activity, only L-Asp13 was essential for inhibition of MurA and MurC (**Figure 30**). This is interesting as L-Asp13 was also crucial for anti-HIV activity (described *vide supra*).<sup>208</sup> Moreover, this indicates that while feglymycin does inhibit cytoplasmic enzymes involved in peptidoglycan biosynthesis, other targets both within and outside of the peptidoglycan biosynthesis pathway need to be considered for antibacterial activity.

**Figure 30.** Residues that impact feglymycin's antimicrobial activity.



To conclude, it is apparent that the secondary structure of feglymycin likely contributes significantly to its anti-HIV and antibacterial properties. While the precise nuances of feglymycin's mechanism of action are not yet understood, we do know that it effects processes

unrelated to the targets of many of the drugs in use today. It is also the first natural inhibitor of MurC. Viral and bacterial resistance will always drive the need for the development of drugs with novel MOAs, and feglymycin could serve as a significant prototype in this regard.

### **3.1.3 Biosynthesis of feglymycin.**

The biosynthesis of feglymycin was elucidated in 2015 by the Süsssmuth group.<sup>219</sup> It was determined that feglymycin belongs to the class of nonribosomally synthesized peptides, and is made in a colinear, rather than an iterative, manner. The study commenced with whole genome sequencing of the producing organism, *Streptomyces* sp. DSM 11171. The biosynthetic gene cluster was then identified by mining for genes that are linked to the biosynthesis of Hpg and Dpg. The feglymycin gene cluster (*feg*) was found to span >73 kb and has up to 19 open reading frames (ORF). The first set of genes is located upstream of the non-ribosomal peptide synthetase encoding genes, and was assigned the function of Hpg synthesis. These genes encode for FegC, FegD, FegG, and FegE which are homologs of enzymes known to be involved in the biosynthesis of Hpg.<sup>220,221</sup> Their specific predicted functions and homology are shown in **Table 25** (entries 3-5, 7). To further illustrate their proposed functions, the biosynthesis of Hpg is shown in **Scheme 93**. To this end, it is expected that FegE converts prephenate into *p*-hydroxyphenylpyruvate, which undergoes benzylic oxidation and decarboxylation as catalyzed by FegD. The resulting *p*-hydroxymandelate is then oxidized to *p*-hydroxybenzoylformate by either FegC or FegG, which both carry a potential hydroxymandelate oxidase function. Finally, FegG is proposed to catalyze the final transamination to provide L-Hpg.

---

<sup>219</sup> Gonsior, M.; Mühlenweg, A.; Tietzmann, M.; Rausch, S.; Poch, A.; Süssmuth, R. D. *ChemBioChem* **2015**, *16*, 2610.

<sup>220</sup> Hubbard, B. K.; Thomas, M. G.; Walsh, C. T. *Chem. Biol.* **2000**, *7*, 931.

<sup>221</sup> Al Toma, R. S.; Brieke, C.; Cryle, M. J.; Süssmuth, R. D. *Nat. Prod. Rep.* **2015**, *32*, 1207.

**Table 25.** Genes of the feglymycin biosynthesis gene cluster and their predicted functions.<sup>a</sup>

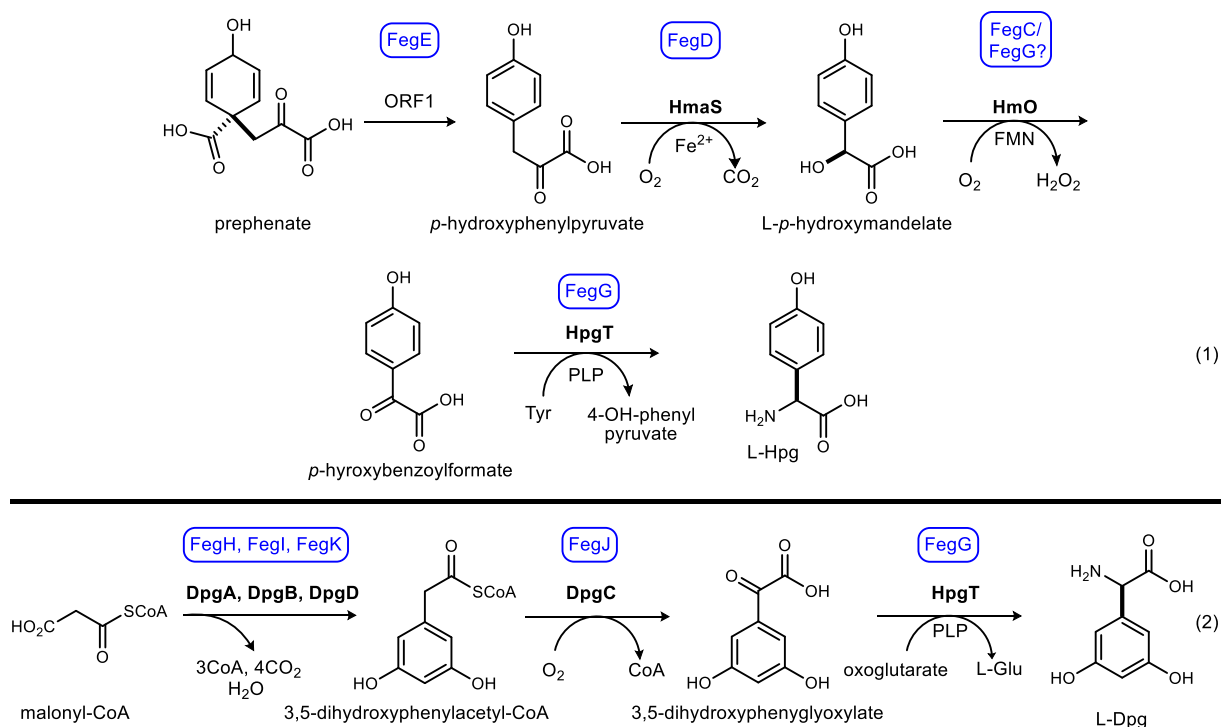
entry	ORF	size (AA)	predicted function/homology	homology similarity/identity (%)
1	<i>fegA</i>	355	3-deoxy-d-arabinoseheptulosonate 7-phosphate (DAHP) synthase	96/92
2	<i>fegB</i>	335	transcriptional regulator	82/72
3	<i>fegC</i>	379	hydroxymandelate oxidase (HmO)	80/88
4	<i>fegD</i>	366	hydroxymandelate synthase (HmaS)	87/92
5	<i>fegE</i>	398	prephenatedehydrogenase (Pdh)	63/73
6	<i>fegF</i>	969	LuxR regulatory protein	65/75
7	<i>fegG</i>	775	hydroxyphenylglycine aminotransferase/hydroxymandelateoxidase fusion protein	77/71
8	<i>fegH</i>	388	3,5-dihydroxyphenylacetyl-CoA Synthetase (DpgA)	89/81
9	<i>fegI</i>	217	enoyl-CoA hydratase (DpgB)	80/72
10	<i>fegJ</i>	435	3,5-dihydroxyphenylacetyl-CoA oxygenase (DpgC)	83/76
11	<i>fegK</i>	270	enoyl-CoA hydratase (DpgD)	92/86
12	<i>fegL</i>	269	a/b-hydrolase	84/74
13	<i>fegM</i>	418	histidine kinase	79/70
14	<i>fegN</i>	217	two-component transcription regulator	93/90
15	<i>fegO</i>	74	antibiotic synthesis protein MbtH	95/78
16	<i>fegP</i>	685	ABC transporter	83/73
17	<i>fegQ</i>	5447	nonribosomal peptide synthase	72/62
18	<i>fegR</i>	7911	nonribosomal peptide synthetase	56/43
19	<i>fegS</i>	3407	nonribosomal peptide synthetase	71/60

<sup>a</sup> Table adapted from reference 219. Genes are from the producing organism, *Streptomyces* sp. DSM11171. Functions were predicted by sequence homology and protein domain analysis.

The feglymycin gene cluster also contains four ORFs, named *fegH/I/J/K*, that code for proteins homologous to DpgA, DpgB, DpgC and DpgD, which are involved in Dpg biosynthesis (**Table 25**, entries 8-11).<sup>221,222</sup> The specific function for each of these proteins is overlaid with the Dpg biosynthetic pathway as shown in **Scheme 93**. It is proposed that FegH-K catalyze the conversion of four malonyl-CoA units to 3,5-dihydroxyphenylacetyl-CoA. This is followed by benzylic oxidation carried out by FegJ, and transamination catalyzed by FegG, which provides L-Dpg.

<sup>222</sup> Pfeifer, V.; Nicholson, G. J.; Ries, J.; Recktenwald, J.; Schefer, A. B.; Shawky, R. M.; Schröder, J.; Wohlleben, W.; Pelzer, S. *J. Biol. Chem.* **2001**, *276*, 38370.

**Scheme 93.** Biosynthesis of Hpg and Dpg.<sup>a</sup>



<sup>a</sup> Enzymes in blue boxes are the proposed enzymes encoded in the *feg* gene cluster.<sup>219</sup> Bold font indicates enzymes previously identified for the production of Hpg and Dpg.<sup>220,222,221</sup>

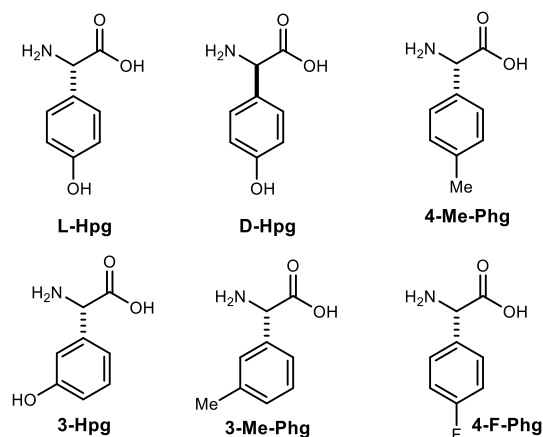
**Table 26** highlights some of the results that implicate FegC's role in the production of L-Hpg, and of feglymycin. As shown, no feglymycin was detected by LCMS upon deletion of the *fegC* gene (**Table 26**, entry 2). However, if the  $\Delta fegC$  mutant was supplemented with L-Hpg, feglymycin was produced (**Table 26**, entry 3). This indicated that FegC is involved in producing L-Hpg. Further support was obtained when the  $\Delta fegC$  mutant was transformed with a non-integrating plasmid that encoded *fegC*, and production was restored (**Table 26**, entry 4). Interestingly, when the  $\Delta fegC$  mutant was fed with other phenylglycine analogues, no feglymycin nor feglymycin derivatives were observed. This was the case for the non-natural enantiomer, D-Hpg, as well as 3-Hpg, 4-Me-Phg, 3-Me-Phg and 4-F-Phg (**Table 26**, entries 5-9). **These results are particularly interesting as they indicate that biosynthesis of feglymycin derivatives is likely inaccessible by mutasynthesis. This necessitates robust methodology for the synthesis of peptides containing non-natural aryl glycinamides.**

**Table 26.** Feeding studies with feglymycin mutant and role of the *fegC* gene.

entry	species (+ supplement)	<i>feg</i> or <i>feg</i> derivative produced? <sup>a</sup>
1	<i>Streptomyces</i> sp. DSM 11171 (wt)	yes
2	$\Delta fegC$	no
3	$\Delta fegC$ + L-Hpg	yes
4 <sup>b</sup>	$\Delta fegC$ + plasmid <i>fegC</i>	yes
5	$\Delta fegC$ + D-Hpg	no
6	$\Delta fegC$ + L-4-Me-Phg	no
7	$\Delta fegC$ + L-3-Hpg	no
8	$\Delta fegC$ + L-3-Me-Phg	no
9	$\Delta fegC$ + L-4-F-Phg	no

<sup>a</sup> Production of feglymycin or feglymycin derivative determined by LC-MS.

<sup>b</sup>  $\Delta fegC$  Mutant was transformed with a non-integrating plasmid encoding *fegC*.

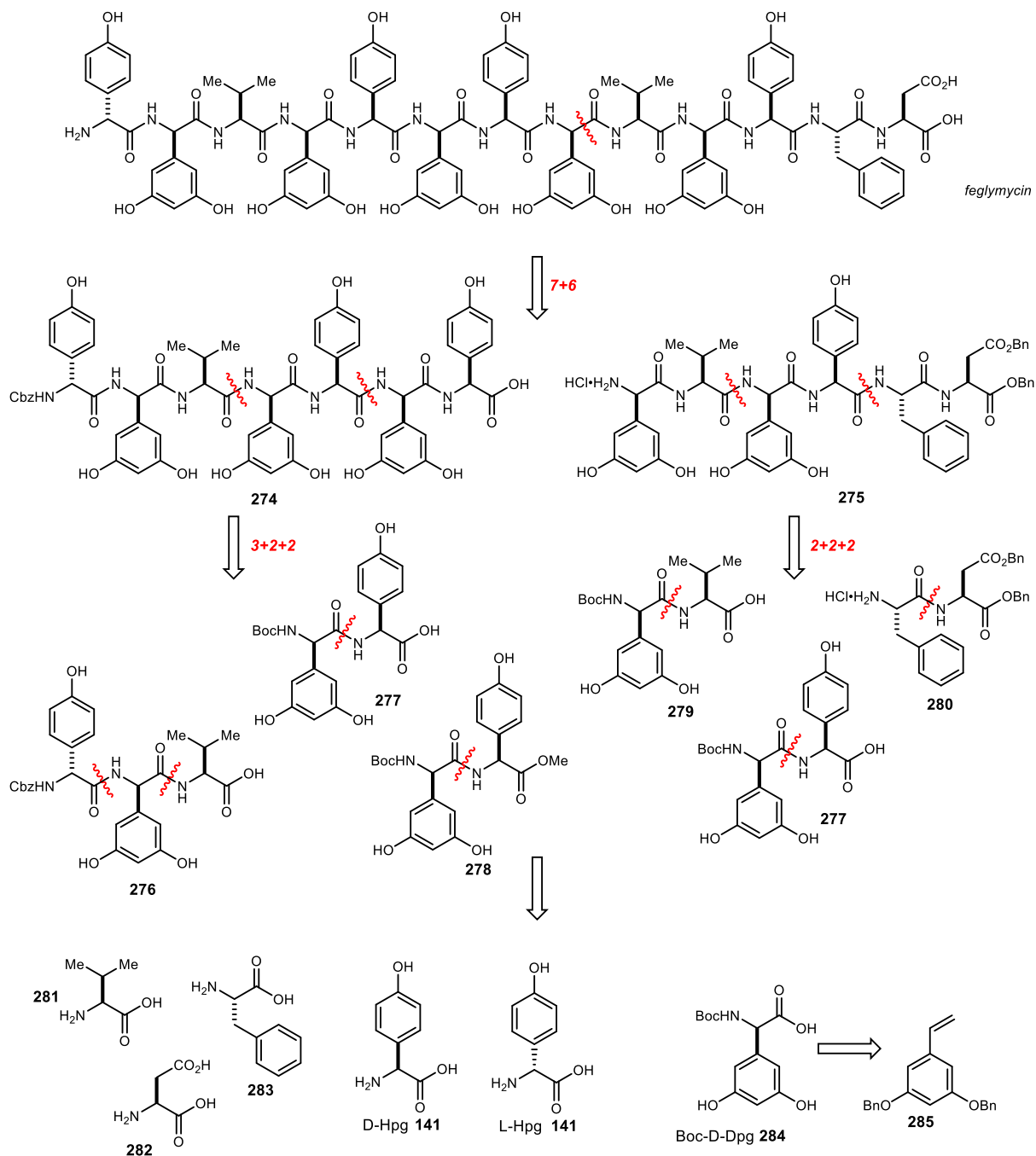


The synthesis of feglymycin is proposed to be carried out by three NRPSs: FegQ (four modules), FegR (six modules), and FegS (three modules) (**Figure 31**). This correlates perfectly to the 13 residues in feglymycin. Interestingly, despite feglymycin containing many repeating motifs, the NRPSs are colinear and not iterative. The first module is the loading module, which is followed by 11 elongation modules, and a termination module with a thioesterase domain. As would be expected, the assembly line contains six epimerization domains in modules 1,2,4,6,8 and 10. These correspond to the six D-amino acids present in feglymycin.

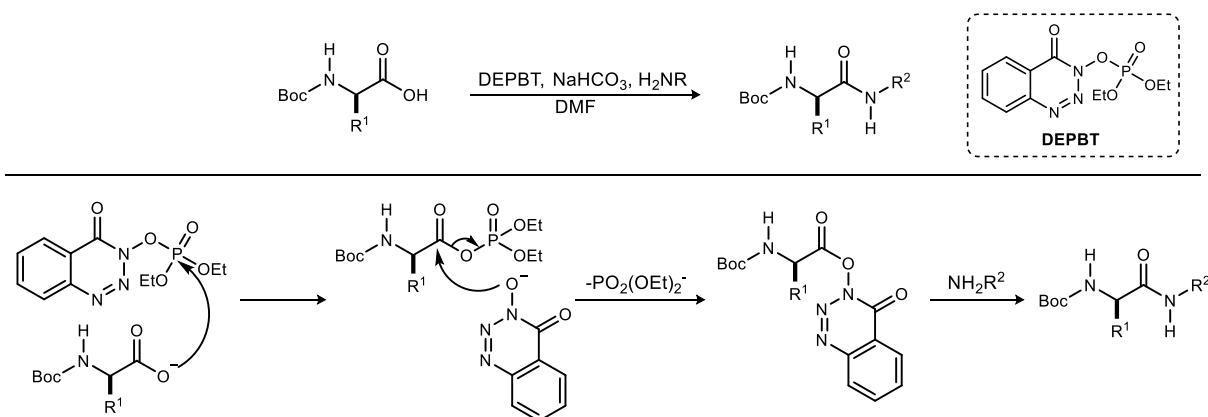


Key to this tactic is the incorporation of Dpg into dipeptide fragments to avoid its activation, and likely epimerization, when coupling to larger fragments. As such, feglymycin would be synthesized by joining *N*-terminal heptapeptide **274** and *C*-terminal hexapeptide **275**. Each of these

**Figure 32.** Süßmuth's convergent retrosynthetic analysis of feglymycin.



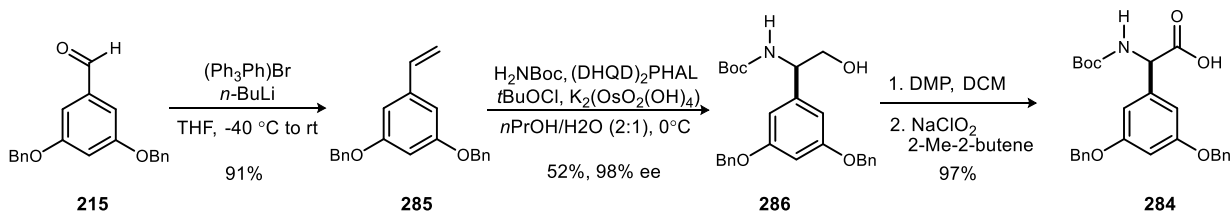
**Scheme 94.** Mechanism of DEPBT-mediated amide coupling.



fragments would be made from tripeptide **276** and dipeptides **277**, **278**, **279**, and **280**. The tri- and dipeptides would be synthesized from commercially available L-Val, L-Asp, L-Phe, L-Hpg and L-Hpg and from D-Dpg which was made via Sharpless aminohydroxylation. The peptide couplings were carried out using 3-(diethoxyphosphoryloxy)-1,2,3-benzotriazin-4(3H)-one (DEPBT)<sup>224</sup> and a mild base (NaHCO<sub>3</sub>) in either THF or DMF. DEPBT was chosen as all other coupling reagents led to epimerization and slow coupling reactions. A representative example of a DEPBT-mediated coupling is shown in **Scheme 94**.

To begin the synthesis, the Dpg residue was prepared in 4 steps and 46% overall yield from the aldehyde **215** (**Scheme 95**). Wittig olefination provided the styrene **285** in 91% yield, which was then subjected to Sharpless aminohydroxylation conditions to provide the *N*-Boc amino alcohol **286** in 52% yield and 98% ee. Finally, DMP oxidation of the alcohol followed by Pinnick oxidation to the carboxylic acid provided the *N*-Boc amino acid **284** in 97% over 2 steps.

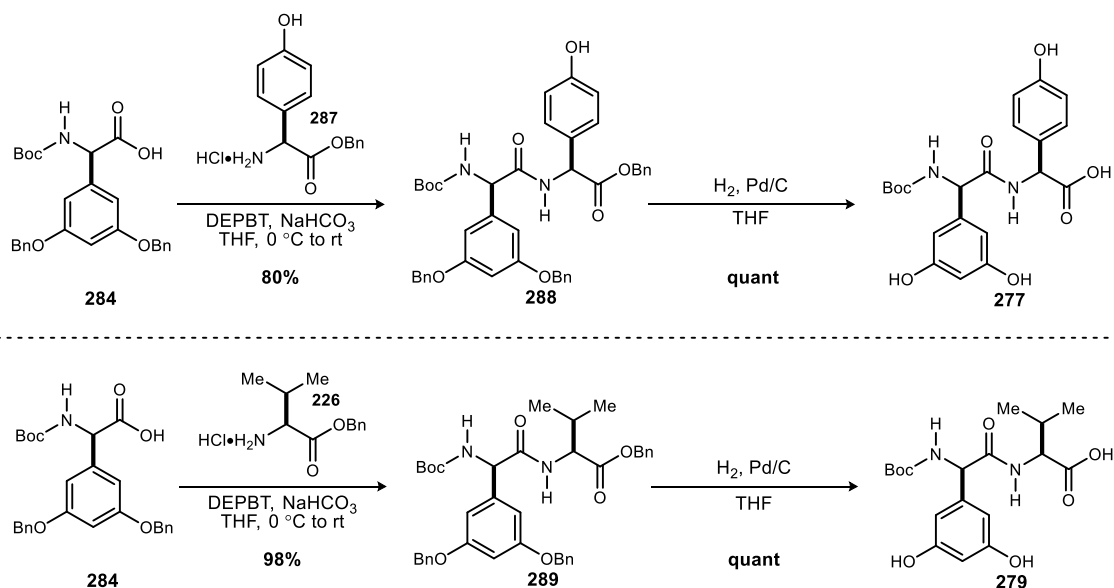
**Scheme 95.** Süßmuth's synthesis of 3,5-dihydroxyphenylglycine.



<sup>224</sup> Li, H.; Jiang, X.; Ye, Y.-h.; Fan, C.; Romoff, T.; Goodman, M. *Org. Lett.* **1999**, *1*, 91.; Ye, Y.-h.; Li, H.; Jiang, X. *Pept. Sci.* **2005**, *80*, 172.

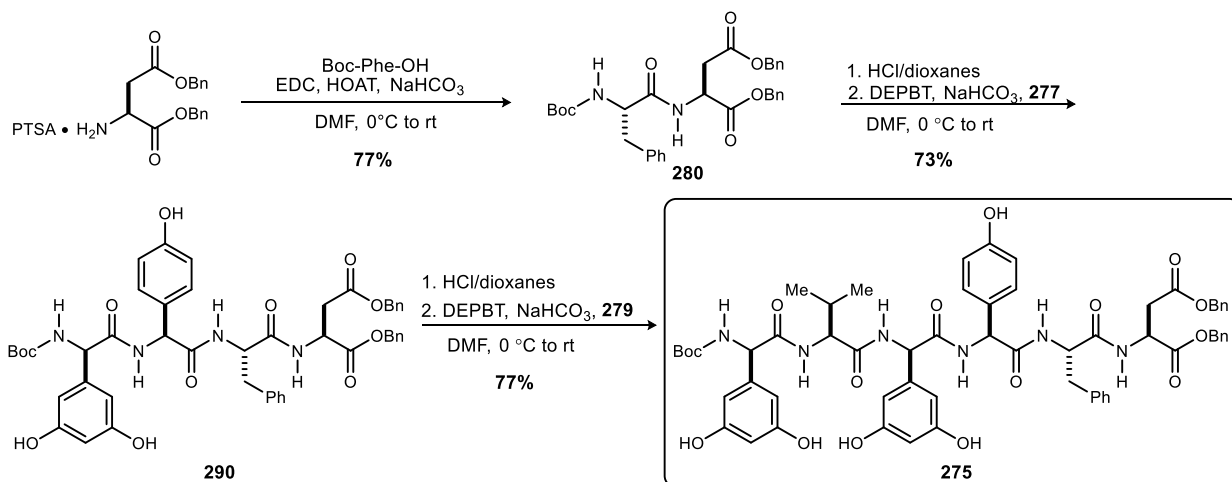


**Scheme 96.** Süssmuth's synthesis of dipeptides **277** and **279**.



To avoid potential epimerization caused by coupling Dpg residues to large amines, Süssmuth first assembled dipeptides **277** and **279** (Scheme 96). These fragments were synthesized in 80% and 98% yield when coupled to HCl-Hpg-OBn and HCl-Val-OBn, respectively. Hydrogenation in both cases was quantitative.

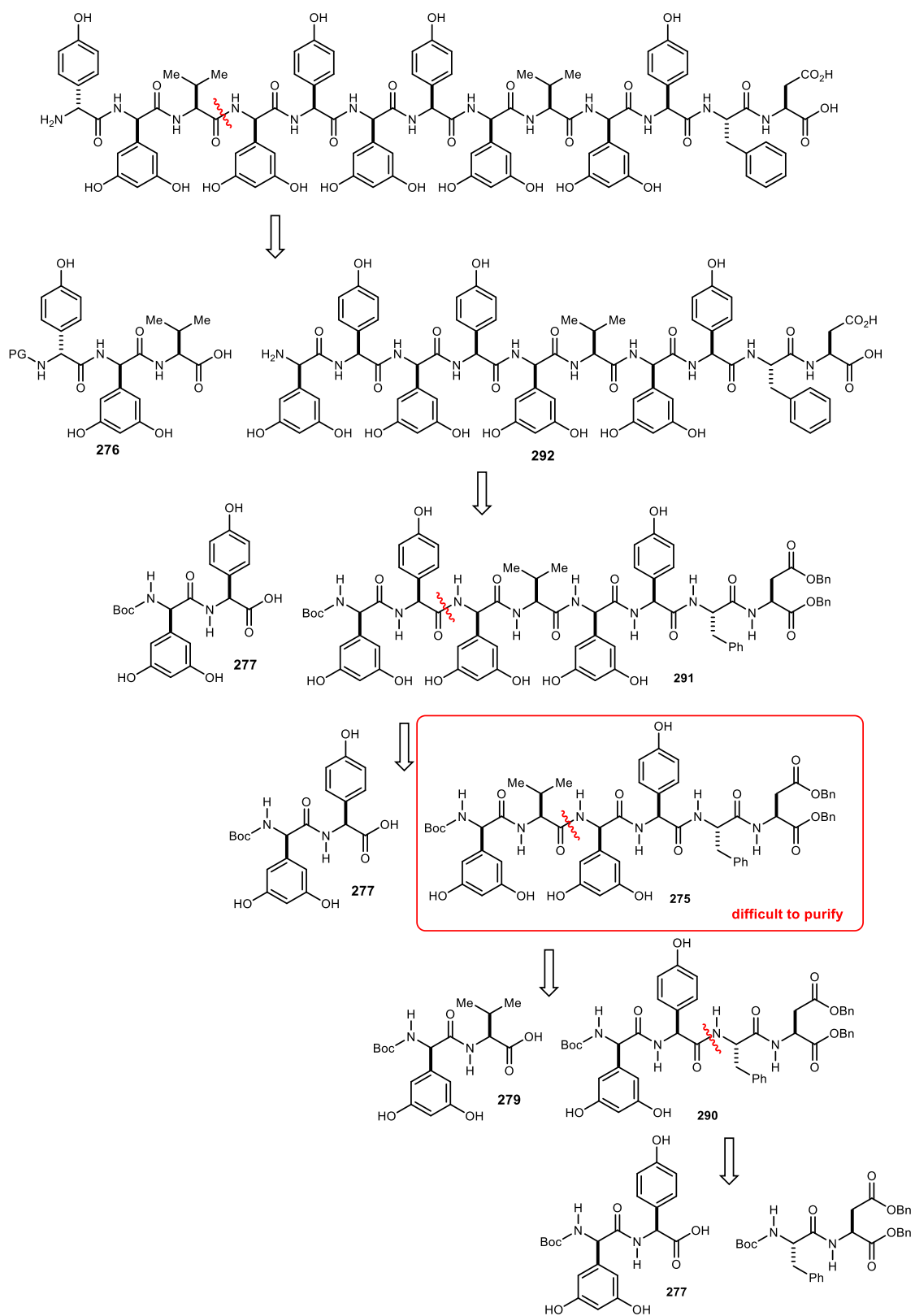
**Scheme 97.** Süssmuth's synthesis of C-terminal hexapeptide **275**.



The D-Dpg-L-Hpg fragment **277** was coupled to the C-terminal dipeptide **280** in 73% yield. The resulting tetrapeptide **290** was further extended by coupling to Boc-Dpg-Val in 77% yield to provide the hexapeptide **275** (**Scheme 97**).

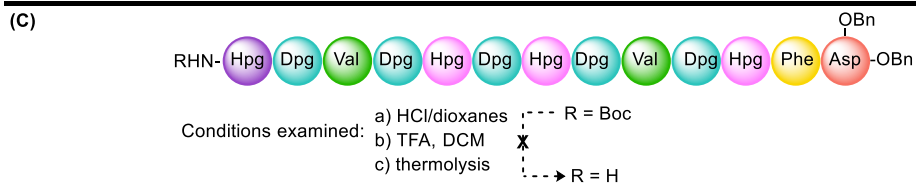
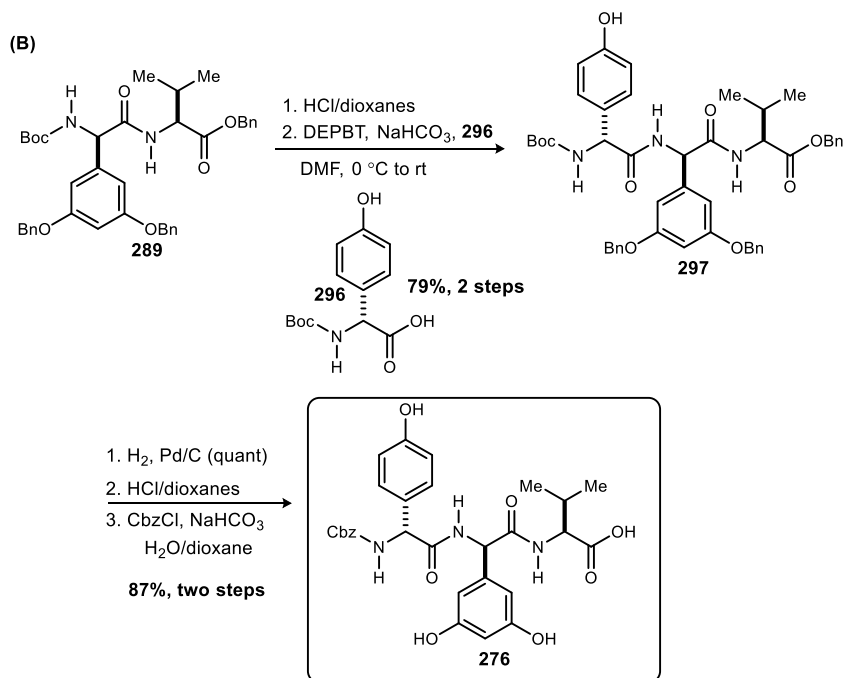
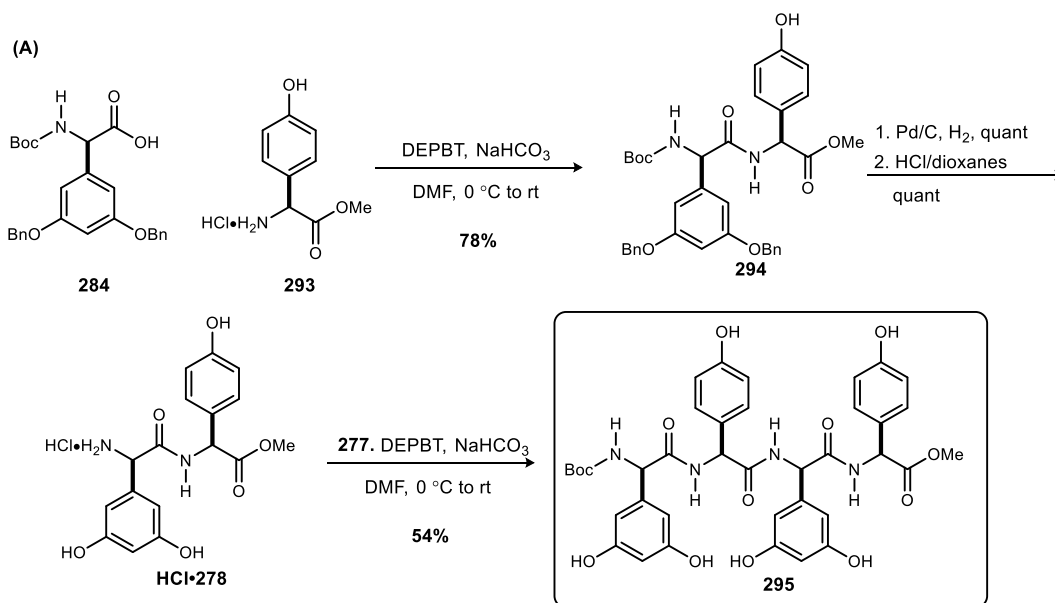
The Süßmuth group originally envisioned on synthesizing (-)-feglymycin by the iterative route shown in **Figure 33**. In this approach the hexapeptide **275** would be extended by iterative coupling to the dipeptide **277** and then tripeptide **276**. However, the hexapeptide **275** proved difficult to purify. Concerns with purification of the octapeptide **291** and decapeptide **292** ultimately precluded moving this route forward.

Figure 33. Süssmuth's iterative retrosynthesis of feglymycin.



Instead, the Süßmuth group pursued the convergent strategy shown in **Figure 32**. To this end, the *N*-terminal heptapeptide **274** would be made by the convergent coupling of tripeptide **276** and tetrapeptide **295** (**Scheme 98**). In the forward direction, the tetrapeptide **295** was made by joining the Boc-Dpg and HCl-Hpg-OMe residues in 78% yield. The benzyl and Boc protecting groups were both removed from the dipeptide methyl ester **HCl·278** in quantitative yield before that fragment was connected to dipeptide **277** (54%, **Scheme 98**). The tripeptide was synthesized by coupling the (*R*)-Boc-Hpg residue to dipeptide **289**. Importantly, after adjoining tetrapeptide **295** and *N*-Boc protected tripeptide **298**, and the hexapeptide **275** to make the protected tridecapeptide, all attempts to remove the *N*-terminal Boc protecting group failed (**Scheme 98**, C). Süßmuth reports decomposition of the tridecapeptide using 4 M HCl in dioxanes or TFA in DCM. The group also tried thermolysis, but the results were not reproducible. Thus the *N*-terminal protecting group was changed to Cbz (**Scheme 98**, B), which could be removed using hydrogenation (**Scheme 101**). To this end, the Cbz-protected tripeptide **276** and tetrapeptide methyl ester **295** were coupled in 52% yield (**Scheme 99**).

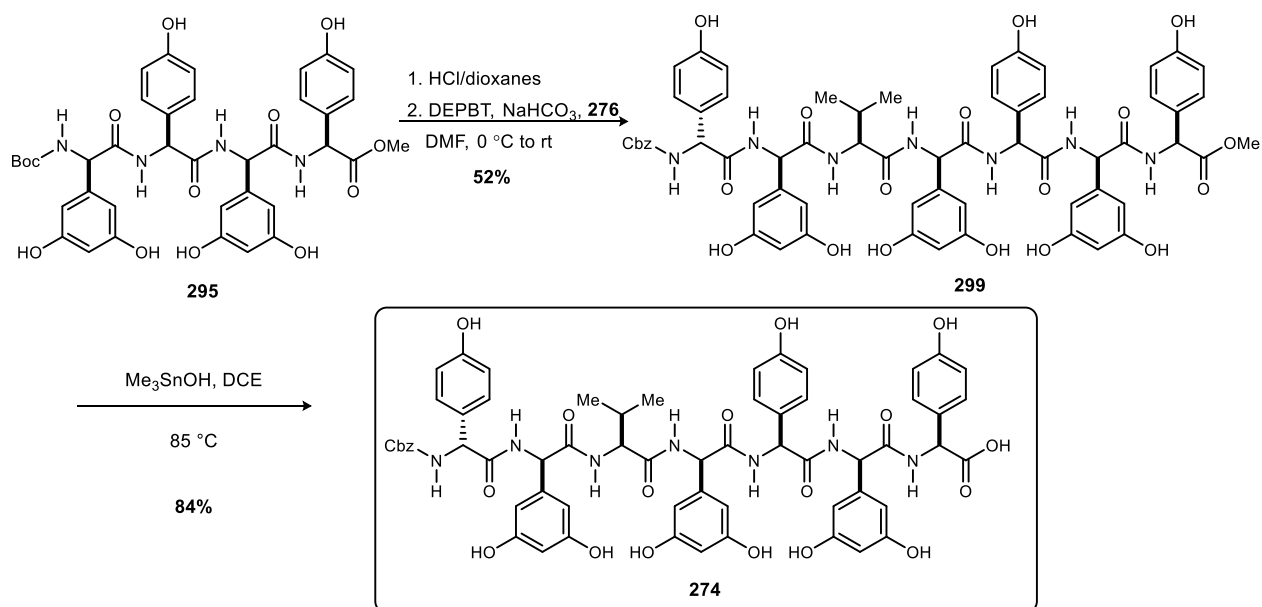
**Scheme 98.** Süßmuth's synthesis of tetrapeptide and tripeptide precursors to *N*-terminal heptapeptide 274.



Care was taken when removing the C-terminal methyl ester, as the strongly basic conditions typically used for cleavage would likely result in Dpg epimerization. Consequently, the group deprotected the ester with trimethyltin hydroxide in DCE at 85 °C (84%, **Scheme 98**). These conditions were initially used by Mascaretti to cleave phenacyl esters linking *N*-Boc-amino acids and peptides to polystyrene resins without noticeable epimerization.<sup>225</sup>

Nicolaou also found success with this reagent when pursuing the synthesis of thiostrepton.<sup>226</sup> They also carried out a formal investigation of its utility where they conducted a rather thorough substrate scope. Of particular relevance to Süßmuth's work was their exploration of Mosher-amide derivatives of Hpg (**Scheme 100**). In this study it was found that while LiOH resulted in extensive epimerization (43:57 dr), Me<sub>3</sub>SnOH caused very little epimerization, providing the acid in 94:6 dr from the starting methyl ester with 96:4 dr.

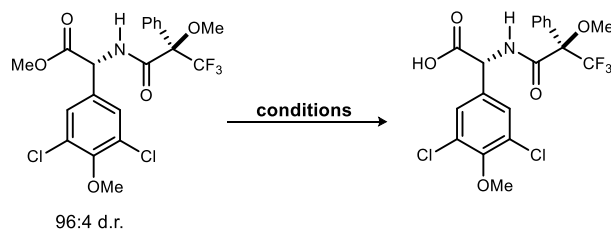
**Scheme 99.** Süßmuth's synthesis of N-terminal heptapeptide 274.



<sup>225</sup> a) Furlán, R. L. E.; Mata, E. G.; Mascaretti, O. A. *Tetrahedron Letters* **1996**, *37*, 5229. b) L. E. Furlán, R.; G. Mata, E.; A. Mascaretti, O. *J. Chem. Soc., Perkin Trans. 1* **1998**, 355.

<sup>226</sup> Thiostrepton synthesis: Nicolaou, K. C.; Safina, B. S.; Zak, M.; Estrada, A. A.; Lee, S. H. *Angewandte Chemie International Edition* **2004**, *43*, 5087.; Nicolaou, K. C.; Zak, M.; Safina, B. S.; Lee, S. H.; Estrada, A. A. *Angewandte Chemie International Edition* **2004**, *43*, 5092. Further evaluation of Me<sub>3</sub>SnOH: Nicolaou, K. C.; Estrada, A. A.; Zak, M.; Lee, S. H.; Safina, B. S. *Angewandte Chemie International Edition* **2005**, *44*, 1378.

**Scheme 100.** Nicolaou's comparison of conditions for methyl ester hydrolysis.



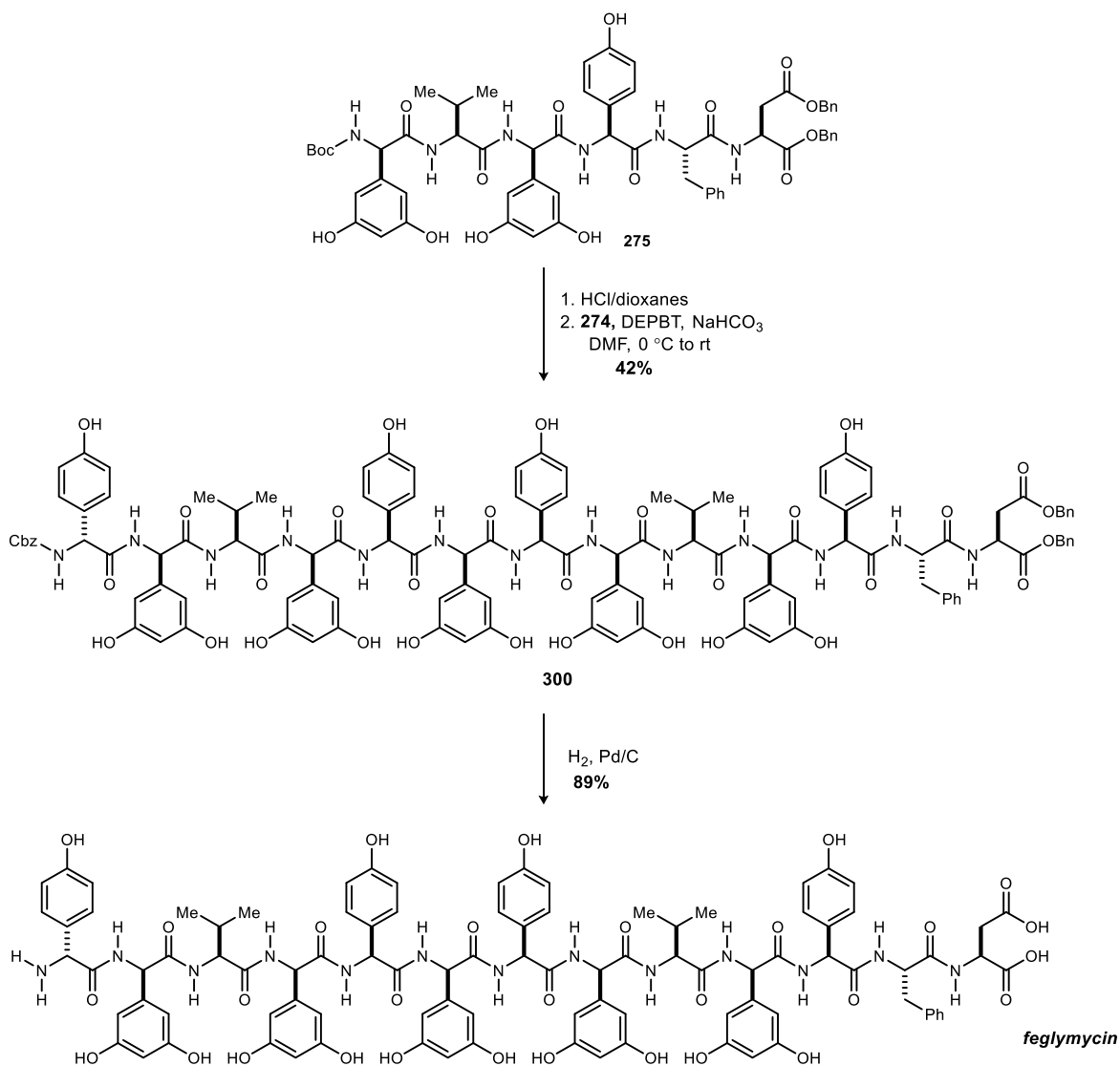
**Conditions:**

Me<sub>3</sub>SnOH (3.0 equiv), 1,2-DCE, 80°C                      94:6 d.r.

LiOH (1.1 equiv), THF, MeOH, H<sub>2</sub>O, 0°C to rt              43:57 d.r.

With both the hexa- and heptapeptides in hand, the two were coupled to afford tridecapeptide **300** in 42% yield (**Scheme 101**). Finally, hydrogenation removed both the *N*-terminal Cbz and *C*-terminal benzyl ester protecting groups to furnish the target compound, feglymycin, in 89% yield. This completed the synthesis in 31 total steps (14 longest linear sequence) and 4% overall yield.

**Scheme 101.** Süßmuth's completion of (-)-feglymycin.



### Fuse's synthesis of feglymycin.

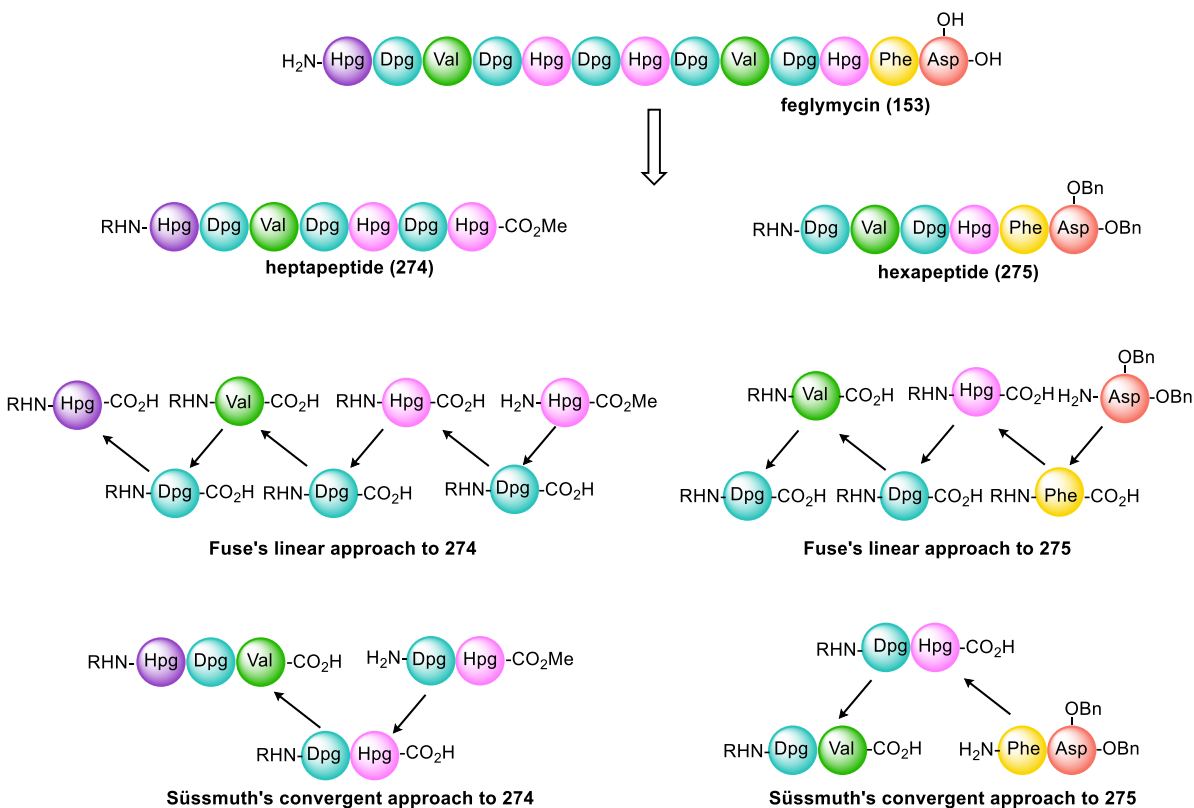
As described above, the lack of a completely effective technology for epimerization-free coupling of Dpg residues precluded a linear approach toward feglymycin. However, in 2016, Fuse developed a micro-flow approach that allowed for the linear synthesis of hexa- and heptapeptides **274** and **275** with minimal epimerization.<sup>227</sup> **Figure 34** highlights the disconnections made by Fuse

<sup>227</sup> Fuse, S.; Mifune, Y.; Nakamura, H.; Tanaka, H. *Nature Communications* **2016**, *7*, 13491.



and Süßmuth. Both groups split the tridecapeptide into a hepta- and hexapeptide. Süßmuth synthesized each fragment via the convergent method described earlier and depicted in the bottom

**Figure 34.** Comparison of Fuse's linear approach and Süßmuth's convergent approach to feglymycin.

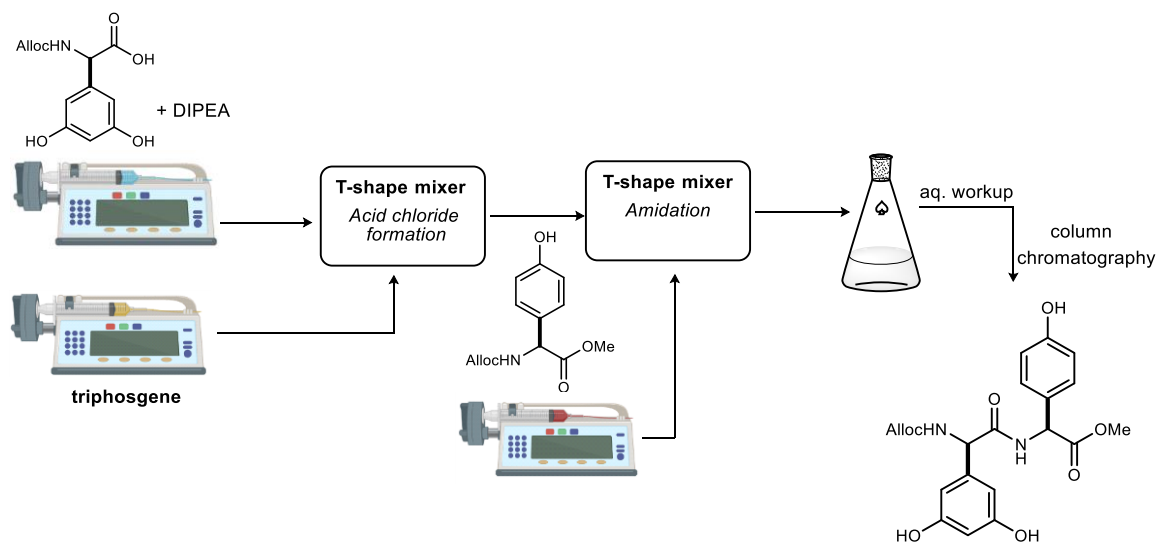


of **Figure 34**. Fuse instead pursued the linear approach, coupling one amino acid at a time.

The ability to carry out the linear synthesis with sensitive aryl glycine residues stemmed from their previous studies, which demonstrated the use of triphosgene as an activating agent.<sup>228</sup> By conducting the reaction in-flow and limiting the residence time to less than one second, the group was able to minimize racemization ( $\leq 3\%$ ). The general approach is illustrated in **Figure 35**. As shown, a solution containing the acid and an organic base, and a solution of triphosgene are added via separate syringe pumps into a T-shape mixer. The acid chloride that is then

<sup>228</sup> Fuse, S.; Tanabe, N.; Takahashi, T. *Chem. Commun.* **2011**, 47, 12661.; Fuse, S.; Mifune, Y.; Takahashi, T. *Angew. Chem. Int. Ed.* **2014**, 53, 851.

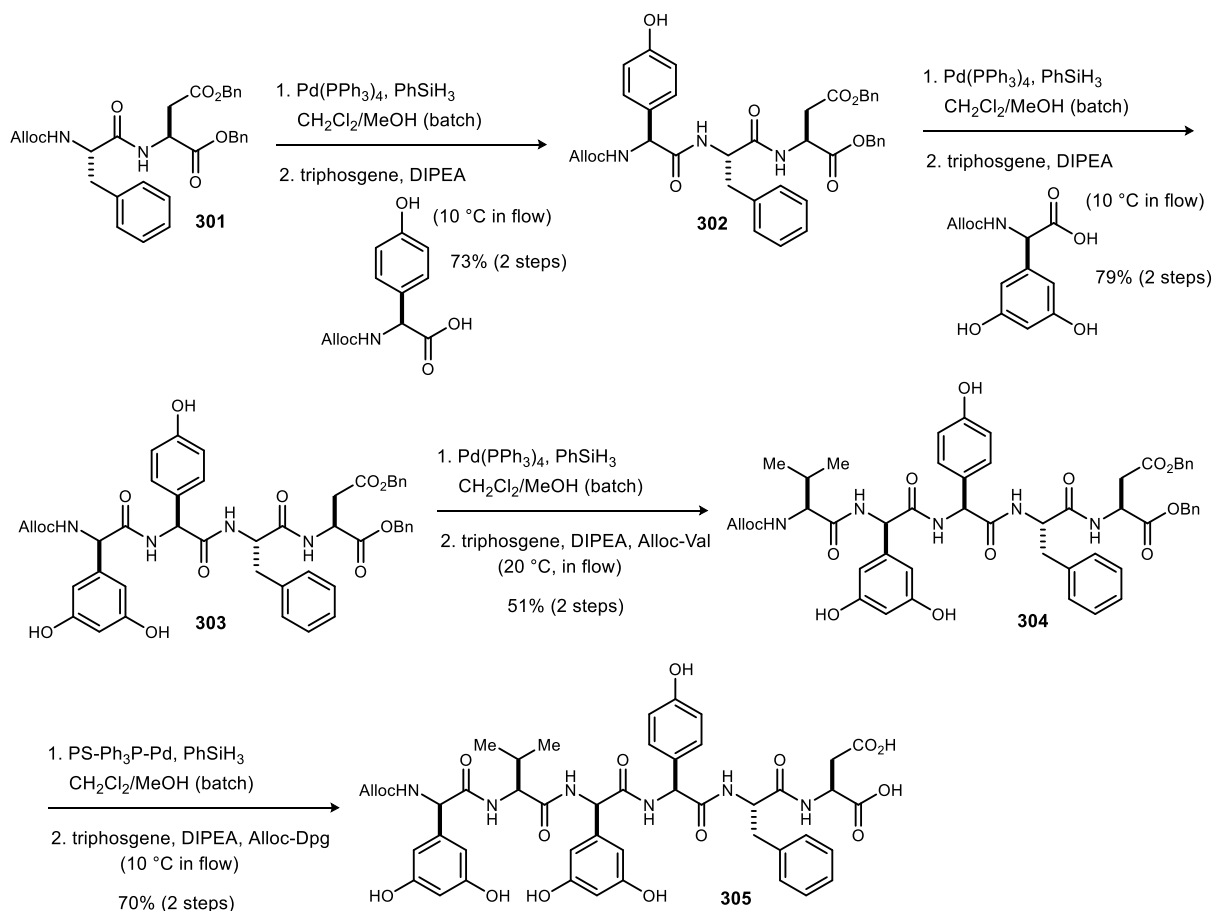
**Figure 35.** Representative schematic for micro-flow amidation.



pumped into a second T-shape mixer along with the amine. The reaction mixture is then pumped into a flask and subjected to aqueous workup. Finally, the crude product is purified by chromatography. The resulting peptide is then subjected to *N*-terminal deprotection and used as the amine nucleophile in the next coupling.

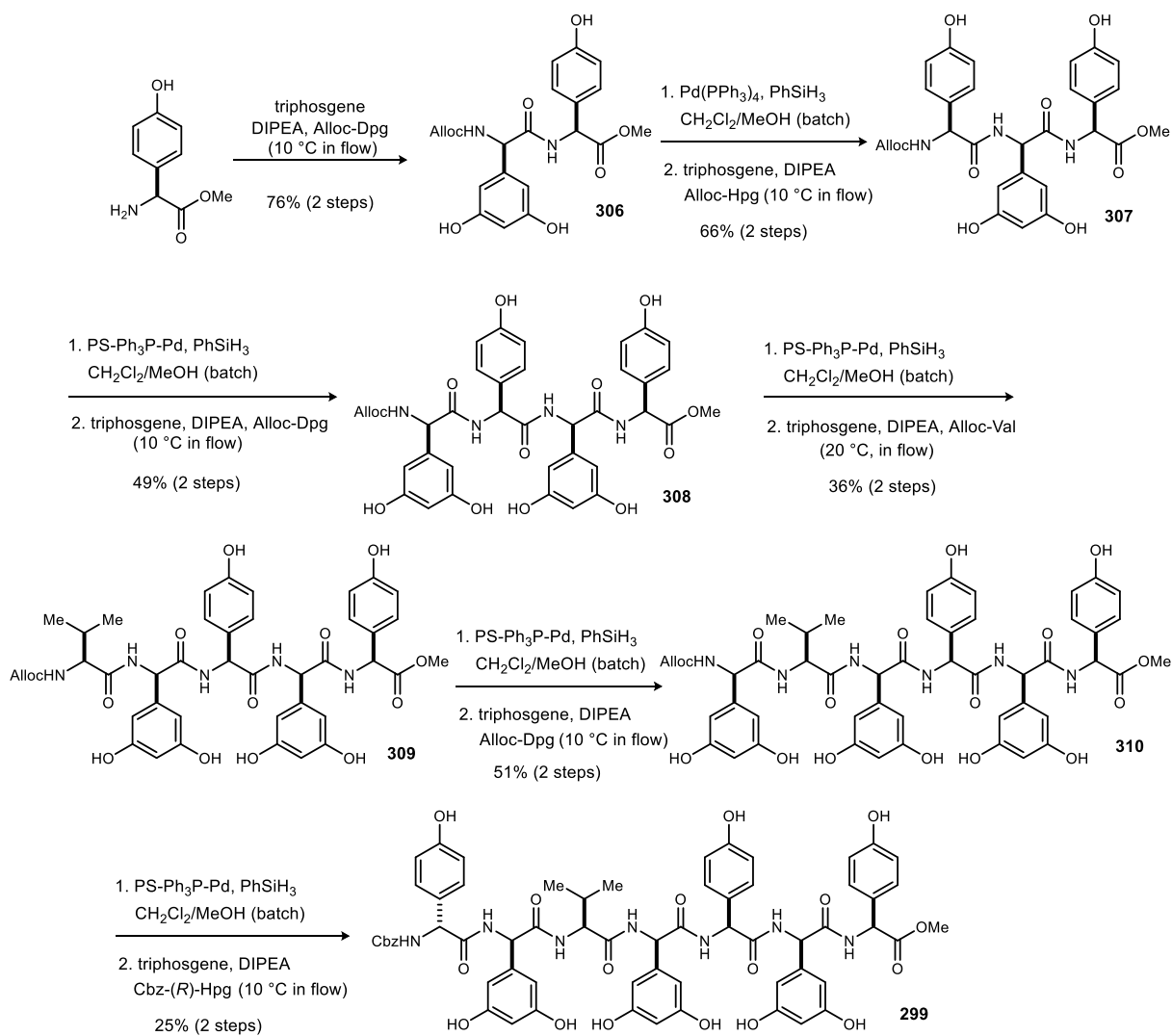
Toward feglymycin, Fuse began with the synthesis of *C*-terminal hexapeptide **275** (Scheme 102). The Alloc-Phe-Asp-CO<sub>2</sub>Bn dipeptide **301** was Alloc-deprotected in a batch reactor and then subjected to micro-flow amidation with Alloc-Hpg to afford the tripeptide **302** (73% yield, 2 steps). The tetrapeptide **303** was synthesized in 79% yield (2 steps) and then coupled again to make the pentapeptide **304** in 51% yield (2 steps). The Alloc group of the pentapeptide was removed using a solid-immobilized Pd catalyst in a batch reactor to assist with the difficult purification of the polar compound. Finally, the hexapeptide **305** was accessed after micro-flow amidation as a single diastereomer (70%, 2 steps).

**Scheme 102.** Fuse's synthesis of *C*-terminal hexapeptide 305.



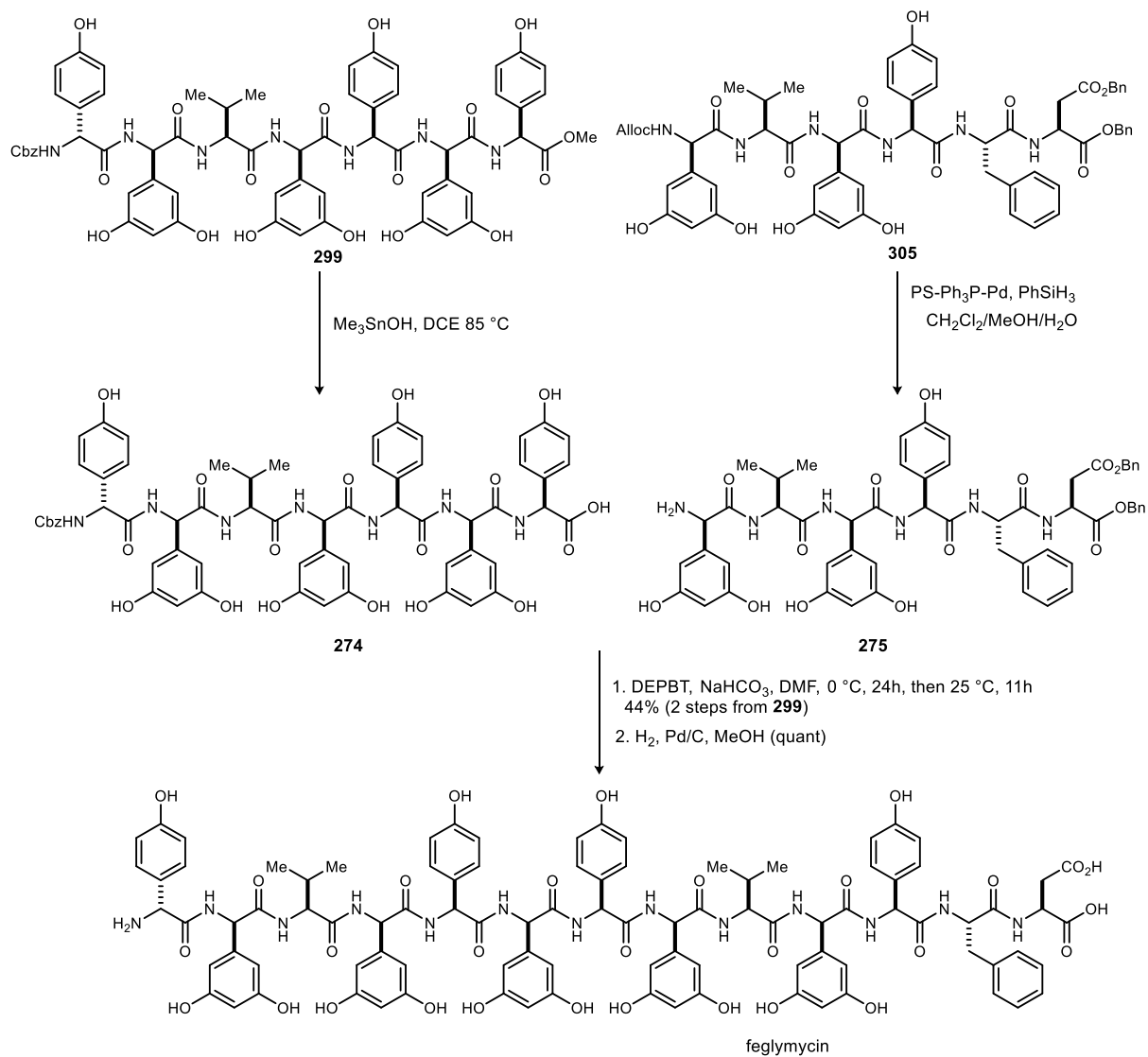
The synthesis of the *N*-terminal heptapeptide **274** proceeded in a similar fashion (**Scheme 103**). In this sequence, the first coupling of the sensitive Dpg residue resulted in epimerization. Solvent had a significant effect on epimerization: when the amine was added as a solution in DMA, epimerization was high (11%), however, when the amine was added as a solution in a 1:2 H<sub>2</sub>O/MeCN mixture, epimerization decreased to 1%. This solvent system was used to add the amine in all subsequent micro-flow amidations toward the heptapeptide, which was synthesized in 1.2% overall yield from Hpg-methyl ester.

**Scheme 103.** Fuse's synthesis of *N*-terminal heptapeptide 299.



Finally, Fuse completed the synthesis of feglymycin in a manner identical to Süssmuth. The hexa- and heptapeptides were coupled after deprotection using DEPBT, and global deprotection of the tridecapeptide was achieved by hydrogenolysis (**Scheme 104**). Overall, this synthesis achieved the notable feat of a linear synthesis that incorporated highly racemizable Dpg residues with minimal epimerization. The micro-flow approach allows for rapid generation of significant quantities of materials and the reaction conditions only generate CO<sub>2</sub> and the HCl salt of DIPEA as byproducts.

**Scheme 104.** Fuse's completion of (-)-feglymycin.

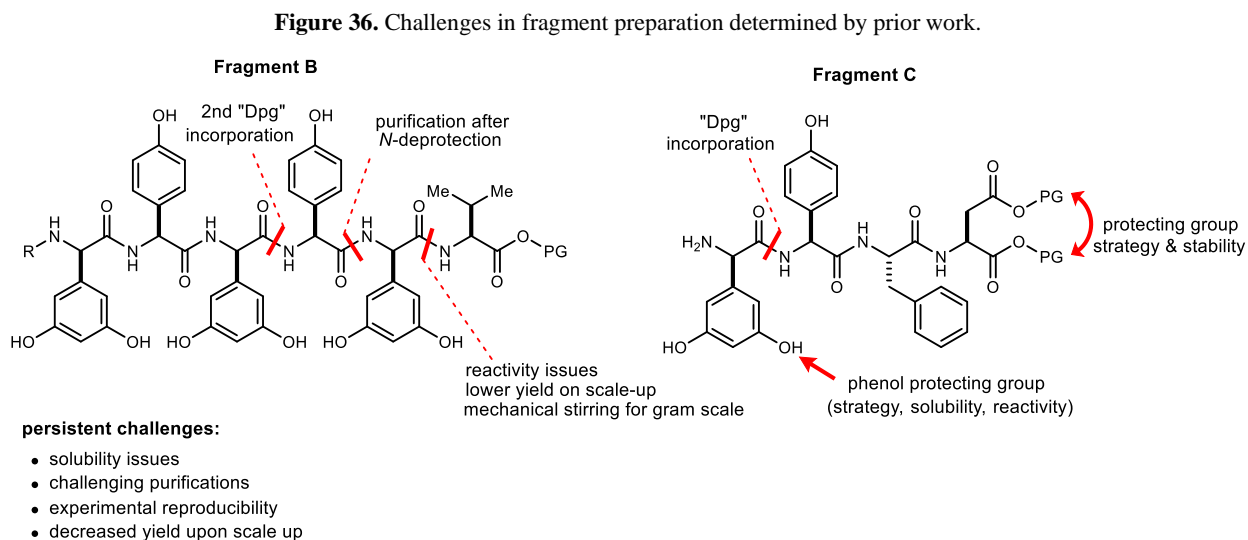


## 3.2 Formal synthesis of (-)-feglymycin

### 3.2.1 Previous work in the Johnston Group<sup>229</sup>

Feglymycin has been a target of interest in the Johnston Laboratory for many years, with several scientists contributing to the design, execution, revision, and optimization of our synthetic strategy. The general retrosynthetic strategy was to split feglymycin into three fragments (A, B, & C, **Scheme 105**). Umpolung amide synthesis would be used to prepare each fragment, which would then be joined together by condensative coupling. To this end, the disconnections were made at the valine residues (i.e. the amide bonds connecting residues 3 and 4, and 9 and 10). This strategy ensured that the condensative couplings would not require activation of the epimerization-prone Hpg and Dpg residues, while providing a C-terminal natural amino acid to be used as a homologation point for UmAS. The original synthetic plan coupled Fragments A and B first, then coupled Fragment AB to C. This was re-designed to first couple Fragments B and C, then couple Fragment BC to A to address protecting group and scale-up challenges that were encountered.<sup>179</sup>

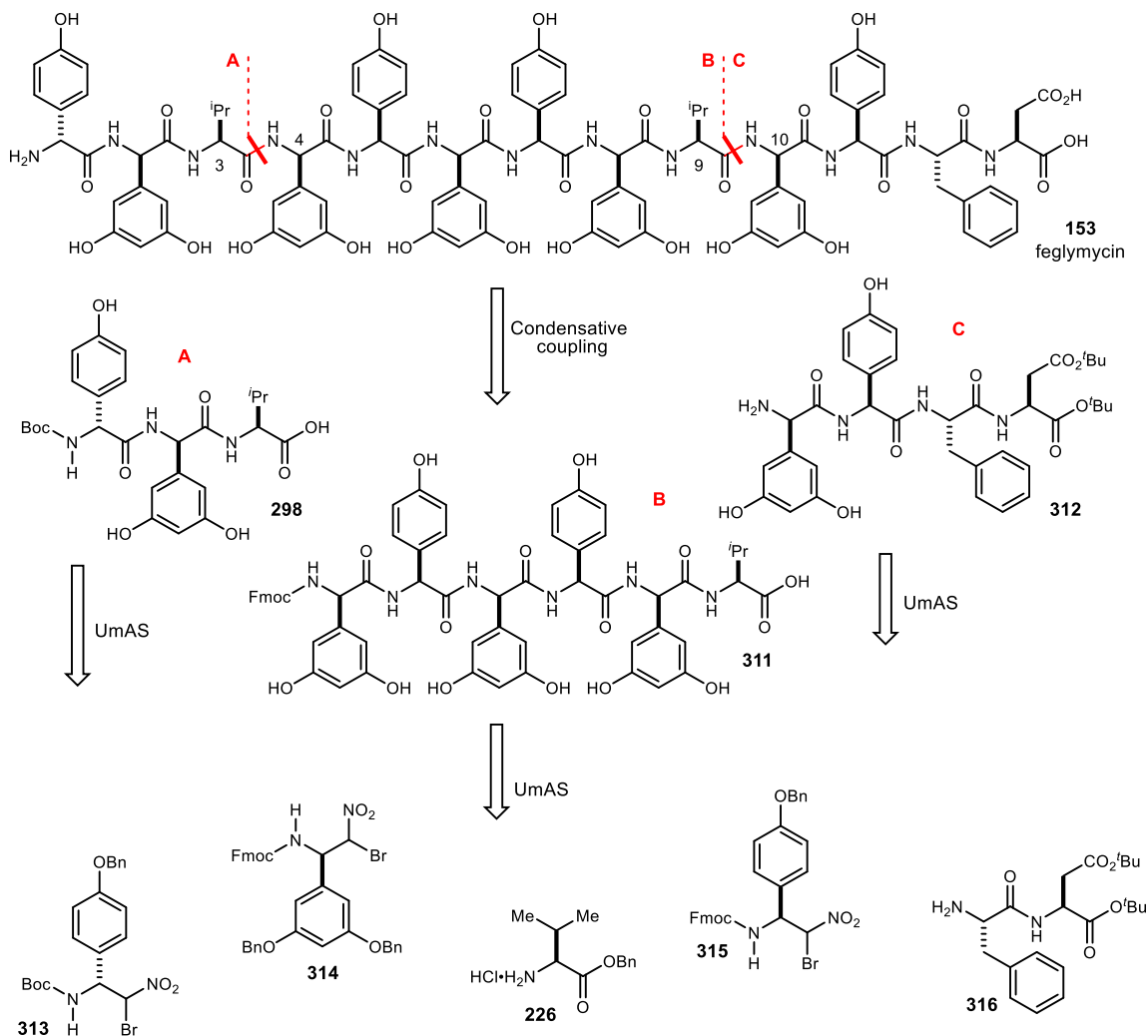
Each of the fragments would be synthesized from canonical amino acids (L-Val, L-Phe, L-Asp) and  $\alpha$ -bromo nitroalkane donors for the nine non-canonical residues. The  $\alpha$ -bromonitroalkanes



<sup>229</sup> Schwieter, K. Tsukanov, S. Doody, A. Makley, D. *Unpublished results.*

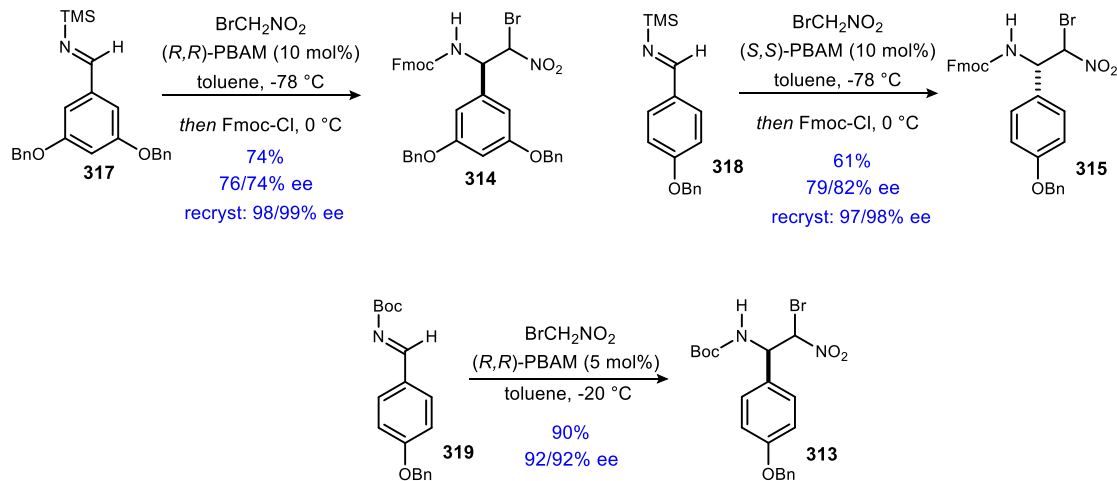
were prepared using an enantioselective aza-Henry reaction. Initially, the Fmoc-protected  $\alpha$ -bromonitroalkanes were prepared to implement an orthogonal protecting group strategy, and to leverage the utility of the aza-Henry reaction with silyl-imine electrophiles developed in our group (**Scheme 106**).<sup>43</sup> The *N*-Boc protected  $\alpha$ -bromonitroalkane **313** was also prepared using the enantioselective aza-Henry reaction.

**Scheme 105.** General retrosynthetic analysis of feglymycin.



Over the course of our lab's pursuit of feglymycin, several challenges presented themselves, which resulted in several revisions and iterations of the synthesis. Some of these challenges are highlighted in **Figure 36**. For all fragments, the protecting group strategy was important and challenging in terms of developing an orthogonal approach. The protecting groups, particularly

**Scheme 106.** *N*-TMS Aldimine approach to Dpg  $\alpha$ -bromonitroalkane donors.<sup>229</sup>



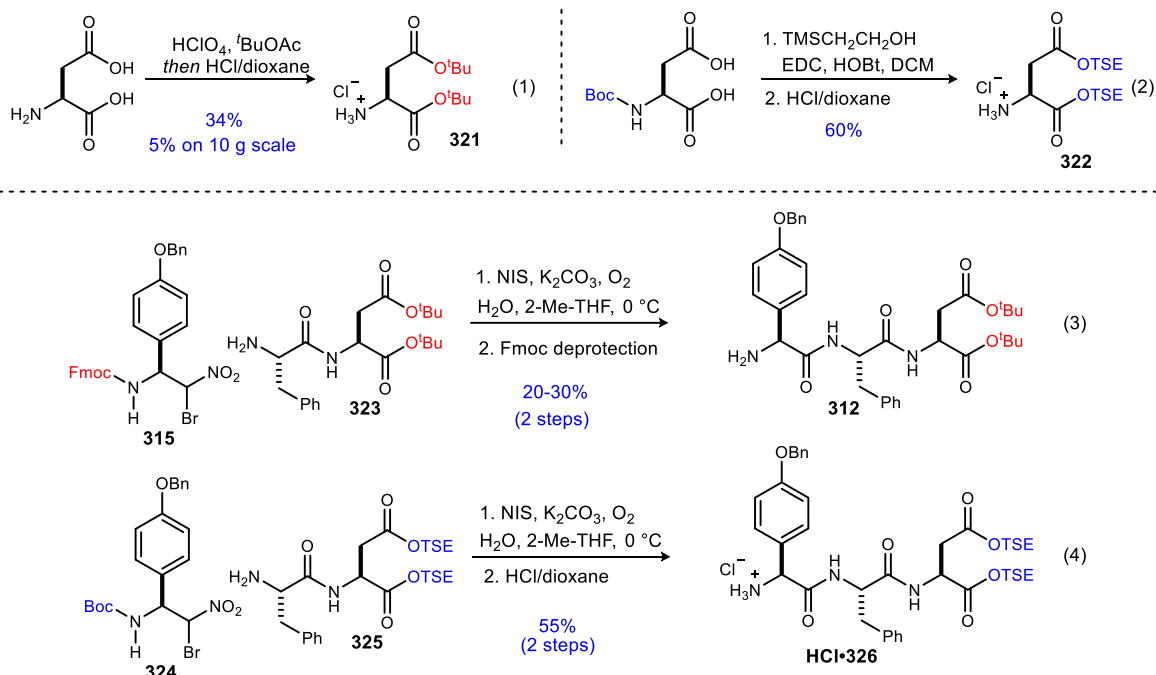
those on the phenols also significantly alter the reactivity and solubility of the fragments and precursors. For all of the fragments, complications arose due to issues with solubility, reactivity, purification, and reaction scale-up.

For example, the *C*-terminus of feglymycin was originally protected as the di-*tert*-butyl ester. This protection was carried out following a known procedure,<sup>230</sup> and gave modest yields on small scale (**Scheme 107**, eq 1). Upon scale-up these yields suffered tremendously, providing only 5% yield on a 10-gram scale (**Scheme 107**, eq 1). A change was made to a trimethylsilylethanol (TSE) protecting group, which could be removed at the same time as the *N*-terminal Boc protecting group on the tridecapeptide. This not only improved the yield of the *N*-Boc-Asp protection (60%, **Scheme 107**, eq 2), but also improved the yield of the tripeptide **312** to 55% after *N*-Boc deprotection (**Scheme 107**, eq 4).

<sup>230</sup> Chen, H.; Feng, Y.; Xu, Z.; Ye, T. *Tetrahedron* **2005**, *61*, 11132.

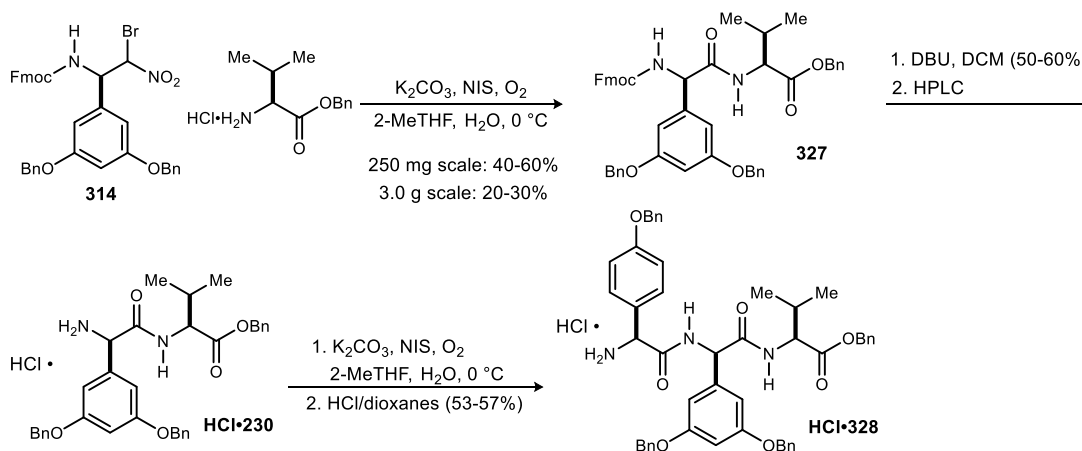


**Scheme 107.** Previous improvements toward the C-terminal tetrapeptide.

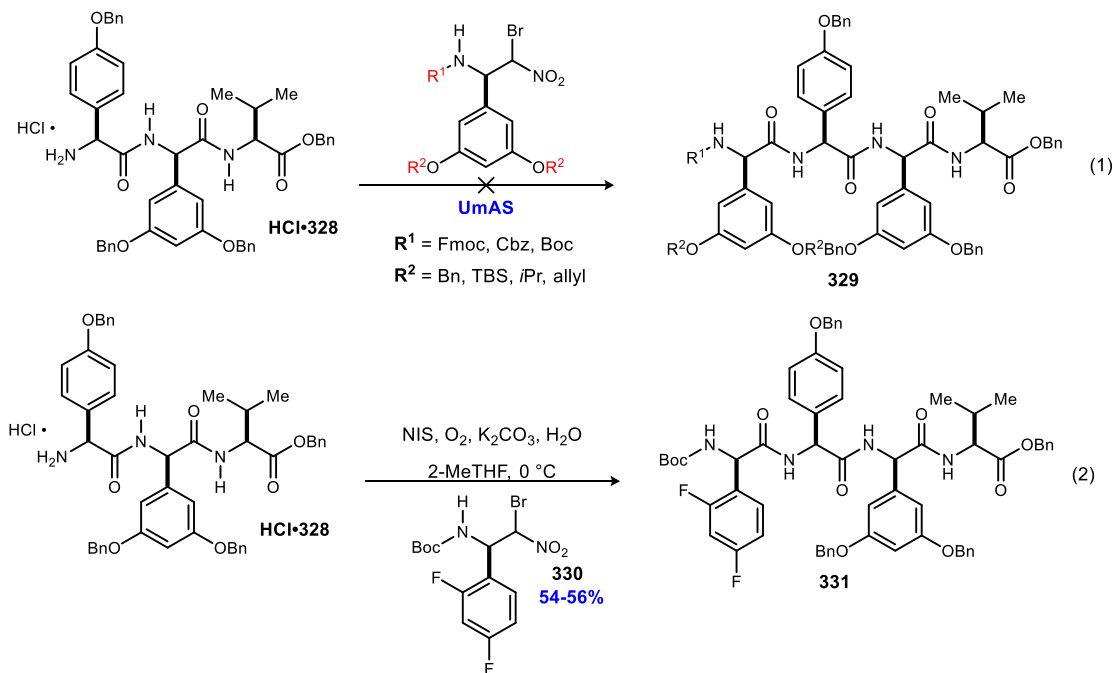


It should be noted that with the exception of the stereochemistry at the *N*-terminal Hpg residue, the preparation of Fragment A parallels that of Fragment B, and thus presented similar challenges. A previously pursued route is shown in **Scheme 108**. To this end, the synthesis of Fragment B began with the coupling of valine to the Dpg donor **314** which, as explained in Chapter 2, was a very complicated reaction. As shown, the coupling between Fmoc-protected Dpg donor **314** and valine gave good yields on small scale, but upon scale-up the yields dropped significantly, and

**Scheme 108.** Previous synthesis of tripeptide 328.



**Scheme 109.** Key observation toward the synthesis of tetrapeptide 329.



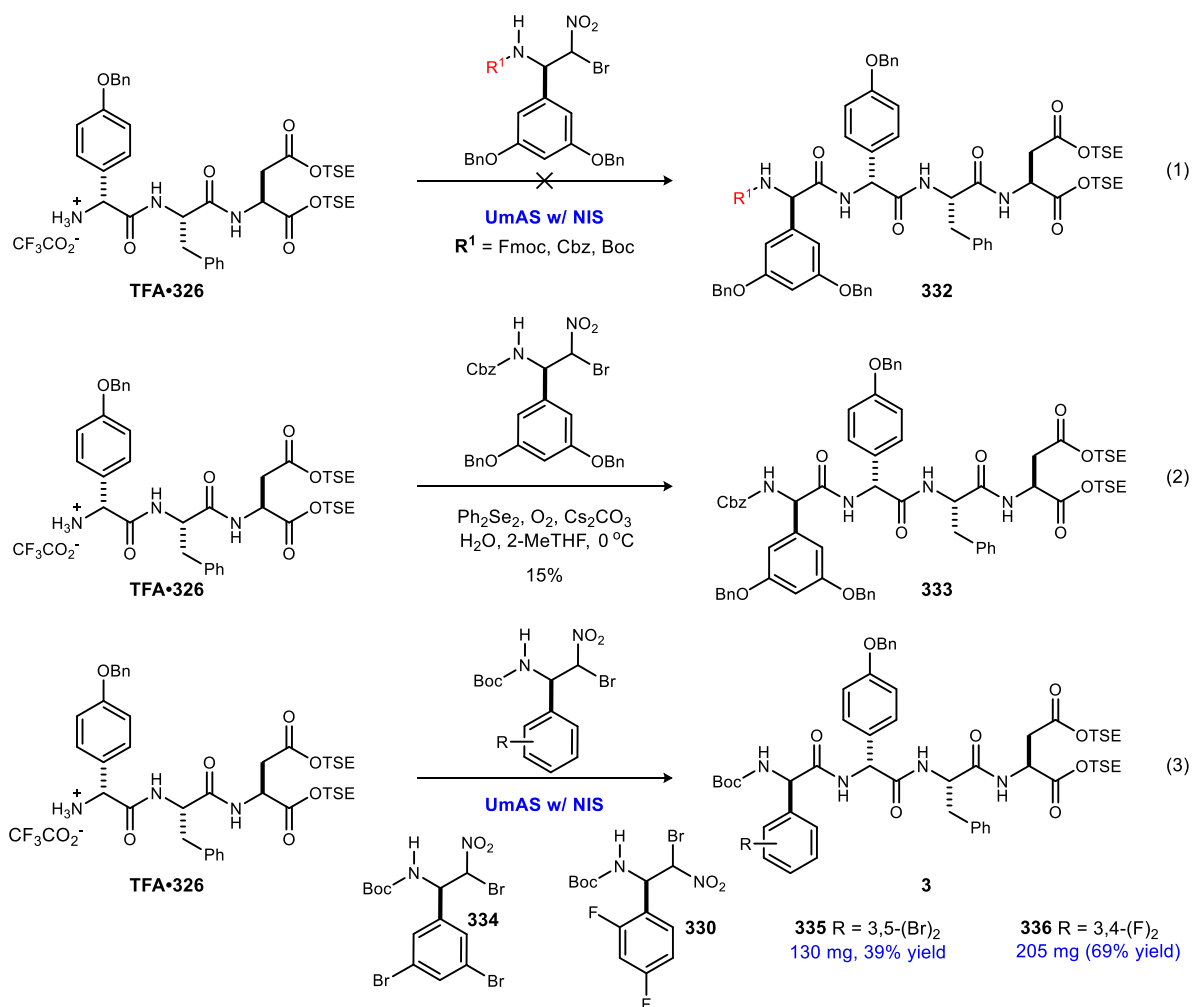
were often not reproducible despite the assistance of a mechanical stirrer. Removal of the Fmoc-protecting group required DBU, and the product had to be purified by preparative HPLC for the ensuing reaction to yield reproducible results.

The completion of Fragment B soon became the bottleneck of this total synthesis, as the incorporation of more than one Dpg unit could not be realized, despite extensive attempts to do so. An array of oxidant systems, solvents, temperatures, concentrations and *N*- and *O*-protecting groups were explored, but to no avail (**Scheme 109**). To better understand these reactions, attempts were made to couple other residues to the tripeptide **328**. A crucial realization was made when the 2,4-difluoro bromonitroalkane analog **320** was coupled to the tripeptide in good yield (**Scheme 109**). This demonstrated that the inability to synthesize tetrapeptide **329** (and the target hexapeptide **311**), was directly related to some inherent quality of the Dpg donor and/or its product.

A similar phenomenon was observed in previous attempts to synthesize Fragment C. Under UmAS conditions using NIS, the Dpg donor could not be coupled to make the tetrapeptide **332** (**Scheme 110**). A change in oxidant to  $(\text{PhSe})_2$  provided some product, albeit in low yield (15%, **Scheme**

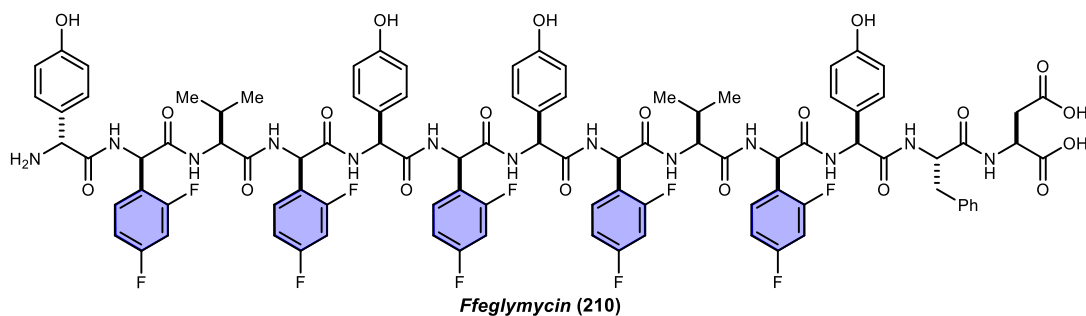
**110**, eq 2). Interestingly, attempts to couple either the 3,5-dibromo or 2,4-difluoro analogues **334** or **330**, were successful in moderate to good yield (**Scheme 110**, eq 3). This mirrored that which was previously observed toward Fragment B, and supported the hypothesis that the electron-rich Dpg donor was particularly unreactive.

**Scheme 110.** Efforts toward C-terminal tetrapeptide.



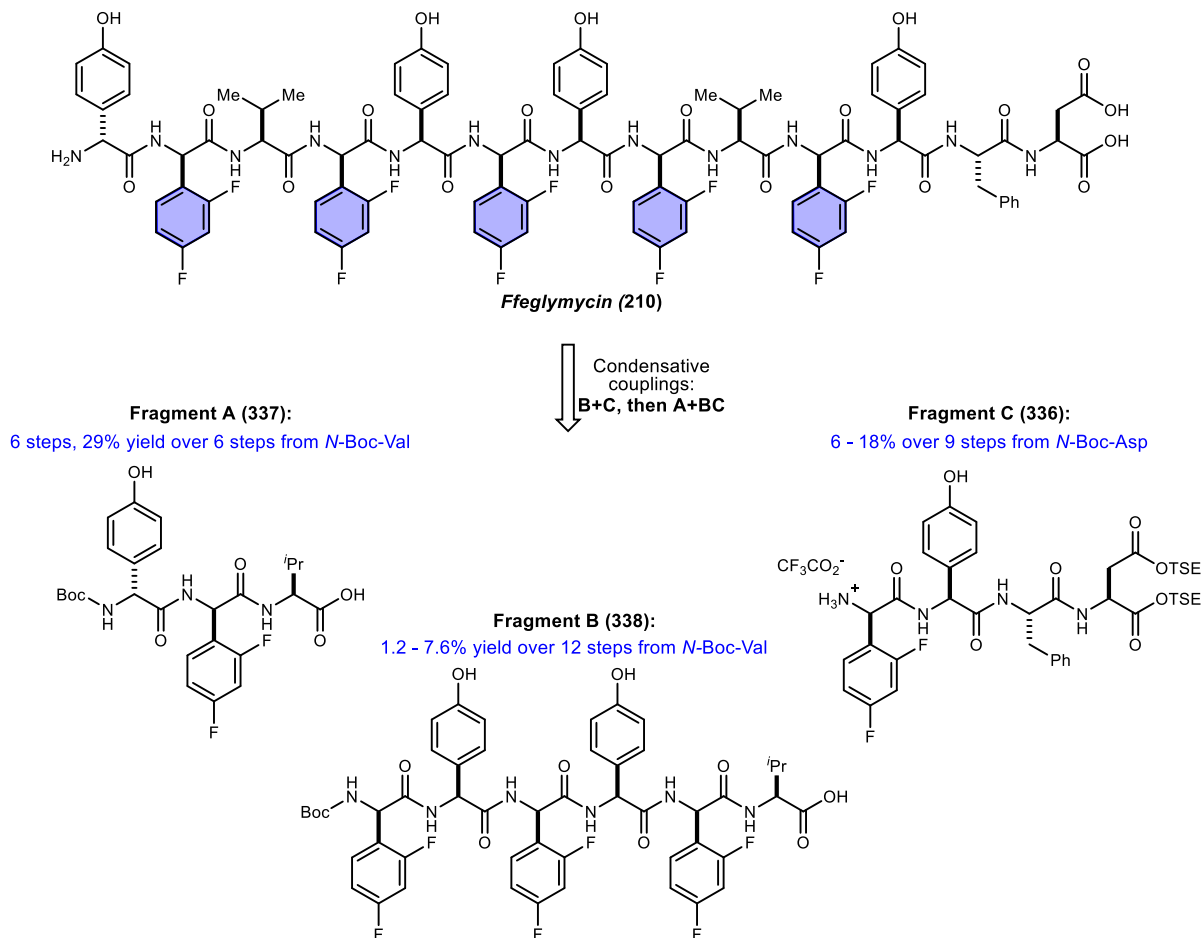
To examine the potential for iterative UmAS couplings to be used in the synthesis of a complex target such as feglymycin, while avoiding the problems associated with the Dpg donor **314**, a model peptide was pursued.<sup>184,229</sup> A fluorinated version of feglymycin – dubbed internally as Ffeglymycin (**Scheme 111**) – where each Dpg residue is replaced with the 2,4-difluoro analog, was selected as the target.

**Scheme 111.** Structure of model peptide Ffeglymycin (210).



The retrosynthesis of Ffeglymycin mirrors that of feglymycin, with the target retrosynthetically deconstructed into three fragments (**Scheme 112**). Each of these fragments were successfully synthesized in good yields using UmAS, demonstrating the utility of the reaction for the preparation of large peptide fragments, and again supporting the hypothesis that the previous shortcomings toward feglymycin could be attributed to the unique qualities of the Dpg donor.

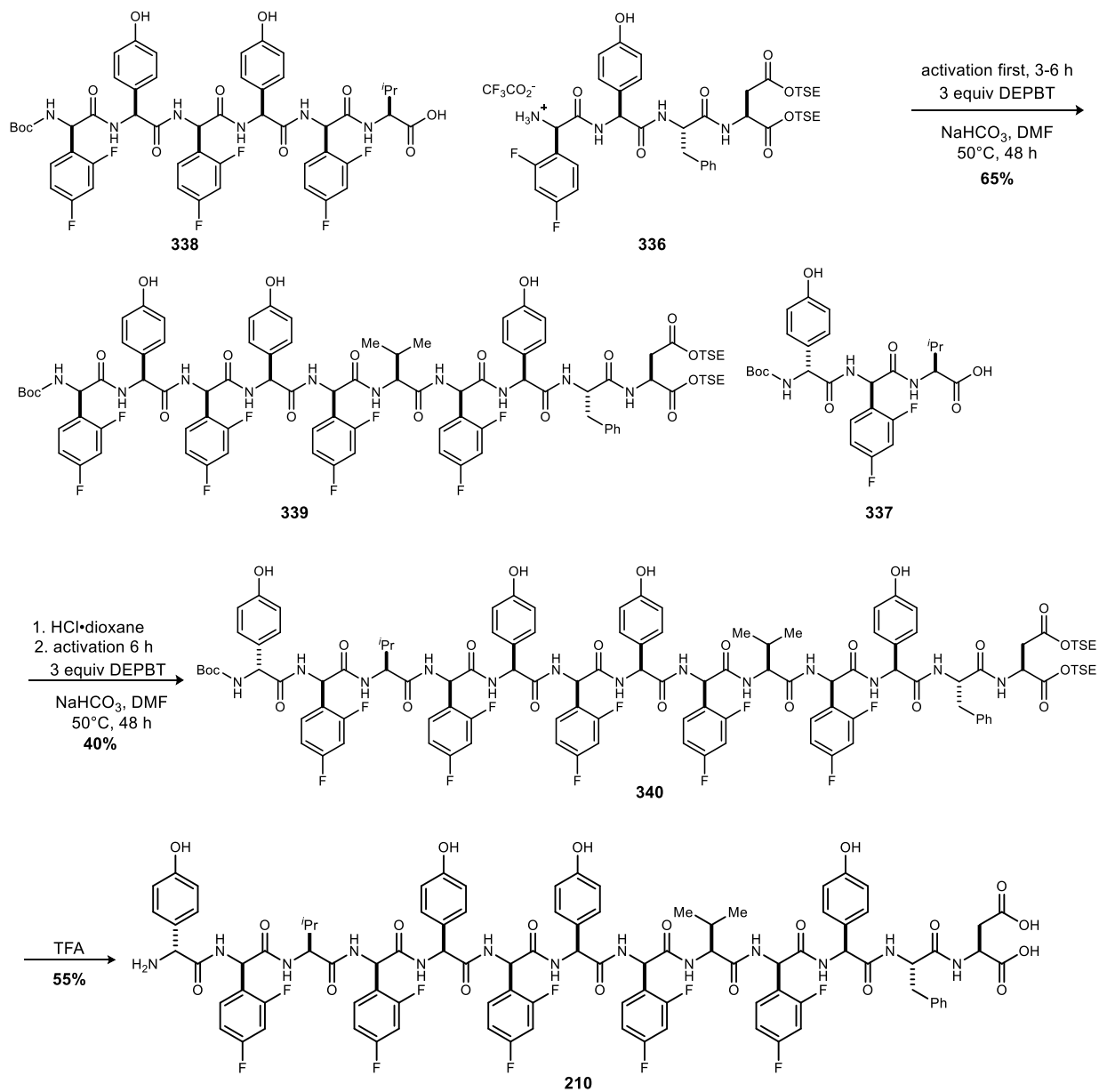
**Scheme 112.** Retrosynthetic analysis and summary of fragment preparation for Ffeglymycin.



The completion of the synthesis of Ffeglymycin is shown in **Scheme 113**. The final condensative couplings were carried out using DEPBT as the coupling reagent, and significant optimization efforts were dedicated to determine the best reaction conditions in terms of stoichiometry, temperature, and concentration. Importantly, a pre-activation period for the carboxylic acid was critical to the success of the reaction, and studies were conducted that established the optimal pre-activation times. To this end, the *C*-terminal tetrapeptide was successfully coupled to the central hexapeptide in 65% yield using DEPBT with a 3 to 6-hour activation period (**Scheme 113**). The resulting decapeptide was Boc-protected and coupled to the *N*-terminal tripeptide in 40% yield to provide the tridecapeptide, which was globally deprotected with TFA in 55% yield (**Scheme 113**). This provided Ffeglymycin in 0.4% overall yield with an 18-step longest linear sequence, and 35 steps overall. The completion of this ambitious feat by Ken Schwieter and Sergey Tsukanov demonstrated that UmAS is indeed a synthetically useful reaction for peptide synthesis. This

reinvigorated our group's aspirations toward achieving the total synthesis of natural (-)-feglymycin.

**Scheme 113.** Completion of Ffeglymycin (210).



### 3.2.2 Retrosynthetic proposal and building block synthesis

The revised retrosynthesis of feglymycin to be pursued in this work was modeled after the successful synthesis of the fluorinated analogue of feglymycin, Ffeglymycin (**Scheme 114**).<sup>229</sup>

Thus, the target was deconstructed into three fragments that would each be synthesized using



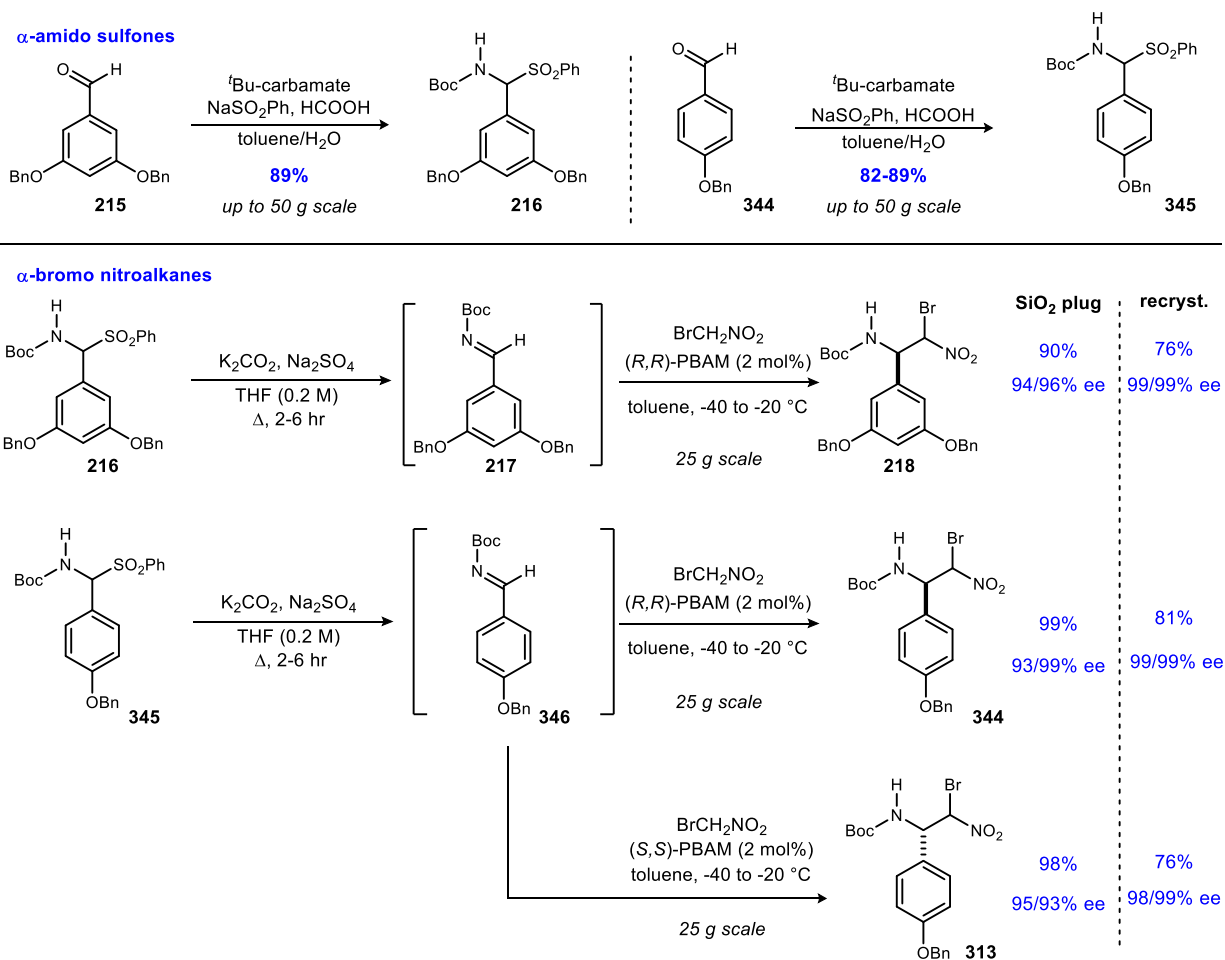
modified to use the more precious aldehyde (instead of the carbamate) as the limiting reagent.<sup>231</sup> The elimination of sulfinate was effected using a mild base, desiccant, and heat (**Scheme 115**). The exclusion of water in these reactions is crucial as the imines are susceptible to hydrolysis. To that extent, they were carried immediately into the aza-Henry reaction following filtration and concentration. More electron deficient *N*-Boc aldimines have displayed a reasonably long shelf-life in our laboratory (stable  $\geq 6$  months at  $-20$  °C), but these electron-rich substrates are particularly sensitive. If the aza-Henry reaction cannot be performed on the same day as the elimination, care should be taken to store the imine at  $-78$  °C under an inert atmosphere, or under high-vacuum at room temperature. The aza-Henry reactions consistently provided high ee material in high yield on 25 g scale. We found that the catalyst loading could be decreased to 2 mol% with no significant effect on yield or enantioselection. Fractional recrystallization consistently produced the  $\alpha$ -bromonitroalkanes with  $>98\%$  ee. Overall, this provided the optically active carboxylic acid surrogates in 3 steps, with high enantiomeric excess, from the corresponding aldehyde. With these building blocks and retrosynthetic plan of attack in hand, we moved forward toward the synthesis of feglymycin.

---

<sup>231</sup> Engberts, J. B. F. N.; Strating, J. *Recl. Trav. Chim. Pays-Bas* **1964**, 83, 733.; For a review see: Petrini, M. *Chem. Rev.* **2005**, 105, 3949.



**Scheme 115.** Synthesis of  $\alpha$ -bromo nitroalkane building blocks for feglymycin.



### 3.2.3 Synthesis of Fragment B

When I was first brought on to this project, the primary impeding factor in our laboratory's pursuit of feglymycin was the synthesis of the central hexapeptide (Fragment B). Extensive efforts were dedicated to improving the yield, reproducibility, and scalability of reactions employing electron-rich aryl  $\alpha$ -bromo nitroalkanes. The saga discussed in Chapter 2 covers these endeavors in detail. Ultimately, studies conducted by Dr. Kazuyuki Tokumaru and myself, which built upon the discoveries of prior lab members<sup>229</sup> concluded with the development of a protocol that uses KI and urea-hydrogen peroxide instead of NIS. This protocol was particularly effective in improving the yield of, and reducing the byproducts produced in, reactions using Dpg donors in UmAS.

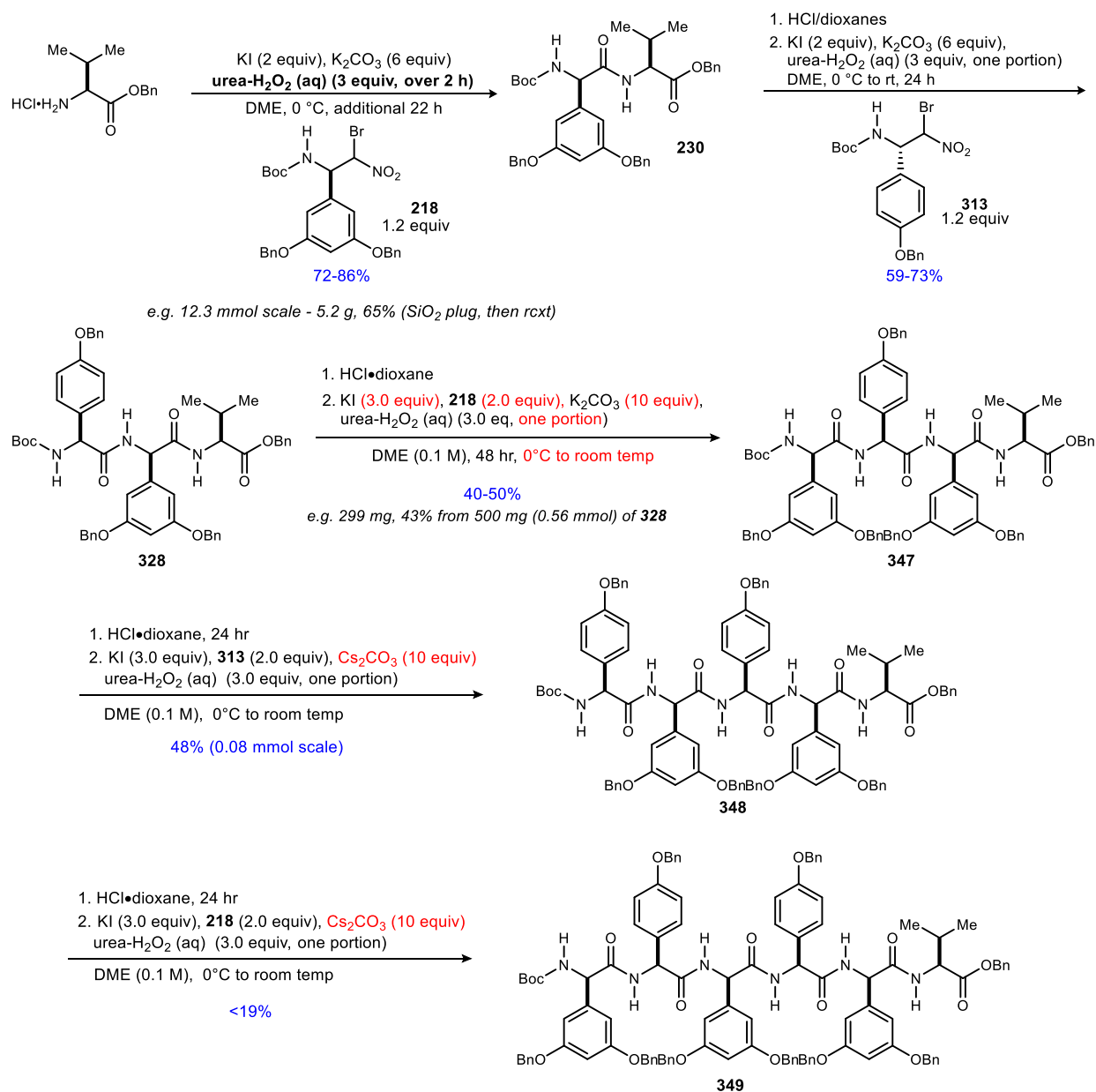
This enabled our synthesis of the challenging Fragment B. To this extent, the synthesis began with the dipeptide **230** (**Scheme 116**). The use of the KI/UHP protocol delivered the dipeptide **230** on multi-gram scale with 72-86% yield. The product was purified by crystallization after a silica plug (**Scheme 116**). This was a considerable improvement over the NIS conditions, which required mechanical stirring on scales >1g along with extensive purification efforts. Similarly, the next coupling afforded the tripeptide **328** in 59-73% yield and the product was purified by recrystallization (**Scheme 116**). In this case, it proved beneficial to add the UHP solution at one time, instead of dropwise, as the presence of water improved solubility. The variability in yields is a result of different reaction times and whether or not the mother liquor was recrystallized.

*It was a joyous occasion when the tetrapeptide **347** was successfully synthesized for the first time in our laboratory using the KI/UHP protocol!* Under standard conditions the tetrapeptide **347** was consistently produced in 20-24% yield. The reaction had low conversion as evidenced by recovered amine. Optimization studies were carried out and it was found that increasing the equivalents of reactants relative to the amine, extending the reaction time, and warming the reaction mixture to room temperature after the addition of UHP provided the tetrapeptide with yields consistently between 40-50% (**Scheme 116**). Due to the poor solubility of the tetrapeptide, the product is purified by trituration with acetonitrile post workup.<sup>232</sup> Further trituration of the resulting solids in hot methanol seems to further break up aggregates and leads to improved reactivity in subsequent couplings. While these optimized yields may be modest, this was still a significant feat considering our prior inability to access product in any capacity. *This success pushed us past a bottleneck that spanned the course of about 8 years, and provided the impetus to continue with the pursuit of feglymycin.*

---

<sup>232</sup> Identification of MeCN trituration as a means of purification for this substrate was done by Dr. Kazuyuki Tokumaru.

**Scheme 116.** Synthesis of central Fragment B via UmAS.



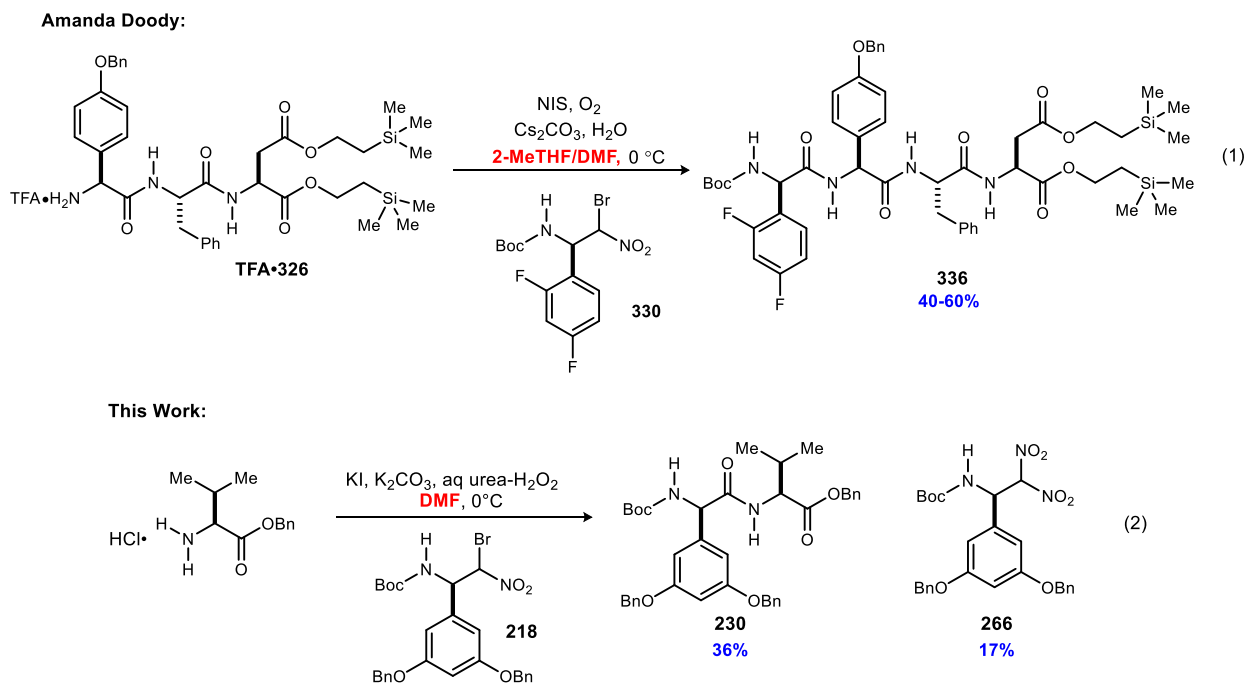
The standard KI/UHP protocol provided the pentapeptide **348** in 16% yield, while the conditions optimized for the tetrapeptide **347** provided the pentapeptide **348** in 27% yield. Interestingly, while a switch from K<sub>2</sub>CO<sub>3</sub> to Cs<sub>2</sub>CO<sub>3</sub> did not substantially improve the yield for tetrapeptide, using 10.0 equivalents of Cs<sub>2</sub>CO<sub>3</sub> for the pentapeptide increased the yield to 48% from 27% (**Scheme 116**). Using these conditions to synthesize the hexapeptide **349** did indeed provide product, but the reaction yield was low, and purification proved difficult.

## DMF as a solvent in UmAS

Given that the tetra-, penta-, and hexapeptides are only soluble in solvents like DMSO or DMF, we wanted to see if we could move away from the ethereal solvents typically used in UmAS. Toward the synthesis of a fluorinated derivative of feglymycin, it was previously demonstrated that a mixture of 2-MeTHF/DMF worked well to address solubility issues en route to **Fragment C** (eq. 1, **Scheme 117**).<sup>183</sup>

Thus, a model reaction was conducted where the standard KI/UHP protocol was applied to synthesize the dipeptide **230** in DMF. While the reaction was still relatively clean, the yield was significantly lower than the reaction run in DME and a large amount of dinitroalkane **266** (17%) formed (**Scheme 117**, eq 2). Presumably DMF would increase the solubility of nitrite and thus increase the likelihood of the ter Meer reaction (see Chapter 2) to form the  $\alpha,\alpha$ -dinitroalkane. DMF was also explored as a cosolvent with DME (25%, 50%, and 75% DMF in DME) but there was no significant change in reaction profile when compared to the test reaction shown in **Scheme 117**.

**Scheme 117.** DMF as a solvent in UmAS.

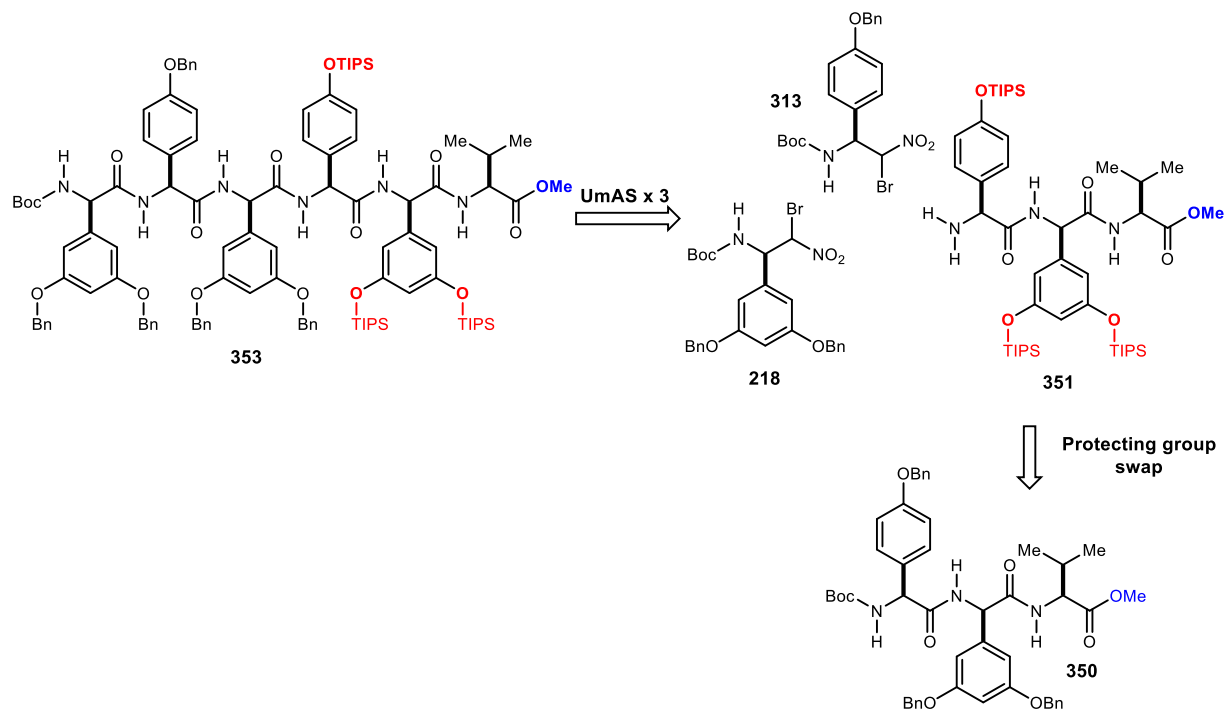


While this served as a good proof of concept that UmAS can be run in DMF, it was not sufficiently promising to explore further down the line for the synthesis of the penta- and hexapeptide B.

### TIPS protected phenols change solubility of Fragment B

It was expected that the solubility issues were caused by the plethora of benzyl protecting groups and so a strategy was devised that would allow us to explore this concept via a protecting group swap (**Figure 37**). It was hypothesized that the use of large TIPS protecting groups on the DPG and HPG residues would serve to break up aggregates and to make the compounds more lipophilic. This route was pursued first before investing time and resources into making TIPS protected  $\alpha$ -bromo nitroalkanes. As shown in **Figure 37**, three of the phenolic benzyl ethers would be replaced with TIPS groups, and in order to remove the benzyl groups without deprotecting the C-terminal valine residue, a C-terminal methyl ester was used. The TIPS protecting group is almost twice the molecular weight of the benzyl protecting group, which brings about concerns later in the synthesis

**Figure 37.** Retrosynthesis of the partially TIPS-protected central fragment of (-)-feglymycin.

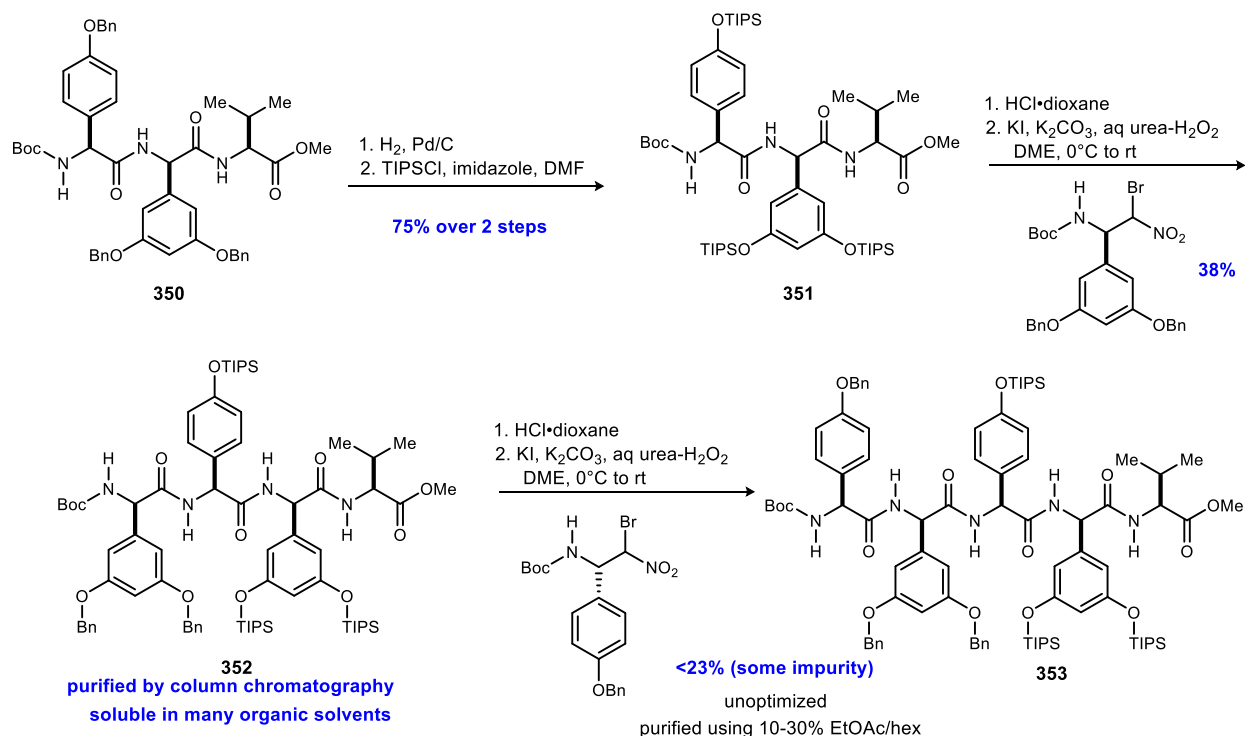


where deprotection would come with a significant loss of mass, so a focus was put on incorporating the minimum number of TIPS groups to achieve an effect.

Thus, the tripeptide was hydrogenated and then TIPS protected to afford **351** in 75% yield over two steps (**Scheme 118**). The next UmAS reaction proceeded in 38% yield, and to our delight the resulting tetrapeptide **352** had tremendously improved solubility. It is soluble in most organic solvents (ethyl acetate, dichloromethane, acetonitrile etc.) and in fact, the compound was purified by column chromatography using ethyl acetate in hexanes. This is a something that was not possible with the fully benzyl protected fragment. Taking this material forward using UmAS provided the pentapeptide in less than 23% yield. The solubility of pentapeptide **353** was drastically improved, but the reaction yield was not, and purification proved challenging.

This approach was not pursued further for the synthesis of (-)-feglymycin since the yields were not significantly improved. Moreover, this route used a protecting group swap and it would be more practical to incorporate the  $\alpha$ -bromo nitroalkanes already TIPS-protected, which would require further optimization at the aza-Henry stage. It was also unknown if the TIPS protected  $\alpha$ -bromo nitroalkanes would behave in a similar fashion to the benzyl protected analogues, and UmAS conditions may need to be re-optimized. Nevertheless, this series of experiments confirmed the hypothesis that the benzyl groups are a key contributor to the solubility issues plaguing this synthesis.

**Scheme 118.** Protecting group swap toward the partially TIPS-protected central fragment of (-)-feglymycin.

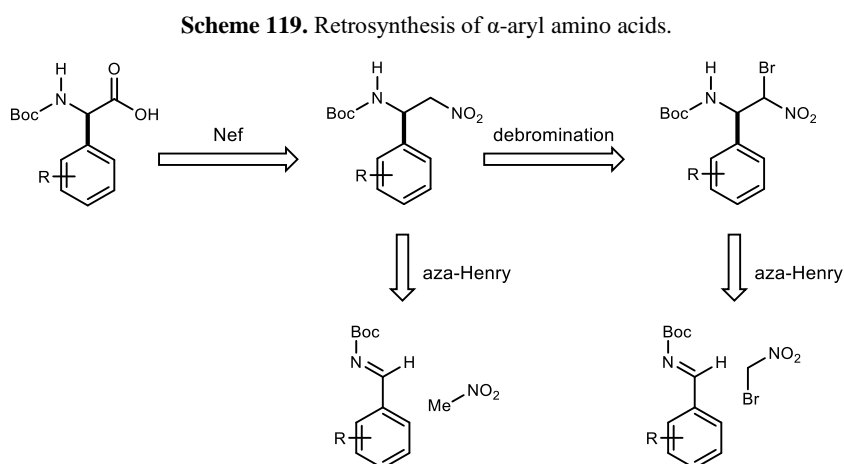


## DEPBT couplings to homologate the tetra- and pentapeptides

*Ultimately, the poor solubility of the penta- and hexapeptide intermediates was an insurmountable issue and prevented UmAS from being utilized as the primary route to access these larger compounds, especially on the scale required to bring material through for a total synthesis.* We thus decided to use iterative amino acid couplings to homologate the tetrapeptide to the penta- and hexapeptide. It was hypothesized that this would enable us to overcome the solubility issues given the greater variety in solvent choice for condensative coupling as compared to UmAS. Importantly, if successful, this would allow for the synthesis of greater amounts of penta- and hexapeptide for characterization. This would facilitate confirmation of their presence in the UmAS reactions and potentially aid the ability to optimize those reactions.

As described in **Chapter 2**, the enantioselective synthesis of aryl glycines is far from trivial. *In fact, as of January 2020, none of the methods developed within the last 20 years have been applied in the total synthesis of any arylglycine containing natural products.* Süßmuth and coworkers as well as Fuse and coworkers both used Sharpless chemistry to access the DPG residue, and purchased the HPG residue.<sup>206,227</sup> Our aim is to avoid the use of osmium and its attendant potential

for imperfect regioselectivity. This required the extensive development of an alternate method, one that leveraged our laboratory's robust and stereoselective means of synthesizing  $\beta$ -amido-nitro- and  $\beta$ -amido- $\alpha$ -bromo nitroalkanes. To this end, the key transformation in the retrosynthetic analysis is the Nef reaction<sup>233, 234</sup> which would convert a  $\beta$ -amido nitroalkane with defined stereochemistry to the corresponding *N*-Boc amino acid (**Scheme 119**). The nitroalkane could be accessed directly through an aza-Henry reaction with nitromethane, or by debromination of the corresponding  $\alpha$ -bromo nitroalkane.



The latter strategy was tested first, and the  $\alpha$ -bromo nitroalkanes were successfully converted to the corresponding nitroalkanes using  $\text{SnCl}_2$  (**Scheme 120**). These reactions work well on small (<1 g) scale, but on larger scale the workup becomes cumbersome as addition of water causes the tin to form an opalescent jelly-like precipitate. This is typically removed using Celite, but multiple iterations can often lead to a diminished yield. It was later found that vigorous stirring with water

<sup>233</sup> Discovery & pioneering studies: a) Konovalov, M. *J. Russ. Phys. Chem. Soc.* **1893**, 25, 509.; b) Meyer, V.; Wurster, C. *Berichte der deutschen chemischen Gesellschaft* **1873**, 6, 1168.; c) Nef, J. U. *Ann.* **1894**, 280, 263.; d) Konowalov, M. *Berichte der deutschen chemischen Gesellschaft* **1896**, 29, 2193.; e) Bamberger, E.; Rüst, E. *Berichte der deutschen chemischen Gesellschaft* **1902**, 35, 45.; f) Lippincott, S. B.; Hass, H. B. *Industrial & Engineering Chemistry* **1939**, 31, 118.; g) Kamlet, M. J.; Kaplan, L. A.; Dacons, J. C. *J. Org. Chem.* **1961**, 26, 4371.; h) Kornblum, N.; Brown, R. A. *J. Am. Chem. Soc.* **1965**, 87, 1742.

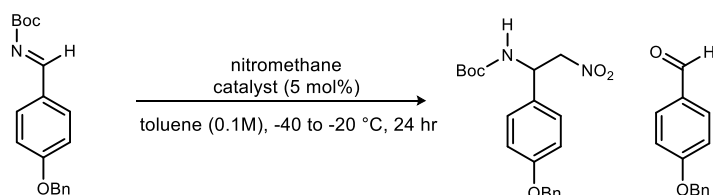
<sup>234</sup> For reviews on the Nef reaction see: Noland, W. E. *Chem. Rev.* **1955**, 55, 137.; Ballini, R.; Petrini, M. *Tetrahedron* **2004**, 60, 1017.; Ballini, R.; Petrini, M. *Adv. Synth. Catal.* **2015**, 357, 2371.





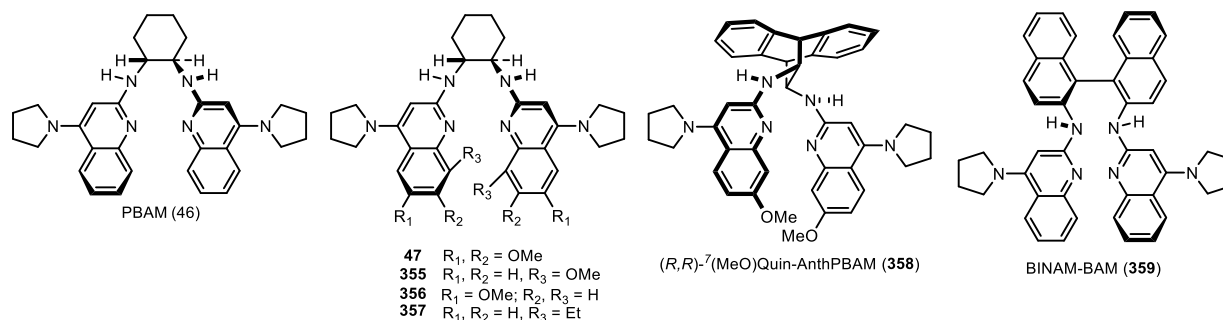
It was also desirable to make the nitroalkane directly through an aza-Henry reaction. This began with a screen of some of the catalysts in the Johnston Laboratory BAM Ligand Library for conversion. **Table 27** describes these initial tests, where the main species found in the crude reaction mixture were the starting imine, the desired nitroalkane, and the product of hydrolysis (the aldehyde). PBAM (**46**) and <sup>6,7</sup>(MeO)<sub>2</sub>PBAM (**47**) as well as their 1:1 salts were tested first

**Table 27.** Catalyst screen and product distribution in BAM catalyzed aza-Henry reactions.



entry <sup>a</sup>	catalyst base	catalyst additive <sup>b</sup>	product distribution (relative ratio) <sup>c</sup>		
			imine	nitroalkane	aldehyde
1	PBAM ( <b>46</b> )	--	3	3	1
2	PBAM ( <b>46</b> )	HOTf	1	5	1
3	PBAM ( <b>46</b> )	HNTf <sub>2</sub>	1	25	4
4	<sup>6,7</sup> (MeO) <sub>2</sub> PBAM ( <b>47</b> )	--	2	1	1
5	<sup>6,7</sup> (MeO) <sub>2</sub> PBAM ( <b>47</b> )	HNTf <sub>2</sub>	0	3	1
6	<sup>8</sup> (MeO)PBAM ( <b>355</b> )	HOTf	75	1	5
7	<sup>8</sup> (MeO)PBAM ( <b>355</b> )	HNTf <sub>2</sub>	29	1	2
8	<sup>6</sup> (MeO)PBAM ( <b>356</b> )	HOTf	1	14	1
9	<sup>8</sup> EtPBAM ( <b>357</b> )	HNTf <sub>2</sub>	44	1	3
10	<sup>7</sup> (MeO)AnthPBAM ( <b>358</b> )	HNTf <sub>2</sub>	5	2	1
11	BINAMBAM ( <b>359</b> )	HNTf <sub>2</sub>	11	2	1
12 <sup>d</sup>	<sup>6,7</sup> (MeO) <sub>2</sub> PBAM ( <b>47</b> )	HNTf <sub>2</sub>	0	14	1
13 <sup>e</sup>	<sup>6,7</sup> (MeO) <sub>2</sub> PBAM ( <b>47</b> )	HNTf <sub>2</sub>	0	5	1

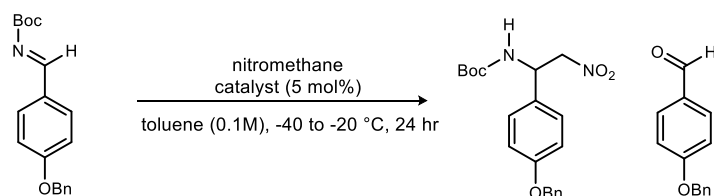
<sup>a</sup>All reactions used 10 equiv. of nitromethane unless otherwise indicated. <sup>b</sup>Catalyst prepared as the 1:1 base:acid salt. <sup>c</sup>Relative ratio determined by <sup>1</sup>H-NMR integration. <sup>d</sup>5.0 Equiv nitromethane. <sup>e</sup>1.2 Equiv nitromethane. Shading emphasizes product distribution: blue = major, purple = second major, red = minor.



and it was observed that the salts performed significantly better in terms of conversion (**Table 27**, entries 1-5). For example,  $^{6,7}(\text{MeO})_2\text{PBAM}$  (free base) resulted in a 2:1 ratio of starting material to product, while the triflimide salt resulted in complete conversion (**Table 27**, entry 4 vs entry 5). We thus proceeded to examine only the salts of the other catalysts. Ultimately, the  $^6(\text{MeO})\text{PBAM}$  (**Table 27**, entry 8),  $^{6,7}(\text{MeO})_2\text{PBAM}$ , and PBAM ligands were used going forward as the rest of the catalysts did not provide good conversion of starting material. The corresponding products were isolated, their ee was determined, and the results are summarized in **Table 20**.

The more electron-rich catalysts ( $^{6,7}(\text{MeO})_2$ - and  $^6(\text{MeO})$ -PBAM) provided better yields than PBAM.  $^{6,7}(\text{MeO})_2\text{PBAM}$  gave the best yield and ee, and we found that decreasing the amount of nitromethane resulted in an increase in ee. The best conditions used 1.2 equivalents of nitromethane, which provided a 70% isolated yield with 98% ee (**Table 20**, entry 7). It should be noted that these conditions did not directly translate to the 3,5-(BnO)<sub>2</sub> derivative. An inseparable mixture of products resulted, which was believed to be the result of a second addition of the resulting nitroalkane to the imine. Further optimization would need to be done on this system to

**Table 28.** Optimization of BAM-catalyzed aza-Henry reaction for amino acid precursors.



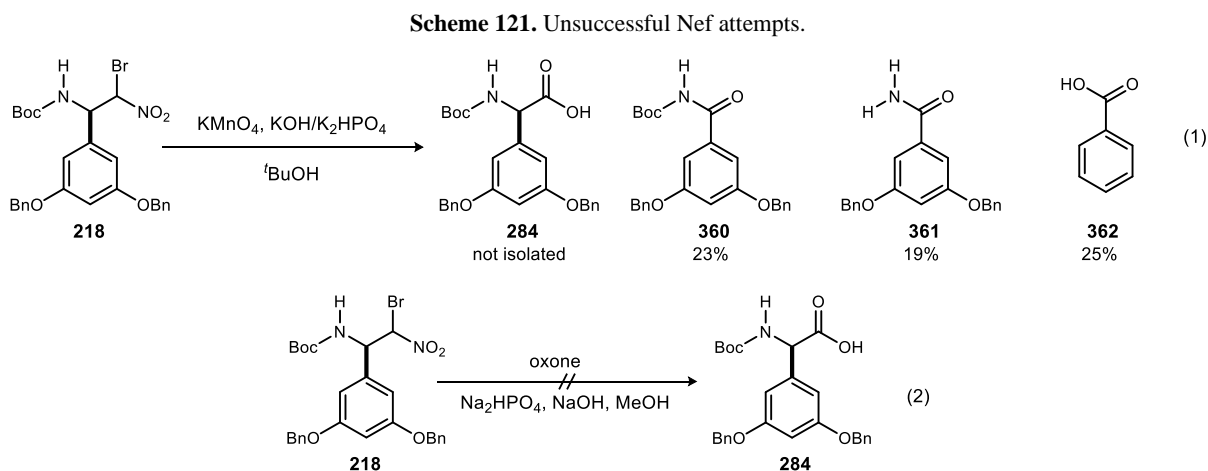
entry	catalyst base	catalyst additive <sup>a</sup>	nitromethane (equiv)	yield <sup>b</sup>	ee (%) <sup>c</sup>
1	PBAM ( <b>46</b> )	HOTf	10	40	85
2	PBAM ( <b>46</b> )	HNTf <sub>2</sub>	10	52	86
3	$^{6,7}(\text{MeO})_2\text{PBAM}$ ( <b>47</b> )	--	10	59	60
4	$^{6,7}(\text{MeO})_2\text{PBAM}$ ( <b>47</b> )	HNTf <sub>2</sub>	10	76	91
5	$^6(\text{MeO})\text{PBAM}$ ( <b>356</b> )	HOTf	10	72	86
6	$^{6,7}(\text{MeO})_2\text{PBAM}$ ( <b>47</b> )	HNTf <sub>2</sub>	5	72	93
7	$^{6,7}(\text{MeO})_2\text{PBAM}$ ( <b>47</b> )	HNTf <sub>2</sub>	1.2	70	98

<sup>a</sup>Catalyst prepared as the 1:1 base:acid salt. <sup>b</sup> Isolated yield. <sup>c</sup>Enantiomeric excess (ee) determined by HPLC using a chiral stationary phase.

make this reaction effective. For this work, the aforementioned tin-promoted debromination was used to make the nitroalkane.

With the nitroalkanes in hand, attention was turned toward effecting the Nef reaction. There are many ways to achieve the nitro to carbonyl conversion (oxidative, reductive, biocatalytic etc).<sup>177</sup> We chose reaction conditions that were i) mild, so as to not remove protecting groups or epimerize the  $\alpha$ -stereocenter, and ii) procedurally simple and safe enough to perform on gram scale.

To this end, potassium permanganate<sup>236</sup> was tested first but these conditions were too strong for the substrate and led to a number of oxidized decomposition products such as the imide and benzamide (**Scheme 121**, eq 1). It also caused benzyl deprotection. Oxone<sup>237</sup> was also not effective, as no conversion of starting material was observed (**Scheme 121**, eq 2). Conversion of a terminal amide to the carboxylic acid using DMF-DMA was also attempted, but it did not provide product.<sup>238</sup>



Gratifyingly, conditions identified by Mioskowski for the conversion of nitroalkanes and bromides to carboxylic acids were fruitful (**Scheme 122**).<sup>239</sup> These mild conditions use sodium nitrite and acetic acid in warm DMSO to effect the transformation. The proposed mechanism is shown in

<sup>236</sup> Saville-Stones, E. A.; Lindell, S. D. *Synlett* **1991**, 1991, 591.

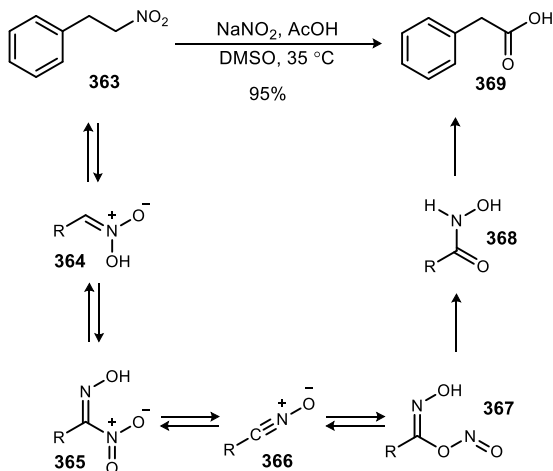
<sup>237</sup> Ceccherelli †, P.; Curini, M.; Marcotullio, M. C.; Epifano, F.; Rosati, O. *Synth. Commun.* **1998**, 28, 3057.

<sup>238</sup> Anelli, P. L.; Brocchetta, M.; Palano, D.; Visigalli, M. *Tetrahedron Lett.* **1997**, 38, 2367.

<sup>239</sup> Matt, C.; Wagner, A.; Mioskowski, C. *J. Org. Chem.* **1997**, 62, 234.

**Scheme 122** where under acidic conditions the nitroalkane is in equilibrium with the *aci*-nitronate **364**. The *aci*-nitronate reacts with a  $\text{NO}^+$  species form the nitrolic acid **365**, which is in equilibrium with the nitrile oxide **366**. Attack of sodium nitrite on the nitrile oxide will form the nitrite ester **367** which loses  $\text{NO}^+$  to generate the hydroxamic acid **368** nitrile oxide. **368** is then hydrolyzed to the carboxylic acid **369**.<sup>239,240</sup>

**Scheme 122.** Proposed mechanism of the Mioskowski-Nef reaction.

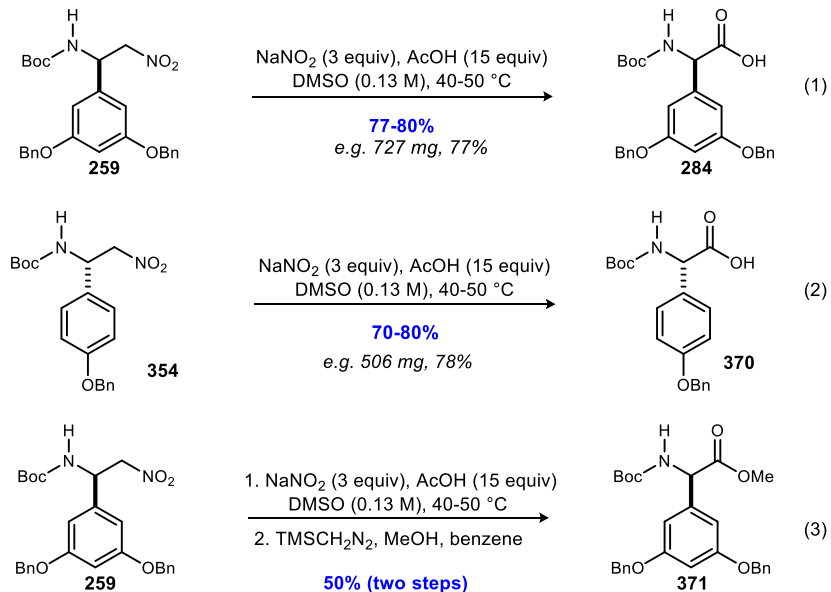


Specifically, conditions used by Palomo *et al.* that used an excess of acetic acid (15 equiv.) worked the best for our substrates (**Scheme 123**).<sup>241</sup> Both the *N*-Boc DPG and *N*-Boc HPG residues were synthesized in high yield (**Scheme 123**, eq 1-2). Additionally, the methyl ester could be synthesized by treatment of the crude acid with TMS-diazomethane (**Scheme 123**, eq 3).<sup>241</sup>

<sup>240</sup> Gissot, A.; N'Gouela, S.; Matt, C.; Wagner, A.; Mioskowski, C. *J. Org. Chem.* **2004**, *69*, 8997.

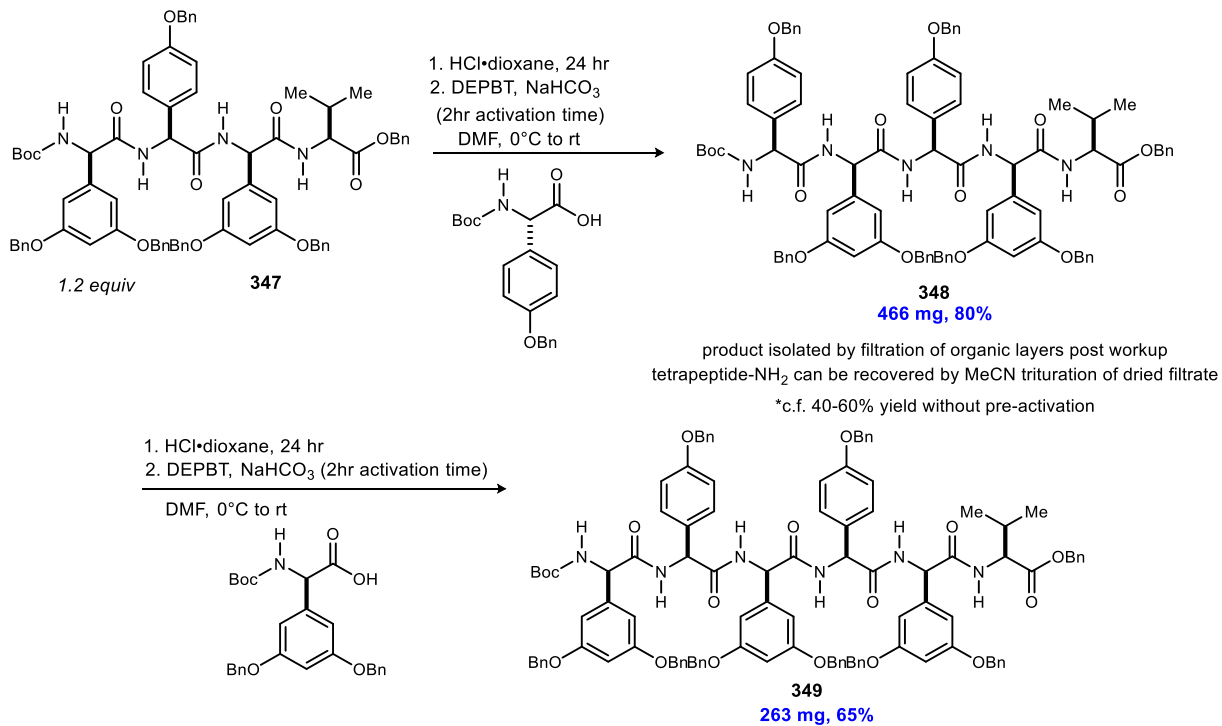
<sup>241</sup> Palomo, C.; Oiarbide, M.; Halder, R.; Laso, A.; López, R. *Angew. Chem. Int. Ed.* **2006**, *45*, 117.

**Scheme 123.** Synthesis of aryl glycine amino acids via the Mioskowski-Nef reaction.



Gratifyingly, iterative employment of the amino acids **284** and **370** to synthesize the hexapeptide B was successful! Using this approach, the *N*-Boc-Hpg residue was coupled in 80% yield to afford

**Scheme 124.** DEPBT couplings to make penta- and hexapeptide B.

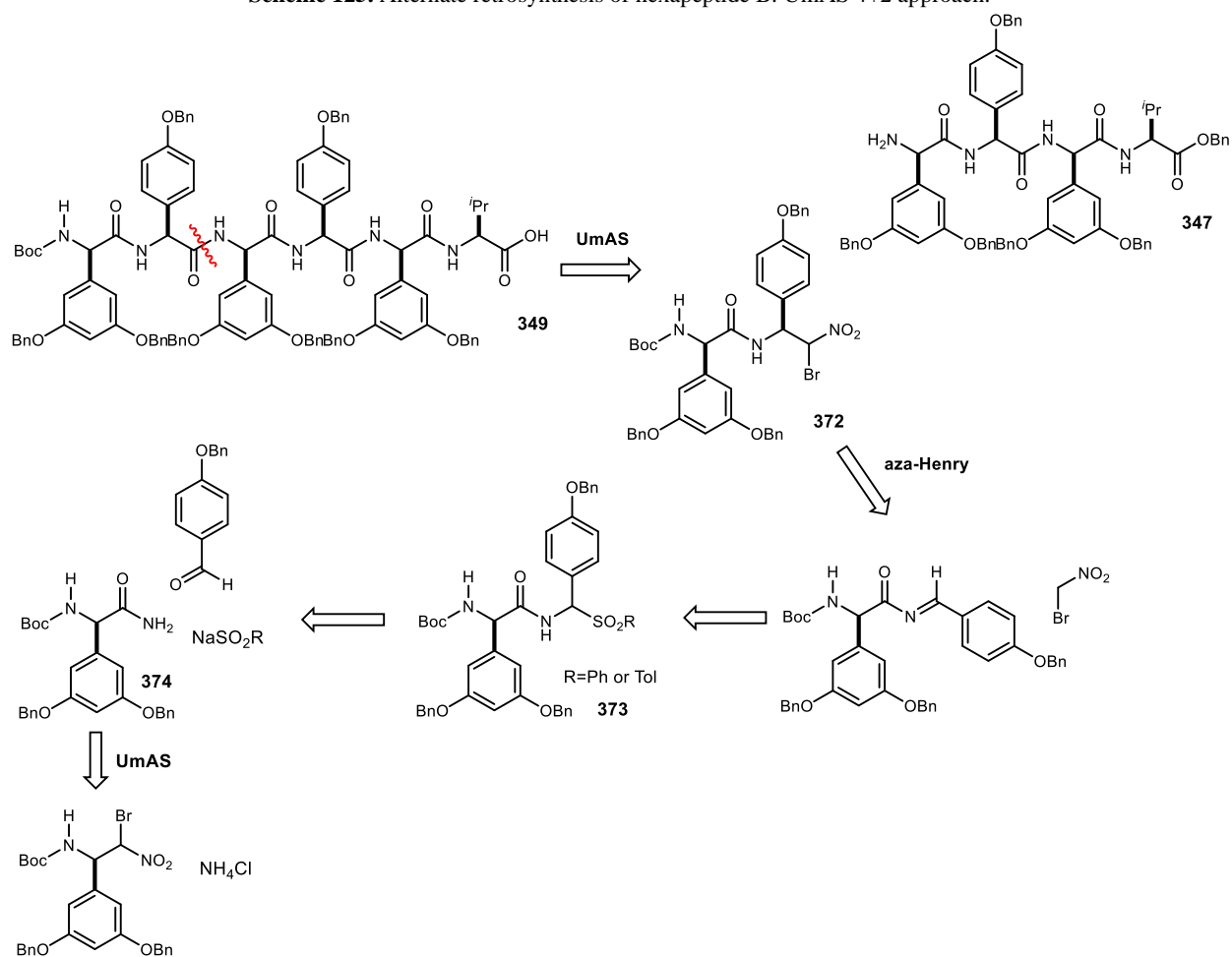


the pentapeptide **348** (Scheme 124). A two-hour pre-activation of the carboxylic acid provided the best yields. The product is purified by trituration and the starting tetrapeptide amine can typically be recovered from the filtrate. The hexapeptide **349** was also synthesized in good yield using a two-hour pre-activation of the acid (65%, Scheme 124). Importantly, no signs of epimerization were observed.

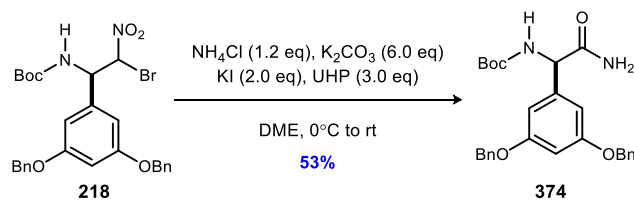
### N→C Convergent 4+2 approach to hexapeptide **349** via UmAS

An alternative to the iterative coupling of the Hpg and Dpg amino acids to make the hexapeptide **349** would be to pursue a convergent approach that couples the tetrapeptide **347** to the dipeptide surrogate **372** (Scheme 125). The approach outlined in Scheme 125 shows how UmAS can be used to build the peptide in the N→C direction. This would avoid activating both the Dpg and Hpg

Scheme 125. Alternate retrosynthesis of hexapeptide B: UmAS 4+2 approach.



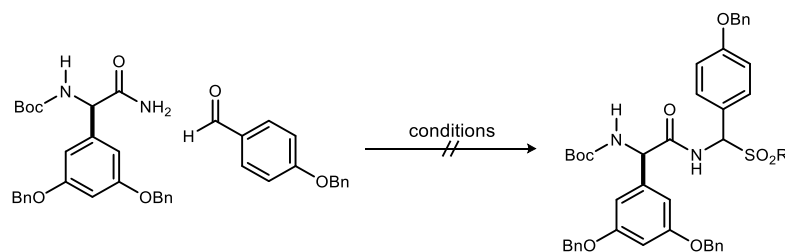
**Scheme 126.** Synthesis of terminal amide 374.



residues. The bromonitroalkane **372** could be made via an aza-Henry reaction, and the requisite sulfone **373** could be made from the primary amide **374**. That amide would also be synthesized via UmAS, thus avoiding any active esters in this route.

In the forward direction, the primary amide **374** needed to make the desired sulfone was synthesized in 53% yield using the KI/UHP UmAS protocol (**Scheme 126**). However, all attempts to make the required sulfone were unsuccessful and gave little to no conversion (**Table 29**). The poor solubility of amide **374** made these reactions difficult since they are driven forward by precipitation of the product.

**Table 29.** Attempts to synthesize sulfones for 4+2 UmAS.



entry <sup>a</sup>	solvent	acid	temperature
1 <sup>a</sup>	DCM <sup>a</sup>	TsOH <sup>b</sup>	rt
2 <sup>a</sup>	DCE <sup>a</sup>	TsOH <sup>c</sup>	60-100 °C
3 <sup>d</sup>	MeOH/H <sub>2</sub> O	HCO <sub>2</sub> H, NaSO <sub>2</sub> <i>p</i> -tol	rt
4 <sup>d</sup>	toluene/H <sub>2</sub> O	HCO <sub>2</sub> H, NaSO <sub>2</sub> <i>p</i> -tol	rt
5 <sup>d</sup>	DCM/MeOH/H <sub>2</sub> O	HCO <sub>2</sub> H, NaSO <sub>2</sub> <i>p</i> -tol	40 °C
6 <sup>d</sup>	toluene/MeOH/H <sub>2</sub> O	HCO <sub>2</sub> H, NaSO <sub>2</sub> <i>p</i> -tol	100 °C
7 <sup>d</sup>	DCM/MeOH/H <sub>2</sub> O	HCO <sub>2</sub> H, NaSO <sub>2</sub> <i>p</i> -tol	40 °C

<sup>a</sup>Reaction run 0.1M in indicated solvent; 1.0 equiv. aldehyde; 1.2 equiv. amide. <sup>b</sup>1.0 equiv.  $\text{MgSO}_4$ . <sup>c</sup>2.0 equiv.  $\text{Na}_2\text{SO}_4$ . <sup>d</sup>Reaction run 0.3 M in indicated solvent; 1.5 equiv. aldehyde; 1.0 equiv. amide; 2 equiv. acid.

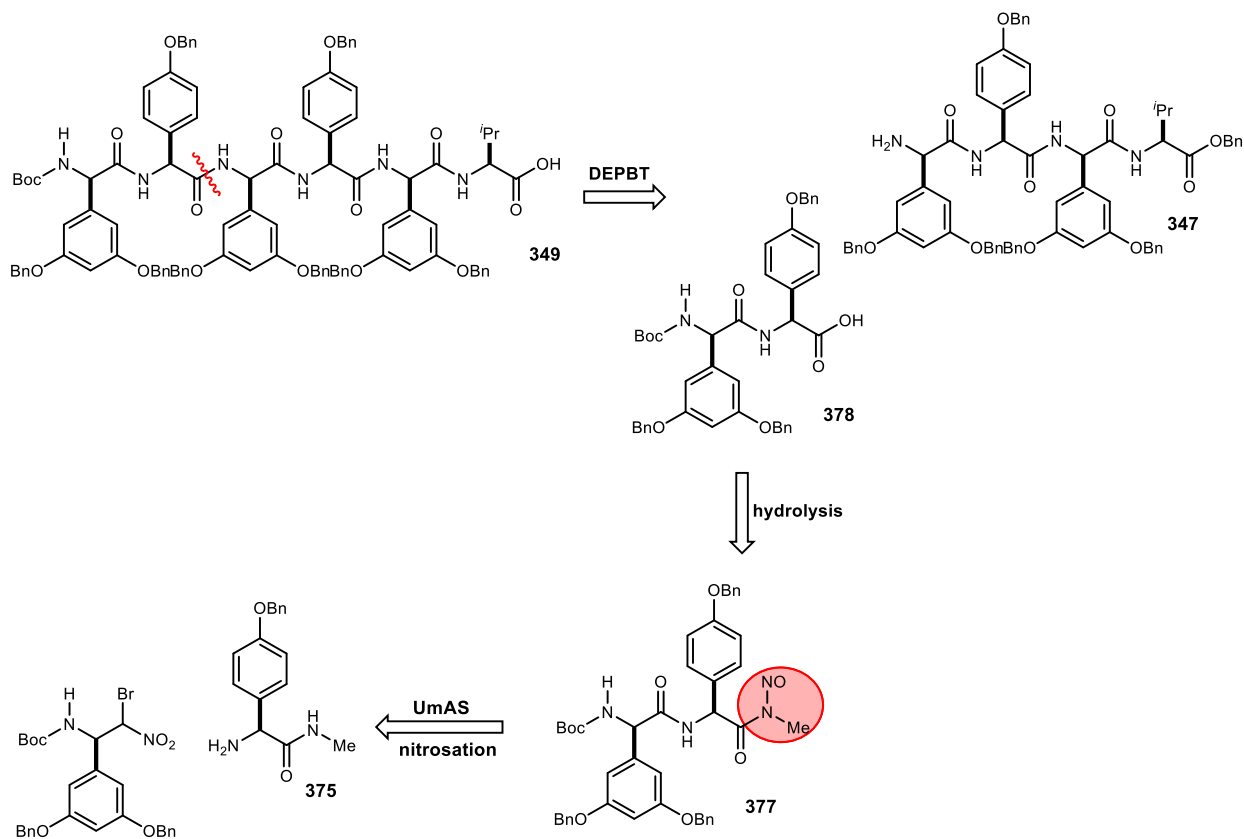


A range of solvent systems and acid sources were tried, but none were effective. Changing the temperature to help with solubility was also explored. We hypothesized that warming the reaction would improve solubility of the starting materials and help drive the reaction forward, but unfortunately, only starting materials were recovered (**Table 29**, entries 2, 5-7).

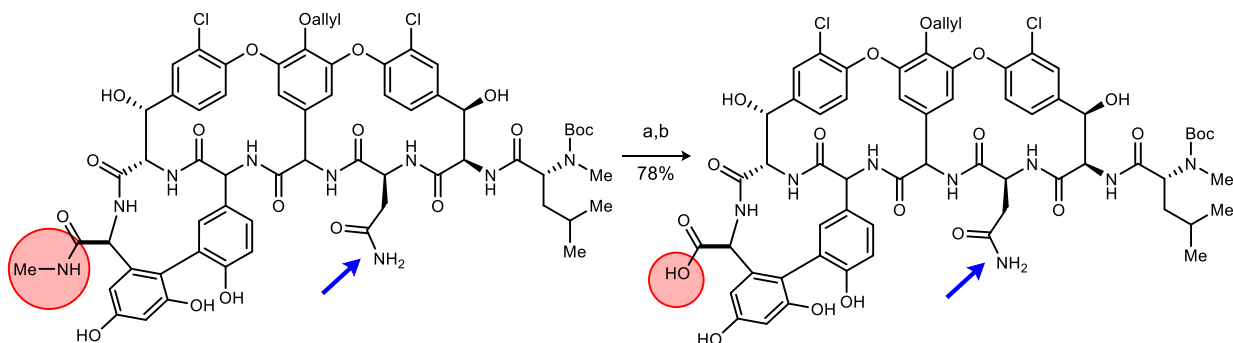
### Convergent 4+2 approach to hexapeptide 349 via DEPBT coupling

An alternate 4+2 approach was devised next and pursued with Dr. Rashanique Quarels. The disconnection would be the same one described in the previous section, but a DEPBT coupling would be used instead of UmAS to attach the fragments (**Scheme 127**).

**Scheme 127.** Revised 4+2 approach to Fragment B.



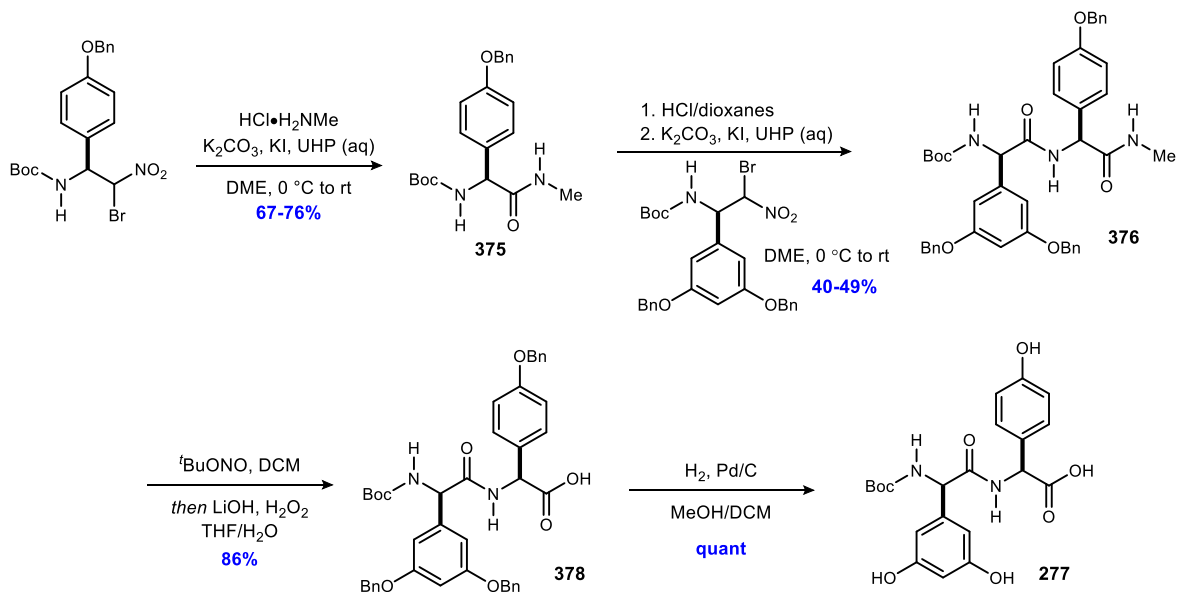
**Scheme 128.** Evans' use of an *N*-methyl amide as a masked carboxylic acid in the synthesis of vancomycin.



a)  $\text{N}_2\text{O}_4$ , NaOAc, DCM/MeCN, 0 °C; b) LiOH, 30%  $\text{H}_2\text{O}_2$ , THF/ $\text{H}_2\text{O}$ , 0 °C, 10 min;  $\text{Na}_2\text{SO}_3$ , 5 min, 0 °C

Inspiration was drawn from Evans' synthesis of vancomycin<sup>242,243</sup> (as well as later studies),<sup>244</sup> where an *N*-methyl amide served as a carboxylic acid protecting group (**Scheme 128**). They were able to selectively nitrosate and hydrolyze the *N*-methyl amide over the backbone amide nitrogens, as well as the primary amide of the asparagine residue, without epimerization.

**Scheme 129.** Masked carboxylic acid approach.



<sup>242</sup> Evans, D. A.; Wood, M. R.; Trotter, B. W.; Richardson, T. I.; Barrow, J. C.; Katz, J. L. *Angew. Chem. Int. Ed.* **1998**, *37*, 2700.

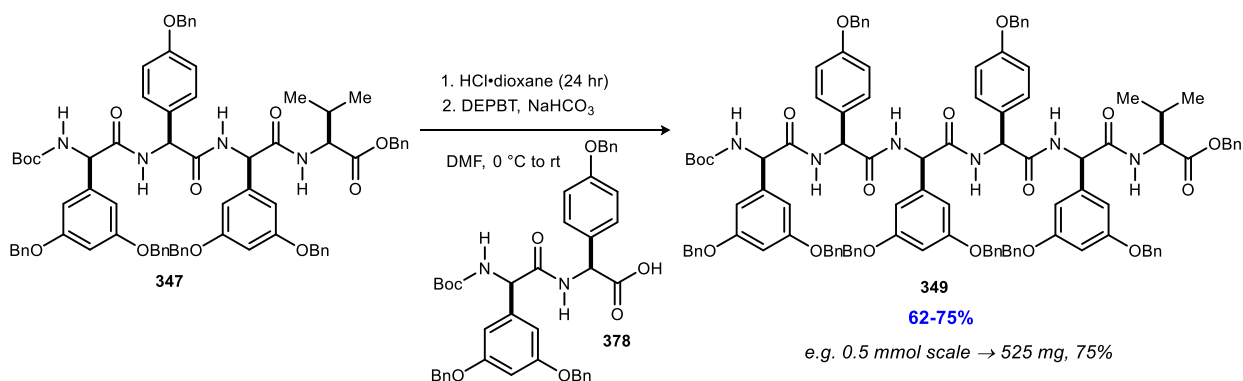
<sup>243</sup> Evans, D. A.; Carter, P. H.; Dinsmore, C. J.; Barrow, J. C.; Katz, J. L.; Kung, D. W. *Tetrahedron Lett.* **1997**, *38*, 4535.

<sup>244</sup> Yedage, S. L.; Bhanage, B. M. *J. Org. Chem.* **2017**, *82*, 5769.

This strategy was selected because it still avoids activation of the sensitive Dpg residue by using UmAS to make the core dipeptide with a C-terminal *N*-methyl amide. In the forward direction, the dipeptide **376** was synthesized by two sequential UmAS couplings using the KI/UHP protocol in good yield on multigram scale (**Scheme 129**). The masked carboxylic acid was revealed by selective *N*-nitrosation of the terminal *N*-Me amide followed by hydrolysis. Finally, hydrogenolysis proceeded with quantitative yield to afford **277**.

With the dipeptide in hand, a convergent approach to the hexapeptide was pursued (**Scheme 130**). The DEPBT coupling with **378** went well, affording the hexapeptide **349** in good yield after trituration in acetonitrile. These reactions were performed on scales up to 0.5 mmol (570 mg of tetrapeptide), with no change in yield. It should also be noted that the crude <sup>1</sup>H-NMR of these reactions were identical to those that activated the DPG carboxylic acid in a 5+1 approach, which supports our conclusion that epimerization was not observed in those reactions.

**Scheme 130.** Convergent 4+2 approach to hexapeptide **349**.



### Completion and purification of the hexapeptide central fragment of (-)-feglymycin

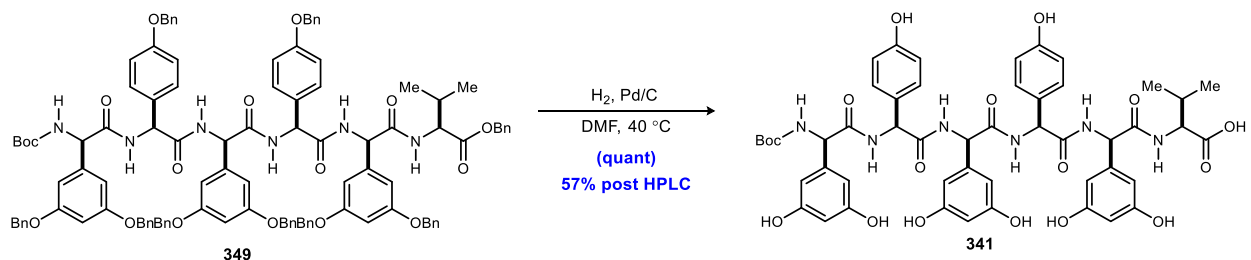
The next hurdle to be cleared was the purification of the hexapeptide. Trituration in acetonitrile followed by an additional trituration in hot methanol gave considerably clean product. However, it was important to ensure high purity of the product prior to its use in the coupling to make the decapeptide. Extensive efforts were made to further purify the fully benzyl protected hexapeptide. Most recrystallization attempts were not successful due to the poor solubility of the compound in many organic solvents (MeOH, EtOH, EtOAc, DCM etc.). When solvents such as DMSO or DMF (with or without co-solvents) were used, some precipitation was observed and only product

collection using nylon or PTFE filters with <15  $\mu\text{M}$  pore size was effective. This protocol was simply not practical on scales >100 mg.

Preparative HPLC was also extensively examined as a means to purify the benzyl protected hexapeptide, but again, the poor solubility caused many problems. Even if DMSO was used as the loading solvent, the product would precipitate throughout the run, causing material to accumulate in the injection loop, on the guard column, and within the C18 column. Manual injection using a variety of solvent systems was explored but did not provide any improvements. Peak shape was often broad, and blank runs would be needed to remove the material completely from the column.

The poor solubility of the hexapeptide could be attributed to the numerous benzyl-protecting groups and thus the hexapeptide was purified after hydrogenolysis. The hydrogenolysis itself was not entirely straightforward, again due to poor solubility. Many solvents and solvent combinations were explored, but ultimately DMF was used. A heat gun was used to get the starting material mostly solubilized in DMF prior to the hydrogenolysis, which was conducted overnight at 40  $^{\circ}\text{C}$ . Since the product was soluble in DMF, the reaction moved forward and went to completion (**Scheme 131**). Initially however, we were unsure of the product's solubility profile, and used DMF to pack the Celite pad that would be used to remove the palladium catalyst. A significant drawback to this was that the DMF would cause palladium black to advance through the Celite with the product. The presence of palladium black posed a problem for purification by HPLC as metal catalysts can clog the guard column and decrease the lifetime of the C18 column. Ultimately, as material was moved forward, the hydrogenolysis was run on scales large enough to produce sufficient quantities of product for solubility studies. The product was soluble in methanol, which became the solvent used to pack and wash the Celite pad. This significantly limited the amount of DMF and palladium black in the filtrate. Ultimately, this provided the hexapeptide for the first time in our laboratory in quantitative yield (although this yield was diminished by HPLC purification) (**Scheme 131**)

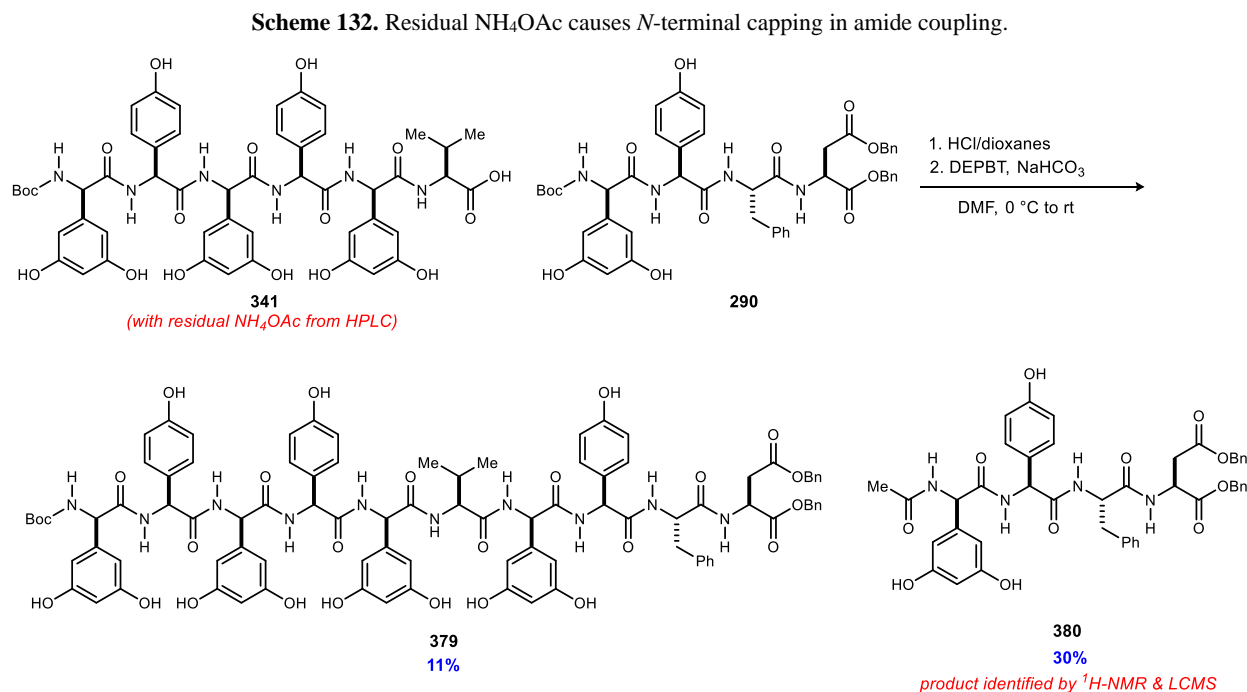
**Scheme 131.** Hydrogenolysis of hexapeptide 349 affords Fragment B.



When the fully benzyl deprotected hexapeptide was purified by preparative HPLC, it was initially injected using DMSO. This, however, caused some of the partially water-soluble product to elute in the solvent front. This would require that the fractions from the solvent front be collected, concentrated, and re-injected, thus reducing the yield. However, when methanol was used to load the compound, the material would be lost to the HPLC, and less than 20% of the product was isolated on several occasions. All fractions and waste were collected and concentrated, but the expected amount of product was not present. It was also not present in the guard column. Presumably, injections using methanol caused precipitation of the product to the extent that it eluted so slowly over time that it was not detected by UV. Ultimately, we stuck with DMSO as the loading solvent since it gave the best recovery of product.

Another aspect of HPLC purification that needed to be addressed was the buffer system. Considering that the product is partially water soluble, it could not be extracted from the HPLC fractions, and thus those fractions would need to be concentrated. This requires heating to remove the water. If 0.1% TFA in acetonitrile/water was used, sharp peaks were observed, but so was Boc-deprotection after concentration. Eventually ammonium acetate was found to be sufficient for good separation and peak shape. However, ammonium acetate was, in our hands, not removable by standard hi-vacuum. It was later found that small amounts of ammonium acetate could be removed by repeated over-night lyophilization, but a more practical approach was desired. In the end, purification needs were met with the use of size exclusion chromatography (gel permeation chromatography). Using Sephadex LH-20 gel, the product (MW = 1011) was easily separated from ammonium acetate (MW = 77). This step was crucial for the success of the next coupling, as evidenced by the reaction shown in **Scheme 132**. When the ammonium acetate was not completely

removed from the hexapeptide, it caused significant capping of the amine nucleophile **290** in the DEPBT coupling to make the decapeptide **379** (**Scheme 132**, 30%).



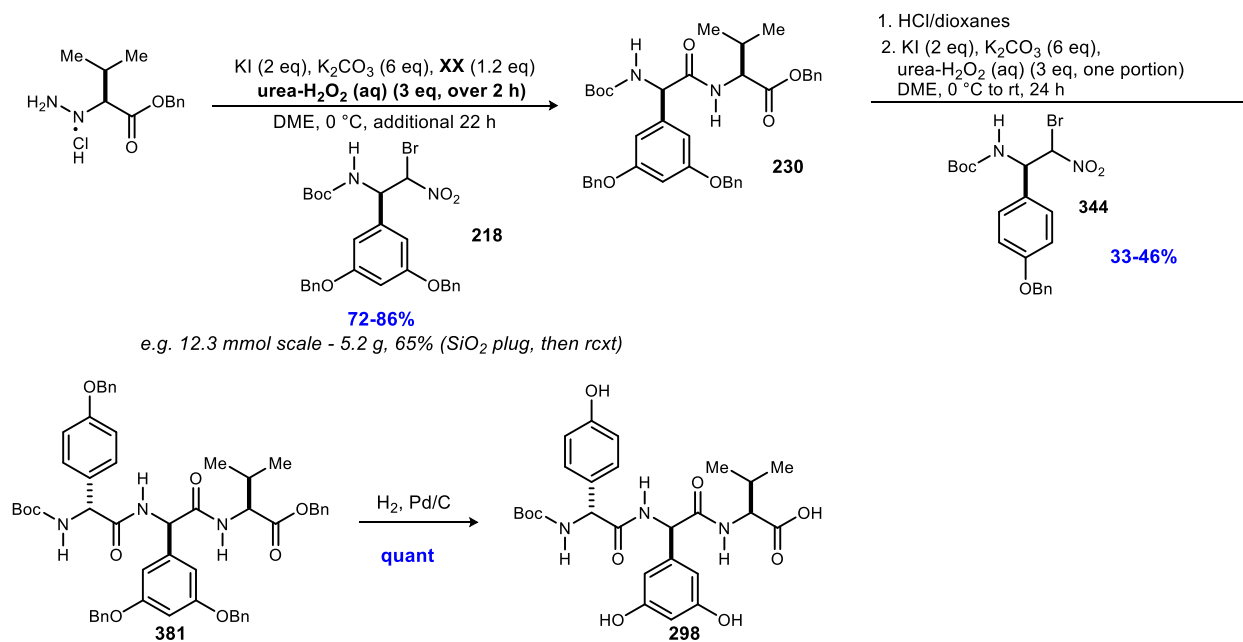
To summarize, trituration was the only suitable purification method for the poorly soluble, fully benzyl-protected hexapeptide **341**. **Gratifyingly, hydrogenation in warm DMF provided the desired Fragment B for the first time in our laboratory!** Purification of the hexapeptide was performed using preparatory HPLC with an ammonium acetate buffer, followed by size-exclusion chromatography to remove residual acetate. It was later found that formic acid could also be used as a buffer in HPLC, with no detectable Boc-deprotection, but size-exclusion would still be needed to remove residual formic acid prior to the next coupling.

### 3.2.4 Synthesis of Fragment A

The synthesis of Fragment A began in the same manner as that for Fragment B. Thus, the coupling of valine and the  $\alpha$ -bromo nitroalkane **218** using the KI/UHP protocol provided the dipeptide in good yield (**Scheme 133**). The UmAS reaction with the D-Hpg donor **344** was significantly lower yielding than the identical reaction with the L-enantiomer (33-46% vs 59-73%). This phenomenon was previously observed when the NIS conditions were used for UmAS.<sup>229</sup> It has been

hypothesized that the configuration of the residue is responsible for the decrease in yield, as this has been a consistent observation by several scientists using multiple stock sources of bromonitroalkane.<sup>229</sup> The hydrogenation of the tripeptide **381** proceeded uneventfully, revealing the carboxylic acid **298** in quantitative yield.

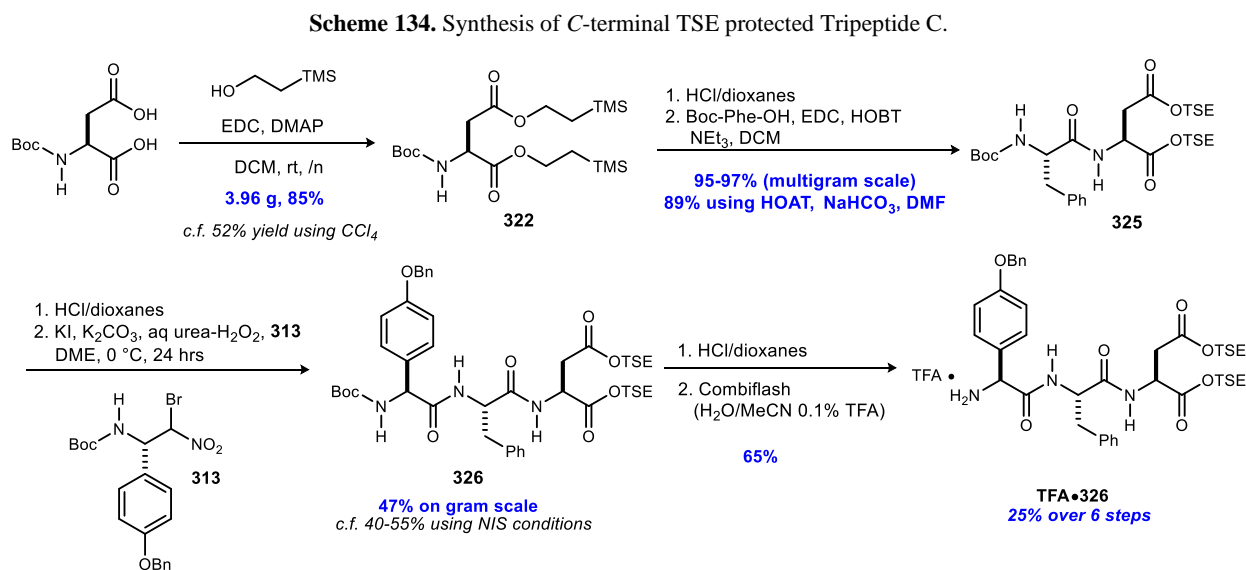
**Scheme 133.** Synthesis of Fragment A.



### 3.2.5 Synthesis of Fragment C & Endgame Strategies

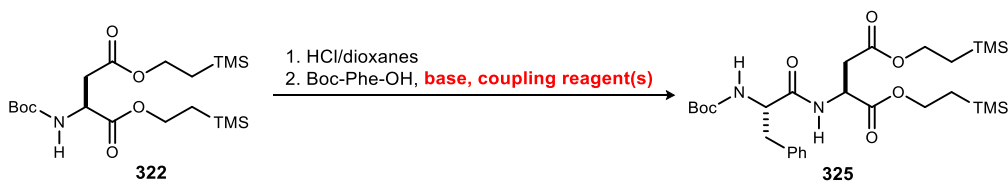
#### Synthesis of Fragment C with C-terminal TSE protecting groups

The synthesis of Fragment C was modeled after the route used for Ffeglymycin, with some modifications that improved the yield of the Steglich esterification, and decreased epimerization during the conventional amide coupling of Boc-Phe to Asp-OTSE. The synthesis began with the Steglich esterification of *N*-Boc aspartic acid, to provide **322**, which proceeded in good yield on gram scale. It was found that a change in solvent from CCl<sub>4</sub> to DCM significantly improved yields (52 vs 85%, **Scheme 134**). Conventional amide coupling to phenyl alanine was carried out next, at which point some epimerization at the  $\alpha$ -position of phenyl alanine was observed by <sup>1</sup>H-NMR. A survey of conditions was performed to determine the best conditions for this coupling (**Table 30**).



As shown in **Table 30** standard conditions for EDC coupling resulted in some epimerization yielding a 7:1 d.r. (**Table 30**, entry 1). Interestingly, the time at which the base was added had a significant effect on the d.r. When triethylamine was added before the amine coupling partner, the d.r. decreased to 3:1 (**Table 30**, entry 2). Changing to a milder base (NaHCO<sub>3</sub>) and HOAt (instead of HOBT) resulted in worse d.r. when run at room temperature (2:1, **Table 30**, entry 3). However, maintaining the reaction at 0 °C improved the d.r. to 9:1 (**Table 30**, entry 4). Using PyBOP or



**Table 30.** Epimerization studies for dipeptide **325**.

entry	base	coupling reagent(s)	d.r. <sup>a</sup>
1 <sup>b,c</sup>	NEt <sub>3</sub>	EDC, HOBT	7:1
2 <sup>b,d</sup>	NEt <sub>3</sub>	EDC, HOBT	3:1
3 <sup>e</sup>	NaHCO <sub>3</sub>	EDC, HOAT	2:1
4 <sup>f</sup>	NaHCO <sub>3</sub>	EDC, HOAT	9:1
5 <sup>g</sup>	DIPEA	PyBOP	5.7:1
6 <sup>g</sup>	DIPEA	PyBrOP	5.1:1
7 <sup>h</sup>	NaHCO <sub>3</sub>	DEPBT	5.9:1

<sup>a</sup>Diastereomeric ratio determined by <sup>1</sup>H-NMR integration in comparison to authentic samples. <sup>b</sup>Reaction run 0.06 M in dry DCM using 1.05 equiv. Boc-Phe-OH, 1.05 equiv. EDC, 1.1 equiv. HOBT, and 2.1 equiv. NEt<sub>3</sub>, room temperature in dry DCM (0.06 M). <sup>c</sup>NEt<sub>3</sub> added after HCl-322. <sup>d</sup>NEt<sub>3</sub> added before HCl-XX. <sup>e</sup>1.0 equiv. Boc-Phe-OH, 1.2 equiv. EDC, 1.2 equiv. HOAT, 1.0 equiv. NaHCO<sub>3</sub>, 0 °C to room temp in DMF (0.25 M). <sup>f</sup>1.0 equiv. Boc-Phe-OH, 1.2 equiv. EDC, 1.2 equiv. HOAT, 1.0 equiv. NaHCO<sub>3</sub>, 0 °C in DMF (0.25 M). <sup>g</sup>1.0 equiv. Boc-Phe-OH, 1.5 equiv. coupling reagent, 3.0 equiv. base, 0 °C to room temperature in DCM (0.1 M). <sup>h</sup>1.1 equiv. Boc-Asp-OTSE, 1.5 equiv. coupling reagent, 2.0 equiv. base, 0 °C to room temperature in DMF (0.05 M).

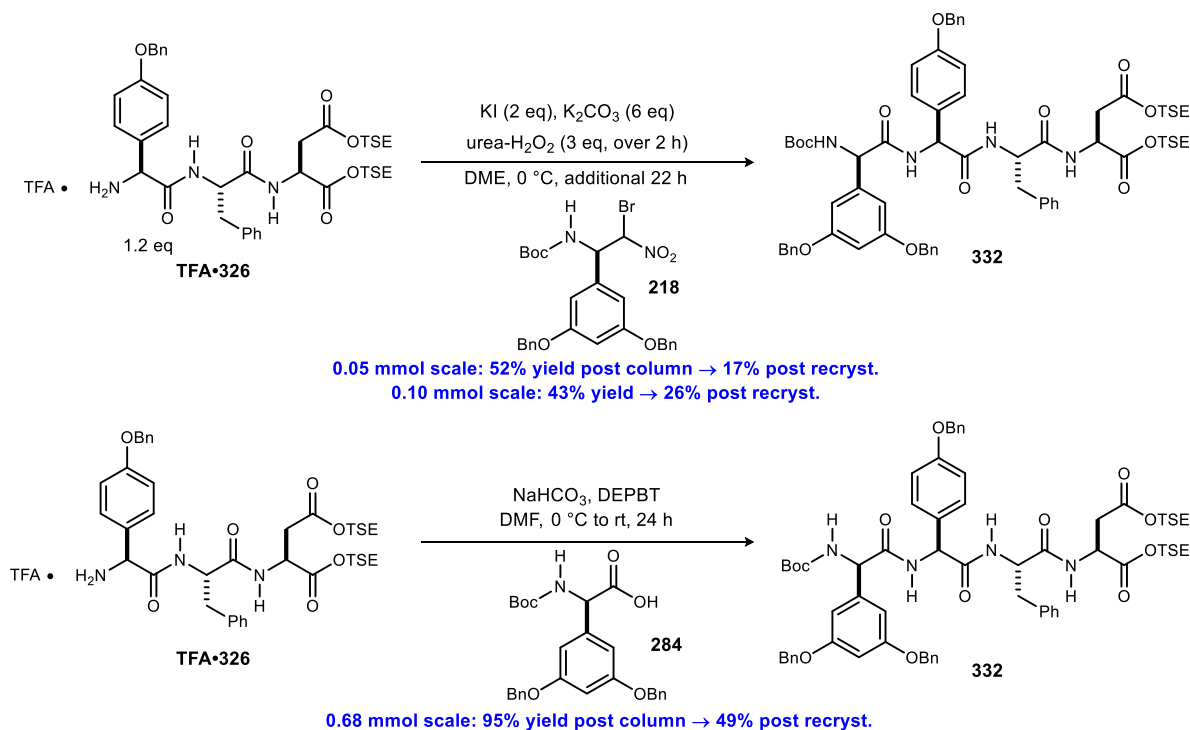
PyBrOP, which are known to work well for sterically hindered *N*-methyl amides,<sup>245</sup> did not provide a significant improvement (**Table 30**, entries 5-6). DEPBT was also examined as the coupling reagent, given its success with very epimerization-prone residues,<sup>224</sup> and to our surprise this reagent did not perform well either (**Table 30**, entry 7). Ultimately, the conditions from entry 1 or entry 4 were used to make this substrate and carry the mixture of diastereomers into the next coupling. The resultant tripeptide was *N*-Boc deprotected and purified by preparative HPLC, separating it from any other diastereomers (**Scheme 134**).

With the dipeptide in hand, the aryl glycine equivalent was coupled. In this case, both the UHP/KI protocol, as well as the NIS protocol, worked equally well to afford the tripeptide in 40-55% yield (**Scheme 134**). The synthesis of the tetrapeptide worked best if the *N*-Boc deprotected tripeptide was purified. This also ensured that a single diastereomer was carried forward.

<sup>245</sup> Coste, J. J., P In *Encyclopedia of Reagents for Organic Synthesis* 2003.; Albericio, F. K., S.A. In *Encyclopedia of Reagents for Organic Synthesis* 2001. ;Coste, J.; Frerot, E.; Jouin, P. *J. Org. Chem.* **1994**, *59*, 2437.

Thus, the HCl salt was purified by reversed phase chromatography. It is important to note here that the fractions from this purification must be concentrated immediately to avoid partial or full TSE deprotection. Finally, the benzyl protected DPG residue could be incorporated. Using the KI/UHP protocol, we witnessed the first successful incorporation into this fragment using UmAS. However, while this reaction was reasonable on small scale, efficient stirring became an issue upon scale up. **Scheme 135** demonstrates the difference in yield between using UmAS or DEPBT to synthesize tetrapeptide C. In this case, DEPBT coupling of the amino acid proved superior with higher yields and cleaner reaction profiles to afford **332**. Ultimately, DEPBT coupling was used when this

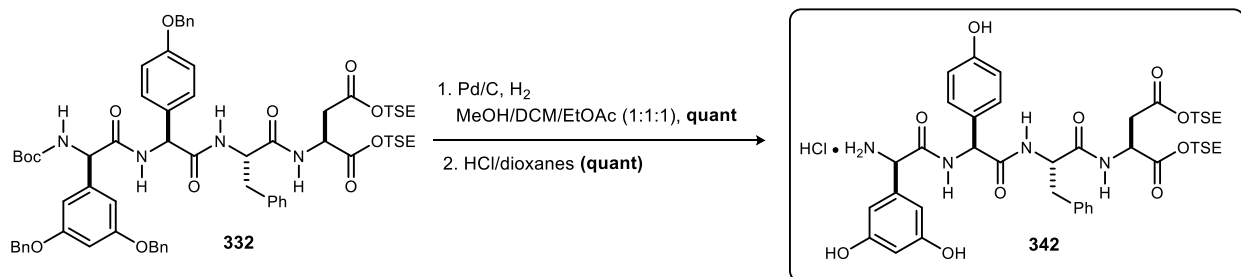
**Scheme 135.** Comparison of UmAS and DEPBT couplings to complete Fragment C.



fragment needed to be made on scale, taking advantage of the solubilizing power of DMF.

Finally, the tetrapeptide **332** was benzyl- and Boc-deprotected to afford **342-HCl** (**Scheme 136**). In this case, care must be taken to closely monitor the *N*-Boc deprotection to avoid premature TSE removal or protodesilylation.

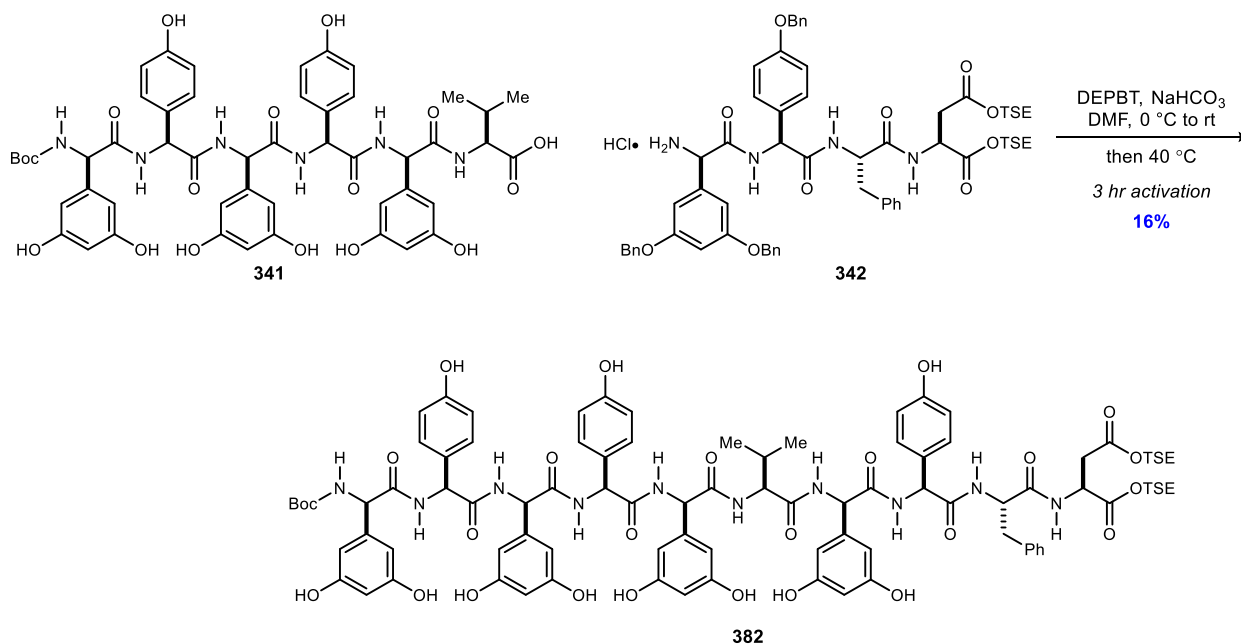
**Scheme 136.** *N*-terminal deprotection of TSE-protected tetrapeptide **332**.



### Endgame attempts using *C*-terminal TSE protecting groups

The ability of the TSE protected tetrapeptide **342** to react with the hexapeptide **341** acid was next tested. It was found that using a 3 hour acid activation at 0 °C, then warming the reaction first to room temperature and then to 40 °C to improve homogeneity, provided our best results (16% yield,

**Scheme 137.** Synthesis of *C*-terminal TSE protected decapeptide **382**.



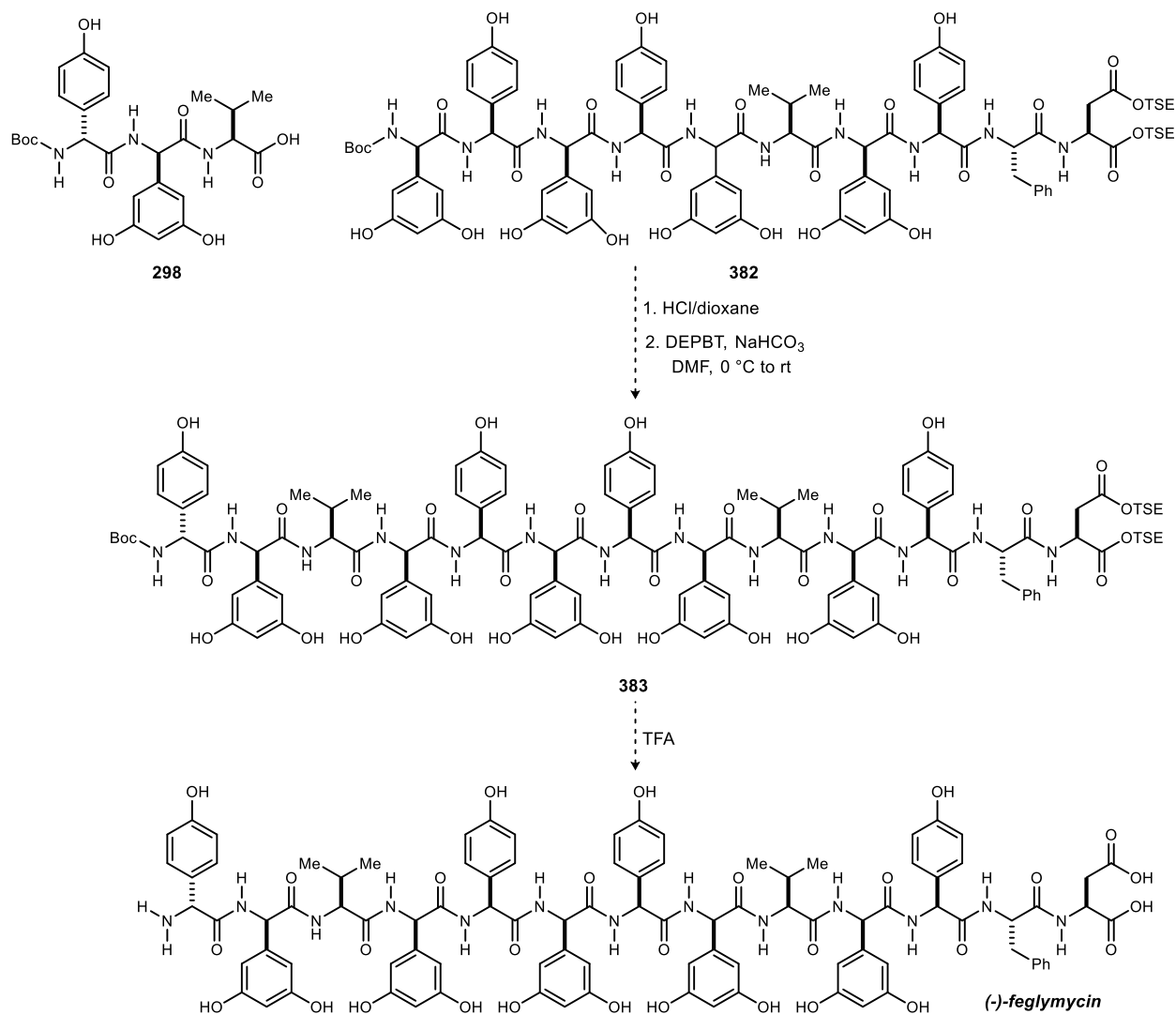
### **Scheme 137).**

We then explored the use of this substrate to make the desired tridecapeptide **383** (**Scheme 138**). During our first attempt, the decapeptide **382** was stirred in HCl/dioxanes for 5 hours, but only

partial deprotection was observed by  $^1\text{H-NMR}$ . A precipitate formed after an additional 5 hours in  $\text{HCl/dioxanes}$ , at which point the material was carried forward into the coupling. Attempts to purify the crude reaction mixture by HPLC were unsuccessful. All attempts gave an extremely broad ( $>2$  minutes) peak. Further purification by size exclusion chromatography was pursued, along with a second round of HPLC, but whether product was present in any of the resultant fractions was unclear due to very broad  $^1\text{H-NMR}$  spectra. A second pursuit began with an overnight Boc deprotection of the decapeptide, which was deemed complete by  $^1\text{H-NMR}$  analysis. In that spectrum, the TSE group appeared in-tact given the integration relative to valine, however there were also signs of decomposition. Nevertheless, the material was taken forward. Again, HPLC purification was attempted, but the peaks were very broad in both the HPLC trace and the resulting  $^1\text{H-NMR}$  spectra of the isolated fractions.

Ultimately, we were unable to recover sufficient amounts of starting materials from the tridecapeptide or decapeptide reactions, which posed a problem this late in the synthesis. At this point, evidence was accumulating that the TSE group was a liability. Desilylated and

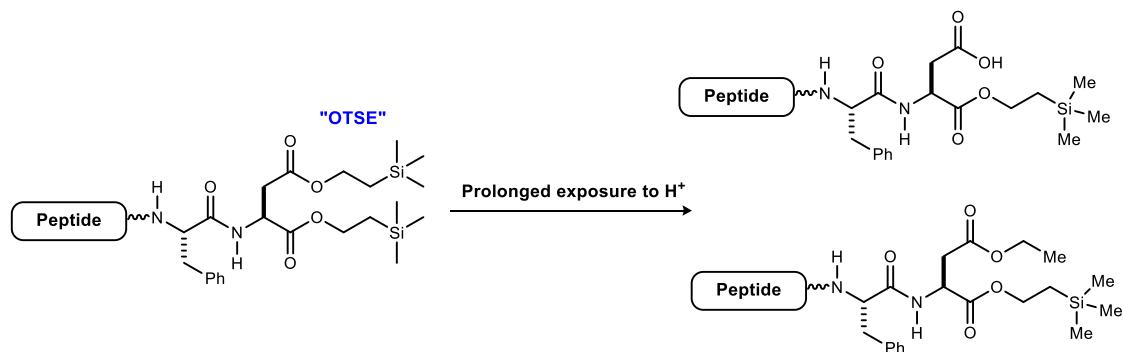
**Scheme 138.** Endgame strategy with C-terminal TSE protecting groups.



protodesilylated materials were identified during Boc deprotection, and during HPLC purification if the compounds were in eluent with 0.1% TFA for extended periods of time (**Figure 38**). These phenomena were inconsistent, and experimental reproducibility suffered. Therefore, this C-terminal protecting group was abandoned for future endeavors. It could however still prove useful

in an alternative retrosynthetic approach, wherein Fragment C is coupled last to the nonapeptide AB.

**Figure 38.** Deprotection and protodesilylation of TSE protecting group.



Products shown represent two of four possible constitutional isomers. The connectivity has not been defined in the isolated products.

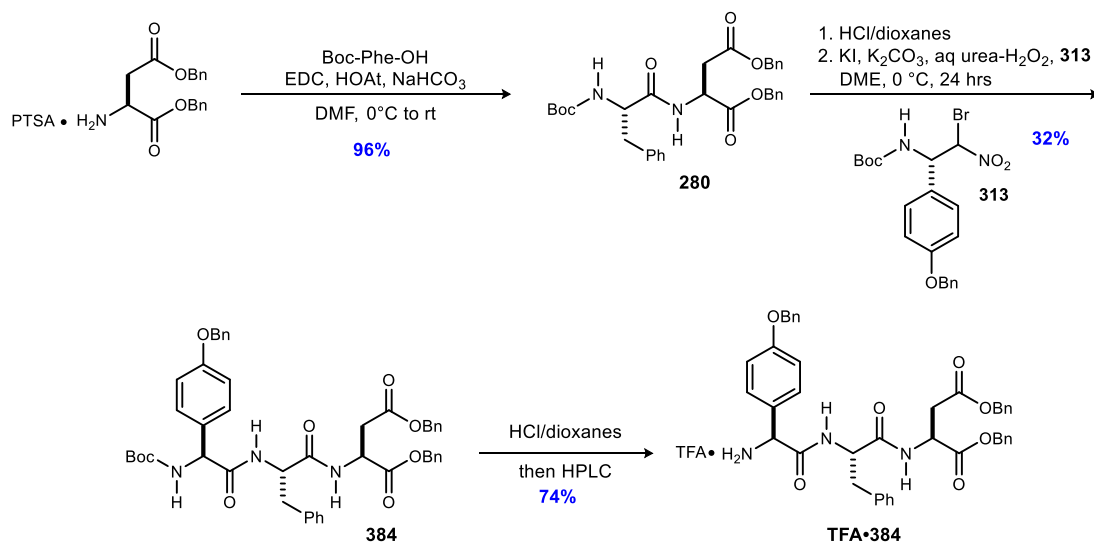
### Synthesis of Fragment C with C-terminal benzyl protecting groups

Given the observed instability of the TSE groups, we sought a more stable and robust C-terminal protecting group. Feglymycin presents a unique challenge for C-terminal protection, as the terminal residue is an aspartic acid. Thus, the approach used not only has to consider protecting group orthogonality and stability in the proposed reaction conditions, but also undesired hydrolysis, and aspartimide formation.<sup>246</sup> To this end, our laboratory has previously explored the use of *t*-butyl esters, and while the tetrapeptide was synthesized, the route took a significant hit in yield early on with the synthesis of the *t*-butyl protected aspartic acid (34%).<sup>179</sup> This was a contributing factor to why a change to TSE protecting groups was originally pursued.<sup>184</sup> Ultimately, benzyl protecting groups were selected for this revised route.

<sup>246</sup> Tam, J. P. R., M.W.; Merrifield, R.B. *Pept. Res.* **1988**, *1*, 6. Mergler, M.; Dick, F.; Sax, B.; Weiler, P.; Vorherr, T. *J. Pept. Sci.* **2003**, *9*, 36.

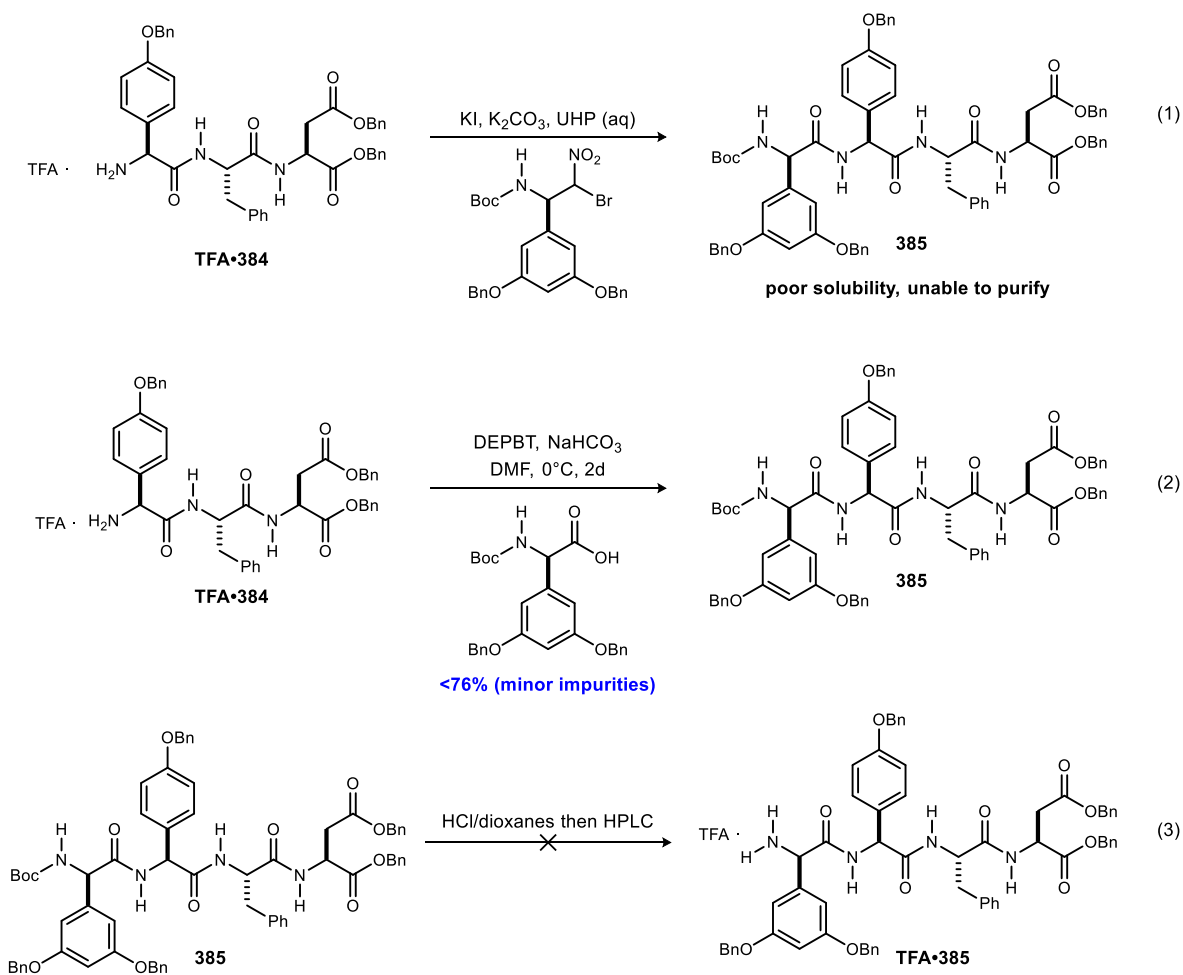
To this end, the coupling of benzyl protected aspartic acid to *N*-Boc phenylalanine was clean and high yielding (**Scheme 139**). The next UmAS reaction proceeded in reasonable yield to give the tripeptide **384**, and given our laboratory's previous experiences with the subsequent coupling, the tripeptide was purified by HPLC prior to homologation (**Scheme 139**)<sup>179,183</sup> Unfortunately, the UmAS reaction to make the tetrapeptide **385** presented some difficulties. The product was unable to be purified from the UmAS approach. It has very poor solubility, and the presence of other impurities made purification by recrystallization difficult (**Scheme 140**, eq 1). The DEPBT coupling approach was effective, but due to the poor solubility of the product, it could only be purified by recrystallization or trituration and removal of minor impurities was difficult (**Scheme 140**, eq 2). *N*-Boc deprotection followed by purification of the HCl salt by HPLC was also

**Scheme 139.** Toward the synthesis of C-terminal benzyl protected Fragment C.



attempted, but it was unsuccessful.

**Scheme 140.** Solubility issues in synthesis of fully benzyl protected Fragment C.

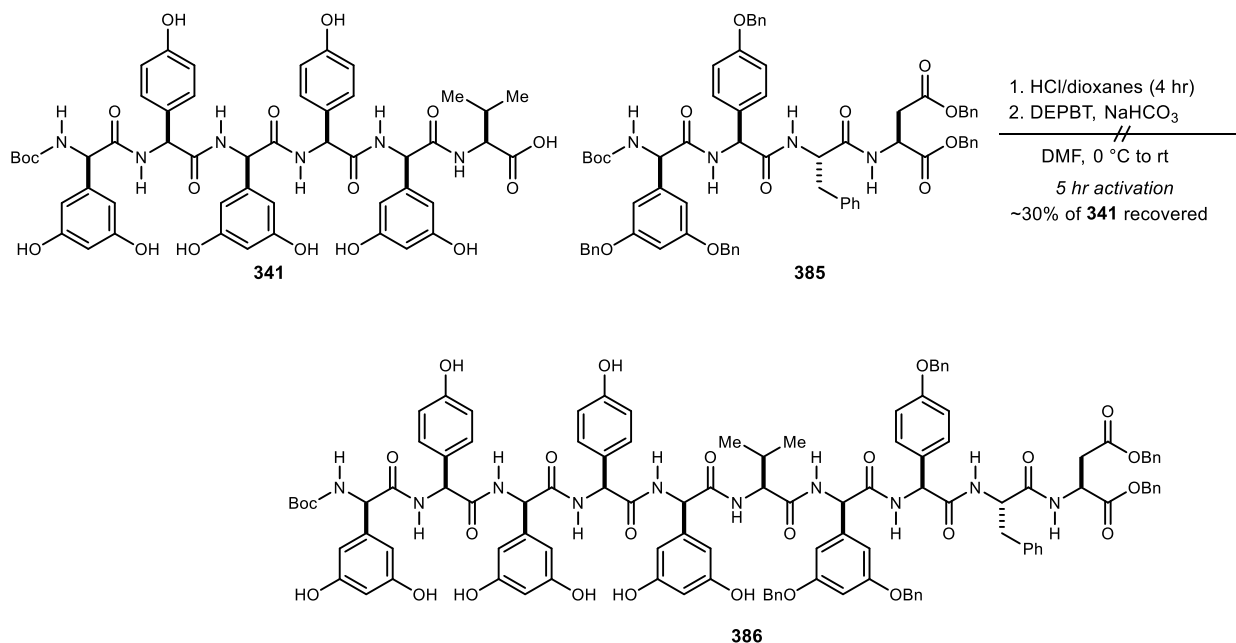




## Endgame attempt using C-terminal benzyl protecting groups

The synthesis of the decapeptide **386** was attempted using the C-terminal tetrapeptide from the DEPBT coupling above (**Scheme 140**, eq 2), but this did not work and most of the starting materials were recovered (**Scheme 141**). It was hypothesized that the poor solubility in conjunction with the steric hindrance caused by the Dpg and Hpg benzyl protecting groups, significantly retarded the nucleophilicity of tetrapeptide **385** and caused the slow reaction rate.

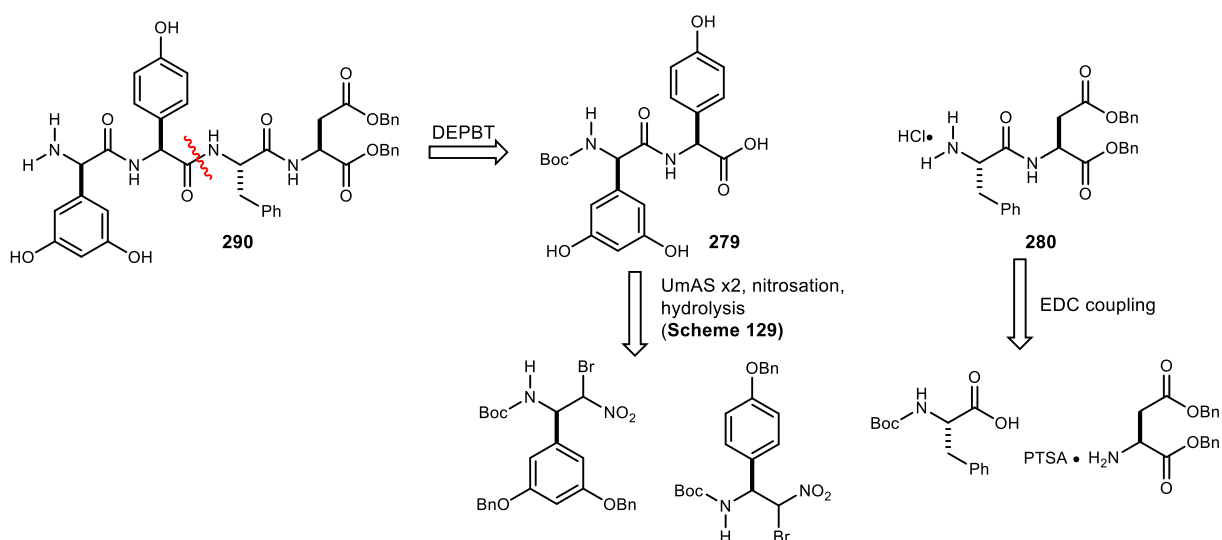
**Scheme 141.** Attempt to synthesize decapeptide **386**.



## Second generation synthesis of Fragment C with C-terminal benzyl protecting groups

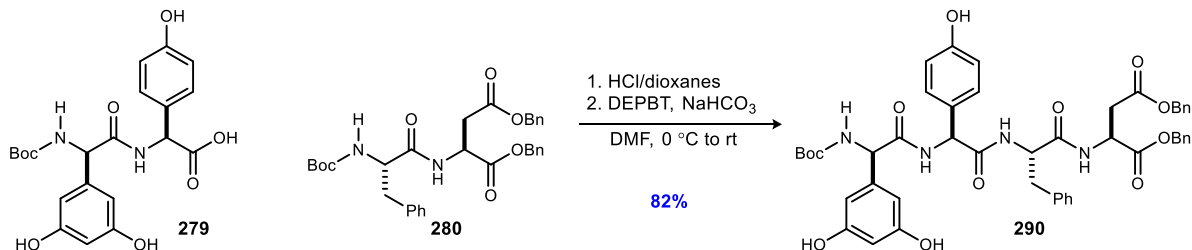
At this point it was evident that the fully benzyl protected tetrapeptide C **385** was not going to be our way forward. It was desirable to keep the benzyl ester protected aspartic acid residue because of its stability and orthogonality to the *N*-terminal protecting group. However, the solubility issues caused by so many benzyl groups was an inherent disadvantage. Free phenols can be tolerated in UmAS, but usually at the expense of reaction yield. To this end, the strategy illustrated in **Figure 39** was used to incorporate the Dpg and Hpg residues as free phenols while keeping the aspartic acid benzyl protected. The dipeptide **279** could be accessed from bromonitroalkanes via the route previously described in **Scheme 129**, and the dipeptide **280** could be made via EDC coupling of the amino acids.

**Figure 39.** Revised retrosynthesis for C-terminal benzyl protected Fragment C.



In the forward fashion, this provided the tetrapeptide **290** in 81% yield. Interestingly, this was one of the few cases where pre-activation of the acid decreased the yield of the reaction (40% vs 81%). Alternatively, this tetrapeptide could be accessed by iterative DEPBT couplings as demonstrated by Süssmuth (see **Süssmuth's synthesis of feglymycin: Scheme 96**), however it would be beneficial to keep the condensative couplings at Dpg residues to a minimum to avoid epimerization.

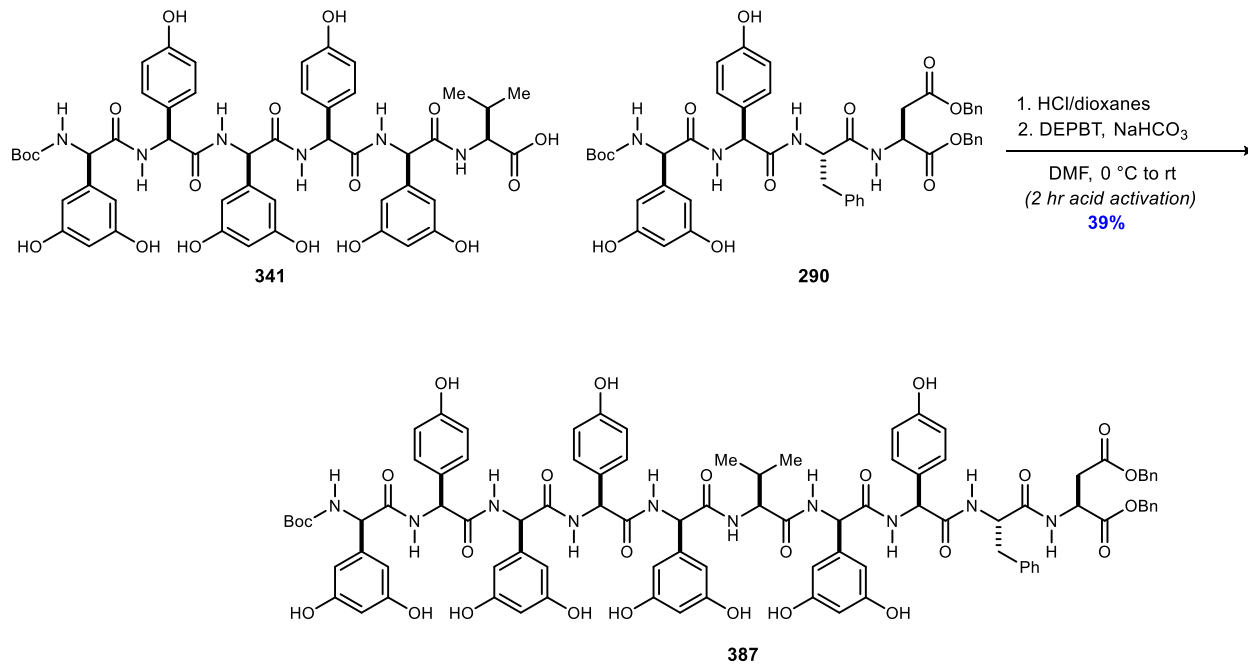
**Scheme 142.** 2+2 amide coupling to synthesize *C*-terminal tetrapeptide **290**.



## Second generation endgame attempts using *C*-terminal benzyl protecting groups

With the desired tetrapeptide in hand, its performance in decapeptide formation was tested. Gratifyingly, with a two-hour activation of the acid, the coupling proceeded with 39% yield. It is worthwhile to note that running the reaction without pre-activation provided <21% yield. These reactions are purified by preparative HPLC and selection of the proper buffer system was crucial for good peak shape and recovery of material. When using 0.1% TFA, sharp peaks were observed but *N*-Boc deprotection prevented adequate recovery of the hexapeptide **341**. Switching to the more basic 0.1% NH<sub>4</sub>OAc system left all of the compounds in tact at the expense of peak shape. Excessive broadening that prevented proper recovery of product was observed. Finally, using 0.1%

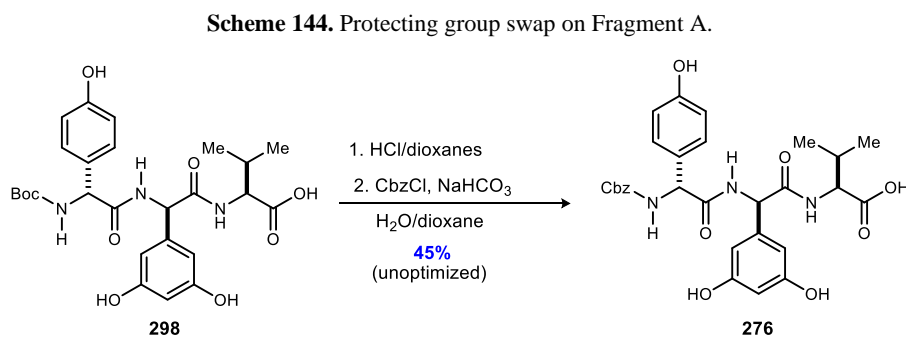
**Scheme 143.** Synthesis of *C*-terminal benzyl protected decapeptide **387**.



formic acid proved best, providing the better peak shape observed with TFA, without any of the undesired *N*-Boc deprotection.

### 3.2.6 Completion of the formal synthesis of (-)-feglymycin

In this approach the *N*-Boc group on Fragment A was changed to a Cbz group for two main reasons: 1) Cbz and *C*-terminal benzyl groups can be removed simultaneously, saving a synthetic step and 2) Süssmuth reported that all attempts to Boc deprotect the tridecapeptide resulted in decomposition of the material.<sup>206</sup> We also observed decomposition during Boc deprotection attempts of the tridecapeptide. For ease of immediate access, tripeptide A was *N*-Boc deprotected, and then *N*-Cbz protected as outlined in **Scheme 144**. Future studies could focus on a protecting

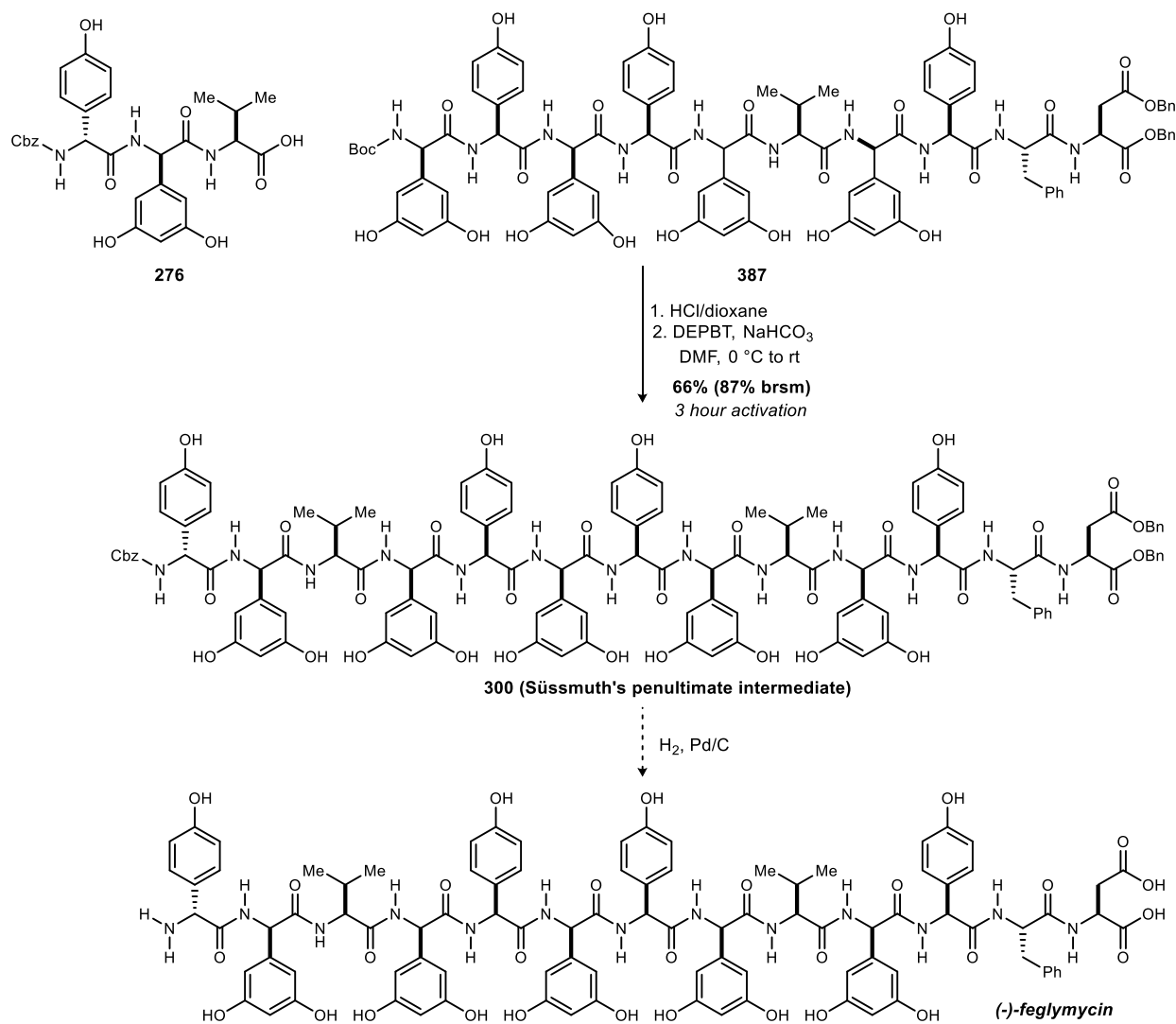


group strategy that would allow for direct access to this fragment without having to do a protecting group swap.

Given Süssmuth's and our joint experience of decomposition during Boc deprotection at the tridecapeptide stage, the Boc deprotection of the decapeptide **387** only ran for one hour. The tripeptide Cbz-**276** was activated for 3 hours at 0 °C before the amine was added, and the reaction was kept cold for 24 hours, then warmed to room temperature for an additional 48 hours. This crude mixture was first subjected to size exclusion chromatography, and LCMS analysis of the fractions showed some promising peaks. The material was further purified by preparative HPLC and ultimately matched Süssmuth's penultimate intermediate, thus completing the formal synthesis of feglymycin. However, the amount of material recovered post-HPLC was minimal (<1 mg). Another reaction was conducted, and the material was again purified by size-exclusion

chromatography, this time taking smaller fraction. This provided pure tridecapeptide in an isolated 66% yield (87% brsm). *The analytical data for the isolated material matched Süßmuth's penultimate material, thus completing the formal synthesis of (-)-feglymycin!* The compound remains to be fully deprotected, which will afford our target, (-)-feglymycin. Preliminary studies on the final deprotection have indicated the presence of (-)-feglymycin by  $^1\text{H-NMR}$ , but at the time of submission of this dissertation, the target remains to be purified and characterized.

**Scheme 145.** Completion of the formal synthesis of (-)-feglymycin.



### 3.2.7 Feglymycin formal synthesis: summary & comparison of final routes

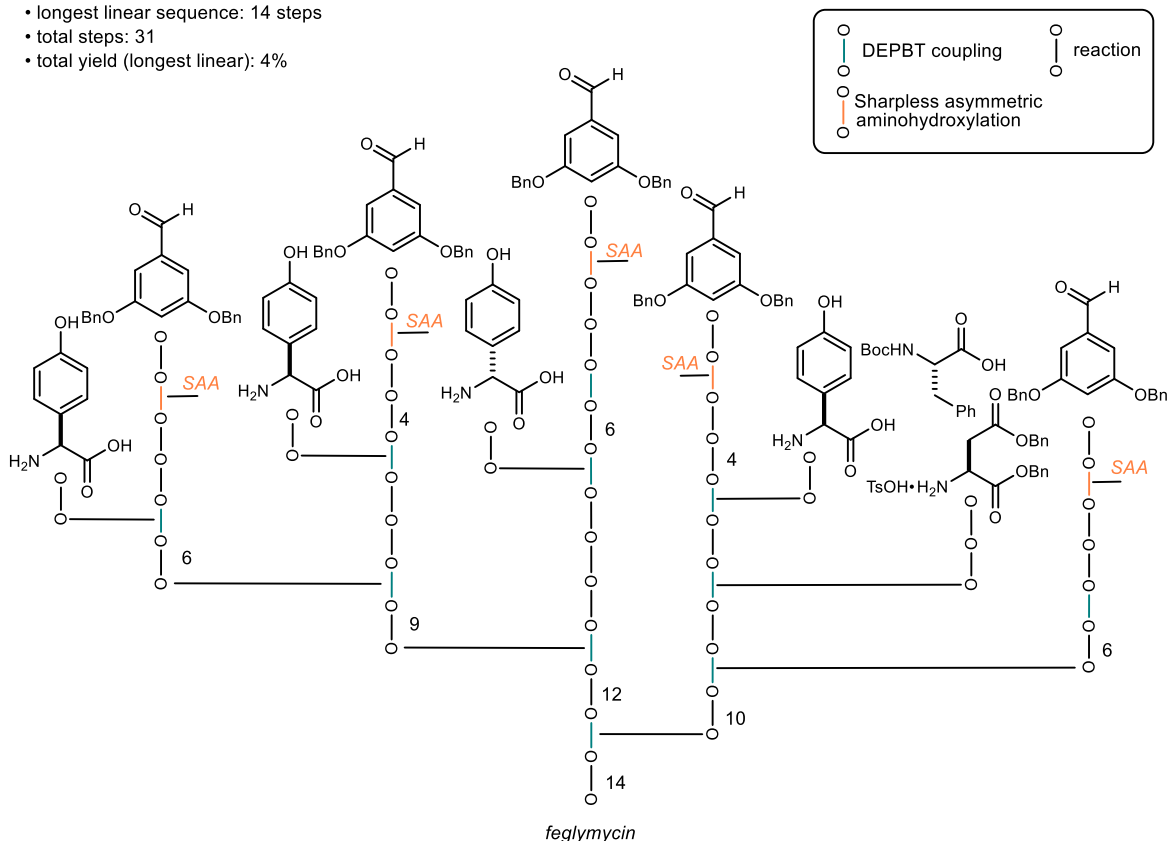
Completing the formal synthesis of (-)-feglymycin was the result of a long-lived collaborative effort that spanned the course of a decade. Consequently, the synthetic route has seen many iterations and re-writes. This section will serve to summarize only the routes that resulted in the formal synthesis of (-)-feglymycin, though it should be noted that each of these pursuits builds on many partial syntheses, as well as the total synthesis of Ffeglymycin.

To date there have been two total syntheses of feglymycin prior to the efforts described herein. Süssmuth's synthesis is summarized in **Scheme 146**.<sup>206</sup> The stereochemistry of the Dpg amino acids was established using the Sharpless asymmetric aminohydroxylation, and the peptide backbone was stitched together primarily with the use of DEPBT as a coupling reagent. DEPBT

**Scheme 146.** Süssmuth's total synthesis diagram.

#### Süssmuth's Synthesis of Feglymycin

- longest linear sequence: 14 steps
- total steps: 31
- total yield (longest linear): 4%



worked particularly well to suppress racemization of Dpg residues during condensative coupling.



tridecapeptide. This was deprotected to afford (-)-feglymycin with a longest linear sequence of 14 steps. Their publication does not describe the preparation of *N*-Alloc-protected Dpg residues, or of the protected Hpg residues, and therefore the total step count cannot be determined. The longest linear sequence and associated total yield is described as starting from the Hpg methyl ester, though it would necessarily be longer, and the total yield would be lower, if the synthesis of the Dpg residue was included. To this end, this synthesis produced (-)-feglymycin in 0.5% overall yield, if it is based on a 14 LLS from the Hpg methyl ester.

We have completed three formal syntheses of (-)-feglymycin, which have been deemed the first-generation (**Scheme 148**), second-generation (**Scheme 149**), and third-generation (**Scheme 150**) approaches. Common to all three of the formal syntheses are the syntheses of Fragments A and C. Fragment A was made using 2 sequential UmAS couplings, followed by benzyl deprotection. Due to observed decomposition of the tridecapeptide during attempted *N*-terminal Boc deprotections, a protecting group swap was performed to generate the *N*-Cbz protected Fragment A with 8-12% total yield based on an 8 step LLS (10 steps total). Currently, the yield of the last Cbz protection is about 40% less than what Süssmuth reports (45% vs 87%), so presumably the total yield will be higher upon optimization of that step.<sup>206</sup> Fragment C was synthesized via DEPBT coupling of the Boc-Dpg-Hpg dipeptide to the Phe-Asp-CO<sub>2</sub>Bn dipeptide. After much experimentation, we arrived at the dibenzyl ester protected *C*-terminal aspartic acid residue. The convergent strategy was pursued so that the Dpg and Hpg residues could be benzyl deprotected prior to coupling to avoid solubility issues with the fully benzyl protected Fragment C. The Boc-Dpg-Hpg dipeptide was made in 19-28% yield over 7 steps (LLS). This is comparable to Süssmuth's synthesis of the identical dipeptide, which they made using Sharpless asymmetric aminohydroxylation and DEPBT couplings. Their route runs the risk of epimerization by activation at the Dpg residue. Nonetheless, they synthesized the dipeptide with 37% total yield over 6 steps from 3,5-dibenzyloxy benzaldehyde.<sup>206</sup> Fragment C was completed by the coupling of the two dipeptides, which resulted in an 11-17% total yield over an 8 step LLS.

What sets each of the formal syntheses apart is the approach to the central hexapeptide, Fragment B. Three approaches were taken, and in each of them the tetrapeptide was synthesized via iterative UmAS couplings in 14-25% total yield over 7 LLS from 3,5-dibenzyloxy benzaldehyde. From the tetrapeptide the hexapeptide was made either by iterative UmAS couplings (first-generation),



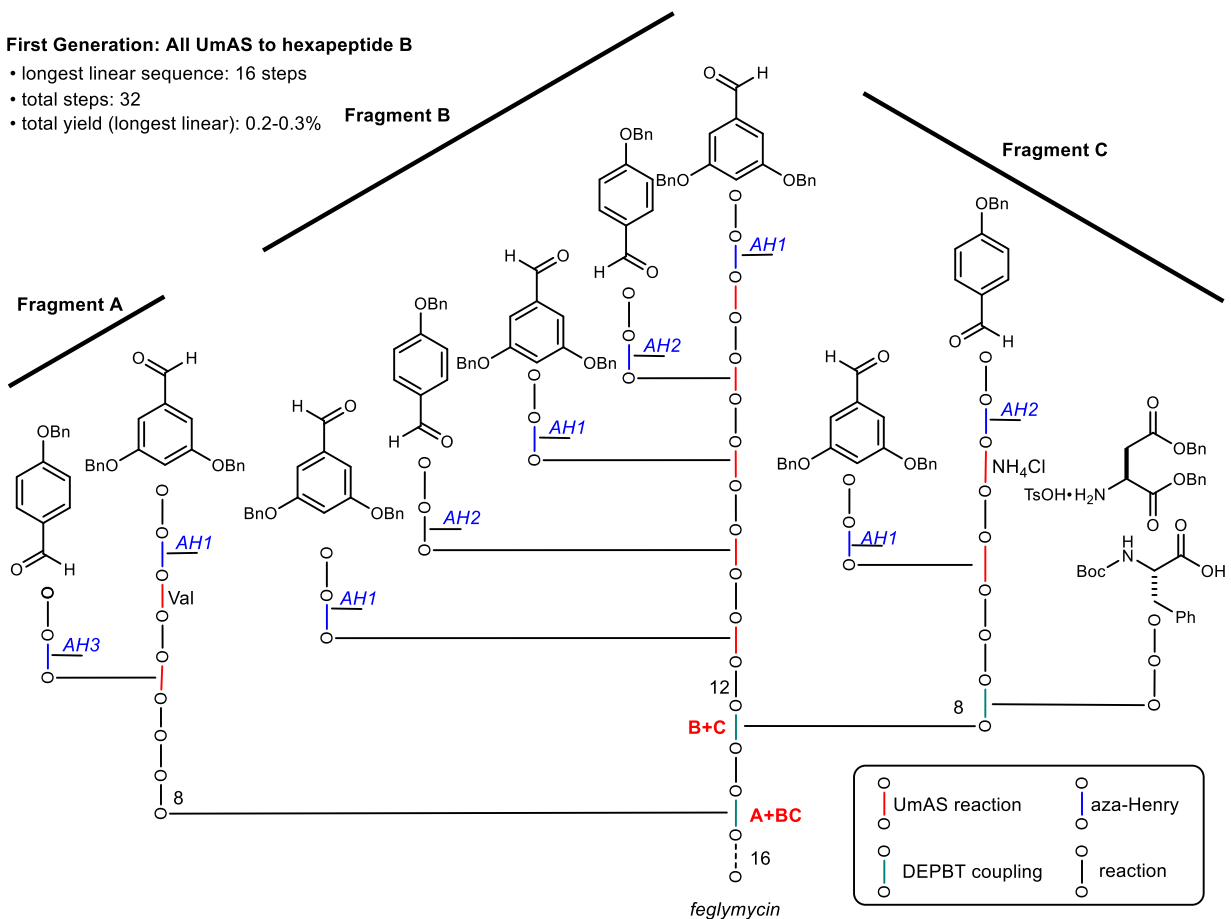
iterative DEPBT couplings (second-generation), or a convergent coupling to a dipeptide (third-generation).

Our first-generation formal synthesis solely depends on UmAS to generate the glycinamide chain

**Scheme 148.** Johnston laboratory formal synthesis: first-generation synthesis diagram.

**First Generation: All UmAS to hexapeptide B**

- longest linear sequence: 16 steps
- total steps: 32
- total yield (longest linear): 0.2-0.3%



in the central hexapeptide (**Scheme 148**). This process ensured that no epimerization would occur at the sensitive aryl glycine residues. While the pentapeptide was synthesized in moderate yield (48%), the yield of the hexapeptide was low (19%) and poor solubility of the intermediates and products made isolation and purification difficult. This resulted in a low yield of Fragment B (0.7-

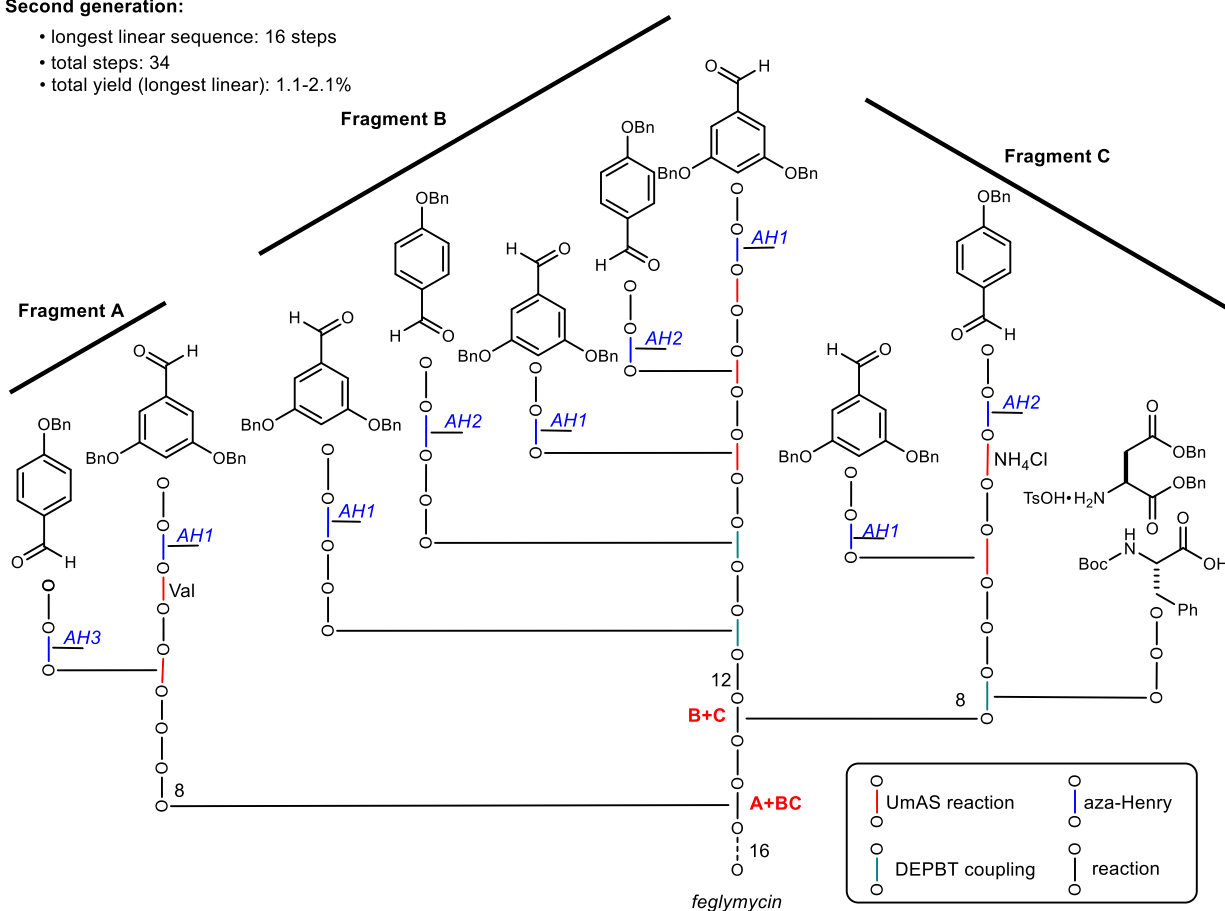
1.3% over 12 steps LLS). Nonetheless, the first-generation formal synthesis was completed with 0.2-0.3% total yield with a 16 LLS (32 steps total).<sup>247</sup>

The second-generation synthesis aimed to address the poor solubility of the penta- and hexapeptide of the central Fragment B by using DEPBT couplings to homologate the tetrapeptide (**Scheme 149**). These reactions could be run in DMF, which was shown to better solubilize the intermediates and products. This improved the yield of the hexapeptide from 0.7-1.3% (first-generation) to 4.7-9.2% total yield over 12 steps (LLS). The second-generation formal synthesis was completed with 1.1 to 2.1% total yield over a longest linear sequence of 16 steps (34 total steps).<sup>247</sup>

**Scheme 149.** Johnston laboratory formal synthesis: second-generation synthesis diagram.<sup>a</sup>

**Second generation:**

- longest linear sequence: 16 steps
- total steps: 34
- total yield (longest linear): 1.1-2.1%



<sup>a</sup>Hpg donors are synthesized in this route (c.f. purchased by Süssmuth); Hpg amino acid could be made in one less step *via* the direct aza-Henry reaction with nitromethane.

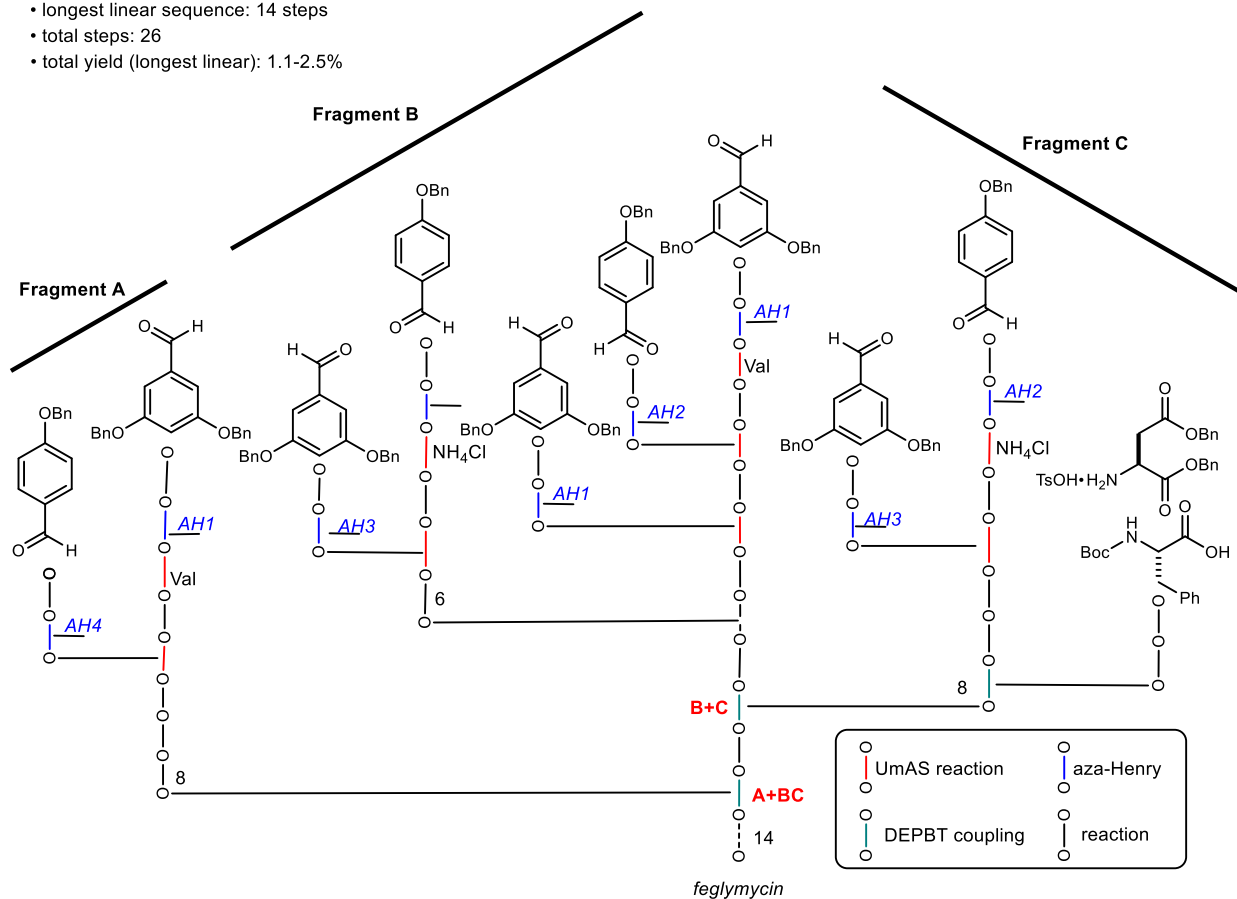
<sup>247</sup> The total yield was calculated using Süssmuth's reported yield for the final global deprotection (89%) – See ref. 206

While the second-generation synthesis significantly improved the overall yield of Fragment B, and the overall yield of feglymycin, it required activation at the Dpg residue, which is something we set out to avoid. It also added two steps to the total step count to account for the synthesis of the amino acids from the  $\alpha$ -bromo nitroalkanes. Our final, third-generation approach hinged on the success of a convergent 4+2 homologation of the tetrapeptide toward Fragment B. This coupling was originally attempted using UmAS, but poor solubility plagued the synthesis of the  $\alpha$ -bromonitroalkane dipeptide surrogate (see section 3.2.3 Synthesis of Fragment B). Thus, the dipeptide carboxylic acid used to make Fragment C was also used to make Fragment B through DEPBT coupling. The dipeptide would still be synthesized by UmAS, thus preventing the activation of any Dpg residues in the formal synthesis of (-)-feglymycin. This convergent approach provided the hexapeptide Fragment B with approximately the same total yield as the second-generation approach (4.9-10.7% total yield based on 10 step LLS). The third-generation formal synthesis decreased the longest linear sequence as well as the total step count, and was ultimately completed with 1.1 to 2.5% total yield over a longest linear sequence of 14 steps (26 total steps).<sup>247</sup>

**Scheme 150.** Johnston laboratory formal synthesis: third-generation synthesis diagram.

**Third generation:**

- longest linear sequence: 14 steps
- total steps: 26
- total yield (longest linear): 1.1-2.5%



To this end, we have constructed routes to (-)-feglymycin that avoid activation of the sensitive Dpg residue for amide coupling. Our formal synthesis is comparable in yield and step count to the previously published routes, and achieves the goal of demonstrating that UmAS, while not intended to replace condensative amide coupling reactions, does complement conventional methods in the context of complex total synthesis. While the feglymycin story highlighted the role that solubility can play in moderating the success of UmAS in complex peptide synthesis, the synthesis of Ffeglymycin predicts a more promising outcome when applying UmAS to soluble complex peptides with unusual aryl glycinamide residues.

## IV. Experimental Section

### 4.1 Characterization of organic molecules

#### General Experimental Section

All reagents and solvents were commercial grade and purified prior to use when necessary. Acetonitrile (MeCN), tetrahydrofuran (THF), dichloromethane (CH<sub>2</sub>Cl<sub>2</sub>), and toluene were dried by passage through a column of activated alumina as described by Grubbs<sup>248</sup> for microscale reactions. Flame-dried (under vacuum) glassware was used for all reactions. Stainless steel syringe needles or cannulae attached to a glass syringe barrel were used to transfer air- and moisture-sensitive liquids. Anhydrous magnesium sulfate (MgSO<sub>4</sub>) was used as a drying agent after extractions unless otherwise indicated.

Thin layer chromatography (TLC) was performed using glass-backed silica gel (250 μm) plates and flash chromatography utilized 230–400 mesh silica gel from Sorbent Technologies. UV light, and/or the use of ceric ammonium molybdate, *p*-anisaldehyde, potassium permanganate or phosphomolybdic acid solutions were used to visualize products.

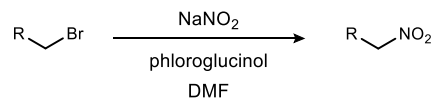
IR spectra were recorded on a Nicolet Avatar 360 spectrophotometer and are reported in wavenumbers (cm<sup>-1</sup>) analyzed as neat films on NaCl plates (transmission). Nuclear magnetic resonance spectra (NMR) were obtained on a Bruker DRX-500 (500 MHz), Bruker AV-400 (400 MHz), or Bruker AV II-600 (600 MHz). Chemical shifts are measured to residual non-deuterated solvent peaks as an internal standard. Mass spectra were recorded by use of chemical ionization (CI), electron impact ionization (EI), or electro-spray ionization (ESI) on a high resolution Thermo Electron Corporation MAT 95XP-Trap by the Indiana University Mass Spectrometry Facility or on a TQ-Orbitrap 3 XL Penn or Orbitrap 2 Classic FPG in the Vanderbilt Mass Spectrometry Core Laboratory. Optical rotations were measured on a Perkin Elmer-341 polarimeter or a Jasco P-2000 polarimeter. Chiral HPLC analysis was conducted on an Agilent 1100 series or an Agilent 1260

---

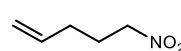
<sup>248</sup> Pangborn, A. B.; Giardello, M. A.; Grubbs, R. H.; Rosen, R. K.; Timmers, F. J. *Organometallics* **1996**, *15*, 1518.

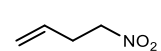
Infinity instrument using the designated ChiralPak column. Absolute configuration was determined by X-ray (see 4.2 X-Ray Crystallographic Data).

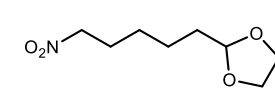
### Synthesis of nitroalkanes



**General procedure for nitrite substitution.** Sodium nitrite (2.0 equiv) was added to a stirred solution of bromide (1.0 equiv) in DMF (0.5 M). Phloroglucinol (1.1 equiv) was added to the reaction mixture, which was poured into ice water upon completion. The mixture was then extracted with Et<sub>2</sub>O, and the combined organics were washed with water, dried, and concentrated. The crude oil was purified by flash column chromatography or distillation.

 **5-Nitropent-1-ene (S1).** Prepared from 5-bromopent-1-ene (10.3 mL, 86.9 mmol) according to the general procedure for nitrite substitution. Flash column chromatography (3-5-10% Et<sub>2</sub>O in hexanes) afforded the desired compound as a yellow oil (4.69 g, 47%). All spectral data matched the literature values.<sup>249,250</sup>

 **4-Nitrobut-1-ene (S2).** Prepared from 4-bromobut-1-ene (15.2 mL, 150 mmol) according to the general procedure for nitrite substitution. Fractional distillation (bp = 85-90 °C, 600 mTorr) afforded the desired compound as a clear oil (7.94 g, 52%). All spectral data matched the literature values.<sup>251</sup>

 **2-(5-Nitropentyl)-1,3-dioxolane (S3).** Prepared from 2-(5-bromopentyl)-1,3-dioxolane according to the general procedure for nitrite substitution with a reaction time of 18 hours. Flash column chromatography (10-15-25-30-40% EtOAc/hexanes) afforded the desired compound as a yellow oil (1.32 g, 41%). R<sub>f</sub> = 0.44 (30% EtOAc/hexanes, CAM stain); IR (film) 2949, 2865, 1554, 1434, 1383, 1142, 1028, 945, 900 cm<sup>-1</sup>;

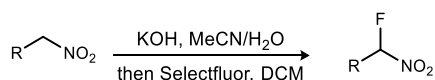
<sup>249</sup> Burkhard, J. A.; Tchitchanov, B. H.; Carreira, E. M. *Angew. Chem. Int. Edit.* **2011**, *50*, 5379.

<sup>250</sup> Cavanagh, C. W.; Aukland, M. H.; Laurent, Q.; Hennessy, A.; Procter, D. J. *Organic & Biomolecular Chemistry* **2016**, *14*, 5286.

<sup>251</sup> Marsh, G. P.; Parsons, P. J.; McCarthy, C.; Corniquet, X. G. *Org. Lett.* **2007**, *9*, 2613.

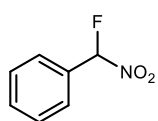
$^1\text{H}$  NMR (400 MHz,  $\text{CDCl}_3$ )  $\delta$  4.84 (t,  $J = 4.7$  Hz, 1H), 4.38 (t,  $J = 7.0$  Hz, 2H), 3.97 - 3.82 (m, 4H), 2.02 (dt,  $J = 14.3, 7.1$  Hz, 2H), 1.69-1.65 (m, 2H), 1.52 - 1.43 (m, 4H);  $^{13}\text{C}$  NMR (100 MHz,  $\text{CDCl}_3$ ) 104.3, 75.7, 65.0, 33.5, 27.4, 26.3, 23.3 ppm; HRMS (ESI): Exact mass calcd for  $\text{C}_8\text{H}_{15}\text{NO}_4$   $[\text{M}-\text{H}]^-$  188.0928, found 188.0934

### Synthesis of $\alpha$ -fluoro nitroalkanes

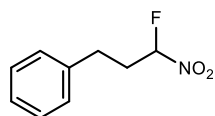


### General Procedure for the Preparation of $\alpha$ -Fluoro Nitroalkanes<sup>252</sup>

A round bottom flask was charged with the nitroalkane (6.05 mmol) and MeCN/ $\text{H}_2\text{O}$  (4.7 mL/9.0 mL). The solution was cooled to 0 °C, solid KOH (97%) (390 mg, 6.05 mmol) was added, and the reaction was vigorously stirred for 1 h at 0 °C. The reaction mixture was chilled to -20 °C to partially precipitate the nitronate salt, and Selectfluor (9.68 mol) was added, followed immediately by  $\text{CH}_2\text{Cl}_2$  (21 mL) which was pre-cooled to -78 °C. This mixture was gradually warmed to 10 °C and monitored by TLC. Upon completion, the resulting biphasic mixture was diluted with diethyl ether and stirred for an additional 10 min before being passed through a pad of Celite ( $\text{Et}_2\text{O}$ ). The water layer was extracted with diethyl ether, and the combined organics were dried ( $\text{MgSO}_4$ ), filtered, and concentrated.



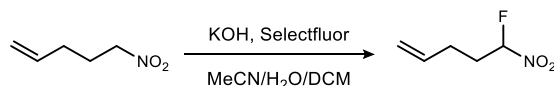
**(Fluoro(nitro)methyl)benzene (54b).** This compound was prepared according to the General Procedure for the Preparation of  $\alpha$ -Fluoro Nitroalkanes using 1.50 g (10.9 mmol) of the nitroalkane. The crude mixture was purified by flash column chromatography (0-2-4% EtOAc/hexanes) to afford the product as a pale-yellow oil (1.27 g, 75%). All spectral data matched the literature values.<sup>252</sup>



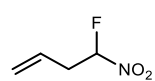
**(3-Fluoro-3-nitropropyl)benzene (54d).** This compound was prepared according to the General Procedure for the Preparation of  $\alpha$ -Fluoro Nitroalkanes using 1.00 g (6.05 mmol) of the nitroalkane. The resulting pale-yellow oil was used without further purification.  $R_f = 0.69$  (20%  $\text{Et}_2\text{O}$ /hexanes); IR (film) 3028, 2932, 1570, 1453,

<sup>252</sup> Hu, H.; Huang, Y.; Guo, Y. *J. Fluorine Chem.* **2012**, *133*, 108.

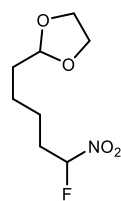
1124, 747, 698  $\text{cm}^{-1}$ ;  $^1\text{H}$  NMR (600 MHz,  $\text{CDCl}_3$ )  $\delta$  7.33 (dd,  $J = 7.5, 7.5$  Hz, 2H), 7.27-7.24 (m, 1H), 7.20 (d,  $J = 7.4$  Hz, 2H), 5.75 (ddd,  $^2J_{\text{HF}} = 50.6$ ,  $^3J_{\text{HH}} = 7.0, 4.0$  Hz, 1H), 2.87-2.77 (m, 2H), 2.56-2.39 (m, 2H);  $^{13}\text{C}$  NMR (150 MHz,  $\text{CDCl}_3$ ) ppm 138.4, 129.0, 128.5, 127.0, 110.4 (d,  $^1J_{\text{CF}} = 239$  Hz), 34.9 (d,  $^2J_{\text{CF}} = 19.8$  Hz), 29.2 (d,  $^3J_{\text{CF}} = 3.3$  Hz);  $^{19}\text{F}$  NMR (376 MHz,  $\text{CDCl}_3$ )  $\delta$  -147.8; HRMS (-ESI): Exact mass calcd for  $\text{C}_9\text{H}_9\text{FNO}_2$   $[\text{M}-\text{H}]^-$  182.0623, found 182.0618.



**5-Fluoro-5-nitropent-1-ene (61).** Prepared according to the General Procedure for the Preparation of  $\alpha$ -Fluoro Nitroalkanes from 5-nitropent-1-ene (**S1**) (2.50 g, 21.7 mmol). The resulting light yellow oil was used without further purification (2.64 g, 91%);  $R_f = 0.70$  (20% EtOAc/hexanes,  $\text{KMnO}_4$  stain); IR (film) 3085, 2929, 2856, 1572, 1359, 1154, 923  $\text{cm}^{-1}$ ;  $^1\text{H}$  NMR (600 MHz,  $\text{CDCl}_3$ )  $\delta$  5.85-5.75 (m, 2H), 5.15-5.11 (m, 2H), 2.33-2.19 (m, 4H);  $^{13}\text{C}$  NMR (150 MHz,  $\text{CDCl}_3$ ) ppm 134.8, 117.5, 110.6 (d,  $^1J_{\text{CF}} = 239.3$  Hz), 32.5 (d,  $^2J_{\text{CF}} = 19.8$  Hz), 27.1 (d,  $^3J_{\text{CF}} = 3.2$  Hz);  $^{19}\text{F}$ -NMR (376 MHz,  $\text{CDCl}_3$ )  $\delta$  -147.5; HRMS (CI gc/ms): Exact mass calcd for  $\text{C}_5\text{H}_9\text{FNO}_2$   $[\text{M}+\text{H}]^+$  134.0612, found 134.0613.



**4-Fluoro-4-nitrobut-1-ene (65).** Prepared according to the General Procedure for the Preparation of  $\alpha$ -Fluoro Nitroalkanes from 4-nitrobut-1-ene (**S2**) (6.29 g, 62.2 mmol). The clear oil was used without further purification (5.79 g, 78%). All spectral data matched the literature values.<sup>252</sup>

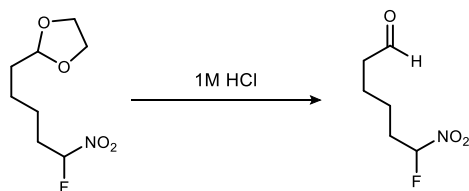


**2-(5-Fluoro-5-nitropentyl)-1,3-dioxolane (S4).**

Prepared according to the General Procedure for the Preparation of  $\alpha$ -Fluoro Nitroalkanes. Concentration afforded the desired compound as a light yellow oil, which was used without further purification (1.37 g, 96%);  $R_f = 0.35$  (20% EtOAc/hexanes, CAM stain); IR (film) 2950, 2874, 1573, 1359, 1144, 1033, 946  $\text{cm}^{-1}$ ;  $^1\text{H}$  NMR (400 MHz,  $\text{CDCl}_3$ )  $\delta$  5.79 (ddd,  $^2J_{\text{HF}} = 50.8$ ,  $J = 6.3, 4.3$  Hz, 1H), 4.84 (t,  $J = 4.6$  Hz, 1H), 3.97-3.82 (m, 4H), 2.22-2.09 (m, 2H), 1.70-1.65 (m, 2H), 1.58-1.55 (m, 1H), 1.53-1.48 (m, 3H);  $^{13}\text{C}$  NMR (100 MHz,  $\text{CDCl}_3$ ) ppm 111.2 ( $^1J_{\text{CF}} = 238$  Hz), 104.2, 65.1, 33.4, 33.2 ( $^2J_{\text{CF}} = 19.6$  Hz), 23.1, 22.8 ( $^3J_{\text{CF}} = 3.0$



Hz);  $^{19}\text{F}$  NMR (376 MHz,  $\text{CDCl}_3$ )  $\delta$  -146.8; HRMS (CI GC/MS): Exact mass calcd for  $\text{C}_8\text{H}_{15}\text{FNO}_4$   $[\text{M}+\text{H}]^+$  208.0981, found 208.0981.



**6-Fluoro-6-nitrohexanal (96).** The acetal (119 mg, 574  $\mu\text{mol}$ ) was stirred for 24 hours in a 1 M aq HCl solution (0.6 mL). The aqueous solution was extracted with dichloromethane. The combined organics were dried ( $\text{Na}_2\text{SO}_4$ ) and concentrated.  $^1\text{H}$  NMR indicated incomplete conversion, so the mixture of acetal and aldehyde was resubjected using 2 M aq HCl. Extraction with dichloromethane followed by concentration afforded the product as a colorless oil (81.6 mg, 87%).  $R_f = 0.28$  (20% EtOAc/hexanes); IR (film) 2941, 2873, 2730, 1721, 1572, 1391, 1351, 1135  $\text{cm}^{-1}$ ;  $^1\text{H}$  NMR (400 MHz,  $\text{CDCl}_3$ )  $\delta$  9.77 (dd,  $J = 1.1, 1.1$  Hz, 1H), 5.81 (ddd,  $^2J_{\text{HF}} = 50.8, J = 6.3, 4.3$  Hz, 1H), 2.50 (td,  $J = 7.1, 1.1$  Hz, 2H), 2.25-2.12 (m, 2H), 1.74-1.66 (m, 2H), 1.52-1.62 (m, 1H), 1.42-1.50 (m, 1H);  $^{13}\text{C}$  NMR (100 MHz,  $\text{CDCl}_3$ ) ppm 201.3, 110.7 (d,  $^1J_{\text{HF}} = 239.3$  Hz), 43.3, 32.9 (d,  $^2J_{\text{HF}} = 19.6$  Hz), 22.3 (d,  $^3J_{\text{HF}} = 3.1$  Hz), 21.0;  $^{19}\text{F}$  NMR (376 MHz,  $\text{CDCl}_3$ )  $\delta$  -146.9; HRMS (ESI): Exact mass calcd for  $\text{C}_6\text{H}_9\text{FNO}_3$   $[\text{M}-\text{H}]^-$  162.0572, found 162.0564.

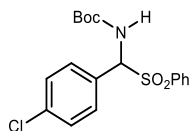
### General Procedure for the Preparation of *N*-Boc $\alpha$ -Amidosulfones.<sup>253,254,255</sup>

To a round-bottomed flask equipped with a stir bar was added *tert*-butyl carbamate (1 equiv), *para*-toluene sulfinic acid sodium salt (2 equiv), MeOH, and water. The corresponding aldehyde (1.5 equiv) was then added, followed by formic acid (2 equiv). The mixture was stirred for 96 h at room temperature. The resulting precipitate was filtered and washed with water and hexanes to afford the desired  $\alpha$ -amidosulfone without further purification.

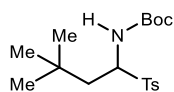
<sup>253</sup> Schwieter, K. E.; Johnston, J. N. *ACS Catalysis* **2015**, *5*, 6559.

<sup>254</sup> Gomez-Bengoia, E.; Linden, A.; Lopez, R.; Mugica-Mendiola, I.; Oiarbide, M.; Palomo, C. *J Am Chem Soc* **2008**, *130*, 7955.

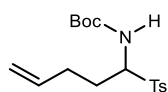
<sup>255</sup> Herrera, R. P.; Sgarzani, V.; Bernardi, L.; Fini, F.; Pettersen, D.; Ricci, A. *The Journal of Organic Chemistry* **2006**, *71*, 9869.



**tert-Butyl ((4-chlorophenyl)(phenylsulfonyl)methyl)carbamate (55a).** The title compound was prepared according to the general procedure and isolated as a white solid in 84% yield. All spectral data matched the literature.<sup>256</sup>



**tert-Butyl (3,3-dimethyl-1-tosylbutyl)carbamate (55d).** The title compound was prepared according to the general procedure and isolated as a white solid in 94% yield. All spectral data matched the literature.<sup>257</sup>



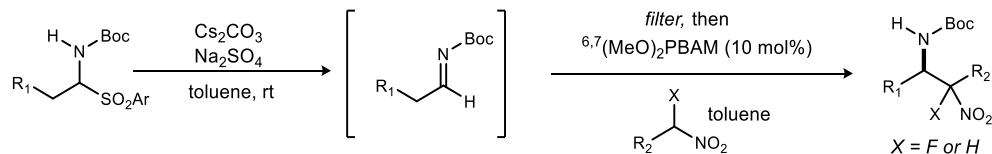
**tert-Butyl (1-tosylpent-4-en-1-yl)carbamate (55c).** Pent-4-enal (8.90 g, 106 mmol) was dissolved in a mixture of MeOH/H<sub>2</sub>O (1:2, 235 mL) in a round-bottomed flask. To the solution was added *tert*-butyl carbamate (8.26 g, 70.5 mmol), *para*-toluene sulfonic acid sodium salt (25.14 g, 141.1 mmol) and formic acid (5.32 mL, 141 mmol). The mixture was stirred at room temperature and the resulting precipitate was filtered and washed with water and hexanes to afford the  $\alpha$ -amidosulfone, which was used without further purification, as a white solid (14.9 g, 62%). Mp 95.2-96.0 °C, 113.2°C (Boc thermolysis);  $R_f = 0.36$  (20% EtOAc/hexanes); IR (film) 3334, 2977, 1720, 1518, 1316, 1165, 1141 cm<sup>-1</sup>; <sup>1</sup>H NMR (400 MHz, CDCl<sub>3</sub>)  $\delta$  7.77 (d,  $J = 8.2$  Hz, 2H), 7.31 (d,  $J = 8.1$  Hz, 2H), 5.82-5.72 (m, 1H), 5.07-5.02 (m, 2H), 4.96 (d,  $J = 10.8$  Hz, 1H), 4.81 (ddd,  $J = 10.8, 10.8, 3.0$  Hz, 1H), 2.40 (s, 3H), 2.38-2.27 (m, 2H), 2.18-2.12 (m, 1H), 1.86-1.78 (m, 1H), 1.21 (s, 9H); <sup>13</sup>C NMR (150 MHz, CDCl<sub>3</sub>) ppm 153.8, 145.0, 136.1, 133.9, 129.8, 129.5, 116.7, 80.8, 70.3, 29.5, 28.0, 25.9, 21.7; HRMS (ESI): Exact mass calcd for C<sub>17</sub>H<sub>25</sub>NNaO<sub>4</sub>S [M+Na]<sup>+</sup> 362.1402, found 362.1401.

## Aza-Henry reactions with $\alpha$ -fluoro and unsubstituted nitroalkanes

### General Procedure A: BAM-catalyzed aza-Henry reaction with alkyl electrophiles.<sup>253</sup>

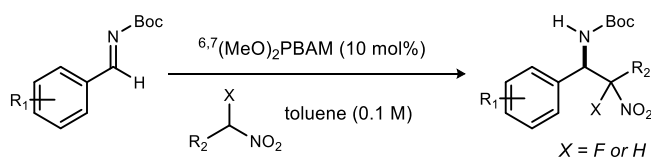
<sup>256</sup> Davis, T. A.; Vilgelm, A. E.; Richmond, A.; Johnston, J. N. *The Journal of Organic Chemistry* **2013**, *78*, 10605.

<sup>257</sup> Schwieter, K. E.; Johnston, J. N. *Chemical Science* **2015**, *6*, 2590.



To a flame-dried vial equipped with a stir bar was added *N*-Boc  $\alpha$ -amidosulfone (100  $\mu\text{mol}$ ),  $\text{Na}_2\text{SO}_4$  (500  $\mu\text{mol}$ ),  $\text{Cs}_2\text{CO}_3$  (500  $\mu\text{mol}$ ) and toluene (500  $\mu\text{L}$ ). The reaction stirred for 3 hours at room temperature. The mixture was filtered through a short pad of Celite into a flame dried vial containing the nitroalkane (1.1 equiv). The Celite was rinsed with an additional 500  $\mu\text{L}$  of toluene into the reaction vial. The reaction mixture was cooled to the indicated temperature and the catalyst (10 mol%) was added. Upon completion, the reaction was filtered through a short plug of silica gel, concentrated, and purified by flash column chromatography if necessary.

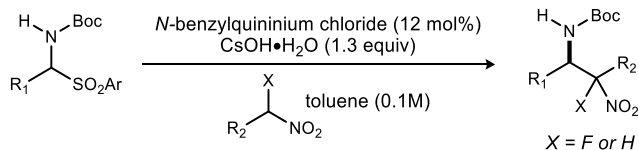
### General Procedure B: BAM catalyzed aza-Henry reaction with aryl aldimines.<sup>258</sup>



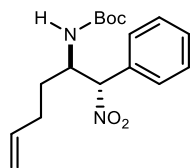
To a flame dried vial equipped with a stir bar was added the nitroalkane (120  $\mu\text{mol}$ ), toluene (500  $\mu\text{L}$ ), and  $^{6,7}(\text{MeO})_2\text{PBAM}$  or  $^{6,7}(\text{MeO})_2\text{PBAM}\cdot\text{HNTf}_2$  (10  $\mu\text{mol}$ ) at room temperature. The mixture was stirred until homogeneous and then cooled to the indicated temperature before the imine (100  $\mu\text{mol}$ ) was added. Upon completion of the reaction, the mixture was quickly flushed through a pad of silica gel and concentrated. The resultant residue was purified by column chromatography to afford the title compound.

### General Procedure C: Phase transfer catalyzed aza-Henry reaction.<sup>253,254</sup>

<sup>258</sup> Vara, B. A.; Johnston, J. N. *J. Am. Chem. Soc.* **2016**, *138*, 13794.



To a flame dried vial equipped with a stir bar was added the *N*-Boc  $\alpha$ -amidosulfone (100  $\mu$ mol), nitroalkane (450  $\mu$ mol), *N*-benzylquininium chloride (12  $\mu$ mol) and toluene (1 mL). The reaction mixture was cooled to the indicated temperature and CsOH $\cdot$ H<sub>2</sub>O (130  $\mu$ mol) was added. The reaction was stirred vigorously at the indicated temperature for 72 hours. Upon completion the reaction mixture was quenched with 1 M aq HCl while still cold, and extracted with dichloromethane. The combined organic layers were washed with 1 M aq HCl, dried, and concentrated. The resultant mixture was purified by column chromatography to afford the desired  $\beta$ -amino nitroalkane.



***tert*-Butyl ((1*S*,2*R*)-1-nitro-1-phenylhex-5-en-2-yl)carbamate (56c).** This compound was prepared according to General Procedure A using *tert*-butyl (1-tosylpent-4-en-1-yl)carbamate (33.9 mg, 100  $\mu$ mol), phenylnitromethane (15.1 mg, 110  $\mu$ mol) and <sup>6,7</sup>(MeO)<sub>2</sub>PBAM (6.3 mg, 10  $\mu$ mol). Flash column chromatography (10-20-40% diethyl ether in hexanes) afforded the product as a white solid (11.2 mg, 35% yield), which was determined the be >20:1 dr and 60% ee by chiral HPLC analysis.

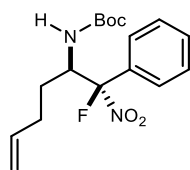
**Phase transfer catalysis:** Prepared according to General Procedure C at -35 °C from *tert*-butyl (1-tosylpent-4-en-1-yl)carbamate (33.9 mg, 100  $\mu$ mol), phenylnitromethane (61.7 mg, 450  $\mu$ mol) and *N*-benzylquininium chloride (5.4 mg, 12  $\mu$ mol). Flash column chromatography (10-20-40% diethyl ether in hexanes) afforded the product as a white solid (10 mg, 31% yield), which was determined to be >11:1 dr and 90/>99% ee by chiral HPLC analysis.

White solid, mp = 122-125 °C<sup>259</sup>; [ $\alpha$ ]<sub>D</sub><sup>20</sup> + 12.4 (*c* 0.24, CHCl<sub>3</sub>)<sup>260</sup>; (Chiralpak AD, 3% *i*PrOH/hexanes, 1.0 mL/min: *t*<sub>r</sub>(*d*<sub>1e1</sub>, major/minor) = 18.6 min, *t*<sub>r</sub>(*d*<sub>1e2</sub>, major/major) = 20.0 min, *t*<sub>r</sub>(*d*<sub>2e1</sub>, minor/minor) = 21.7 min, *t*<sub>r</sub>(*d*<sub>2e2</sub>, minor/major) = 24.7 min). *R*<sub>f</sub> = 0.23 (10%

<sup>259</sup> The melting point was measured on >20:1 dr material.

<sup>260</sup> The optical rotation measured on >11:1 dr, 86/99% ee material.

EtOAc/hexanes); IR (film) 3374, 2978, 2918, 1683, 1542, 1522, 1367, 1165  $\text{cm}^{-1}$ ;  $^1\text{H}$  NMR (600 MHz,  $\text{CDCl}_3$ )  $\delta$  7.48-7.46 (m, 2H), 7.39-7.38 (m, 3H), 5.76 (dddd,  $J=17.0, 10.3, 6.8, 6.5$  Hz, 1H), 5.65 (d,  $J = 7.1$  Hz, 1H), 5.05-5.00 (br m, 2H), 4.42-4.39 (m, 2H), 2.25-2.21 (m, 1H), 2.14-2.07 (m, 1H), 1.74-1.66 (m, 2H), 1.30 (s, 9H);  $^{13}\text{C}$  NMR (150 MHz,  $\text{CDCl}_3$ ) ppm 155.0, 137.0, 132.3, 129.9, 128.9, 128.4, 116.0, 93.8, 80.1, 53.0, 30.36, 30.2, 28.3; HRMS (ESI): Exact mass calcd for  $\text{C}_{17}\text{H}_{23}\text{N}_2\text{O}_4$  [M-H], 319.1663, found 319.1654.



**tert-Butyl ((1R,2R)-1-fluoro-1-nitro-1-phenylhex-5-en-2-yl) (56d).** This compound was prepared according to General Procedure A using *tert*-butyl (1-tosylpent-4-en-1-yl)carbamate (500 mg, 1.47 mmol), (fluoro(nitro)methyl)benzene (274 mg, 1.77  $\mu\text{mol}$ ) and  $^{6,7}(\text{OMe})_2\text{PBAM}\cdot\text{HNTf}_2$

(267 mg, 295  $\mu\text{mol}$ ).  $^{19}\text{F}$ -NMR analysis of the crude mixture showed a 5.2:1 dr. Flash column chromatography (2-4-6% EtOAc/hexanes) afforded the product as a white solid (263 mg, 53% yield), which was determined by chiral HPLC analysis to be 83% ee for the major *anti* diastereomer and >99% ee for the minor *syn* diastereomer. Absolute and relative stereochemistry was determined by X-Ray analysis of a single crystal of the major diastereomer grown by slow evaporation of dichloromethane. See **4.2 X-Ray Crystallographic Data** for more details.

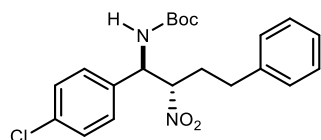
When 10 mol% catalyst was used the product was isolated in 43% yield as a 5.8:1 mixture of diastereomers with 87/<99% ee.

White solid, mp = 77-81  $^{\circ}\text{C}$ <sup>261</sup>;  $[\alpha]_D^{20} + 4.0$  ( $c$  0.45,  $\text{CHCl}_3$ )<sup>262</sup>; Agilent 1100 Series, Chiralpak AD-H, 4% EtOH/hexanes, 1.0 mL/min, 25  $^{\circ}\text{C}$ :  $t_r(d_{1e1}, \text{major/major}) = 5.6$  min,  $t_r(d_{1e2}, \text{major/minor}) = 6.7$  min,  $t_r(d_{2e1}, \text{minor/major}) = 11.7$  min,  $t_r(d_{2e2}, \text{minor/minor}) = 16.7$  min).  $R_f = 0.57$  (20% EtOAc/hexanes); IR (film) 3334, 2980, 2934, 1705, 1571, 1515, 1161  $\text{cm}^{-1}$ ;  $^1\text{H}$  NMR (400 MHz,  $\text{CDCl}_3$ )  $\delta$  7.74 (dd,  $J = 7.9, 1.7$  Hz, 2H), 7.45-7.38 (m, 3H), 5.84-5.74 (m, 1H), 5.15 (dddd,  $J = 10.9, 10.9, 2.6$  Hz,  $^3J_{\text{HF}} = 27.1$  Hz, 1H), 5.10-5.04 (m, 2H), 4.41 (d,  $J = 10.8$  Hz, 1H), 2.28-2.21 (m, 1H), 2.16 (ddd,  $J = 22.4, 14.8, 7.5$  Hz, 1H), 1.71-1.62 (m, 1H), 1.58-1.51 (m, 1H), 1.23 (s, 9H);  $^{13}\text{C}$  NMR (100 MHz,  $\text{CDCl}_3$ ) 154.9, 136.6, 131.6 (d,  $^2J_{\text{CF}} = 23.3$  Hz), 131.0, 128.6 (d,  $^4J_{\text{CF}} = 1.1$  Hz), 126.0 (d,  $^3J_{\text{CF}} = 8.7$  Hz), 120.3 (d,  $^1J_{\text{CF}} = 242.9$ ), 116.4, 80.4, 54.1 (d,  $^2J_{\text{CF}} = 20.8$  Hz),

<sup>261</sup> The melting point was measured on 16:1 dr material.

<sup>262</sup> The optical rotation was measured on 16:1 dr, 83/99% ee material.

29.7, 28.3 (d,  $^3J_{CF} = 3.9$  Hz), 28.1 ppm;  $^{19}\text{F}$ -NMR (376 MHz) -141.4, HRMS (-ESI): Exact mass calcd for  $\text{C}_{17}\text{H}_{23}\text{FN}_2\text{NaO}_4$   $[\text{M}+\text{Na}]^+$  361.1540, found 361.1539.

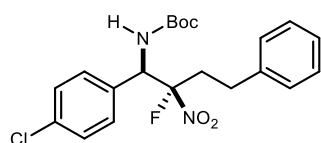


**tert-Butyl ((1R,2S)-1-(4-chlorophenyl)-2-nitro-4-phenylbutyl)carbamate (56e).** This compound was prepared according to General Procedure **B** using *tert*-butyl (*E*)-(4-chlorobenzylidene)carbamate (24.0 mg, 100  $\mu\text{mol}$ ), 3-(nitropropyl)benzene (19.8 mg, 120  $\mu\text{mol}$ ) and  $^{6,7}(\text{OMe})_2\text{PBAM}\cdot\text{HNTf}_2$  (9.1 mg, 10  $\mu\text{mol}$ ).

Flash column chromatography (10-20% EtOAc/hexanes) afforded the product as a white solid (20 mg, 49% yield), which was determined to be >20:1 dr and 87/51% ee by chiral HPLC analysis. Recrystallization from ethyl acetate provided >20:1 dr and 96% ee material.

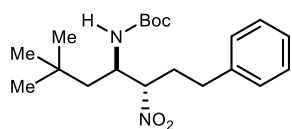
**Phase transfer catalysis:** Prepared according to General Procedure **C** at  $-55$   $^\circ\text{C}$  from *tert*-butyl ((4-chlorophenyl)(phenylsulfonyl)methyl)carbamate (38.2 mg, 100  $\mu\text{mol}$ ), 3-(nitropropyl)benzene (74.3 mg, 450  $\mu\text{mol}$ ) and *N*-benzylquininium chloride (5.4 mg, 12  $\mu\text{mol}$ ). Analysis of the crude  $^1\text{H}$ -NMR spectrum showed a 94% yield. Chiral HPLC analysis of the crude mixture showed the product was 3:1 dr with 30/8% ee.

White solid, mp = 159-161  $^\circ\text{C}$ ;  $[\alpha]_D^{20} -36$  ( $c$  0.43,  $\text{CHCl}_3$ ); Chiralpak AD-H, 10% *i*PrOH/hexanes, 1.0 mL/min, 25  $^\circ\text{C}$ :  $t_r(d_{1e1}, \text{major/minor}) = 9.2$  min,  $t_r(d_{2e1}, \text{minor/minor}) = 11.7$  min,  $t_r(d_{2e2}, \text{minor/major}) = 13.0$  min,  $t_r(d_{1e2}, \text{major/major}) = 25.5$  min;  $R_f = 0.26$  (10% EtOAc/hexanes); IR (film) 3386, 2977, 1683, 1547, 1519, 1494, 1367, 1160  $\text{cm}^{-1}$ ;  $^1\text{H}$  NMR (400 MHz,  $\text{CDCl}_3$ )  $\delta$  7.31-7.27 (m, 4H), 7.24-7.20 (m, 1H), 7.11 (d,  $J = 8.4$  Hz, 4H), 5.12 (br s, 2H), 4.74 (br s, 1H), 2.74 (ddd,  $J = 13.9, 9.1, 4.8$  Hz, 1H), 2.54 (ddd,  $J = 13.9, 8.1, 8.1$  Hz, 1H), 2.40-2.30 (m, 1H), 2.10-2.01 (m, 1H), 1.41 (s, 9H);  $^{13}\text{C}$  NMR (150 MHz,  $\text{CDCl}_3$ ) ppm 154.7, 139.4, 135.0, 134.7, 129.2, 128.7, 128.5, 128.2, 126.6, 90.1, 80.9, 56.3, 31.9, 31.5, 28.2; HRMS (-ESI): Exact mass calcd for  $\text{C}_{21}\text{H}_{24}\text{ClN}_2\text{O}_4$   $[\text{M}-\text{H}]^-$  403.1430, found 403.1422.



**tert-Butyl ((1R,2S)-1-(4-chlorophenyl)-2-fluoro-2-nitro-4-phenylbutyl)carbamate (56f).** This compound was prepared according to General Procedure **C** at  $-35$   $^\circ\text{C}$  from *tert*-butyl ((4-chlorophenyl)(phenylsulfonyl)methyl)carbamate (38.2 mg, 100  $\mu\text{mol}$ ), (3-fluoro-3-nitropropyl)benzene (82.4 mg, 450  $\mu\text{mol}$ ) and *N*-benzylquininium chloride (5.4 mg, 12  $\mu\text{mol}$ ). The

crude reaction mixture was purified by flash column chromatography (SiO<sub>2</sub>, 10-20% diethyl ether in hexanes) to provide the product (33 mg, 79%) as a 2.8:1 mixture of diastereomers. The major diastereomer (*syn*) was found to be 60% ee and the minor (*anti*) was found to be 24% ee by chiral HPLC analysis (Chiralpak IA, 5% EtOH/hexanes, 1.0 mL/min, 30 °C:  $t_r(d_{1e1}, \text{minor/major}) = 6.6$  min,  $t_r(d_{2e1}, \text{major/minor}) = 7.1$  min,  $t_r(d_{2e2}, \text{major/major}) = 9.8$  min,  $t_r(d_{1e2}, \text{minor/minor}) = 14.3$  min). All other spectral data matched the literature.<sup>258</sup> Absolute and relative stereochemistry was determined by X-Ray analysis of a single crystal of the major diastereomer grown by slow liquid/liquid diffusion with ethyl acetate/hexanes. See **4.2 X-Ray Crystallographic Data** for more details.

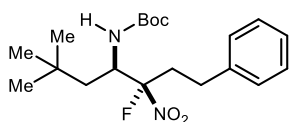


**tert-Butyl ((3*S*,4*R*)-6,6-dimethyl-3-nitro-1-phenylheptan-4-yl)carbamate (56g).** This compound was prepared according to the General Procedure A using *tert*-butyl (3,3-dimethyl-1-

tosylbutyl)carbamate (35.5 mg, 100  $\mu\text{mol}$ ), (3-nitropropyl)benzene (18.2 mg, 110  $\mu\text{mol}$ ) and <sup>6,7</sup>(MeO)<sub>2</sub>PBAM (6.3 mg, 10  $\mu\text{mol}$ ) at -55 °C for 48 hours. <sup>1</sup>H NMR analysis of the crude reaction mixture showed a 1:1 mixture of diastereomers which were separated and purified by flash column chromatography (5-10-20% Et<sub>2</sub>O in hexanes) to afford the major diastereomer (4.3 mg, 12%) and the minor diastereomer (3.5 mg, 10%), both as white solids with 20% and 11% ee respectively as determined by chiral HPLC analysis. Absolute and relative stereochemistry was determined by X-Ray analysis of a single crystal of the major diastereomer grown by slow evaporation of benzene. See **4.2 X-Ray Crystallographic Data** for more details.

**Phase transfer catalysis:** Prepared according to General Procedure C at -55 °C using *tert*-butyl (3,3-dimethyl-1-tosylbutyl)carbamate (35.5 mg, 100  $\mu\text{mol}$ ), (3-nitropropyl)benzene (74.3 mg, 450  $\mu\text{mol}$ ) and *N*-benzylquininium chloride (5.4 mg, 12  $\mu\text{mol}$ ). Analysis of the crude <sup>1</sup>H NMR showed >20:1 dr with a 94% yield (<sup>1</sup>H NMR). The reaction mixture was purified by column chromatography (5-10-20% diethyl ether in hexanes) to provide the product as a white solid (33 mg, 90% yield), which was determined to be >20:1 dr and >99% ee by chiral HPLC analysis.

**Major diastereomer (anti):** White solid, mp = 115-119 °C;  $[\alpha]_D^{20} +20.4$  ( $c$  0.67,  $\text{CHCl}_3$ )<sup>263</sup>; Chiralpak AD-H, 5% *i*PrOH/hexanes, 1.0 mL/min, 30 °C:  $t_r(e_1, \text{major}) = 6.6$  min,  $t_r(e_2, \text{minor}) = 7.4$  min;  $R_f = 0.17$  (10%  $\text{Et}_2\text{O}$ /hexanes); IR (film) 3344, 2956, 1703, 1548, 1366, 1167  $\text{cm}^{-1}$ ;  $^1\text{H}$  NMR (600 MHz,  $\text{CDCl}_3$ )  $\delta$  7.29 (dd,  $J = 7.5, 7.5$  Hz, 2H), 7.21 (dd,  $J = 7.4, 7.4$  Hz, 1H), 7.17 (d,  $J = 7.3$  Hz, 1H), 4.55-4.51 (m, 2H), 4.06 (ddd,  $J = 13.8, 4.9, 4.9$  Hz, 1H), 2.71 (dddd,  $J = 14.7, 9.7, 4.9, 4.9$  Hz, 1H), 2.64-2.59 (m, 1H), 2.40-2.34 (m, 1H), 1.43 (s, 9H), 1.15 (dd,  $J = 14.8, 10.1$  Hz, 1H), 0.97-0.93 (m, 1H), 0.91 (s, 9H);  $^{13}\text{C}$  NMR (150 MHz,  $\text{CDCl}_3$ ) ppm 155.0, 140.0, 128.8, 128.6, 126.6, 91.6, 80.3, 50.4, 43.5, 32.3, 31.9, 30.4, 29.7, 28.5; HRMS (+ESI): Exact mass calcd for  $\text{C}_{20}\text{H}_{33}\text{N}_2\text{O}_4$   $[\text{M}+\text{H}]^+$  365.2435, found 365.2423.



**Minor diastereomer (syn):** White solid, mp = 117-119 °C;  $[\alpha]_D^{20} +8.7$  ( $c$  0.09,  $\text{CHCl}_3$ )<sup>264</sup>; Chiralpak IC, 10% *i*PrOH/hexanes, 1.0 mL/min, 25 °C:  $t_r(e_1, \text{major}) = 3.9$  min,  $t_r(e_2, \text{minor}) = 4.4$  min;  $R_f = 0.33$  (10%  $\text{Et}_2\text{O}$ /hexanes); IR (film) 3449, 3355, 1957, 2867, 1714, 1554, 1504, 1366, 1168  $\text{cm}^{-1}$ ;  $^1\text{H}$  NMR (600 MHz,  $\text{CDCl}_3$ )  $\delta$  7.30 (dd,  $J = 7.7, 7.7$  Hz, 2H), 7.22 (dd,  $J = 7.4, 7.4$  Hz, 1H), 7.18 (d,  $J = 7.1$  Hz, 2H), 4.95 (d,  $J = 10.0$  Hz, 1H), 4.44 (ddd,  $J = 8.9, 5.1, 3.9$  Hz, 1H);  $^{13}\text{C}$  NMR (150 MHz,  $\text{CDCl}_3$ ) ppm 155.4, 139.8, 128.8, 128.7, 126.6, 91.3, 80.1, 48.7, 46.1, 32.5, 31.8, 30.5, 29.7, 28.5; HRMS (ESI): Exact mass calcd for  $\text{C}_{20}\text{H}_{32}\text{N}_2\text{NaO}_4$   $[\text{M}+\text{Na}]^+$  387.2254, found 387.2237. ***tert*-Butyl ((3*S*,4*R*)-3-fluoro-6,6-dimethyl-3-nitro-1-phenylheptan-4-yl)carbamate (56h).** This compound was prepared according to the General Procedure C at -35 °C using *tert*-butyl (3,3-dimethyl-1-tosylbutyl)carbamate (35.5 mg, 100  $\mu\text{mol}$ ), (3-fluoro-3-nitropropyl)benzene (82.4 mg, 450  $\mu\text{mol}$ ), and *N*-benzylquininium chloride (5.4 mg, 12  $\mu\text{mol}$ ). Analysis of the crude  $^{19}\text{F}$  NMR showed 7.2:1 dr. The diastereomers were separated by column chromatography (5-10-20% diethyl ether in hexanes) to provide a combined 84% yield (31.9 mg). The major *syn* diastereomer was isolated as a white solid in >20:1 dr with 91% ee and the minor *anti* diastereomer was isolated in >20:1 dr with 76% ee as determined by chiral HPLC analysis. Absolute and relative stereochemistry was determined by X-Ray analysis of a single crystal of both the major and minor diastereomers. A single crystal of the major *syn* diastereomer was grown by slow evaporation of toluene at 0 °C. A

<sup>263</sup> Optical rotation measured on >99% ee material

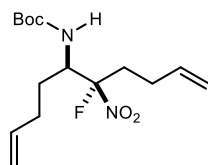
<sup>264</sup> Optical rotation measured on 11% ee material



single crystal of the minor *anti* diastereomer was grown by slow evaporation of benzene. See **4.2 X-Ray Crystallographic Data** for more details.

**Major diastereomer (syn):** White solid, mp = 91-93 °C;  $[\alpha]_D^{20} +24.7$  (*c* 0.92, CHCl<sub>3</sub>); Chiralpak OD-H, 2% *i*PrOH/hexanes, 1.0 mL/min, 25 °C:  $t_r(e_1, \text{major}) = 3.6$  min,  $t_r(e_2, \text{minor}) = 4.0$  min;  $R_f = 0.53$  (10% Et<sub>2</sub>O/hexanes); IR (film) 3352, 2958, 2869, 1716, 1564, 1502, 1368, 1163 cm<sup>-1</sup>; <sup>1</sup>H NMR (600 MHz, CDCl<sub>3</sub>)  $\delta$  7.29-7.27 (br m, 2H), 7.22-7.20 (br m, 1H), 7.15 (d, *J* = 7.2 Hz, 2H), 4.94 (d, *J* = 10.3 Hz, 1H), 4.35 (apparent dd, <sup>3</sup>*J*<sub>HH</sub> = 10.2 Hz, <sup>3</sup>*J*<sub>HF</sub> = 20.2 Hz, 1H), 2.95-2.90 (m, 1H), 2.59-2.46 (series of m, 3H), 1.59 (br d, *J* = 13.5 Hz, 1H), 1.44 (s, 9H), 1.07 (dd, *J* = 14.4, 10.2 Hz, 1H), 0.95 (s, 9H); <sup>13</sup>C NMR (150 MHz, CDCl<sub>3</sub>) 155.1, 139.3, 128.8, 128.5, 126.7, 122.6 (d, <sup>1</sup>*J*<sub>CF</sub> = 244.7 Hz), 80.7, 51.6 (d, <sup>2</sup>*J*<sub>CF</sub> = 29.4 Hz), 42.7, 36.3 (d, <sup>2</sup>*J*<sub>CF</sub> = 20.8 Hz), 29.5, 28.4, 28.4 (d, <sup>3</sup>*J*<sub>CF</sub> = 3.4 Hz); <sup>19</sup>F NMR (376 MHz, CDCl<sub>3</sub>)  $\delta$  -131.3; HRMS (ESI): Exact mass calcd for C<sub>20</sub>H<sub>31</sub>FN<sub>2</sub>NaO<sub>4</sub> [M+Na]<sup>+</sup> 405.2160, found 405.2160.

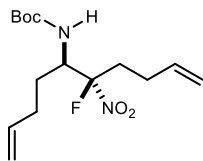
**Minor diastereomer (anti):** White solid, mp = 98-103 °C;  $[\alpha]_D^{20} -25.9$  (*c* 0.21, CHCl<sub>3</sub>); Chiralpak AD-H, 3% EtOH/hexanes, 0.8 mL/min, 25 °C:  $t_r(e_1, \text{major}) = 5.2$  min,  $t_r(e_2, \text{minor}) = 6.0$  min.  $R_f = 0.33$  (10% Et<sub>2</sub>O/hexanes); <sup>1</sup>H NMR (600 MHz, CDCl<sub>3</sub>)  $\delta$  7.28 (br dd, *J* = 7.3, 6.8 Hz, 2H), 7.21 (dd, *J* = 7.4, 7.4 Hz, 1H), 7.14 (d, *J* = 7.3 Hz, 2H), 4.58 (dddd, <sup>3</sup>*J*<sub>HF</sub> = 24.5 Hz, <sup>3</sup>*J*<sub>HH</sub> = 9.8, 9.8, 1.4 Hz, 1H), 4.45 (d, *J* = 9.6 Hz, 1H), 2.74 (ddd, *J* = 12.7, 12.7, 4.5 Hz, 1H), 2.68-2.58 (m, 1H), 2.52 (ddd, *J* = 12.6, 12.6, 4.5 Hz, 1H), 2.39-2.33 (m, 1H), 1.43 (s, 9H), 1.33-1.29 (m, 2H), 0.92 (s, 9H); <sup>13</sup>C NMR (150 MHz, CDCl<sub>3</sub>) ppm 155.2, 139.3, 128.7, 128.4, 126.6, 123.4 (<sup>1</sup>*J*<sub>CF</sub> = 246 Hz), 80.8, 52.6 (<sup>2</sup>*J*<sub>CF</sub> = 22 Hz), 42.8, 35.7 (<sup>2</sup>*J*<sub>CF</sub> = 21 Hz), 30.2, 29.5, 28.5, 28.3 (<sup>3</sup>*J*<sub>CF</sub> = 4 Hz); <sup>19</sup>F NMR (376 Hz, CDCl<sub>3</sub>)  $\delta$  -140.1; HRMS (ESI): Exact mass calcd for C<sub>20</sub>H<sub>31</sub>FN<sub>2</sub>NaO<sub>4</sub> [M+Na]<sup>+</sup> 405.2166, found 405.2158.



***tert*-Butyl ((5*R*,6*S*)-6-fluoro-6-nitrodeca-1,9-dien-5-yl)carbamate (*syn*-62).**

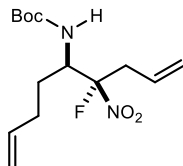
Prepared according to general procedure C using *tert*-butyl (1-tosylpent-4-en-1-yl)carbamate (340 mg, 1.00 mmol), 5-fluoro-5-nitropent-1-ene (666 mg, 5.00 mmol), CsOH·H<sub>2</sub>O (218 mg, 1.30 mmol), *N*-benzyl quininium chloride (54.1 mg, 0.12 mmol) and toluene (666 mL). Concentration after workup afforded a 5.4:1 mixture of diastereomers (<sup>19</sup>F NMR) which were purified by column chromatography (2-5-8-10% diethyl ether in hexanes) to provide an oil (280.8 mg, 89%). The major diastereomer **9** was obtained as a viscous oil and found to be 91% ee by chiral HPLC (Chiralpak IC: 2% *i*PrOH/hexanes, 1.0

mL/min:  $t_r$  ( $e_1$  major) = 4.7 min,  $t_r$  ( $e_2$  minor) = 6.7 min).  $[\alpha]_D^{24} +29.5$  ( $c$  0.74,  $\text{CHCl}_3$ );<sup>265</sup>  $R_f$  = 0.68 (20% EtOAc/hexanes); IR (film) 3419, 3340, 2981, 2932, 1720, 1570, 1503, 1164  $\text{cm}^{-1}$ ;  $^1\text{H}$  NMR (400 MHz,  $\text{CDCl}_3$ )  $\delta$  5.81-5.67 (m, 2H), 5.06-4.99 (m, 4H), 4.87 (d,  $J$  = 10.6 Hz, 1H), 4.26 (ddd,  $^3J_{\text{HF}}$  = 22.3 Hz,  $J$  = 11.2, 2.7 Hz, 1H), 2.46–2.15 (series of multiplets, 4H), 2.09 (dd,  $J$  = 14.8, 7.5 Hz, 1H), 1.99-1.92 (m, 1H), 1.85-1.78 (m, 1H), 9.06 (s, 9H), 1.29-1.19 (m, 1H);  $^{13}\text{C}$  NMR (100 MHz,  $\text{CDCl}_3$ ) 155.3, 136.6, 135.3, 122.2 (d,  $^1J_{\text{CF}}$  = 244 Hz), 116.5, 116.4, 80.7, 53.9 (d,  $^2J_{\text{CF}}$  = 28.4 Hz), 33.9 (d,  $^2J_{\text{CF}}$  = 20.9 Hz), 29.64, 29.60, 28.3, 26.2 (d,  $^3J_{\text{CF}}$  = 3.4 Hz);  $^{19}\text{F}$  NMR (376 MHz,  $\text{CDCl}_3$ )  $\delta$  -132.5; HRMS (ESI): Exact mass calcd for  $\text{C}_{15}\text{H}_{25}\text{FN}_2\text{NaO}_4$   $[\text{M}+\text{Na}]^+$  339.1696, found 339.1700.



***tert*-Butyl ((5*R*,6*S*)-6-fluoro-6-nitrodeca-1,9-dien-5-yl)carbamate (*anti*-62).**

The minor diastereomer *anti*-62 was obtained as a white solid and found to be 98% ee by chiral HPLC (Chiralpak IA: 5% EtOH/hexanes, 1.0 mL/min:  $t_r$  ( $e_1$  major) = 4.04 min,  $t_r$  ( $e_2$  minor) = 4.48 min). Mp = 47.5-49.0 °C;  $[\alpha]_D^{24} -20.5$  ( $c$  0.57,  $\text{CHCl}_3$ );  $R_f$  = 0.68 (20% EtOAc/hexanes); IR (film) 3419, 3340, 2981, 2932, 1720, 1570, 1503, 1164  $\text{cm}^{-1}$ ;  $^1\text{H}$  NMR (400 MHz, acetone- $d_6$ )  $\delta$  6.47 (d,  $J$  = 9.2 Hz, 1H), 5.84-5.71 (m, 2H), 5.08-4.96 (br m, 4H), 4.41 (dddd,  $^3J_{\text{HF}}$  = 22.8 Hz,  $J$  = 11.6, 9.9, 2.7 Hz, 1H), 2.50-2.34 (m, 1H), 2.31-2.12 (m, 3H), 1.96-1.87 (m, 1H), 1.73 (dddd,  $J$  = 17.1, 8.2, 8.2, 5.3 Hz, 1H), 1.43 (s, 9H), 1.41-1.27 (m, 2H);  $^{13}\text{C}$  NMR (100 MHz, acetone- $d_6$ ) ppm 156.9, 137.8, 136.8, 123.9 (d,  $^1J_{\text{CF}}$  = 245.9 Hz), 116.5, 116.4, 80.1, 55.4 (d,  $^2J_{\text{CF}}$  = 21.9 Hz), 34.0 (d,  $^2J_{\text{CF}}$  = 21.6 Hz), 28.6, 27.9 ( $^3J_{\text{CF}}$  = 3.3 Hz), 26.8 (d,  $^3J_{\text{CF}}$  = 3.9 Hz);  $^{19}\text{F}$  NMR (376 MHz,  $\text{CDCl}_3$ )  $\delta$  -132.5.

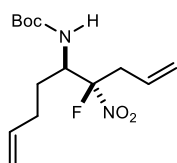


***tert*-Butyl ((4*S*,5*R*)-4-fluoro-4-nitronona-1,8-dien-5-yl)carbamate (*syn*-66).**

Prepared according to the general procedure using *tert*-butyl (1-tosylpent-4-en-1-yl)carbamate (3.42 g, 10.1 mmol), 4-fluoro-4-nitrobut-1-ene (5.40 g, 45.3 mmol),  $\text{CsOH}\cdot\text{H}_2\text{O}$  (2.20 g, 13.1 mmol), *N*-benzyl quininium chloride (682 mg, 1.51 mmol) and toluene (100 mL). Concentration after workup afforded an 8.2:1 mixture of diastereomers which were purified by column chromatography (3-5-8-10% diethyl ether in hexanes) to provide the title compound (2.53 g, 83%). The major diastereomer 8 was obtained as a white solid and found to be 95% ee by chiral HPLC (Chiralpak IC: 5% *i*PrOH/hexanes, 1.0

<sup>265</sup> Optical rotation measured for 94% ee material.

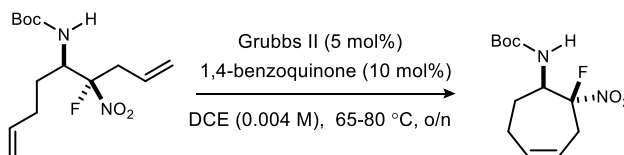
mL/min:  $t_r$  ( $e_1$  major) = 4.4 min,  $t_r$  ( $e_2$  minor) = 6.5 min). Mp = 39.3-40.9 °C;  $[\alpha]_D^{23}$  +24.2 (c 0.74, CHCl<sub>3</sub>);  $R_f$  = 0.68 (20% EtOAc/hexanes); IR (film) 3333, 2980, 2932, 1707, 1570, 1505, 1454, 1392, 1368, 1345, 1248, 1165 cm<sup>-1</sup>; <sup>1</sup>H NMR (400 MHz, CDCl<sub>3</sub>)  $\delta$  5.81-5.63 (m, 2H), 5.26-5.19 (m, 2H), 5.06-5.01 (m, 2H), 4.89 (d,  $J$  = 10.8 Hz, 1H), 4.28 (ddd,  $J$  = 22.3, 11.2, 2.7 Hz, 1H), 3.00 (td,  $J$  = 21.8, 8.0 Hz, 1H), 2.96-2.87 (m, 1H), 2.22-2.13 (m, 1H), 2.13-2.04 (m, 1H), 1.86-1.78 (m, 1H), 1.45 (s, 9H), 1.28-1.19 (m, 1H); <sup>13</sup>C NMR (100 MHz, CDCl<sub>3</sub>) ppm 155.3, 136.6, 126.9 (d, <sup>3</sup> $J_{CF}$  = 3.7 Hz), 123.0, 121.8 (d, <sup>1</sup> $J_{CF}$  = 243.7 Hz), 116.4, 80.7, 53.8 (d, <sup>2</sup> $J_{CF}$  = 28.2 Hz), 39.1 (d, <sup>2</sup> $J_{CF}$  = 20.7 Hz), 29.6, 28.6, 28.4; <sup>19</sup>F NMR (376 MHz, CDCl<sub>3</sub>)  $\delta$  -132.0; HRMS (ESI): Exact mass calcd for C<sub>14</sub>H<sub>23</sub>FN<sub>2</sub>NaO<sub>4</sub> [M+Na]<sup>+</sup> 325.1540, found 325.1529.



**tert-Butyl ((4*R*,5*R*)-4-fluoro-4-nitronona-1,8-dien-5-yl) (*anti*-66).** Obtained as a white solid and found to be 90% ee by chiral HPLC (Chiralcel AD-H: 3% EtOH/hexanes, 1.0 mL/min:  $t_r$  ( $e_1$  major) = 4.6 min,  $t_r$  ( $e_2$  minor) = 5.2 min). Mp = 72.5-74.0 °C;  $[\alpha]_D^{23}$  -17.4 (c 0.52, CHCl<sub>3</sub>);  $R_f$  = 0.54 (20% EtOAc/hexanes); IR

(film) 3313, 2980, 2930, 1697, 1569, 1524, 1368, 1250, 1165 cm<sup>-1</sup>; <sup>1</sup>H NMR (600 MHz, CDCl<sub>3</sub>)  $\delta$  5.74-5.73 (m, 2H), 5.22-5.17 (m, 2H), 5.03-5.00 (m, 2H), 4.48 (br m, 1H), 4.45 (ddd, <sup>3</sup> $J_{HF}$  = 20.8 Hz,  $J$  = 10.3, 2.4 Hz, 1H), 3.03-2.94 (m, 1H), 2.91-2.86 (m, 1H), 2.19-2.13 (m, 1H), 2.05 (ddd, <sup>3</sup> $J_{HF}$  = 22.4 Hz,  $J$  = 7.6, 7.6 Hz, 1H), 1.53-1.46 (m, 1H), 1.46 (s, 9H), 1.44-1.38 (m, 1H); <sup>13</sup>C NMR (100 MHz, CDCl<sub>3</sub>) ppm 155.4, 136.3, 127.1 (d, <sup>3</sup> $J_{CF}$  = 3.5 Hz), 122.4, 122.3 (d, <sup>1</sup> $J_{CF}$  = 245.5 Hz), 116.5, 80.9, 54.2 (d, <sup>2</sup> $J_{CF}$  = 20.8 Hz), 39.0 (d, <sup>2</sup> $J_{CF}$  = 21.0 Hz), 29.6, 28.4, 27.8 (<sup>3</sup> $J_{CF}$  = 3.1 Hz); <sup>19</sup>F NMR (376 MHz, CDCl<sub>3</sub>)  $\delta$  -140.4.

### Grubbs ring closing metathesis and derivatization of cycloheptyl substrates



**tert-Butyl ((1*R*,2*S*)-2-fluoro-2-nitrocyclohept-4-en-1-yl)carbamate (67a).** A solution of *tert*-butyl ((4*S*,5*R*)-4-fluoro-4-nitronona-1,8-dien-5-yl)carbamate *syn*-66 (183 mg, 605  $\mu$ mol) in 1,2-dichloroethane (151 mL) was subjected to 2 cycles of freeze-pump-thaw (-196 °C) and the flask was back-filled with nitrogen. Grubbs II catalyst (25.7 mg, 30.3  $\mu$ mol) and 1,4-benzoquinone (6.5 mg, 60  $\mu$ mol) were added to the flask, which was subjected to 2 additional cycles of free-pump-

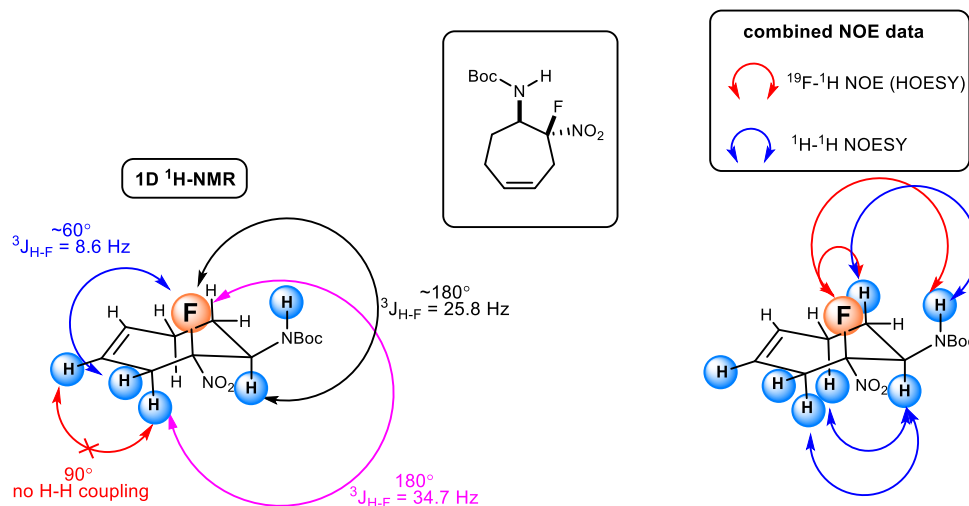
thaw, backfilled with nitrogen, and heated at 70-80 °C for 18 hours. The reaction was cooled to room temperature and concentrated. The residue was purified by flash column chromatography (10-15-20-30% Et<sub>2</sub>O in hexanes) to afford the desired product as a white solid (148 mg, 89%). Mp = 76.5-77.0 °C;  $[\alpha]_D^{20} +93.0$  (*c* 0.11, CHCl<sub>3</sub>)<sup>266</sup>; R<sub>f</sub> = 0.42 (20% EtOAc/hexanes); IR (film) 3317, 2978, 2832, 1715, 1568, 1504, 1393, 1367, 1248, 1170, 801 cm<sup>-1</sup>; <sup>1</sup>H NMR (600 MHz, CDCl<sub>3</sub>) δ 6.13-6.09 (m, 1H), 5.59-5.55 (m, 1H), 4.78 (d, *J* = 9.6 Hz, 1H), 4.63 (dddd, <sup>3</sup>J<sub>HF</sub> = 34.7 Hz, *J* = 10.9, 10.9, 3.8 Hz, 1H), 3.16 (dd, <sup>3</sup>J<sub>HF</sub> = 34.7 Hz, *J* = 15.5 Hz, 1H), 2.69 (ddd, *J* = 15.7, 4.8 Hz, <sup>3</sup>J<sub>HF</sub> = 8.6 Hz, 1H), 2.33 (ddd, *J* = 15.2, 7.5, 7.5 Hz, 1H), 2.21 (br dd, *J* = 13.3, 13.3 Hz, 1H), 2.03-1.98 (m, 1H), 1.52-1.45 (m, 1H), 1.39 (s, 9H); <sup>13</sup>C NMR (150 MHz, CDCl<sub>3</sub>) ppm 154.3, 135.8, 121.5, 118.7 (<sup>1</sup>J<sub>CF</sub> = 243.8 Hz), 80.8, 57.4 (<sup>2</sup>J<sub>CF</sub> = 19 Hz), 33.9 (<sup>2</sup>J<sub>CF</sub> = 23 Hz), 29.6, 28.3, 24.2; <sup>19</sup>F NMR (376 MHz, CDCl<sub>3</sub>) δ -139.7. HRMS (ESI): Exact mass calcd for C<sub>12</sub>H<sub>19</sub>FN<sub>2</sub>NaO<sub>4</sub> [M+Na]<sup>+</sup> 297.1227, found 297.1224.

Relative stereochemistry was assigned using 1D and 2D NMR (Figure 40). First, the C-H connectivity was determined by HSQC, COSY and HMBC. The coupling constants (*J*<sub>HH</sub> and *J*<sub>HF</sub>) were used to assign axial and equatorial positions around the ring. This was further confirmed by NOE interactions. Both <sup>1</sup>H-<sup>1</sup>H-NOESY and <sup>19</sup>F-<sup>1</sup>H NOE (HOESY) experiments were run, and the through space interactions further supported the assigned stereochemistry.

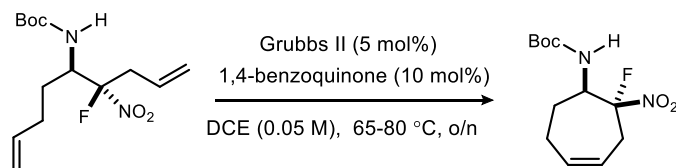
---

<sup>266</sup> Optical rotation measured on material with >99:1 r.r. which was obtained from a single diastereomer (>99% ee) of the linear precursor

Figure 40. Key NMR correlations for the stereochemical assignment of 67a.

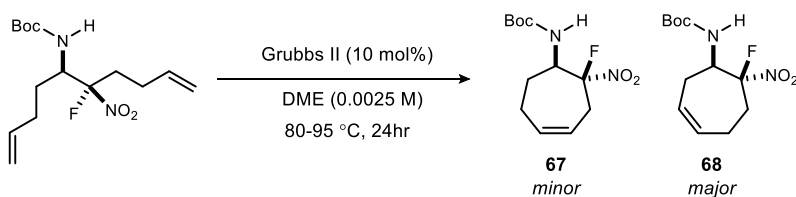


Absolute and relative stereochemistry were confirmed by X-Ray analysis of a single crystal of the major diastereomer grown by slow diffusion of hexanes into ethyl acetate. See **4.2 X-Ray Crystallographic Data** for more details. Further evidence was obtained by X-ray crystallography that confirmed the absolute and relative stereochemistry of the (1*R*,2*R*) diastereomer **67b**.



**tert-Butyl ((1*R*,2*R*)-2-fluoro-2-nitrocyclohept-4-en-1-yl)carbamate (67b)**. A solution of *tert*-butyl ((4*R*,5*R*)-4-fluoro-4-nitronona-1,8-dien-5-yl)carbamate *anti*-**66** (39 mg, 129  $\mu$ mol) in DCE (2.6 mL) was subjected to 2 cycles of freeze-pump-thaw (-196  $^{\circ}$ C) and the flask was back-filled with nitrogen. Grubbs II catalyst (5.6 mg, 6.45  $\mu$ mol) and 1,4-benzoquinone (1.4 mg, 12.9  $\mu$ mol) were added to the flask, which was subjected to 2 additional cycles of free-pump-thaw, backfilled with nitrogen, and heated at 70-80  $^{\circ}$ C for 18 hours. The reaction was cooled to room temperature and concentrated. The residue was purified by flash column chromatography (10-15-20-30% Et<sub>2</sub>O/hexanes) to afford the desired product as a white solid (24.3 mg, 69%). Mp = 110.5-111.2

°C,  $[\alpha]_D^{23} +22.4$  (*c* 0.54, CHCl<sub>3</sub>)<sup>267</sup>; *R<sub>f</sub>* = 0.51 (20% EtOAc/hexanes); IR (film) 3265, 2977, 2932, 1703, 1561, 1367, 1165 cm<sup>-1</sup>; <sup>1</sup>H NMR (600 MHz, CDCl<sub>3</sub>) δ 6.05 (br s, 1H), 5.54-5.50 (m, 1H), 4.95 (d, *J* = 7.9 Hz, 1H), 4.42 (br m, 1H), 3.12 (ddd, <sup>3</sup>*J*<sub>HF</sub> = 23.9, *J* = 13.8, 6.5 Hz, 1H), 2.79 (d, *J* = 14.8 Hz, 1H), 2.36–2.30 (m, 1H), 2.27–2.21 (m, 1H), 1.99 (appt d, *J* = 4.1 Hz, 2H), 1.43 (s, 9H); <sup>13</sup>C NMR (150 MHz, CDCl<sub>3</sub>) ppm 155.0, 135.8, 120.8 (d, <sup>3</sup>*J*<sub>CF</sub> = 7.9 Hz), 119.3 (d, <sup>1</sup>*J*<sub>CF</sub> = 240 Hz), 80.7, 56.3 (d, <sup>2</sup>*J*<sub>CF</sub> = 23.2 Hz), 33.3 (d, <sup>2</sup>*J*<sub>CF</sub> = 23.2 Hz), 29.8 (d, <sup>3</sup>*J*<sub>CF</sub> = 6.6 Hz). 28.4, 24.3; <sup>19</sup>F NMR (376 MHz, CDCl<sub>3</sub>) δ -114.3; HRMS (ESI): Exact mass calcd for C<sub>12</sub>H<sub>19</sub>FN<sub>2</sub>NaO<sub>4</sub> [M+Na]<sup>+</sup> 297.1227, found 297.1241. Absolute and relative stereochemistry were determined by X-Ray analysis of a single crystal of the major diastereomer grown by slow evaporation of ethyl acetate. See **4.2 X-Ray Crystallographic Data** for more details.

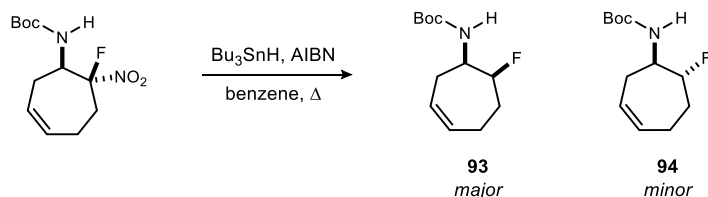


***tert*-Butyl ((1*R*,7*S*)-7-fluoro-7-nitrocyclohept-3-en-1-yl)carbamate (68).** A solution of *tert*-butyl ((5*R*,6*R*)-6-fluoro-6-nitrodeca-1,9-dien-5-yl)carbamate (150 mg, 474 μmol) in DME (215 mL) was subjected to 3 cycles of freeze-pump-thaw (-196 °C) and the flask was back-filled with nitrogen. Grubbs II catalyst (40.3 mg, 47.4 μmol) was added to the flask, which was subjected to 2 additional cycles of free-pump-thaw, backfilled with nitrogen, and refluxed for 24 hours. The reaction was cooled to room temperature and concentrated to afford a 1:2.5 **11**:**12** mixture of regioisomers. The residue was purified by flash column chromatography (10-15-17-20% Et<sub>2</sub>O/hexanes) to afford the cyclized products (81.5 mg, 75%). The major regioisomer **12** was obtained as a clear oil;  $[\alpha]_D^{24} +34.1$  (*c* 0.45, CHCl<sub>3</sub>);<sup>268</sup> *R<sub>f</sub>* = 0.51 (20% EtOAc/hexanes); IR (film) 3323, 2977, 2922, 2851, 1719, 1569, 1367, 1248, 1169 cm<sup>-1</sup>; <sup>1</sup>H NMR (600 MHz, CDCl<sub>3</sub>) δ 5.98-5.93 (m, 1H), 5.84-5.80 (m, 1H), 4.83 (d, *J* = 9.6 Hz, 1H), 4.55 (dddd, <sup>3</sup>*J*<sub>HF</sub> = 25.4 Hz, *J* = 10.3, 10.3, 1.6 Hz, 1H), 2.52 (br dd, *J* = 13.7, 13.7 Hz, 1H), 2.41-2.27 (m, 4H), 2.23-2.18 (m, 1H), 1.39

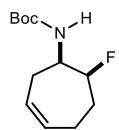
<sup>267</sup> Optical rotation measured on material derived from aza-Henry adduct with 90% ee

<sup>268</sup> Optical rotation measured on material that was >99:1 rr, and derived from aza-Henry adduct with 99% ee

(s, 9H);  $^{13}\text{C}$  NMR (125 MHz,  $\text{CDCl}_3$ ) ppm 154.4, 132.5, 127.8, 122.2 ( $^1J_{\text{CF}} = 241.5$  Hz), 80.8, 53.3 ( $^2J_{\text{CF}} = 18.5$  Hz), 35.2 ( $^2J_{\text{CF}} = 22.1$  Hz), 30.6, 28.3, 21.4;  $^{19}\text{F}$  NMR (376 MHz,  $\text{CDCl}_3$ )  $\delta$  -138.5; HRMS (ESI): Exact mass calcd for  $\text{C}_{12}\text{H}_{19}\text{FN}_2\text{NaO}_4$   $[\text{M}+\text{Na}]^+$  297.1227, found 297.1233.



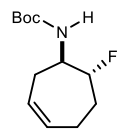
**Reductive denitration of 68.** To a flame-dried vial was added the fluoronitroalkane (34.0 mg, 124  $\mu\text{mol}$ , 16:1 mixture of regioisomers) and dry benzene (620  $\mu\text{L}$ ). To a separate flame-dried vial was added tributyltin hydride (334  $\mu\text{L}$ , 1.24 mmol) and of dry benzene (884  $\mu\text{L}$ ). Both vials were subjected to three cycles of freeze-pump-thaw and backfilled with inert gas. To the flask containing tributyltin hydride was added AIBN (16.2 mg, 49.6  $\mu\text{mol}$ ) and the resulting mixture was added to a refluxing solution of the fluoronitroalkane in 100  $\mu\text{L}$  portions every 25 minutes until the reaction was complete (as indicated by TLC). This reaction was complete after the addition of 450  $\mu\text{L}$  of the stock solution (123  $\mu\text{L}$ , 458  $\mu\text{mol}$  of  $\text{Bu}_3\text{SnH}$  and 6.1 mg, 37  $\mu\text{mol}$  of AIBN). The reaction was cooled to room temperature and concentrated to yield a 1.8:1 mixture of diastereomers ( $^{19}\text{F}$  NMR). Column chromatography (2-5-8-10-15%  $\text{Et}_2\text{O}$  in hexanes) provided both diastereomers (14.9 mg, 52%).



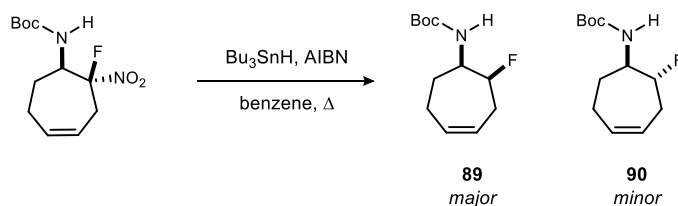
**tert-Butyl ((1R,7S)-7-fluorocyclohept-3-en-1-yl)carbamate (93).** The major diastereomer **S6** was isolated as a clear oil. Clear oil,  $[\alpha]_D^{23} +18.3$  ( $c$  0.06,  $\text{CHCl}_3$ );<sup>269</sup>  $R_f = 0.63$  (20%  $\text{EtOAc}$ /hexanes); IR (film) 3360, 2960, 1923, 2853, 1670, 1464, 1261, 1093, 1019, 802  $\text{cm}^{-1}$ ;  $^1\text{H}$  NMR (600 MHz,  $\text{CDCl}_3$ )  $\delta$  5.91-5.88 (m, 1H), 5.74-5.71 (m, 1H), 4.95 (d,  $J = 7.5$  Hz, 1H), 4.85 (dd,  $^2J_{\text{HF}} = 46.4$  Hz,  $J = 5.6$  Hz, 1H), 3.80 (ddd,  $^3J_{\text{HF}} = 27.7$  Hz,  $J = 10.3$ ,

<sup>269</sup> Derived from aza-Henry adduct with 86% ee

10.3 Hz, 1H), 2.62 (ddd,  $J = 12.4, 12.4, 3.0$  Hz, 1H), 2.38-2.33 (m, 1H), 2.03 (ddd,  $J = 15.8, 7.7, 1.2$  Hz, 1H), 1.98-1.91 (m, 2H), 1.83-1.73 (m, 1H), 1.45 (s, 9H);  $^{13}\text{C}$  NMR (150 MHz,  $\text{CDCl}_3$ ) ppm 155.2, 133.5, 128.0, 95.3 ( $^1J_{\text{CF}} = 172.7$  Hz), 79.7, 51.3 ( $^2J_{\text{CF}} = 18.6$  Hz), 30.3 ( $^2J_{\text{CF}} = 21.1$  Hz), 28.5, 28.4 ( $^3J_{\text{CF}} = 5.2$  Hz), 20.8 ( $^3J_{\text{CF}} = 6.7$  Hz);  $^{19}\text{F}$  NMR (376 MHz,  $\text{CDCl}_3$ )  $\delta$  -193.6. HRMS (ESI): Exact mass calcd for  $\text{C}_{12}\text{H}_{20}\text{FNNaO}_2$   $[\text{M}+\text{Na}]^+$  252.1376, found 252.1365.

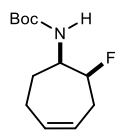


**tert-Butyl ((1*R*,7*R*)-7-fluorocyclohept-3-en-1-yl)carbamate (94).** The minor diastereomer **S7** was isolated as a white solid; mp = 82.5-83.5 °C;  $[\alpha]_D^{24}$  -10.6 ( $c$  0.19,  $\text{CHCl}_3$ );<sup>269</sup>  $R_f = 0.56$  (20% EtOAc/hexanes);  $^1\text{H}$  NMR (600 MHz,  $\text{CDCl}_3$ )  $\delta$  5.94-5.91 (m, 1H), 5.69-5.65 (m, 1H), 4.62 (dddd,  $^2J_{\text{HF}} = 46.2$  Hz,  $J = 9.9, 3.3, 3.3$  Hz), 3.85 (br m, 1H), 2.60-2.58 (br m, 1H), 2.40-2.36 (m, 1H), 2.16 (ddd,  $J = 15.4, 8.0, 6.9$  Hz, 1H), 1.99-1.94 (m, 1H), 1.91-1.88 (m, 1H), 1.87-1.84 (m, 1H), 1.44 (s, 9H);  $^{13}\text{C}$  NMR (150 MHz,  $\text{CDCl}_3$ ) ppm 155.2, 133.9, 127.1, 94.3, (d,  $^1J_{\text{CF}} = 174.3$  Hz), 79.6, 51.3, ( $^2J_{\text{CF}} = 18.8$  Hz), 29.2 (d,  $^2J_{\text{CF}} = 21.1$  Hz), 28.4, 28.1 (d,  $^3J_{\text{CF}} = 3.2$  Hz), 21.3 (d,  $^3J_{\text{CF}} = 6.6$  Hz);  $^{19}\text{F}$  NMR (376 Hz,  $\text{CDCl}_3$ )  $\delta$  -176.7.

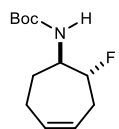


**Reductive denitration of 67.** To a flame-dried flask was added the fluoronitroalkane (350 mg, 1.28 mmol) and dry benzene (6.4 mL). To a separate flame-dried flask was added tributyltin hydride (2.58 mL, 9.6 mmol) and dry benzene (6.9 mL). Both flasks were subjected to three cycles of freeze-pump-thaw and backfilled with inert gas. To the flask containing tributyltin hydride was added AIBN (126 mg, 765  $\mu\text{mol}$ ) and the resulting mixture was added to a refluxing solution of the fluoronitroalkane in 0.5 to 1.0 mL portions every 25 minutes until the reaction was complete as indicated by TLC. This reaction was complete after the addition of 7.3 mL of the stock solution (1.99 mL, 7.42 mmol of  $\text{Bu}_3\text{SnH}$  and 97.2 mg, 592  $\mu\text{mol}$  of AIBN). The reaction was cooled to room temperature and concentrated to yield a 1.7:1 mixture of diastereomers ( $^{19}\text{F}$  NMR). Column chromatography (2-5-8-10-15%  $\text{Et}_2\text{O}$  in hexanes) provided both diastereomers (263 mg, 90%).





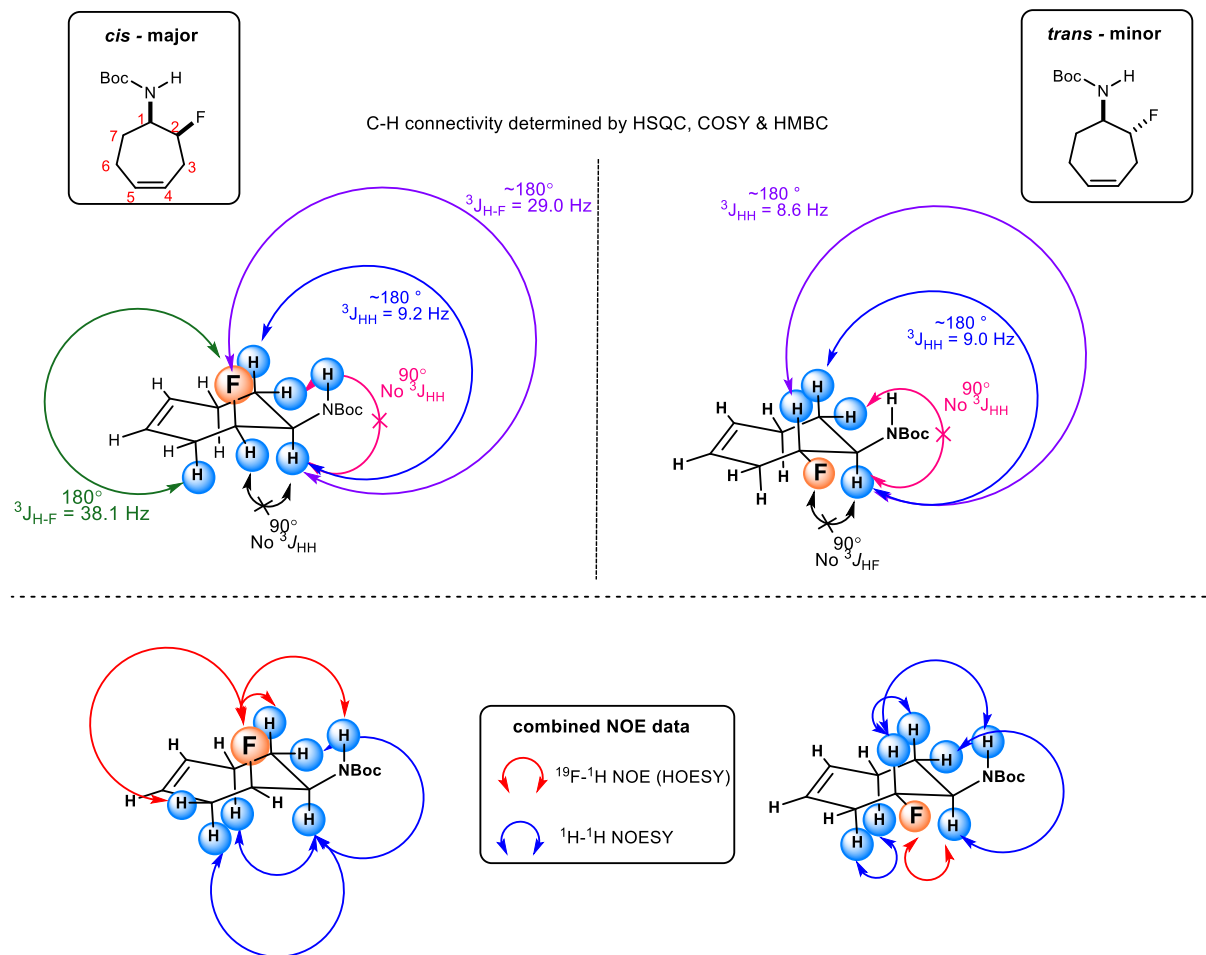
**tert-Butyl ((1*R*,2*S*)-2-fluorocyclohept-4-en-1-yl)carbamate (89).** The major diastereomer was isolated as a white solid; mp = 60.3-61.4 °C;  $[\alpha]_D^{23} +42.1$  (*c* 0.50, CHCl<sub>3</sub>);<sup>270</sup> *R<sub>f</sub>* = 0.59 (20% EtOAc/hexanes); IR (film) 3343, 2977, 2935, 1698, 1503, 1366, 1249, 1169 cm<sup>-1</sup>; <sup>1</sup>H NMR (600 MHz, CDCl<sub>3</sub>) δ 5.96-5.92 (m, 1H), 5.56-5.52 (m, 1H), 4.94 (br s, 1H), 4.78 (dd, <sup>2</sup>*J*<sub>HF</sub> = 48.3 Hz, *J* = 6.9 Hz, 1H), 3.80 (br dt, <sup>3</sup>*J*<sub>HF</sub> = 29.0, *J* = 9.21 Hz, 1H), 2.67-2.61 (m, 1H), 2.30 (ddd, <sup>3</sup>*J*<sub>HF</sub> = 38.1 Hz, *J* = 16.0, 1.6 Hz, 1H), 2.23 (dddd, *J* = 15.6, 7.7, 7.7, 1.9 Hz, 1H), 2.05 (br dd, *J* = 13.2, 13.2 Hz, 1H), 1.73-1.70 (m, 1H), 1.63-1.55 (m, 1H), 1.44 (s, 9H); <sup>13</sup>C NMR (100 MHz, CDCl<sub>3</sub>) ppm 155.1, 133.6, 124.2 (<sup>3</sup>*J*<sub>CF</sub> = 5.7 Hz), 91.1 (<sup>1</sup>*J*<sub>CF</sub> = 174 Hz), 79.7, 56.2 (<sup>2</sup>*J*<sub>CF</sub> = 19.4 Hz), 30.0 (<sup>2</sup>*J*<sub>CF</sub> = 22.4 Hz), 28.5, 27.5, 24.8; <sup>19</sup>F NMR (376 MHz, CDCl<sub>3</sub>) δ -197.0 Hz. HRMS (ESI): Exact mass calcd for C<sub>12</sub>H<sub>20</sub>FNNaO<sub>2</sub> [M+Na]<sup>+</sup> 252.1376, found 252.1378.



**tert-Butyl ((1*R*,2*R*)-2-fluorocyclohept-4-en-1-yl)carbamate (90).** The minor diastereomer was isolated as a white solid; mp = 120.5–121.3 °C.  $[\alpha]_D^{23} -30.4$  (*c* 0.67, CHCl<sub>3</sub>);<sup>270</sup> *R<sub>f</sub>* = 0.54 (20% EtOAc/hexanes); IR (film) 3360, 2985, 2940, 1683, 1526, 1445, 1320, 1264, 1246, 1172 cm<sup>-1</sup>; <sup>1</sup>H NMR (600 MHz, CDCl<sub>3</sub>) δ 5.93-5.89 (m, 1H), 5.63-5.59 (m, 1H), 4.68 (br s, 1H), 4.15 (dddd, <sup>2</sup>*J*<sub>HF</sub> = 48.6 Hz, *J* = 8.6, 8.6, 4.9 Hz, 1H), 3.82 (br m, 1H), 2.56-2.46 (m, 2H), 2.16-2.11 (m, 1H), 2.08-2.06 (m, 1H), 2.03-2.01 (m, 1H), 1.43 (s, 9H), 1.41-1.35 (m, 1H); <sup>13</sup>C NMR (100 MHz, CDCl<sub>3</sub>) ppm 155.5, 134.8, 124.2 (<sup>3</sup>*J*<sub>CF</sub> = 14.5 Hz), 92.7 (<sup>1</sup>*J*<sub>CF</sub> = 177 Hz), 79.7, 57.9 (<sup>2</sup>*J*<sub>CF</sub> = 19.3 Hz), 31.7 (<sup>2</sup>*J*<sub>CF</sub> = 23.1 Hz), 30.9 (<sup>3</sup>*J*<sub>CF</sub> = 6.3 Hz), 28.5, 24.0; <sup>19</sup>F NMR (376 MHz, CDCl<sub>3</sub>) δ -171.4.

<sup>270</sup> Derived from aza-Henry adduct with 91% ee

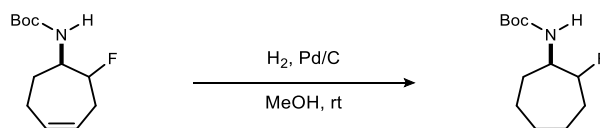
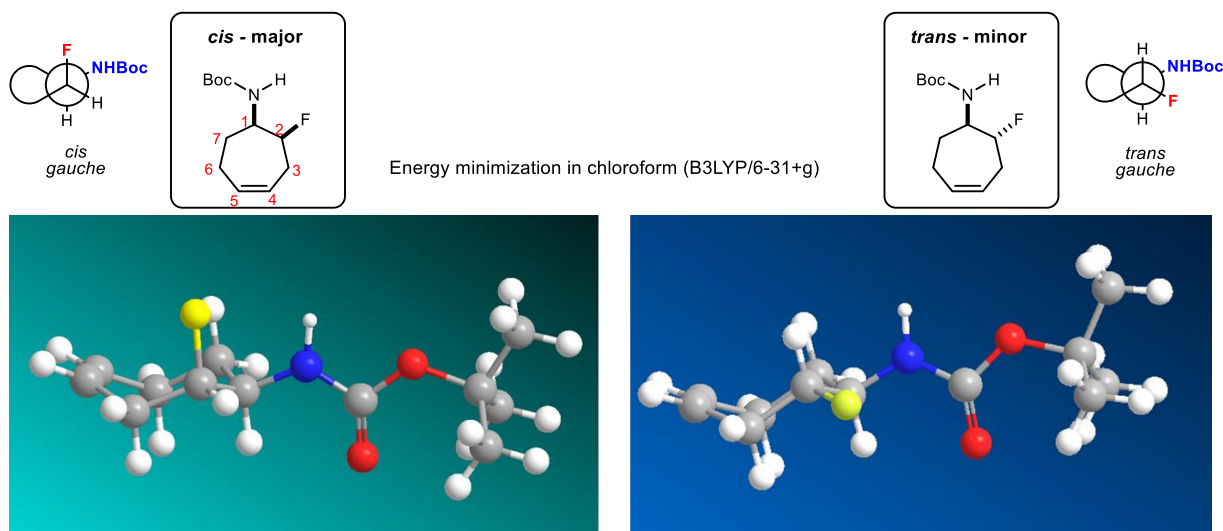
Figure 41. Key NMR correlations for the stereochemical assignment of the major and minor diastereomers from reductive denitration of 67.



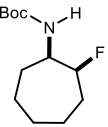
Relative stereochemistry was assigned using 1D and 2D NMR (**Figure 1**). First, the C-H connectivity was determined by HSQC, COSY and HMBC. The coupling constants ( $J_{HH}$  and  $J_{HF}$ ) were used to assign axial and equatorial positions around the ring. This was further confirmed by NOE interactions. Both  $^1\text{H}-^1\text{H}$ -NOESY and  $^{19}\text{F}-^1\text{H}$  NOE (HOESY) experiments were run, and the through space interactions further supported the assigned stereochemistry. Finally, energy minimization in chloroform (B3LYP/6-31+g), showed that the conformation used when assigning stereochemistry by NMR, were the lowest energy conformations for the respective diastereomers (Figure 42).<sup>271</sup>

<sup>271</sup> Calculations were performed by Thomas J. Struble.

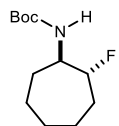
Figure 42. Lowest energy conformations of cis and trans cycloheptenyl  $\beta$ -fluoroamines 89 and 90.



**General procedure for alkene hydrogenation.** A solution of the cycloheptene in MeOH (0.05 M) was added to a round bottom flask charged with Pd/C (10% by weight) under an inert atmosphere. The flask was evacuated and backfilled with hydrogen three times then let stir under a hydrogen atmosphere. Upon completion, the reaction was filtered through a pad of Celite to afford the desired compound.

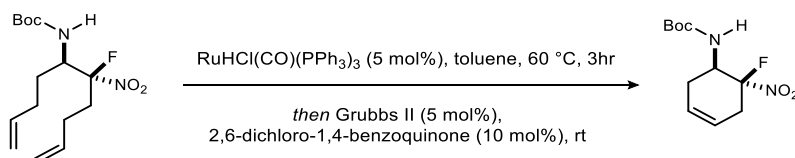
 **tert-Butyl ((1*R*,2*S*)-2-fluorocycloheptyl)carbamate (91).** Under an argon atmosphere, MeOH (100 mL) was added to a solution of *tert*-butyl ((1*R*,2*S*)-2-fluorocyclohept-4-en-1-yl)carbamate (1.10 g, 4.80 mmol) in DCM (1.5 mL). Pd/C (10% w/w, 110 mg) was added to the solution, the flask was evacuated and backfilled with hydrogen three times and stirred under a hydrogen atmosphere. Upon completion, the reaction was filtered through a pad of Celite and concentrated. The resultant solid was dissolved in EtoAc and passed through a plug of silica gel to afford the desired compound as a white solid (1.16 g, quant).

Mp = 52.0-53.0 °C;  $[\alpha]_D^{23} +29.7$  (*c* 0.60, CHCl<sub>3</sub>);<sup>272</sup>  $R_f = 0.70$  (20% EtOAc/hexanes, ninhydrin stain); IR (film) 3332, 2977, 2933, 2865, 1716, 1502, 1366, 1172 cm<sup>-1</sup>; <sup>1</sup>H NMR (600 MHz, CDCl<sub>3</sub>) δ 4.97 (d, *J* = 5.9 Hz, 1H), 4.83 (d, <sup>1</sup>*J*<sub>HF</sub> = 48.9 Hz, 1H), 3.68 (ddd, <sup>2</sup>*J*<sub>HF</sub> = 30.3 Hz, *J* = 9.6, 9.6 Hz, 1H), 1.97-1.90 (m, 1H), 1.85-1.68 (series of multiplets, 4H), 1.64-1.57 (m, 2H), 1.57-1.48 (m, 2H), 1.43 (br s, 10H); <sup>13</sup>C NMR (150 MHz, CDCl<sub>3</sub>) ppm 155.3, 94.7 (d, <sup>1</sup>*J*<sub>CF</sub> = 172 Hz), 79.5, 54.9 (d, <sup>2</sup>*J*<sub>CF</sub> = 18.8 Hz), 31.2 (d, <sup>2</sup>*J*<sub>CF</sub> = 21.0 Hz), 28.7 (d, <sup>3</sup>*J*<sub>CF</sub> = 4.4 Hz), 28.5, 27.3, 24.9, 20.6 (d, <sup>3</sup>*J*<sub>CF</sub> = 5.7 Hz); <sup>19</sup>F NMR (376 MHz, CDCl<sub>3</sub>) δ -194.0.



***tert*-Butyl ((1*R*,2*R*)-2-fluorocycloheptyl)carbamate (92).** Prepared according to the general procedure using *tert*-butyl ((1*R*,2*R*)-2-fluorocyclohept-4-en-1-yl)carbamate (54 mg, 0.19 mmol). The product was obtained as a white solid (53.5 mg, 98%). Mp = 90.5-91.5 °C;  $[\alpha]_D^{24} -8.2$  (*c* 1.02, CHCl<sub>3</sub>);  $R_f = 0.60$  (20% EtOAc/hexanes); IR (film) 3366, 2980, 2941, 2861, 1683, 1525, 1244, 1170, 994 cm<sup>-1</sup>; <sup>1</sup>H NMR (600 MHz, CDCl<sub>3</sub>) δ 4.65 (br s, 1H), 4.39 (dddd, <sup>2</sup>*J*<sub>HF</sub> = 48.5 Hz, *J* = 7.6, 5.7, 5.7 Hz, 1H), 3.71 (br m, 1H), 1.92-1.87 (m, 3H), 1.72-1.60 (m, 3H), 1.56-1.48 (m, 1H), 1.47-1.39 (m, 12 H); <sup>13</sup>C NMR (150 MHz, CDCl<sub>3</sub>) ppm 155.6, 96.6 (<sup>1</sup>*J*<sub>CF</sub> = 173 Hz), 79.6, 56.6 (<sup>2</sup>*J*<sub>CF</sub> = 22.2 Hz), 31.8 (<sup>2</sup>*J*<sub>CF</sub> = 21.3 Hz), 30.6 (<sup>3</sup>*J*<sub>CF</sub> = 7.5 Hz), 28.6, 27.9, 24.4, 21.3 (<sup>3</sup>*J*<sub>CF</sub> = 8.0 Hz); <sup>19</sup>F NMR (376 MHz, CDCl<sub>3</sub>) δ -169.7. HRMS (ESI): Exact mass calcd for C<sub>12</sub>H<sub>22</sub>FNNaO<sub>2</sub> [M+Na]<sup>+</sup> 254.1532, found 254.1542.

### Tandem isomerization/ring closing metathesis

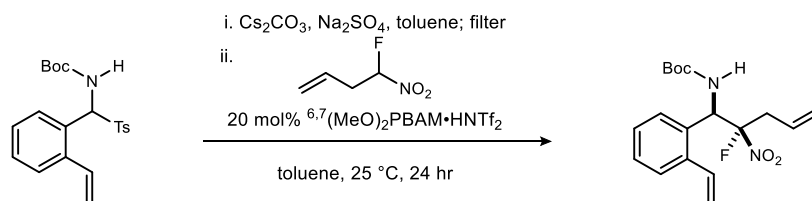


***tert*-Butyl ((1*R*,6*S*)-6-fluoro-6-nitrocyclohex-3-en-1-yl)carbamate (113).** Under an inert atmosphere RuHCl(CO)(PPh<sub>3</sub>)<sub>3</sub> (248 mg, 260 μmol) was added to a solution of *tert*-butyl ((5*R*,6*S*)-6-fluoro-6-nitrodeca-1,9-dien-5-yl)carbamate (1.64 g, 5.20 mmol) in dry toluene (52 mL), and the solution was degassed (freeze-pump-thaw, -196 °C), backfilled with nitrogen, and then stirred at

<sup>272</sup> Optical rotation measured on ≥97% ee material

60 °C for three hours or until complete conversion was observed by NMR. Upon completion, the flask was cooled to room temperature, Grubbs II catalyst (221 mg, 260  $\mu\text{mol}$ ) and 2,6-dichloro-1,4-benzoquinone (138 mg, 780  $\mu\text{mol}$ )<sup>273</sup> were added, and the solution was then degassed (freeze-pump-thaw, -196 °C), backfilled with nitrogen, and stirred at room temperature overnight. Concentration followed by column chromatography (10-15-20% Et<sub>2</sub>O in hexanes) provided the desired product as a white solid (1.21 g, 90%). Mp = 59.5-61.5 °C;  $[\alpha]_D^{24} +38.4$  (*c* 0.55, CHCl<sub>3</sub>);  $R_f = 0.49$  (20% EtOAc/hexanes, ninhydrin stain); IR (film) 3321, 2980, 1710, 1571, 1512, 1367, 1250, 1159 cm<sup>-1</sup>; <sup>1</sup>H NMR (600 MHz, CDCl<sub>3</sub>)  $\delta$  5.76-5.74 (m, 1H), 5.62-5.60 (m, 1H), 4.71 (br s, 1H), 4.71-4.64 (br m, 1H), 3.26 (ddd, <sup>3</sup>*J*<sub>HF</sub> = 35.2 Hz, *J* = 20.0, 1.5 Hz, 1H), 2.74-2.67 (m, 1H), 2.64 (br ddd, *J* = 17.4, 5.3, 5.3 Hz, 1H), 2.16 (br dd, *J* = 13.0, 12.7 Hz, 1H), 1.40 (s, 9H); <sup>13</sup>C NMR (150 MHz, CDCl<sub>3</sub>) ppm 154.6, 124.9, 120.9, 118.5 (d, <sup>1</sup>*J*<sub>CF</sub> = 240.2 Hz), 80.8, 50.0 (d, <sup>2</sup>*J*<sub>CF</sub> = 20.9 Hz), 35.3 (d, <sup>2</sup>*J*<sub>CF</sub> = 23.2 Hz), 30.4, 28.3; <sup>19</sup>F NMR (376 MHz, CDCl<sub>3</sub>)  $\delta$  139.6. HRMS (ESI): Exact mass calcd for C<sub>11</sub>H<sub>17</sub>FN<sub>2</sub>NaO<sub>4</sub> [M+Na]<sup>+</sup> 283.1065, found 283.1065.

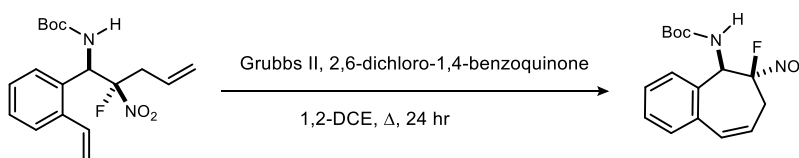
### Synthesis of benzannulated derivatives



***tert*-Butyl ((1*R*,2*S*)-2-fluoro-2-nitro-1-(2-vinylphenyl)pent-4-en-1-yl)carbamate (126).** To a flame-dried flask was added the *N*-Boc  $\alpha$ -amido sulfone (200 mg, 516  $\mu\text{mol}$ ), Cs<sub>2</sub>CO<sub>3</sub> (841 mg, 2.58 mmol), Na<sub>2</sub>SO<sub>4</sub> (367 mg, 2.58 mmol) and toluene (5.2 mL). The reaction was monitored by <sup>1</sup>H NMR, and after approximately 3 hours, it was filtered through a plug of dry Celite that was rinsed with toluene (1 mL) into a flask containing 1-fluoro-1-nitrobut-1-ene (73.8 mg, 619  $\mu\text{mol}$ ) and 6,7-(MeO)<sub>2</sub>PBAM·HNTf<sub>2</sub> (46.9 mg, 51.6  $\mu\text{mol}$ ). The reaction mixture was stirred for 24 hours and filtered through a plug of SiO<sub>2</sub> (EtOAc) to afford an 8.3:1 mixture of diastereomers. The crude oil was purified by column chromatography (5-10-20% diethyl ether in hexanes) to provide a colorless foam (135.2 mg, 76%) that was determined to be a 7.5:1 mixture of diastereomers (92

<sup>273</sup> On a small (<500 mg) scale, 10 mol% of the 2,6-dichloro-1,4-benzoquinone is used.

and 75% ee, respectively) by chiral HPLC (Chiralpak IC: 2% EtOH/hexanes, 1.0 mL/min:  $t_r$  (d<sub>1e1</sub> minor, minor) = 4.0 min,  $t_r$  (d<sub>2e2</sub> minor, major) = 4.7 min,  $t_r$  (d<sub>1e2</sub> major, major) = 5.2 min,  $t_r$  (d<sub>2e2</sub> major, minor) = 6.1 min). Characterized as a 7.5:1 ratio of diastereomers:  $[\alpha]_D^{23} +90.0$  ( $c$  0.73, CHCl<sub>3</sub>)<sup>274</sup>;  $R_f$  = 0.6 (20% EtOAc/hexanes); IR (film) 3424, 3322, 2924, 2853, 1696, 1571, 1503, 1367, 1249, 1169 cm<sup>-1</sup>; <sup>1</sup>H NMR (600 MHz, CDCl<sub>3</sub>)  $\delta$  7.50 (d,  $J$  = 8.7 Hz, 1H), 7.38-7.33 (m, 2H), 7.32-7.25 (m, 2H), 5.98 (dd,  $J$  = 22.9, 10.0 Hz, 1H), 5.70 (d,  $J$  = 17.2 Hz, 1H), 5.61-5.43 (series of m, 3H), 5.16 (d,  $J$  = 10.1 Hz, 1H), 5.10 (d,  $J$  = 17.0 Hz, 1H), 2.87 (ddd, <sup>3</sup> $J_{HF}$  = 33.8 Hz,  $J$  = 14.9, 8.1 Hz, 1H), 2.33 (ddd,  $J$  = 14.8, 7.4, 7.4 Hz, 1H), 1.38 (s, 9H); <sup>13</sup>C NMR (150 MHz, CDCl<sub>3</sub>) ppm 154.4, 138.6, 134.4, 132.6, 129.4, 128.7, 127.6, 126.8, 126.4, 122.7, 122.2 (<sup>1</sup> $J_{CF}$  = 247.1 Hz), 119.3, 81.0, 53.8 (<sup>2</sup> $J_{CF}$  = 19.9 Hz), 39.0 (<sup>2</sup> $J_{CF}$  = 21.0 Hz), 28.3; <sup>19</sup>F NMR (376 MHz, CDCl<sub>3</sub>)  $\delta$  -139.1; HRMS (ESI): Exact mass calcd for C<sub>18</sub>H<sub>23</sub>FNaN<sub>2</sub>O<sub>4</sub> [M+Na]<sup>+</sup> 373.1534, found 373.1537. Relative stereochemistry was assigned by conversion to the carbocycle **127** and subsequent X-ray analysis. See **4.2 X-Ray Crystallographic Data** for more details.



***tert*-Butyl ((5*R*,6*S*)-6-fluoro-6-nitro-6,7-dihydro-5*H*-benzo[7]annulen-5-yl)carbamate (**127**).**

To a solution of the diene (88.0 mg, 251  $\mu$ mol) in 1,2-dichloroethane (5.0 mL) was added Grubbs II catalyst (10.7 mg, 12.6  $\mu$ mol) and 2,6-dichloro-1,4-benzoquinone (4.4 mg, 25  $\mu$ mol), and the solution was subjected to 2 cycles of freeze-pump-thaw (liquid N<sub>2</sub>), backfilled with nitrogen, and warmed to reflux at 80-90 °C overnight. The reaction mixture was concentrated and the crude residue (12.4:1 dr) was purified by flash column chromatography (5-10-20% Et<sub>2</sub>O in hexanes) to afford the desired product as a white solid (78.8 mg, 97%). Mp = 146.5-148.5 °C;  $[\alpha]_D^{23} -185$  ( $c$  0.57, CHCl<sub>3</sub>)<sup>275</sup>;  $R_f$  = 0.36 (20% EtOAc/hexanes, KMnO<sub>4</sub> stain); IR (film) 3334, 2979, 1709, 1567, 1500, 1368, 1162 cm<sup>-1</sup>; <sup>1</sup>H NMR (600 MHz, CDCl<sub>3</sub>)  $\delta$  7.39-7.33 (m, 3H), 7.23 (d,  $J$  = 7.31 Hz, 1H), 6.88 (d,  $J$  = 10.5 Hz, 1H), 6.21-6.16 (m, 1H), 5.87 (dd, <sup>3</sup> $J_{HF}$  = 25.7 Hz,  $J$  = 10.2 Hz, 1H), 5.36 (d,  $J$  = 9.8 Hz, 1H), 2.83 (dd,  $J$  = 15.5, 7.7 Hz, 1H), 2.52 (dddd, <sup>3</sup> $J_{HF}$  = 17.4,  $J$  = 15.2, 4.8, 1.9 Hz,

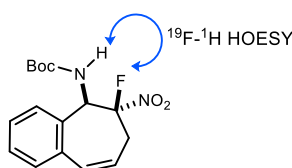
<sup>274</sup> Optical rotation measured on material with >7.5:1 dr, 92/75% ee.

<sup>275</sup> Optical rotation measured on >50:1 dr material derived from an aza-Henry adduct with 92% ee.

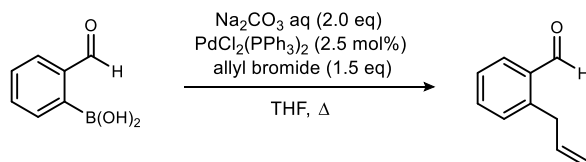
1H), 1.41 (s, 9H); <sup>13</sup>C NMR (150 MHz, CDCl<sub>3</sub>) ppm 154.4, 135.9, 133.8, 133.5, 129.1, 128.7, 128.3, 127.3 (d, <sup>1</sup>J<sub>CF</sub> = 247.7 Hz), 125.5, 125.4 (d, <sup>3</sup>J<sub>CF</sub> = 9.0 Hz), 81.1, 56.4 (d, <sup>2</sup>J<sub>CF</sub> = 17.7 Hz), 34.5 (d, <sup>2</sup>J<sub>CF</sub> = 24.3 Hz), 28.3; <sup>19</sup>F NMR (376 MHz, CDCl<sub>3</sub>) δ -128.5; HRMS (ESI): Exact mass calcd for C<sub>16</sub>H<sub>19</sub>FN<sub>2</sub>O<sub>4</sub> [M+K]<sup>+</sup> 361.0960, found 361.0963.

Relative stereochemistry was assigned by 2D-NMR experiments. All peaks were assigned by HSQC and COSY. NOE experiments were used to determine the relative stereochemistry and a key NOE interaction was observed between the fluorine and the amide N-H (Figure 43).

Figure 43. Key <sup>19</sup>F-<sup>1</sup>H HOESY interaction for the benzannulated cycloheptene 127



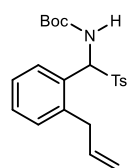
Absolute and relative stereochemistry was further determined by X-Ray analysis of a single crystal of the major diastereomer grown by slow evaporation with ethyl acetate. See **4.2 X-Ray Crystallographic Data** for more details.



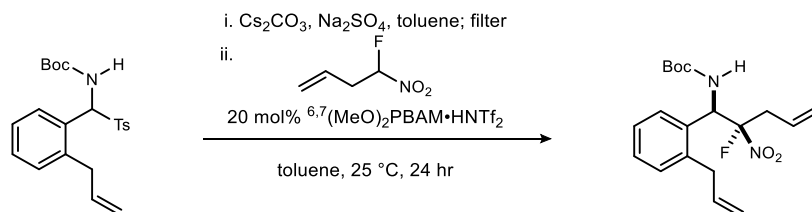
**2-Allylbenzaldehyde (S4).** Prepared according to a modified literature procedure.<sup>276</sup> In a three-neck round bottom flask (2-formylphenyl)boronic acid (500 mg, 3.33 mmol) and allyl bromide (433 μL, 5.00 mmol) were dissolved in THF (16.7 mL). Argon was bubbled through the reaction mixture for 30 minutes and PdCl<sub>2</sub>(PPh<sub>3</sub>)<sub>2</sub> (87.8 mg, 125 μmol) was added, followed by a degassed aqueous solution of Na<sub>2</sub>CO<sub>3</sub> (6.7 mL, 1.0 M). The reaction mixture was refluxed for 5 hours, then cooled to room temperature, diluted with water, extracted with DCM, washed with brine, and then

<sup>276</sup> PEACOCK, L. R.; CHAPMAN, R. S. L.; SEDGWICK, A. C.; MAHON, M. F.; AMANS, D.; BULL, S. D. *ORG. LETT.* **2015**, *17*, 994.

dried and concentrated. The crude mixture was purified by column chromatography (1-2-3% Et<sub>2</sub>O/hexanes) to afford the aldehyde (197 mg, 41%). All spectral data matched the literature.<sup>277</sup>



**tert-Butyl ((2-allylphenyl)(tosyl)methyl)carbamate (128).** Prepared according to the General Procedure for the Preparation of *N*-Boc  $\alpha$ -Amidosulfones.<sup>277</sup> from 2-allyl benzaldehyde (298 mg, 2.04 mmol) and isolated as a white solid (222 mg, 35%). Mp 111.0-113.0 °C; *R*<sub>f</sub> = 0.54 (30% EtOAc/hexanes); IR (film) 3346, 2979, 1702, 1368, 1319, 1161, 1142 cm<sup>-1</sup>; <sup>1</sup>H NMR (600 MHz, CDCl<sub>3</sub>)  $\delta$  7.80 (d, *J* = 8.0 Hz, 2H), 7.55 (d, *J* = 7.4 Hz, 1H), 7.38-7.32 (series of multiplets, 4H), 7.25 (br m, 1H), 6.22 (d, *J* = 10.6 Hz, 1H), 6.02-5.95 (m, 1H), 5.66 (d, *J* = 10.4 Hz, 1H), 5.11 (dd, *J* = 10.1, 1.4 Hz, 1H), 5.03 (d, *J* = 17.0 Hz, 1H), 3.62 (dd, *J* = 16.4, 5.7 Hz, 1H), 3.48 (dd, *J* = 16.2, 6.2 Hz, 1H), 2.42 (s, 3H), 1.25 (s, 9H); <sup>13</sup>C NMR (150 MHz, CDCl<sub>3</sub>) ppm 153.5, 145.1, 139.9, 136.2, 134.6, 130.5, 130.0, 129.9, 129.6, 129.5, 127.9, 127.2, 117.0, 81.1, 69.5, 37.5, 28.1, 21.8; HRMS (ESI): Exact mass calcd for C<sub>22</sub>H<sub>27</sub>NNaO<sub>4</sub>S [M+Na]<sup>+</sup> 424.1553, found 424.1553.

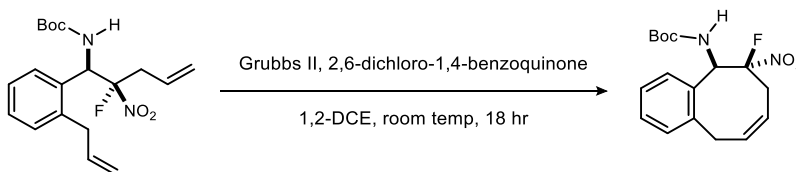


**tert-Butyl ((1*R*,2*S*)-1-(2-allylphenyl)-2-fluoro-2-nitropent-4-en-1-yl)carbamate (129).** To a flame-dried flask was added *tert*-butyl ((2-allylphenyl)(tosyl)methyl)carbamate (80.3 mg, 200  $\mu$ mol), Cs<sub>2</sub>CO<sub>3</sub> (326 mg, 1.00 mmol), Na<sub>2</sub>SO<sub>4</sub> (142 mg, 1.00 mmol) and toluene (1 mL). The reaction was monitored by <sup>1</sup>H NMR and upon completion was filtered through a plug of dry Celite that was rinsed with toluene (1 mL), into a flask containing 1-fluoro-1-nitrobut-1-ene (28.6 mg, 240  $\mu$ mol) and 6,7-(MeO)<sub>2</sub>PBAM·HNTf<sub>2</sub> (36.3 mg, 40.0  $\mu$ mol). The reaction mixture was stirred overnight and filtered through a plug of SiO<sub>2</sub> (Et<sub>2</sub>O) to afford a crude 16:1 mixture of diastereomers. The crude oil was purified by column chromatography (5-10-20% Et<sub>2</sub>O/hexanes) to provide 55.6 mg (76%) of a 24:1 mixture of diastereomers which were determined to be 96 and

<sup>277</sup> WATSON, I. D. G.; RITTER, S.; TOSTE, F. D. *J. AM. CHEM. SOC.* **2009**, *131*, 2056.



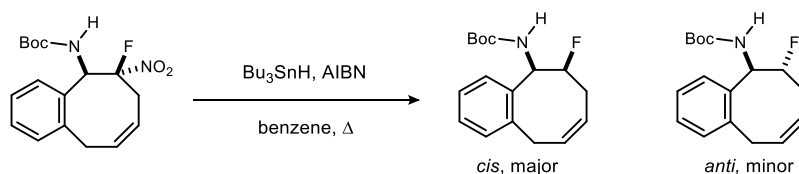
88% ee by chiral HPLC (Chiralpak AD-H: 4% *i*PrOH/hexanes, 1.0 mL/min:  $t_r$  (d<sub>1e1</sub> major, minor) = 11.1 min,  $t_r$  (d<sub>2e2</sub> minor, minor) = 12.7 min,  $t_r$  (d<sub>1e2</sub> minor, major) = 20.3 min,  $t_r$  (d<sub>2e2</sub> major, major) = 22.4 min). Characterized as a 24:1 ratio of diastereomers:  $[\alpha]_D^{23}$  -31.5 (*c* 0.43, CHCl<sub>3</sub>);  $R_f$  = 0.64 (20% EtOAc/hexanes); IR (film) 3306, 2958, 2922, 2851, 1708, 1572, 1492, 1367, 1169 cm<sup>-1</sup>; <sup>1</sup>H NMR (600 MHz, CDCl<sub>3</sub>)  $\delta$  7.34-7.27 (m, 4H), 6.04-5.99 (m, 1H), 5.93 (dd, *J* = 21.8, 9.9 Hz, 1H), 5.57 (ddd, *J* = 24.6, 8.4, 8.4 Hz, 1H), 5.36 (d, *J* = 9.6 Hz, 1H), 5.19-5.11 (m, 4H), 3.68 (dd, *J* = 15.7, 7.4 Hz, 1H), 3.60 (dd, *J* = 15.4, 4.5 Hz, 1H), 2.94 (ddd, <sup>3</sup>*J*<sub>HF</sub> = 34.2 Hz, *J* = 14.9, 8.2 Hz, 1H), 2.44 (ddd, *J* = 14.7, 7.4, 7.4 Hz, 1H), 1.38 (s, 9H); <sup>13</sup>C NMR (150 MHz, CDCl<sub>3</sub>) ppm 154.4, 139.1, 136.7, 133.8, 130.1, 129.3, 127.6, 126.9 (d, <sup>3</sup>*J*<sub>CF</sub> = 4.3 Hz), 126.5 (d, <sup>3</sup>*J*<sub>CF</sub> = 3.1 Hz), 123.1, 122.2 (d, <sup>1</sup>*J*<sub>CF</sub> = 246.3 Hz), 117.2, 80.9, 53.6 (d, <sup>2</sup>*J*<sub>CF</sub> = 19.2 Hz), 39.2 (d, <sup>2</sup>*J*<sub>CF</sub> = 20.6 Hz), 37.5, 28.8; <sup>19</sup>F NMR (376 MHz, CDCl<sub>3</sub>)  $\delta$  -137.9 (*syn* diastereomer, major), 139.1 (*anti* diastereomer, minor); HRMS (ESI): Exact mass calcd for C<sub>19</sub>H<sub>25</sub>FN<sub>2</sub>NaO<sub>4</sub> [M+Na]<sup>+</sup> 387.1691, found 387.1691.



***tert*-Butyl ((5*R,Z*)-6-fluoro-6-nitro-5,6,7,10-tetrahydrobenzo[8]annulen-5-yl)carbamate (130).** To a solution of *tert*-butyl ((1*R,2S*)-1-(2-allylphenyl)-2-fluoro-2-nitropent-4-en-1-yl)carbamate (45.0 mg, 123  $\mu$ mol) in 1,2-dichloroethane (25 mL) was added Grubbs II catalyst (10.5 mg, 12.3  $\mu$ mol) and 2,6-dichloro-1,4-benzoquinone (4.4 mg, 24  $\mu$ mol), and the solution was subjected to 2 cycles of freeze-pump-thaw (liquid nitrogen), backfilled with nitrogen, and stirred at room temperature. After 18 hours, the reaction mixture was concentrated and the crude residue was purified by flash column chromatography (10-15-20% Et<sub>2</sub>O in hexanes) to afford the desired product as a white solid (39.0 mg, 94%). Mp = 86.5-88.0 °C;  $[\alpha]_D^{23}$  -9.3 (*c* 0.43, CHCl<sub>3</sub>)<sup>278</sup>;  $R_f$  = 0.53 (20% EtOAc/hexanes, KMnO<sub>4</sub> stain); IR (film) 3323, 2977, 1708, 1566, 1503, 1367, 1248,

<sup>278</sup> Derived from aza-Henry adduct with >24:1 dr, 90%/83% ee

1163  $\text{cm}^{-1}$ ;  $^1\text{H}$  NMR (600 MHz,  $\text{CDCl}_3$ , peaks for major rotamer listed)  $\delta$  7.34 (dd,  $J = 7.3, 7.3$  Hz, 1H), 7.30 (dd,  $J = 7.2, 7.2$  Hz, 1H), 7.25 (br s, 1H), 7.23 (br s, 1H), 6.14 (dd,  $^3J_{\text{HF}} = 26.5$  Hz,  $J = 9.7$  Hz, 1H), 5.97 (dddd,  $J = 12.0, 5.1, 5.1, 2.7$  Hz, 1H), 5.58 (d,  $J = 9.4$  Hz, 1H), 5.42 (m, 1H), 4.09 (br d,  $J = 19.7$  Hz, 1H), 3.54 (dd,  $J = 19.8, 5.04$  Hz, 1H), 2.37-2.35 (br m, 1H), 2.27 (ddd,  $^3J_{\text{HF}} = 15.0, J = 9.0, 6.8$  Hz, 1H), 1.40 (s, 9H);  $^{13}\text{C}$  NMR (150 MHz,  $\text{CDCl}_3$ ) ppm 154.6, 137.0, 135.2, 134.2, 130.9, 129.1, 127.8, 126.1, 121.3 (d,  $^1J_{\text{CF}} = 244.8$  Hz), 118.2 (d,  $^3J_{\text{CF}} = 12.3$  Hz), 81.0, 53.9 (d,  $^2J_{\text{CF}} = 16.2$  Hz), 38.1, 31.6 (d,  $^2J_{\text{CF}} = 23.2$  Hz), 28.3;  $^{19}\text{F}$  NMR (376 MHz,  $\text{CDCl}_3$ )  $\delta$  -132.4; HRMS (ESI): Exact mass calcd for  $\text{C}_{17}\text{H}_{21}\text{FN}_2\text{NaO}_4$   $[\text{M}+\text{Na}]^+$  359.1378, found 359.1377.

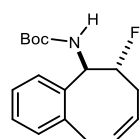


**Reductive denitration of 130.** To a flame-dried vial was added the fluoronitroalkane (30.0 mg, 89.2  $\mu\text{mol}$ ) and dry benzene (446  $\mu\text{L}$ ). To a separate flame-dried vial was added tributyltin hydride (120  $\mu\text{L}$ , 446 mmol) and dry benzene (318  $\mu\text{L}$ ). Both vials were subjected to three cycles of freeze-pump-thaw and backfilled with inert gas. To the flask containing tributyltin hydride was added AIBN (5.9 mg, 35.7  $\mu\text{mol}$ ) and the resulting mixture was added to a refluxing solution of the fluoronitroalkane in 100  $\mu\text{L}$  portions every 25 minutes until the reaction was complete (as indicated by TLC). The reaction was cooled to room temperature and concentrated to yield a 1:1 mixture of diastereomers ( $^{19}\text{F}$  NMR). Column chromatography (5-10-15%  $\text{Et}_2\text{O}$  in hexanes) provided both diastereomers (12.4 mg, 44% *cis* and 9.7 mg, 37% *trans*).

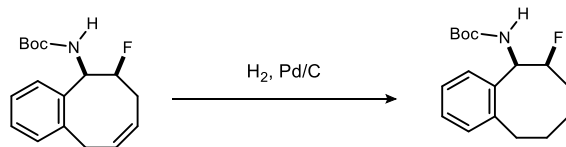
**tert-Butyl ((5R,6S,Z)-6-fluoro-5,6,7,10-tetrahydrobenzo[8]annulen-5-yl)carbamate (131).** The major diastereomer was isolated as a white solid (12.4 mg, 44%), mp = 114.5-116.0  $^\circ\text{C}$ ;  $[\alpha]_D^{23} +46$  (c 0.40,  $\text{CHCl}_3$ )<sup>279</sup>;  $R_f = 0.63$  (20%  $\text{EtOAc}$ /hexanes,  $\text{KMnO}_4$  stain); IR (film) 3441, 3021, 2960, 2923, 2851, 1716, 1491, 1366, 1167, 719  $\text{cm}^{-1}$ ;  $^1\text{H}$  NMR (400 MHz,  $\text{CDCl}_3$ )  $\delta$  7.29-7.15 (m, 4H), 5.82 (d,  $J = 8.9, 8.0, 5.1, 2.9$  Hz, 1H),

<sup>279</sup> Derived from aza-Henry adduct with >24:1 dr, 90%/83% ee

5.76 (br d,  $J = 8.2$  Hz, 1H), 5.49-5.43 (br m, 1H), 5.24 (ddd,  $^3J_{\text{HF}} = 32.2$  Hz,  $J = 8.9, 2.8$  Hz, 1H), 4.79 (dddd,  $^2J_{\text{HF}} = 50.0$  Hz,  $J = 11.6, 4.7, 3.2$  Hz, 1H), 3.88 (br d,  $J = 19.6$  Hz, 1H), 3.40 (dd,  $J = 19.6, 5.1$  Hz, 1H), 2.09 (dddd,  $^3J_{\text{HF}} = 13.1, J = 9.4, 7.1, 4.6$  Hz, 1H), 1.90-1.79 (m, 1H), 1.44 (s, 9H);  $^{13}\text{C}$  NMR (100 MHz,  $\text{CDCl}_3$ ) ppm 155.3, 136.9, 136.7, 134.7, 130.1, 127.8, 127.2, 125.8, 120.7 (d,  $^3J_{\text{CF}} = 16.3$  Hz), 93.0 (d,  $^1J_{\text{CF}} = 180.6$  Hz), 80.0, 52.8 (d,  $^2J_{\text{CF}} = 16.0$  Hz), 38.1, 28.57, 28.55;  $^{19}\text{F}$  NMR (376 MHz,  $\text{CDCl}_3$ )  $\delta$  -189.9; HRMS (ESI): Exact mass calcd for  $\text{C}_{17}\text{H}_{22}\text{FNNaO}_2$   $[\text{M}+\text{Na}]^+$  314.1532, found 314.1517.



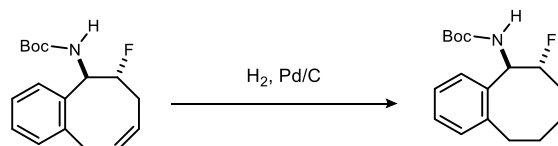
**tert-Butyl ((5R,6R,Z)-6-fluoro-5,6,7,10-tetrahydrobenzo[8]annulen-5-yl)carbamate (132).** The minor diastereomer was isolated as a white solid (9.7 mg, 37%), mp = 125.0-128.0 °C;  $[\alpha]_D^{23} +14$  ( $c$  0.57,  $\text{CHCl}_3$ )<sup>279</sup>;  $R_f = 0.53$  (20% EtOAc/hexanes,  $\text{KMnO}_4$  stain);  $^1\text{H}$  NMR (600 MHz,  $\text{CDCl}_3$ )  $\delta$  7.25-7.24 (br m, 2H), 7.19-7.16 (m, 2H), 5.91-5.87 (m, 1H), 5.56 (dddd,  $J = 18.2$  Hz,  $J = 9.1, 2.4, 2.4$  Hz, 1H), 5.29 (br s, 1H), 5.26 (br s, 1H), 4.40 (dddd,  $^2J_{\text{HF}} = 50.3$  Hz,  $J = 9.4, 3.9, 2.2$  Hz, 1H), 3.97 (br s, 1H), 3.40 (dd,  $J = 19.6, 4.9$  Hz, 1H), 2.09 (dddd,  $J = 15.4, 11.2, 8.5, 4.0$  Hz, 1H), 1.95 (m, 1H), 1.41 (br s, 9H);  $^{13}\text{C}$  NMR (150 MHz,  $\text{CDCl}_3$ ) ppm 155.6, 139.2, 137.2, 133.5, 130.6, 127.8, 127.4, 124.4, 122.3, 97.1 (d,  $^1J_{\text{CF}} = 183.9$  Hz), 80.0, 55.0, 38.3, 28.5, 27.7 (d,  $^2J_{\text{CF}} = 20.7$  Hz);  $^{19}\text{F}$  NMR (376 MHz,  $\text{CDCl}_3$ )  $\delta$  -183.0.



**tert-Butyl ((5R,6S)-6-fluoro-5,6,7,8,9,10-hexahydrobenzo[8]annulen-5-yl)carbamate (133).**

Prepared according to the general procedure using *tert*-butyl ((5R,6S,Z)-6-fluoro-5,6,7,10-tetrahydrobenzo[8]annulen-5-yl)carbamate (9.2 mg, 31.6  $\mu\text{mol}$ ) with a modified solvent system (3:1:1 MeOH:DCM:toluene). Filtration through Celite followed by concentration afforded the product as a white solid (9.2 mg, quantitative yield). Mp = 108.0-109.5 °C;  $[\alpha]_D^{23} +3.6$  ( $c$  0.73,  $\text{CHCl}_3$ );  $R_f = (0.43, 20\%$  EtOAc, ninhydrin stain); Chemical shifts reported for major rotamer:  $^1\text{H}$  NMR (600 MHz,  $\text{CDCl}_3$ )  $\delta$  7.24-7.20 (m, 2H), 7.18-7.14 (m, 2H), 5.75 (d,  $J = 8.4$  Hz, 1H), 5.27 (ddd,  $^3J_{\text{HF}} = 34.0$  Hz,  $J = 8.9, 1.9$  Hz, 1H), 4.78 (dddd,  $^2J_{\text{HF}} = 48.8$  Hz,  $J = 10.8, 5.4, 2.7$  Hz, 1H), 2.92 (br ddd,  $J = 14.4, 14.4, 1.6$  Hz, 1H), 2.81 (ddd,  $J = 14.2, 5.2, 2.8$  Hz, 1H), 2.06-2.02 (br m,

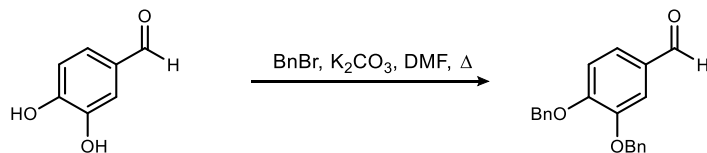
1H), 1.96-1.90 (m, 1H), 1.77 (br dd,  $J = 12.7, 12.7$  Hz, 1H), 1.46-1.40 (m, 1H), 1.43 (s, 9H), 1.34-1.25 (m, 1H), 0.94 (ddd,  $^3J_{\text{HF}} = 23.3$  Hz,  $J = 10.7, 10.7$  Hz, 1H);  $^{13}\text{C}$  NMR (150 MHz,  $\text{CDCl}_3$ ) ppm 155.3, 141.1, 135.3, 129.8, 127.9, 126.4, 95.8 (d,  $^1J_{\text{CF}} = 175.9$  Hz), 80.0, 51.8 (d,  $^2J_{\text{CF}} = 16.7$  Hz), 34.0, 32.0, 30.0 (d,  $^2J_{\text{CF}} = 19.2$  Hz), 28.6, 21.5 (d,  $^3J_{\text{CF}} = 12.8$  Hz);  $^{19}\text{F}$  NMR (376 MHz,  $\text{CDCl}_3$ )  $\delta$  -191.1.



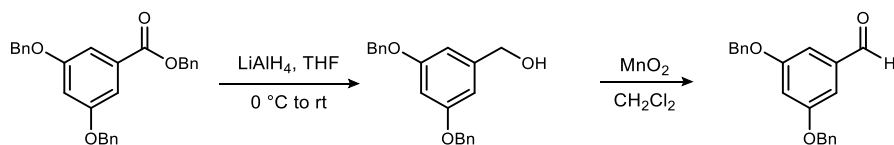
***tert*-Butyl ((5*R*,6*R*)-6-fluoro-5,6,7,8,9,10-hexahydrobenzo[8]annulen-5-yl)carbamate (134).**

Prepared according to the general procedure using *tert*-butyl ((5*R*,6*R,Z*)-6-fluoro-5,6,7,10-tetrahydrobenzo[8]annulen-5-yl)carbamate (5.7 mg, 19.6  $\mu\text{mol}$ ) with a modified solvent system (4:1 EtOAc/DCM). Filtration through Celite followed by concentration afforded the product as a white solid (5.7 mg, 99%). Mp = 147.0-149.0  $^\circ\text{C}$ ;  $[\alpha]_D^{24} -9.8$  ( $c$  0.49,  $\text{CHCl}_3$ );  $R_f = 0.52$  (20% EtOAc/hexanes, ninhydrin stain); IR (film) 3350, 2925, 1687, 1533, 1174  $\text{cm}^{-1}$ ;  $^1\text{H}$  NMR (600 MHz,  $\text{CDCl}_3$ )  $\delta$  7.24-7.19 (series of m, 3H), 7.14-7.12 (m, 1H), 5.25 (br s, 2H), 4.38 (dd,  $^2J_{\text{HF}} = 49.5$  Hz,  $J = 8.7$  Hz, 1H), 3.06 (br s, 1H), 2.81 (dd,  $J = 13.7, 2.2$  Hz, 1H), 2.12-2.10 (m, 1H), 1.96 (dddd,  $J = 15.8, 15.9, 10.3, 4.0$  Hz, 1H), 1.86 (br dd,  $J = 23.9, 12.9$  Hz, 1H), 1.66 (br m, 1H), 1.25 (s, 9H), 1.10 (dd,  $J = 14.7, 10.3$  Hz, 1H), 1.03 (dd, 15.2, 10.1 Hz, 1H), 0.89-0.87 (m, 1H), 0.86-0.82 (m, 1H);  $^{13}\text{C}$  NMR (150 MHz,  $\text{CDCl}_3$ ) ppm 155.6, 141.1, 137.7, 130.2, 128.0, 126.6, 124.7 ( $^1J_{\text{CF}} = 182.3$  Hz), 96.3, 79.9, 53.9, 34.1, 32.5, 30.3 ( $^2J_{\text{CF}} = 21.0$  Hz), 29.8, 21.7;  $^{19}\text{F}$  NMR (376 MHz,  $\text{CDCl}_3$ )  $\delta$  -180.3; HRMS (ESI): Exact mass calcd for  $\text{C}_{17}\text{H}_{24}\text{FNNaO}_2$   $[\text{M}+\text{Na}]^+$  316.1683, found 316.1684.

## Umpolung Amide Synthesis: preparation of substrates and synthesis of suspected byproducts



**(3,4)-Bis(benzyloxy)benzaldehyde (212).** In a flame-dried flask equipped with a stir bar and reflux condenser, (3,4)-dihydroxybenzaldehyde (5.00 g, 36.2 mmol) was dissolved in dry DMF (100 mL) under an argon atmosphere. Benzyl bromide (10.0 mL, 84.4 mmol) was added dropwise to the solution, followed by  $K_2CO_3$  (10.0 g, 72.5 mmol). The reaction was heated at reflux for 5 hours, cooled to 0 °C, and poured into 500 mL of  $Et_2O$ . Water was added and the aqueous layer was extracted twice with  $Et_2O$ . The combined organic layers were washed with  $H_2O$  and brine, dried ( $Na_2SO_4$ ), and concentrated. The crude solid was dissolved in hot  $EtOAc$  (25 mL), and hexanes (100 mL) was added. The solution was stirred overnight at room temperature, and the precipitate was collected by filtration and washed with hexanes to afford the desired aldehyde as a cream-colored solid (10.1 g, 88%). All spectral data matched literature values.<sup>280</sup>



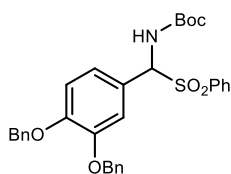
**(3,5)-bis(Benzyloxy)phenylmethanol (S4).** In a flame-dried flask equipped with a stir bar, the benzyl ester (20.0 g, 47.1 mmol) was dissolved in dry THF (470 mL) and cooled to 0 °C. Lithium aluminum hydride (3.57 g, 94.2 mmol) was added portionwise, the reaction mixture was stirred for 10 minutes, and then warmed to room temperature and stirred for 1 hour. The reaction mixture was cooled in an ice-water bath,  $H_2O$  (4 mL) was added, and it was then treated with 15% aq  $NaOH$  (4 mL) and  $H_2O$  (12 mL). The mixture was warmed to room temperature,  $MgSO_4$  (34 g)

<sup>280</sup> Gissot, A.; Wagner, A.; Mioskowski, C. *Tetrahedron* **2004**, *60*, 6807.

was added, and the reaction was stirred for 15 minutes before it was filtered through Celite and concentrated. The resulting solid was recrystallized from EtOAc/hexanes to provide the desired product as a white solid (11.4 g, 76%). All spectral data ( $^1\text{H}$   $^{13}\text{C}$  NMR) matched the literature values.<sup>281,282</sup>

**(3,5)-Bis(benzyloxy)benzaldehyde (53b).** In a flame-dried flask equipped with a stir bar, (3,5)-bis(benzyloxy)phenylmethanol (10.3 g, 32.2 mmol) was dissolved in dry dichloromethane (64 mL) under an argon atmosphere. To the solution was added  $\text{MnO}_2$  (19.6 g, 224 mmol), and the reaction was stirred for 48 h at room temperature. The reaction mixture was filtered through Celite and concentrated to provide the desired aldehyde as a white solid (9.57 g, 94%). All spectral data matched the literature values.<sup>282</sup>

**General procedure for the preparation of aryl *N*-Boc  $\alpha$ -amidosulfones.**<sup>283</sup> To a solution of aldehyde (1.2 equiv) in toluene, was added *tert*-butyl carbamate (1.0 equiv) and sodium benzene sulfinate dihydrate (2.0 equiv). Formic acid (2.0 equiv) was added dropwise followed by  $\text{H}_2\text{O}$  and the reaction was stirred for the indicated amount of time. Toluene was added, and the white precipitate was collected by vacuum filtration, washing with toluene to provide the desired  $\alpha$ -amidosulfone without further purification.



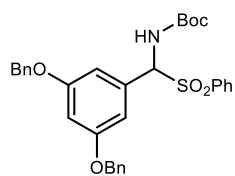
***tert*-Butyl ((3,4-bis(benzyloxy)phenyl)(phenylsulfonyl)methyl) carbamate (213).** Prepared according to the general procedure using (3,5)-bis(benzyloxy)benzaldehyde (9.09 g, 28.6 mmol) in toluene (79 mL), *tert*-butylcarbamate (2.79 g, 23.8 mmol), sodium benzenesulfinate dihydrate (4.76

g, 23.8 mmol), formic acid (1.79 mL, 47.6 mmol) and  $\text{H}_2\text{O}$  (15 mL). The mixture was stirred for 9 days and the white precipitate was collected by vacuum filtration, to provide the desired product as a white solid (7.69 g, 58%).  $^1\text{H}$  NMR (400 MHz,  $\text{DMSO-}d_6$ )  $\delta$  8.67 (d,  $J = 10.6$  Hz, 1H), 7.84 (d,  $J = 7.3$  Hz, 2H), 7.74 (t,  $J = 7.0$  Hz, 1H), 7.65 (d,  $J = 7.0$  Hz, 2H), 7.45-7.34 (m, 13H), 5.96 (d,  $J = 10.5$  Hz, 1H), 5.18 (s, 2H), 5.10 (d,  $J = 3.2$  Hz, 2H), 1.23 (s, 9H);  $^{13}\text{C}$  NMR (100 MHz,  $\text{DMSO-}d_6$ ) 154.0, 149.0, 147.9, 137.2, 137.1, 137.0, 133.8, 128.4, 127.9, 127.85, 127.77, 127.61, 127.56, 127.4, 123.4, 122.8, 115.7, 113.6, 79.3, 74.4, 70.4, 69.9, 27.9.

<sup>281</sup> Denmark, S. E.; Regens, C. S.; Kobayashi, T. *J. Am. Chem. Soc.* **2007**, *129*, 2774.

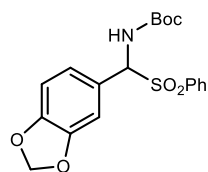
<sup>282</sup> Srinivas, B. T. V.; Maadhur, A. R.; Bojja, S. *Tetrahedron* **2014**, *70*, 8161.

<sup>283</sup> Kanazawa, A. M.; Denis, J.-N.; Greene, A. E. *The Journal of Organic Chemistry* **1994**, *59*, 1238.



**tert-Butyl ((3,5-bis(benzyloxy)phenyl)(phenylsulfonyl)methyl)carbamate (216).** Prepared according to the general procedure using (3,5)-bis(benzyloxy)benzaldehyde (4.30 g, 13.6 mmol) in toluene (37.6 mL), *tert*-butylcarbamate (1.32 g, 11.3 mmol), sodium benzenesulfinate dihydrate (4.52

g, 22.6 mmol), formic acid (850  $\mu$ L, 22.6 mmol) and H<sub>2</sub>O (7.5 mL). The mixture was stirred for 8 days, at which point toluene (15 mL) was added, and the white precipitate was collected by vacuum filtration, to provide the desired product as a white solid (5.61 g, 74%). <sup>1</sup>H NMR (400 MHz, DMSO-*d*<sub>6</sub>)  $\delta$  8.65 (d, *J* = 10.8 Hz, 1H), 7.83 (d, *J* = 7.5 Hz, 2H), 7.73 (t, *J* = 7.4 Hz, 1H), 7.61 (t, *J* = 7.7 Hz, 2H), 7.39 (m, 10H), 6.97 (d, *J* = 2.0 Hz, 2H), 6.69 (s, 1H), 5.96 (d, *J* = 10.7 Hz, 1H), 5.05 (s, 4H), 1.20 (s, 9H); <sup>13</sup>C NMR (100 MHz, DMSO-*d*<sub>6</sub>) ppm 159.1, 154.0, 137.1, 136.8, 133.9, 132.4, 129.2, 129.0, 128.5, 127.9, 127.9, 109.1, 102.7, 79.3, 74.5, 69.5, 27.8.

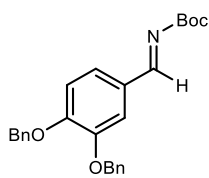


**tert-Butyl (benzo[d][1,3]dioxol-5-yl(phenylsulfonyl)methyl)carbamate (245).** Prepared according to the general procedure using piperonal (1.00 g, 6.66 mmol) in toluene (22 mL), *tert*-butylcarbamate (650 mg, 5.55 mmol), sodium benzene sulfinate dihydrate (2.22 g, 11.1 mmol), formic acid (420  $\mu$ L, 11.1

mmol) and H<sub>2</sub>O (6.4 mL). The mixture was stirred for 8 days, at which point toluene was added, and the white precipitate was collected by vacuum filtration to provide the desired product as a white solid (1.53 g, 59%). <sup>1</sup>H NMR (400 MHz, DMSO-*d*<sub>6</sub>)  $\delta$  8.62 (d, *J* = 10.7 Hz, 1H), 7.87 (d, *J* = 7.4, 2H), 7.73 (t, *J* = 7.3 Hz, 1H), 7.64 (t, *J* = 7.7 Hz, 2H), 7.32 (d, *J* = 1.2 Hz, 1H), 7.10 (dd, *J* = 8.1, 1.4 Hz, 1H), 6.94 (d, *J* = 8.0 Hz, 1H), 6.07 (s, 2H), 5.96 (d, *J* = 10.7 Hz, 1H), 1.19 (s, 9H); <sup>13</sup>C NMR (100 MHz, DMSO-*d*<sub>6</sub>) 153.9, 148.1, 147.1, 137.1, 133.8, 129.1, 129.0, 124.3, 123.6, 109.9, 107.8, 101.3, 79.3, 74.1, 27.8.

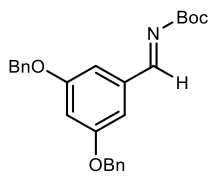
### General procedure for the synthesis of *N*-Boc imines.

To a flame-dried 2-neck flask equipped with a stir bar and reflux condenser was added *N*-Boc- $\alpha$ -amidophenylsulfone, potassium carbonate (5.0 equiv), and sodium sulfate (5.0 equiv). Dry THF was added and the solution was heated at reflux until complete as indicated by <sup>1</sup>H NMR. The reaction mixture was filtered through an oven-dried glass frit, concentrated, and carried forward without further purification.



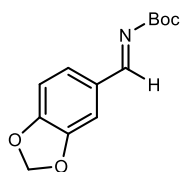
**tert-Butyl (E)-(3,4-bis(benzyloxy)benzylidene)carbamate (219).** Prepared according to the general procedure using *tert*-butyl ((3,4-bis(benzyloxy)phenyl)(phenylsulfonyl)methyl)carbamate (2.00 g, 3.57 mmol), potassium carbonate (2.47 g, 17.9 mmol) and sodium sulfate (2.54 g, 17.9

mmol) and THF (17.9 mL). The mixture was heated at reflux for 6 hours, filtered, and concentrated to provide the product as a yellow oil (1.50 g, quant). <sup>1</sup>H NMR (400 MHz, CDCl<sub>3</sub>) δ 8.81 (s, 1H), 7.66 (d, *J* = 1.9 Hz, 1H), 7.39-7.35 (m, 10H), 7.32 (dd, *J* = 7.1, 1.4 Hz, 2H), 6.98 (d, *J* = 8.3 Hz, 1H), 5.23 (s, 2H), 5.19 (s, 2H), 1.58 (s, 9H).



**tert-Butyl (E)-(3,5-bis(benzyloxy)benzylidene)carbamate (217).** Prepared according to the general procedure using *tert*-butyl ((3,5-bis(benzyloxy)phenyl)(phenylsulfonyl)methyl)carbamate (3.00 g, 5.36 mmol), potassium carbonate (3.70 g, 26.8 mmol), sodium sulfate (3.80 g, 26.8 mmol), and THF (26.8 mL). The mixture was heated at reflux for 6 hours, filtered, and concentrated to

provide the product as a yellow oil (2.12 g, 95%). <sup>1</sup>H NMR (400 MHz, CDCl<sub>3</sub>) δ 8.76 (s, 1H), 7.39-7.32 (m, 10H), 7.16 (d, *J* = 2.3 Hz, 2H), 6.81 (t, *J* = 2.3 Hz, 1H), 5.07 (s, 4H), 1.59 (s, 9H).



**(3,4) tert-Butyl (E)-(benzo[d][1,3]dioxol-5-ylmethylene)carbamate (246).**

Prepared according to the general procedure using *tert*-butyl (benzo[d][1,3]dioxol-5-yl(phenylsulfonyl)methyl)carbamate (1.00 g, 2.55 mmol), potassium carbonate (1.77 g, 12.8 mmol), sodium sulfate (1.81 g, 12.8

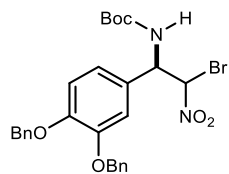
mmol), and THF (25 mL). The mixture was heated at reflux for 6 hours, then stirred at room temperature overnight, filtered, and concentrated to provide the *N*-Boc imine without further purification (646 mg, quant). <sup>1</sup>H NMR (400 MHz, CDCl<sub>3</sub>) δ 8.79 (s, 1H), 7.50 (d, *J* = 1.5 Hz, 1H), 7.34 (dd, *J* = 8.4, 1.6 Hz, 1H), 6.87 (d, *J* = 8.0 Hz, 1H), 6.05 (s, 2H), 1.57 (s, 9H).

### General procedure for aza-Henry reactions with bromonitromethane or nitromethane.

In a flame-dried flask equipped with a stir bar, the *N*-Boc imine (1.0 equiv) was dissolved in toluene and cooled to -40 °C. PBAM was added and the reaction mixture was stirred for 10 minutes. Bromonitromethane (1.5 equiv) or nitromethane (10 equiv) was added dropwise, and the reaction mixture was warmed to -20 °C, and stirred for 24 hours. Upon completion of the reaction,

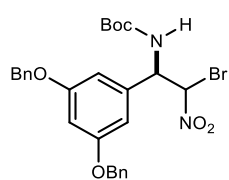


the mixture was filtered through a plug of silica gel (EtOAc), and concentrated to afford the bromonitroalkane after recrystallization with EtOAc/hexanes.



**tert-Butyl ((1R)-1-(3,4-bis(benzyloxy)phenyl)-2-bromo-2-nitroethyl)carbamate (220).** Prepared according to the general procedure using *tert*-butyl (*E*)-(3,5-bis(benzyloxy)benzylidene)carbamate (1.70 g, 4.07 mmol), toluene (41 mL), (*R,R*)-PBAM (103 mg, 204  $\mu$ mol), and

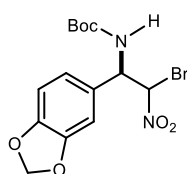
bromonitromethane (426  $\mu$ L, 6.11 mmol). Upon completion, the reaction mixture was filtered through a plug of silica gel (EtOAc), and concentrated to provide the bromonitroalkane as a 1:2.3 mixture of diastereomers (1.81 g, 80%). The diastereomers were determined to be 76 and 83% ee by chiral HPLC analysis (Chiralpak AD-H, 10% EtOH/hexanes, 1.0 mL/min,  $t_r$  ( $d_{1e1}$ , major, minor) = 40.9 min,  $t_r$  ( $d_{2e1}$ , minor, minor) = 45.8 min,  $t_r$  ( $d_{1e1}$ , major, major) = 49.1 min,  $t_r$  ( $d_{2e2}$ , minor, major) = 96.4 min). Recrystallization from EtOAc/hexanes afforded the bromonitroalkane as a 1:2 mixture of diastereomers with >99 and >99% ee (1.50 g, 66%). Mp 157.0–161.0  $^{\circ}$ C;  $R_f$  = 0.37 (20% EtOAc/hexanes); IR (film) 3359, 2980, 1684, 1562, 1516, 1164, 856  $\text{cm}^{-1}$ ; 1:2 mixture of diastereomers:  $^1\text{H}$  NMR (400 MHz,  $\text{CDCl}_3$ )  $\delta$  7.90 (d,  $J$  = 9.7 Hz, 1H), 7.76 (d,  $J$  = 10.0 Hz, 1H), 7.47–7.30 (m, 22H), 7.01 (dd,  $J$  = 8.2, 6.9 Hz, 2H), 6.96 (d,  $J$  = 8.2 Hz, 1H), 6.90 (d,  $J$  = 7.8 Hz, 1H), 6.57 (d,  $J$  = 8.1 Hz, 1H), 6.50 (d,  $J$  = 9.6 Hz, 1H), 5.30 (dd,  $J$  = 9.2, 9.0 Hz, 1H), 5.24 (dd,  $J$  = 9.7, 9.7 Hz, 1H), 5.12 (d,  $J$  = 4.0 Hz, 4H), 5.09 (s, 4H), 1.38 (s, 9H), 1.33 (s, 9H);  $^{13}\text{C}$  NMR (100 MHz,  $\text{DMSO}-d_6$ ) ppm 154.7, 154.2, 148.5, 148.4, 148.1, 148.0, 137.14, 137.06, 137.0, 136.9, 128.5 (2C), 128.4 (8C), 127.85, 127.83, 127.76 (2C), 127.74 (4C), 127.5 (4C), 121.3, 120.8, 114.1, 113.9, 113.8, 113.7, 83.6, 81.3, 79.0 (2C), 70.2 (2C), 69.9 (2C), 58.3, 57.7, 28.1, 28.0; HRMS (ESI): Exact mass calcd for  $\text{C}_{27}\text{H}_{29}\text{BrN}_2\text{O}_6\text{Na}$  [ $\text{M}+\text{Na}$ ] $^+$  579.1107, found 579.1126.



**tert-Butyl ((1R)-1-(3,5-bis(benzyloxy)phenyl)-2-bromo-2-nitroethyl)carbamate (218).** Prepared according to the general procedure using *tert*-butyl (*E*)-(3,5-bis(benzyloxy)benzylidene)carbamate (1.95 g, 4.66 mmol), toluene (46.6 mL), (*R,R*)-PBAM (118 mg, 233  $\mu$ mol), and

bromonitromethane (487  $\mu$ L, 6.99 mmol). Upon completion, the reaction was filtered through a plug of silica gel (EtOAc), and concentrated to provide the bromonitroalkane as a 1:1.1 mixture of diastereomers ( $^1\text{H}$  NMR). The diastereomers were determined to be 85 and 94% ee by chiral HPLC analysis (Chiralpak OD-H, 5% EtOH/hexanes, 1.0 mL/min,  $t_r$  ( $d_{1e1}$ , major, minor) = 18.0 min,

$t_r(d_{1e2}, \text{major, major}) = 20.4 \text{ min}$ ,  $t_r(d_{2e1}, \text{minor, minor}) = 22.6 \text{ min}$ ,  $t_r(d_{2e2}, \text{minor, major}) = 26.9 \text{ min}$ . Recrystallization from EtOAc/hexanes afforded the bromonitroalkane as a 1:1.6 mixture of diastereomers with >99 and >99% ee (1.95 g, 75%). Mp 161.0–164.0 °C;  $R_f = 0.54$  (20% EtOAc/hexanes); IR (film) 3362, 2983, 2357, 1686, 1561, 1164  $\text{cm}^{-1}$ ; 1:1.6 mixture of diastereomers:  $^1\text{H NMR}$  (400 MHz, DMSO- $d_6$ )  $\delta$  7.93 (d,  $J = 9.6 \text{ Hz}$ , 1H), 7.79 (d,  $J = 10.0 \text{ Hz}$ , 1H), 7.45–7.30 (m, 20 H), 6.77 (s, 2H), 6.71 (d,  $J = 2.0 \text{ Hz}$ , 2H), 6.65 (d,  $J = 10.0 \text{ Hz}$ , 1H), 6.64 (d,  $J = 2.0 \text{ Hz}$ , 2H), 6.52 (d,  $J = 9.6 \text{ Hz}$ , 1H), 5.35 (dd,  $J = 9.6, 9.0 \text{ Hz}$ , 1H), 5.25 (dd,  $J = 9.6, 9.4 \text{ Hz}$ , 1H), 5.07 (s, 4H), 5.05 (s, 4H), 1.38 (s, 9H), 1.33 (s, 9H);  $^{13}\text{C NMR}$  (100 MHz, DMSO- $d_6$ ) ppm 159.4 (2C), 159.3 (2C), 154.5, 154.0, 138.1, 138.0, 136.6 (2C), 136.5 (2C), 128.2 (8C), 127.7 (4C), 127.66 (8C), 107.1 (2C), 106.6 (2C), 101.53, 101.48, 83.5, 80.5, 78.9 (2C), 69.3 (4C), 58.4, 57.8, 27.9, 27.8; HRMS (ESI): Exact mass calcd for  $\text{C}_{27}\text{H}_{29}\text{N}_2\text{O}_6\text{Na}$   $[\text{M}+\text{Na}]^+$  579.1136, found 579.1107.



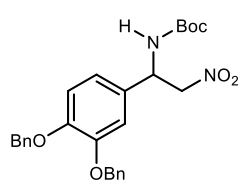
**tert-Butyl**

**((1R)-1-(benzo[d][1,3]dioxol-5-yl)-2-bromo-2-**

**nitroethyl)carbamate (239)**. Prepared according to the general procedure using (3,4)-*tert*-butyl (*E*)-(benzo[d][1,3]dioxol-5-ylmethylene)carbamate (635 mg, 2.55 mmol), toluene (26 mL), (*R,R*)-PBAM (130 mg, 255  $\mu\text{mol}$ ), and

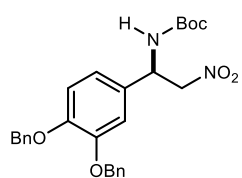
bromonitromethane (267  $\mu\text{L}$ , 3.83 mmol). Upon completion of the reaction, the mixture was filtered through a plug of silica gel (EtOAc), and concentrated to provide the bromonitroalkane as a 1:1.1 mixture of diastereomers. The diastereomers were determined to be 93 and 93% ee by chiral HPLC analysis Chiralpak AD-H, 8% EtOH/hexanes, 1.0 mL/min,  $t_r(d_{1e1}, \text{major}) = 18.6 \text{ min}$ ,  $t_r(d_{2e1}, \text{minor}) = 20.7 \text{ min}$ ,  $t_r(d_{1e2}, \text{major}) = 21.8 \text{ min}$ ,  $t_r(d_{2e2}, \text{major}) = 27.2 \text{ min}$ . Recrystallization from EtOAc/hexanes afforded the bromonitroalkane as a 1:1 mixture of diastereomers with >99 and >99% ee (498 mg, 50%). Mp 149.0–153.0 °C;  $R_f = 0.36$  (20% EtOAc/hexanes); IR (film) 3366, 2979, 2902, 2359, 2340, 1683, 1563, 1247, 932  $\text{cm}^{-1}$ ; 1:1 mixture of diastereomers:  $^1\text{H NMR}$  (400 MHz, DMSO- $d_6$ )  $\delta$  7.92 (d,  $J = 9.6 \text{ Hz}$ , 1H), 7.77 (d,  $J = 9.6 \text{ Hz}$ , 1H), 7.09 (s, 1H), 7.04 (d,  $J = 1.2 \text{ Hz}$ , 1H), 6.87–6.83 (m, 4H), 6.54 (d,  $J = 8.4 \text{ Hz}$ , 1H), 6.50 (d,  $J = 10.0 \text{ Hz}$ , 1H), 6.03 (s, 2H), 6.02 (s, 2H), 5.25 (dd,  $J = 19.6, 9.6 \text{ Hz}$ , 2H), 1.38 (s, 9H), 1.33 (s, 9H);  $^{13}\text{C NMR}$  (150 MHz, DMSO- $d_6$ ) 154.6, 154.1, 147.51, 147.47, 147.36 (2C), 129.91 (2C), 129.52 (2C), 122.2, 121.6, 108.3 (2C), 108.1 (2C), 108.0, 107.6, 101.3, 101.2, 83.2, 81.1, 79.1

(2C), 58.3, 57.9, 28.0, 27.9; HRMS (ESI): Exact mass calcd for C<sub>14</sub>H<sub>17</sub>BrN<sub>2</sub>O<sub>6</sub>Na [M+Na]<sup>+</sup> 411.0168, found 411.0180.



**tert-Butyl ((±)-1-(3,4-bis(benzyloxy)phenyl)-2-nitroethyl)carbamate**

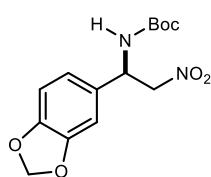
**((rac)224).** Prepared according to the general procedure using *tert*-butyl (*E*)-(3,4-bis(benzyloxy)benzylidene)carbamate (150 mg, 360 μmol), toluene (3.6 mL), (*rac*)-PBAM (18.2 mg, 36 μmol), and nitromethane (193 μL, 3.60 mmol) at room temperature. Upon completion of the reaction, the mixture was filtered through a plug of silica gel (EtOAc), and concentrated. Recrystallization (EtOAc/hexanes) afforded the nitroalkane as a white solid (41.8 mg, 24%). Chiral HPLC analysis (Chiralpak OD-H, 12% EtOH/hexanes, 1.0 mL/min) *t<sub>r</sub>*(*e*<sub>1</sub>) = 17.7 min, *t<sub>r</sub>*(*e*<sub>2</sub>) = 22.7 min; *R<sub>f</sub>* = 0.46 (30% EtOAc/hexanes); IR (film) 3361, 2978, 2932, 1690, 1555, 1379, 1255, 1165 cm<sup>-1</sup>; <sup>1</sup>H NMR (400 MHz, CDCl<sub>3</sub>) δ 7.45-7.42 (m, 4H), 7.39-7.31 (m, 6H), 6.91 (d, *J* = 8.3 Hz, 1H), 6.88 (d, *J* = 1.8 Hz, 1H), 6.81 (dd, *J* = 8.3, 2.0 Hz, 1H), 5.25 (d, *J* = 5.5 Hz, 1H), 5.14 (s, 4H), 5.13-5.11 (m, 1H), 4.76 (br s, 1H), 4.60 (dd, *J* = 12.4, 5.7 Hz, 1H), 1.44 (s, 9H); <sup>13</sup>C NMR (100 MHz, CDCl<sub>3</sub>) ppm 154.6, 149.3, 149.2, 136.9, 136.8, 129.9, 128.5, 127.9, 127.8, 127.4, 127.2, 119.4, 115.1, 113.7, 80.6, 78.7, 77.2, 71.5, 71.1, 28.2; HRMS (ESI): Exact mass calcd for C<sub>27</sub>H<sub>30</sub>N<sub>2</sub>O<sub>6</sub>Na [M+Na]<sup>+</sup> 501.2002, found 501.2022.



**tert-Butyl ((*R*)-1-(3,4-bis(benzyloxy)phenyl)-2-nitroethyl)carbamate**

**(224).** Prepared according to the general procedure using *tert*-butyl (*E*)-(3,4-bis(benzyloxy)benzylidene)carbamate (1.49 g, 3.57 mmol), toluene (36 mL), (*R,R*)-PBAM (181 mg, 357 μmol), and nitromethane (2.87 mL, 53.6 mmol). Upon completion of the reaction, the mixture was filtered through a plug of silica gel (EtOAc), and concentrated. Column chromatography (10-25-30% EtOAc/hexanes) afforded the product as a white solid (831 mg, 49%). The compound was determined to be 66% ee by chiral HPLC analysis (Chiralpak OD-H, 12% EtOH/hexanes, 1.0 mL/min) *t<sub>r</sub>*(*e*<sub>1</sub>, major) = 16.8 min, *t<sub>r</sub>*(*e*<sub>2</sub>, minor) = 21.7 min; mp 123.0–124.5 °C; [*α*]<sub>D</sub><sup>20</sup> -19.5 (*c* 1.00, CHCl<sub>3</sub>); *R<sub>f</sub>* = 0.49 (30% EtOAc/hexanes); IR (film) 3371, 2981, 1688, 1549, 1515, 1455, 1430, 1383, 1272, 1169, 1142, 1026, 733, 695 cm<sup>-1</sup>; <sup>1</sup>H NMR (400 MHz, CDCl<sub>3</sub>) δ 7.43 (t, *J* = 6.4 Hz, 4H), 7.39-7.31 (m, 6H), 6.90 (d, *J* = 8.4 Hz, 1H), 6.87 (d, *J* = 2.0 Hz, 1H), 6.80 (dd, *J* = 8.0, 2.0 Hz, 1H), 5.25 (d, *J* = 6.0 Hz, 1H), 5.14 (s, 5H), 4.76 (br s,

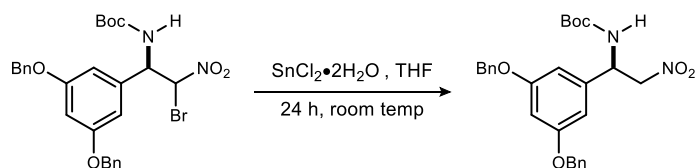
1H), 4.59 (dd,  $J = 12.4, 5.6$  Hz, 1H), 1.43 (s, 9H);  $^{13}\text{C}$  NMR (100 MHz,  $\text{CDCl}_3$ ) ppm 154.8, 149.5, 149.4, 137.1, 137.0, 130.1, 128.7, 128.1, 128.0, 127.6, 127.4, 119.6, 115.2, 113.9, 80.8, 78.9, 71.7, 71.3, 52.8, 28.4; HRMS (ESI): Exact mass calcd for  $\text{C}_{27}\text{H}_{30}\text{N}_2\text{O}_6\text{Na}$   $[\text{M}+\text{Na}]^+$  501.2002, found 501.1979.



***tert*-Butyl (*R*)-(1-(benzo[*d*][1,3]dioxol-5-yl)-2-nitroethyl)carbamate (250).**

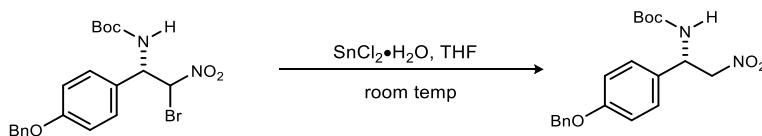
Prepared according to the general procedure using *tert*-butyl (*E*)-(benzo[*d*][1,3]dioxol-5-ylmethylene)carbamate (106 mg, 255  $\mu\text{mol}$ ), toluene (2.55 mL), (*R,R*)-PBAM (12.9 mg, 25  $\mu\text{mol}$ ), and nitromethane (137  $\mu\text{L}$ , 2.55 mmol) at  $-50$   $^\circ\text{C}$ . Upon completion of the reaction, the mixture was filtered through a plug of silica gel (EtOAc) and concentrated. Column chromatography (10-20-30% EtOAc/hexanes) afforded the nitroalkane as a white solid (29.2 mg, 37%). The compound was determined to be 78% ee by chiral HPLC analysis (Chiralpak OD-H, 9% EtOH/hexanes, 1.0 mL/min)  $t_r(e_1, \text{major}) = 18.7$  min,  $t_r(e_2, \text{minor}) = 22.7$  min; mp 134.0–136.5  $^\circ\text{C}$ ;  $[\alpha]_D^{20} -28.6$  ( $c$  0.97,  $\text{CHCl}_3$ );  $R_f = 0.33$  (20% EtOAc/hexanes); IR (film) 3335, 2978, 2911, 1698, 1553, 1499, 1374, 1249, 1166, 1039, 930, 859, 813  $\text{cm}^{-1}$ ;  $^1\text{H}$  NMR (400 MHz,  $\text{CDCl}_3$ )  $\delta$  6.80-6.75 (m, 3H), 5.97 (s, 2H), 5.26 (dd,  $J = 12.6, 6.0$  Hz, 1H), 5.20 (s, 1H), 4.80 (s, 1H), 4.64 (dd,  $J = 12.5, 5.7$  Hz, 1H), 1.44 (s, 9H);  $^{13}\text{C}$  NMR (100 MHz,  $\text{CDCl}_3$ ) ppm 154.6, 148.3, 147.8, 130.6, 119.8, 108.7, 106.7, 101.3, 80.7, 78.9, 52.7, 28.2; HRMS (ESI): Exact mass calcd for  $\text{C}_{14}\text{H}_{18}\text{N}_2\text{O}_6$   $[\text{M}+\text{Na}]^+$  333.1063, found 333.1067.

**Synthesis of nitroalkanes by debromination of  $\alpha$ -bromo nitroalkanes.**



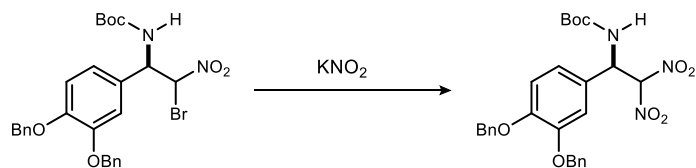
***tert*-Butyl (*R*)-(1-(3,5-bis(benzyloxy)phenyl)-2-nitroethyl)carbamate (259).** *tert*-Butyl ((1*R*)-1-(3,5-bis(benzyloxy)phenyl)-2-bromo-2-nitroethyl)carbamate (112 mg, 200  $\mu\text{mol}$ ) was dissolved in THF (2 mL) and  $\text{SnCl}_2 \cdot \text{H}_2\text{O}$  (67.7 mg, 300  $\mu\text{mol}$ ) was added. The mixture stirred for 24 hours,  $\text{H}_2\text{O}$  was added, the aqueous layer was extracted with  $\text{Et}_2\text{O}$ , and the collected organic layers were dried ( $\text{Na}_2\text{SO}_4$ ) and concentrated. Column chromatography (5-10-15-25-30% ethyl acetate in

hexanes) of the residue provided the desired nitroalkane as a white solid (70.8 mg, 74% yield). The compound was determined to be >99% ee by chiral HPLC analysis (Chiralpak IB 20% *i*PrOH/hexanes, 1.0 mL/min,  $t_r$  ( $e_1$ , major) = 9.89 min); mp = 124–126 °C;  $[\alpha]_D^{20}$  -30.2 ( $c$  0.75, CHCl<sub>3</sub>);  $R_f$  = 0.60 (30% EtOAc/hexanes); IR (film) 3362, 2980, 2932, 1697, 1607, 1597, 1556, 1512, 1378, 1163, 1056, 910, 851, 735, 697 cm<sup>-1</sup>; <sup>1</sup>H NMR (400 MHz, CDCl<sub>3</sub>)  $\delta$  7.41-7.35 (m, 10H), 6.57 (s, 1H), 6.55 (s, 2H), 5.32 (br s, 2H), 5.01 (s, 4H), 4.66 (br s, 1H), 4.64 (dd,  $J$  = 12.2, 2.8 Hz, 1H), 1.45 (s, 9H); <sup>13</sup>C NMR (100 MHz, CDCl<sub>3</sub>) ppm 160.6, 154.9, 139.5, 136.5, 128.8, 128.3, 127.7, 105.8, 101.9, 80.8, 78.9, 70.3, 52.9, 28.4; HRMS (ESI): Exact mass calcd for C<sub>27</sub>H<sub>30</sub>N<sub>2</sub>O<sub>6</sub>Na [M+Na]<sup>+</sup> 501.2002, found 501.1997.

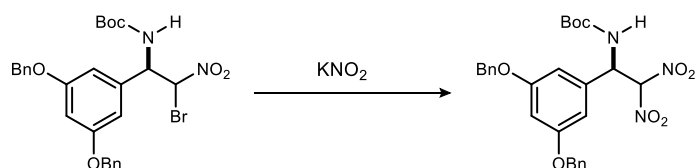


***tert*-Butyl (S)-1-(4-(benzyloxy)phenyl)-2-nitroethylcarbamate (354).** *tert*-Butyl ((1*S*)-1-(4-(benzyloxy)phenyl)-2-bromo-2-nitroethyl)carbamate (557 mg, 1.00 mmol) was dissolved in THF (10 mL) and SnCl<sub>2</sub>·H<sub>2</sub>O (339 mg, 1.50 mmol) was added. The mixture was stirred for 2 hours and water was added upon completion as indicated by TLC. The aqueous layer was extracted with Et<sub>2</sub>O and the collected organic layers were dried (Na<sub>2</sub>SO<sub>4</sub>) and concentrated. Column chromatography (15-30% ethyl acetate in hexanes) provided the nitroalkane as a white solid (354 mg, 74%). Mp = 126-130 °C;  $[\alpha]_D^{20}$  +31 ( $c$  0.88, CHCl<sub>3</sub>);  $R_f$  = 0.31 (20% EtOAc/hexanes); IR (film) 3353, 2978, 1701, 1556, 1511, 1245, 1167 cm<sup>-1</sup>; <sup>1</sup>H NMR (400 MHz, CDCl<sub>3</sub>)  $\delta$  7.43-7.32 (m, 5H), 7.23 (d,  $J$  = 8.4 Hz, 2H), 6.97 (d,  $J$  = 8.4 Hz, 2H), 5.32 (br dd,  $J$  = 14.1, 8.0 Hz, 1H), 5.19 (br s, 1H), 5.06 (s, 2H), 4.83 (br s, 1H), 4.67 (dd,  $J$  = 12.4, 5.8 Hz, 1H), 1.45 (s, 9H); <sup>13</sup>C NMR (100 MHz, CDCl<sub>3</sub>) ppm 158.9, 154.6, 136.6, 129.1, 128.6, 128.0, 127.6, 127.4, 115.4, 80.6, 78.8, 70.0, 52.4, 28.2; HRMS (ESI): Exact mass calcd for C<sub>20</sub>H<sub>25</sub>N<sub>2</sub>O<sub>5</sub> [M+H]<sup>+</sup> 373.1758, found 373.1753.

## Synthesis of $\alpha,\alpha$ -dinitroalkanes by nitrite substitution.



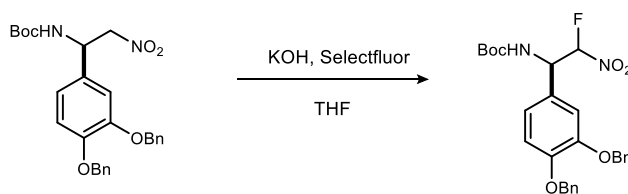
***tert*-Butyl ((1*R*)-1-(3,4-bis(benzyloxy)phenyl)-2,2-dinitroethyl)carbamate (223).** Potassium nitrite (214 mg, 2.51 mmol) was dissolved in H<sub>2</sub>O (500  $\mu$ L) and DME/MeOH (2:1, 1.6 mL). *tert*-Butyl ((1*R*)-1-(3,4-bis(benzyloxy)phenyl)-2-bromo-2-nitroethyl)carbamate (200 mg, 359  $\mu$ mol) was dissolved in DME/MeOH (2:1, 2.5 mL) and added to the potassium nitrite solution. After 5 days the reaction mixture was cooled to 0  $^{\circ}$ C, 1 N HCl (10 mL) was added, and the yellow precipitate was collected, washed with H<sub>2</sub>O and dried under vacuum. Column chromatography (5-10-15-25-30% ethyl acetate in hexanes) afforded the product as a cream-colored solid (23.4 mg, 13%). Mp 125.0–127.5  $^{\circ}$ C;  $[\alpha]_D^{20}$  -2.3 (*c* 0.62, CHCl<sub>3</sub>);  $R_f$ =0.34 (30% EtOAc/hexanes); IR (film) 3370, 2981, 2929, 1688, 1576, 1516, 1455, 1369, 1323, 1269, 1162, 1022, 857, 734, 696  $\text{cm}^{-1}$ ; <sup>1</sup>H NMR (400 MHz, CDCl<sub>3</sub>)  $\delta$  7.42-7.31 (m, 10H), 6.91 (d, *J* = 8.4 Hz, 1H), 6.87 (d, *J* = 2.0 Hz, 1H), 6.82 (dd, *J* = 8.3, 2.1 Hz, 1H), 6.51 (br s, 1H), 5.84 (br s, 1H), 5.61 (d, *J* = 9.0 Hz, 1H), 5.14 (s, 4H), 1.42 (s, 9H); <sup>13</sup>C NMR (100 MHz, CDCl<sub>3</sub>) ppm 154.6, 150.2, 149.5, 136.8, 136.7, 128.7, 128.24, 128.16, 127.6, 127.3, 125.7, 120.2, 115.2, 114.2, 111.8, 81.8, 71.8, 71.3, 55.0, 28.3; HRMS (CI): Exact mass calcd for C<sub>27</sub>H<sub>29</sub>N<sub>3</sub>O<sub>8</sub> 523.1949, found 523.1926.



***tert*-Butyl ((1*R*)-1-(3,5-bis(benzyloxy)phenyl)-2,2-dinitroethyl)carbamate (266).** Potassium nitrite (153 mg, 179  $\mu$ mol) was dissolved in H<sub>2</sub>O (300  $\mu$ L) and MeOH (1.2 mL) was added followed by a solution of *tert*-butyl ((1*R*)-1-(3,5-bis(benzyloxy)phenyl)-2-bromo-2-nitroethyl)carbamate (400 mg, 720  $\mu$ mol) in MeOH (5 mL). After 1 hour, MeCN (3 mL) was added followed by DME (1 mL). Over the course of 96 hours, potassium nitrite (368 mg, 4.62

mmol) was added along with 900  $\mu\text{L}$  of water. The reaction mixture was cooled to 0  $^{\circ}\text{C}$ , 1 N HCl (14 mL) was added, and the precipitate was collected and washed with  $\text{H}_2\text{O}$ . Column chromatography (10-25-30-40% ethyl acetate in hexanes) provided the product as a white solid (58.1 mg, 15%). Mp 151.0–152.0  $^{\circ}\text{C}$ ;  $[\alpha]_D^{20}$  -6.2 ( $c$  0.50,  $\text{CHCl}_3$ );  $R_f$ =0.30 (30% EtOAc/hexanes); IR (film) 3362, 2924, 2360, 1688, 1597, 1572, 1302, 1164, 732, 692,  $\text{cm}^{-1}$ ;  $^1\text{H}$  NMR (400 MHz,  $\text{CDCl}_3$ )  $\delta$  7.40-7.33 (m, 10H), 6.59 (s, 1H), 6.56 (br s, 1H), 6.53 (d,  $J$  = 1.6 Hz, 2H), 5.95 (br s, 1H), 5.72 (d,  $J$  = 7.6 Hz, 1H), 5.01 (s, 4H), 1.43 (s, 9H);  $^{13}\text{C}$  NMR (100 MHz,  $\text{CDCl}_3$ ) ppm 160.9, 154.6, 136.3, 135.3, 128.9, 128.4, 127.7, 111.8, 106.2, 102.7, 81.9, 70.5, 55.1, 28.3; HRMS (CI): Exact mass calcd for  $\text{C}_{27}\text{H}_{29}\text{N}_3\text{O}_8$   $[\text{M}]^+$  523.1949, found 523.1935.

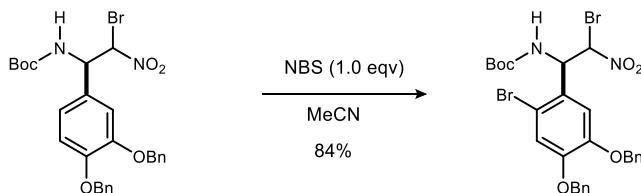
### Fluorination of nitroalkane 61a.



### *tert*-Butyl ((1*R*)-1-(3,4-bis(benzyloxy)phenyl)-2-fluoro-2-nitroethyl)carbamate (257).

Prepared according to a modified literature protocol.<sup>252</sup> *tert*-Butyl ((*R*)-1-(3,4-bis(benzyloxy)phenyl)-2-nitroethyl)carbamate (388 mg, 810  $\mu\text{mol}$ ) was dissolved in THF (620  $\mu\text{L}$ ),  $\text{H}_2\text{O}$  (1.2 mL) was added and the mixture was cooled to 0  $^{\circ}\text{C}$ . Solid KOH (52.2 mg, 810  $\mu\text{mol}$ ) was added and the mixture was stirred for 30 mins. Additional THF (200  $\mu\text{L}$ ) was added, and the mixture was stirred for another 30 mins and then cooled to -20  $^{\circ}\text{C}$ . Dichloromethane (2 mL, pre-cooled to -78  $^{\circ}\text{C}$ ) was added, followed immediately by Selectfluor (330 mg, 931  $\mu\text{mol}$ ). The reaction mixture was warmed slowly to 10  $^{\circ}\text{C}$ , stirred for 2 hours, then warmed to room temperature and stirred for 3 hours. The mixture was diluted with 1:1  $\text{Et}_2\text{O}$ /hexanes, the layers were separated, the aqueous layer was extracted ( $\text{Et}_2\text{O}$ ) and the combined organic layers were dried ( $\text{Na}_2\text{SO}_4$ ) and concentrated. Column chromatography (10-15-20-25-30% ethyl acetate in hexanes) followed by recrystallization ( $\text{EtOAc}$ /hexanes) afforded the desired product as a white solid (139 mg, 35%). Mp 144.0-147.5  $^{\circ}\text{C}$ ;  $R_f$ =0.58 (30%  $\text{EtOAc}$ /hexanes); IR (film) 3333, 2925, 2854, 1710, 1576, 1511, 1455, 1369, 1254, 1162, 1022, 736, 697  $\text{cm}^{-1}$ ; 2:1 mixture of diastereomers:  $^1\text{H}$ -NMR

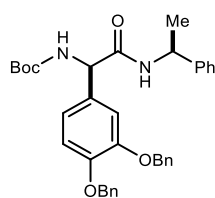
(400 MHz, CDCl<sub>3</sub>) δ 7.46-7.30 (m, 20H), 6.93 (d, *J* = 8.3 Hz, 1H), 6.90-6.80 (m, 5H), 6.19 (br d, <sup>2</sup>*J*<sub>HF</sub> = 51.1 Hz, 1H), 5.90 (br d, <sup>2</sup>*J*<sub>HF</sub> = 48.9 Hz, 1H), 5.49 (dd, <sup>2</sup>*J*<sub>HF</sub> = 22.5, *J* = 8.7 Hz, 1H), 5.34-5.22 (m, 2H), 5.16 (s, 4H), 5.13 (d, *J* = 2.4 Hz, 4H), 5.02 (d, *J* = 6.6 Hz, 1H), 1.46 (s, 9H), 1.42 (s, 9H); <sup>19</sup>F-NMR (400 MHz, CDCl<sub>3</sub>) δ -156.99, -160.22; <sup>13</sup>C NMR (100 MHz, CDCl<sub>3</sub>) ppm 154.8, 154.6, 150.2, 149.9, 149.4, 149.2, 136.91 (d, <sup>3</sup>*J*<sub>CF</sub> = 9.4 Hz), 136.89 (d, <sup>3</sup>*J*<sub>CF</sub> = 8.4 Hz), 128.7 (8C), 128.2, 128.12, 128.08, 128.06, 127.7, 127.6, 127.3 (4C), 127.1, 124.7, 121.5, 120.2, 115.1 (2C), 114.9, 114.1, 110.0 (d, <sup>1</sup>*J*<sub>CF</sub> = 242.8 Hz), 109.1 (d, <sup>1</sup>*J*<sub>CF</sub> = 243.7), 81.4, 81.3, 71.73, 71.71, 71.3, 71.2, 56.5 (d, <sup>2</sup>*J*<sub>CF</sub> = 20.8 Hz), 55.7 (d, <sup>2</sup>*J*<sub>CF</sub> = 19.3 Hz), 28.4, 28.3; HRMS (ESI): Exact mass calcd for C<sub>27</sub>H<sub>29</sub>FN<sub>2</sub>O<sub>6</sub>Na [M+Na]<sup>+</sup> 519.1907, found 519.1896.



**tert-Butyl ((1R)-1-(4,5-bis(benzyloxy)-2-bromophenyl)-2-bromo-2-nitroethyl)carbamate (259).** The α-bromonitroalkane (300 mg, 538 μmol) was dissolved in MeCN (5.4 mL). The solution was cooled to 0 °C and *N*-bromosuccinimide (105 mg, 592 μmol) was added. The mixture was warmed slowly to room temperature and stirred for 18 hours. Upon full conversion as indicated by <sup>1</sup>H NMR, the MeCN was removed in vacuo. The crude residue was reconstituted in ethyl acetate, washed with satd aq Na<sub>2</sub>S<sub>2</sub>O<sub>3</sub> and brine, dried (Na<sub>2</sub>SO<sub>4</sub>), and concentrated. Column chromatography (5-10-15-25% ethyl acetate in hexanes) afforded the desired product as an amorphous solid with 1:1 dr (286.4 mg, 84%). *R*<sub>f</sub> = 0.66 (30% EtOAc/hexanes); IR (film) 3419, 3033, 2979, 2930, 1702, 1599, 1568, 1501, 1455, 1368, 1352, 1258, 1213, 1162, 1023, 909, 858, 735, 697 cm<sup>-1</sup>; <sup>1</sup>H NMR (400 MHz, CDCl<sub>3</sub>) δ 7.45-7.31 (m, 20H), 7.12 (s, 1H), 7.11 (s, 1H), 6.87 (s, 1H), 6.84 (s, 1H), 6.39 (br s, 2H), 6.01 (br d, *J* = 7.6 Hz, 1H), 5.91 (dd, *J* = 9.0, 3.6 Hz, 1H), 5.61 (dd, *J* = 8.8, 5.3 Hz, 1H), 5.39 (d, *J* = 7.4 Hz, 1H), 5.18-5.07 (m, 8H), 1.45 (br s, 18H); <sup>13</sup>C NMR (100 MHz, CDCl<sub>3</sub>) ppm 154.6, 154.2, 150.3, 148.6, 148.2, 136.5, 136.3, 136.1, 128.60, 128.59, 128.6, 128.2, 128.1, 128.0, 127.39, 127.34, 127.3, 118.8, 118.7, 116.2, 115.4, 113.8, 83.6, 81.1, 78.4, 71.8, 71.3, 57.5, 56.9, 28.2; HRMS (ESI): Exact mass calcd for C<sub>27</sub>H<sub>28</sub>Br<sub>2</sub>N<sub>2</sub>NaO<sub>6</sub> [M+Na]<sup>+</sup> 657.0212, found 657.0238.



## Umpolung Amide Synthesis using NIS protocol.



*tert*-Butyl

**((*R*)-1-(3,4-bis(benzyloxy)phenyl)-2-oxo-2-(((*S*)-1-**

**phenylethyl)amino)ethyl) carbamate (221).** *tert*-Butyl ((*R*)-1-(3,4-

bis(benzyloxy)phenyl)-2-bromo-2-nitroethyl)carbamate (50.0 mg, 89.6  $\mu$ mol)

was dissolved in DME (900  $\mu$ L). H<sub>2</sub>O (8.08  $\mu$ L, 448  $\mu$ mol) and  $\alpha$ -

methylbenzylamine (13.9  $\mu$ L, 108  $\mu$ mol) were added, followed by K<sub>2</sub>CO<sub>3</sub> (30.9 mg, 224  $\mu$ mol)

and NIS (10.1 mg, 44.8  $\mu$ mol). The reaction was stirred for 48 h, diluted with EtOAc, and quenched

with AcOH. Water was added and the aqueous layer was extracted with EtOAc, washed twice with

saturated aq Na<sub>2</sub>S<sub>2</sub>O<sub>3</sub>, and brine, dried (Na<sub>2</sub>SO<sub>4</sub>), and concentrated. Column chromatography (8-12-20-

25-30 % ethyl acetate in hexanes) afforded the desired amide as a brown oil (29.4 mg, 58%). [ $\alpha$ ]<sub>D</sub><sup>20</sup>

-59.9 (*c* 0.73, CHCl<sub>3</sub>) R<sub>f</sub> = 0.37 (30% EtOAc/hexanes); IR (film) 3315, 3031, 2965, 2925, 1653,

1508, 1260, 1165; <sup>1</sup>H NMR (400 MHz, CDCl<sub>3</sub>) 7.44-7.43 (m, 4H), 7.37-7.24 (m, 11H), 6.94 (s,

1H), 6.91-6.88 (m, 2H), 5.81 (d, *J* = 5.9 Hz, 1H), 5.69 (s, 1H), 5.14 (s, 2H), 5.11 (s, 2H), 5.05 (dq,

*J* = 5.8, 5.6 Hz, 1H), 4.98 (s, 1H), 1.40 (s, 9H), 1.32 (d, *J* = 5.5 Hz, 3H), <sup>13</sup>C NMR (100 MHz,

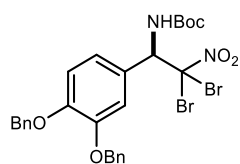
CDCl<sub>3</sub>) ppm 169.4, 153.5, 149.4, 149.2, 142.7, 137.3, 137.1, 131.8, 128.9, 128.6, 128.03, 127.99,

127.7, 127.5, 127.4, 126.3, 120.8, 115.3, 113.7, 77.4, 71.4, 71.3, 49.3, 28.4, 21.5; HRMS (ESI):

Exact mass calcd for C<sub>35</sub>H<sub>38</sub>N<sub>2</sub>O<sub>5</sub>Na [M+Na]<sup>+</sup> 589.2678, found 589.2668.

In addition, dibromonitroalkane **225** was detected by crude <sup>1</sup>H-NMR and was spectroscopically

identical to an authentic sample.



*tert*-Butyl

**((*R*)-1-(3,4-bis(benzyloxy)phenyl)-2,2-dibromo-2-**

**nitroethyl)carbamate (225).** Isolated as a brown solid. Mp 102.5–105.0 °C;

[ $\alpha$ ]<sub>D</sub><sup>20</sup> -9.8 (*c* 0.15, CHCl<sub>3</sub>); R<sub>f</sub> = 0.50 (30% EtOAc/hexanes); IR (film) 3320,

2921, 2852, 2359, 2341, 1717, 1541, 1509, 1473, 1457, 1259, 1161, 1141,

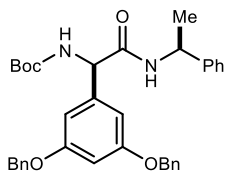
736, 696 cm<sup>-1</sup>; <sup>1</sup>H NMR (600 MHz, CDCl<sub>3</sub>)  $\delta$  7.45-7.35 (m, 10H), 7.02 (d, *J* = 1.9 Hz, 1H), 6.99

(dd, *J* = 8.3, 1.7 Hz, 1H), 6.92 (d, *J* = 8.3 Hz, 1H), 5.66 (s, 1H), 5.17 (s, 2H), 5.16 (s, 2H), 4.94 (s,

1H), 1.47 (s, 9H); <sup>13</sup>C NMR (150 MHz, CDCl<sub>3</sub>) ppm 154.3, 150.0, 149.5, 136.9, 136.8, 131.0,

129.0, 128.7, 128.6, 128.2, 128.1, 128.0, 127.6, 127.3, 126.5, 120.3, 118.0, 115.1, 113.7, 81.7,

71.6, 71.3, 46.0, 28.4.



**tert-Butyl**

**((R)-1-(3,5-bis(benzyloxy)phenyl)-2-oxo-2-(((S)-1-**

**phenylethyl)amino)ethyl)carbamate (229).** *tert*-Butyl ((1*R*)-1-(3,5-

**bis(benzyloxy)phenyl)-2-bromo-2-nitroethyl)carbamate (100 mg, 179  $\mu$ mol)**

was dissolved in DME (1.8 mL). H<sub>2</sub>O (16.2  $\mu$ L, 896  $\mu$ mol) and  $\alpha$ -

methylbenzylamine (27.8  $\mu$ L, 215  $\mu$ mol) were added, followed by K<sub>2</sub>CO<sub>3</sub> (61.9 mg, 448  $\mu$ mol)

and NIS (20.2 mg, 89.6  $\mu$ mol). The reaction was stirred for 48 h, diluted with EtOAc, and quenched

with AcOH. Water was added and the aqueous layer was extracted with EtOAc, washed twice with

saturated aq Na<sub>2</sub>S<sub>2</sub>O<sub>3</sub>, and brine, dried (Na<sub>2</sub>SO<sub>4</sub>), and concentrated. Column chromatography (8-15-25-

30 % ethyl acetate in hexanes) afforded the desired amide as a brown oil (36.2 mg, 36%). ;  $[\alpha]_D^{20}$

-38.6 (*c* 0.66, CHCl<sub>3</sub>)  $R_f$  = 0.41 (30% EtOAc/hexanes); IR (film) 3315, 2977, 2923, 1699, 1655,

1597, 1496, 1454, 1368, 1161, 1053, 698; <sup>1</sup>H NMR (400 MHz, CDCl<sub>3</sub>) 7.39-7.26 (m, 15H), 6.60

(br d, *J* = 22.4 Hz, 3H), 6.04 (d, *J* = 6.0 Hz, 1H), 5.83 (br s, 1H), 5.09 (m, 2H), 4.99 (s, 4H), 1.41

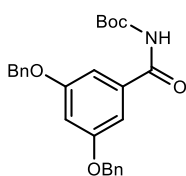
(s, 9H), 1.35 (d, *J* = 6.8 Hz, 3H), <sup>13</sup>C NMR (100 MHz, CDCl<sub>3</sub>) ppm 168.8, 160.3, 155.4, 142.6,

140.7, 136.6, 136.1, 128.6, 128.2, 128.0, 127.6, 127.53, 127.49, 127.4, 126.1, 106.2, 102.0, 80.1,

70.0, 49.1, 28.2, 21.3.

In addition, imide **236** was observed by crude <sup>1</sup>H-NMR and was spectroscopically identical (<sup>1</sup>H-

NMR) to a pure sample.<sup>284</sup>



**tert-Butyl (3,5-bis(benzyloxy)benzoyl)carbamate (236).** Isolated as a white

solid. Mp 133.0–135.5 °C;  $R_f$  = 0.15 (20% EtOAc/hexanes); IR (film) 3248,

2978, 1746, 1680, 1593, 1518, 1456, 1161, 1048 cm<sup>-1</sup>; <sup>1</sup>H NMR (400 MHz,

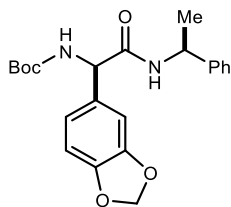
CDCl<sub>3</sub>)  $\delta$  7.83 (br s, 1H), 7.41-7.31 (m, 10H), 6.99 (d, *J* = 2.4 Hz, 2H), 6.76 (d, *J*

= 2.2 Hz, 1H), 5.04 (s, 4H), 1.51 (s, 9H); <sup>13</sup>C NMR (100 MHz, CDCl<sub>3</sub>) ppm 164.8, 160.3, 149.5,

136.3, 135.7, 128.8, 128.4, 127.8, 106.7, 106.3, 82.9, 70.6, 28.2; HRMS (ESI): Exact mass calcd

for C<sub>26</sub>H<sub>27</sub>NO<sub>5</sub>Na [M+Na]<sup>+</sup> 456.1787, found 456.1776.

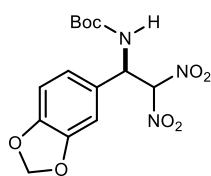
<sup>284</sup> Analytically pure imide **66b** was isolated (174 mg, 30%) by Dr. Kazuyuki Tokumaru during the synthesis of imine **55b**, prepared according to the general procedure for the synthesis of *N*-Boc imines using *tert*-butyl ((3,5-bis(benzyloxy)phenyl)(phenylsulfonyl)methyl)carbamate (750 mg, 1.34 mmol), potassium carbonate (926 mg, 6.70 mmol), sodium sulfate (952 mg, 6.70 mmol), and THF (7.5 mL).



**tert-Butyl ((R)-1-(benzo[d][1,3]dioxol-5-yl)-2-oxo-2-(((S)-1-phenylethyl)amino)ethyl)carbamate (248).**

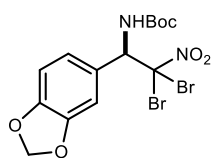
*tert*-Butyl ((1*R*)-1-(benzo[*d*][1,3]dioxol-5-yl)-2-bromo-2-nitroethyl)carbamate (30.0 mg, 77.0 μmol) was dissolved in DME (770 μL). H<sub>2</sub>O (6.9 μL, 385 μmol) and α-methylbenzylamine (11.9 μL, 92.0 μmol) were added, followed by K<sub>2</sub>CO<sub>3</sub> (26.6 mg, 193 μmol) and NIS (17.3 mg, 77.0 μmol). The reaction was stirred for 48 h, diluted with EtOAc, and quenched with 1 N HCl. Water was added and the aqueous layer was extracted with EtOAc, washed twice with satd aq Na<sub>2</sub>S<sub>2</sub>O<sub>3</sub>, and brine, dried (Na<sub>2</sub>SO<sub>4</sub>), and concentrated. Column chromatography (8-12-20-25-30 % ethyl acetate in hexanes) afforded the desired amide as a brown oil (8.6 mg, 28%);  $[\alpha]_D^{20}$  -64.5 (*c* 0.70, CHCl<sub>3</sub>) *R*<sub>f</sub> = 0.38 (30% EtOAc/hexanes); IR (film) 3314, 2977, 2928, 1700, 1655, 1504, 1489, 1447, 1392, 1367, 1247, 1167, 1095, 1040, 933, 803, 759, 699; <sup>1</sup>H NMR (400 MHz, DMSO-*d*<sub>6</sub>) 8.50 (d, *J* = 7.6 Hz, 1H), 7.31 (s, 2H), 7.30 (d, *J* = 1.6, 2H), 7.21 (m, 2H), 6.99 (s, 1H), 6.90 (dd, *J* = 8.0, 1.6 Hz, 1H), 6.86 (d, *J* = 8.0 Hz, 1H), 5.99 (d, *J* = 2.0 Hz, 2H), 5.12 (d, *J* = 8.8 Hz, 1H), 4.83 (qd, *J* = 7.2, 7.2 Hz, 1H), 1.36 (s, 9H), 1.27 (d, *J* = 7.0, 3H) <sup>13</sup>C NMR (100 MHz, DMSO-*d*<sub>6</sub>) ppm 169.3, 154.8, 147.1, 146.6, 144.2, 132.8, 128.2, 126.7, 126.0, 123.1, 120.6, 107.9, 107.5, 101.0, 78.4, 70.1, 48.1, 28.2, 22.3; HRMS (ESI): Exact mass calcd for C<sub>22</sub>H<sub>26</sub>N<sub>2</sub>O<sub>5</sub>Na [M+Na]<sup>+</sup> 421.1739, found 421.1726.

In addition, dinitroalkane **249** (5.5 mg, 20%) and dibromonitroalkane **S5** (2.5 mg, 5%) were isolated.



**tert-Butyl (R)-1-(benzo[d][1,3]dioxol-5-yl)-2,2-dinitroethyl)carbamate**

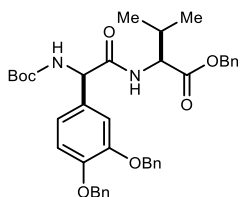
**(249).** Isolated as viscous yellow oil. *R*<sub>f</sub> = 0.31 (30% EtOAc/hexanes); IR (film) 3325, 2958, 2922, 2852, 2359, 1709, 1583, 1505, 1489, 1448, 1369, 1252, 1159, 1040 cm<sup>-1</sup>; <sup>1</sup>H NMR (600 MHz, CDCl<sub>3</sub>) δ 6.81 (s, 3H), 6.59 (br s, 1H), 6.00 (s, 2H), 5.90 (br s, 1H), 5.70 (d, *J* = 4.8 Hz, 1H), 1.44 (s, 9H); <sup>13</sup>C NMR (150 MHz, CDCl<sub>3</sub>) ppm 154.8, 148.8, 131.1, 120.8, 111.9, 109.2, 107.2, 101.9, 82.0, 55.1, 28.2; HRMS (CI) Exact mass calcd for C<sub>14</sub>H<sub>18</sub>N<sub>3</sub>O<sub>8</sub> [MH]<sup>+</sup> 356.1088 found 356.1076.



**tert-Butyl (R)-1-(benzo[d][1,3]dioxol-5-yl)-2,2-dibromo-2-nitroethyl)carbamate (S5).**

Isolated as a yellow oil.  $[\alpha]_D^{20}$  -11.2 (*c* 0.11, CHCl<sub>3</sub>); *R*<sub>f</sub> = 0.49 (30% EtOAc/hexanes); IR (film) 3315, 2960, 2922, 2851, 2360, 1717, 1565, 1505, 1490, 1447, 1393, 1369, 1251, 1162, 1097, 1039, 932,

861, 799, 699  $\text{cm}^{-1}$ ;  $^1\text{H NMR}$  (600 MHz,  $\text{CDCl}_3$ )  $\delta$  6.98 (dd,  $J = 8.0, 1.5$  Hz, 1H), 6.92 (d,  $J = 1.8$  Hz, 1H), 6.83 (d,  $J = 8.0$  Hz, 1H), 6.00 (s, 2H), 5.68 (s, 1H), 4.99 (s, 1H), 1.48 (s, 9H);  $^{13}\text{C NMR}$  (150 MHz,  $\text{CDCl}_3$ ) ppm 154.3, 148.8, 148.7, 127.3, 120.9, 117.9, 108.9, 107.5, 101.8, 81.8, 46.0, 28.4.



### Benzyl

### *((R)-2-(3,4-bis(benzyloxy)phenyl)-2-((tert-*

**butoxycarbonyl)amino)acetyl)-L-valinate (227).** *tert*-Butyl ((1*R*)-1-(3,4-bis(benzyloxy)phenyl)-2-bromo-2-nitroethyl)carbamate (100 mg, 179  $\mu\text{mol}$ ) was dissolved in DME (1.80 mL).  $\text{H}_2\text{O}$  (16.0  $\mu\text{l}$  897  $\mu\text{mol}$ ) and (*L*)-valine

benzyl ester-HCl (52.5 mg, 215  $\mu\text{mol}$ ) were added, followed by  $\text{K}_2\text{CO}_3$  (99.0 mg, 718  $\mu\text{mol}$ ) and NIS (20.2 mg, 89.0  $\mu\text{mol}$ ). The reaction was stirred for 48 h, diluted with EtOAc, and quenched with AcOH. Water was added and the aqueous layer was extracted with EtOAc, washed twice with satd aq  $\text{Na}_2\text{S}_2\text{O}_3$ , and brine, dried ( $\text{Na}_2\text{SO}_4$ ), and concentrated. Column chromatography (10-15-20-25-30 % EtOAc/hexanes) followed by preparatory HPLC afforded the desired amide as a light pink solid (19.9 mg, 17%). MP 121.0-125.0  $^\circ\text{C}$ ;  $[\alpha]_D^{20}$  -53.3 ( $c$  0.55,  $\text{CHCl}_3$ );  $R_f$  = 0.19 (20% EtOAc/hexanes); IR (film) 3318, 2967, 1735, 1659, 1509;  $^1\text{H NMR}$  (400 MHz,  $\text{CDCl}_3$ )  $\delta$  7.41 (d,  $J = 7.4$  Hz, 2H), 7.37-7.29 (m, 11H), 6.99 (s, 1H), 6.89 (s, 2H), 6.23 (d,  $J = 7.9$  Hz, 1H), 5.60 (s, 1H), 5.19 (d,  $J = 12.2$  Hz, 1H), 5.12 (d,  $J = 6.0$  Hz, 5H), 5.04 (br s, 1H), 4.58 (dd,  $J = 9.0, 4.6$ , 1H), 2.08 (dq,  $J = 13.1, 6.6, 6.6$  Hz, 1H), 1.41 (s, 9H), 0.72 (d,  $J = 6.8$  Hz, 3H), 0.63 (d,  $J = 6.8$  Hz, 3H);  $^{13}\text{C NMR}$  (100 MHz  $\text{CDCl}_3$ ) ppm 171.7, 170.1, 155.1, 149.6, 149.1, 137.2, 137.1, 135.3, 128.8, 128.7, 128.6, 128.5, 128.01, 127.95, 127.6, 127.4, 120.7, 115.5, 113.6, 80.3, 71.40, 71.36, 67.3, 58.9, 57.1, 31.5, 28.4, 19.0, 17.3; HRMS (ESI): Exact mass calcd for  $\text{C}_{39}\text{H}_{44}\text{N}_2\text{O}_7\text{Na}$   $[\text{M}+\text{Na}]^+$  675.3046, found 675.3066.

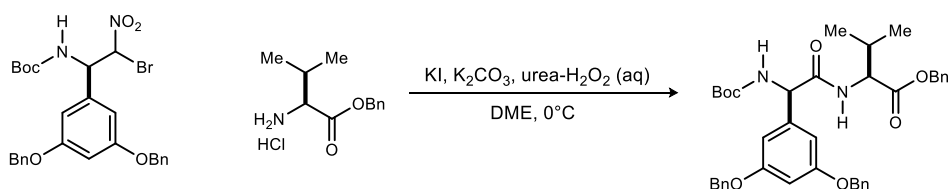
### Umpolung Amide Synthesis using the KI/Urea-hydrogen peroxide protocol.

**General procedure for the amidation of  $\alpha$ -bromo nitroalkane with an amine:** To a vigorously stirred mixture of amine (0.10 mmol),  $\alpha$ -bromo nitroalkane (0.12 mmol, 1.2 equiv), potassium iodide<sup>285</sup> (0.20 mmol, 2.0 equiv) and potassium carbonate (0.60 mmol, 6.0 equiv)<sup>286</sup> in 1,2-

<sup>285</sup> For best results, the potassium iodide should be ground by mortar & pestle prior to use.

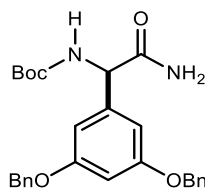
<sup>286</sup> Potassium carbonate should be added just before addition of the urea-hydrogen peroxide solution to prevent decomposition of the bromonitroalkane.

dimethoxyethane (1.0 mL) was added a freshly prepared solution of urea-hydrogen peroxide in water (3.0 M solution, 0.10 mL, 0.30 mmol, 3.0 equiv) over 2 h by syringe pump at 0 °C. After the addition was complete, the mixture was stirred for an additional 22 h at the same temperature. Aqueous sodium thiosulfate was then added and the mixture was extracted with ethyl acetate. The organic layers were washed with 1 M HCl and brine, dried (sodium sulfate) and concentrated *in vacuo*. The residue was purified by flash column chromatography or recrystallization to give pure amide product.



**Benzyl ((*R*)-2-(3,5-bis(benzyloxy)phenyl)-2-((*tert*-butoxycarbonyl)amino)acetyl)-*L*-valinate (230).** Following the general procedure, the  $\alpha$ -bromo nitroalkane (67 mg, 120  $\mu$ mol) and the amine (24 mg, 100  $\mu$ mol) provided the amide after flash column chromatography (silica gel, 10-50% ethyl acetate in hexanes) as a colorless solid (47 mg, 72% yield);<sup>287</sup> Mp = 107-109 °C (recrystallized from diethyl ether/hexanes);  $[\alpha]_D^{20}$  -34 (*c* 0.49, CHCl<sub>3</sub>),  $R_f$  = 0.46 (30% EtOAc/hexanes); IR (film) 3319, 2977, 2924, 1699, 1655, 1596, 1496, 1454, 1368, 1161, 1053, 698 cm<sup>-1</sup>; <sup>1</sup>H NMR (400 MHz, CDCl<sub>3</sub>)  $\delta$  7.40-7.31 (series of m, 15H), 6.63 (d, *J* = 2.1 Hz, 2H), 6.54 (dd, *J* = 2.3, 2.3 Hz, 1H), 6.21 (d, *J* = 9.0 Hz, 1H), 5.66 (br s, 1H), 5.18 (d, *J* = 12.2 Hz, 1H), 5.12 (d, *J* = 12.2 Hz, 1H), 5.05 (br s, 1H), 5.00 (s, 4H), 4.57 (d, *J* = 9.0, 4.7 Hz, 1H), 2.14-2.03 (m, 1H), 1.41 (s, 9H), 0.74 (d, *J* = 6.9 Hz, 3H), 0.65 (d, *J* = 6.9 Hz, 3H); <sup>13</sup>C NMR (100 MHz, CDCl<sub>3</sub>) ppm 171.6, 169.7, 160.6, 155.1, 140.8, 136.8, 135.3, 128.83, 128.78, 128.7, 128.6, 128.5, 128.4, 128.2, 127.8, 127.7, 106.7, 106.4, 102.4, 80.3, 70.3, 67.3, 59.2, 57.2, 31.5, 28.4, 19.0, 17.3; HRMS (ESI): Exact mass calcd for C<sub>39</sub>H<sub>45</sub>N<sub>2</sub>O<sub>7</sub> [M+H]<sup>+</sup> 653.3221, found 653.3225.

<sup>287</sup> On gram-scale, the crude residue is passed through a short silica plug (ethyl acetate), concentrated, and then recrystallized from diethyl ether.

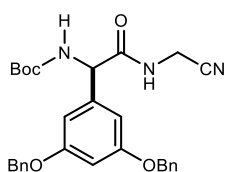


**tert-Butyl**

**(R)-(2-amino-1-(3,5-bis(benzyloxy)phenyl)-2-**

**oxoethyl)carbamate (374).**

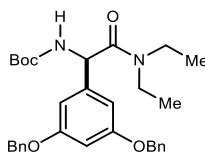
This compound was prepared according to the General Procedure using the bromonitroalkane (250 mg, 44.8  $\mu\text{mol}$ ) and ammonium chloride (28.8 mg, 53.8  $\mu\text{mol}$ ). The crude mixture was purified by flash column chromatography (5-10-20% methanol in dichloromethane) to afford the product as a white foam (110 mg, 53%).  $[\alpha]_D^{20}$  -110 (*c* 0.38,  $\text{CHCl}_3$ );  $R_f$  = 0.51 (5% MeOH/DCM); IR (film) 3360, 3200, 1676, 1661, 1596, 1529, 1160  $\text{cm}^{-1}$ ;  $^1\text{H}$  NMR (400 MHz,  $\text{CDCl}_3$ )  $\delta$  7.37 (br m, 10 H), 6.65 (s, 2H), 6.55 (s, 1H), 5.89 (br s, 2H), 5.56 (br s, 1H), 5.17 (br s, 1H), 4.95 (br s, 4H), 1.41 (s, 9H);  $^{13}\text{C}$  NMR (100 MHz,  $\text{CDCl}_3$ ) ppm 172.0, 160.5, 155.4, 141.7, 140.7, 136.7, 128.7, 128.2, 127.7, 106.3, 102.1, 80.4, 70.2, 58.5, 28.5; HRMS (ESI): Exact mass calcd for  $\text{C}_{27}\text{H}_{31}\text{N}_2\text{O}_5$   $[\text{M}+\text{H}]^+$  463.2227, found 463.2251.



**tert-Butyl (R)-(1-(3,5-bis(benzyloxy)phenyl)-2-((cyanomethyl)amino)-2-**

**oxoethyl)carbamate (268).**

This compound was prepared according to the General Procedure using the bromonitroalkane (66.9 mg, 120  $\mu\text{mol}$ ), aminoacetonitrile bisulfate (15.4 mg, 100  $\mu\text{mol}$ ), and  $\text{K}_2\text{CO}_3$  (8.0 equiv.). The crude mixture was purified by flash column chromatography (10-20-50% ethyl acetate in hexanes) to afford the product as a tan foam (16.9 mg, 34%)<sup>288</sup>;  $[\alpha]_D^{20}$  -67 (*c* 0.25,  $\text{CHCl}_3$ );  $R_f$  = 0.46 (50% EtOAc/hexanes) IR (film) 3350, 3287, 3068, 2981, 2930, 1686, 1659, 1609, 1522, 1448, 1369, 1252, 1167  $\text{cm}^{-1}$ ;  $^1\text{H}$  NMR (400 MHz,  $\text{CHCl}_3$ )  $\delta$  7.37-7.32 (m, 10H), 6.76 (s, 1H), 6.60 (s, 2H), 6.52 (dd,  $J$  = 2.0, 2.0 Hz, 1H), 5.83 (s, 1H), 5.23 (s, 1H), 4.94 (d,  $J$  = 11.3 Hz, 2H), 4.89 (d,  $J$  = 11.2 Hz, 2H), 4.10 (dd,  $J$  = 17.5, 5.9 Hz, 1H), 4.00 (dd,  $J$  = 17.5, 5.7 Hz, 1H), 1.44 (s, 9H);  $^{13}\text{C}$  NMR (100 MHz,  $\text{CHCl}_3$ ) ppm 170.5, 160.7, 155.6, 139.5, 136.7, 128.8, 128.3, 127.8, 115.7, 106.4, 102.5, 81.0, 70.3, 58.6, 28.5, 27.9; HRMS (ESI): Exact mass calcd for  $\text{C}_{29}\text{H}_{32}\text{N}_3\text{O}_5$   $[\text{M}+\text{H}]^+$  502.2336, found 502.2344.



**tert-Butyl**

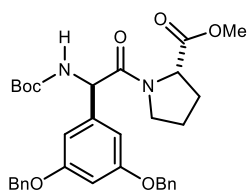
**(R)-(1-(3,5-bis(benzyloxy)phenyl)-2-(diethylamino)-2-**

**oxoethyl)carbamate (269).**

This compound was prepared according to the

<sup>288</sup> Analysis of the crude material by  $^1\text{H}$ -NMR using an internal standard indicated a 55% yield.

General Procedure using the bromonitroalkane (66.9 mg, 120  $\mu\text{mol}$ ) and diethylamine (10.4  $\mu\text{L}$ , 100  $\mu\text{mol}$ ). The crude mixture (66% NMR yield) was purified by flash column chromatography (15-30% ethyl acetate in hexanes) to afford the product as a tan foam (26.9 mg, 52%).  $[\alpha]_D^{20}$  -97 (*c* 0.23,  $\text{CHCl}_3$ );  $R_f$  = 0.41 (30% EtOAc/hexanes); IR (film) 3308, 2975, 2929, 1709, 1640, 1596, 1453, 1161  $\text{cm}^{-1}$ ;  $^1\text{H}$  NMR (600 MHz,  $\text{CHCl}_3$ )  $\delta$  7.41-7.30 (series of m, 10H), 6.64 (s, 2H), 6.56 (s, 1H), 5.98 (br s, 1H), 5.44 (s,  $J$  = 7.9 Hz, 1H), 5.02 (d,  $J$  = 11.8 Hz, 2H), 5.00 (d,  $J$  = 11.2 Hz, 2H), 3.45 (ddd,  $J$  = 13.8, 13.8, 6.8 Hz, 1H), 3.26 (ddd,  $J$  = 14.1, 14.1, 7.1 Hz, 2H), 3.06 (ddd,  $J$  = 14.6, 14.6, 7.3 Hz, 1H), 1.42 (s, 9H), 1.09 (dd,  $J$  = 7.1, 7.1 Hz, 3H), 0.95 (dd,  $J$  = 7.1, 7.1 Hz, 3H);  $^{13}\text{C}$  NMR (150 MHz,  $\text{CHCl}_3$ ) ppm 169.0, 160.4, 155.2, 140.9, 136.8, 128.7, 128.1, 127.7, 106.8, 102.3, 79.7, 70.2, 55.2, 41.7, 40.6, 28.5, 13.9, 12.8; HRMS (ESI): Exact mass calcd for  $\text{C}_{31}\text{H}_{39}\text{N}_2\text{O}_5$   $[\text{M}+\text{H}]^+$  519.2853, found 519.2835.

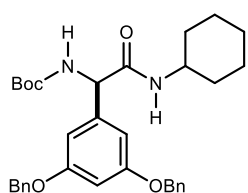


#### Methyl

#### ((*R*)-2-(3,5-bis(benzyloxy)phenyl)-2-((*tert*-

butoxycarbonyl)amino)acetyl)-L-prolinate (270). This compound was prepared according to the General Procedure using the bromonitroalkane (84.8 mg, 152  $\mu\text{mol}$ ) and L-proline methyl ester hydrochloride (21.0 mg, 127  $\mu\text{mol}$ ).

The crude mixture was purified by flash column chromatography (15-25-30-40% ethyl acetate in hexanes) to afford the product as a white foam (44.3 mg, 77%).  $[\alpha]_D^{20}$  -130 (*c* 0.50,  $\text{CHCl}_3$ );  $R_f$  = 0.24 (30% EtOAc/hexanes) IR (film) 3418, 2977, 1746, 1711, 1649, 1596, 1495, 1434, 1162  $\text{cm}^{-1}$ ;  $^1\text{H}$  NMR (400 MHz,  $\text{CHCl}_3$ )  $\delta$  7.42-7.29 (series of m, 10H), 6.62 (d,  $J$  = 1.9 Hz, 2H), 6.57 (dd,  $J$  = 2.1, 2.1 Hz, 1H), 6.04 (d,  $J$  = 7.4 Hz, 1H), 5.33 (d,  $J$  = 7.5 Hz, 1H), 5.02 (s, 4H), 4.34 (dd,  $J$  = 8.1, 3.5 Hz, 1H), 3.75 (s, 3H), 3.66-3.61 (m, 1H), 3.08-3.02 (m, 1H), 2.02-1.89 (m, 2H), 1.73-1.70 (m, 2H), 1.41 (s, 9H);  $^{13}\text{C}$  NMR (100 MHz,  $\text{CHCl}_3$ ) ppm 172.3, 168.5, 160.0, 154.7, 139.7, 136.6, 128.5, 127.9, 127.4, 106.8, 102.2, 79.6, 69.9, 59.2, 56.5, 52.3, 46.6, 28.9, 28.3, 24.5; HRMS (ESI): Exact mass calcd for  $\text{C}_{33}\text{H}_{39}\text{N}_2\text{O}_7$   $[\text{M}+\text{H}]^+$  575.2752, found 575.2759.



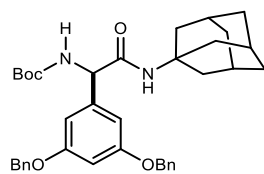
#### *tert*-Butyl

#### (*R*)-1-(3,5-bis(benzyloxy)phenyl)-2-(cyclohexylamino)-2-

oxoethyl)carbamate (271). This compound was prepared according to the General Procedure using the bromonitroalkane (66.9 mg, 120  $\mu\text{mol}$ ) and cyclohexylamine (11.4  $\mu\text{L}$ , 100  $\mu\text{mol}$ ).

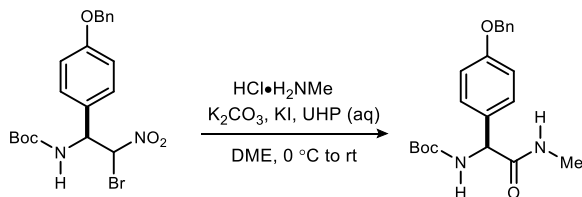
The reaction was warmed to room temperature after the addition of urea hydrogen peroxide and stirred for 24 hours. The crude mixture was purified by flash column chromatography (15-30-50% ethyl acetate in hexanes) to

afford the product as a light brown foam (41.3 mg, 76%).  $[\alpha]_D^{20}$  -54 (*c* 0.45, CHCl<sub>3</sub>);  $R_f$  = 0.47 (30% EtOAc/hexanes, CAM stain); IR (film) 3295, 2931, 2856, 1684, 1648, 1597, 1522, 1165 cm<sup>-1</sup>; <sup>1</sup>H NMR (400 MHz, CHCl<sub>3</sub>)  $\delta$  7.41-7.32 (m, 10H), 6.60 (s, 2H), 6.55 (dd, *J* = 1.8, 1.8 Hz, 1H), 5.84 (s, 1H), 5.49 (d, *J* = 7.8 Hz, 1H), 5.00 (br s, 5H), 3.75-3.66 (m, 1H), 1.88 (br d, *J* = 10.0 Hz, 1H), 1.71-1.65 (m, 2H), 1.59-1.56 (m, 2H), 1.49 (s, 9H), 1.35-1.26 (m, 2H), 1.16-1.04 (m, 2H), 0.99-0.88 (m, 1H); <sup>13</sup>C NMR (100 MHz, CHCl<sub>3</sub>) ppm 168.6, 160.2, 155.1, 141.1, 136.6, 128.5, 128.0, 127.5, 106.1, 101.9, 79.9, 70.0, 58.6, 48.5, 32.7, 32.5, 28.3, 25.3, 24.6, 24.5; HRMS (ESI): Exact mass calcd for C<sub>33</sub>H<sub>41</sub>N<sub>2</sub>O<sub>5</sub> [M+H]<sup>+</sup> 545.3010, found 545.3016.



**tert-Butyl ((R)-2-(((3S,5S,7S)-adamantan-1-yl)amino)-1-(3,5-bis(benzyloxy)phenyl)-2-oxoethyl)carbamate (272).** This compound was prepared according to the General Procedure using the bromonitroalkane (66.9 mg, 120  $\mu$ mol) and 1-adamantamine (15.1 mg, 100  $\mu$ mol). The crude mixture was purified by flash column chromatography (15-30-50% ethyl acetate in hexanes) to afford the product (58.9 mg, 37%) as a foam. The compound was further purified by preparative HPLC for characterization purposes (0-40% MeCN/H<sub>2</sub>O, 0.1% HCOOH, retention time = 11.6 min) to provide the title compound as a white foam.  $[\alpha]_D^{20}$  -59 (*c* 0.45, CHCl<sub>3</sub>);  $R_f$  = 0.61 (30% EtOAc/hexanes); IR (film) 3320, 2909, 2851, 1659, 1596, 1162 cm<sup>-1</sup>; <sup>1</sup>H NMR (600 MHz, CHCl<sub>3</sub>)  $\delta$  7.42-7.37 (m, 8H), 7.32 (dd, *J* = 7.2 Hz, 2H), 6.59 (br s, 2H), 6.56 (dd, *J* = 2.1, 2.1 Hz, 1H), 5.82 (s, 1H), 5.22 (s, 1H), 5.02 (s, 4H), 4.90 (s, 1H), 2.04 (br s, 3H) 1.87 (d, *J* = 2.3 Hz, 6H), 1.64 (br s, 6H), 1.42 (s, 9H); <sup>13</sup>C NMR (150 MHz, CHCl<sub>3</sub>) ppm 168.7, 160.5, 155.4, 141.7, 136.9, 128.8, 128.2, 127.7, 106.4, 102.1, 80.0, 70.3, 59.1, 52.5, 41.5, 36.4, 29.6, 28.5; HRMS (ESI): Exact mass calcd for C<sub>38</sub>H<sub>44</sub>N<sub>2</sub>O<sub>5</sub> [M+H]<sup>+</sup> 597.3323, found 597.3300.

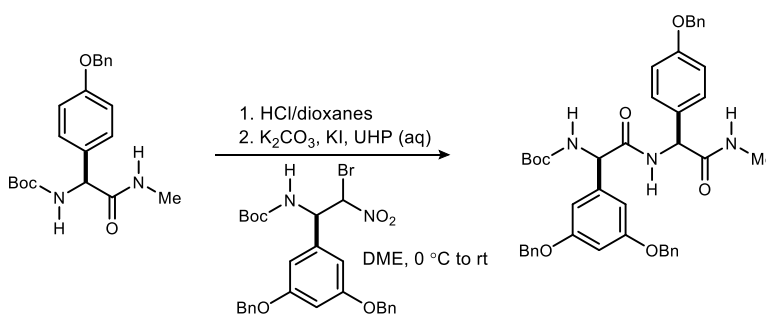
### Synthesis of Dipeptide 277



**tert-Butyl ((S)-1-(4-(benzyloxy)phenyl)-2-(methylamino)-2-oxoethyl)carbamate (375).** This compound was prepared according to the UmAS General Procedure using *tert*-butyl ((1S)-1-(4-



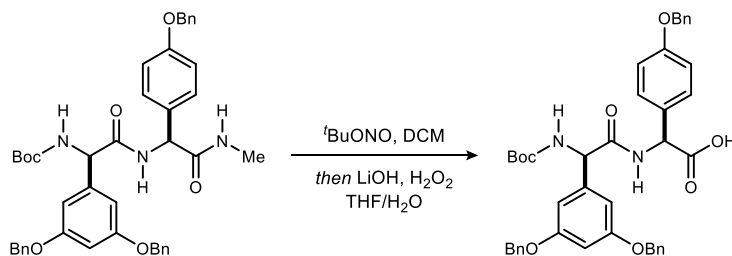
(benzyloxy)phenyl)-2-bromo-2-nitroethyl)carbamate (3.00 g, 6.65 mmol)<sup>289</sup> and methyl amine hydrochloride (539 mg, 7.98 mmol). The crude mixture was purified by flash column chromatography (25-40% ethyl acetate in hexanes) to afford the product as a white solid (1.64 g, 67%). MP = 147-151 °C;  $[\alpha]_D^{20}[\alpha]_n^{2C} +77.3$  (*c* 0.53, CHCl<sub>3</sub>); *R<sub>f</sub>* = 0.4 (40% EtOAc/ hexanes); IR (film) 3302, 2977, 1657, 1556, 1527, 1511, 1366, 1249, 1171 cm<sup>-1</sup>; <sup>1</sup>H NMR (600 MHz, CDCl<sub>3</sub>) δ 7.42-7.36 (m, 4H), 7.33-7.31 (m, 1H), 7.27 (d, *J* = 8.9 Hz, 2H), 6.93 (d, *J* = 8.7 Hz, 2H), 5.94 (s, 1H), 5.81 (s, 1H), 5.04 (s, 2H), 2.77 (d, *J* = 4.9 Hz, 3H), 1.26 (s, 9H); <sup>13</sup>C NMR (150 MHz, CDCl<sub>3</sub>) ppm 171.1, 158.9, 155.4, 136.9, 131.1, 128.7, 128.6, 128.2, 127.6, 115.4, 80.1, 70.2, 58.0, 24.5, 26.6; HRMS (ESI): Exact mass calcd for C<sub>21</sub>H<sub>27</sub>N<sub>2</sub>O<sub>4</sub> [M+H]<sup>+</sup> 371.1965, found 371.1967.



**tert-Butyl ((R)-2-(((S)-1-(4-(benzyloxy)phenyl)-2-(methylamino)-2-oxoethyl)amino)-1-(3,5-bis(benzyloxy)phenyl)-2-oxoethyl)carbamate (376).** This compound was prepared according to the UmAS General Procedure using *tert*-butyl (*S*)-1-(4-(benzyloxy)phenyl)-2-(methylamino)-2-oxoethyl)carbamate (1.12 g, 3.03 mmol) and  $\alpha$ -bromo nitroalkane (1.69 g, 3.03 mmol). After aqueous urea-hydrogen peroxide addition, the reaction was stirred at 0 °C for an additional hour before stirring at room temperature overnight. The crude mixture was purified by flash column chromatography (25-75% ethyl acetate in hexanes) to afford the product as a white solid (1.02 g, 47%). MP = 211-215 °C;  $[\alpha]_D^{20}[\alpha]_n^{2C} -12.2$  (*c* 0.53, CHCl<sub>3</sub>); *R<sub>f</sub>* = 0.3 (60% EtOAc/hexanes); IR (film) 3297, 3034, 2980, 2361, 1685, 1641, 1606, 1513, 1164 cm<sup>-1</sup>; <sup>1</sup>H NMR (600 MHz, DMSO-*d*<sub>6</sub>) δ 8.78 (d, *J* = 7.9 Hz, 1H), 8.23 (d, *J* = 4.1 Hz, 1H), 7.42-7.30 (m, 16H), 7.21 (d, *J* = 8.6 Hz,

<sup>289</sup> Lim, V. T., S. V. ; Doody, A. ; Johnston, J. N., Enantioselective Synthesis of  $\alpha$ -Bromonitroalkanes for Umpolung Amide Synthesis: Preparation of *tert*-Butyl ((1*R*)-1-(4-(benzyloxy)phenyl)-2-bromo-2-nitroethyl)carbamate. *Organic Syntheses* **2016**, 93, 88.

2H), 6.88 (d,  $J = 8.7$  Hz, 2H), 6.76 (d,  $J = 1.8$  Hz, 2H), 6.54 (t,  $J = 2.1$  Hz, 1H), 5.34 (d,  $J = 7.6$  Hz, 2H), 4.99 (br s, 6H), 2.59 (d,  $J = 4.6$  Hz, 3H), 1.40 (s, 9H);  $^{13}\text{C}$  NMR (150 MHz, DMSO- $d_6$ ) ppm 170.2, 169.3, 159.3, 157.7, 154.9, 140.9, 137.0, 136.9, 130.9, 128.43, 128.41, 127.9, 127.8, 127.76, 127.5, 114.4, 106.4, 100.7, 78.5, 69.3, 69.1, 57.4, 55.5, 28.2, 25.6; HRMS (ESI): Exact mass calcd for  $\text{C}_{43}\text{H}_{46}\text{N}_3\text{O}_7$   $[\text{M}+\text{H}]^+$  716.3330, found 716.3335.

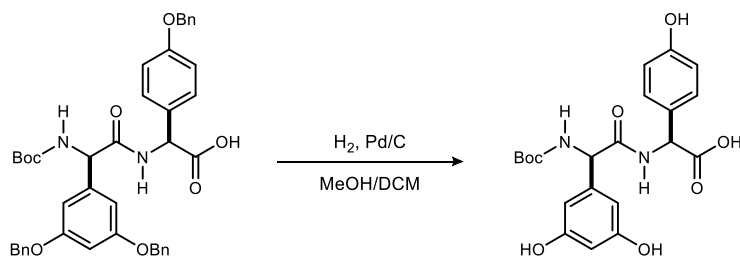


**(S)-2-(4-(benzyloxy)phenyl)-2-((R)-2-(3,5-bis(benzyloxy)phenyl)-2-((tert-butoxycarbonyl)amino)acetamido)acetic acid (378).** *tert*-Butyl ((*R*)-2-(((*S*)-1-(4-(benzyloxy)phenyl)-2-(methylamino)-2-oxoethyl)amino)-1-(3,5-bis(benzyloxy)phenyl)-2-oxoethyl)carbamate (1.16 g, 1.62 mmol) was prepared as a 0.05 M suspension in  $\text{CH}_2\text{Cl}_2$  at room temperature. *tert*-Butyl nitrite (0.1 M) was added in one portion and the consumption of starting amide was monitored by TLC.<sup>290</sup> Upon complete conversion of *N*-methyl amide the reaction becomes homogenous, the solution was then diluted with diethyl ether and concentrated in vacuo three times, subjected to high vacuum, and used without further purification. The *N*-nitroso-*N*-methyl amide intermediate was dissolved in a 3:1 THF/ $\text{H}_2\text{O}$  (0.05 M) and cooled to 0 °C.<sup>291</sup> After 30 minutes at 0 °C, LiOH (155 mg, 6.48 mmol) and 30%  $\text{H}_2\text{O}_2$  (2.94 mL, 25.9 mmol) were added in succession. The reaction was monitored by TLC for completion (30 minutes). The reaction was quenched with sodium bisulfite at 0 °C and stirred for an additional 10 minutes. The reaction mixture was transferred to a separatory funnel and extracted with  $\text{CH}_2\text{Cl}_2$ . The aqueous layer was acidified to pH 3 and re-extracted with  $\text{CH}_2\text{Cl}_2$  two times. The combined organic layers were washed with brine, dried with  $\text{Na}_2\text{SO}_4$ , filtered, and concentrated. The residue was purified by

<sup>290</sup> Yedage, S. L.; Bhanage, B. M. *J. Org. Chem.* **2017**, *82*, 5769.

<sup>291</sup> Ellman, J. A. R., S.D.; Lacour, J. *J. Am. Chem. Soc.* **1997**, *119*, 3419.

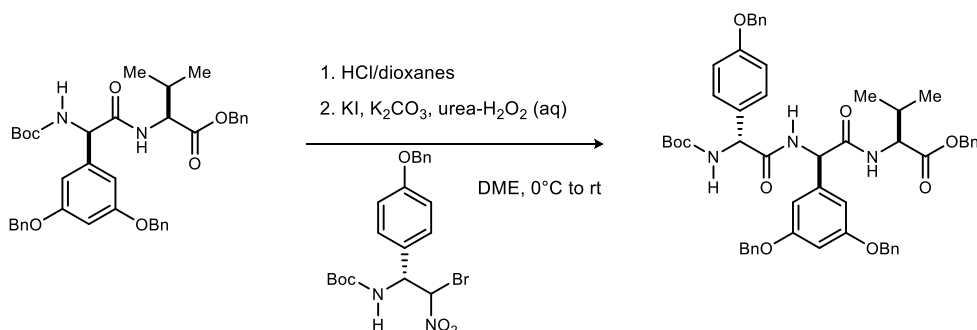
flash column chromatography (60% ethyl acetate in hexanes → 2-10% methanol in dichloromethane) to afford the product as a white solid (881 mg, 78%). MP = 96-101°C;  $[\alpha]_D^{20}$  -1.1 (*c* 0.53, CHCl<sub>3</sub>); R<sub>f</sub> = 0.3 (10% MeOH/CH<sub>2</sub>Cl<sub>2</sub>); IR (film) 3321, 3033, 2977, 2361, 1660, 1602, 1510, 1453, 1370, 1295, 1245, 1161 cm<sup>-1</sup>; <sup>1</sup>H NMR (600 MHz, CDCl<sub>3</sub>) δ 7.71 (br s, 1H), 7.36-7.31 (m, 15H), 7.28 (d, *J* = 7.2 Hz, 2H), 7.24 (d, *J* = 8.5 Hz, 2H), 6.55 (s, 2H), 6.51 (s, 1H), 5.97 (d, *J* = 8.9 Hz, 1H), 5.87 (s, 1H), 5.58 (d, *J* = 6.3 Hz, 1H), 4.94 (br s, 1H), 4.88-4.81 (br s, 6H), 1.40 (s, 9H) [COOH not observed due to broadening]; <sup>13</sup>C NMR (150 MHz, CDCl<sub>3</sub>) ppm 172.9, 169.6, 160.4, 159.0, 156.3, 140.2, 136.9, 136.7, 128.71, 128.66, 128.5, 128.2, 128.1, 127.8, 127.6, 115.1, 106.1, 102.2, 81.4, 70.2, 70.0, 56.9, 55.8, 28.4; HRMS (ESI): Exact mass calcd for C<sub>42</sub>H<sub>43</sub>N<sub>2</sub>O<sub>8</sub> [M+H]<sup>+</sup> 703.3014, found 703.3018.



**(S)-2-((R)-2-((tert-butoxycarbonyl)amino)-2-(3,5-dihydroxyphenyl)acetamido)-2-(4-hydroxyphenyl)acetic acid (277).** A 0.05 M solution of (S)-2-(4-(benzyloxy)phenyl)-2-((R)-2-(3,5-bis(benzyloxy)phenyl)-2-((tert-butoxycarbonyl)amino)acetamido)acetic acid (1.50 g, 2.13 mmol) in 1:1 methanol/dichloromethane was prepared. Palladium on carbon (10%) was added to the stirred solution, the flask was sealed with a septum, and the atmosphere was evacuated and refilled with argon three times. The reaction was evacuated (50 Torr) and refilled with hydrogen three times. The reaction was monitored by TLC, and upon completion after two hours, the reaction was evacuated by removing the hydrogen balloon, and filtered through a pad of Celite and washed with methanol. The crude mixture was purified by flash column chromatography (2-20% methanol in dichloromethane) to afford the product as an off-white solid (878 mg, 95%). MP = 102-105 °C;  $[\alpha]_D^{20}$  +3.0 (*c* 0.53, MeOH); R<sub>f</sub> = 0.1 (20% MeOH/CH<sub>2</sub>Cl<sub>2</sub>); IR (film) 3389, 2360, 1646, 1159 cm<sup>-1</sup>; <sup>1</sup>H NMR (400 MHz, DMSO-*d*<sub>6</sub>) δ 9.23 (br s, 2H), 8.33 (s, 1H), 7.07 (d, *J* = 7.8 Hz, 2H), 7.07 (br s, 1H), 6.64 (d, *J* = 8.1 Hz, 2H), 6.25 (s, 2H), 6.10 (s, 1H), 5.11 (d, *J* = 7.7 Hz, 1H), 5.02 (d, *J*

= 6.9 Hz, 1H), 1.38 (s, 9H) [ArOH not observed due to broadening, 2H]; <sup>13</sup>C NMR (100 MHz, DMSO-*d*<sub>6</sub>) ppm 172.7, 169.2, 158.2, 156.7, 154.8, 140.9, 128.2, 114.8, 105.4, 101.7, 78.4, 57.6, 56.7, 48.7, 28.2; HRMS (ESI).<sup>292</sup>

### Synthesis of Fragment A of feglymycin.

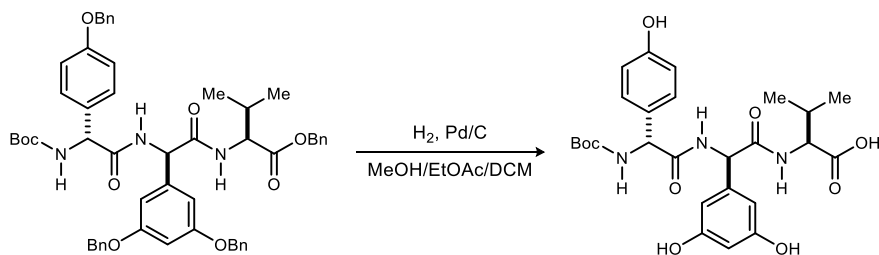


**Benzyl ((R)-2-((R)-2-(4-(benzyloxy)phenyl)-2-((tert-butoxycarbonyl)amino)acetamido)-2-(3,5-bis(benzyloxy)phenyl)acetyl)-L-valinate (381).** The dipeptide (1.00 g, 1.53 mmol) was dissolved in 4 M HCl/dioxanes (20 mL) and stirred under argon. Upon complete deprotection (approx. 1 hour), the volatiles were removed by vacuum (50 Torr). Diethyl ether was added to the flask and the mixture was concentrated to remove residual HCl. This was repeated twice and the resulting white foam was dried under high vacuum for an hour. The bromonitroalkane (831 mg, 1.84 mmol) was added to the flask, followed by DME (15.3 mL), and the mixture was cooled to 0 °C. Potassium iodide (508 mg, 3.06 mmol) was added, followed by potassium carbonate (2.11 g, 15.3 mmol). A freshly prepared solution of 3 M urea-hydrogen peroxide in water was then added (1.53 mL, 4.59 mmol), and the reaction was stirred under an oxygen atmosphere at 0 °C for 2 hours, and then at room temperature for 24 hours. The reaction was quenched with satd aq Na<sub>2</sub>S<sub>2</sub>O<sub>4</sub> and the aqueous layers were extracted several times with ethyl acetate. The organic layers were combined and washed with Na<sub>2</sub>S<sub>2</sub>O<sub>4</sub> followed by 1M HCl and brine.<sup>293</sup> The organic layers were concentrated, and the resultant solid was recrystallized from diethyl ether to provide the product

<sup>292</sup> HRMS was unable to be obtained prior to submission of this document due to the lockdown put in place by the COVID-19 pandemic. Please contact the author for final details.

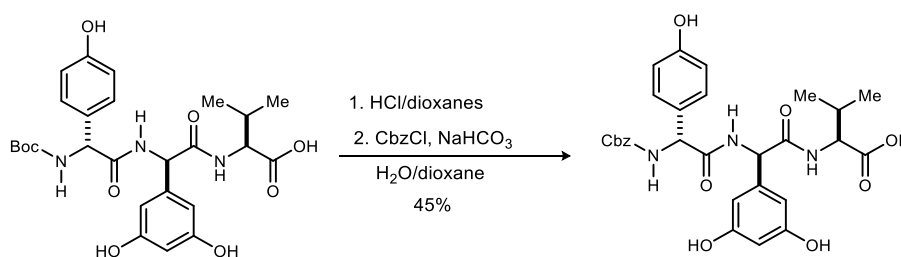
<sup>293</sup> At this point on large scale, a lot of precipitate may be present. If so, the solids are collected prior to concentration.

as a light yellow solid (616 mg, 45%). Mp = 184-185 °C;  $[\alpha]_D^{20} +24$  ( $c$  0.50,  $\text{CHCl}_3$ ),  $R_f = (0.41, 1\% \text{ MeOH/DCM})$ ; IR (film) 3376, 3280, 2967, 1739, 1714, 1639, 1607, 1541, 1510, 1452, 1380, 1243, 1163  $\text{cm}^{-1}$ ;  $^1\text{H NMR}$  (600 MHz,  $\text{DMSO-}d_6$ )  $\delta$  8.76 (d,  $J = 8.2$  Hz, 2H), 7.42-7.31 (m, 23H), 6.91 (d,  $J = 8.6$  Hz, 2H), 6.63 (br s, 2H), 6.50 (br s, 1H), 5.65 (d,  $J = 7.9$  Hz, 1H), 5.41 (d,  $J = 8.3$  Hz, 1H), 5.19 (d,  $J = 12.5$  Hz, 1H), 5.16 (d,  $J = 12.4$  Hz, 1H), 4.96-4.88 (series of m, 6H), 4.21 (dd,  $J = 8.3, 6.4$  Hz, 1H), 2.04 (dq,  $J = 13.4, 6.7, 6.7$  Hz, 1H), 1.37 (s, 9H), 0.79 (d,  $J = 6.8$  Hz, 3H), 0.74 (d,  $J = 6.8$  Hz, 3H);  $^{13}\text{C NMR}$  (150 MHz,  $\text{DMSO-}d_6$ ) ppm 171.7, 170.5, 170.2, 159.7, 158.2, 155.3, 141.7, 137.4, 137.3, 136.3, 131.5, 129.1, 128.93, 128.89, 128.8, 128.6, 128.5, 128.3, 128.2, 128.1, 128.0, 114.8, 106.0, 101.3, 78.8, 69.7, 69.5, 66.5, 57.9, 57.2, 55.9, 30.7, 28.6, 19.3, 18.3; HRMS (ESI): Exact mass calcd for:  $\text{C}_{54}\text{H}_{58}\text{N}_3\text{O}_9$   $[\text{M}+\text{H}]^+$  892.4168, found 892.4194



**((*R*)-2-((*R*)-2-((tert-butoxycarbonyl)amino)-2-(4-hydroxyphenyl)acetamido)-2-(3,5-dihydroxyphenyl)acetyl)-*L*-valine (298).** A 0.05 M solution of (benzyl ((*R*)-2-((*R*)-2-(4-(benzyloxy)phenyl)-2-((tert-butoxycarbonyl)amino)acetamido)-2-(3,5-bis(benzyloxy)phenyl)acetyl)-*L*-valinate (1.39 g, 1.56 mmol) in 1:1:1 methanol/ethyl acetate/dichloromethane was prepared. Palladium on carbon (10%) was added to the stirred solution, and the flask was sealed with a septum. The flask was evacuated and refilled with argon, and the process was repeated twice. The reaction flask was evacuated and refilled with hydrogen three times. The reaction was monitored by TLC. After 4 hours the reaction was evacuated by removing the hydrogen balloon without removing the needle or septa. The reaction mixture was filtered through a pad of Celite and washed with methanol. The volatiles were removed,  $\text{CH}_2\text{Cl}_2$  was added to the resultant residue and the solvent was removed at reduced pressure. This was repeated twice and the resulting purple foam was dried under high vacuum for an hour (878 mg, 97%).;  $[\alpha]_D^{20} -75$  ( $c$  0.52, MeOH);  $R_f = 0.4$  (20% methanol in dichloromethane); MP = 209-215

°C; IR (film) XXXX  $\text{cm}^{-1}$ ; <sup>294</sup> <sup>1</sup>H NMR (600 MHz, DMSO-*d*<sub>6</sub>)  $\delta$  9.35 (br s, 1H), 9.12 (s, 2H), 8.41 (d, *J* = 7.7 Hz, 1H), 8.28 (d, *J* = 7.8 Hz, 1H), 7.18 (d, *J* = 8.4 Hz, 3H), 6.65 (d, *J* = 8.5 Hz, 2H), 6.22 (d, *J* = 1.8 Hz, 2H), 6.08 (s, 1H), 5.40 (d, *J* = 7.5 Hz, 1H), 5.24 (d, *J* = 8.4 Hz, 1H), 4.12 (dd, *J* = 8.5, 5.9 Hz, 1H), 2.01-1.98 (m, 1H), 1.37 (s, 9H), 0.77 (d, *J* = 6.9 Hz, 3H), 0.73 (d, *J* = 6.8 Hz, 3H) [COOH not observed due to broadening]; <sup>13</sup>C NMR (150 MHz, DMSO-*d*<sub>6</sub>) ppm 172.9, 170.01, 169.98, 158.0, 156.7, 154.8, 140.5, 129.1, 128.5, 114.9, 105.4, 101.7, 78.4, 57.1, 57.0, 56.0, 30.3, 28.2, 19.0, 17.8; HRMS (ESI): Exact mass calcd for C<sub>26</sub>H<sub>32</sub>N<sub>3</sub>O<sub>9</sub> [M-H]<sup>-</sup> 530.2139, found 530.2123.



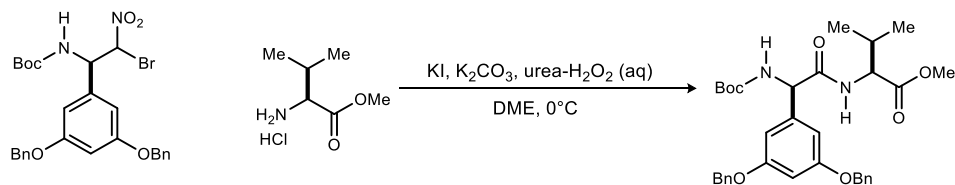
**((*R*)-2-((*R*)-2-(((benzyloxy)carbonyl)amino)-2-(4-hydroxyphenyl)acetamido)-2-(3,5-dihydroxyphenyl)acetyl)-L-valine (276).** Following a literature procedure,<sup>295</sup> the tripeptide (154 mg, 289  $\mu\text{mol}$ ) was dissolved in 4 M HCl/dioxanes (2 mL) and stirred under argon. After one hour the volatiles were removed. Diethyl ether was added to the flask and the mixture was concentrated to remove excess HCl. This was repeated twice and the resulting white foam was dried under high vacuum for an hour. The amine salt was then dissolved in a 1:1 mixture of H<sub>2</sub>O/dioxane (2.9 mL), and NaHCO<sub>3</sub> (58.4 mg, 695  $\mu\text{mol}$ ) was added to the flask. This mixture was added dropwise via syringe pump over 45 minutes to a separate flask containing CbzCl (41  $\mu\text{L}$ , 260  $\mu\text{mol}$ ) in dioxane (700  $\mu\text{L}$ ). The reaction mixture stirred for an additional 45 minutes, and then water was added. The aqueous phase was washed with ethyl acetate, and then acidified to pH 3 with 1 M HCl. The suspension was then extracted with ethyl acetate, and the combined organic layers were washed with 1M HCl, water, and brine. The organic phase was then dried (Na<sub>2</sub>SO<sub>4</sub>) and concentrated to

<sup>294</sup> This data point was unable to be obtained prior to submission of this document due to the lockdown put in place by the COVID-19 pandemic. Please contact the author for further details.

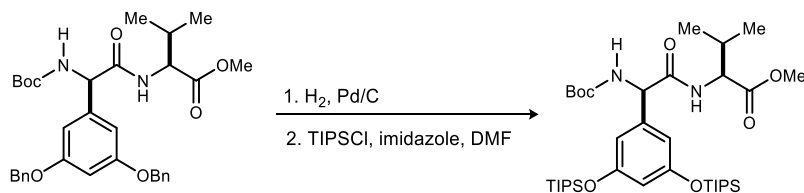
<sup>295</sup> Dettner, F.; Hänchen, A.; Schols, D.; Toti, L.; Nußer, A.; Süßmuth, R. D. *Angew. Chem. Int. Ed.* **2009**, *48*, 1856.

afford the desired tripeptide as a white solid (74 mg, 45%). All spectral data matched the literature.<sup>295</sup>

### Synthesis of Fragment B and related derivatives

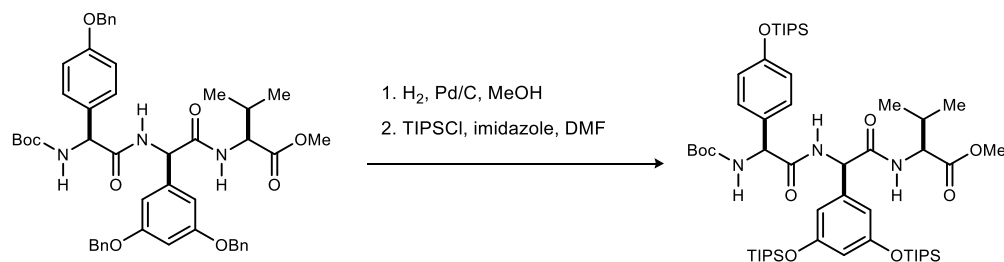


**Methyl ((*R*)-2-(3,5-bis(benzyloxy)phenyl)-2-((*tert*-butoxycarbonyl)amino)acetyl)-*L*-valinate (S6).** This compound was prepared according to the General Procedure using the bromonitroalkane (1.99 g, 3.58 mmol) and *N*-Boc-*L*-valine methyl ester hydrochloride (500 mg, 2.98 mmol). The crude mixture was purified by recrystallization (diethyl ether) to afford the title compound as a white solid (763 mg, 43%). Mp = 106-108 °C;  $[\alpha]_D^{20}$  -49 (*c* 0.50, CHCl<sub>3</sub>),  $R_f$  = 0.29 (30% EtOAc/hexanes); IR (film) 3316, 2968, 1743, 1655, 1597, 1521, 1452, 1368, 1164 cm<sup>-1</sup>; <sup>1</sup>H NMR (400 MHz, CDCl<sub>3</sub>) δ 7.42-7.30 (series of m, 10H), 6.66 (d, *J* = 1.8 Hz, 2H), 6.56 (dd, *J* = 2.1, 2.1 Hz, 1H), 6.27 (d, *J* = 8.8 Hz, 1H), 5.72 (br s, 1H), 5.09 (br s, 1H), 5.01 (s, 4H), 4.54 (dd, *J* = 9.0, 4.9 Hz, 1H), 3.73 (s, 3H), 2.08 (dq, *J* = 13.6, 6.2, 6.2 Hz, 1H), 1.43 (s, 9H), 0.78 (d, *J* = 6.8 Hz, 3H), 0.71 (d, *J* = 6.9 Hz, 3H); <sup>13</sup>C NMR (100 MHz, CDCl<sub>3</sub>) ppm 171.9, 169.5, 160.4, 154.9, 140.6, 136.6, 128.5, 128.0, 127.5, 106.2, 102.1, 80.1, 70.0, 58.9, 57.0, 52.2, 31.3, 28.2, 18.7, 17.3 ppm; HRMS (ESI): Exact mass calcd for C<sub>33</sub>H<sub>41</sub>N<sub>2</sub>O<sub>7</sub> [M+H]<sup>+</sup> 577.2908, found 577.2914.



**Methyl ((*R*)-2-(3,5-bis((triisopropylsilyl)oxy)phenyl)-2-((*tert*-butoxycarbonyl)amino)acetyl)-*L*-valinate (S7).** Methyl ((*R*)-2-(3,5-bis(benzyloxy)phenyl)-2-((*tert*-butoxycarbonyl)amino)acetyl)-*L*-valinate (150 mg, 260 μmol) was dissolved in a 1:1 mixture of methanol/DCM (2.6 mL) and the flask was purged with argon. 10% Pd/C (30 mg) was added and

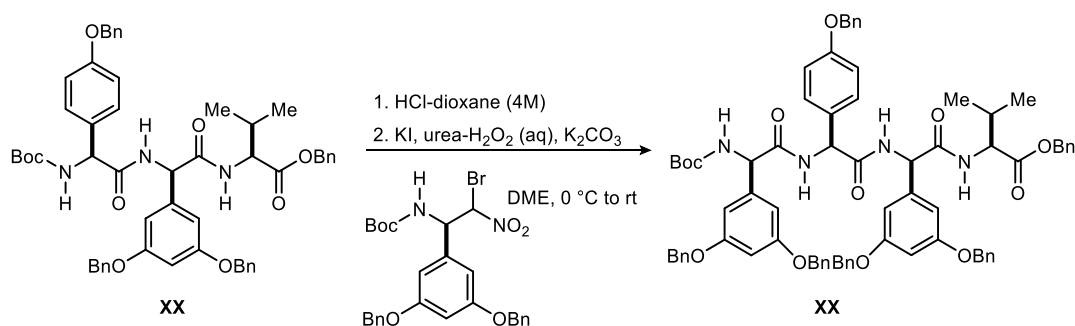
the flask was evacuated (house vacuum, 50 mmHg), backfilled with argon, evacuated again, and backfilled with hydrogen. Upon completion of the reaction, the mixture was filtered through Celite and concentrated. The resulting material was dissolved in dry DMF (260  $\mu\text{L}$ ) under an argon atmosphere and imidazole (70.8 mg, 1.04 mmol) was added, followed by TIPS-Cl (134  $\mu\text{L}$ , 624  $\mu\text{mol}$ ). The material was poured into ice-water, extracted with ethyl acetate, washed with  $\text{NaHCO}_3$ , ice-water, and brine. The organic layer was dried ( $\text{Na}_2\text{SO}_4$ ) and concentrated. Column chromatography ( $\text{SiO}_2$ , 5-10-20% ethyl acetate in hexanes) afforded the title compound as a white foam (84.8 mg, 46% over 2 steps).  $[\alpha]_D^{20}$  -48 ( $c$  0.45,  $\text{CHCl}_3$ );  $R_f$  = 0.68 (30% EtOAc/hexanes); IR (film) 3331, 2946, 2894, 2868, 1668, 1591, 1455, 1172, 883  $\text{cm}^{-1}$ ;  $^1\text{H}$  NMR (600 MHz,  $\text{CDCl}_3$ )  $\delta$  6.50 (s, 2H), 6.35 (dd,  $J$  = 1.8, 1.8 Hz, 1H), 6.09 (br s, 1H), 5.68 (br s, 1H), 5.00 (br s, 1H), 4.54 (dd,  $J$  = 8.9, 4.8 Hz, 1H), 3.73 (s, 3H), 2.05 (dq,  $J$  = 13.3, 6.3, 6.3 Hz, 1H), 1.40 (s, 9H), 1.23 (sept,  $J$  = 9.0 Hz, 6H), 1.08 (d,  $J$  = 7.7 Hz, 36H), 0.76 (d,  $J$  = 6.7 Hz, 3H), 0.69 (d,  $J$  = 6.8 Hz, 3H);  $^{13}\text{C}$  NMR (150 MHz,  $\text{CDCl}_3$ ) ppm 171.9, 169.6, 157.4, 154.8, 140.4, 111.9, 111.4, 79.8, 77.2, 77.0, 76.8, 58.6, 57.0, 52.2, 31.5, 28.3, 18.8, 17.9, 17.4, 12.7; HRMS (ESI): Exact mass calcd for  $\text{C}_{37}\text{H}_{68}\text{N}_2\text{O}_7\text{Si}_2$   $[\text{M}]^+$  709.4638, found 709.4625.



**Methyl ((R)-2-(3,5-bis((triisopropylsilyl)oxy)phenyl)-2-((S)-2-((tert-butoxycarbonyl)amino)-2-(4-((triisopropylsilyl)oxy)phenyl)acetamido)acetyl)-L-valinate (351).** The tripeptide (81.6 mg, 100  $\mu\text{mol}$ ) was dissolved in methanol (1 mL) and the flask was purged with argon. Pd/C (8 mg) was added and the flask was evacuated (house vacuum), backfilled with argon, evacuated again, and backfilled with hydrogen. Upon completion of the reaction, the mixture was filtered through Celite and concentrated. The resulting material was dissolved in dry DMF (100  $\mu\text{L}$ ) under an argon atmosphere, imidazole (40.8 mg, 600  $\mu\text{mol}$ ) was added, followed by TIPS-Cl (77  $\mu\text{L}$ , 360  $\mu\text{mol}$ ). The material was poured into ice-water, extracted with ethyl acetate, washed with

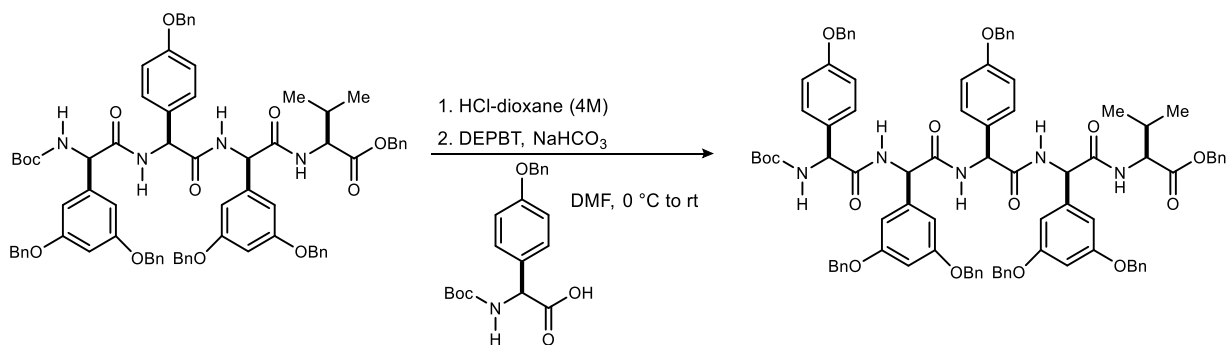


NaHCO<sub>3</sub>, ice-water, and then brine. The organic layer was dried (Na<sub>2</sub>SO<sub>4</sub>) and concentrated. Column chromatography (SiO<sub>2</sub>, 15-30% ethyl acetate in hexanes) afforded the title compound as a white foam (69.7 mg, 75% over 2 steps).  $R_f = 0.39$  (20% EtOAc/hexanes);  $[\alpha]_D^{20} +7.6$  ( $c$  0.50, CHCl<sub>3</sub>); IR (film) 3315, 2944, 2892, 2867, 1702, 1656, 1591, 1508, 1460, 1263, 1172 cm<sup>-1</sup>; <sup>1</sup>H NMR (600 MHz, DMSO-*d*<sub>6</sub>)  $\delta$  8.72 (d,  $J = 8.2$  Hz, 1H), 8.68 (d,  $J = 8.3$  Hz, 1H), 7.26 (d,  $J = 7.6$  Hz, 3H), 6.71 (d,  $J = 8.6$  Hz, 2H), 6.58 (s, 2H), 6.16 (s, 1H), 5.58 (d,  $J = 7.8$  Hz, 1H), 5.37 (d,  $J = 8.6$  Hz, 1H), 4.21 (dd,  $J = 8.9, 6.0$  Hz, 1H), 3.67 (s, 3H), 1.98 (qd,  $J = 13.3, 6.6$  Hz, 1H), 1.38 (s, 9H), 1.20 (septet,  $J = 6.9$  Hz, 6H), 1.19 (septet,  $J = 7.3$  Hz, 3H), 1.03 (d,  $J = 5.4$  Hz, 18H), 1.02 (d,  $J = 6.2$  Hz, 36H), 0.74 (d,  $J = 6.7$  Hz, 3H), 0.67 (d,  $J = 6.7$  Hz, 3H); <sup>13</sup>C NMR (150 MHz, CDCl<sub>3</sub>) ppm 171.8, 169.8, 169.7, 155.8, 154.8, 154.5, 141.2, 131.5, 128.3, 118.9, 111.8, 109.7, 78.2, 56.9, 56.4, 55.2, 51.8, 30.4, 28.1, 18.7, 17.7, 17.6, 12.00, 11.99; HRMS (ESI): Exact mass calcd for C<sub>54</sub>H<sub>96</sub>N<sub>3</sub>O<sub>9</sub>Si<sub>3</sub> [M+H]<sup>+</sup> 1014.6449, found 1014.6486.



**Benzyl ((*R*)-2-((*S*)-2-(4-(benzyloxy)phenyl)-2-((*R*)-2-(3,5-bis(benzyloxy)phenyl)-2-((*tert*-butoxycarbonyl)amino)acetamido)acetamido)-2-(3,5-bis(benzyloxy)phenyl)acetyl)-L-valinate (347).** The tripeptide (1.03 g, 1.15 mmol) was dissolved in 4 M HCl/dioxanes (10 mL) and stirred under argon. Upon complete deprotection, the volatiles were removed under reduced pressure. Diethyl ether was added to the flask and the mixture was concentrated to remove excess HCl. This was repeated twice and the resulting colorless foam was dried under high vacuum for an hour. The bromonitroalkane (1.29 g, 2.31 mmol) was added to the flask, followed by DME (11.5 mL), and the mixture was cooled to 0 °C. Potassium iodide (572 mg, 3.45 mmol) was added, followed by potassium carbonate (1.60 g, 11.5 mmol). A freshly prepared solution of 3 M urea hydrogen peroxide in water was then added (1.15 mL, 3.45 mmol) and the reaction was stirred under an oxygen atmosphere (balloon) at 0 °C for 2 hours, and then at room temperature for 24

hours. The reaction was quenched with sat'd aq Na<sub>2</sub>S<sub>2</sub>O<sub>4</sub> and the aqueous layers were extracted several times with ethyl acetate. The organic layers were combined and washed with Na<sub>2</sub>S<sub>2</sub>O<sub>4</sub> followed by 1 M HCl and brine.<sup>296</sup> The organic layers were concentrated, and the resultant residue was triturated with MeCN. The solids were collected, washed with MeCN, and dried. The resulting product could be further purified by trituration with hot methanol to provide the product as a cream-colored solid (815 mg, 57%) over 2 steps.<sup>297</sup> Mp = 226-231 °C; IR (film) 3298, 3034, 2967, 1632, 1600, 1510, 1158 cm<sup>-1</sup>; <sup>1</sup>H NMR (600 MHz, DMSO-*d*<sub>6</sub>)<sup>298</sup> δ 9.10 (s, 1H), 8.84 (s, 1H), 8.76 (s, 1H), 7.40-7.28 (m, 31H obsd),<sup>299</sup> 6.82 (d, *J* = 6.0 Hz, 2H), 6.77 (s, 2H), 6.65 (s, 2H), 6.52 (s, 1H), 6.47 (s, 1H), 5.78 (d, *J* = 5.5 Hz, 1H), 5.67 (d, *J* = 6.5 Hz, 1H), 5.42 (d, *J* = 7.4 Hz, 1H), 5.19 (d, *J* = 12.1 Hz, 1H), 5.15 (d, *J* = 12.2 Hz, 1H), 5.05-4.81 (m, 10H), 4.21 (br s, 1H), 2.08-1.98 (br m, 1H), 1.39 (s, 9H), 0.78 (d, *J* = 5.6 Hz, 3H), 0.72 (d, *J* = 5.3 Hz, 3H); <sup>13</sup>C NMR (150 MHz, DMSO-*d*<sub>6</sub>) ppm 171.7, 170.1, 169.9, 169.7, 159.7, 158.2, 155.2, 141.7, 141.6, 137.4, 137.30, 137.25, 136.3, 131.3, 128.9, 128.92, 128.88, 128.8, 128.7, 128.6, 128.5, 128.3, 128.2, 128.1, 127.9, 114.6, 106.7, 106.0, 101.4, 101.1, 78.9, 69.8, 69.7, 69.5, 66.5, 57.9, 57.6, 55.9, 55.3, 30.7, 28.6, 19.2, 18.3; HRMS (ESI): Exact mass calcd for C<sub>76</sub>H<sub>77</sub>N<sub>4</sub>O<sub>12</sub> [M+H]<sup>+</sup> 1237.5533, found 1237.5535.



**Benzyl ((*R*)-2-((*S*)-2-(4-(benzyloxy)phenyl)-2-((*R*)-2-((*S*)-2-(4-(benzyloxy)phenyl)-2-((tert-butoxycarbonyl)amino)acetamido)-2-(3,5-bis(benzyloxy)phenyl)acetamido)acetamido)-2-(3,5-bis(benzyloxy)phenyl)acetyl)-*L*-valinate (348).** The tetrapeptide (587 mg, 475 μmol) was

<sup>296</sup> At this point on large scale, a lot of precipitate may be present. If so, the solids are collected prior to concentration.

<sup>297</sup> Due to aggregation and limited solubility, optical rotation and R<sub>f</sub> are not reported for this compound.

<sup>298</sup> Boc N-H not observed due to broadening

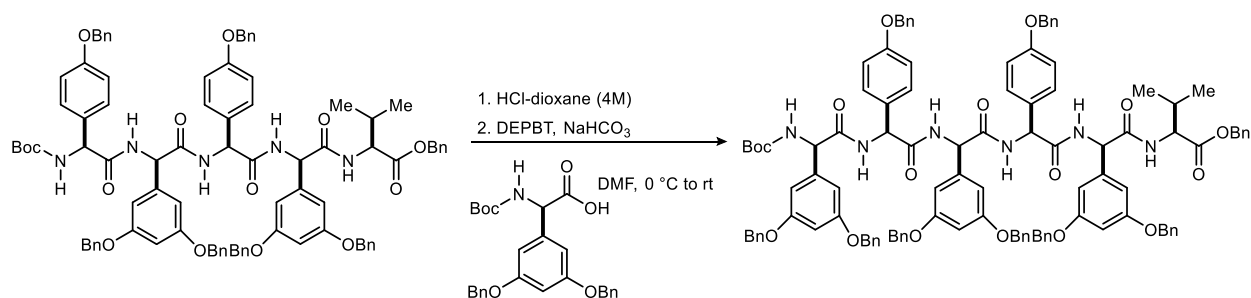
<sup>299</sup> Region should integrate to 32 (6xOCH<sub>2</sub>C<sub>6</sub>H<sub>5</sub> + 2 ArCH (Hpg-OBn)). However, 31H observed, due to broadening.

stirred as a suspension in 4M HCl/dioxanes (25 mL) under argon for 24 hours. The volatiles were removed and diethyl ether was added to the flask and the mixture was concentrated to remove excess HCl. This was repeated twice and the resulting solids were dried under high vacuum. In a separate flame-dried round-bottom flask, the amino acid (141 mg, 396  $\mu$ mol) was dissolved in DMF (6 mL) and the solution was cooled to 0 °C. To the flask was added DEPBT (355 mg, 1.19 mmol) and NaHCO<sub>3</sub> (133 mg, 1.58 mmol), and the mixture was stirred for 2 hours. The HCl salt of the amine was added as a solid, and DMF (2 mL) was used to transfer any residual amine from the flask. The reaction mixture stirred at 0 °C for 2 hours and then at room temperature for 48 hours. The reaction was quenched with water and the aqueous layers were extracted several times with ethyl acetate. The organic layers were combined and washed with copious amounts of ice water followed by NaHCO<sub>3</sub> and brine. The organic layers were allowed to sit for 10 minutes before the precipitated solids were collected by filtration and washed with ethyl acetate and MeCN.<sup>300</sup> The solids were resuspended and stirred with hot methanol for 30 minutes, filtered, and dried on high vacuum to afford the product as a cream colored solid (466 mg, 80% over 2 steps).<sup>301</sup> IR (neat) 3291, 3032, 2929, 1632, 1596, 1160, 1053, 734 cm<sup>-1</sup>; <sup>1</sup>H NMR (600 MHz, DMSO-*d*<sub>6</sub>)  $\delta$  9.21 (d, *J* = 6.8 Hz, 1H), 9.15 (d, *J* = 6.9 Hz, 1H), 8.81 (d, *J* = 7.9 Hz, 1H), 8.72 (d, *J* = 7.6 Hz, 1H), 7.43-7.28 (m, 39H), 7.25 (d, *J* = 7.2 Hz, 1H), 6.91 (d, *J* = 9.5 Hz, 2H), 6.83 (d, *J* = 8.4 Hz, 2H), 6.65 (br s, 2H), 6.56 (br s, 2H), 6.47 (s, 2H), 6.43 (s, 1H), 5.85 (d, *J* = 7.3 Hz, 1H), 5.75 (d, *J* = 7.0 Hz, 1H), 5.72 (d, *J* = 7.8 Hz, 1H), 5.42 (d, *J* = 7.6 Hz, 1H), 5.20 (d, *J* = 12.4 Hz, 2H), 5.15 (d, *J* = 12.4 Hz, 2H), 4.95-4.75 (series of m, 12H), 4.23 (br m, 1H), 2.04 (dq, *J* = 12.9, 6.5, 6.5 Hz, 1H), 1.37 (s, 9H), 0.79 (d, *J* = 6.1 Hz, 3H), 0.73 (d, *J* = 5.6 Hz, 3H); <sup>13</sup>C NMR (150 MHz, DMSO-*d*<sub>6</sub>) ppm 171.3, 169.9, 169.6, 169.5, 168.6, 159.21, 159.19, 157.7, 154.8, 141.2, 141.1, 136.9, 136.8, 136.7, 135.7, 131.2, 130.8, 128.6, 128.45, 128.39, 128.37, 128.33, 128.29, 128.2, 128.0, 127.8, 127.73, 127.70, 127.6, 127.5, 127.4, 114.3, 114.1, 105.5, 105.4, 100.8, 100.7, 78.3, 69.2, 69.05, 68.99, 66.0, 57.3, 56.7, 55.3, 54.7, 30.3, 28.1, 18.7, 17.8; HRMS (ESI): Exact mass calcd for C<sub>91</sub>H<sub>90</sub>N<sub>5</sub>O<sub>14</sub> [M+H]<sup>+</sup> 1476.6479, found 1476.6507.

---

<sup>300</sup> On a smaller (<100  $\mu$ mol) scale, the organic layers were filtered to remove any initial precipitate and then concentrated. The resulting film was triturated with MeCN, and the solids were collected by filtration and washed with MeCN. The collected solids were combined with the first precipitate and triturated with hot methanol.

<sup>301</sup> Due to aggregation and limited solubility, optical rotation and R<sub>f</sub> are not reported for this compound.



**Benzyl ((R)-2-((S)-2-(4-(benzyloxy)phenyl)-2-((R)-2-((S)-2-(4-(benzyloxy)phenyl)-2-((R)-2-(3,5-bis(benzyloxy)phenyl)-2-((tert-butoxycarbonyl)amino)acetamido)acetamido)-2-(3,5-bis(benzyloxy)phenyl)acetamido)acetamido)-2-(3,5-bis(benzyloxy)phenyl)acetyl)-L-valinate (349).** The pentapeptide (450 mg, 305  $\mu\text{mol}$ ) was stirred as a suspension in 4M HCl/dioxanes (25 mL) under argon for 24 hours. The volatiles were removed, diethyl ether was added to the flask, and the mixture was concentrated to remove excess HCl. This was repeated twice and the resulting solids were dried under high vacuum. In a separate flame-dried round-bottom flask, the amino acid (118 mg, 254  $\mu\text{mol}$ ) was dissolved in DMF (4 mL) and the solution was cooled to 0 °C. To the flask was added DEPBT (228 mg, 762  $\mu\text{mol}$ ) and  $\text{NaHCO}_3$  (85.4 mg, 1.02 mmol), and the mixture was stirred for 2 hours. The HCl salt of the amine was added as a solid, and DMF (1 mL) was used to transfer any residual amine from the flask. The reaction mixture was stirred at 0 °C for 2 hours and then at room temperature for 48 hours. The mixture was quenched with water and the aqueous layers were extracted several times with ethyl acetate. The organic layers were combined and washed with copious amounts of ice water followed by  $\text{NaHCO}_3$  and brine. The organic layers were allowed to sit for 10 minutes before the precipitated solids were collected by filtration and washed with ethyl acetate and MeCN. The filtrate was concentrated, and the resulting film was triturated with MeCN. The solids were collected by filtration, washed with MeCN, and combined with the first precipitate. The combined solids were suspended and stirred with hot methanol for 30 minutes, filtered, and dried on high vacuum to afford the product as a cream colored solid (372 mg, 80% over 2 steps).<sup>302</sup> IR (neat) 3927, 2926, 1632, 1596, 1159, 734, 694  $\text{cm}^{-1}$ ;  $^1\text{H}$  NMR (600 MHz,  $\text{DMSO-}d_6$ )  $\delta$  Please refer to Supporting Information 2 for the  $^1\text{H}$  NMR spectra;  $^{13}\text{C}$  NMR

<sup>302</sup> Due to aggregation and limited solubility, optical rotation and  $R_f$  are not reported for this compound.

(150 MHz, DMSO-*d*<sub>6</sub>) ppm – Please refer to Supporting Information 2 for the <sup>13</sup>C NMR spectra; HRMS (ESI): Exact mass calcd for C<sub>113</sub>H<sub>109</sub>N<sub>6</sub>O<sub>17</sub> [M+H]<sup>+</sup> 1821.7844, found 1821.7870.

Due to aggregation, limited solubility, and multiple conformers in solution, the structure of **349** was primarily assigned using 2D-NMR. Key assignments are shown in Figure 45 and Figure 44. The structure was further supported by HRMS, and by full characterization of the benzyl-deprotected derivative **341**.

Figure 44. Key  $^1\text{H}$ - $^{13}\text{C}$  HSQC crosspeaks for the structural assignment of hexapeptide 349.

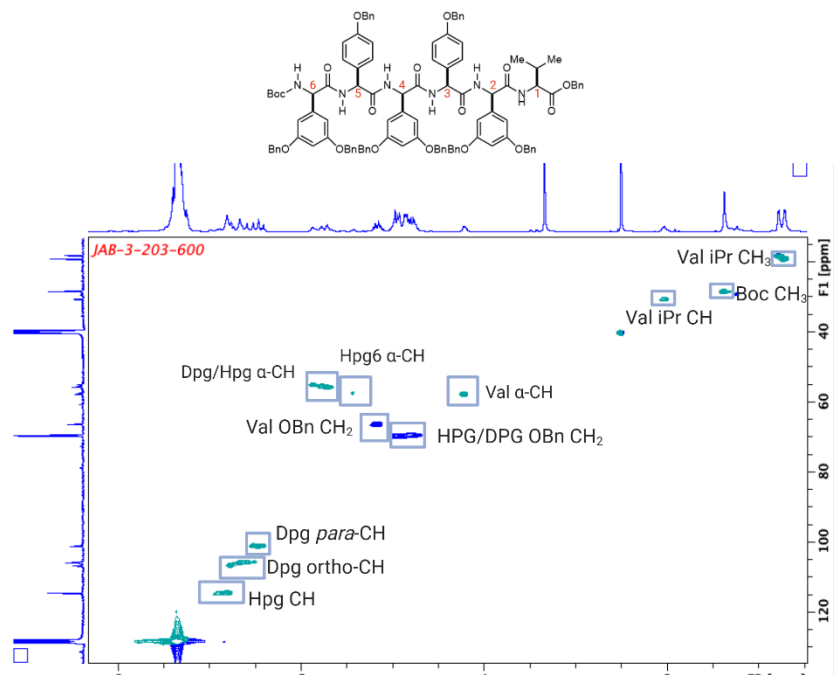
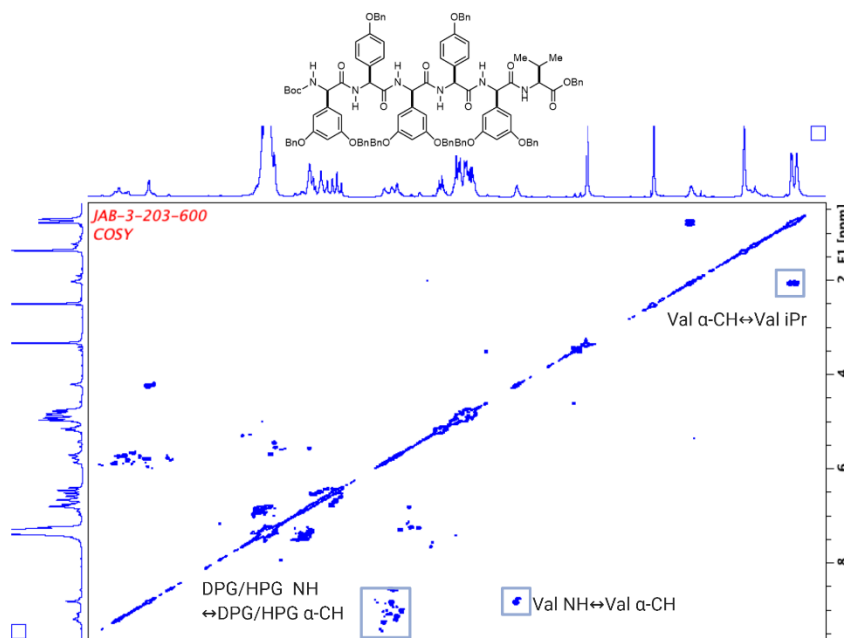
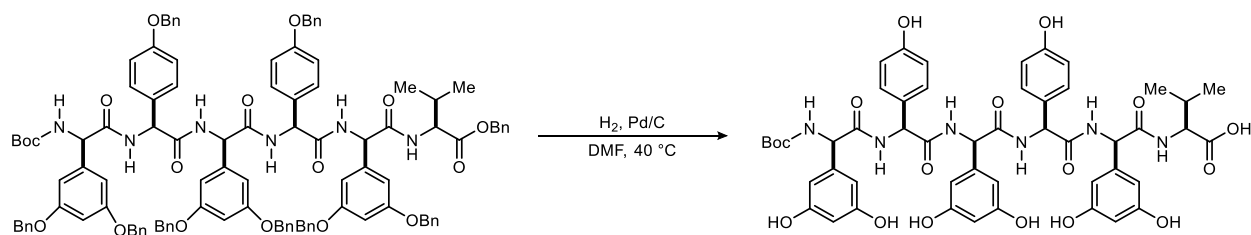


Figure 45. Key  $^1\text{H}$ - $^1\text{H}$  COSY crosspeaks for the structural assignment of hexapeptide 349.





**((R)-2-((S)-2-((R)-2-((S)-2-((R)-2-((tert-Butoxycarbonyl)amino)-2-(3,5-dihydroxyphenyl)acetamido)-2-(4-hydroxyphenyl)acetamido)-2-(3,5-dihydroxyphenyl)acetamido)-2-(4-hydroxyphenyl)acetamido)-2-(3,5-dihydroxyphenyl)acetyl)-L-valine (341).**

Hexapeptide **349** (311 mg, 171  $\mu$ mol) was suspended in warm DMF and stirred under argon until dissolved. Pd/C (10%, 150 mg) was added and the flask was evacuated and backfilled with hydrogen gas three times. The mixture was stirred at 40  $^{\circ}$ C for 8 hours. The flask was evacuated and backfilled with argon, and an additional 150 mg of Pd/C was added to the flask. The flask was evacuated and backfilled with hydrogen gas three times, and the mixture was stirred at 40  $^{\circ}$ C overnight. The reaction mixture was filtered through Celite, and the pad was rinsed with MeOH and DMF. The volatiles were removed to afford the product as a deep purple foam (175 mg, quant). The hexapeptide was further purified by preparatory HPLC according to the table below (retention time = 9.8 – 10.0 min). De-salting was achieved by size exclusion chromatography (Sephadex LH-20, MeOH), which afforded the product as a fluffy white solid after lyophilization (98.3 mg, 57%).

Solvent A: 95:5 H<sub>2</sub>O/MeCN (10 mM NH<sub>4</sub>OAc)

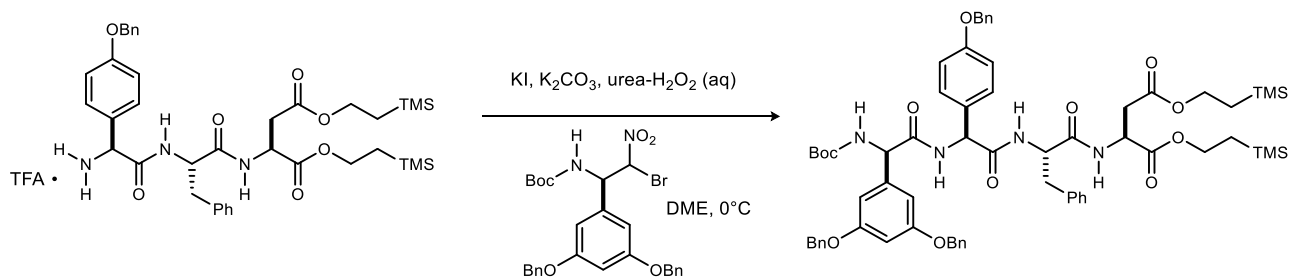
Solvent B: 95:5 MeCN/H<sub>2</sub>O (10 mM NH<sub>4</sub>OAc)

Flow rate: 20 mL/min

Time	%B
0.00	0.0
3.00	0.0
10.00	20.0
17.00	20.0
18.00	95.0
20.00	95.0
21.00	0.0
22.50	0.0

White solid; mp = 224-234 °C (decomp);  $[\alpha]_D^{20}$  -32.0 (*c* 0.50, MeOH);  $R_f$  = 0.1 (30% MeOH/DCM + 0.1% AcOH);<sup>303</sup> IR (neat) 3289, 1634, 1369, 1157, 1004, 681  $\text{cm}^{-1}$ ;  $^1\text{H}$  NMR (600 MHz, DMSO- $d_6$ )<sup>304</sup>  $\delta$  9.27 (br s, 3H), 9.10 (br s, 4H), 8.87 (d,  $J$  = 7.7 Hz, 1H), 8.80 (d,  $J$  = 7.7 Hz, 1H), 8.73 (d,  $J$  = 8.0 Hz, 1H), 8.51 (d,  $J$  = 7.5 Hz, 1H), 8.34 (d,  $J$  = 8.3 Hz, 1H), 7.07 (d,  $J$  = 8.6 Hz, 2H), 7.06 (d,  $J$  = 9.1 Hz, 2H), 7.03 (d,  $J$  = 7.0 Hz, 1H), 6.57 (d,  $J$  = 6.9 Hz, 2H), 6.56 (d,  $J$  = 7.9 Hz, 2H), 6.28 (br s, 2H), 6.25 (br s, 2H), 6.22 (br s, 2H), 6.10 (br s, 1H), 6.07 (br s, 1H), 6.06 (br s, 1H), 5.67 (d,  $J$  = 8.2 Hz, 1H), 5.62 (d,  $J$  = 7.7 Hz, 1H), 5.53 (d,  $J$  = 7.8 Hz, 1H), 5.48 (d,  $J$  = 8.1 Hz, 1H), 5.21 (d,  $J$  = 8.3 Hz, 1H), 4.12 (dd,  $J$  = 8.3, 6.0 Hz, 1H), 2.00 (dq,  $J$  = 13.0, 6.5, 6.5 Hz, 1H), 1.40 (s, 9H), 0.77 (d,  $J$  = 6.7 Hz, 3H), 0.73 (d,  $J$  = 6.7 Hz, 3H);  $^{13}\text{C}$  NMR (150 MHz, DMSO- $d_6$ ) ppm 173.0, 169.9, 169.6, 169.5, 169.3, 169.1, 158.1, 158.0, 157.9, 156.55, 156.48, 154.6, 140.9, 140.7, 140.3, 128.9, 128.8, 127.9, 127.9, 114.7, 105.5, 105.4, 105.4, 101.6, 78.4, 57.3, 57.2, 55.8, 54.9, 54.8, 30.4, 28.2, 19.1; HRMS (ESI): Exact mass calcd for  $\text{C}_{50}\text{H}_{54}\text{N}_6\text{NaO}_{17}$   $[\text{M}+\text{Na}]^+$  1033.3438, found 1033.3439.

### Synthesis of Fragment C and related derivatives



#### Bis(2-(trimethylsilyl)ethyl)

#### ((*S*)-2-(4-(benzyloxy)phenyl)-2-((*R*)-2-(3,5-

bis(benzyloxy)phenyl)-2-((*tert*-butoxycarbonyl)amino)acetamido)acetyl)-L-phenylalanyl-L-aspartate (332). Following the general procedure, the  $\alpha$ -bromo nitroalkane (28 mg, 50  $\mu\text{mol}$ ) and the TFA salt of the amine<sup>305</sup> (50 mg, 60  $\mu\text{mol}$ ) provided the amide after flash column

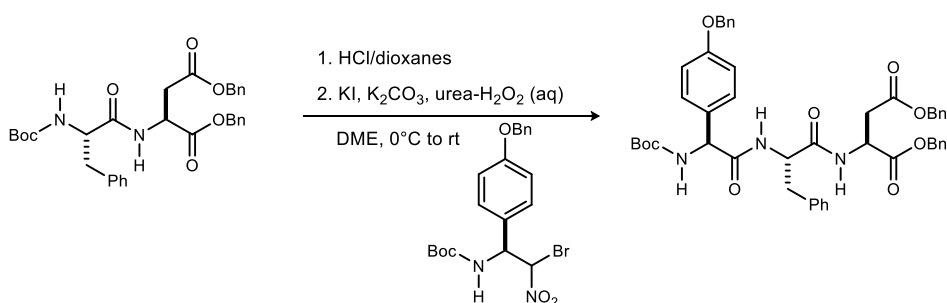
<sup>303</sup> This compound streaks on the TLC plate.

<sup>304</sup> Seven of nine phenolic O-H observed

<sup>305</sup> Schwieter, K. E., Vanderbilt University, 2016.



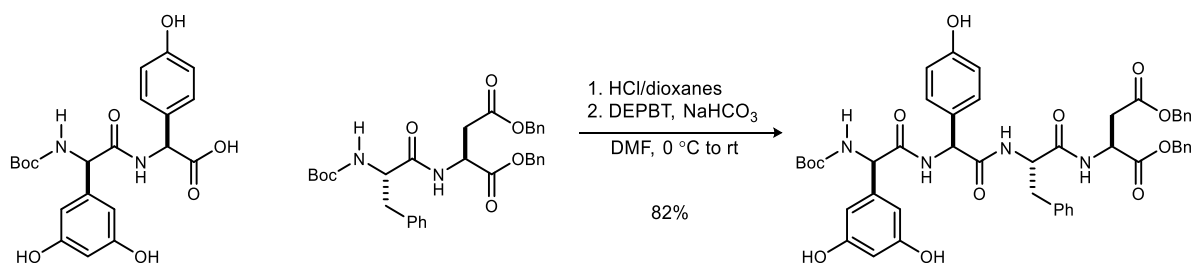
chromatography (silica gel, 20-50 % ethyl acetate in hexanes) as a white solid (30 mg, 52% yield). Mp = 200-206 °C (recrystallized from acetonitrile/water);  $[\alpha]_D^{20}$  -8.2 (*c* 0.58, CHCl<sub>3</sub>),  $R_f$  = 0.78 (50% EtOAc/hexanes); IR (film) 3281, 3065, 2955, 1737, 1639, 1519, 1452, 1381, 1296, 1248, 1167, 1051, 843 cm<sup>-1</sup>; <sup>1</sup>H NMR (400 MHz, CDCl<sub>3</sub>, 328K)<sup>306</sup> δ 7.42-7.20 (series of m, 20H), 6.97 (d, *J* = 9.3 Hz, 2H), 6.82 (d, *J* = 8.7 Hz, 2H), 6.72-6.69 (br m, 2H), 6.59 (d, *J* = 2.1 Hz, 2H), 6.57 (dd, *J* = 2.1, 2.1 Hz, 1H), 6.37 (d, *J* = 7.7 Hz, 1H), 5.55 (d, *J* = 5.6 Hz, 1H), 5.25 (d, *J* = 6.3 Hz, 1H), 5.07 (d, *J* = 5.9 Hz, 1H), 5.00-4.95 (m, 6H), 4.73 (ddd, *J* = 8.1, 5.0, 5.0 Hz, 1H), 4.67 (d, *J* = 14.3, 7.2 Hz, 1H), 4.26-4.22 (m, 2H), 4.16 (ddd, *J* = 9.4, 7.7, 3.5 Hz, 2H), 3.24 (dd, *J* = 13.8, 6.3 Hz, 1H), 3.06 (dd, *J* = 14.1, 7.2 Hz, 1H), 2.86 (dd, *J* = 16.8, 4.7 Hz, 1H), 2.70 (dd, *J* = 16.8, 5.4 Hz, 1H), 1.45 (s, 9H), 1.03-0.94 (m, 4H), 0.06 (s, 9H), 0.04 (s, 9H); <sup>13</sup>C NMR (100 MHz, CDCl<sub>3</sub>) ppm 170.5, 170.3, 170.1, 169.5, 160.2, 158.5, 155.3, 140.1, 136.60, 136.58, 136.2, 129.4, 128.9, 128.6, 128.5, 128.43, 128.39, 128.1, 127.85, 127.81, 127.5, 127.3, 126.9, 114.9, 106.0, 102.2, 80.1, 69.9, 69.6, 64.1, 63.2, 58.2, 56.7, 54.1, 48.6, 38.4, 36.1, 28.4, 17.3, 17.1, -1.6; HRMS (ESI): Exact mass calcd for C<sub>65</sub>H<sub>80</sub>N<sub>4</sub>NaO<sub>12</sub>Si<sub>2</sub> [M+Na]<sup>+</sup> 1187.5209, found 1187.5171.



**Dibenzyl**                      **((S)-2-(4-(benzyloxy)phenyl)-2-((tert-butoxycarbonyl)amino)acetyl)-L-phenylalanyl-L-aspartate (384)**. The dipeptide (860 mg, 1.53 mmol) was dissolved in 4 M HCl/dioxanes (15 mL) and stirred under argon. Upon complete deprotection, the volatiles were removed. Diethyl ether was added to the flask and the mixture was concentrated to remove excess HCl. This was repeated twice and the resulting white foam was dried under high vacuum for an

<sup>306</sup> Refer to Supporting Information 2 for <sup>1</sup>H spectra at 298 and 328K

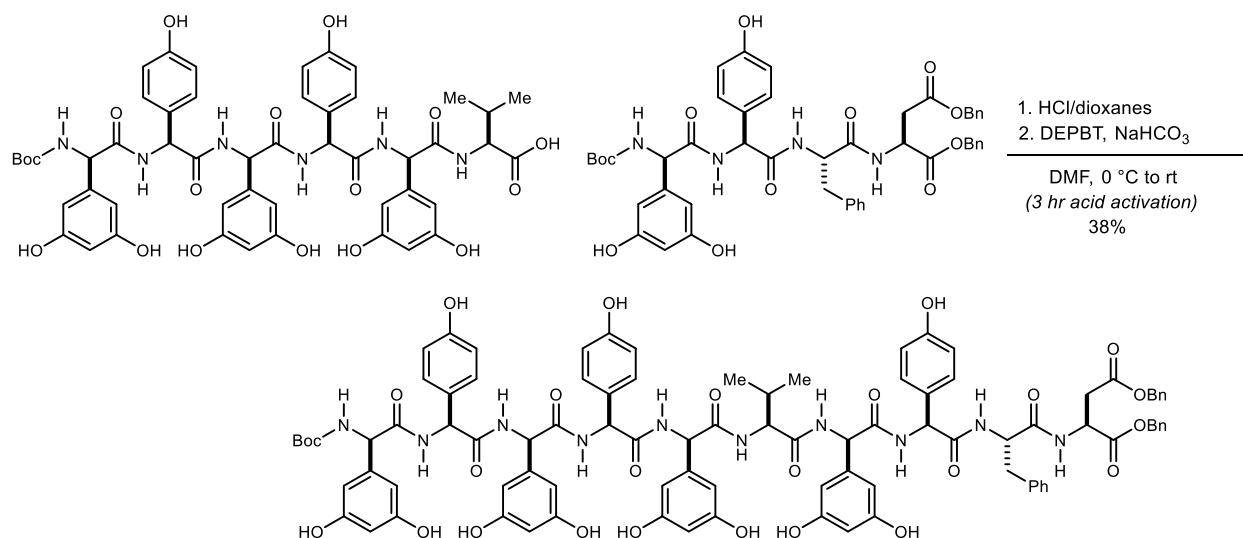
hour. The bromonitroalkane (831 mg, 1.84 mmol) was added to the flask followed by DME (15 mL), and the mixture was cooled to 0 °C. Potassium iodide (508 mg, 3.06 mmol) was added followed by potassium carbonate (1.27 g, 9.18 mmol). A freshly prepared solution of 3 M urea hydrogen peroxide in water was then added (1.53 mL, 4.59 mmol) and the reaction was stirred under an oxygen atmosphere at 0 °C for 2 hours, and then at room temperature for 24 hours. The reaction was quenched with satd aq Na<sub>2</sub>S<sub>2</sub>O<sub>4</sub> and the aqueous layers were extracted several times with ethyl acetate. The organic layers were combined and washed with aq Na<sub>2</sub>S<sub>2</sub>O<sub>4</sub>, 1 M HCl and brine, dried (Na<sub>2</sub>SO<sub>4</sub>), filtered and concentrated. The resulting residue was purified by flash column chromatography (SiO<sub>2</sub>, 30-50% ethyl acetate in hexanes) to provide the product as a white solid (429 mg, 35% over two steps). Mp = 108-111 °C; [ $\alpha$ ]<sub>D</sub><sup>20</sup> +35 (c 0.49, CHCl<sub>3</sub>); R<sub>f</sub> = 0.67 (50% EtOAc/hexanes); IR (film) 3285, 3064, 3033, 2978, 1736, 1693, 1646, 1510, 1242, 1169 cm<sup>-1</sup>; <sup>1</sup>H NMR (600 MHz, CDCl<sub>3</sub>)  $\delta$  7.40-7.36 (m, 4H), 7.35-7.28 (m, 11H), 7.24-7.19 (m, 3H), 7.11 (dd, *J* = 7.9, 1.5 Hz, 2H), 7.08 (d, *J* = 8.5 Hz, 2H), 6.87 (d, *J* = 8.7 Hz, 2H), 6.80 (br s, 1H), 6.24 (d, *J* = 7.7 Hz, 1H), 5.45 (br s, 1H), 5.11 (s, 2H), 5.04 (d, *J* = 12.2 Hz, 2H), 5.01 (d, *J* = 12.1 Hz, 2H), 4.96 (s, 1H), 4.80 (dd, *J* = 8.0, 4.9, 4.9 Hz, 1H), 4.63 (dd, *J* = 13.6, 6.5 Hz, 1H), 3.11 (dd, *J* = 14.1, 6.2 Hz, 1H), 2.99 (dd, *J* = 14.1, 7.0 Hz, 1H), 2.94 (dd, *J* = 17.1, 4.7 Hz, 1H), 2.78 (dd, *J* = 17.0, 4.3 Hz, 1H), 1.39 (s, 9H); <sup>13</sup>C NMR (150 MHz, CDCl<sub>3</sub>) ppm 170.5, 170.3, 170.2, 170.0, 159.0, 155.4, 136.9, 136.1, 135.4, 135.2, 129.4, 128.8, 128.75, 128.73, 128.66, 128.63, 128.60, 128.55, 128.50, 128.2, 127.6, 127.2, 115.6, 80.5, 70.1, 67.7, 67.0, 58.8, 54.2, 48.9, 37.7, 36.3, 28.4; HRMS (ESI): Exact mass calcd for C<sub>47</sub>H<sub>49</sub>N<sub>3</sub>O<sub>9</sub> [M]<sup>+</sup> 800.3542, found 800.3527.



**Dibenzyl ((*S*)-2-((*R*)-2-((*tert*-butoxycarbonyl)amino)-2-(3,5-dihydroxyphenyl)acetamido)-2-(4-hydroxyphenyl)acetyl)-*L*-phenylalanyl-*L*-aspartate (290).** Prepared according to a literature

procedure.<sup>295</sup> The *N*-Boc-Phe-Asp-OBn dipeptide (190 mg, 339  $\mu\text{mol}$ ) was stirred as a solution in 4M HCl/dioxanes (5 mL) under argon for one hour. The volatiles were removed, diethyl ether was added to the flask, and the mixture was concentrated to remove excess HCl. This was repeated twice and the resulting solids were dried under high vacuum. In a separate flame-dried round-bottom flask, the amino acid (122 mg, 282  $\mu\text{mol}$ ) was dissolved in DMF (5.6 mL) and the solution was cooled to 0 °C. To the flask was added DEPBT (253 mg, 846  $\mu\text{mol}$ ) and  $\text{NaHCO}_3$  (94.8 mg, 1.13 mmol). The HCl salt of the amine was added as a solid, and DMF (250  $\mu\text{L}$ ) was used to transfer any residual amine from the flask. The reaction mixture was stirred at 0 °C for 2 hours and then at room temperature for 48 hours. The mixture was quenched with water and the aqueous layers were extracted several times with ethyl acetate. The organic layers were combined and washed with copious amounts of ice water followed by  $\text{NaHCO}_3$  and brine. The organic layers were dried ( $\text{Na}_2\text{SO}_4$ ) and concentrated. The resulting residue was purified by column chromatography (2-5-10% MeOH in dichloromethane) to afford the product as a white solid (196 mg, 82%). All spectral data matched the literature.<sup>295</sup>

## Endgame strategies toward feglymycin



**Dibenzyl ((S)-2-((R)-2-((S)-2-((R)-2-((S)-2-((R)-2-((S)-2-((R)-2-((tert-butoxycarbonyl)amino)-2-(3,5-dihydroxyphenyl)acetamido)-2-(4-hydroxyphenyl)acetamido)-2-(3,5-dihydroxyphenyl)acetamido)-2-(4-hydroxyphenyl)acetamido)-2-(3,5-dihydroxyphenyl)acetamido)-3-methylbutanamido)-2-(3,5-dihydroxyphenyl)acetamido)-2-(4-hydroxyphenyl)acetyl)-L-phenylalanyl-L-aspartate (348).** The tetrapeptide (32.5 mg, 37  $\mu\text{mol}$ ) was stirred in 4M HCl/dioxanes (500  $\mu\text{L}$ ) under argon for 1 hour. The volatiles were removed and diethyl ether was added to the vial and the mixture was concentrated to remove excess HCl. This was repeated twice and the resulting solids were dried under high vacuum. In a separate flame-dried vial, the amino acid (26 mg, 30.9  $\mu\text{mol}$ ) was dissolved in DMF (500  $\mu\text{L}$ ) and the solution was cooled to 0 °C. To the vial was added DEPBT (30.3 mg, 101  $\mu\text{mol}$ ) and NaHCO<sub>3</sub> (11.4 mg, 135  $\mu\text{mol}$ ), and the mixture was stirred for 3 hours. The HCl salt of the amine was added as a solid, and DMF (175  $\mu\text{L}$ ) was used to transfer any residual amine from the vial. The reaction mixture stirred at 0 °C for 2 hours and then at room temperature for 48 hours. The reaction was quenched with a few drops of water the mixture was concentrated. The crude material was purified by preparative HPLC (retention time = 15.1 min) according to the table below to afford the product as a cream-colored solid (22.7 mg, 38%). Mp >275 °C;  $[\alpha]_D^{20}$  -20 (*c* 0.82, MeOH);  $R_f$  = 0.07 (20% MeOH/DCM); IR (film) 3294, 2965, 2922, 1731, 1645, 1515, 1159  $\text{cm}^{-1}$ ; <sup>1</sup>H NMR (600 MHz,

DMSO-*d*<sub>6</sub>) δ 9.29-9.10 (series of br s, 10H)<sup>307</sup>, 8.84 (d, *J* = 7.9 Hz, 1H), 8.72 (d, *J* = 6.3 Hz, 1H), 8.68 (d, *J* = 7.3 Hz, 1H), 8.56 (d, *J* = 8.0 Hz, 1H), 8.53-8.47 (m, 3H), 8.41 (d, *J* = 8.2 Hz, 1H), 8.17 (d, *J* = 6.7 Hz, 1H), 7.35-7.29 (m, 12H), 7.23-7.16 (series of m, 5H), 7.07 (appt dd, *J* = 7.9, 7.9 Hz, 3H), 7.08 (d, *J* = 8.1 Hz, 1H), 6.97-6.94 (m, 2H), 6.57-6.55 (m, 6H), 6.29 (dd, *J* = 13.2, 1.7 Hz, 4H), 6.22-6.21 (m, 3H), 6.10-6.09 (m, 2H), 6.06 (d, *J* = 1.8 Hz, 2H), 5.63 (d, *J* = 7.7 Hz, 2H), 5.54 (d, *J* = 8.1 Hz, 1H), 5.49 (d, *J* = 7.9 Hz, 1H), 5.45 (d, *J* = 7.2 Hz, 1H), 5.32 (d, *J* = 7.5 Hz, 1H), 5.21 (d, *J* = 8.4 Hz, 1H), 5.09-5.01 (m, 4H), 4.73-4.69 (m, 1H), 4.55 (br dd, *J* = 13.3, 8.2 Hz, 1H), 4.38 (br dd, *J* = 7.5, 7.5 Hz, 1H), 2.99-2.97 (m 1H), 2.86-2.71 (series of m, 3H), 1.88 (dq, *J* = 13.3, 6.6, 6.6 Hz, 1H), 1.38 (s, 9H), 0.62 (d, *J* = 6.5 Hz, 3H), 0.59 (d, *J* = 6.5 Hz, 3H); <sup>13</sup>C NMR (150 MHz, DMSO-*d*<sub>6</sub>) ppm: Please refer to the Supporting Information 2 for the <sup>13</sup>C NMR spectrum ; HRMS (ESI): Exact mass calcd for C<sub>93</sub>H<sub>93</sub>N<sub>10</sub>O<sub>26</sub> [M-H]<sup>-</sup> 1765.6268, found 1765.6323.

Solvent A: H<sub>2</sub>O (0.1% HCOOH)

Solvent B: MeCN (0.1% HCOOH)

Flow rate: 20 mL/min

Time	%B
0.00	0.0
2.00	20.0
20.00	75.0
22.00	95.0
23.00	95.0
23.50	20.0
24.00	20.0

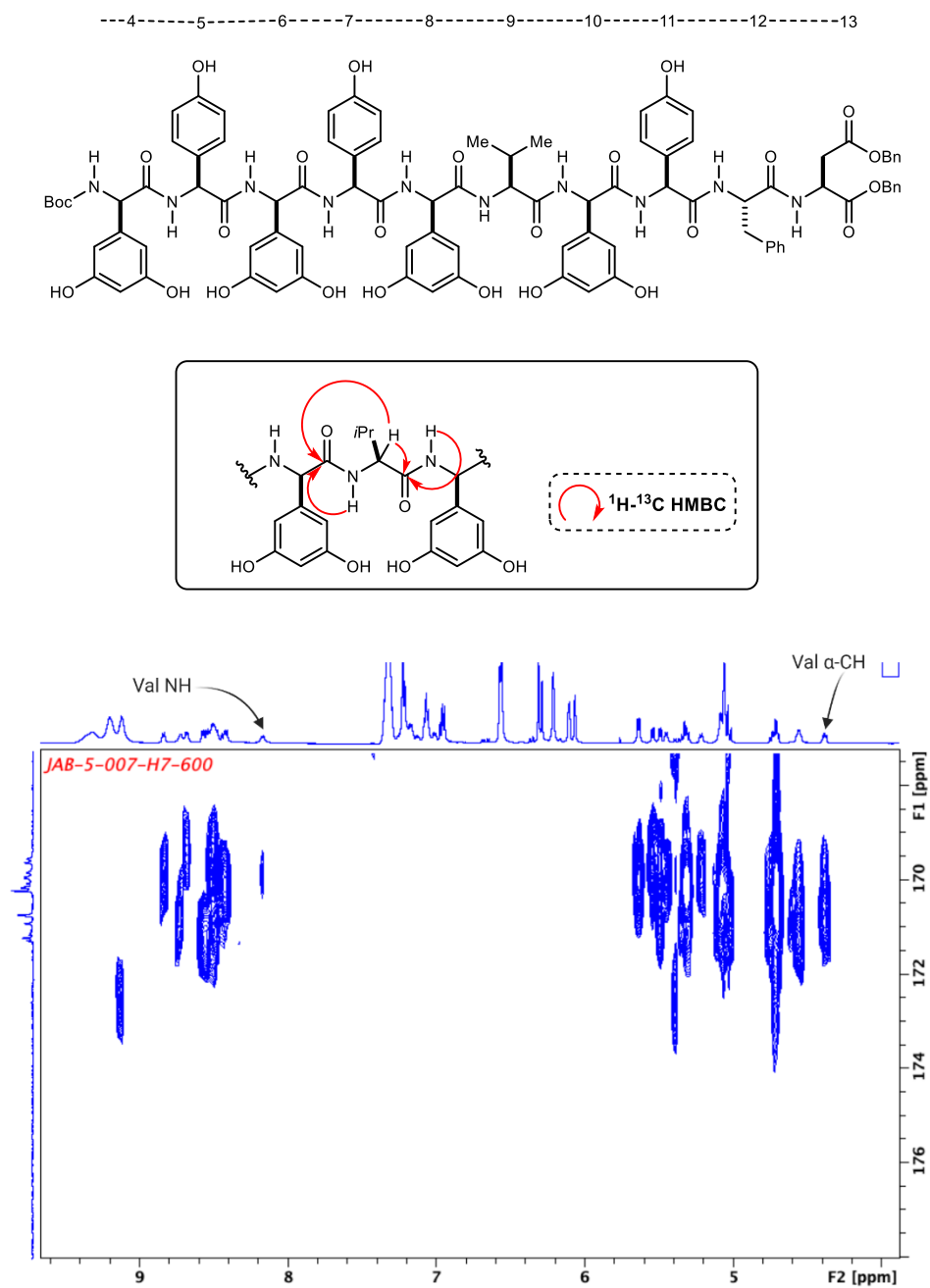
2D NMR and HRMS were used as the primary methods for structural elucidation of decapeptide **348**. Please refer to the Supporting Information 2 for the 2D spectra. One key observation that supports the connection between the tetra- and hexapeptides results from the connecting valine residue. Backbone carbonyl carbons of residues 4-8, and 10-11 are difficult to distinguish from one another. Similarly, the N-H and α-CH peaks for each of those residues are also difficult to assign with certainty. However, the valine NH and α-CH are distinct and were assigned by HSQC and COSY. HMBC then showed that the two resonances had correlations to two distinct carbonyl carbons. The shared carbonyl correlation would be indicative of the carbonyl at Dpg8, which is to

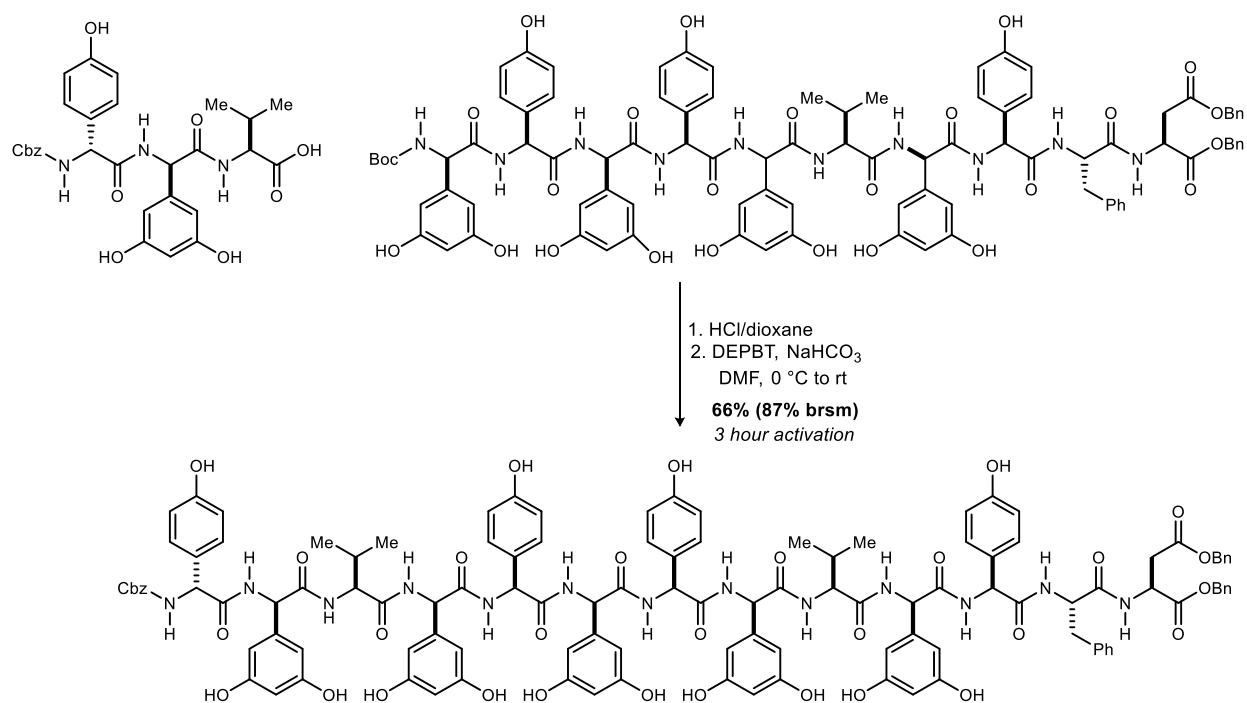
---

<sup>307</sup> 10 of 11 phenolic O-H observed

be expected from the starting materials. The second correlation from the Val  $\alpha$ -CH to a separate carbonyl would be indicative of the connection forged in the coupling reaction. That carbonyl also has a correlation to Dpg NH. While the residue associated with the specific Dpg NH cannot be explicitly assigned as previously mentioned, this serves to support that there was an amide bond formed between Val9 and a Dpg residue. (Figure 46).

Figure 46. Key  $^1\text{H}$ - $^{13}\text{C}$  HMBC crosspeaks for the structural assignment of decapeptide 348.





**Dibenzyl** ((S)-2-((R)-2-((S)-2-((R)-2-((S)-2-((R)-2-((S)-2-((R)-2-((S)-2-((R)-2-((R)-2-((benzyloxy)carbonyl)amino)-2-(4-hydroxyphenyl)acetamido)-2-(3,5-dihydroxyphenyl)acetamido)-3-methylbutanamido)-2-(3,5-dihydroxyphenyl)acetamido)-2-(4-hydroxyphenyl)acetamido)-2-(3,5-dihydroxyphenyl)acetamido)-2-(4-hydroxyphenyl)acetamido)-2-(3,5-dihydroxyphenyl)acetamido)-3-methylbutanamido)-2-(3,5-dihydroxyphenyl)acetamido)-2-(4-hydroxyphenyl)acetyl)-L-phenylalanyl-L-aspartate (**300**). The decapeptide (13.0 mg, 7.35  $\mu\text{mol}$ ) was stirred in 4M HCl/dioxanes (500  $\mu\text{L}$ ) under argon for 1 hour. The volatiles were removed and diethyl ether was added to the vial and the mixture was concentrated to remove excess HCl. This was repeated twice and the resulting solids were dried under high vacuum. In a separate flame-dried vial, the amino acid (3.8 mg, 6.7  $\mu\text{mol}$ ) was dissolved in DMF (90  $\mu\text{L}$ ) and the solution was cooled to 0 °C. To the vial was added DEPBT (6.0 mg, 20  $\mu\text{mol}$ ) and NaHCO<sub>3</sub> (2.3 mg, 27  $\mu\text{mol}$ ), and the mixture was stirred for 3 hours. The HCl salt of the amine was added as a solid, and DMF (120  $\mu\text{L}$ ) was used to transfer any residual amine from the vial. The reaction mixture stirred at 0 °C for 2 hours and then at room temperature for 48 hours. The reaction was quenched with a few drops of water and the mixture was concentrated. The crude material was purified by size exclusion chromatography (Sephadex LH-



20, MeOH) to provide the product as a cream film (9.8 mg, 66%). Mp >275 °C;  $[\alpha]_D^{20}$  -29 (c 0.46, MeOH);  $R_f$  not determined due to excessive streaking of the compound on the TLC plate;  $^1\text{H}$  NMR (600 MHz,  $\text{DMSO-}d_6$ )  $\delta$  Please refer to Supporting Information 2 for the  $^1\text{H}$ -NMR spectrum;  $^{13}\text{C}$  NMR (150 MHz,  $\text{DMSO-}d_6$ ) ppm: Please refer to the Supporting Information 2 for the  $^{13}\text{C}$  NMR spectrum; HRMS (ESI): Exact mass calcd for  $\text{C}_{117}\text{CaH}_{116}\text{N}_{13}\text{O}_{32}$   $[\text{M}+\text{Ca}]^+$  1127.3709, found 1127.3717.

## 4.2 X-Ray Crystallographic Data

Details of crystallographic refinement for compounds 56d, 56f, syn-56h, anti-56h, and 56g.

**General Methods.** A suitable crystal of each sample was selected for analysis and mounted in a polyimide loop. All measurements were made on a Rigaku Oxford Diffraction Supernova Eos CCD with filtered Cu-K $\alpha$  radiation at a temperature of 100 K. Using Olex2,<sup>308</sup> the structure was solved with the ShelXT structure solution program using Direct Methods and refined with the ShelXL refinement package<sup>309</sup> using Least Squares minimization.

### Compound 56d

A disordered vinyl group was modeled over two positions without restraint. The absolute configuration was determined on the basis of the Flack parameter.

### Compounds 56f, syn-56h, anti-56h, and 56g.

Structures were refined without restraint. The absolute configuration was determined on the basis of the Flack parameter in each case.

### Compound syn-66

This compound was modeled without restraint.

### Compound anti-66

A disordered tertiary butyl group was modeled over two positions with similarity restraints placed on its atom thermal parameters. The absolute configuration was determined on the basis of the Flack parameter.

### Compound 67a

This compound was modeled without restraint. The absolute configuration was determined on the basis of the Flack parameter.

---

<sup>308</sup> Dolomanov, O. V.; Bourhis, L. J.; Gildea, R. J.; Howard, J. A. K.; Puschmann, H. *J Appl Crystallogr* **2009**, *42*, 339.

<sup>309</sup> Sheldrick, G. M. *Acta Crystallogr A* **2008**, *64*, 112.

**Compound 67b**

This compound was modeled without restraint. The absolute configuration was determined on the basis of the Flack parameter.

**Compound 127**

This compound was modeled without restraint. The absolute configuration was determined on the basis of the Flack parameter.

**Table 1. Crystal data and structure refinement for 56d.**

Identification code	56d
Empirical formula	$C_{17}H_{23}FN_2O_4$
Formula weight	338.37
Temperature	99.98(10) K
Wavelength	1.54184 Å
Crystal system	Monoclinic
Space group	P 1 21 1
Unit cell dimensions	$a = 10.32624(13)$ Å $\alpha = 90^\circ$ $b = 15.5828(2)$ Å $\beta = 106.1130(14)^\circ$ $c = 11.74267(16)$ Å $\gamma = 90^\circ$
Volume	1815.30(4) Å <sup>3</sup>
Z	4
Density (calculated)	1.238 Mg/m <sup>3</sup>
Absorption coefficient	0.794 mm <sup>-1</sup>
F(000)	720
Crystal size	0.189 x 0.158 x 0.101 mm <sup>3</sup>
Theta range for data collection	3.918 to 72.965°.
Index ranges	$-9 \leq h \leq 12$ , $-19 \leq k \leq 19$ , $-14 \leq l \leq 14$
Reflections collected	24691
Independent reflections	6879 [R(int) = 0.0290]
Completeness to theta	= 67.684° 99.8 %
Absorption correction	Gaussian
Max. and min. transmission	1.000 and 0.811

Refinement method Full-matrix least-squares on  $F^2$   
Data / restraints / parameters 6879 / 1 / 458  
Goodness-of-fit on  $F^2$  1.027  
Final R indices [ $I > 2\sigma(I)$ ]  $R1 = 0.0273$ ,  $wR2 = 0.0640$   
R indices (all data)  $R1 = 0.0307$ ,  $wR2 = 0.0687$   
Absolute structure parameter 0.02(5)  
Largest diff. peak and hole 0.187 and  $-0.207 \text{ e}/\text{\AA}^{-3}$

**Table 2. Crystal data and structure refinement for 56f.**

Identification code	56f
Empirical formula	C <sub>21</sub> H <sub>24</sub> ClFN <sub>2</sub> O <sub>4</sub>
Formula weight	422.87
Temperature	100.01(10) K
Wavelength	1.54184 Å
Crystal system	Monoclinic
Space group	P 1 21 1
Unit cell dimensions	a = 12.8885(3) Å $\alpha$ = 90° b = 5.3127(2) Å $\beta$ = 95.058(2)° c = 15.1705(4) Å $\gamma$ = 90°
Volume	1034.72(5) Å <sup>3</sup>
Z	2
Density (calculated)	1.357 Mg/m <sup>3</sup>
Absorption coefficient	1.972 mm <sup>-1</sup>
F(000)	444
Crystal size	0.249 x 0.034 x 0.017 mm <sup>3</sup>
Theta range for data collection	2.924 to 72.299°.
Index ranges	-15 ≤ h ≤ 15, -5 ≤ k ≤ 6, -18 ≤ l ≤ 15
Reflections collected	13856
Independent reflections	3635 [R(int) = 0.0387]
Completeness to theta	= 67.684° 99.9 %
Absorption correction	Gaussian
Max. and min. transmission	1.000 and 0.731

Refinement method    Full-matrix least-squares on  $F^2$   
Data / restraints / parameters    3635 / 1 / 265  
Goodness-of-fit on  $F^2$     1.049  
Final R indices [ $I > 2\sigma(I)$ ]     $R1 = 0.0361$ ,  $wR2 = 0.0916$   
R indices (all data)     $R1 = 0.0372$ ,  $wR2 = 0.0927$   
Absolute structure parameter     $-0.010(13)$   
Largest diff. peak and hole     $0.537$  and  $-0.220 \text{ e}/\text{\AA}^{-3}$

**Table 3. Crystal data and structure refinement for syn-56h.**

Identification code	syn-56h	
Empirical formula	$C_{20}H_{31}FN_2O_4$	
Formula weight	382.47	
Temperature	100.00(10) K	
Wavelength	1.54184 Å	
Crystal system	Orthorhombic	
Space group	P2 <sub>1</sub> 2 <sub>1</sub> 2 <sub>1</sub>	
Unit cell dimensions	a = 11.50004(6) Å	$\alpha = 90^\circ$
	b = 18.45454(10) Å	$\beta = 90^\circ$
	c = 30.36728(18) Å	$\gamma = 90^\circ$
Volume	6444.79(6) Å <sup>3</sup>	
Z	12	
Density (calculated)	1.183 Mg/m <sup>3</sup>	
Absorption coefficient	0.722 mm <sup>-1</sup>	
F(000)	2472	
Crystal size	0.465 x 0.375 x 0.246 mm <sup>3</sup>	
Theta range for data collection	2.802 to 72.268°.	
Index ranges	-14 ≤ h ≤ 13, -22 ≤ k ≤ 22, -27 ≤ l ≤ 37	
Reflections collected	35099	
Independent reflections	12498 [R(int) = 0.0245]	
Completeness to theta = 67.684°	100.0 %	
Absorption correction	Gaussian	
Max. and min. transmission	1.000 and 0.340	



Refinement method Full-matrix least-squares on  $F^2$   
Data / restraints / parameters 12498 / 0 / 748  
Goodness-of-fit on  $F^2$  1.046  
Final R indices [ $I > 2\sigma(I)$ ]  $R1 = 0.0306$ ,  $wR2 = 0.0764$   
R indices (all data)  $R1 = 0.0315$ ,  $wR2 = 0.0771$   
Absolute structure parameter  $-0.01(3)$   
Largest diff. peak and hole  $0.165$  and  $-0.265 \text{ e}/\text{\AA}^{-3}$

**Table 4. Crystal data and structure refinement for anti-56h.**

Identification code	anti-56h	
Empirical formula	$C_{20}H_{31}FN_2O_4$	
Formula weight	382.47	
Temperature	100.01(10) K	
Wavelength	1.54184 Å	
Crystal system	Hexagonal	
Space group	$P6_1$	
Unit cell dimensions	$a = 11.84190(10)$ Å	$\alpha = 90^\circ$
	$b = 11.84190(10)$ Å	$\beta = 90^\circ$
	$c = 27.22040(10)$ Å	$\gamma = 120^\circ$
Volume	3305.73(6) Å <sup>3</sup>	
Z	6	
Density (calculated)	1.153 Mg/m <sup>3</sup>	
Absorption coefficient	0.704 mm <sup>-1</sup>	
F(000)	1236	
Crystal size	0.415 x 0.077 x 0.065 mm <sup>3</sup>	
Theta range for data collection	4.311 to 72.268°.	
Index ranges	-14 ≤ h ≤ 14, -14 ≤ k ≤ 14, -33 ≤ l ≤ 33	
Reflections collected	50607	
Independent reflections	4353 [R(int) = 0.0349]	
Completeness to theta = 67.684°	100.0 %	
Absorption correction	Gaussian	
Max. and min. transmission	1.000 and 0.580	

Refinement method Full-matrix least-squares on  $F^2$   
Data / restraints / parameters 4353 / 1 / 250  
Goodness-of-fit on  $F^2$  1.052  
Final R indices [ $I > 2\sigma(I)$ ]  $R1 = 0.0232$ ,  $wR2 = 0.0584$   
R indices (all data)  $R1 = 0.0235$ ,  $wR2 = 0.0586$   
Absolute structure parameter 0.04(3)  
Largest diff. peak and hole 0.140 and  $-0.148 \text{ e}/\text{\AA}^{-3}$

**Table 5. Crystal data and structure refinement for 56g.**

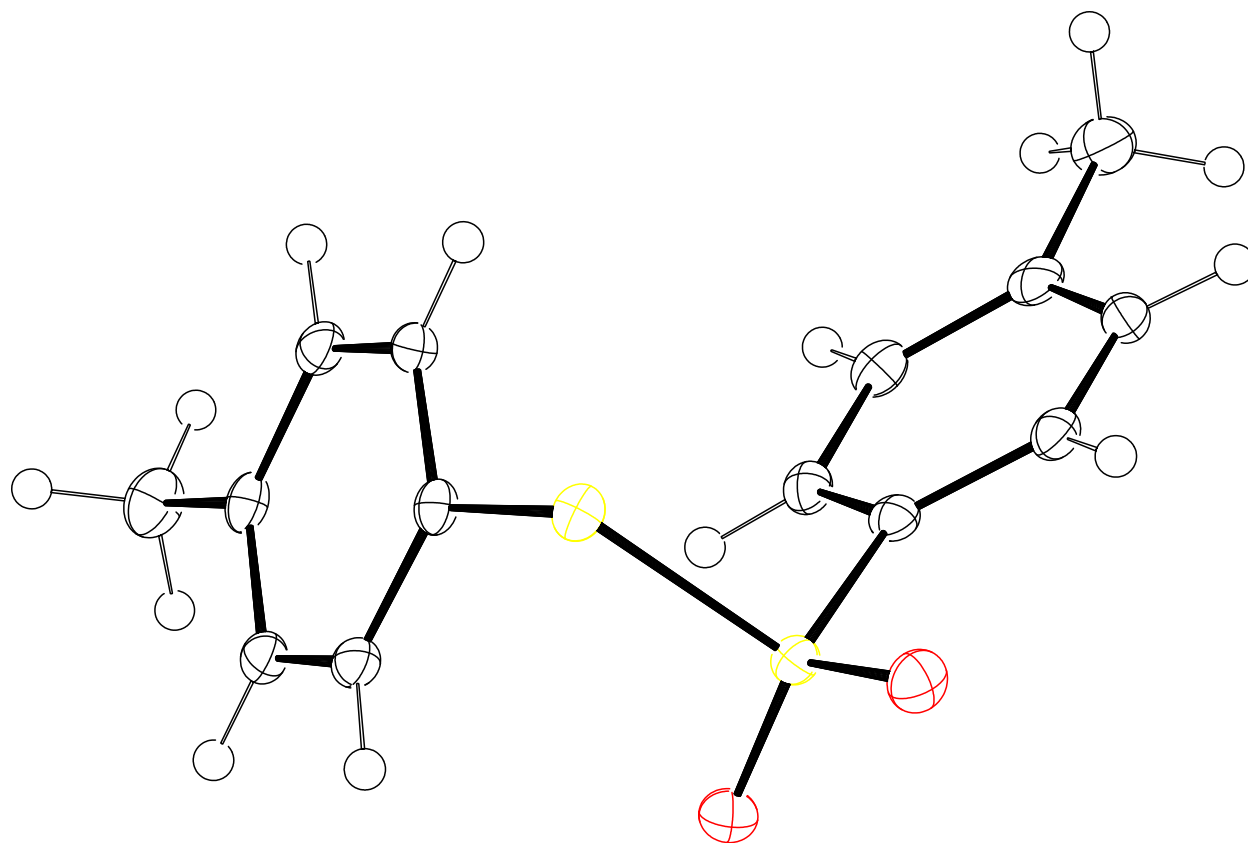
Identification code	6g
Empirical formula	$C_{20}H_{32}N_2O_4$
Formula weight	364.47
Temperature	100.01(10) K
Wavelength	1.54184 Å
Crystal system	Hexagonal
Space group	$P6_1$
Unit cell dimensions	$a = 11.84105(5)$ Å $\alpha = 90^\circ$ $b = 11.84105(5)$ Å $\beta = 90^\circ$ $c = 27.02804(15)$ Å $\gamma = 120^\circ$
Volume	$3281.90(3)$ Å <sup>3</sup>
Z	6
Density (calculated)	1.106 Mg/m <sup>3</sup>
Absorption coefficient	0.618 mm <sup>-1</sup>
F(000)	1188
Crystal size	0.346 x 0.152 x 0.107 mm <sup>3</sup>
Theta range for data collection	4.311 to 72.350°.
Index ranges	$-14 \leq h \leq 14$ , $-14 \leq k \leq 14$ , $-31 \leq l \leq 33$
Reflections collected	62164
Independent reflections	4242 [R(int) = 0.0423]
Completeness to theta	= 67.684° 100.0 %
Absorption correction	Gaussian
Max. and min. transmission	1.000 and 0.474

Refinement method Full-matrix least-squares on  $F^2$   
Data / restraints / parameters 4242 / 1 / 241  
Goodness-of-fit on  $F^2$  1.083  
Final R indices [ $I > 2\sigma(I)$ ]  $R1 = 0.0276$ ,  $wR2 = 0.0742$   
R indices (all data)  $R1 = 0.0278$ ,  $wR2 = 0.0744$   
Absolute structure parameter 0.00(6)  
Largest diff. peak and hole 0.160 and  $-0.140 \text{ e}/\text{\AA}^{-3}$

**Table 6. Crystal data and structure refinement for syn-66.**

Identification code	jab-2-299
Empirical formula	C <sub>14</sub> H <sub>14</sub> O <sub>2</sub> S <sub>2</sub>
Formula weight	278.37
Temperature	100.01(10) K
Wavelength	1.54184 Å
Crystal system	Monoclinic
Space group	P 1 21/c 1
Unit cell dimensions	a = 13.1032(2) Å $\alpha$ = 90° b = 6.48550(12) Å $\beta$ = 92.2750(15)° c = 15.1824(3) Å $\gamma$ = 90°
Volume	1289.20(4) Å <sup>3</sup>
Z	4
Density (calculated)	1.434 Mg/m <sup>3</sup>
Absorption coefficient	3.666 mm <sup>-1</sup>
F(000)	584
Crystal size	0.388 x 0.123 x 0.026 mm <sup>3</sup>
Theta range for data collection	3.376 to 72.267°.
Index ranges	-16 ≤ h ≤ 16, -7 ≤ k ≤ 7, -18 ≤ l ≤ 18
Reflections collected	13961
Independent reflections	2519 [R(int) = 0.0300]
Completeness to theta	= 67.684° 100.0 %
Absorption correction	Gaussian
Max. and min. transmission	1.000 and 0.443

Refinement method Full-matrix least-squares on  $F^2$   
Data / restraints / parameters 2519 / 0 / 165  
Goodness-of-fit on  $F^2$  1.054  
Final R indices [ $I > 2\sigma(I)$ ]  $R_1 = 0.0310$ ,  $wR_2 = 0.0821$   
R indices (all data)  $R_1 = 0.0333$ ,  $wR_2 = 0.0842$   
Extinction coefficient n/a  
Largest diff. peak and hole 0.524 and  $-0.343 \text{ e}/\text{\AA}^{-3}$



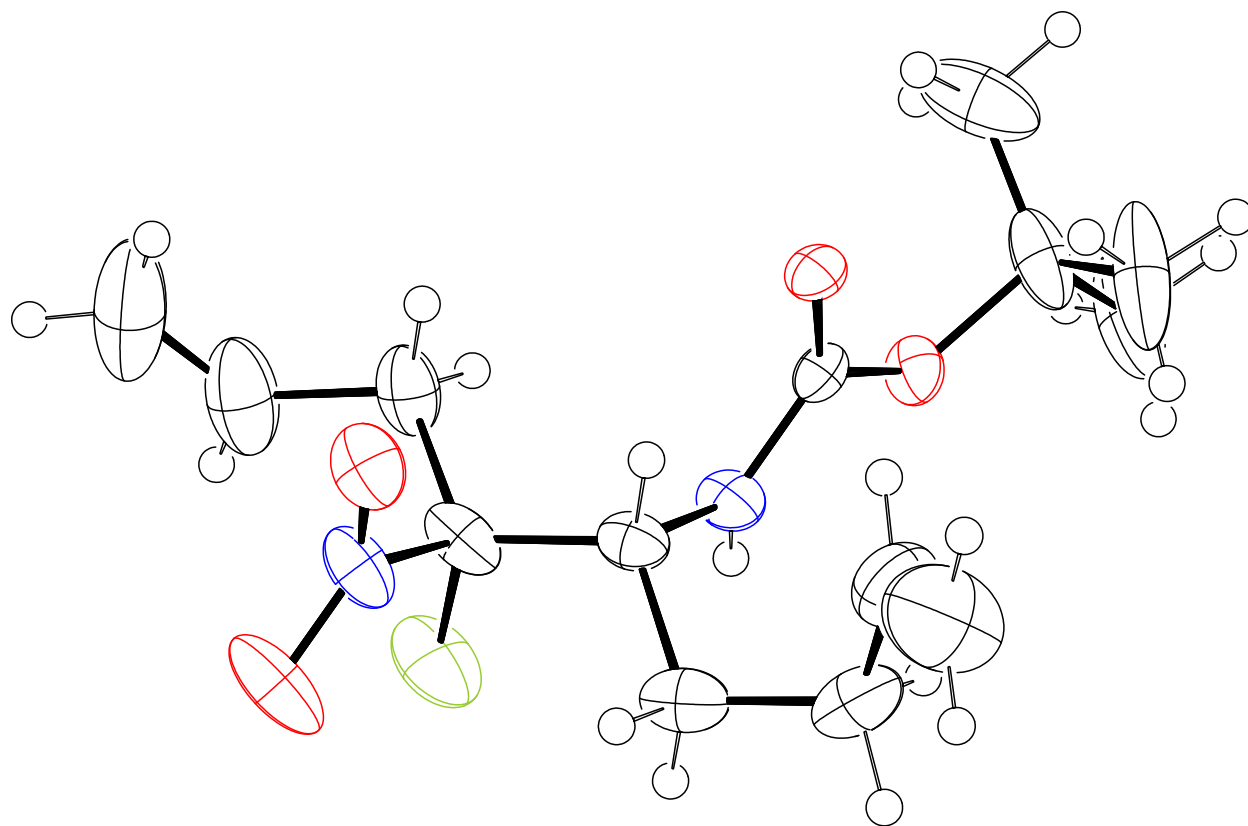
ORTEP diagram shown at 50% probability.



**Table 7. Crystal data and structure refinement for anti-66.**

Identification code	jab-2-251-d2
Empirical formula	C <sub>14</sub> H <sub>23</sub> FN <sub>2</sub> O <sub>4</sub>
Formula weight	302.34
Temperature	100.3(7) K
Wavelength	1.54184 Å
Crystal system	Orthorhombic
Space group	P2 <sub>1</sub> 2 <sub>1</sub> 2 <sub>1</sub>
Unit cell dimensions	a = 11.68912(15) Å      α = 90° b = 16.9694(2) Å      β = 90° c = 17.4982(2) Å      γ = 90°
Volume	3470.91(7) Å <sup>3</sup>
Z	8
Density (calculated)	1.157 Mg/m <sup>3</sup>
Absorption coefficient	0.768 mm <sup>-1</sup>
F(000)	1296
Crystal size	0.199 x 0.1 x 0.049 mm <sup>3</sup>
Theta range for data collection	3.628 to 72.213°.
Index ranges	-9 ≤ h ≤ 14, -18 ≤ k ≤ 20, -21 ≤ l ≤ 21
Reflections collected	19583
Independent reflections	6712 [R(int) = 0.0262]
Completeness to theta	= 67.684° 100.0 %
Absorption correction	Gaussian
Max. and min. transmission	1.000 and 0.775

Refinement method Full-matrix least-squares on  $F^2$   
Data / restraints / parameters 6712 / 114 / 425  
Goodness-of-fit on  $F^2$  1.071  
Final R indices [ $I > 2\sigma(I)$ ]  $R1 = 0.0358$ ,  $wR2 = 0.0928$   
R indices (all data)  $R1 = 0.0383$ ,  $wR2 = 0.0945$   
Absolute structure parameter 0.09(5)  
Extinction coefficient n/a  
Largest diff. peak and hole 0.220 and  $-0.213 \text{ e}/\text{\AA}^{-3}$



ORTEP diagram shown at 50% probability. One of two molecules in the asymmetric unit shown for clarity.

**Table 1. Crystal data and structure refinement for 67a.**

Identification code	jab-2-223-d1
Empirical formula	C <sub>12</sub> H <sub>19</sub> FN <sub>2</sub> O <sub>4</sub>
Formula weight	274.29
Temperature	100.00(10) K
Wavelength	1.54184 Å
Crystal system	Orthorhombic
Space group	P2 <sub>1</sub> 2 <sub>1</sub> 2 <sub>1</sub>
Unit cell dimensions	a = 9.19261(6) Å $\alpha = 90^\circ$
	b = 16.71461(14) Å $\beta = 90^\circ$
	c = 18.49978(11) Å $\gamma = 90^\circ$
Volume	2842.51(3) Å <sup>3</sup>
Z	8
Density (calculated)	1.282 Mg/m <sup>3</sup>
Absorption coefficient	0.887 mm <sup>-1</sup>
F(000)	1168
Crystal size	0.273 x 0.197 x 0.129 mm <sup>3</sup>
Theta range for data collection	3.564 to 72.163°.
Index ranges	-11 ≤ h ≤ 11, -17 ≤ k ≤ 20, -22 ≤ l ≤ 22
Reflections collected	26676
Independent reflections	5571 [R(int) = 0.0282]
Completeness to theta = 67.684°	99.9 %
Absorption correction	Gaussian
Max. and min. transmission	1.000 and 0.733
Refinement method	Full-matrix least-squares on F <sup>2</sup>
Data / restraints / parameters	5571 / 0 / 349

Goodness-of-fit on  $F^2$  1.056

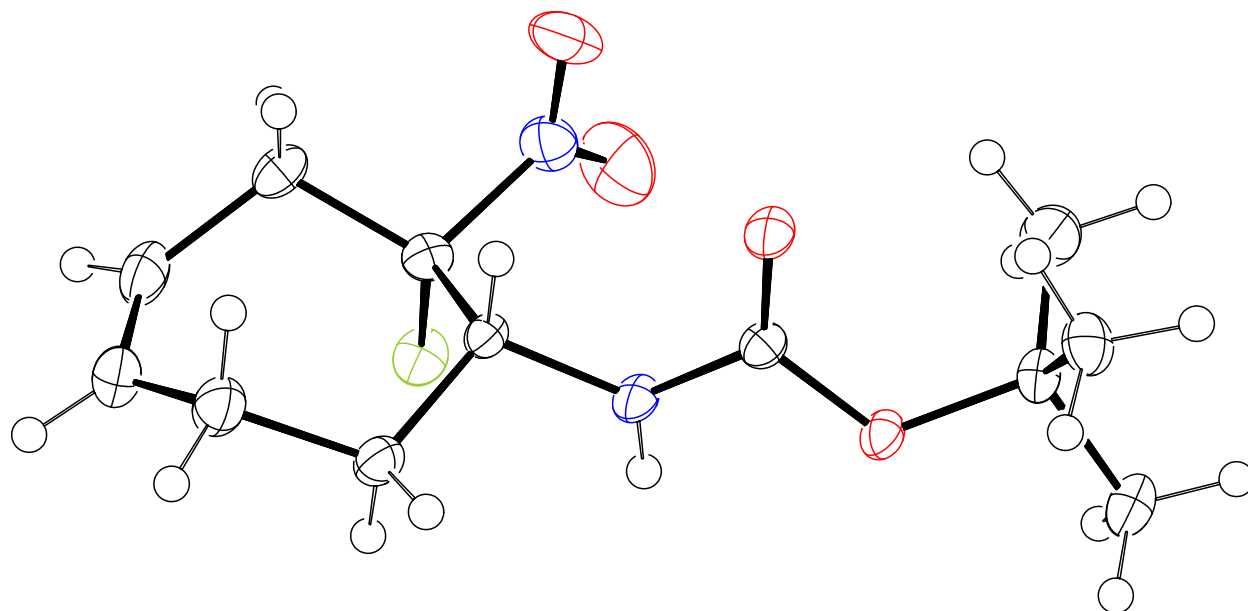
Final R indices [ $I > 2\sigma(I)$ ]  $R_1 = 0.0298$ ,  $wR_2 = 0.0783$

R indices (all data)  $R_1 = 0.0305$ ,  $wR_2 = 0.0788$

Absolute structure parameter 0.02(4)

Extinction coefficient n/a

Largest diff. peak and hole 0.602 and -0.262  $e/\text{\AA}^{-3}$



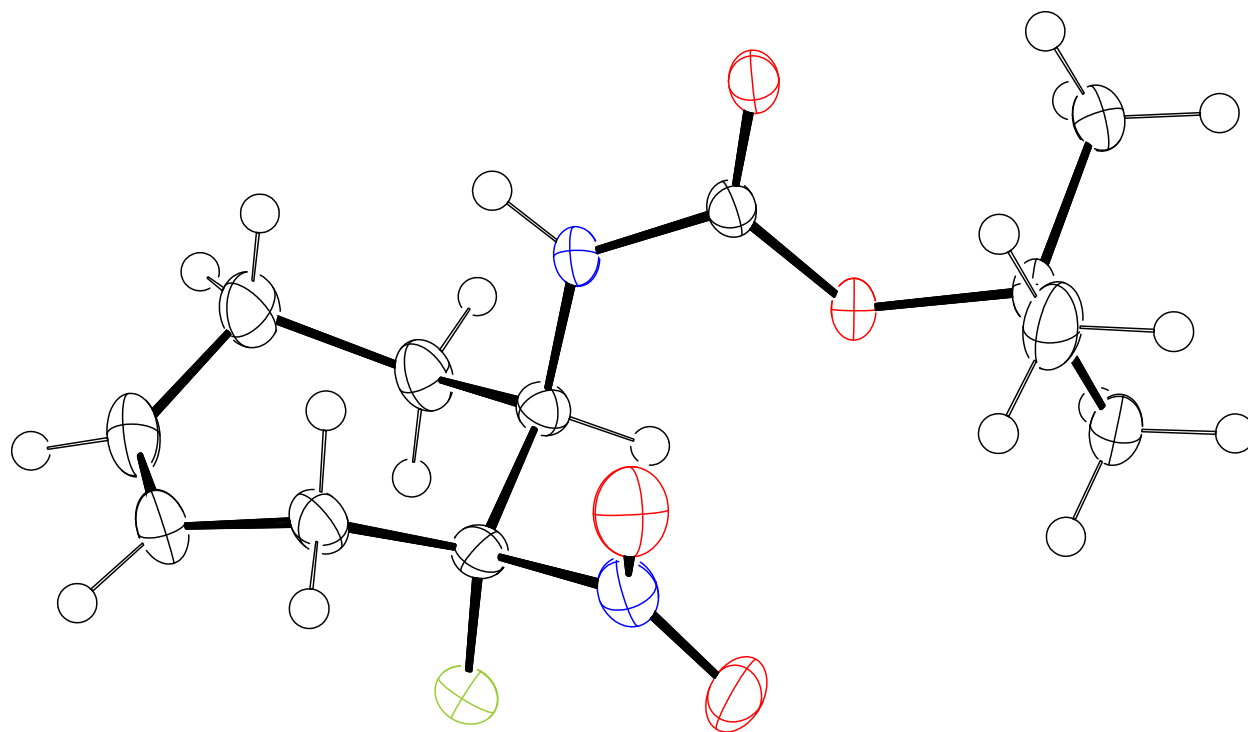
ORTEP diagram shown at 50% probability. One of two molecules in the asymmetric unit are omitted for clarity.

**Table 8. Crystal data and structure refinement for 67b.**

Identification code	jab-2-229_f30-36
Empirical formula	C <sub>12</sub> H <sub>19</sub> FN <sub>2</sub> O <sub>4</sub>
Formula weight	274.29
Temperature	99.96(11) K
Wavelength	1.54184 Å
Crystal system	Orthorhombic
Space group	P2 <sub>1</sub> 2 <sub>1</sub> 2 <sub>1</sub>
Unit cell dimensions	a = 11.5478(8) Å α = 90° b = 11.9104(9) Å β = 90° c = 20.651(3) Å γ = 90°
Volume	2840.3(5) Å <sup>3</sup>
Z	8
Density (calculated)	1.283 Mg/m <sup>3</sup>
Absorption coefficient	0.888 mm <sup>-1</sup>
F(000)	1168
Crystal size	0.25 x 0.198 x 0.164 mm <sup>3</sup>
Theta range for data collection	4.282 to 73.850°.
Index ranges	-14 ≤ h ≤ 14, -14 ≤ k ≤ 13, -25 ≤ l ≤ 24
Reflections collected	23476
Independent reflections	5531 [R(int) = 0.0375]
Completeness to theta	= 67.684° 100.0 %
Absorption correction	Gaussian
Max. and min. transmission	1.000 and 0.617

Refinement method Full-matrix least-squares on  $F^2$   
Data / restraints / parameters 5531 / 0 / 349  
Goodness-of-fit on  $F^2$  1.173  
Final R indices [ $I > 2\sigma(I)$ ]  $R_1 = 0.0396$ ,  $wR_2 = 0.0951$   
R indices (all data)  $R_1 = 0.0561$ ,  $wR_2 = 0.1349$   
Absolute structure parameter  $-0.01(4)$   
Extinction coefficient n/a  
Largest diff. peak and hole  $0.370$  and  $-0.452 \text{ e}/\text{\AA}^{-3}$





ORTEP diagram shown at 50% probability. One of two molecules in the asymmetric unit shown for clarity.

**Table 9. Crystal data and structure refinement for 127.**

Identification code	jab-3-104
Empirical formula	C <sub>16</sub> H <sub>19</sub> FN <sub>2</sub> O <sub>4</sub>
Formula weight	322.33
Temperature	99.94(12) K
Wavelength	1.54184 Å
Crystal system	Monoclinic
Space group	P 1 21 1
Unit cell dimensions	a = 9.91261(14) Å      α = 90° b = 5.23713(10) Å      β = 100.8469(18)° c = 15.5639(4) Å      γ = 90°
Volume	793.54(3) Å <sup>3</sup>
Z	2
Density (calculated)	1.349 Mg/m <sup>3</sup>
Absorption coefficient	0.885 mm <sup>-1</sup>
F(000)	340
Crystal size	0.189 x 0.162 x 0.113 mm <sup>3</sup>
Theta range for data collection	2.891 to 72.231°
Index ranges	-12 ≤ h ≤ 12, -6 ≤ k ≤ 6, -16 ≤ l ≤ 18
Reflections collected	20361
Independent reflections	3063 [R(int) = 0.0330]
Completeness to theta	= 67.684° 99.9 %
Absorption correction	Gaussian
Max. and min. transmission	1.000 and 0.768

Refinement method Full-matrix least-squares on  $F^2$

Data / restraints / parameters 3063 / 1 / 211

Goodness-of-fit on  $F^2$  1.064

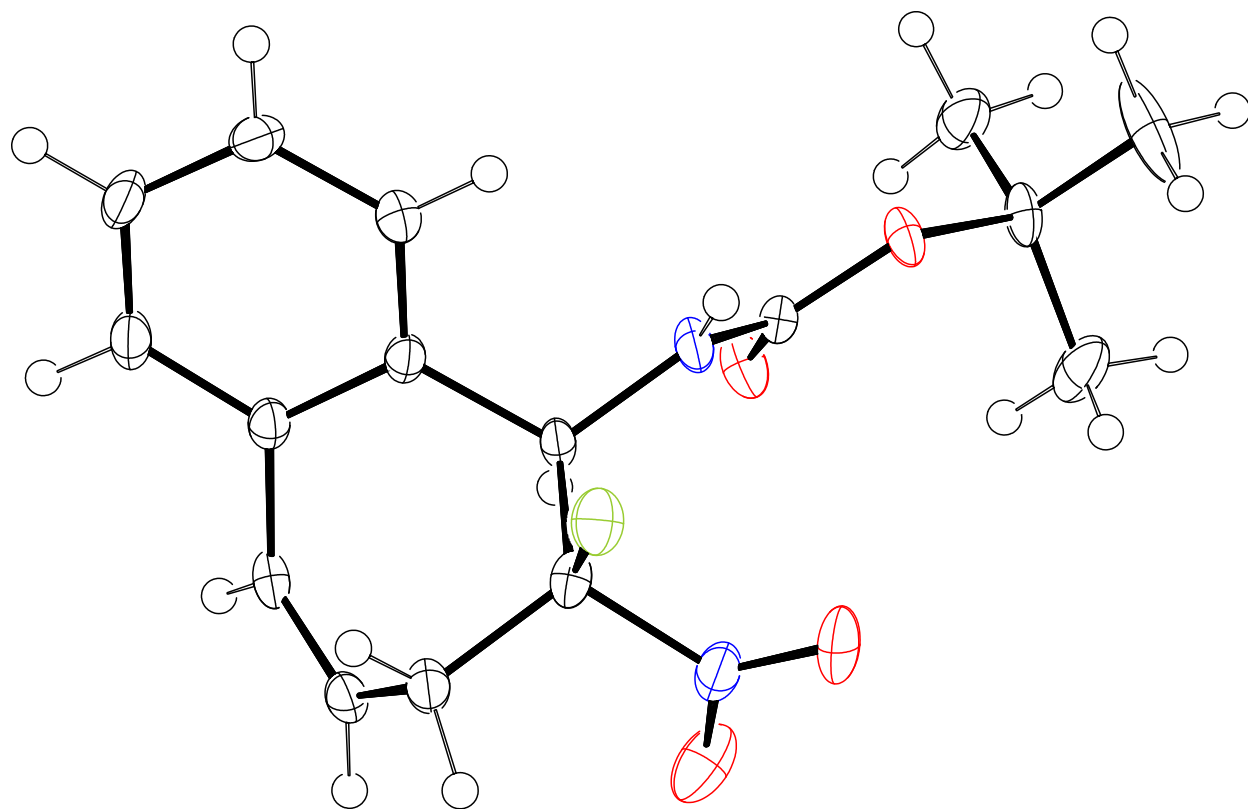
Final R indices [ $I > 2\sigma(I)$ ]  $R_1 = 0.0310$ ,  $wR_2 = 0.0759$

R indices (all data)  $R_1 = 0.0322$ ,  $wR_2 = 0.0781$

Absolute structure parameter 0.03(6)

Extinction coefficient n/a

Largest diff. peak and hole 0.307 and -0.204  $e/\text{\AA}^{-3}$



ORTEP diagram shown at 50% probability.